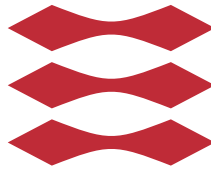


Methods and Algorithms for Economic MPC in Power Production Planning

Leo Emil Sokoler

DTU



Kongens Lyngby 2015
PHD-2015-377

Technical University of Denmark
Department of Applied Mathematics and Computer Science
Richard Petersens Plads, building 324,
2800 Kongens Lyngby, Denmark
Phone +45 4525 3031
compute@compute.dtu.dk
www.compute.dtu.dk

PHD-2015-377, ISSN 0909-3192

Preface

This thesis was prepared at the Department of Applied Mathematics and Computer Science at the Technical University of Denmark in partial fulfilment of the requirements for acquiring the Ph.D. degree in engineering. The project was funded jointly by DONG Energy and the Danish Ministry of Higher Education and Science under the Industrial Ph.D. program, project 11-117435.

The thesis presents novel models and algorithms for power production planning. We apply economic model predictive control (EMPC) for economic dispatch with minimum generation cost. A portfolio system is introduced for demonstration purposes. The portfolio system consists of generators with diverse operational features and capabilities. Extensions of certainty-equivalent EMPC are proposed to account for the inherent uncertainties associated with renewable energy sources. Moreover, we develop tailored optimization algorithms to accommodate the proposed EMPC schemes to large-scale energy systems.

The thesis consists of a summary report and a collection of eleven research papers. The research papers were written during the period April 2012 to September 2015. One paper has been published in a peer-reviewed scientific journal, and three papers have been accepted for publication in peer-reviewed scientific journals. Seven papers have been published at peer-reviewed scientific conferences.

Kgs. Lyngby, October 2015



Leo Emil Sokoler

Acknowledgements

First of all, I would like to thank my supervisors at DTU Compute, John B. Jørgensen, Henrik Madsen, and Niels K. Poulsen. I especially thank my main supervisor John B. Jørgensen for his guidance and suggestions. Without his expertise in optimization and control, this thesis would not be possible. During my time at DTU Compute, I had the pleasure of working with great colleagues. Oscar Borries, Rasmus Halvgaard, Tobias G. Hovgaard, Laura Standardi, and Lars N. Petersen all have been true friends. Special thanks to Anders Skajaa and Martin S. Andersen for always keeping their door open, and for hours of technical discussions.

Thanks also go to my supervisors and colleagues at DONG Energy. My main industrial supervisor Kristian Edlund, for sharing his deep knowledge on energy systems and for his constant support. Simon Børresen, Tommy Mølbak, and Klaus Hilger deserve special thanks as well. Also, I acknowledge Peter Vinter and Runi Beræentsen for their contribution to the work on isolated power systems presented in this thesis.

While at the University of Wisconsin Madison in 2010 during my masters program, I had the pleasure of working with Prof. Stephen J. Wright and Prof. James B. Rawlings. This shaped me into a researcher, and I am grateful for having worked with such competent, passionate, and dedicated people.

Finally, I would like to express the gratitude for my friends and family, in particular for my wife, Mette. She is an invaluable source of support, love, and inspiration. This thesis is dedicated to her, and to my greatest joy in life, our beloved daughter Asta.

Summary (English)

This thesis concerns methods and algorithms for power production planning in contemporary and future power systems. Power production planning is a task that involves decisions across different time scales and planning horizons. Hours-ahead to days-ahead planning is handled by solving a mixed-integer linear program for unit commitment and economic dispatch of the system power generators. We focus on a minutes-ahead planning horizon, where unit commitment decisions are fixed. Economic model predictive control (EMPC) is employed to determine an optimal dispatch for a portfolio of power generators in real-time. A generator can represent a producer of electricity, a consumer of electricity, or possibly both. Examples of generators are heat pumps, electric vehicles, wind turbines, virtual power plants, solar cells, and conventional fuel-fired thermal power plants. Although this thesis is mainly concerned with EMPC for minutes-ahead production planning, we show that the proposed EMPC scheme can be extended to days-ahead planning (including unit commitment) as well.

The power generation from renewable energy sources such as wind and solar power is inherently uncertain and variable. A portfolio with a high penetration of renewable energy is therefore a stochastic system. To accommodate the need for EMPC of stochastic systems, we generalize certainty-equivalent EMPC (CE-EMPC) to mean-variance EMPC (MV-EMPC). In MV-EMPC, the objective function is a trade-off between the expected cost and the cost variance. Simulations show that MV-EMPC reduces cost and risk compared to CE-EMPC. The simulations also show that the economic performance of CE-EMPC can be much improved using a constraint back-off heuristic.

Efficient solution of the optimal control problems (OCPs) that arise in EMPC

is important, as the OCPs are solved online. We present special-purpose algorithms for EMPC of linear systems that exploit the high degree of structure in the OCPs. A Riccati-based homogeneous and self-dual interior-point method is developed for the special case, where the OCP objective function is a linear function. We design an algorithm based on the alternating direction method of multipliers (ADMM) to solve input-constrained OCPs with convex objective functions. The OCPs that occur in EMPC of dynamically decoupled subsystems, e.g. power generators, have a block-angular structure. Subsystem decomposition algorithms based on ADMM and Dantzig-Wolfe decomposition are proposed to solve these OCPs. Subproblems that arise in the decomposition algorithms are solved using structure-exploiting algorithms. To reduce computation time of the EMPC algorithms further, warm-start and early-termination strategies are employed. Benchmarks show that the special-purpose algorithms are significantly faster than current state-of-the-art solvers.

As a potential application area of EMPC, we study power production planning in small isolated power systems. A critical part of power production planning in small isolated power systems is operational reserve planning. The operational reserves are activated to balance production and consumption in real-time. An EMPC scheme is presented for activation of operational reserves. Simulations based on a Faroe Islands case study show that significant cost savings can be achieved using this strategy. For efficient planning of the operational reserves, we present an optimal reserve planning problem (ORPP). The ORPP is a contingency-constrained unit commitment problem that addresses low inertia challenges in small isolated power systems.

In summary, the main contributions of this thesis are:

- A mean-variance optimization strategy for EMPC of linear stochastic systems.
- Tailored algorithms for solution of the OCPs that arise in EMPC of linear stochastic systems.
- Methods for power production planning in small isolated power; the ORPP for unit commitment and economic dispatch, and an EMPC scheme for activation of operational reserves.

Summary (Danish)

Denne afhandling omhandler produktionsplanlægning i nuværende og fremtidige energisystemer. Produktionsplanlægning involverer beslutninger på forskellige tidsskalaer og med forskellige planlægningshorisonter. Planlægning på time- til dagsniveau håndteres ved at løse et lineært blandet heltalsprogram til binding (unit commitment, UC) og økonomisk indmelding (economic dispatch) af systemets elektriske generatorer. Vi fokuserer på planlægning med en minutbaseret horisont, hvor generatorernes bindingsmønster er fastlagt. Økonomisk model prædiktiv regulering (economic model predictive control, EMPC) anvendes til, at bestemme en optimal køreplan for en portefølje af elektriske generatorer i realtid. En elektrisk generator kan repræsentere en producent af elektricitet, en forbruger af elektricitet, eller begge dele. Eksempler på generatorer er varmepumper, elbiler, vindmøller, virtuelle kraftværker, solpaneler, og konventionelle termiske kraftværker. Selvom denne afhandling fokuserer på minutbaseret produktionsplanlægning vises det, at EMPC tilgangen kan generaliseres til planlægning på time- og dagsniveau (inklusive binding af generatorer).

Elproduktion baseret på vedvarende energikilder, som f.eks. vind- og vandkraft, er usikker og variabel. En portefølje af generatorer med en stor andel af vedvarende produktion, er derfor et stokastisk system. Behovet for EMPC af stokastiske systemer imødekommes ved at generalisere sikkerhedsækvivalens EMPC (certainty-equivalent EMPC, CE-EMPC) til middelværdi-varians EMPC (mean-variance EMPC, MV-EMPC). I MV-EMPC formuleres objektfunktionen som en afvejning af de forventede driftsomkostninger og variansen af driftsomkostningerne. Simuleringer viser, at MV-EMPC reducerer både omkostninger og risiko sammenlignet med CE-EMPC. Det vises også, at CE-EMPC kan forbedres betydeligt ved anvendelse af en (back-off) heuristik, der modifi-

cerer systemets begrænsninger.

I EMPC løses et kontrolproblem (optimal control problem, OCP) med samme frekvens som systemets sample tid. Effektive algoritmer til løsning af EMPC kontrolproblemer er vigtige, idet kontrolproblemerne løses i realtid. Afhandlingen præsenterer skræddersyede algoritmer til EMPC af lineære systemer, der udnytter strukturen i kontrolproblemerne. En Riccati-baseret homogen og selvdual indrepunktsmetode, udvikles til specialtilfældet hvor kontrolproblemets omkostningsfunktion er en lineær funktion. En algoritme baseret på den alternerende multiplikator metode (alternating direction method of multipliers, ADMM), designes til løsning af input-begrænsede kontrolproblemer med konvekse objektfunktioner. Kontrolproblemer der opstår i forbindelse med EMPC af dynamisk afkoblede systemer, som f.eks. elektriske generatorer, har en blokangulær struktur. Disse kontrolproblemer løses effektivt af dekompositions algoritmer baseret på ADMM og Dantzig-Wolfe dekomposition. Subproblemer i dekompositionsalgoritmerne løses via skræddersyede optimeringsalgoritmer. Strategier til initialisering (warm start) og tidlig afslutning (early-termination) reducerer beregningstiden for de foreslåede EMPC algoritmer yderligere. Sammenligner viser, at de skræddersyede algoritmer er betydeligt hurtigere end eksisterende state-of-the-art metoder til løsning af kontrolproblemer.

Som et potentielt anvendelsesområde for EMPC, studeres produktionsplanlægning i små isolerede \emptyset -systemer. Reserveplanlægning er en kritisk del af produktionsplanlægningen i små isolerede \emptyset -systemer. Reserverne aktiveres til balancerings af forbrug og produktion i realtid. En EMPC-baseret strategi udvikles til aktivering af reserver. Et konceptuelt case studie af Færøerne viser, at denne strategi reducerer driftsomkostningerne signifikant. Til planlægning af reserver, præsenteres et optimalt reserve beregnings problem (optimal reserve planning problem, ORPP). Dette problem er et hændelses-begrænset (contingency-constrained) UC problem, der er specialiseret til små \emptyset -systemer med varierende inertier.

Hovedbidragene i denne afhandling kan opsummeres som:

- En middelværdi-varians optimeringsstrategi til EMPC af lineære stokastiske systemer.
- Skræddersyede algoritmer til EMPC af lineære stokastiske systemer.
- Metoder til produktionsplanlægning i små isolerede \emptyset -systemer. Herunder det introducerede ORPP til økonomisk indmelding og binding af generatorer, og en EMPC-baseret strategi til aktivering af reserver.

List of publications

Peer-reviewed papers

The following papers have been published or submitted for publication in international journals or in conference proceedings during the project period. They constitute the main contributions of the Ph.D. project. We advise the reader to pick up on the specific details in the papers after reading the summary report.

- [A] L. E. Sokoler, G. Frison, K. Edlund, A. Skajaa, and J. B. Jørgensen. A Riccati Based Homogeneous and Self-Dual Interior-Point Method for Linear Economic Model Predictive Control. In *IEEE Multi-conference on Systems and Control*, pages 592–598, 2013.
- [B] L. E. Sokoler, K. Edlund, L. Standardi, and J. B. Jørgensen. A Decomposition Algorithm for Optimal Control of Distributed Energy Systems. In *4th IEEE/PES Innovative Smart Grid Technologies Europe (ISGT Europe)*, pages 1–5, 2013.
- [C] L. E. Sokoler, A. Skajaa, G. Frison, R. Halvgaard, and J. B. Jørgensen. A Warm-Started Homogeneous and Self-Dual Interior-Point Method for Linear Economic Model Predictive Control. In *52th IEEE Conference on Decision and Control (CDC)*, pages 3677–3683, 2013.
- [D] L. E. Sokoler, G. Frison, M. S. Andersen, and J. B. Jørgensen. Input-Constrained Model Predictive Control via the Alternating Direction Method of Multipliers. In *European Control Conference (ECC)*, pages 115–120, 2014.

- [E] L. E. Sokoler, L. Standardi, K. Edlund, N. K. Poulsen, H. Madsen, and J. B. Jørgensen. A Dantzig-Wolfe Decomposition Algorithm for Linear Economic Model Predictive Control of Dynamically Decoupled Subsystems. *Journal of Process Control*, 24(8):1225–1236, 2014.
- [F] L. E. Sokoler, B. Dammann, H. Madsen, and J. B. Jørgensen. A Mean-Variance Criterion for Economic Model Predictive Control of Stochastic Linear Systems. In *53rd IEEE Conference on Decision and Control (CDC)*, pages 5907–5914, 2014.
- [G] L. E. Sokoler, B. Dammann, H. Madsen, and J. B. Jørgensen. A Decomposition Algorithm for Mean-Variance Economic Model Predictive Control of Stochastic Linear Systems. In *IEEE Multi-conference on Systems and Control*, pages 1086–1093, 2014.
- [H] L. E. Sokoler, P. Vinter, R. Bærentsen, K. Edlund, and J. B. Jørgensen. Contingency-Constrained Unit Commitment in Meshed Isolated Power Systems. *IEEE Transactions on Power Systems*, 2015. To appear.
- [I] L. E. Sokoler, K. Edlund, and J. B. Jørgensen. Application of Economic MPC to Frequency Control in a Single-Area Power System. In *54th IEEE Conference on Decision and Control (CDC)*, pages 2635–2642, 2015.
- [J] L. E. Sokoler, P. J. Dinesen, and J. B. Jørgensen. A Hierarchical Algorithm for Integrated Scheduling and Control with Applications to Power Systems. *IEEE Transactions on Control Systems Technology*, 2015. To appear.
- [K] L. E. Sokoler, G. Frison, A. Skajaa, R. Halvgaard, and J. B. Jørgensen. A Homogeneous and Self-Dual Interior-Point Linear Programming Algorithm for Economic Model Predictive Control. *IEEE Transactions on Automatic Control*, 2015. To appear.

Contents

Preface	i
Acknowledgements	iii
Summary (English)	v
Summary (Danish)	vii
List of publications	ix
I Summary Report: Introduction and Background	1
1 Introduction	3
1.1 Future Power Systems	3
1.2 Thesis Contribution and Organization	5
2 Energy Systems	9
2.1 Energy Value Chain	9
2.2 Planning Hierarchy	11
2.3 Generator Model	14
2.4 Portfolio Model	16
3 Model Predictive Control	19
3.1 Linear Stochastic Systems	20
3.2 Filtering and Prediction	21
3.3 Certainty Equivalent MPC	22
3.4 Objective Functions	23
3.5 Economic MPC	24

3.6	Stability	25
3.7	Online Optimization	25
4	Convex Optimization	29
4.1	Convex Optimization Problems	29
4.2	Linear Programming IPM	31
4.3	Dantzig-Wolfe Decomposition Algorithm	36
4.4	Alternating Direction Method of Multipliers	40
II	Summary Report: Main Contributions	45
5	Economic MPC in Power Production Planning	47
5.1	Contributions	47
5.2	Portfolio Constraints	48
5.3	Portfolio Cost Function	49
5.4	Certainty-Equivalent Economic MPC	51
5.5	Mean-Variance Economic MPC	54
5.6	Regularization	61
5.7	Summary	61
6	Algorithms for Economic MPC	65
6.1	Contributions	65
6.2	Riccati-Based Linear Programming IPM	66
6.3	Subsystem Decomposition	71
6.4	Scenario Decomposition	79
6.5	Summary	84
7	Isolated Power Systems	85
7.1	Contributions	85
7.2	The Faroe Islands	86
7.3	Single-Area Model	87
7.4	Operating Reserves	88
7.5	Unit Commitment	90
7.6	Frequency Control	105
7.7	Summary	114
8	Conclusions	117
8.1	Future Work	118
	Bibliography	120

III	Publications	141
A	A Riccati Based Homogeneous and Self-Dual Interior-Point Method for Linear Economic Model Predictive Control	143
B	A Decomposition Algorithm for Optimal Control of Distributed Energy Systems	151
C	A Warm-Started Homogeneous and Self-Dual Interior-Point Method for Linear Economic Model Predictive Control	157
D	Input-Constrained Model Predictive Control via the Alternating Direction Method of Multipliers	165
E	A Dantzig-Wolfe Decomposition Algorithm for Linear Economic Model Predictive Control of Dynamically Decoupled Subsystems	173
F	A Mean-Variance Criterion for Economic Model Predictive Control of Stochastic Linear Systems	187
G	A Decomposition Algorithm for Mean-Variance Economic Model Predictive Control of Stochastic Linear Systems	197
H	Contingency-Constrained Unit Commitment in Meshed Isolated Power Systems	207
I	Application of Economic MPC to Frequency Control in a Single-Area Power System	219
J	A Hierarchical Algorithm for Integrated Scheduling and Control with Applications to Power Systems	229
K	A Homogeneous and Self-Dual Interior-Point Linear Programming Algorithm for Economic Model Predictive Control	241

Part I

Summary Report: Introduction and Background

Introduction

This chapter describes the transition of contemporary fossil-based power systems into power systems with a high penetration of renewable energy sources. The increased electricity generation of renewable energy sources, motivates the use of economic model predictive control (EMPC) for power production planning. This chapter also states the main contributions and the organization of the thesis.

1.1 Future Power Systems

Many countries have ambitious political climate and energy targets to reduce CO₂ emissions [Eur15a, Bro13, Eur15b]. The Renewable Energy Directive states that 20% of total EU energy consumption in 2020 should be produced by renewable energy sources. Binding national 2020 renewable energy targets for each Member State forms an integral part of EU energy policy. Wind power, solar power, hydro power, and sustainable biomass-sourced power will account for the majority of future renewable energy production [Eur14]. Fig. 1.1 shows the 2020 renewable energy targets for each EU Member State.

Integration of renewable energy sources is challenging, due to their inherent variable and uncertain nature. Wind turbines depend on the wind, and solar

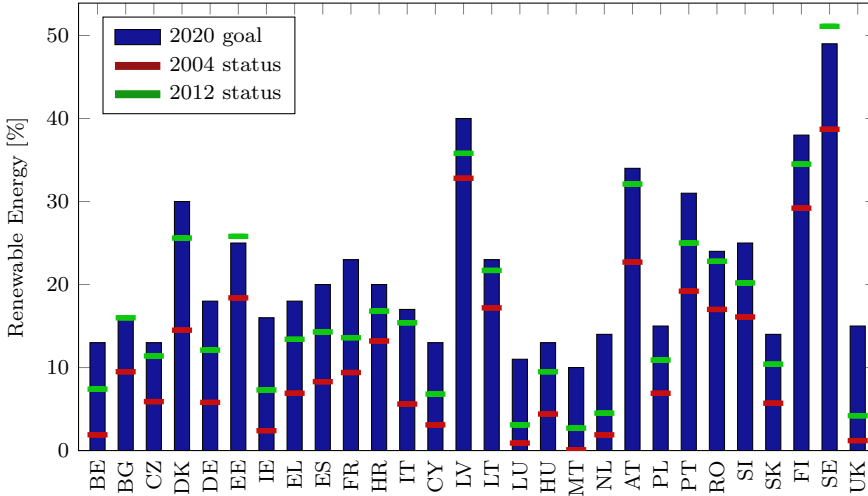


Figure 1.1: Binding national 2020 renewable energy targets for each EU Member State [Eur15b].

cells depend on the solar radiation [Pin13]. Hydro power is an attractive source of renewable energy, because of its flexibility and its storage capabilities. Hydro power is a key factor behind the high 2020 renewable energy targets set by Austria, Sweden, and Finland. Countries with poor conditions for hydro power rely more heavily on wind and solar power. As an example, wind power accounted for approximately 40% of the total Danish energy consumption in 2014 [Ene15]. This percentage is expected to increase. Denmark has set the goal of being completely independent of fossil fuels by 2050 [ED11].

To handle fluctuations in the generation of renewable energy sources, flexible solutions are needed on both the production and the consumption side of energy. Distributed energy resources, such as heat pumps, electric vehicles, and local combined heat and power plants, as well as household electrical appliances, can provide flexibility in the form of e.g. load shifting, balancing services, and energy storage [ED10, ED11, MPH⁺15]. Virtual power plants (VPPs) are aggregates of smaller distributed energy resources [BK10, YTP09, SMT11, LKMB10, HI08, MRKG11]. Commercial VPPs are aimed at market related activities such as maximizing profit and overcoming market barriers (e.g. market barriers may prevent small power generators from submitting bids in the electricity market). Technical VPPs help maintain power quality, reliability and security of supply [PRS07, You10]. Fig. 1.2 is a conceptual illustration of a future power grid, and Fig. 1.3 illustrates the VPP technology.

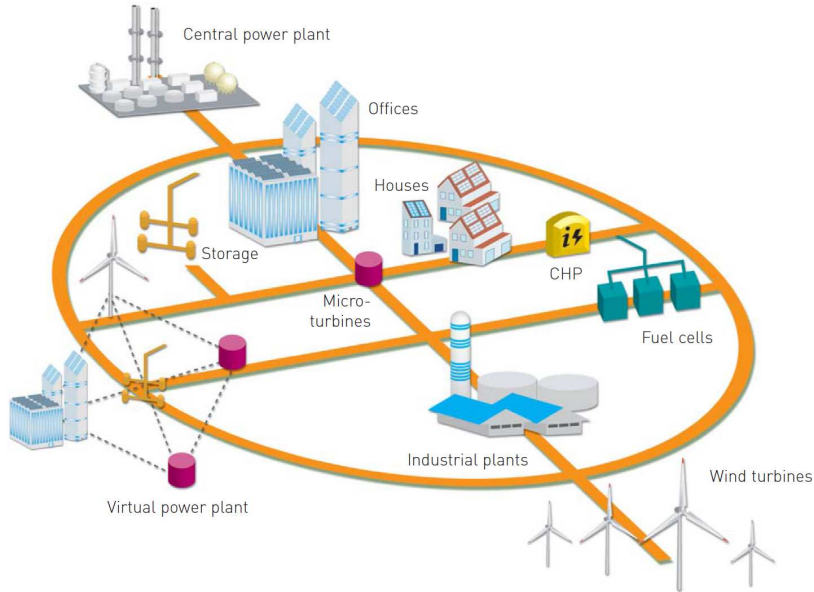


Figure 1.2: Conceptual illustration of a future power grid [Eur06].

This thesis focuses on power system operations from the power producer's point of view. Linear EMPC is applied to operate a portfolio of power generators with minimum generation cost. In a conventional portfolio, the power generation is mainly based on fossil fuels such as coal, natural gas, and petroleum (and in some cases nuclear power). The power production of fossil-based generators is deterministic in nature. Deterministic power management strategies are therefore adequate to control conventional fossil-based portfolios. A portfolio based on a large share of renewable energy sources is a stochastic system. Accordingly, EMPC schemes are developed for control of stochastic systems. The EMPC schemes have several important applications in control of future power systems. We present special purpose algorithms to accommodate the proposed EMPC schemes for large-scale energy systems.

1.2 Thesis Contribution and Organization

The emphasis of this thesis is on the formulation and solution of the optimal control problems (OCPs) that arise in EMPC of linear stochastic systems, and their applications in power production planning. Fig. 1.4 shows the research areas of the thesis papers, within a power production planning framework. Some of the

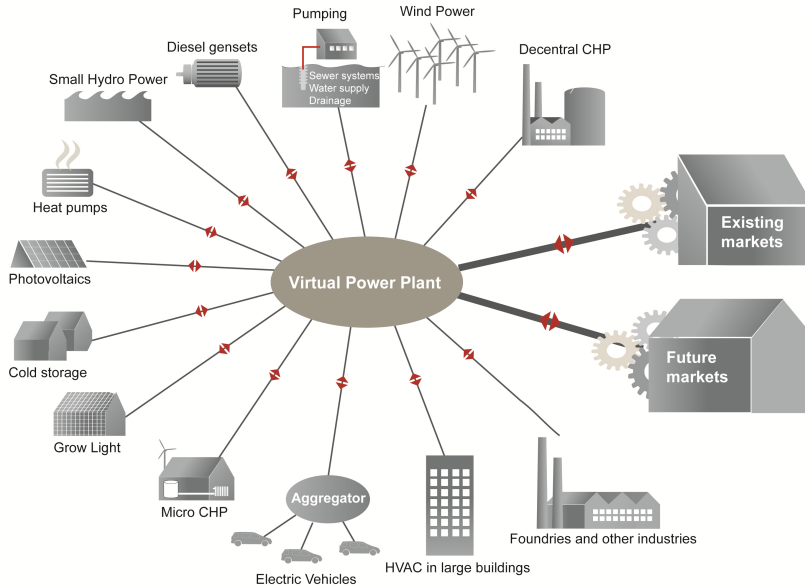


Figure 1.3: A VPP is an aggregate of smaller distributed energy resources [Twe13].

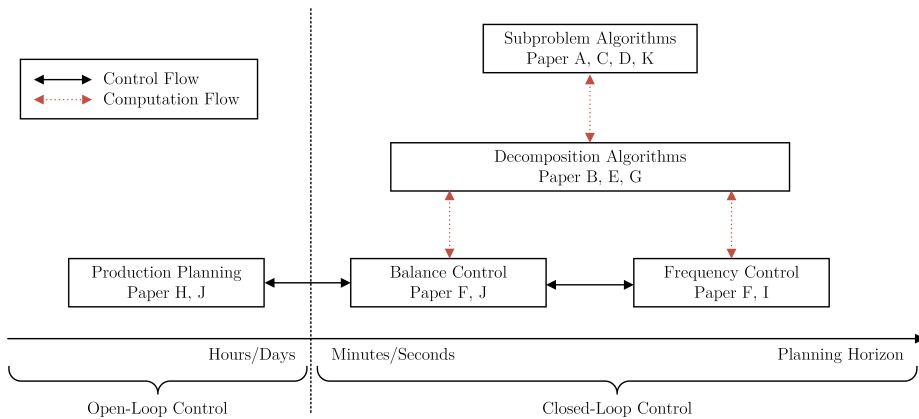


Figure 1.4: Overview of thesis papers.

papers have overlapping areas. The papers are divided into two main groups. Open-loop control concerns production scheduling with a day-ahead planning horizon, and closed-loop control concerns production scheduling with a planning horizon ranging from a few seconds up to several minutes. A key difference between the two groups is that computations within the closed-loop control group

are time critical, because they are performed online. Efficient algorithms are therefore important for the tractability of EMPC schemes within this group. Production scheduling is in the open-loop control group. Production scheduling involves solving a mixed-integer linear program (MILP) for unit commitment (UC) and economic dispatch of the system power generators. Balance control computes corrections to the nominal production plan (provided by the production scheduling algorithm) in real-time, based on updated forecasts, setpoint corrections, measurements, and a dynamic model of the system. Frequency control is applied to keep the system frequency close to its nominal value. This is important to avoid blackouts in the system. Balance and frequency control become increasingly important, as more renewable energy sources are integrated into the power system. The key contributions of this thesis are described in the following two sections.

1.2.1 Formulation of the OCP

Certainty-equivalent EMPC (CE-EMPC) is the most widely used form of EMPC. CE-EMPC replaces random variables in the OCP by conditional expectations. This means that the variance of the random variables is neglected. In power production planning, disregarding the uncertainty (e.g. variations in the electricity price, electricity consumption, and generation of renewable energy) leads to violations of the system constraints and inefficient use of resources. Paper [F](#) and Paper [I](#) show that CE-EMPC performs poorly under uncertainty, both for balance control and for frequency control. To overcome this challenge, Paper [F](#) generalizes CE-EMPC to mean-variance EMPC (MV-EMPC). In MV-EMPC the OCP objective function is formulated as a bi-criterion that trades off cost expectation and cost variance. MV-EMPC reduces both cost and risk compared to CE-EMPC. Paper [E](#) demonstrates regularization techniques for improving the closed-loop performance of EMPC under uncertainty.

Paper [H](#) develops a novel optimal reserve planning problem (ORPP) for UC and economic dispatch of generators in an isolated power system. A Faroe Islands case study show that the production plan provided by the ORPP is robust against contingencies. In the particular case study, blackouts and power outages are avoided at a cost increase of less than 3%. Paper [J](#) presents a hierarchical algorithm for integrated scheduling and control. The algorithm establishes a formal connection between production scheduling and balance control in power system operations. Moreover, it accommodates the need for frequent rescheduling of power generation using updated forecasts of renewable energy production. Paper [I](#) presents a novel EMPC scheme for activation of operational reserves in a single-area power system. In this scheme, the OCP objective function is formulated as a bi-criterion that trades off cost of generation and setpoint track-

ing. Simulations show that significant cost savings can be achieved using the proposed EMPC scheme, compared to conventional setpoint-based EMPC and frequency-based PI control.

1.2.2 Solution of the OCP

The performance and reliability of the optimization algorithms solving the OCPs that arise in EMPC are important, as the optimization problems are solved online. Convex optimization algorithms for EMPC form an important contribution of this thesis. Paper B and Paper E develop decomposition algorithms for EMPC of dynamically decoupled subsystems. These algorithms are based on the alternating direction method of multipliers (ADMM) and Dantzig-Wolfe decomposition. Power generators in a portfolio system are an example of dynamically decoupled subsystems. Paper G overcomes tractability issues of MV-EMPC by solving a convex relaxation of the OCP associated with MV-EMPC using a new ADMM-based decomposition algorithm.

Paper A, Paper C, and Paper K, provide a homogeneous and self-dual interior-point method (IPM) for EMPC of linear systems with linear constraints and linear objective functions. Paper D presents an ADMM-based algorithm for input-constrained EMPC with convex objective functions. These algorithms can be used independently, or as subproblem solvers in the proposed decomposition algorithms. The EMPC algorithms are implemented in MATLAB and C. Warm-start and early-termination strategies are applied to increase the performance of the algorithms further. Benchmarks show that the EMPC algorithms are significantly faster than state-of-the-art solvers for solution of the OCPs. Moreover, while memory becomes an issue for general-purpose solvers, the decomposition algorithms facilitate EMPC of large-scale energy systems.

1.2.3 Thesis Organization

We have organized this thesis as follows. Part I and Part II constitute the summary report, and Part III is the collection of research papers. Part I of the summary report is an introduction and background. It describes energy systems, model predictive control (MPC), and convex optimization algorithms, in general terms. The intention of Part I is only to provide references and background material for Part II and Part III of the thesis. Part II summarizes the contributions of the research papers. Part II is divided into three main sections: a section on OCP formulations, a section on OCP algorithms, and a section on planning and control applications in small isolated power systems.

Energy Systems

This chapter provides an overview of power production planning using a top-down view of energy systems. A hierarchical planning architecture is introduced, and we discuss the integration of EMPC into this architecture. This chapter also introduces a linear power portfolio system. The portfolio system consists of a collection of power generators. A power generator can represent a producer of electricity, a consumer of electricity, or possibly both.

2.1 Energy Value Chain

Producers and consumers of electricity are connected to each other via the power grid. Fig. 2.1 illustrates a typical grid topology. Power producers are connected to the transmission grid, which is a high-voltage grid. Power substations step transmission voltages down to distribution voltages that are distributed to end-users via distribution grids.

In liberalized power systems, the energy value chain is divided into commercial and non-commercial activities. Sales, consumption and generation are commercial activities, while transmission and distribution are non-commercial activities. Fig. 2.2 illustrates the system setup [HJB13]. Retailers (including wholesalers)

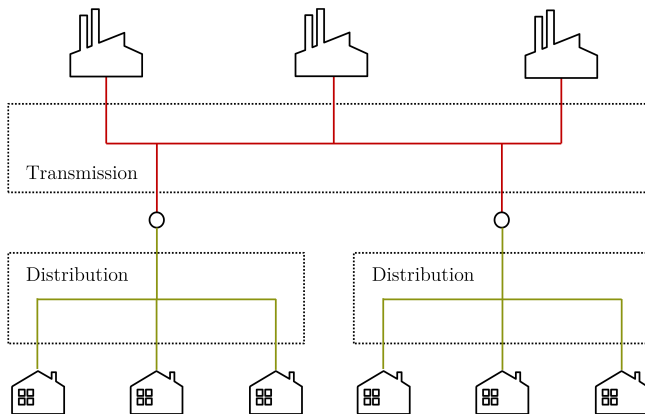


Figure 2.1: A typical power grid topology.

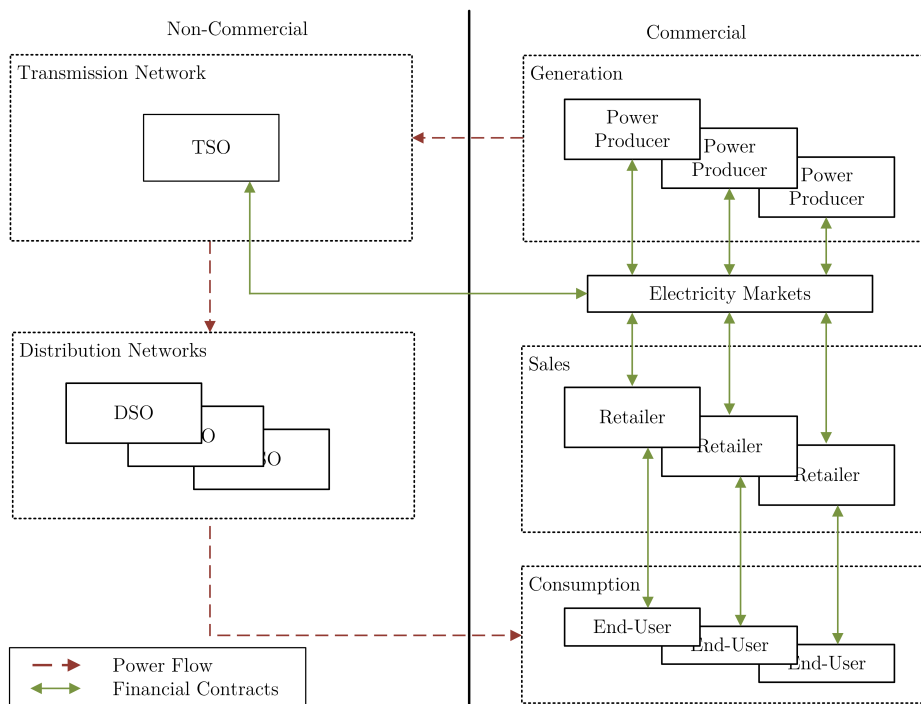


Figure 2.2: Overview of a liberalized electricity market.

and power producers are commercial actors. They buy and sell power in the electricity markets. End-users buy their electricity via the retailers. The trans-

mission system and the distribution system are operated by non-commercial actors. The transmission system operator (TSO) is responsible for the daily operation and maintenance of the transmission grid. The TSO is also responsible for security of supply and power quality. The TSO relies on ancillary services that are traded in special capacity markets. Each distribution network is managed by a distribution system operator (DSO). The DSO is responsible for a stable supply of electricity within its geographical area. The DSO also collects consumption (production) data from the end-users. These data are used for financial settlements with the retailers, and to monitor the need to expand the grid capacity.

Electricity is bought and sold in electricity markets. Markets vary from geographical area to geographical area. A majority of the energy is usually traded in a day-ahead market. Intraday markets make it possible to adjust the contracted positions within the day of operation. Imbalances from the contracted positions are settled in a balancing market. To balance production and consumption in real-time, the TSO relies on operating reserves that are bought in markets for ancillary services. There are different reserve markets, each with specific requirements for the reserve activation time and for the size of the reserve. Usually, there is also a real-time (regulating power) market, where the market players can submit bids for up and down regulation to the TSO. Regulating power is mainly activated to solve persistent imbalance problems, while operating reserves are activated to ensure stable operation of the system. For more details on markets and actors, we refer to e.g. [PHB⁺13, Hal14, HJB13, Zug13, MCM⁺14].

2.2 Planning Hierarchy

After the day-ahead electricity market is cleared, each power producer receives a reference profile specifying the amount of electricity they have sold. The power producer's main objective is then to determine the most economical production plan that accommodates the reference profile.

Fig. 2.3 is a diagram of the power production planning hierarchy from a power producer's point of view. The system level covers the upper three layers of the planning hierarchy. This level involves coordinated decisions for the entire portfolio of generators. In the top system level layer is business planning, where portfolio modifications are planned. The next two layers are the production planning layer and the balance control layer. The production planning layer is responsible for unit commitment and economic dispatch of the portfolio power generators, given the reference profile. This involves solving the UC problem. We refer to the production plan provided by the UC problem, as the nominal

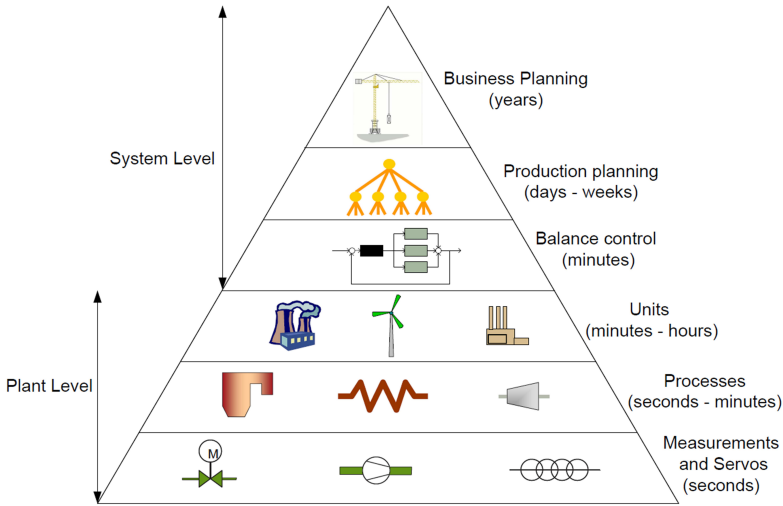


Figure 2.3: Power production planning hierarchy [Edl10].

production plan. The planning horizon of the UC problem is up to several days, while its resolution is in the order of minutes. The UC problem is an MILP. The solution time of the UC problem can be several minutes or even hours, depending on the portfolio size and the number (and type) of operating constraints. Consequently, the production plan can only be updated with a relatively low frequency.

The production planning layer is a pure open-loop control layer. To account for imbalances between power production and reference profile, a balance control layer is employed. The balance control layer is a closed-loop control layer. Closed-loop control is necessary, as the controlled system is a stochastic system. In particular, it is not possible to predict the generation of renewable energy sources exactly. Moreover, the TSO provides corrections to the reference profile in real-time (e.g. via activation of regulating power and operational reserves). As more renewable energy is integrated into the grid, forecasts become less accurate, and the reserve and real-time markets become more critical for the TSO to balance production and consumption on a grid level. This means that the need for continuously adjusting the nominal production plan increases for the power producers.

Fig. 2.4 is a schematic diagram of the production planning layer and the balance control layer. This thesis applies EMPC for balance control. The EMPC-based balance controller exploits information on updated forecasts, setpoint-corrections, and measurements, to continuously adjust the nominal production

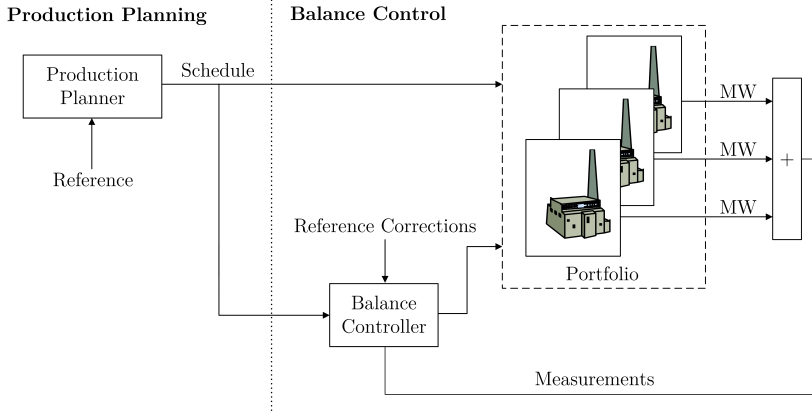


Figure 2.4: The production planning and balance control layer [Edl10].

plan. Discrete decisions such as on/off decisions are considered as fixed parameters by the balance controller. The planning horizon of the balance controller is usually less than one hour, and its sampling rate is in the order of seconds. Using a fine-grained temporal resolution allows the balance controller to act based on a dynamic model of the system. Features that make EMPC well-suited for balance control are its predictive ability, economically efficient operation, easy integration of constraints, direct support of multiple-input multiple-output (MIMO) systems, and flexibility in the formulation of the OCP.

2.2.1 Integration of Scheduling and Control

Paper J presents an EMPC scheme for integrated scheduling and control. The OCP solved in this scheme involves decisions on two time scales. Binary variables occur as scheduling (slow time-scale) decisions in the OCP, and continuous variables occur as control (fast time-scale) decisions in the OCP. A hierarchical algorithm is proposed for solution the OCP. The algorithm consists of two optimization levels. The upper level (scheduling level) solves an MILP with a low frequency. The lower level (control level) solves a linear program (LP) with a high frequency. The main advantage of the proposed approach is that it requires online solution of an LP rather than an MILP.

The hierarchical algorithm is tested using a power portfolio case study, in which production scheduling and balance control are integrated. The idea is to replace the production planner and the balance controller in Fig. 2.4 by a single EMPC scheme. For this EMPC scheme, the OCP is an MILP that includes

binary unit commitment variables. Moreover, the OCP is defined to have a long prediction horizon and a fine-grained temporal resolution. A single-layer EMPC scheme is attractive from an economic point of view, as it collects the degrees of freedom of production planning and balance control in a single optimization problem. The disadvantage is that the resulting OCP is a large-scale MILP. Direct solution of the large-scale MILP is computationally intractable in real-time. Simulations show that the hierarchical algorithm reduces the computation to solve the large-scale MILP (to near-optimality) by several orders of magnitude. Hence, the hierarchical algorithm allows frequent redispatch of the system power generators. This is important for cost-efficient operation of power systems with a high penetration of renewable energy sources.

Hierarchical decomposition of unit commitment and balance control is widely adopted in power system operations [SC13, WW13]. Paper J demonstrates that this hierarchical decomposition can be interpreted as an approximation of the proposed EMPC scheme for integrated scheduling and control.

2.3 Generator Model

EMPC requires a model of the controlled system. This section presents a generic power generator model. A power generator refers to a unit that can either produce or consume power, or possibly both. Electric vehicles, heat pumps, combined heat and power plants, wind turbines, thermal power plants, and VPPs, are examples of power generators. By convention, the negative sign is used for power consumption and the positive sign is used for power production.

Power generators are modeled at different levels of detail, depending on the application of interest [WW13, Deb88, KBL94, KCLB14, And12b]. The main focus of this thesis is on the formulation and the solution of the OCPs, and not on modeling of energy systems. We model a power generator as a time-invariant system. In transfer function form, the nominal system is

$$Z_g(s) = G_{g,u}(s)U_g(s) + G_{g,d}(s)D_g(s), \quad (2.1)$$

where $U_g(s) \in \mathbb{R}^{n_{g,u}}$ is the generator input, $D_g(s) \in \mathbb{R}^{n_{g,d}}$ is a known disturbance, and $Z(s) \in \mathbb{R}^{n_{g,z}}$ is the generator output. $G_{g,u}(s)$ and $G_{g,d}(s)$ are transfer functions. Transfer functions can be identified based on experimental step responses of a system [Lju99]. References [Hal14, Hov13, Sta15, EMB09] provide (approximate) models for a variety of power generators in the form (2.1), e.g. heat pumps in residential buildings [HPMJ12], electric vehicles with vehicle-to-grid capabilities [HPM⁺12], solar tanks [HBP⁺12], cold rooms in refrigeration systems [HLEJ12], and conventional thermal power plants [EMB09].

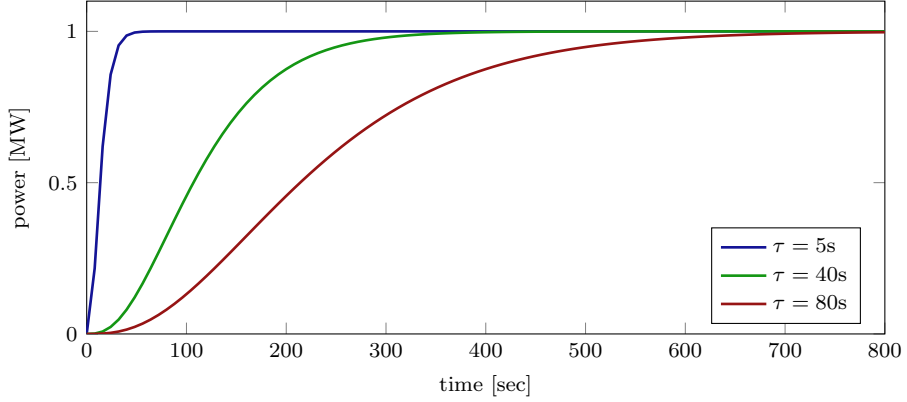


Figure 2.5: Step response of the third-order system (2.2) for three different time constants.

As an example, consider the special case of (2.1) where

$$Z_g(s) = \frac{1}{(\tau s + 1)^3} (U_g(s) + D_g(s)). \quad (2.2)$$

In this single-input single-output (SISO) system, $U_g(s)$ is the power production setpoint, and $Z_g(s)$ is the power production. Fig. 2.5 shows the step response for the system (2.2). Three different time constants are considered. In case $\tau = 5\text{s}$, the third-order system (2.2) can represent a small agile power plant such as a diesel generator. When $\tau = 40\text{s}$, the model may represent a medium-sized gas turbine, and for $\tau = 80\text{s}$, it may represent a large fuel-fired thermal power plant.

In discrete state-space form, we write the system (2.1) as

$$x_{g,k+1} = A_g x_{g,k} + B_g u_{g,k} + E_g d_{g,k}, \quad (2.3a)$$

$$z_{g,k} = C_{g,z} x_{g,k}. \quad (2.3b)$$

In this model structure, $(A_g, B_g, E_g, C_{g,z})$ are the state-space matrices, $x_{g,k} \in \mathbb{R}^{n_{g,x}}$ is the (internal) system state, $u_{g,k} \in \mathbb{R}^{n_{g,u}}$ is the system input, $d_{g,k} \in \mathbb{R}^{n_{g,d}}$ is the known disturbance, and $z_{g,k} \in \mathbb{R}^{n_{g,z}}$ is the system output.

In general, the power generator model (2.3) is a MIMO system. Outputs of the system may include e.g. the state-of-charge for an electric vehicle, the room temperature for a heat pump in a residential building, and the reservoir level for a pumped storage hydro plant. We assume that the power production

(consumption) is part of the system output. This is written as

$$z_{g,k}^p = \Upsilon z_{g,k}, \quad (2.4)$$

where $\Upsilon \in \mathbb{R}^{1 \times n_{g,z}}$ is a vector of multipliers and $z_{g,k}^p$ is the power production of the generator. For the SISO system (2.2), $\Upsilon = 1$.

2.4 Portfolio Model

Define M power generators in the form (2.3)

$$x_{g_j,k+1} = A_{g_j} x_{g_j,k} + B_{g_j} u_{g_j,k} + E_{g_j} d_{g_j,k}, \quad j \in \mathcal{M}, \quad (2.5a)$$

$$z_{g_j,k} = C_{g_j,z} x_{g_j,k}, \quad j \in \mathcal{M}, \quad (2.5b)$$

where $\mathcal{M} = \{1, 2, \dots, M\}$. Using (2.4), the total power production by the M generators is expressed as

$$z_{T,k} = \sum_{j \in \mathcal{M}} z_{g_j,k}^p = \sum_{j \in \mathcal{M}} \Upsilon_j z_{g_j,k} = \sum_{j \in \mathcal{M}} \Upsilon_j C_{g_j,z} x_{g_j,k}. \quad (2.6)$$

The portfolio model (2.5) and (2.6) is written compactly as

$$x_{P,k+1} = A_P x_{P,k} + B_P u_k + E_P d_{P,k}, \quad (2.7a)$$

$$z_{P,k} = C_{P,z} x_{P,k}, \quad (2.7b)$$

in which

$$z_{P,k} = \begin{bmatrix} z_{g_1,k} \\ z_{g_2,k} \\ \vdots \\ z_{g_M,k} \\ z_{T,k} \end{bmatrix}, \quad x_{P,k} = \begin{bmatrix} x_{g_1,k} \\ x_{g_2,k} \\ \vdots \\ x_{g_M,k} \end{bmatrix}, \quad u_{P,k} = \begin{bmatrix} u_{g_1,k} \\ u_{g_2,k} \\ \vdots \\ u_{g_M,k} \end{bmatrix}, \quad d_{P,k} = \begin{bmatrix} d_{g_1,k} \\ d_{g_2,k} \\ \vdots \\ d_{g_M,k} \end{bmatrix}, \quad (2.8)$$

and

$$A_P = \mathbf{blkdiag}(A_{g_1}, A_{g_2}, \dots, A_{g_M}),$$

$$B_P = \mathbf{blkdiag}(B_{g_1}, B_{g_2}, \dots, B_{g_M}),$$

$$E_P = \mathbf{blkdiag}(E_{g_1}, E_{g_2}, \dots, E_{g_M}),$$

using MATLAB notation. Finally

$$C_{P,z} = \begin{bmatrix} C_{g_1,z} & & & & \\ & C_{g_2,z} & & & \\ & & \ddots & & \\ & & & C_{g_M,z} & \\ \Upsilon_1 C_{g_1,z} & \Upsilon_2 C_{g_2,z} & \cdots & \Upsilon_M C_{g_M,z} & \end{bmatrix}.$$

In the portfolio model (2.7), $\mathbf{x}_{P,k} \in \mathbb{R}^{n_{P,x}}$, $\mathbf{u}_{P,k} \in \mathbb{R}^{n_{P,u}}$, $\mathbf{d}_{P,k} \in \mathbb{R}^{n_{P,d}}$ and $\mathbf{z}_{P,k} \in \mathbb{R}^{n_{P,z}}$. The system dimensions are

$$\begin{aligned} n_{P,x} &= \sum_{j \in \mathcal{M}} n_{g_j,x}, & n_{P,u} &= \sum_{j \in \mathcal{M}} n_{g_j,u}, \\ n_{P,d} &= \sum_{j \in \mathcal{M}} n_{g_j,d}, & n_{P,z} &= \sum_{j \in \mathcal{M}} n_{g_j,z} + 1. \end{aligned}$$

The system (2.7) is a generator portfolio model. The model consists of dynamically decoupled subsystems (power generators) that are linked via the aggregated variables (2.6). The aggregated variables represent the total power production of the portfolio. Utilizing structure in the state-space matrices is an important part of implementing efficient algorithms for EMPC. In this thesis, (2.7) is used for conceptual studies of EMPC in power production planning. Modelling individual power generators for the portfolio is studied in e.g. [Hal14, Hov13, Sta15, EMB09].

To model the uncertain and variable behavior of generators based on renewable energy sources, we augment the system (2.7) by stochastic terms. The resulting system is a linear stochastic state-space model in the form

$$\mathbf{x}_{P,k+1} = A_P \mathbf{x}_{P,k} + B_P \mathbf{u}_k + E_P \mathbf{d}_{P,k} + \mathbf{w}_{P,k}, \quad (2.9a)$$

$$\mathbf{z}_{P,k} = C_{P,z} \mathbf{x}_{P,k}, \quad (2.9b)$$

$$\mathbf{y}_{P,k} = C_{P,y} \mathbf{x}_{P,k} + \mathbf{v}_{P,k}. \quad (2.9c)$$

$\mathbf{y}_{P,k} \in \mathbb{R}^{n_{P,y}}$ is the system measurement, $\mathbf{w}_{P,k} \in \mathbb{R}^{n_{P,x}}$ is the process noise, and $\mathbf{v}_{P,k} \in \mathbb{R}^{n_{P,y}}$ is the measurement noise. We use bold letters to denote random variables. Realizations of the random variables are written in normal letters. Generally, a number of the controlled outputs may only be available via state estimation, i.e. $C_{P,y} \neq C_{P,z}$.

CHAPTER 3

Model Predictive Control

The portfolio system (2.9) is a linear stochastic system. This chapter gives a brief introduction to MPC of linear stochastic systems. Economic cost functions motivate the use of EMPC over setpoint-based MPC. This chapter also addresses stability of MPC and EMPC. Finally, we provide an overview of algorithms for efficient solution of the OCPs that arise in MPC and EMPC.

MPC is a technology for control of constrained dynamic systems. Due to its inherent ability to handle constraints, time delays, and multivariate systems, MPC has become one of the most successful control technologies in the process industries [QB03, Raw00, RM09, Mac02, Mos95, Ros03, GSD05, KH05, CB07, ML99, MRRS00, JHR11]. Recent developments demonstrate that MPC is a promising technology for control of energy systems as well [HLEJ12, HLSJ12, HBP⁺12, MSSVP14, HPMJ12, PEH⁺13, Hal14, HPM⁺12, SPJS13, EBJ11, ZH14, MQLS11]. The basic idea of MPC is to optimize the predicted behavior of a dynamic model over a finite horizon. At each sampling instant, the system state is estimated and an OCP is formed and solved. The solution of the OCP provides a sequence of inputs. Only the first input in this sequence is applied to the controlled system, and the process is repeated at the following sampling instant. In this way, a closed-loop input trajectory is synthesized using feedback. Fig. 3.1 is a block diagram of MPC.

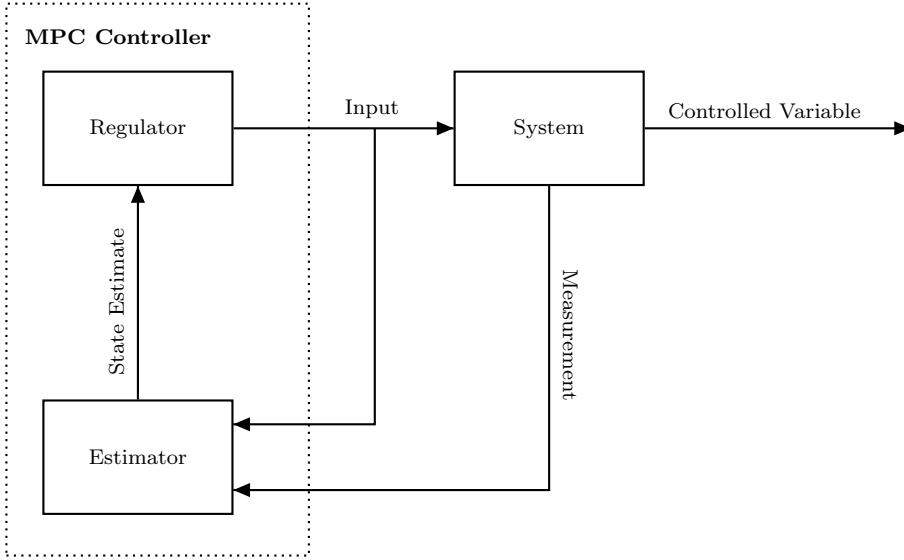


Figure 3.1: Block diagram of MPC.

3.1 Linear Stochastic Systems

We consider linear stochastic state-space systems in the form

$$\mathbf{x}_{k+1} = A\mathbf{x}_k + B\mathbf{u}_k + E\mathbf{d}_k + \mathbf{w}_k, \quad (3.1a)$$

$$\mathbf{y}_k = C_y\mathbf{x}_k + \mathbf{v}_k, \quad (3.1b)$$

$$\mathbf{z}_k = C_z\mathbf{x}_k. \quad (3.1c)$$

(A, B, E, C_y, C_z) are the state-space matrices, $\mathbf{x}_k \in \mathbb{R}^{n_x}$ is the system state, $\mathbf{u}_k \in \mathbb{R}^{n_u}$ is the system input, $\mathbf{d}_k \in \mathbb{R}^{n_d}$ is the known disturbance, $\mathbf{y}_k \in \mathbb{R}^{n_y}$ is the measured output, and $\mathbf{z}_k \in \mathbb{R}^{n_z}$ is the controlled variable. Moreover, $\mathbf{w}_k \in \mathbb{R}^{n_w}$ is the process noise, and $\mathbf{v}_k \in \mathbb{R}^{n_v}$ is the measurement noise. Note that the portfolio system (2.9) is in the form (3.1). We assume that the process noise, \mathbf{w}_k , and the measurement noise, \mathbf{v}_k , are independent and identically distributed random variables with

$$\mathbf{w}_k \sim N(0, R_w), \quad (3.2a)$$

$$\mathbf{v}_k \sim N(0, R_v). \quad (3.2b)$$

The system (3.1) may be derived from input-output models such as finite impulse response (FIR) models, autoregressive moving average exogenous (ARMAX) models, Box-Jenkins models, and transfer function models [BJ76, VD96, Lju99,

[JJ07]. In addition, (3.1) arises when linear continuous differential equations are discretized.

3.2 Filtering and Prediction

The system state, (3.1a), and output, (3.1c), are estimated based on measurements. Accurate estimates are critical for the performance of MPC. This section provides Kalman filter equations for state estimation and prediction with minimum prediction error variance [Kal60]. By assumption, the process noise, \mathbf{w}_k , and the measurement noise, \mathbf{v}_k , are uncorrelated. Reference [JHR11] treats the more general case with correlated process and measurement noise.

Define the information structure

$$\mathcal{I}_k = \{\mathcal{I}_{k-1}, u_{k-1}, d_{k-1}, y_k\},$$

with $\mathcal{I}_0 = y_0$. Moreover, introduce the conditional means

$$\begin{aligned}\hat{\mathbf{x}}_{k+j|k} &= E[\mathbf{x}_{k+j}|\mathcal{I}_k], \\ \hat{\mathbf{y}}_{k+j|k} &= E[\mathbf{y}_{k+j}|\mathcal{I}_k], \\ \hat{\mathbf{z}}_{k+j|k} &= E[\mathbf{z}_{k+j}|\mathcal{I}_k],\end{aligned}$$

and the conditional covariance matrix

$$P_{k+j|k} = V[\mathbf{x}_{k+j}|\mathcal{I}_k].$$

The filtered estimate $\hat{\mathbf{x}}_{k|k}$, and the covariance matrix $P_{k|k}$, are computed as

$$e_k = y_k - \hat{y}_{k|k-1} = y_k - C_y \hat{\mathbf{x}}_{k|k-1}, \quad (3.3a)$$

$$R_{e,k} = C_y P_{k|k-1} C_y^T + R_v, \quad (3.3b)$$

$$\kappa_k = P_{k|k-1} C_y^T R_{e,k}^{-1}, \quad (3.3c)$$

$$P_{k|k} = P_{k|k-1} - \kappa_k R_{e,k} \kappa_k^T, \quad (3.3d)$$

$$\hat{\mathbf{x}}_{k|k} = \hat{\mathbf{x}}_{k|k-1} + \kappa_k e_k. \quad (3.3e)$$

κ_k is the Kalman filter gain, e_k is the innovation, and $R_{e,k}$ is the innovation covariance matrix.

The j -step ahead predictions for the system state and its covariance matrix are

$$\hat{\mathbf{x}}_{k+j+1|k} = A \hat{\mathbf{x}}_{k+j|k} + B u_{k+j} + E d_{k+j}, \quad j \geq 0, \quad (3.4a)$$

$$P_{k+j+1|k} = A P_{k+j|k} A^T + R_w, \quad j \geq 0. \quad (3.4b)$$

The j -step ahead predictions for the system output and measurement are

$$\hat{z}_{k+j|k} = C_z \hat{x}_{k+j|k}, \quad j \geq 0, \quad (3.5a)$$

$$\hat{y}_{k+j|k} = C_y \hat{x}_{k+j|k}, \quad j \geq 0. \quad (3.5b)$$

For proof and details, we refer to [MR93, PR03, MB02].

3.3 Certainty Equivalent MPC

The most common form of MPC is MPC based on the separation and certainty equivalence principle. This form of MPC is referred to as CE-EMPC. In CE-MPC, random variables are replaced by conditional expectations. Control of (3.1) is thereby simplified to control of a deterministic system that is governed by the Kalman filter equations (3.3), (3.4) and (3.5).

Define the prediction and control horizon

$$\mathcal{N}_i = \{0 + i, 1 + i, \dots, N + i\}, \quad (3.6)$$

where N is the horizon length. Subscript i shifts the horizon by i steps. For compact notation, we introduce the vectors

$$u = \begin{bmatrix} u_k \\ u_{k+1} \\ u_{k+2} \\ \vdots \\ u_{k+N-1} \end{bmatrix}, \quad \hat{x} = \begin{bmatrix} \hat{x}_{k+1|k} \\ \hat{x}_{k+2|k} \\ \hat{x}_{k+3|k} \\ \vdots \\ \hat{x}_{k+N|k} \end{bmatrix}, \quad \hat{z} = \begin{bmatrix} \hat{z}_{k+1|k} \\ \hat{z}_{k+2|k} \\ \hat{z}_{k+3|k} \\ \vdots \\ \hat{z}_{k+N|k} \end{bmatrix}. \quad (3.7)$$

The OCP solved in CE-MPC is

$$\min_{u, \hat{x}, \hat{z}} \phi(u, \hat{x}, \hat{z}), \quad (3.8a)$$

$$\text{s.t. } \hat{x}_{k+j+1|k} = A \hat{x}_{k+j|k} + B u_{k+j} + E d_{k+j}, \quad j \in \mathcal{N}_0, \quad (3.8b)$$

$$\hat{z}_{k+j|k} = C_z \hat{x}_{k+j|k}, \quad j \in \mathcal{N}_1, \quad (3.8c)$$

$$(u, \hat{x}, \hat{z}) \in \mathbb{X}. \quad (3.8d)$$

The function $\phi : \mathbb{R}^{Nn_u} \times \mathbb{R}^{Nn_x} \times \mathbb{R}^{Nn_z} \mapsto \mathbb{R}$ is the objective function. Constraints (3.8b) and (3.8c) are the state-space constraints. These constraints model the predicted behavior of the system (3.1). The filtered estimate, $\hat{x}_{k|k}$, is a fixed parameter in (3.8b). This parameter is obtained from (3.3). Constraint (3.8d) accounts for operational constraints such as input limits, input-rate limits, and output limits. The objective function, ϕ , may be non-linear and the constraint

set \mathbb{X} can be non-convex. We only consider the case where ϕ is a convex function over \mathbb{X} , and \mathbb{X} is a closed and convex set. Under these assumptions, the OCP (3.8) is a convex optimization problem.

Let $(u^*, \hat{x}^*, \hat{z}^*)$ denote a solution of (3.8) and define the function

$$u_k^* = \mu(\hat{x}_{k|k}, \{d_{k+j}\}_{j \in \mathcal{N}_0}), \quad (3.9)$$

such that u_k^* is the first component of u^* . The function (3.9) is a control law for the system (3.1). Evaluating the control law requires solution of the convex optimization problem (3.8).

3.4 Objective Functions

In conventional MPC, the objective function (3.8a) penalizes deviations from a target operating point [Raw00]. The objective function may also include regularization terms. We write the objective function as

$$\phi(u, x, z) = \phi^{\text{SP}}(u, x, z) + \phi^{\text{reg}}(u, x, z). \quad (3.10)$$

The function $\phi^{\text{SP}}(u, x, z)$ is a setpoint-based objective function and $\phi^{\text{reg}}(u, x, z)$ is a function composed of regularization terms. A widely used setpoint-based objective function is

$$\phi_{\ell_2}^{\text{SP}}(u, x, z) = \sum_{j \in \mathcal{N}_0} \|Q(z_{k+j+1} - \bar{z})\|_2^2 + \|R(u_{k+j} - \bar{u})\|_2^2, \quad (3.11)$$

where (\bar{u}, \bar{z}) is the target operating point. The entries in $Q \in \mathbb{R}^{n_z \times n_z}$, and $R \in \mathbb{R}^{n_u \times n_u}$, are penalty weights that can be adjusted to tune the controller. Examples of regularization functions for (3.10) are

$$\phi_{\ell_1}^{\text{reg}}(u, x, z) = \sum_{j \in \mathcal{N}_0} \|S_{\ell_1} \Delta u_{k+j}\|_1, \quad (3.12a)$$

$$\phi_{\ell_2}^{\text{reg}}(u, x, z) = \sum_{j \in \mathcal{N}_0} \|S_{\ell_2} \Delta u_{k+j}\|_2^2. \quad (3.12b)$$

As for (3.11), $S_{\ell_1}, S_{\ell_2} \in \mathbb{R}^{n_u \times n_u}$ are weight matrices. The input-rate, Δu_{k+j} , is defined as

$$\Delta u_{k+j} = u_{k+j} - u_{k+j-1}, \quad (3.13)$$

Regularization is important to make the closed-loop trajectory of the controlled system well-behaved [PJ09, SSE+14, HLJB12]. Figure 3.2 illustrates the regularization functions (3.12). The function (3.12a) assigns a linear penalty to

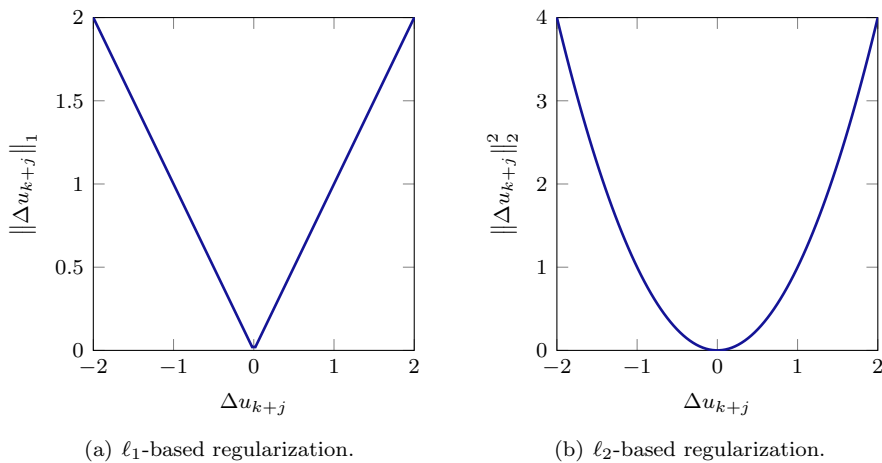


Figure 3.2: Illustration of the regularization functions (3.12).

the input-rate, and the function (3.12b) assigns a quadratic penalty to the input-rate. Generally, ℓ_1 -regularization induces sparsity in the solution, while ℓ_2 -regularization favors smooth solutions [BV04]. A combination of ℓ_1 and ℓ_2 -regularization is used to obtain smooth and sparse solutions.

3.5 Economic MPC

Economic optimization in contemporary industrial systems that utilize MPC is usually composed of several layers. In the real-time optimization layer (RTO), a static optimization problem is solved to determine the most cost-efficient steady-state (target operating point) for the system. The target operating point is sent to the supervisory control layer, where setpoint-based MPC is applied to steer the system to the desired steady-state. The RTO layer and the supervisory control layer have different time scales. Therefore, there is no guarantee that such a hierarchical approach operates the system in an economically efficient way during setpoint transitions. Moreover, steady-state operation may not be the best strategy in terms of economics. To overcome these challenges, EMPC has been introduced as an alternative to setpoint-based MPC [DAR11, Grü13, RAB12, AAR12, EDC14].

In EMPC, the OCP objective function, (3.8a), is an economic cost function. This allows cost information from the RTO layer to be included directly in the

supervisory control layer, which is responsible for closed-loop operation of the system. Including an economic cost function, $\phi^{\text{eco}}(u, x, z)$, in (3.10), yields

$$\phi(u, x, z) = \phi^{\text{eco}}(u, x, z) + \phi^{\text{sp}}(u, x, z) + \phi^{\text{reg}}(u, x, z). \quad (3.14)$$

When $\phi^{\text{sp}}(u, x, z)$ and $\phi^{\text{reg}}(u, x, z)$ are zero, (3.14) is a pure economic objective function. In some cases, regularization terms are incorporated into $\phi^{\text{eco}}(u, x, z)$, e.g. when a price for input-rate movements is available (this price can be related to wear and tear of the system components). The use of an economic objective function is a key concept for MPC in power production planning [HLJ11, MQLS11, HPMJ12, HPM⁺12, SEJ15, SSE⁺14, ZH14, MSSVP14, RSR13, BTS10]. Applications of EMPC in power production planning include flexible consumption for refrigeration systems, [HLEJ12, HLSJ12], cost-efficient building climate control [HPMJ12, MQLS11], control of heat ventilation and air conditioning systems for grid regulation services [MSSVP14], activation of operational reserves for frequency control [SEJ15], charging and discharging electric vehicles using electricity price forecasts [HPM⁺12], control of residential heat pumps for energy storage [PEH⁺13, Hal14], control of solar tanks based on weather and consumption forecasts [HBP⁺12], and design of sustainable policies for mitigating climate change [CDPH12].

3.6 Stability

Stability of MPC has been established for a variety of OCPs [AAR12, DAR11, RBJ⁺08, PN00, QB03, Grü13, JH05, MRRS00, RM93, GPSW12, BGW14]. The stability proofs are mainly based on Lyapunov stability theory. References [RBJ⁺08, MRRS00, RM93] provide stability proofs for setpoint-based MPC with a terminal cost and/or terminal constraints. These stability proofs are not directly applicable to MPC with an economic objective function. References [AAR12, DAR11] prove stability of EMPC with a terminal cost. Stability of EMPC without a terminal cost is addressed in [Grü13, GPSW12, BGW14]. A method to achieve stability that works well in practice, is simply to use sufficiently long prediction horizons [HPJJ12, JH05, PN00, Grü13, LS15, Jør05]. In our work, we adopt this approach. The use of long prediction horizons makes EMPC algorithms that scale well in the horizon length, N , important.

3.7 Online Optimization

MPC requires the solution of an OCP in every sampling instant. For this reason, the use of MPC has conventionally been limited to small systems with

slow dynamics. Modern algorithms, combined with increased computing power, have extended the use of MPC to larger systems with dynamics even in the kHz range. Efficient algorithms for solution of OCPs are based on multi-parametric programming [TJB03, BMDP02, SDG00, Pis12], IPMs [WB10, SFE⁺13, RWR98, SKC10, ESJ09, RJM09, Wri97, DZZ⁺12], active-set methods [BB06, FBD08, JRJ04, Wri97], and first-order methods [RJM09, JGR⁺14].

References [RWR98, JFGND12] present structure-exploiting IPMs for setpoint-based MPC with an ℓ_2 -penalty. A similar algorithm is proposed in [VBN02] for setpoint-based MPC with an ℓ_1 -penalty. Reference [SFS⁺15] provides a Riccati-based homogenous and self-dual IPM for EMPC with a linear objective function. Reference [SAY13] develops a warm-start strategy for homogeneous and self-dual IPMs. Reference [SFS⁺15] reports that this warm-start strategy reduces the average number of IPM iterations by 35-40% in an EMPC power portfolio case study. Splitting methods [BV04, Roc70] and gradient-based methods [HL13, JGR⁺14], have been developed for distributed setpoint-based MPC of dynamically coupled systems [CSZ⁺12, SL12], ℓ_1 -regularized setpoint-based MPC [AHW12], mean-variance EMPC [SDMJ14a], and setpoint-based MPC with an ℓ_2 -penalty [JGR⁺14, KF12, KF11, SFAJ14]. Reference [SSE⁺14] introduces an ADMM-based decomposition algorithm and a Dantzig-Wolfe decomposition algorithm for EMPC of dynamically decoupled subsystems. Warm-start and early-termination strategies are employed to increase the computational performance of the decomposition algorithms.

Generally, the best choice of algorithm for solving the OCP is highly dependent on the problem structure, as well as the accuracy required for the solution. Multi-parametric programming methods compute the control law defined by (3.9) offline. In this way, the online computations can be implemented as a lookup table. The main issue with multi-parametric programming methods is that the computation time can grow exponentially with the problem size (horizon length, number of states, and number of inputs). Multi-parametric programming methods are therefore limited to small problems. IPMs produce high-accuracy solutions using a few computationally expensive iterations. In contrast to this, first-order methods produce less accurate solutions using many computationally inexpensive iterations. For some problems, first-order methods determine a fairly accurate solution within a relatively small number of iterations [KCLB14, BPC⁺11].

3.7.1 State Elimination

Depending on the size and structure of the OCP, one formulation of the OCP may be preferable over another, from a computational point of view. State con-

densing eliminates the system states and outputs from the OCP. This results in a smaller less structured OCP. Algorithms that rely on state condensing are especially efficient for solution of the OCP when the length of the prediction horizon, N , is small and the state dimension, n_x , is large [FJ13]. State condensing is applied several times in this thesis. For convenience, we outline a procedure for state condensing below.

Consider the OCP (3.8). Using the state equation (3.8b), it follows that

$$\hat{x}_{k+1|k} = A\hat{x}_{k|k} + Bu_k + Ed_k, \quad (3.15a)$$

$$\hat{x}_{k+2|k} = A\hat{x}_{k+1|k} + Bu_{k+1} + Ed_{k+1}, \quad (3.15b)$$

$$\vdots$$

$$\hat{x}_{k+N|k} = A\hat{x}_{k+N-1|k} + Bu_{k+N-1} + Ed_{k+N-1}. \quad (3.15c)$$

Repeated substitution of the system states gives

$$\hat{x}_{k+j|k} = A^j \hat{x}_{k|k} + \sum_{i=0}^{j-1} A^{j-i-1} Bu_{k+i} + \sum_{i=0}^{j-1} A^{j-i-1} Ed_{k+i}, \quad j \in \mathcal{N}_1. \quad (3.16)$$

Define the impulse response matrices (Markov parameters)

$$H_{u,j} = C_z A^{j-1} B, \quad j \in \mathcal{N}_1,$$

$$H_{d,j} = C_z A^{j-1} E, \quad j \in \mathcal{N}_1.$$

The system outputs defined by (3.8c), can be written in the form

$$\hat{z}_{k+j|k} = C_z A^j \hat{x}_{k|k} + \sum_{i=0}^{j-1} H_{u,j-i} u_{k+i} + \sum_{i=0}^{j-1} H_{d,j-i} d_{k+i}, \quad j \in \mathcal{N}_1. \quad (3.17)$$

Equations (3.16) and (3.17) show that

$$\hat{x} = L_x(u; d, \hat{x}_{k|k}), \quad (3.18a)$$

$$\hat{z} = L_z(u; d, \hat{x}_{k|k}), \quad (3.18b)$$

where L_x and L_z are affine functions, and $d = [d_k^T \ d_{k+1}^T \ \cdots \ d_{k+N-1}^T]^T$. I.e. the state and the outputs can be written as affine functions of the input, u , the disturbance, d , and the filtered estimate, $\hat{x}_{k|k}$. The semi-colons in (3.18) separate the OCP optimization variable, u , from the OCP parameters, d and $\hat{x}_{k|k}$.

The function L_x is defined as

$$L_x(u; d, \hat{x}_{k|k}) = \Phi \hat{x}_{k|k} + \Gamma_u u + \Gamma_d d, \quad (3.19)$$

where $\Phi = [(C_z A)^T \quad (C_z A^2)^T \quad \cdots \quad (C_z A^N)^T]^T$ and

$$\Gamma_u = \begin{bmatrix} H_{u,1} & & & & \\ H_{u,2} & H_{u,1} & & & \\ \vdots & \vdots & \ddots & & \\ H_{u,N} & H_{u,N-1} & \cdots & H_{u,1} & \end{bmatrix}, \quad \Gamma_d = \begin{bmatrix} H_{d,1} & & & & \\ H_{d,2} & H_{d,1} & & & \\ \vdots & \vdots & \ddots & & \\ H_{d,N} & H_{d,N-1} & \cdots & H_{d,1} & \end{bmatrix}.$$

The function L_z is defined similarly. Using the expressions (3.18), the states, \hat{x} , and the outputs, \hat{z} , can be eliminated from the OCP (3.8).

Convex Optimization

This chapter presents convex optimization algorithms for EMPC of linear stochastic systems. A homogeneous and self-dual linear programming IPM is outlined. LPs arise in EMPC of linear systems with linear constraints and linear objective functions. We present a Dantzig-Wolfe decomposition algorithm for block-angular LPs. Block-angular LPs occur in EMPC of dynamically decoupled subsystems, such as power generators in the portfolio system (2.9). An ADMM algorithm is proposed for convex optimization problems with separable objective functions. This type of problem is solved in MV-EMPC. Part II of the thesis provides tailored EMPC implementations of the proposed algorithms.

4.1 Convex Optimization Problems

Define the convex optimization problem [BV04]

$$\min_x f(x), \tag{4.1a}$$

$$\text{s.t. } g_i(x) = 0, \quad i = 1, 2, \dots, m_E, \tag{4.1b}$$

$$h_i(x) \leq 0, \quad i = 1, 2, \dots, m_I, \tag{4.1c}$$

where $x \in \mathbb{R}^n$ is the optimization variable, and:

- The objective function f is a convex function.
- The equality constraint functions g_1, \dots, g_{m_E} are affine functions.
- The inequality constraint functions h_1, \dots, h_{m_I} are convex functions.

4.1.1 Karush-Kuhn-Tucker Conditions

The Lagrangian associated with (4.1) is

$$\mathcal{L}(x, y, z) = f(x) + \sum_{i=1}^{m_E} y_i g_i(x) + \sum_{i=1}^{m_I} z_i h_i(x). \quad (4.2)$$

where $y_1, \dots, y_{m_E} \in \mathbb{R}$ and $z_1, \dots, z_{m_I} \in \mathbb{R}$ are dual variables, and

$$y = [y_1 \quad y_2 \quad \cdots \quad y_{m_E}]^T, \\ z = [z_1 \quad z_2 \quad \cdots \quad z_{m_I}]^T.$$

The Karush-Kuhn-Tucker (KKT) conditions for (4.1) are

$$\nabla_x \mathcal{L}(x, y, z) = 0, \quad (4.3a)$$

$$g_i(x) = 0, \quad i = 1, 2, \dots, m_E, \quad (4.3b)$$

$$h_i(x) \leq 0, \quad i = 1, 2, \dots, m_I, \quad (4.3c)$$

$$z_i \geq 0, \quad i = 1, 2, \dots, m_I, \quad (4.3d)$$

$$z_i h_i(x) = 0, \quad i = 1, 2, \dots, m_I. \quad (4.3e)$$

Condition (4.3a) is the Lagrangian stationarity condition. Conditions (4.3b) and (4.3c) are the primal feasibility conditions. Condition (4.3d) is the dual feasibility condition, and condition (4.3e) is the complementary slackness condition. Problem (4.1) is a convex optimization problem. The KKT conditions (4.3) are therefore necessary and sufficient for an optimal solution of (4.1). I.e. a point, (x^*, y^*, z^*) , satisfying (4.3) is a global solution of (4.1), and vice-versa. The KKT conditions (4.3) assume that f , g_1, \dots, g_{m_E} , and h_1, \dots, h_{m_I} are differentiable functions. Reference [Rus07] provides generalized KKT conditions that hold for non-differentiable functions as well.

4.2 Linear Programming IPM

This section presents a homogeneous and self-dual IPM for solution of the LP

$$\min_x g^T x, \quad (4.4a)$$

$$\text{s.t. } Ax = b, \quad (4.4b)$$

$$Cx \leq d. \quad (4.4c)$$

The data in (4.4) are $g \in \mathbb{R}^n$, $A \in \mathbb{R}^{m_E \times n}$, $b \in \mathbb{R}^{m_E}$, $C \in \mathbb{R}^{m_I \times n}$, and $d \in \mathbb{R}^{m_I}$. The LP (4.4) is the special case of (4.1) where $f(x)$ is a linear function, g_1, \dots, g_{m_E} are affine functions, and h_1, \dots, h_{m_I} are affine functions. We write this as

$$\begin{aligned} f(x) &= g^T x, \\ g_i(x) &= a_i^T x - b_i, & i = 1, 2, \dots, m_E, \\ h_i(x) &= c_i^T x - d_i, & i = 1, 2, \dots, m_I, \end{aligned}$$

with $a_1, \dots, a_{m_E} \in \mathbb{R}^n$, $b_1, \dots, b_{m_E} \in \mathbb{R}$, $c_1, \dots, c_{m_I} \in \mathbb{R}^n$, and $d_1, \dots, d_{m_I} \in \mathbb{R}$. In addition

$$\begin{aligned} A &= [a_1 \ a_2 \ \cdots \ a_{m_E}]^T, \\ b &= [b_1 \ b_2 \ \cdots \ b_{m_E}]^T, \\ C &= [c_1 \ c_2 \ \cdots \ c_{m_I}]^T, \\ d &= [d_1 \ d_2 \ \cdots \ d_{m_I}]^T, \end{aligned}$$

The Lagrangian associated with (4.4) is

$$\mathcal{L}(x, y, z) = g^T x + y^T (Ax - b) + z^T (Cx - d),$$

and the dual LP of (4.4) can be written in the form

$$\max_{y, z} -b^T y - d^T z, \quad (4.5a)$$

$$\text{s.t. } A^T y + C^T z = -g, \quad (4.5b)$$

$$z \geq 0. \quad (4.5c)$$

The KKT conditions for (4.4) are

$$A^T y + C^T z + g = 0, \quad (4.6a)$$

$$Ax - b = 0, \quad (4.6b)$$

$$Cx - d \leq 0, \quad (4.6c)$$

$$z \geq 0, \quad (4.6d)$$

$$z_i (c_i^T x_i - d_i) = 0, \quad i = 1, 2, \dots, m_I. \quad (4.6e)$$

For convenience, introduce the slack variables

$$s_i = d_i - c_i^T x, \quad i = 1, 2, \dots, m_I.$$

and $s = [s_1 \ \cdots \ s_{m_I}]$. This way, the KKT conditions (4.6) can be written as

$$A^T y + C^T z + g = 0, \quad (4.7a)$$

$$Ax - b = 0, \quad (4.7b)$$

$$Cx - d + s = 0, \quad (4.7c)$$

$$(z, s) \geq 0, \quad (4.7d)$$

$$ZS\mathbf{1} = 0, \quad (4.7e)$$

where $S = \mathbf{diag}(s)$, $Z = \mathbf{diag}(z)$, and $\mathbf{1}$ is a vector of all ones.

4.2.1 Homogeneous and Self-Dual Model

The solution of the KKT system (4.6) provides the solution of the primal LP (4.4), (x^*, s^*) , and the solution of the dual LP (4.5), (y^*, z^*) . Conventional IPMs solve the KKT system using a Newton-type of method. Homogeneous and self-dual IPMs solve the related LP

$$\min_x 0, \quad (4.8a)$$

$$\text{s.t. } A^T \tilde{y} + C^T \tilde{z} + g\tau = 0, \quad (4.8b)$$

$$A\tilde{x} - b\tau = 0, \quad (4.8c)$$

$$C\tilde{x} - d\tau + \tilde{s} = 0, \quad (4.8d)$$

$$-g^T \tilde{x} - b^T \tilde{y} - d^T \tilde{z} + \kappa = 0, \quad (4.8e)$$

$$(\tilde{z}, \tilde{s}, \tau, \kappa) \geq 0, \quad (4.8f)$$

in which $\tilde{x} \in \mathbb{R}^n$, $\tilde{y} \in \mathbb{R}^{m_E}$, $\tilde{z} \in \mathbb{R}^{m_I}$, and $\tau, \kappa \in \mathbb{R}$. The LP (4.8) is a pure feasibility problem.

A strict complementary solution of (4.8), $(\tilde{x}^*, \tilde{y}^*, \tilde{z}^*, \tilde{s}^*, \tau^*, \kappa^*)$, satisfies $\tilde{z}_1 \tilde{s}_1 = 0, \dots, \tilde{z}_{m_I} \tilde{s}_{m_I} = 0$, and $\tau^* \kappa^* = 0$. Moreover, one of the following conditions hold [AGMX96, YTM94, XHY96]:

- If $\tau^* > 0$, and $\kappa^* = 0$: The scaled solution $(x^*, y^*, z^*, s^*) = (\tilde{x}^*, \tilde{y}^*, \tilde{z}^*, \tilde{s}^*)/\tau^*$ is a primal-dual optimal solution of (4.4) and (4.5).
- If $\tau^* = 0$, and $\kappa^* > 0$: The problem (4.4) is infeasible or unbounded. Either $-b^T \tilde{y}^* - d^T \tilde{z}^* > 0$ (primal infeasible and dual unbounded) or $g^T \tilde{x}^* < 0$ (primal unbounded and dual infeasible).

Homogeneous and self-dual IPMs determine a strict complementarity solution of (4.8) [YTM94, XHY96]. If the problem is infeasible or unbounded, the solution satisfies $\tau^* = 0$ and $\kappa^* > 0$. The ability to detect infeasible or unbounded problems is a special feature of homogeneous and self-dual IPMs. An additional advantage of homogeneous and self-dual IPMs is that they can be warm-started efficiently. In [SAY13] warm-start reduces the number of IPM iterations by 30-75% for the NETLIB collection of test problems. Warm-start capabilities are convenient in MPC applications, as the OCP is solved in a receding horizon manner. Conventional IPMs do not have similar warm-start capabilities as homogeneous and self-dual IPMs.

4.2.2 Predictor-Corrector Algorithm

We present a homogeneous and self-dual IPM for solution of (4.8). The method is based on Mehrotra's predictor-corrector method. Proofs and details are provided in e.g. [Meh92, NW06, YTM94, XHY96, ART03, Stu02, SAY13, Ye97, Wri96]. Mehrotra's predictor-corrector method is a path-following algorithm that tracks the central path. The central path is a smooth curve that connects an initial point to a complementary solution of (4.8).

For compact notation, introduce

$$\theta = (\tilde{x}, \tilde{y}, \tilde{z}, \tilde{s}, \tau, \kappa), \quad (4.9)$$

and let θ^i refer to the i 'th iterate generated by the proposed algorithm. The initial point is $\theta^0 = (\tilde{x}^0, \tilde{y}^0, \tilde{z}^0, \tilde{s}^0, \tau^0, \kappa^0)$.

A solution of (4.8) is defined by

$$(\tilde{z}, \tilde{s}, \kappa, \tau) \geq 0, \quad (4.10a)$$

and

$$V(\theta) = \begin{bmatrix} V_1(\theta) \\ V_2(\theta) \\ V_3(\theta) \\ V_4(\theta) \\ V_5(\theta) \\ V_6(\theta) \end{bmatrix} = \begin{bmatrix} A^T \tilde{y} + C^T \tilde{z} + g\tau \\ A\tilde{x} - b\tau \\ C\tilde{x} - d\tau + \tilde{s} \\ -g^T \tilde{x} - b^T \tilde{y} - d^T \tilde{z} + \kappa \\ \tilde{Z}\tilde{S}\mathbf{1} \\ \tau\kappa \end{bmatrix} = \begin{bmatrix} 0 \\ 0 \\ 0 \\ 0 \\ 0 \\ 0 \end{bmatrix}. \quad (4.10b)$$

As in (4.7), $\tilde{Z} = \mathbf{diag}(\tilde{z})$ and $\tilde{S} = \mathbf{diag}(\tilde{s})$ are diagonal matrices.

Define the complementary gap

$$\mu^i = \frac{(\tilde{z}^i)^T \tilde{s}^i + \tau^i \kappa^i}{m_I + 1}. \quad (4.11)$$

The central path is given as

$$\mathcal{C} = \{\theta \mid V(\theta) = \gamma r^0, (\tilde{z}, \tilde{s}, \kappa, \tau) \geq 0, \gamma \in [0, 1]\}. \quad (4.12)$$

where

$$r^0 = \begin{bmatrix} V_1(\theta^0) \\ V_2(\theta^0) \\ V_3(\theta^0) \\ V_4(\theta^0) \\ \mu^0 \mathbf{1} \\ \mu^0 \end{bmatrix} = \begin{bmatrix} A^T \tilde{y}^0 + C^T \tilde{z}^0 + g \tau^0 \\ A \tilde{x}^0 - b \tau^0 \\ C \tilde{x}^0 - d \tau^0 + \tilde{s}^0 \\ -g^T \tilde{x}^0 - b^T \tilde{y}^0 - d^T \tilde{z}^0 + \kappa^0 \\ ((\tilde{z}^0)^T \tilde{s}^0 + \tau^0 \kappa^0) / (m_I + 1) \mathbf{1} \\ ((\tilde{z}^0)^T \tilde{s}^0 + \tau^0 \kappa^0) / (m_I + 1) \end{bmatrix}.$$

For $\gamma = 0$, the central path (4.12) defines a point, θ^* , that satisfies the conditions (4.10), i.e. a solution of (4.8). Mehrotra's predictor-corrector method generates iterates, $\theta^0, \theta^1, \dots, \theta^*$, along the central path as $\gamma \rightarrow 0$. It is trivial to construct an initial point, θ^0 , for this procedure. E.g.

$$\theta^0 = (\tilde{x}^0, \tilde{y}^0, \tilde{z}^0, \tilde{s}^0, \tau^0, \kappa^0) = (\mathbf{0}, \mathbf{0}, \mathbf{1}, \mathbf{1}, 1, 1), \quad (4.13)$$

lies on the central path for $\gamma = 1$.

The optimization search direction is computed by solving the linear system of equations

$$J_V(\theta^i) \Delta \theta^i = -\bar{V}(\theta^i), \quad (4.14)$$

where $J_V(\theta^i)$ is the Jacobian of V evaluated at θ^i . It follows from (4.10b) that

$$J_V(\theta^i) = \begin{bmatrix} 0 & A^T & C^T & 0 & g & 0 \\ A & 0 & 0 & 0 & -b & 0 \\ C & 0 & 0 & I & -d & 0 \\ -g^T & -b^T & -d^T & 0 & 0 & 1 \\ 0 & 0 & \tilde{S}^i & \tilde{Z}^i & 0 & 0 \\ 0 & 0 & 0 & 0 & \kappa^i & \tau^i \end{bmatrix}. \quad (4.15)$$

The right-hand side in (4.14) is defined as

$$\bar{V}(\theta^i) = \begin{bmatrix} (1 - \gamma^i) V_1(\theta^i) \\ (1 - \gamma^i) V_2(\theta^i) \\ (1 - \gamma^i) V_3(\theta^i) \\ (1 - \gamma^i) V_4(\theta^i) \\ V_5(\theta^i) + \Delta \tilde{Z}_{\text{aff}}^i \Delta \tilde{S}_{\text{aff}}^i - \gamma^i \mu_{\text{aff}}^i \mathbf{1} \\ V_6(\theta^i) + \Delta \tau_{\text{aff}}^i \Delta \kappa_{\text{aff}}^i - \gamma^i \mu_{\text{aff}}^i \end{bmatrix}.$$

In this definition, $\Delta \tilde{Z}_{\text{aff}}^i = \mathbf{diag}(\Delta \tilde{z}_{\text{aff}}^i)$, $\Delta \tilde{S}_{\text{aff}}^i = \mathbf{diag}(\Delta \tilde{s}_{\text{aff}}^i)$, $\Delta \tau_{\text{aff}}^i$, and $\Delta \kappa_{\text{aff}}^i$, are second order corrector terms [NW06, Meh92], μ_{aff}^i is the affine complementarity gap, and γ^i is the centering parameter. These quantities are computed

based on an affine-scaling direction

$$\Delta\theta_{\text{aff}} = (\Delta\tilde{x}_{\text{aff}}, \Delta\tilde{y}_{\text{aff}}, \Delta\tilde{z}_{\text{aff}}, \Delta\tilde{s}_{\text{aff}}, \Delta\tau_{\text{aff}}, \Delta\kappa_{\text{aff}}).$$

The affine-scaling direction is obtained by solving the system (4.14) with $\bar{V}(\theta^i)$ replaced by $V(\theta^i)$. Accordingly, we define the affine variables

$$\begin{aligned}\tilde{z}_{\text{aff}}^i &= \tilde{z}^i + \alpha_{\text{aff}}^i \Delta\tilde{z}_{\text{aff}}^i, & \tilde{s}_{\text{aff}}^i &= \tilde{s}^i + \alpha_{\text{aff}}^i \Delta\tilde{s}_{\text{aff}}^i, \\ \tau_{\text{aff}}^i &= \tau^i + \alpha_{\text{aff}}^i \Delta\tau_{\text{aff}}^i, & \kappa_{\text{aff}}^i &= \kappa^i + \alpha_{\text{aff}}^i \Delta\kappa_{\text{aff}}^i,\end{aligned}$$

where α_{aff}^i is a damping parameter that keeps the affine variables within the non-negative orthant (4.10a)

$$\alpha_{\text{aff}}^i = \max \left\{ a_{\text{aff}} \in [0, 1] \mid \begin{bmatrix} \tilde{z}^i \\ \tau^i \\ \tilde{s}^i \\ \kappa^i \end{bmatrix} + a_{\text{aff}} \begin{bmatrix} \Delta\tilde{z}_{\text{aff}}^i \\ \Delta\tau_{\text{aff}}^i \\ \Delta\tilde{s}_{\text{aff}}^i \\ \Delta\kappa_{\text{aff}}^i \end{bmatrix} \geq 0 \right\}.$$

The affine complementarity gap is

$$\mu_{\text{aff}}^i = \frac{(\tilde{z}_{\text{aff}}^i)^T \tilde{s}_{\text{aff}}^i + \tau_{\text{aff}}^i \kappa_{\text{aff}}^i}{m_I + 1},$$

and the centering parameter γ^i is computed as

$$\gamma^i = \left[\frac{\mu_{\text{aff}}^i}{\mu^i} \right]^3 = \left[\frac{((\tilde{z}_{\text{aff}}^i)^T \tilde{s}_{\text{aff}}^i + \tau_{\text{aff}}^i \kappa_{\text{aff}}^i)}{((\tilde{z}^i)^T \tilde{s}^i + \tau^i \kappa^i)} \right]^3. \quad (4.16)$$

Equation (4.16) updates the centering parameter according to the effectiveness of the affine-scaling direction. When $\mu_{\text{aff}}^i \approx \mu^i$, only small progress towards the optimal solution can be made in the affine-scaling direction. In this case, (4.16) yields $\gamma^i \approx 1$, which forces the search direction towards the central path. Substantial progress can usually be made in the affine-scaling direction in an iteration that follows a step with aggressive centering.

To classify a solution as optimal, we use the stopping criteria [ART03]

$$\varrho_E^i \leq \epsilon_E, \quad \varrho_I^i \leq \epsilon_I, \quad \varrho_D^i \leq \epsilon_D, \quad \varrho_O^i \leq \epsilon_O. \quad (4.17)$$

Moreover, the problem is considered to be infeasible if $\tau^i \leq \epsilon_\tau \max(1, \kappa^i)$, and

$$\varrho_E^i \leq \epsilon_E, \quad \varrho_I^i \leq \epsilon_I, \quad \varrho_D^i \leq \epsilon_D, \quad \varrho_G^i \leq \epsilon_G. \quad (4.18)$$

ϵ_τ , ϵ_E , ϵ_I , ϵ_D , ϵ_O and ϵ_G are user-defined tolerance parameters, and

$$\begin{aligned}\varrho_D &= \|V_1(\theta)\|_\infty / \max(1, \|[H^T \ F^T \ g]\|_\infty), \\ \varrho_E &= \|V_2(\theta)\|_\infty / \max(1, \|[F \ b]\|_\infty), \\ \varrho_I &= \|V_3(\theta)\|_\infty / \max(1, \|[H \ I \ c]\|_\infty), \\ \varrho_G &= |L - \kappa| / \max(1, \|[g^T \ b^T \ c^T \ 1]\|_\infty), \\ \varrho_O &= |L| / (\tau + |-b^T \tilde{y} - c^T \tilde{z}|).\end{aligned}$$

Algorithm 1 Homogeneous and self-dual IPM for (4.8)

```

 $\mu \leftarrow (\tilde{z}^T \tilde{s} + \tau \kappa) / (m_I + 1)$ 
while not converged do
  COMPUTE AFFINE-SCALING DIRECTION
   $\Delta \theta_{\text{aff}} \leftarrow -J_V(\theta)^{-1} V(\theta)$ 
   $\alpha_{\text{aff}} \leftarrow \max \{a_{\text{aff}} \in [0, 1] \mid (\tilde{z}, \tau, \tilde{s}, \kappa) + a_{\text{aff}}(\Delta \tilde{z}_{\text{aff}}, \Delta \tau_{\text{aff}}, \Delta \tilde{s}_{\text{aff}}, \Delta \kappa_{\text{aff}}) \geq 0\}$ 
   $\tilde{s}_{\text{aff}} \leftarrow \tilde{s} + \alpha_{\text{aff}} \Delta \tilde{s}_{\text{aff}}, \quad \kappa_{\text{aff}} \leftarrow \kappa + \tilde{\alpha}_{\text{aff}} \Delta \kappa_{\text{aff}}$ 
   $\tilde{z}_{\text{aff}} \leftarrow \tilde{z} + \alpha_{\text{aff}} \Delta \tilde{z}_{\text{aff}}, \quad \tau_{\text{aff}} \leftarrow \tau + \tilde{\alpha}_{\text{aff}} \Delta \tau_{\text{aff}}$ 
   $\mu_{\text{aff}} \leftarrow (\tilde{z}_{\text{aff}}^T \tilde{s}_{\text{aff}} + \tau_{\text{aff}} \kappa_{\text{aff}}) / (m_I + 1)$ 
   $\gamma \leftarrow (\mu_{\text{aff}} / \mu)^3$ 
  COMPUTE SEARCH DIRECTION
   $\Delta \theta \leftarrow -J_V(\theta)^{-1} \bar{V}(\theta)$ 
   $\alpha \leftarrow \max \{a \in [0, 1] \mid (\tilde{z}, \tau, \tilde{s}, \kappa) + a(\Delta \tilde{z}, \Delta \tau, \Delta \tilde{s}, \Delta \kappa) \geq 0\}$ 
   $\tilde{x} \leftarrow \tilde{x} + \nu \alpha \Delta \tilde{x}, \quad \tilde{s} \leftarrow \tilde{s} + \nu \alpha \Delta \tilde{s}, \quad \kappa \leftarrow \kappa + \nu \alpha \Delta \kappa$ 
   $\tilde{y} \leftarrow \tilde{y} + \nu \alpha \Delta \tilde{y}, \quad \tilde{z} \leftarrow \tilde{z} + \nu \alpha \Delta \tilde{z}, \quad \tau \leftarrow \tau + \nu \alpha \Delta \tau$ 
   $\mu \leftarrow (\tilde{z}^T \tilde{s} + \tau \kappa) / (m_I + 1)$ 
end while

```

$L = g^T \tilde{x} - (-b^T \tilde{y} - d^T \tilde{z})$ is the duality gap. Algorithm 1 outlines the proposed homogeneous and self-dual IPM. To keep the iterates well inside the interior of the non-negative orthant, (4.10a), a damping parameter $\nu \in [0.95; 0.999]$ is introduced. Conditions (4.17) and (4.18) are the stopping criteria for Algorithm 1.

4.3 Dantzig-Wolfe Decomposition Algorithm

This section presents a Dantzig-Wolfe decomposition algorithm for solution of LPs in the form

$$\min_x g^T x, \quad (4.19a)$$

$$\text{s.t. } Ax \leq b, \quad (4.19b)$$

with the block-angular structure

$$g = \begin{bmatrix} g_1 \\ g_2 \\ \vdots \\ g_p \end{bmatrix}, \quad x = \begin{bmatrix} x_1 \\ x_2 \\ \vdots \\ x_p \end{bmatrix}, \quad A = \begin{bmatrix} A_{l_1} & A_{l_2} & \cdots & A_{l_p} \\ A_{s_1} & & & \\ & A_{s_2} & & \\ & & \ddots & \\ & & & A_{s_p} \end{bmatrix}, \quad b = \begin{bmatrix} b_l \\ b_{s_1} \\ \vdots \\ b_{s_p} \end{bmatrix}. \quad (4.20)$$

The indices $j \in \mathcal{J} = \{1, \dots, p\}$ are subsystem indices. The vector $g_j \in \mathbb{R}^{n_j}$ is the cost associated with subsystem j , $x_j \in \mathbb{R}^{n_j}$ is the decision variable for subsystem j , $A_{l_j} \in \mathbb{R}^{m_l \times n_j}$ is the linking constraint matrix for subsystem j , and $A_{s_j} \in \mathbb{R}^{m_{s_j} \times n_j}$ is the constraint matrix for subsystem j . The right-hand side of the linking constraints is $b_l \in \mathbb{R}^{m_l}$, and the right-hand side of the constraints for subsystem j is $b_{s_j} \in \mathbb{R}^{m_{s_j}}$. Note that the block-angular LP (4.19) is a special case of (4.4).

Using the definitions (4.20), we write (4.19) as

$$\min_x \sum_{j \in \mathcal{J}} g_j^T x_j, \quad (4.21a)$$

$$\text{s.t. } A_{s_j} x_j \leq b_{s_j}, \quad j \in \mathcal{J}, \quad (4.21b)$$

$$\sum_{j \in \mathcal{J}} A_{l_j} x_j \leq b_l. \quad (4.21c)$$

In the extreme case, $m_l = 0$, there are no linking constraints. For this case, the problem (4.21) decouples into p independent subproblems. Conversely, when $m_{s_1} = \dots = m_{s_p} = 0$, there are no subsystem constraint blocks. Algorithms based on Dantzig-Wolfe decomposition are generally most efficient when m_l is small compared to the overall number of constraints, i.e. when the problem has relatively few linking constraints. The OCP that arises in EMPC of the portfolio system (2.9) is block-angular LPs with relatively few linking constraints.

4.3.1 Extreme Point Representation

Dantzig-Wolfe decomposition exploits that a convex set can be characterized by its extreme points and its extreme rays [CCMGB06, DW60, Mar99]. Define

$$\mathbb{G}_j = \{x_j \mid A_{s_j} x_j \leq b_{s_j}\}, \quad j \in \mathcal{J},$$

such that (4.21b) can be written as $x_j \in \mathbb{G}_j$ for $j \in \mathcal{J}$. For simplicity, assume that every \mathbb{G}_j is bounded. It follows that

$$\mathbb{G}_j = \left\{ x_j \mid x_j = \sum_{i \in \mathcal{I}_j} \lambda_j^i x_j^i, \sum_{i \in \mathcal{I}_j} \lambda_j^i = 1, \lambda_j^i \geq 0 \text{ for all } i \in \mathcal{I}_j \right\}, \quad j \in \mathcal{J}, \quad (4.22)$$

where x_j^i are the extreme points of \mathbb{G}_j , and λ_j^i are convex combination multipliers. The set of indices associated with the extreme points of \mathbb{G}_j is denoted \mathcal{I}_j . Since every \mathbb{G}_j is bounded, the representation (4.22) does not include extreme rays.

Replacing the decision variables in (4.21) by convex combination multipliers yields

$$\min_{\lambda} \sum_{j \in \mathcal{J}} \sum_{i \in \mathcal{I}_j} g_j^i \lambda_j^i, \quad (4.23a)$$

$$\text{s.t.} \quad \sum_{j \in \mathcal{J}} \sum_{i \in \mathcal{I}_j} A_{l_j}^i \lambda_j^i \leq b_l, \quad (4.23b)$$

$$\sum_{i \in \mathcal{I}_j} \lambda_j^i = 1, \quad j \in \mathcal{J}, \quad (4.23c)$$

$$\lambda_j^i \geq 0, \quad j \in \mathcal{J}, \quad i \in \mathcal{I}_j, \quad (4.23d)$$

where we have defined

$$A_{l_j}^i = A_{l_j} x_j^i, \quad j \in \mathcal{J}, \quad i \in \mathcal{I}_j, \quad (4.24a)$$

$$g_j^i = g_j^T x_j^i, \quad j \in \mathcal{J}, \quad i \in \mathcal{I}_j. \quad (4.24b)$$

Problem (4.23) is referred to as the master problem.

Given a solution, λ^* , to the master problem (4.23), a solution to the original problem, (4.21), is obtained as

$$x_j^* = \sum_{i \in \mathcal{I}_j} \lambda_j^{i*} x_j^i, \quad j \in \mathcal{J}.$$

The number of optimization variables and constraints in the master problem (4.23), increases with the number of extreme points. The number of extreme points can be exponential in the size of the original problem (4.21). It is therefore computationally inefficient to solve the master problem directly. The Dantzig-Wolfe decomposition algorithm generates extreme points in an iterative manner [SSE⁺14].

4.3.2 Column Generation Procedure

The dual LP of (4.23) may be stated as

$$\max_{\alpha, \beta} \quad -\alpha^T b_l + \sum_{j \in \mathcal{J}} \beta_j, \quad (4.25a)$$

$$\text{s.t.} \quad -(A_{l_j}^i)^T \alpha + \beta_j \leq g_j^i, \quad j \in \mathcal{J}, \quad i \in \mathcal{I}_j, \quad (4.25b)$$

$$\alpha \geq 0, \quad (4.25c)$$

in which α and β are the dual variables associated with the linking constraints, (4.23b), and the convexity constraints, (4.23c), respectively.

The necessary and sufficient optimality conditions for (4.23) and (4.25) are

$$\sum_{j \in \mathcal{J}} \sum_{i \in \mathcal{I}_j} A_{l_j}^i \lambda_j^i \leq b_l, \quad (4.26a)$$

$$\sum_{i \in \mathcal{I}_j} \lambda_j^i = 1, \quad j \in \mathcal{J}, \quad (4.26b)$$

$$\lambda_j^i \geq 0, \quad j \in \mathcal{J}, \quad i \in \mathcal{I}_j, \quad (4.26c)$$

$$g_j^i + (A_{l_j}^i)^T \alpha - \beta_j \geq 0, \quad j \in \mathcal{J}, \quad i \in \mathcal{I}_j, \quad (4.26d)$$

$$\alpha \geq 0, \quad (4.26e)$$

$$\lambda_j^i (g_j^i + (A_{l_j}^i)^T \alpha - \beta_j) = 0, \quad j \in \mathcal{J}, \quad i \in \mathcal{I}_j, \quad (4.26f)$$

Reference [DW60, DW60, SSE⁺14] presents a column generation procedure for solution of (4.26). In this procedure, a restricted master problem is solved. The restricted master problem is defined as

$$\min_{\lambda} \sum_{j \in \mathcal{J}} \sum_{i \in \tilde{\mathcal{I}}_j} g_j^i \lambda_j^i, \quad (4.27a)$$

$$\text{s.t.} \quad \sum_{j \in \mathcal{J}} \sum_{i \in \tilde{\mathcal{I}}_j} A_{l_j}^i \lambda_j^i \leq b_l, \quad (4.27b)$$

$$\sum_{i \in \tilde{\mathcal{I}}_j} \lambda_j^i = 1, \quad j \in \mathcal{J}, \quad (4.27c)$$

$$\lambda_j^i \geq 0, \quad j \in \mathcal{J}, \quad i \in \tilde{\mathcal{I}}_j, \quad (4.27d)$$

where $\tilde{\mathcal{I}}_j \subseteq \mathcal{I}_j$, for $j \in \mathcal{J}$. The restricted master problem is simply (4.23), defined over a subset of the extreme points.

Let $(\tilde{\lambda}, \tilde{\alpha}, \tilde{\beta})$ denote a primal-dual solution of the restricted master problem, (4.27). Reference [SSE⁺14] shows that the solution

$$\begin{aligned} \alpha^* &= \tilde{\alpha}, \\ \beta_j^* &= \tilde{\beta}_j, \quad j \in \mathcal{J}, \\ \lambda_j^{i*} &= \begin{cases} \tilde{\lambda}_j^i & \text{if } i \in \tilde{\mathcal{I}}_j \\ 0 & \text{if } i \in \mathcal{I}_j \setminus \tilde{\mathcal{I}}_j \end{cases}, \quad j \in \mathcal{J}, \quad i \in \mathcal{I}_j, \end{aligned}$$

satisfies the KKT conditions (4.26), provided that the optimal objective value of the subproblem

$$\min_{\tilde{x}_j} \varphi_j = (g_j + A_{l_j}^T \alpha^*)^T \tilde{x}_j - \beta_j^* \quad (4.28a)$$

$$\text{s.t.} \quad A_{s_j} \tilde{x}_j \leq b_{s_j}, \quad (4.28b)$$

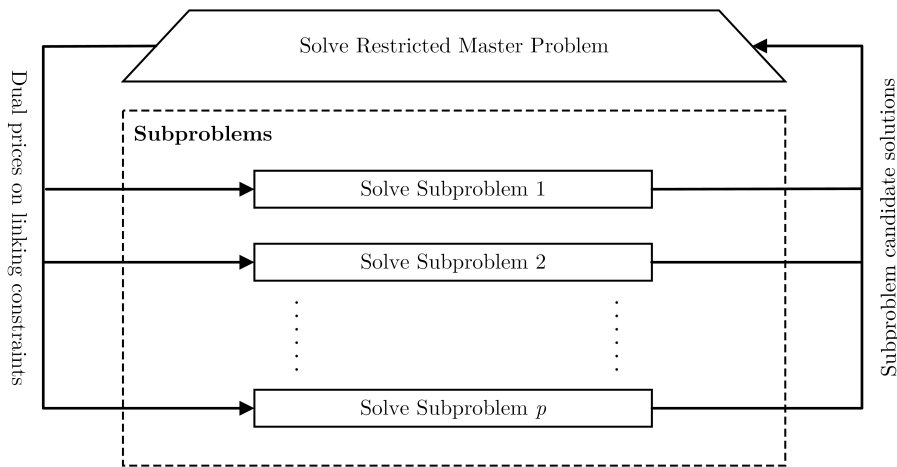


Figure 4.1: Flowchart of the Dantzig-Wolfe decomposition algorithm.

is non-negative for each $j \in \mathcal{J}$.

Algorithm 2 outlines the Dantzig-Wolfe decomposition algorithm. Extreme points are generated by solving subproblems in the form (4.28). The algorithm terminates if $\varphi_j \geq \epsilon$ for all $j \in \mathcal{J}$. The parameter ϵ is a user-defined tolerance parameter. Fig. 4.1 is a flowchart of Algorithm 2. For proofs and details, we refer to [CCMGB06, DW60, Mar99, SSE⁺14].

4.4 Alternating Direction Method of Multipliers

This section presents an ADMM algorithm for solution of the convex optimization problem

$$\min_x f_1(x_1) + f_2(x_2), \quad (4.29a)$$

$$\text{s.t. } A_1x_1 + A_2x_2 = b, \quad (4.29b)$$

where $x = (x_1, x_2)$. We assume that f_1 and f_2 are convex (not necessarily differentiable) functions. The problem dimensions are $x_1 \in \mathbb{R}^{n_1}$, $x_2 \in \mathbb{R}^{n_2}$, $A_1 \in \mathbb{R}^{m \times n_1}$, and $A_2 \in \mathbb{R}^{m \times n_2}$. Problem (4.29) is the special case of (4.1),

Algorithm 2 Dantzig-Wolfe Decomposition Algorithm for (4.23)

```

i = 0, converged = false
while not converged do
   $\tilde{\mathcal{I}} \leftarrow \{0, 1, \dots, i\}$ 
  COMPUTE PROBLEM DATA
  for  $j \in \mathcal{J}$  do
     $A_{l_j}^i = A_{l_j} x_j^i$ 
     $g_j^i = g_j^T x_j^i$ 
  end for
  SOLVE RESTRICTED MASTER PROBLEM
   $(\lambda^*, \alpha^*, \beta^*) \leftarrow \text{solve (4.27) with } \tilde{\mathcal{I}}_j = \tilde{\mathcal{I}} \text{ for } j \in \mathcal{J}$ 
  SOLVE SUBPROBLEMS
  for  $j \in \mathcal{J}$  do
     $(\varphi_j^*, \tilde{x}_j^*) \leftarrow \text{solve (4.28)}$ 
  end for
  CHECK IF CONVERGED
  if  $\varphi_j \geq \varepsilon$  for  $j \in \mathcal{J}$  then
    converged = true
  else
    UPDATE EXTREME POINTS
    for  $j \in \mathcal{J}$  do
       $x_j^{i+1} = \tilde{x}_j^*$ 
    end for
     $i \leftarrow i + 1$ 
  end if
end while

```

where $m_E = m$, $m_I = 0$, and

$$\begin{aligned}
 f(x) &= f_1(x_1) + f_2(x_2), \\
 g_i(x) &= a_{1,i}^T x_1 + a_{2,i}^T x_2 - b_i, \quad i = 1, 2, \dots, m.
 \end{aligned}$$

$a_{1,1}, \dots, a_{1,m} \in \mathbb{R}^n$, $a_{2,1}, \dots, a_{2,m} \in \mathbb{R}^n$, and $b_1, \dots, b_m \in \mathbb{R}$. Moreover

$$\begin{aligned}
 A_1 &= [a_{1,1} \quad a_{1,2} \quad \cdots \quad a_{1,m}]^T, \\
 A_2 &= [a_{2,1} \quad a_{2,2} \quad \cdots \quad a_{2,m}]^T, \\
 b &= [b_1 \quad b_2 \quad \cdots \quad b_m]^T.
 \end{aligned}$$

ADMM is a powerful algorithm for solving large-scale structured convex optimization problems in the form (4.29) [BPC⁺11]. In particular, ADMM gives rise to distributed algorithms for the OCPs that arise in EMPC of linear stochastic systems [SSE⁺14, SDM⁺14a].

The indicator function is often used to pose convex optimization problems in the form (4.29). The indicator function of a set \mathbb{A} is defined as

$$I_{\mathbb{A}}(x) = \begin{cases} 0 & \text{if } x \in \mathbb{A}, \\ \infty & \text{otherwise.} \end{cases} \quad (4.30)$$

The indicator function of a convex set is a non-differentiable convex function [BV04].

4.4.1 ADMM Recursions

The Lagrangian of the convex optimization problem (4.29) is

$$\mathcal{L}(x, y) = f_1(x_1) + f_2(x_2) + y^T(A_1x_1 + A_2x_2 - b),$$

where $y \in \mathbb{R}^m$ is the dual variable associated with the equality constraints (4.29b). Let ∂ denote the subdifferential operator [BL11]. A stationary point of the Lagrangian satisfies

$$0 \in \partial_{x_1} \mathcal{L}(x, y) = \partial_{x_1} f_1(x_1) + A_1^T y, \quad (4.31a)$$

$$0 \in \partial_{x_2} \mathcal{L}(x, y) = \partial_{x_2} f_2(x_2) + A_2^T y, \quad (4.31b)$$

The KKT conditions for (4.29) are the primal feasibility condition (4.29b), and the dual feasibility conditions (4.31).

The ADMM recursions for solution of (4.29) are

$$x_1^{i+1} = \underset{x_1}{\operatorname{argmin}} \mathcal{L}_\rho(x_1, x_2^i, y^i), \quad (4.32a)$$

$$x_2^{i+1} = \underset{x_2}{\operatorname{argmin}} \mathcal{L}_\rho(x_1^{i+1}, x_2, y^i), \quad (4.32b)$$

$$y^{i+1} = y^i + \rho(A_1x_1^{i+1} + A_2x_2^{i+1} - b). \quad (4.32c)$$

The augmented Lagrangian with penalty parameter $\rho > 0$ is defined as

$$\mathcal{L}_\rho(x, y) = \mathcal{L}(x, y) + \frac{\rho}{2} \|A_1x + A_2x - b\|_2^2.$$

The recursions (4.32) alternate between an x_1 -minimization, (4.32a), and an x_2 -minimization, (4.32b). Finally, (4.32c) is a dual variable update.

It is convenient to express the recursions (4.32) in a scaled form. The scaled

Algorithm 3 ADMM algorithm for the solution of (4.29)

```

converged = false
while not converged do
  ADMM RECURSIONS
   $x_1 \leftarrow \operatorname{argmin}_{x_1} f_1(x_1) + \rho/2 \|Ax_1 + A_2x_2 - b + u\|_2^2$ 
   $x_2 \leftarrow \operatorname{argmin}_{x_2} f_2(x_2) + \rho/2 \|Ax_1 + A_2x_2 - b + u\|_2^2$ 
   $u \leftarrow u + \rho(A_1x_1 + A_2x_2 - b)$ 
  CHECK IF CONVERGED
  if  $\|r\|_2 \leq \epsilon_P$  and  $\|s\|_2 \leq \epsilon_D$  then
    converged = true
  end if
end while

```

ADMM recursions are

$$x_1^{i+1} = \operatorname{argmin}_{x_1} f_1(x_1) + \rho/2 \|Ax_1 + A_2x_2^i - b + u^i\|_2^2, \quad (4.33a)$$

$$x_2^{i+1} = \operatorname{argmin}_{x_2} f_2(x_2) + \rho/2 \|Ax_1^{i+1} + A_2x_2 - b + u^i\|_2^2, \quad (4.33b)$$

$$u^{i+1} = u^i + \rho(A_1x_1^{i+1} + A_2x_2^{i+1} - b). \quad (4.33c)$$

where $u = (1/\rho)y$ is a scaled dual variable. Under mild assumptions, the ADMM recursions, (4.33), converge to a solution of (4.29). References [BV04, BPC⁺11, Roc70, BL00, HUL01] provide proofs and details.

Algorithm 3 outlines the ADMM algorithm. To detect an optimal solution in Algorithm 3, we use the stopping criteria [BPC⁺11]

$$\|r^i\|_2 \leq \epsilon_P^i, \quad (4.34a)$$

$$\|s^i\|_2 \leq \epsilon_D^i. \quad (4.34b)$$

$\epsilon_P^i > 0$ and $\epsilon_D^i > 0$ are primal and dual tolerance parameters. These parameters are defined as

$$\epsilon_P^i = \epsilon_A \sqrt{m} + \epsilon_R \max\{\|A_1x_1^i\|_2, \|A_2x_2^i\|_2, \|b\|_2\},$$

$$\epsilon_D^i = \epsilon_A \sqrt{n_1} + \epsilon_R \|A_1^T y^i\|_2,$$

where $\epsilon_A > 0$ and $\epsilon_R > 0$ are user-defined (absolute and relative) tolerance parameters. Moreover

$$r^{i+1} = A_1x_1^{i+1} + A_2x_2^{i+1} - b, \quad (4.35a)$$

$$s^{i+1} = \rho A_1^T A_2(x_2^{i+1} - x_2^i). \quad (4.35b)$$

Reference [HL13] establishes a linear convergence rate of ADMM. The empirical convergence rate of ADMM can be much faster, and is highly problem-dependent [KCLB14, WBAW12]. Several tuning strategies have been proposed to speed-up convergence of ADMM for individual problems. One extension of Algorithm 3 is to replace $A_1 x_1^{i+1}$ by $\alpha A_1 x_1^{i+1} - (1 - \alpha)(A_2 x_2^i - b)$ in the recursions (4.33). This strategy is known as over-relaxation [BPC⁺11]. The parameter $\alpha \in [0, 2]$ is tuned to the particular application. Another critical tuning parameter is the penalty parameter ρ [JGR⁺14, JGR⁺14, HL13, GTSJ13]. References [BPC⁺11, GTSJ13] provide adaptive updating strategies for ρ .

Part II

Summary Report: Main Contributions

Economic MPC in Power Production Planning

This chapter presents novel EMPC schemes for power production planning. Control of the portfolio system (2.9) is considered. A small demonstration example shows that CE-EMPC performs poorly under uncertainty in terms of economics. MV-EMPC is introduced to account for the system uncertainty in a more economically efficient manner. We employ regularization techniques to obtain well-behaved closed-loop control of the portfolio system.

5.1 Contributions

The OCP solved in EMPC consists of an economic objective function and a number of operating constraints. The performance and reliability of EMPC depend on the formulation of the OCP. Uncertainty management is important for EMPC of stochastic systems, such as the power portfolio system (2.9). In CE-EMPC, uncertain parameters in the OCP are replaced by conditional expectations. Paper F shows that CE-EMPC can be economically inefficient in practice. The main issue with CE-EMPC is that the approach disregards the variance of the uncertain parameters. Paper F introduces MV-EMPC for linear stochastic systems. In MV-EMPC, the OCP objective function is a bi-criterion

that trades off cost expectation and cost variance. Simulations show that MV-EMPC outperforms CE-EMPC economically. Paper G presents a novel ADMM-based decomposition algorithm for MV-EMPC, to overcome tractability issues of the EMPC scheme. Paper E illustrates that regularization is critical for the closed-loop performance of EMPC.

We have organized this chapter as follows. Section 5.2 describes common operating constraints for the portfolio of power generators, and section 5.3 defines an economic objective function for the system. Section 5.4 defines CE-EMPC for the portfolio system. A two-generator case study is presented for demonstration purposes. Section 5.5 generalizes CE-EMPC to MV-EMPC, and introduces a back-off heuristic to improve the economic performance of CE-EMPC. Section 5.6 discusses regularization techniques under uncertainty. Section 5.7 summarizes the main contributions of this chapter.

5.2 Portfolio Constraints

The portfolio system (2.9) is a collection of power generators in the form (2.5). Each generator is associated with a number of operating constraints. These operating constraints often have a linear representation [Hal14,Hov13,HPM⁺12,HBP⁺12,EMB09,HLEJ12,HPMJ12,Sta15]. We consider input constraints

$$\underline{u}_{g_j,k} \leq u_{g_j,k} \leq \bar{u}_{g_j,k}, \quad j \in \mathcal{M}, \quad (5.1)$$

and input-rate constraints

$$\Delta \underline{u}_{g_j,k} \leq \Delta u_{g_j,k} \leq \Delta \bar{u}_{g_j,k}, \quad j \in \mathcal{M}. \quad (5.2)$$

The input-rate, $\Delta u_{g_j,k}$, is defined as in (3.13). As an example, (5.1) and (5.2) represent charging and discharging limits for an electric vehicle. For a heat-pump in a residential heating system, (5.1) and (5.2) restrict the work of the compressor. In a commercial refrigeration system, (5.1) and (5.2) limit the evaporator heat duty. For the power plant model in [EMB09], (5.1) limits the power production setpoint to the feasible range of setpoints, and (5.2) limits the setpoint rate of change. Section 5.3 introduces soft output constraints for the portfolio system.

Using the definitions (2.8), we write the constraints (5.1) and (5.2), in the compact form

$$\underline{u}_{P,k} \leq u_{P,k} \leq \bar{u}_{P,k}, \quad (5.3a)$$

$$\Delta \underline{u}_{P,k} \leq \Delta u_{P,k} \leq \Delta \bar{u}_{P,k}, \quad (5.3b)$$

where

$$\underline{u}_{P,k} = \begin{bmatrix} \underline{u}_{g_1,k} \\ \underline{u}_{g_2,k} \\ \vdots \\ \underline{u}_{g_M,k} \end{bmatrix}, \quad \bar{u}_{P,k} = \begin{bmatrix} \bar{u}_{g_1,k} \\ \bar{u}_{g_2,k} \\ \vdots \\ \bar{u}_{g_M,k} \end{bmatrix}, \quad \Delta \underline{u}_{P,k} = \begin{bmatrix} \Delta \underline{u}_{g_1,k} \\ \Delta \underline{u}_{g_2,k} \\ \vdots \\ \Delta \underline{u}_{g_M,k} \end{bmatrix}, \quad \Delta \bar{u}_{P,k} = \begin{bmatrix} \Delta \bar{u}_{g_1,k} \\ \Delta \bar{u}_{g_2,k} \\ \vdots \\ \Delta \bar{u}_{g_M,k} \end{bmatrix}.$$

5.3 Portfolio Cost Function

Let $p_{g_j,k}$ denote the price of utilization for power generator j , and define

$$p_{P,k} = \begin{bmatrix} p_{g_1,k} \\ p_{g_2,k} \\ \vdots \\ p_{g_M,k} \end{bmatrix}.$$

The utilization cost for the portfolio system (2.9), over N time steps, is

$$\psi_u(u_P, z_P) = \sum_{j \in \mathcal{M}} \sum_{k \in \mathcal{N}_0} p_{g_j,k}^T u_{g_j,k} = \sum_{k \in \mathcal{N}_0} p_{P,k}^T u_{P,k}. \quad (5.4)$$

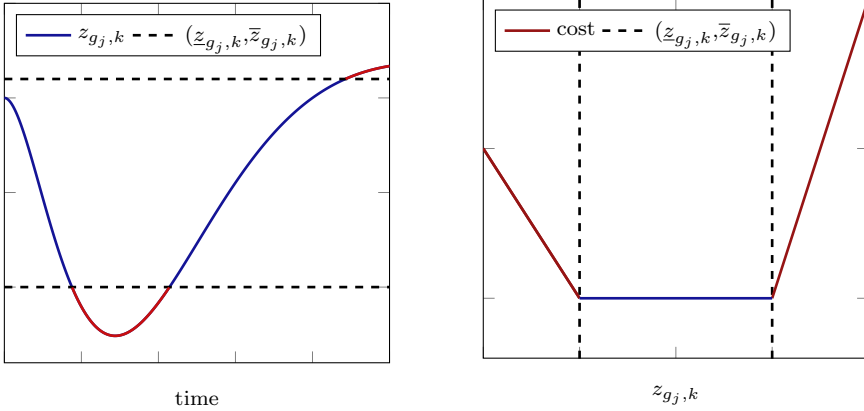
u_P and z_P are stacked vectors as in (3.7).

Let $(\underline{z}_{g_j,k}, \bar{z}_{g_j,k})$ be the desired operating range for the output of power generator j , and let $(\underline{z}_{T,k}, \bar{z}_{T,k})$ be the desired operating range for the portfolio power production. The desired operating range can be related to the state-of-charge of the battery in an electric vehicle, the room temperature in a residential heating system, the food temperature in a commercial refrigeration system, and the reference profile (electricity sold in the day-ahead electricity market) for the portfolio power production. The cost of operating the system outside its desired operating range, over N time steps, is

$$\begin{aligned} \psi_z(u_P, z_P) &= \sum_{k \in \mathcal{N}_1} \underline{q}_{T,k}^T \max(\underline{z}_{T,k} - z_{T,k}, 0) + \bar{q}_{T,k}^T \max(z_{T,k} - \bar{z}_{T,k}, 0) \\ &+ \sum_{j \in \mathcal{M}} \sum_{k \in \mathcal{N}_1} \underline{q}_{g_j,k}^T \max(\underline{z}_{g_j,k} - z_{g_j,k}, 0) + \bar{q}_{g_j,k}^T \max(z_{g_j,k} - \bar{z}_{g_j,k}, 0), \end{aligned} \quad (5.5)$$

or in a compact form

$$\psi_z(u_P, z_P) = \sum_{k \in \mathcal{N}_1} \underline{q}_{P,k}^T \max(\underline{z}_{P,k} - z_{P,k}, 0) + \bar{q}_{P,k}^T \max(z_{P,k} - \bar{z}_{P,k}, 0), \quad (5.6)$$



(a) A cost is imposed for operating the system outside its desired operating range. In this figure, cost intervals are indicated by red.

(b) The cost of operating the system outside its desired operating range is proportional to the distance from the operating range.

Figure 5.1: Illustration of the output related cost function (5.6).

in which we have defined

$$\underline{z}_{P,k} = \begin{bmatrix} \underline{z}_{g_1,k} \\ \underline{z}_{g_2,k} \\ \vdots \\ \underline{z}_{g_M,k} \\ \underline{z}_{T,k} \end{bmatrix}, \quad \bar{z}_{P,k} = \begin{bmatrix} \bar{z}_{g_1,k} \\ \bar{z}_{g_2,k} \\ \vdots \\ \bar{z}_{g_M,k} \\ \bar{z}_{T,k} \end{bmatrix}, \quad \underline{q}_{P,k} = \begin{bmatrix} \underline{q}_{g_1,k} \\ \underline{q}_{g_2,k} \\ \vdots \\ \underline{q}_{g_M,k} \\ \underline{q}_{T,k} \end{bmatrix}, \quad \bar{q}_{P,k} = \begin{bmatrix} \bar{q}_{g_1,k} \\ \bar{q}_{g_2,k} \\ \vdots \\ \bar{q}_{g_M,k} \\ \bar{q}_{T,k} \end{bmatrix}. \quad (5.7)$$

$\underline{q}_{P,k}$ and $\bar{q}_{P,k}$ contain prices for the individual generators, as well as for the portfolio power production. $\underline{q}_{T,k}$ and $\bar{q}_{T,k}$ can be the prices for balancing power. Using components such as batteries in electric vehicles, compressors in heat pumps, and evaporators in cold storage systems, outside their desired operating range, may be associated with a price for wear and tear of the components. These prices define $\underline{q}_{g_j,k}$ and $\bar{q}_{g_j,k}$ for the power generators. The maximum function in (5.6) is evaluated element-wise, such that for a vector $v \in \mathbb{R}^n$

$$\max(v, 0) = \begin{bmatrix} \max(v_1, 0) \\ \max(v_2, 0) \\ \vdots \\ \max(v_n, 0) \end{bmatrix}.$$

Fig. 5.1 illustrates the cost function (5.6) for a single power generator. The

EMPC objective function for the power portfolio system (2.9) is defined as

$$\psi(u_P, z_P) = \psi_u(u_P, z_P) + \psi_z(u_P, z_P), \quad (5.8)$$

where ψ_u and ψ_z are defined as in (5.4) and (5.6), respectively.

5.4 Certainty-Equivalent Economic MPC

This section introduces CE-EMPC for the portfolio system (2.9). We assume that the process noise, $w_{P,k}$, and the measurement noise, $v_{P,k}$, are independent and identically distributed random variables with

$$w_{P,k} \sim N(0, R_{P,w}), \quad (5.9a)$$

$$v_{P,k} \sim N(0, R_{P,v}). \quad (5.9b)$$

To keep the notation simple, we let $k = 0$ denote the current time step and write $\hat{x}_k = \hat{x}_{k|0}$ for conditional expectations. Introduce the auxiliary variables

$$\rho_{P,k}^d = \begin{bmatrix} \rho_{g_1,k}^d \\ \rho_{g_2,k}^d \\ \vdots \\ \rho_{g_M,k}^d \\ \rho_{T,k}^d \end{bmatrix}, \quad \rho_{P,k}^u = \begin{bmatrix} \rho_{g_1,k}^u \\ \rho_{g_2,k}^u \\ \vdots \\ \rho_{g_M,k}^u \\ \rho_{T,k}^u \end{bmatrix}.$$

The OCP solved in CE-EMPC of the portfolio system (2.9) is the LP

$$\min_{u_P, \hat{x}_P, \hat{z}_P, \rho_P^d, \rho_P^u} \sum_{k \in \mathcal{N}_0} p_{P,k}^T u_{P,k} + \sum_{k \in \mathcal{N}_1} q_{P,k}^T \rho_{P,k}^d + \bar{q}_{P,k}^T \rho_{P,k}^u, \quad (5.10a)$$

$$\text{s.t. } \hat{x}_{P,k+1} = A_P \hat{x}_{P,k} + B_P u_{P,k} + E_P d_{P,k}, \quad k \in \mathcal{N}_0, \quad (5.10b)$$

$$\hat{z}_{P,k} = C_{P,z} \hat{x}_{P,k}, \quad k \in \mathcal{N}_1, \quad (5.10c)$$

$$\underline{u}_{P,k} \leq u_{P,k} \leq \bar{u}_{P,k}, \quad k \in \mathcal{N}_0, \quad (5.10d)$$

$$\Delta \underline{u}_{P,k} \leq \Delta u_{P,k} \leq \Delta \bar{u}_{P,k}, \quad k \in \mathcal{N}_0, \quad (5.10e)$$

$$\underline{z}_{P,k} - \rho_{P,k}^d \leq \hat{z}_{P,k} \leq \bar{z}_{P,k} + \rho_{P,k}^u, \quad k \in \mathcal{N}_1, \quad (5.10f)$$

$$\rho_{P,k}^d \geq 0, \quad k \in \mathcal{N}_1, \quad (5.10g)$$

$$\rho_{P,k}^u \geq 0, \quad k \in \mathcal{N}_1. \quad (5.10h)$$

The optimization variables in (5.10) are

$$u_P = \begin{bmatrix} u_{P,0} \\ u_{P,1} \\ \vdots \\ u_{P,N-1} \end{bmatrix}, \quad \hat{x}_P = \begin{bmatrix} \hat{x}_{P,1} \\ \hat{x}_{P,2} \\ \vdots \\ \hat{x}_{P,N} \end{bmatrix}, \quad \hat{z}_P = \begin{bmatrix} \hat{z}_{P,1} \\ \hat{z}_{P,2} \\ \vdots \\ \hat{z}_{P,N} \end{bmatrix},$$

and

$$\rho_P^d = \begin{bmatrix} \rho_{P,1}^d \\ \rho_{P,2}^d \\ \vdots \\ \rho_{P,N}^d \end{bmatrix}, \quad \rho_P^u = \begin{bmatrix} \rho_{P,1}^u \\ \rho_{P,2}^u \\ \vdots \\ \rho_{P,N}^u \end{bmatrix}.$$

Constraints (5.10a) and (5.10c) are the state-space constraints. These constraints are governed by the Kalman filter equations, defined in Section 3.2. Constraints (5.10d) and (5.10e) follow from (5.3). Constraints (5.10f), (5.10g), and (5.10h), are a model of (5.6), based on soft output constraints [PJ09, KM00, Ken75, MRRS00, ZJM10]. Let $(u_P^*, \hat{x}_P^*, \hat{z}_P^*, \rho_P^{d*}, \rho_P^{u*})$ denote an optimal solution of (5.10). The auxiliary variables ρ_P^{d*} and ρ_P^{u*} clearly satisfy

$$\begin{aligned} \rho_{P,k}^{d*} &= \max(\underline{z}_{P,k} - \hat{z}_{P,k}^*, 0), & k \in \mathcal{N}_1, \\ \rho_{P,k}^{u*} &= \max(\hat{z}_{P,k}^* - \bar{z}_{P,k}, 0), & k \in \mathcal{N}_1, \end{aligned}$$

This shows that (5.10a) provides a linear model of (5.8) for the OCP (5.10).

5.4.1 Two-Generator Case Study

A power portfolio CE-EMPC case study is considered. The case study portfolio consists of two generators; a cheap/slow generator (Generator 1), and an expensive/fast generator (Generator 2). It is common that small agile generators have a high price of utilization, while larger less flexibly generators have a low price of utilization [EIA14]. We model the case study generators as third-order systems in the form (2.2). The resulting portfolio system, (2.9), is discretized using a sampling time of $T_s = 5$ s. The OCP (5.10) is solved in a receding horizon manner. The controller objective is to coordinate the most cost-efficient power production, given a time-varying reference for the total power production. The reference is required to be satisfied with a ± 0.5 MW margin. The cost of not satisfying the demand (with this margin) is 360EUR/MWh in both the up and the down direction. The scenario length is 30 minutes, which corresponds to 360 time steps. Full information about the initial state is given, $x_{P,0} = 0$, and

$$w_{P,k} \sim N(0, \sigma B B^T), \quad (5.11a)$$

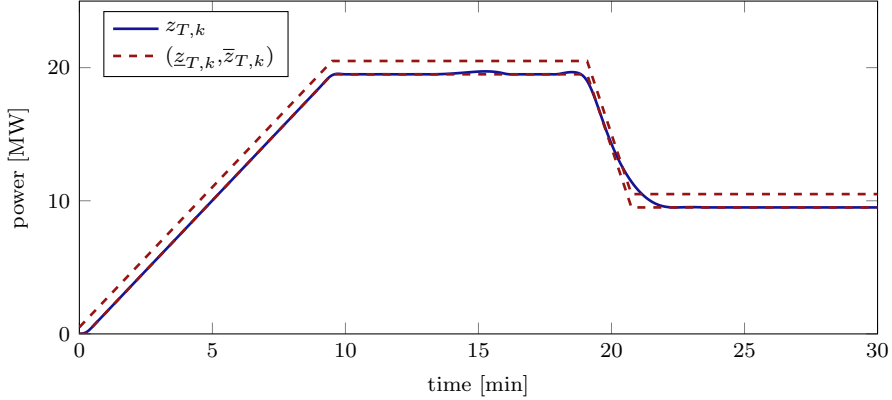
$$v_{P,k} \sim N(0, \sigma I). \quad (5.11b)$$

The prediction horizon is $N = 60$ time steps. Table 5.1 lists the case study parameters. The parameters are constant over the entire prediction and control horizon.

Fig. 5.2 and Fig. 5.3 show a closed-loop simulation with $\sigma = 0$. The cheap

Table 5.1: Case study parameters.

	τ_i	$p_{g_i,k}$	$\underline{u}_{g_i,k}$	$\bar{u}_{g_i,k}$	$\Delta\underline{u}_{g_i,k}$	$\Delta\bar{u}_{g_i,k}$
Generator 1	20	0.25	0	5	-1	1
Generator 2	50	0.125	0	20	-0.2	0.2

**Figure 5.2:** Closed-loop simulation with $\sigma = 0$: Portfolio power production and power production reference with a ± 0.5 MW margin.

generator produces the majority of the energy. The expensive generator is activated to keep the total power production within the desired operating range. Around $t = 20$ min a situation with surplus power occurs. The cost for this is EUR 8. The total operating cost is EUR 679. Fig. 5.4 and Fig. 5.5 show a closed-loop simulation with $\sigma = 1$. In this simulation, the total power production is outside the desired operating range a significant part of the time. The cost for this is EUR 36, which is an increase of a factor 4.5 in imbalance costs, compared to the noise-free simulation. Over the course of longer time horizons, the power imbalances increase the overall operating cost significantly.

CE-EMPC operates the system as close as possible to its constraints. This works well in a noise-free setting. In the presence of uncertainty, random perturbations drive the system to a state outside its desired operating range. For power production planning applications, this can cause e.g. faults in generator components, overflow of hydro storage reservoirs, decay of food products in refrigeration systems, as well as blackouts in small isolated power systems [SEJ15]. For the two-generator case study, CE-EMPC leads to expensive power imbalances that can potentially be avoided. Also observe that the power production setpoint levels behave irregularly when $\sigma = 1$. In particular, the setpoint levels for Generator 1 fluctuate at a high rate. Such an aggressive control of a

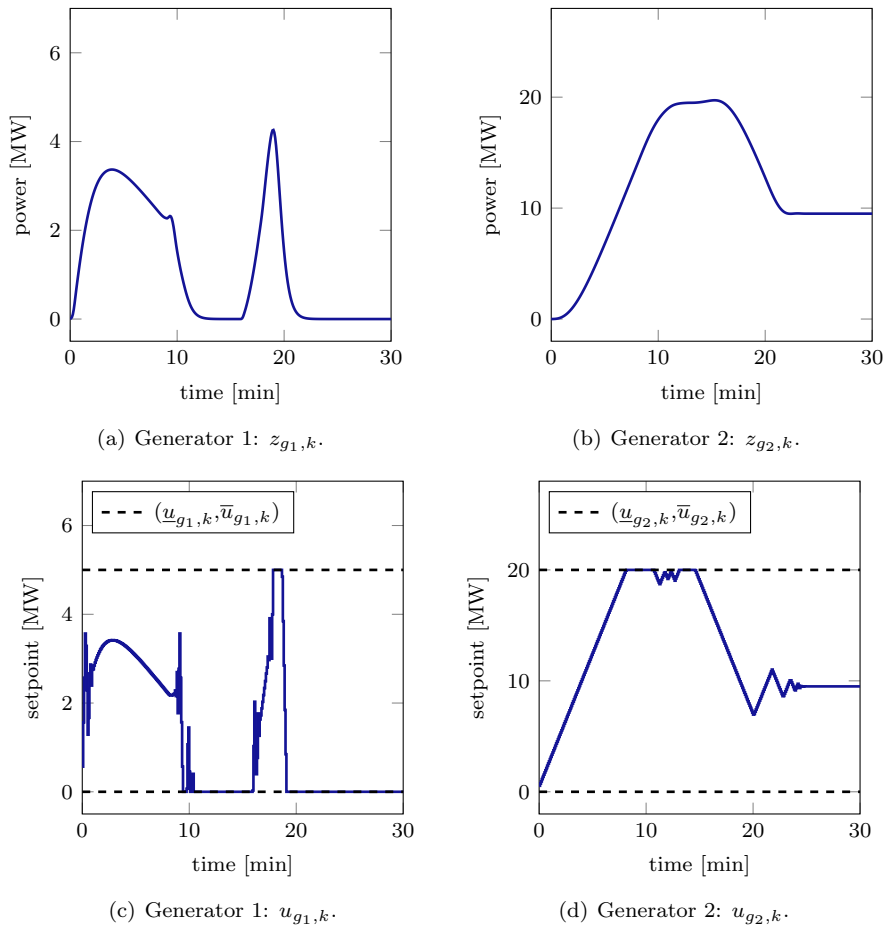


Figure 5.3: Closed-loop simulation with $\sigma = 0$: Generator power production and setpoint levels.

generator is unfit for practical use due to e.g. wear and tear of the generator components and model uncertainties [PJ09].

5.5 Mean-Variance Economic MPC

This section provides an overview of MV-EMPC for linear stochastic systems. For proof and details, we refer to Paper F and Paper G. Reference [CSFJ15]

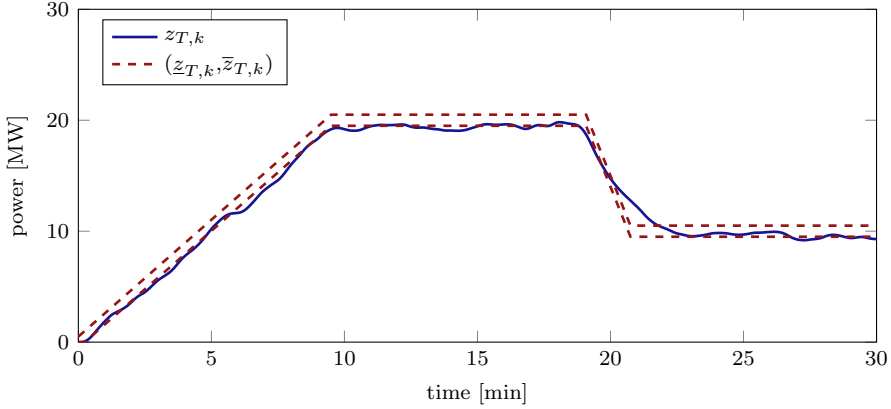


Figure 5.4: Closed-loop simulation with $\sigma = 1$: Portfolio power production and power production reference with a ± 0.5 MW margin.

describes MV-EMPC for non-linear systems with uncertain model parameters.

Consider the evolution of the linear stochastic system (3.1) (this includes the portfolio system (2.9)) over the horizon \mathcal{N}_0 . For simplicity, assume that $d_k = 0$, for $k \in \mathcal{N}_0$. Similar to (3.18), we can write the state and output variables as affine functions of the input sequence $\{u_k\}_{k \in \mathcal{N}_0}$, the current state \mathbf{x}_k , and the process noise sequence $\{\mathbf{w}_k\}_{k \in \mathcal{N}_0}$. This means that

$$\begin{aligned}\mathbf{x} &= L_x(u; \mathbf{x}_k, \mathbf{w}), \\ \mathbf{z} &= L_z(u; \mathbf{x}_k, \mathbf{w}),\end{aligned}$$

where L_x and L_z are affine functions, and $\mathbf{x} \in \mathbb{R}^{Nn_x}$, $\mathbf{z} \in \mathbb{R}^{Nn_z}$, $u \in \mathbb{R}^{Nn_u}$, and $\mathbf{w} \in \mathbb{R}^{Nn_w}$, are stacked vectors as in (3.7).

Define the function

$$\varphi(u; \mathbf{x}_k, \mathbf{w}) = \phi(u, L_x(u; \mathbf{x}_k, \mathbf{w}), L_z(u; \mathbf{x}_k, \mathbf{w})),$$

where ϕ is the EMPC cost function, e.g. (3.14). The OCP solved in CE-EMPC can be stated as

$$\min_{u \in \mathcal{U}} \Psi_{CE} = \varphi(u; E[\mathbf{x}_k], E[\mathbf{w}]).$$

\mathcal{U} is an input constraint set derived from (3.8d). Fig. 5.6 shows a histogram of $\varphi(u_P^*; x_{P,0|0}, w_P)$ for the two-generator case study, based on 10000 realizations of the process noise \mathbf{w}_P . The vector u_P^* is the open-loop input trajectory obtained by solving (5.10), and $x_{P,0|0}$ is the known initial state. The operating cost

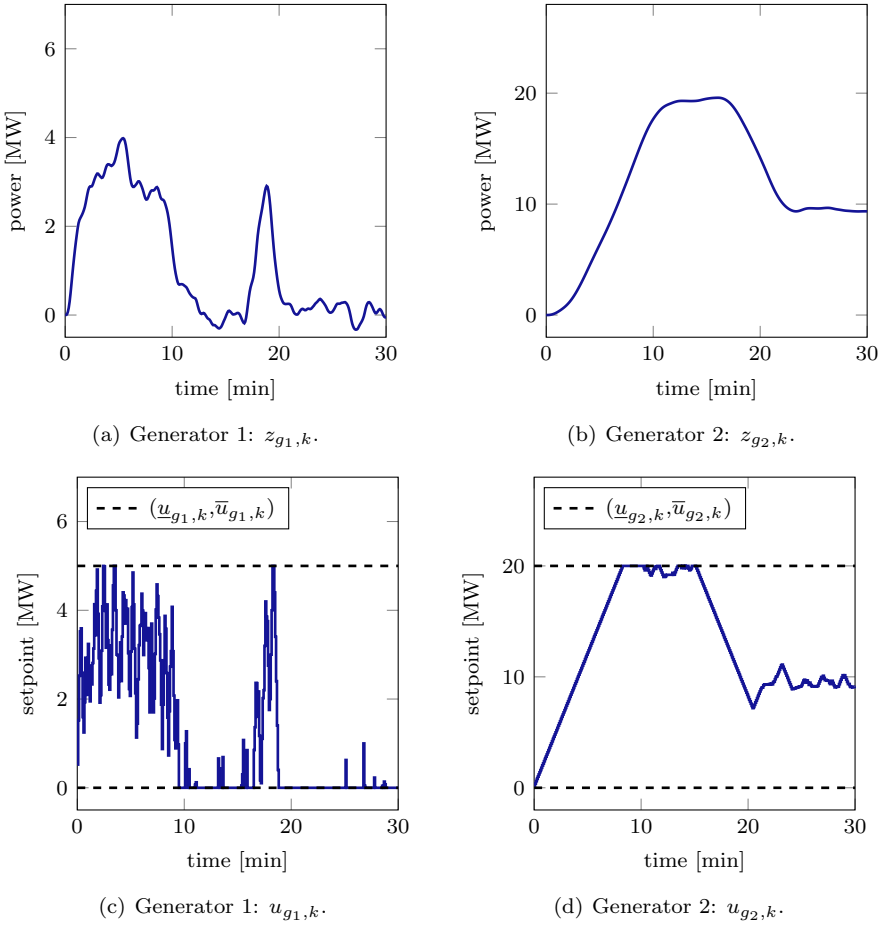


Figure 5.5: Closed-loop simulation with $\sigma = 1$: Generator power production and setpoint levels.

resulting from the case $w_P = E[\mathbf{w}_P] = 0$ is indicated in Fig. 5.6. For almost all the considered realizations of the process noise, the operating cost is larger than for this case. The average cost over the 10000 simulations is EUR 695. Thus, while CE-EMPC performs well when the uncertain parameters are equal to their expected values, it does not perform well on average. The fundamental issue with CE-EMPC is that

$$\varphi(u^*; E[\mathbf{x}_k], E[\mathbf{w}]) \neq E[\varphi(u^*; \mathbf{x}_k, \mathbf{w})].$$

I.e. minimizing over $\varphi(u; E[\mathbf{x}_k], E[\mathbf{w}])$, as in CE-EMPC, does not necessarily minimize the expected cost. The two-generator case study is an example where

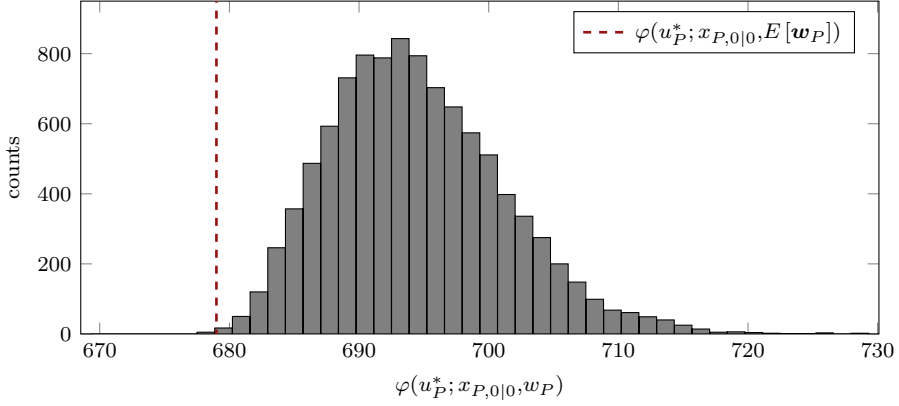


Figure 5.6: Operating costs for 10000 realizations of the process noise \mathbf{w}_P .

this situation clearly occurs. The OCP solved in MV-EMPC is defined as

$$\min_{u \in \mathcal{U}} \Psi_{MV} = \alpha E[\varphi(u; \mathbf{x}_k, \mathbf{w})] + (1 - \alpha)V[\varphi(u; \mathbf{x}_k, \mathbf{w})]. \quad (5.12)$$

The OCP (5.12) trades off cost expectation and cost variance. α is a user-defined risk-aversion parameter. The formulation (5.12) can be interpreted as a classical Markowitz mean-variance optimization approach [Ste01, Mar52]. This approach is convenient for EMPC, as it includes a risk measure in the objective function. Moreover, in contrast to CE-EMPC, it considers the actual cost expectation, $E[\varphi(u; \mathbf{x}_k, \mathbf{w})]$, rather than $\varphi(u; E[\mathbf{x}_k], E[\mathbf{w}])$.

Closed-form expressions for the expected value $E[\varphi(u; \mathbf{x}_k, \mathbf{w})]$ and the variance $V[\varphi(u; \mathbf{x}_k, \mathbf{w})]$ are generally not available. This is addressed by introducing the sample estimates

$$E[\varphi(u; \mathbf{x}_k, \mathbf{w})] \approx \mu = \frac{1}{S} \sum_{s \in \mathcal{S}} \varphi(u; \mathbf{x}_k, w^s), \quad (5.13a)$$

$$V[\varphi(u; \mathbf{x}_k, \mathbf{w})] \approx s^2 = \frac{1}{S-1} \sum_{s \in \mathcal{S}} (\varphi(u; \mathbf{x}_k, w^s) - \mu)^2, \quad (5.13b)$$

where $\{w^s\}_{s \in \mathcal{S}}$ is a set of S samples from the distribution of \mathbf{w} , and $\mathcal{S} = \{1, 2, \dots, S\}$. To keep the notation simple, (5.13) assumes that the current state $\mathbf{x}_k = x_k$ is a known parameter. If \mathbf{x}_k is a random variable, scenarios can be introduced for this variable accordingly. Monte Carlo-based approximations such as (5.13) have been considered for conventional MPC with probabilistic constraints in [CF13a, CF13b, MB12b, PGL12, SCFM12, SFFM14, ZSSM13].

For a sufficiently large number of scenarios, S

$$\Psi_{MV} \approx \alpha\mu + (1 - \alpha)s^2. \quad (5.14)$$

Paper F defines the OCP solved in MV-EMPC of linear stochastic systems as

$$\min_{u \in \mathcal{U}, \{x^s, z^s, \varphi^s\}_{s \in \mathcal{S}}, \mu} \alpha\mu + \tilde{\alpha} \sum_{s \in \mathcal{S}} (\varphi^s - \mu)^2, \quad (5.15a)$$

$$\text{s.t. } x_{k+1}^s = Ax_k^s + Bu_k + w_k^s, \quad k \in \mathcal{N}_0, \quad s \in \mathcal{S}, \quad (5.15b)$$

$$z_k^s = Cz_k^s, \quad k \in \mathcal{N}_1, \quad s \in \mathcal{S}, \quad (5.15c)$$

$$\varphi^s = \phi(u, x^s, z^s), \quad s \in \mathcal{S}, \quad (5.15d)$$

$$\mu = \frac{1}{S} \sum_{s \in \mathcal{S}} \varphi^s. \quad (5.15e)$$

$\tilde{\alpha} = (1 - \alpha)/(S - 1)$. The optimization variables in (5.15) are the input vector $u \in \mathbb{R}^{Nn_u}$, the state vectors $x^1, x^2, \dots, x^S \in \mathbb{R}^{Nn_x}$, the output vectors $z^1, z^2, \dots, z^S \in \mathbb{R}^{Nn_z}$, the costs $\varphi^1, \varphi^2, \dots, \varphi^S \in \mathbb{R}$, and the average cost $\mu \in \mathbb{R}$. The objective function (5.15a) is the mean-variance approximation (5.14). Constraint (5.15d) assigns the cost associated with scenario s to the variable φ^s . The OCP solved in CE-EMPC (3.8) corresponds to the special case where $S = 1$ and $w_k^1 = E[w_k]$, for $k \in \mathcal{N}_0$.

As a performance indicator for a given input-sequence, $u^* \in \mathbb{R}^{Nn_u}$, we define

$$\bar{\Psi}_{MV} = \alpha\bar{\mu} + (1 - \alpha)\bar{s}^2. \quad (5.16)$$

where

$$\bar{\mu} = \frac{1}{S} \sum_{s \in \mathcal{S}} \varphi(u^*; x_k, \tilde{w}^s), \quad (5.17a)$$

$$\bar{s}^2 = \frac{1}{S - 1} \sum_{s \in \mathcal{S}} (\varphi(u^*; x_k, \tilde{w}^s) - \bar{\mu})^2, \quad (5.17b)$$

Expressions (5.14) and (5.16) differ in the set of uncertainty scenarios. We use $\{w^s\}_{s \in \mathcal{S}}$ for optimization, and $\{\tilde{w}^s\}_{s \in \mathcal{S}}$ for performance evaluation. Paper F demonstrates MV-EMPC using a case study, which is similar to the two-generator case study. Fig. 5.7 shows a plot of the average cost, $\bar{\mu}$, as a function of the standard deviation, \bar{s} , for this case study. In an open-loop setting, MV-EMPC reduces both cost expectation and cost variance compared to CE-EMPC. Each value of α provides a different mean-variance trade-off option. The OCP (5.15) assumes that no recourse exists in the future. Therefore, MV-EMPC may be overly conservative when applied in a receding horizon manner [SFFM14,

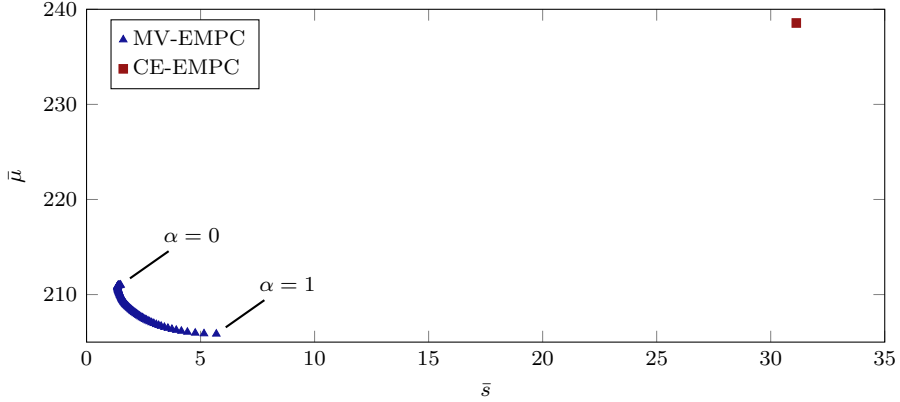


Figure 5.7: Open-loop efficient frontier for $\alpha = [0; 1]$. Points on the efficient frontier are computed by solving (5.15) with $S = 2048$ realizations of the process noise vector, \mathbf{w} .

[LSE13]. To account for future recourse, Paper F introduces an extended two-stage OCP for MV-EMPC. The two-stage OCP is

$$\min_{\{u^s \in \mathcal{U}, x^s, z^s, \varphi^s\}_{s \in \mathcal{S}}, \mu} \alpha \mu + \tilde{\alpha} \sum_{s \in \mathcal{S}} (\varphi^s - \mu)^2, \quad (5.18a)$$

$$\text{s.t. } x_{k+1}^s = Ax_k^s + Bu_k^s + w_k^s, \quad k \in \mathcal{N}_0, \quad s \in \mathcal{S}, \quad (5.18b)$$

$$z_k^s = C_z x_k^s, \quad k \in \mathcal{N}_1, \quad s \in \mathcal{S}, \quad (5.18c)$$

$$\varphi^s = \phi(u^s, x^s, z^s), \quad s \in \mathcal{S}, \quad (5.18d)$$

$$\mu = \frac{1}{S} \sum_{s \in \mathcal{S}} \varphi^s, \quad (5.18e)$$

$$u_k^{s_1} = u_k^{s_2}, \quad s_1, s_2 \in \mathcal{S}, \quad k \in \mathcal{Q}. \quad (5.18f)$$

In this formulation, the input variables are scenario-dependent. Constraint (5.18f) is a non-anticipativity constraint stating that the input variables should be equal over all the scenarios for time steps $k \in \mathcal{Q} = \{0, 1, \dots, q\}$ [LSE13]. q is a user-defined parameter. The single-stage OCP (5.15) is the special case of (5.18) where $q = N$. Paper F shows that two-stage MV-EMPC is economically more efficient than both single-stage MV-EMPC and CE-EMPC.

5.5.1 Constraint Back-Off Heuristic

Fig. 5.8 illustrates the typical behavior of MV-EMPC and CE-EMPC for 100 output realizations. The realization associated with the case $w_k = E[w_k]$,

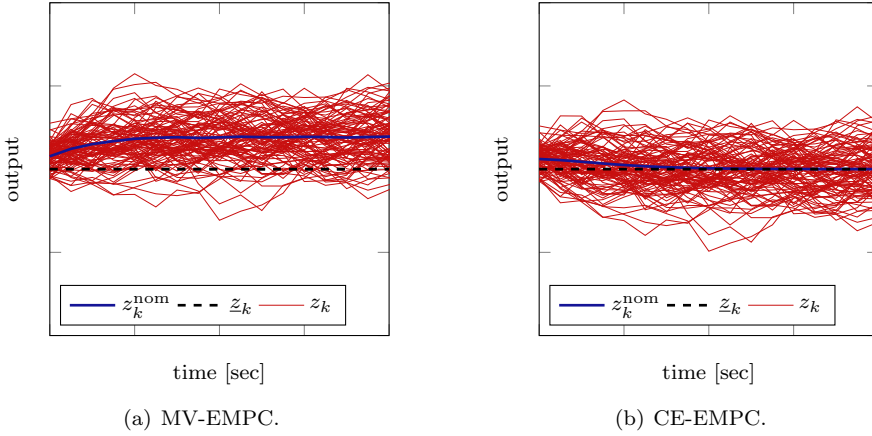


Figure 5.8: EMPC constraint management.

is denoted z_k^{nom} . CE-EMPC operates the system as close as possible to its constraints. This is inefficient for control of stochastic systems, as a significant part of the output realizations end up below the minimum desired output level. In MV-EMPC, the system is operated with a safety margin from the minimum desired output level. The safety margin is an integral part the OCP solved MV-EMPC. A way to achieve similar behavior for CE-EMPC is to use constraint back-off [VB02, ASS08]. E.g. for the power portfolio system, we can redefine the desired output levels, such that

$$\underline{z}_{P,k} := \underline{z}_{P,k} - \underline{\eta}_k, \quad k \in \mathcal{N}_1, \quad (5.19a)$$

$$\bar{z}_{P,k} := \bar{z}_{P,k} + \bar{\eta}_k, \quad k \in \mathcal{N}_1, \quad (5.19b)$$

where $\underline{\eta}_k$ and $\bar{\eta}_k$ are vectors of back-off parameters. The main advantage of using CE-EMPC over MV-EMPC is that the OCP solved in CE-EMPC is much smaller than the OCP solved in MV-EMPC. Paper F provides an example where back-off modified CE-EMPC performs as well as MV-EMPC in terms of economics. For large systems, back-off modified CE-EMPC involves a large number of back-off parameters. Tuning the back-off parameters can be challenging, especially when the process noise follows a non-Gaussian distribution. Also, when back-off is introduced in an EMPC setting, the OCP objective function is no longer directly related to the system operating cost. Consequently, there is no way to guarantee the economic performance of back-off modified CE-EMPC. In MV-EMPC, the only tuning parameter is the risk-aversion parameter, α , which trades off cost expectation and cost variance. MV-EMPC handles the case with non-Gaussian process noise in a straightforward way.

5.6 Regularization

The objective function (5.8) is a pure economic objective function. Regularization terms can be added to the objective function to change the behavior of the controlled system, e.g. to reduce the variability of the setpoint levels in Fig. 5.5. Paper E investigates the use of a weighted ℓ_1 -regularization term for this purpose. An advantage of using ℓ_1 -regularization in the OCP (5.10), is that the resulting optimization problem remains an LP. Paper E and Paper K show that OCPs in this problem class can be solved efficiently.

This section demonstrates that ℓ_1 -regularization improves the behavior of the closed-loop input trajectories for the two-generator case study. We define ℓ_1 -regularization for the two-generator case study as

$$\phi_{\ell_1}^{\text{reg}}(u_P, x_P, z_P) = \sum_{k \in \mathcal{N}_0} \|R\Delta u_{P,k}\|_1, \quad (5.20)$$

where $R = rI$. In some cases, regularization has an economic interpretation. For example, setpoint changes are related to wear-and-tear of a power generator. The ℓ_1 -regularization term (5.20) can be interpreted as a linear cost for setpoint changes. It is convenient to have an economic interpretation of the regularization terms, since the introduction of tuning parameters in the OCP objective function, conflicts with the fundamental idea of EMPC. Fig. 5.9 and Fig. 5.10 show closed-loop simulations for different values of the noise parameter, σ , and the regularization weight, r . The effect of the regularization is most clearly observed in the generator setpoint levels (system inputs). At the expense of slightly less tight control on the total power production, the setpoint levels become less volatile when the regularization weight, r , is increased. Note that less tight control on the total power production does not necessarily lead to more violations of the soft output constraints.

5.7 Summary

This chapter addressed two main challenges of EMPC for linear stochastic systems. We introduced MV-EMPC to handle the system uncertainty in an economically efficient manner, and regularization techniques were employed to achieve well-behaved closed-loop control. The EMPC schemes were tested using a two-generator case study. Simulations show that MV-EMPC outperforms CE-MPC in terms of economics. By varying the risk-aversion parameter, α , MV-EMPC provides different mean-variance trade-off specifications for the system operating cost. To avoid conservative closed-loop control, a two-stage extension

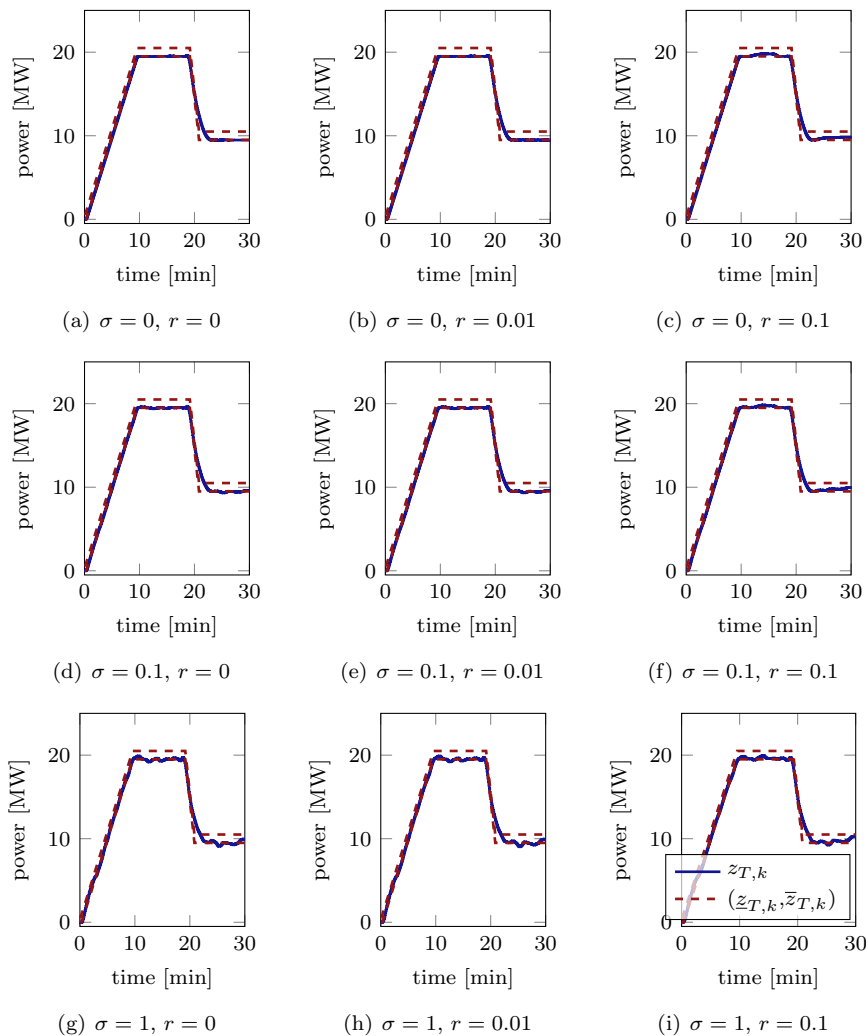


Figure 5.9: Total power production. Slightly less tight control on the total power production is observed when the regularization parameter, r , is increased.

of MV-EMPC was presented. We introduced a back-off heuristic to improve the economic performance of CE-EMPC. Back-off modified CE-EMPC can perform as well as MV-EMPC. On the other hand, back-off modified CE-EMPC does not guarantee the economic performance of the system in the same way as MV-EMPC, and it can be difficult to tune. We also illustrated that ℓ_1 -regularization

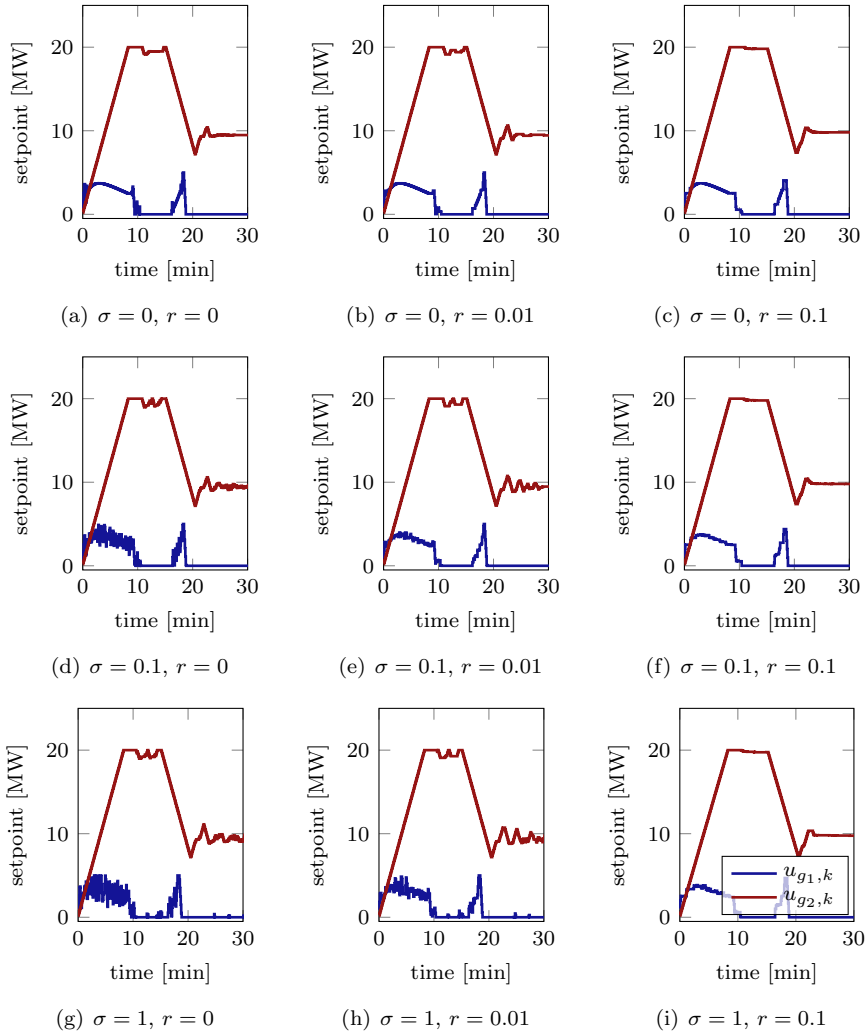


Figure 5.10: Power generator setpoint levels. Increasing the regularization parameter, r , reduces the variance of the setpoint levels.

reduces the input variance significantly for the two-generator case study, without a significant increase in the overall cost function. Ideally, the regularization terms have an economic interpretation, such that the economic interpretation of the OCP objective function in EMPC is preserved.

Algorithms for Economic MPC

Computationally tractable EMPC schemes require efficient algorithms for solution of the OCPs. The contributions of this chapter are special-purpose algorithms for EMPC in power production planning. The algorithms exploit the high degree of structure in the OCPs to reduce computational time and memory requirements. We provide benchmarks that compare the proposed algorithms to current state-of-the-art solvers.

6.1 Contributions

Paper [A](#), Paper [C](#) and Paper [K](#) develop a homogeneous and self-dual IPM for EMPC of linear systems with linear constraints and linear objective functions. The IPM is combined with a tailored Riccati iteration procedure to exploit the problem structure. In addition, the warm-start procedure of [\[SAY13\]](#) is employed to reduce the number of IPM iterations. The Riccati-based IPM scales linearly in the length of the prediction horizon, N . This is convenient, as stability of EMPC schemes often may be achieved for a sufficiently large N . Paper [B](#) and Paper [E](#) provide a Dantzig-Wolfe decomposition algorithm and an ADMM-based decomposition algorithm for EMPC of dynamically decoupled

subsystems. The subsystem decomposition algorithms are well-suited for EMPC of the portfolio system (2.9), as they scale linearly in the number of power generators, M . Paper G presents a scenario decomposition algorithm for MV-EMPC that scales linearly in the number of uncertainty scenarios, S . The algorithm solves a convex relaxation of the OCP that arises in MV-EMPC using ADMM. An algorithm for MV-EMPC that scales well in S is critical for the tractability of this EMPC scheme. Subproblems that occur in the proposed decomposition algorithms can be solved efficiently using the Riccati-based IPM of Paper K and the ADMM-based algorithm of Paper D.

We have organized this chapter as follows. Section 6.2 presents the Riccati-based homogeneous and self-dual IPM for EMPC of linear systems with linear constraints and linear objective functions. The subsystem decomposition algorithms for EMPC of dynamically decoupled subsystems are outlined in Section 6.3, and Section 6.4 describes the scenario decomposition algorithm for MV-EMPC. Section 6.5 provides a summary of this chapter.

6.2 Riccati-Based Linear Programming IPM

The OCP that arises in EMPC of linear systems with linear constraints and linear objective functions can be posed as an LP. A fairly general OCP within this problem class is (5.10). Paper K develops a tailored homogeneous and self-dual IPM for (5.10). This section provides a brief overview of the algorithm.

Algorithm 1 is a general-purpose homogeneous and self-dual IPM for solution of the LP (4.4). To avoid conflicting notation, we write the LP as

$$\min_t g^T t, \quad (6.1a)$$

$$\text{s.t. } Ft = b, \quad (6.1b)$$

$$Ht \leq c \quad (6.1c)$$

The most time-consuming numerical operations in Algorithm 1 are solving the two linear systems of equations

$$J_V(\theta)\Delta\theta_{\text{aff}} = -V(\theta), \quad (6.2a)$$

$$J_V(\theta)\Delta\theta = -\bar{V}(\theta). \quad (6.2b)$$

The systems (6.2a) and (6.2b) determine the optimization search direction for the IPM. Both systems can be written in the form

$$J_V(\theta)\Delta\theta = r, \quad (6.3)$$

where r is an arbitrary right-hand side.

Using the definitions (4.9) and (4.15), we write (6.3) as

$$F^T \Delta \tilde{v} + H^T \Delta \tilde{w} + g\tau = r_1, \quad (6.4a)$$

$$b\Delta\tau - F\Delta\tilde{t} = r_2, \quad (6.4b)$$

$$c\Delta\tau - H\Delta\tilde{t} - \Delta\tilde{s} = r_3, \quad (6.4c)$$

$$g^T \Delta\tilde{t} + b^T \Delta\tilde{v} + c^T \Delta\tilde{w} - \Delta\kappa = r_4, \quad (6.4d)$$

$$\tilde{W}^i \Delta\tilde{s} + \tilde{S}^i \Delta\tilde{w} = r_5, \quad (6.4e)$$

$$\kappa^i \Delta\tau + \tau^i \Delta\kappa = r_6. \quad (6.4f)$$

r_1, r_2, r_3, r_4, r_5 , and r_6 are arbitrary right-hand sides.

Paper K shows that the solution of (6.4) can be obtained by solving the system

$$\begin{bmatrix} 0 & F^T & H^T \\ -F & 0 & 0 \\ -H & 0 & (\tilde{W}^i)^{-1} \tilde{S}^i \end{bmatrix} \begin{bmatrix} f_1 & h_1 \\ f_2 & h_2 \\ f_3 & h_3 \end{bmatrix} = \begin{bmatrix} r_1 & -g \\ r_2 & -b \\ r_3 & -c \end{bmatrix}, \quad (6.5)$$

and subsequent computation of

$$\begin{aligned} \Delta\tau &= \frac{r_6 - \tau^i (g^T f_1 + b^T f_2 + c^T f_3)}{\kappa^i + \tau^i (g^T h_1 + b^T h_2 + c^T h_3)}, \\ \Delta\tilde{t} &= f_1 + h_1 \Delta\tau, \\ \Delta\tilde{v} &= f_2 + h_2 \Delta\tau, \\ \Delta\tilde{w} &= f_3 + h_3 \Delta\tau, \\ \Delta\kappa &= g^T \Delta\tilde{t} + b^T \Delta\tilde{v} + c^T \Delta\tilde{w} - r_4, \\ \Delta\tilde{s} &= (\tilde{W}^i)^{-1} (r_5 - \tilde{S}^i \Delta\tilde{w}), \end{aligned}$$

where $r_3 := r_3 + (\tilde{W}^i)^{-1} r_5$ and $r_6 := r_6 + \tau^i r_4$.

Paper K expresses the OCP (5.10) as an LP in the form (6.1). In this formulation, F and H are highly structured matrices. Consequently, the system (6.5) becomes highly structured as well. Paper K solves the system (6.5) using a Riccati iteration procedure, which is specifically tailored to the OCP (5.10). The Riccati iteration procedure consists of two parts. The first part is a variable elimination procedure that reduces (6.5) into a standard system. The second part of the procedure solves the standard system using a discrete Riccati recursion [AM12, RWR98, DFH09, Jøø05, WB10, FJ13, RCRW97]. The overall complexity of the Riccati iteration procedure is $O(N(n_u + n_x + n_z)^3)$. Computations that scale cubically in the Riccati iteration procedure are only performed one single time in every IPM iteration, as system factorizations are

stored within the IPM iteration. Subsequent solutions of (6.5) within the IPM iteration have complexity $O(N(n_u + n_x + n_z)^2)$. It is convenient to have an algorithm that scales linearly in the length of the prediction horizon, N , as stability of EMPC schemes often may be achieved by selecting a sufficiently large value of N [HPJJ12, JH05, PN00, Grü13, LS15, Jør05, JFGND12].

Solving (6.4) directly using sparse linear algebra routines is linear to quadratic in N , while general-purpose solvers using dense linear algebra routines scale cubically in N [ZB09]. When the state dimension, n_x , is large compared to the number of inputs, n_u , condensing methods are more efficient than Riccati-based methods for solving (6.4) [FJ13]. Condensing methods eliminate the state and output variables from (6.4), to form and solve a smaller, but less structured system. Condensing methods scale quadratically to cubically in N . Condensing-based solvers are therefore not well-suited to OCPs with long prediction horizons. As a rule of thumb, condensing-based solvers are more efficient than Riccati-based solvers, roughly when $n_x \geq Nn_u$ [FJ13]. The condensing method of [FJ13] can replace the proposed Riccati iteration procedure to solve (6.4) in the IPM, when $n_x \geq Nn_u$.

6.2.1 Warm-Start

We apply the strategy of [SAY13] to warm-start the proposed homogeneous and self-dual IPM. Let $(\bar{t}, \bar{v}, \bar{w}, \bar{s})$ denote a candidate primal-dual solution of (6.1). The warm-start is defined as

$$\tilde{t}^0 = \lambda \bar{t}, \tag{6.6a}$$

$$\tilde{v}^0 = \lambda \bar{v}, \tag{6.6b}$$

$$\tilde{s}^0 = \lambda \bar{s} + (1 - \lambda)\mathbf{1}, \tag{6.6c}$$

$$\tilde{w}^0 = \lambda \bar{w} + (1 - \lambda)\mathbf{1}, \tag{6.6d}$$

$$\tau^0 = 1, \tag{6.6e}$$

$$\kappa^0 = (\tilde{w}^0)^T \tilde{s}^0 / m_I. \tag{6.6f}$$

The point defined by (6.6) is a combination of the candidate point, $(\bar{t}, \bar{v}, \bar{w}, \bar{s})$, and the standard cold-start

$$(\tilde{t}, \tilde{v}, \tilde{w}, \tilde{s}, \tau, \kappa) = (\mathbf{0}, \mathbf{0}, \mathbf{1}, \mathbf{1}, 1, 1). \tag{6.7}$$

The parameter $\lambda \in [0, 1]$ in (6.6) is a tuning parameter. When $\lambda = 0$, the initial point becomes the standard cold-start, and for $\lambda = 1$ the initial point coincides with the candidate point. For homogeneous and self-dual IPMs, the standard cold-start, (6.7), is perfectly centralized with respect to the central path. This

is a key feature that makes warm-start work well for homogeneous and self-dual IPMs [SAY13]. As λ is decreased from one towards zero, the initial point becomes better centralized, while the distance from the candidate point (and possibly the solution) is increased.

The performance of the proposed warm-start strategy depends on the quality of the candidate point. In EMPC, the OCP is solved in a receding horizon manner. A primal-dual solution of (6.1) is therefore available from the previous sampling time. This makes it possible to construct a candidate point using the shift-initialization approach [DFH09], as follows: For the LP formulation of (5.10), the optimization variable t consists of the components

$$t = [u_{P,0}^T \quad \hat{x}_{P,1}^T \quad \rho_{P,1}^T \quad u_{P,1}^T \quad \hat{x}_{P,2}^T \quad \rho_{P,2}^T \quad \dots \quad u_{P,N-1}^T \quad \hat{x}_{P,N}^T \quad \rho_{P,N}^T]^T.$$

As an example, consider the solution of (6.1) at time step $k = 0$, for $N = 3$

$$t^* = [u_{P,0}^{*T} \quad \hat{x}_{P,1}^{*T} \quad \rho_{P,1}^{*T} \quad u_{P,1}^{*T} \quad \hat{x}_{P,2}^{*T} \quad \rho_{P,2}^{*T} \quad u_{P,2}^{*T} \quad \hat{x}_{P,3}^{*T} \quad \rho_{P,3}^{*T}]^T,$$

The following candidate point is then used at time step $k = 1$

$$\bar{t} = [u_{P,1}^{*T} \quad \hat{x}_{P,2}^{*T} \quad \rho_{P,2}^{*T} \quad u_{P,2}^{*T} \quad \hat{x}_{P,3}^{*T} \quad \rho_{P,3}^{*T} \quad u_{P,2}^{*T} \quad \hat{x}_{P,3}^{*T} \quad \rho_{P,3}^{*T}]^T. \quad (6.8)$$

Thus, \bar{t} is constructed by shifting the components of t^* forward in time. The final (three) components of \bar{t} can be chosen in several ways [DFH09]. We use a steady-state approach, where the final components of t^* are repeated two times in \bar{t} . Note that when N is large, we expect the initialization strategy for the last components of \bar{t} to be less significant. As for \bar{t} , we left-shift the optimal slack variables, s^* , and the optimal dual variables, v^* and w^* , to construct \bar{s} , \bar{v} and \bar{w} .

6.2.2 Benchmark

LPempc is a tailored MATLAB and C implementation of Algorithm 1. The algorithm utilizes the proposed Riccati iteration procedure to solve (6.5). Moreover, multiplications involving the structured matrices F and H , are implemented as specialized linear algebra routines.

Paper K compares LPempc to IPMs from the following software packages: Gurobi, MOSEK, SeDuMi, LIPSOL and GLPK. These state-of-the-art IPMs are mainly written in low-level language such as FORTRAN and C, and they rely on tailored linear algebra routines for solution of large-scale sparse LPs. The comparison also includes the simplex method provided by CPLEX, as well as FORCES [DZZ⁺12] and CVXGEN [MB12a] that are IPMs based on automatic code generation. The

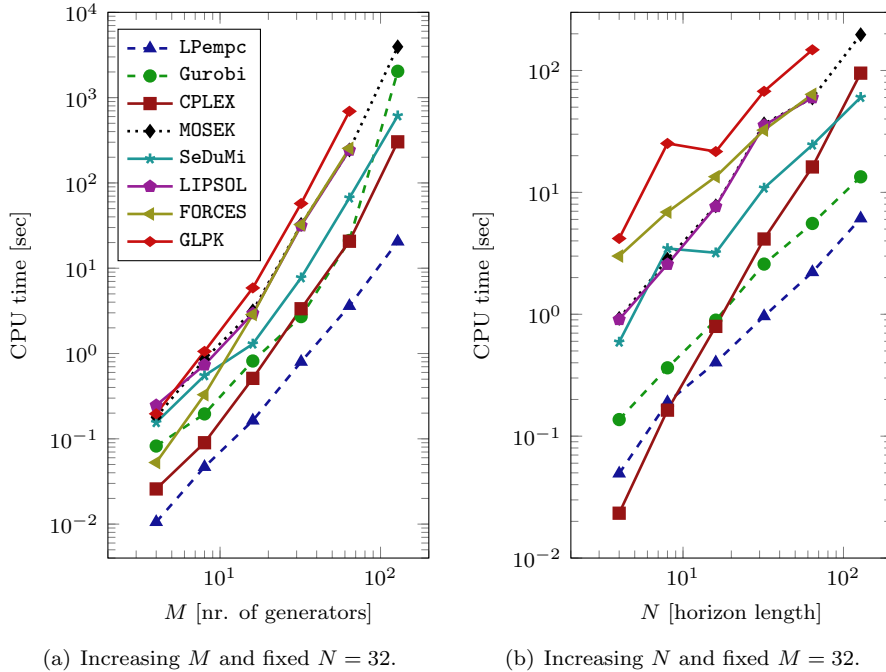


Figure 6.1: CPU time to solve (5.10) as a function of the number of power generators, M , and the horizon length, N .

algorithms are compared using a power portfolio case study, which is similar to the two-generator case study. The case study involves control of M generators in the form (2.2).

Fig. 6.1 depicts the CPU time to solve the OCP (5.10) as a function of the number of power generators, M , and the length of the prediction horizon, N . For large problems, LPempc is faster than all other solvers by a significant margin. In general, code generation-based solvers such as CVXGEN and FORCES are most competitive for small-dimensional problems [DZZ⁺12]. Code generation in CVXGEN fails for problems larger than $M = 4$ and $N = 12$. Therefore, Fig. 6.1 does include results for CVXGEN.

Fig. 6.2 compares the CPU time to solve (5.10) in a closed-loop simulation with $M = 15$ power generators, noise parameter $\sigma = 1$, and a horizon length of $N = 200$ time steps. Only the most competitive solvers are considered in this benchmark. Fig. 6.2 shows that LPempc is up to an order of magnitude faster than CPLEX, Gurobi, SeDuMi and MOSEK, depending on the problem data. On

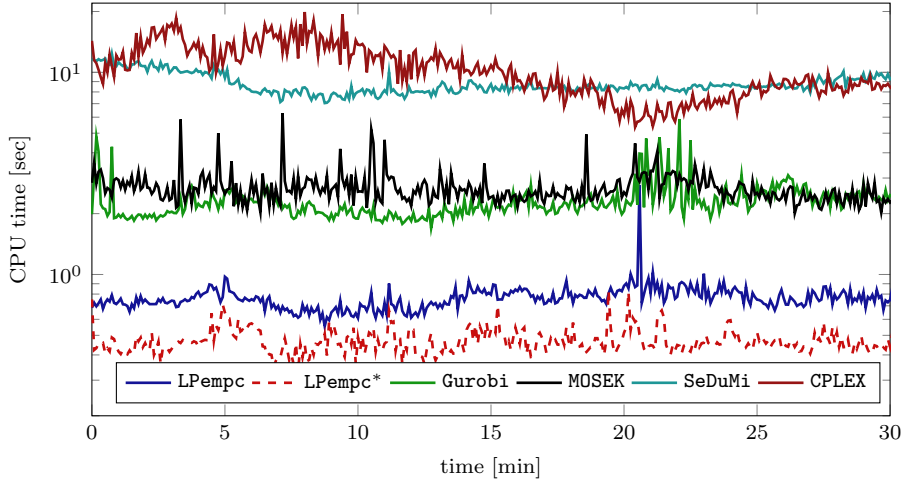


Figure 6.2: CPU time to solve (5.10). Timings are performed over a 30 min closed-loop simulation with $M = 15$ power generators and a horizon length of $N = 200$ time steps. Warm-start is indicated by an asterisk (*) for LPempc.

average, LPempc is approximately 5 times faster than Gurobi, 6 times faster than MOSEK, 19 times faster than SeDuMi, and 22 times faster than CPLEX. Warm-start reduces the average number of IPM iterations by approximately 40%. Paper K shows that warm-start works well, even for large values of the noise parameter, σ .

6.3 Subsystem Decomposition

The portfolio system (2.9) may include a large number of generators, e.g. it can represent a virtual power plant that is made up of thousands of distributed energy resources. When the number of generators, M , is large, EMPC algorithms that scale well in M are attractive. The generators (2.5) are dynamically decoupled. Paper E presents two decomposition algorithms for EMPC of dynamically decoupled subsystems. The algorithms are based on Dantzig-Wolfe decomposition and ADMM. This section outlines the two decomposition algorithms.

Using the definitions in (2.9), we write the OCP (5.10) as

$$\min_{u_P, \hat{x}_P, \hat{z}_P, \rho_P^d, \rho_P^u} \sum_{k \in \mathcal{N}_0} p_{P,k}^T u_{P,k} + \sum_{k \in \mathcal{N}_1} \underline{q}_{P,k}^T \rho_{P,k}^d + \bar{q}_{P,k}^T \rho_{P,k}^u, \quad (6.9a)$$

subject to

$$\hat{x}_{g_j,k+1} = A_{g_j} \hat{x}_{g_j,k} + B_{g_j} u_{g_j,k} + E_{g_j} d_{g_j,k}, \quad j \in \mathcal{M}, \quad k \in \mathcal{N}_0, \quad (6.9b)$$

$$\hat{z}_{g_j,k} = C_{g_j,z} \hat{x}_{g_j,k}, \quad j \in \mathcal{M}, \quad k \in \mathcal{N}_1, \quad (6.9c)$$

$$\underline{u}_{g_j,k+j} \leq u_{g_j,k} \leq \bar{u}_{g_j,k}, \quad j \in \mathcal{M}, \quad k \in \mathcal{N}_0, \quad (6.9d)$$

$$\Delta \underline{u}_{g_j,k} \leq \Delta u_{g_j,k} \leq \Delta \bar{u}_{g_j,k}, \quad j \in \mathcal{M}, \quad k \in \mathcal{N}_0, \quad (6.9e)$$

$$\underline{z}_{g_j,k} - \rho_{g_j,k}^d \leq z_{g_j,k} \leq \bar{z}_{g_j,k} + \rho_{g_j,k}^u, \quad j \in \mathcal{M}, \quad k \in \mathcal{N}_1, \quad (6.9f)$$

$$\rho_{g_j,k}^d \geq 0, \quad j \in \mathcal{M}, \quad k \in \mathcal{N}_1, \quad (6.9g)$$

$$\rho_{g_j,k}^u \geq 0, \quad j \in \mathcal{M}, \quad k \in \mathcal{N}_1, \quad (6.9h)$$

$$\hat{z}_{T,k} = \sum_{j \in \mathcal{M}} \Upsilon_j C_{g_j,z} x_{g_j,k}, \quad k \in \mathcal{N}_1, \quad (6.9i)$$

$$\underline{z}_{T,k} - \rho_{T,k}^d \leq z_{T,k} \leq \bar{z}_{T,k} + \rho_{T,k}^u, \quad k \in \mathcal{N}_1, \quad (6.9j)$$

$$\rho_{T,k}^d \geq 0, \quad k \in \mathcal{N}_1, \quad (6.9k)$$

$$\rho_{T,k}^u \geq 0, \quad k \in \mathcal{N}_1. \quad (6.9l)$$

Constraints (6.9b), (6.9c), (6.9d), (6.9e), (6.9f), (6.9g) and (6.9h) are generator-level constraints. Constraint (6.9i) connects the generator-level state variables, $\hat{x}_{g_1,k}, \dots, \hat{x}_{g_M,k}$, with the portfolio-level power production variable, $\hat{z}_{T,k}$. Constraints (6.9j), (6.9k) and (6.9l) are portfolio-level constraints. Accordingly, (5.4) and (5.5) show that the objective function, (6.9a), can be split into generator-level costs and a portfolio-level cost.

Paper E poses the OCP (6.9) as a block-angular LP in the form (4.21). To avoid conflicting notation, we write this problem as

$$\min_t \sum_{j \in \mathcal{J}} g_j^T t_j, \quad (6.10a)$$

$$\text{s.t. } F_{g_j} t_j \leq b_{g_j}, \quad j \in \mathcal{J}, \quad (6.10b)$$

$$\sum_{j \in \mathcal{J}} F_{l_j} t_j \leq b_l. \quad (6.10c)$$

In this formulation of (6.9), the subsystem constraints (6.10b) are generator-level constraints, and the linking constraints (6.10c) are portfolio-level constraints. Finally, $\mathcal{J} = \{1, 2, \dots, M, M+1\}$, where M is the number of generators.

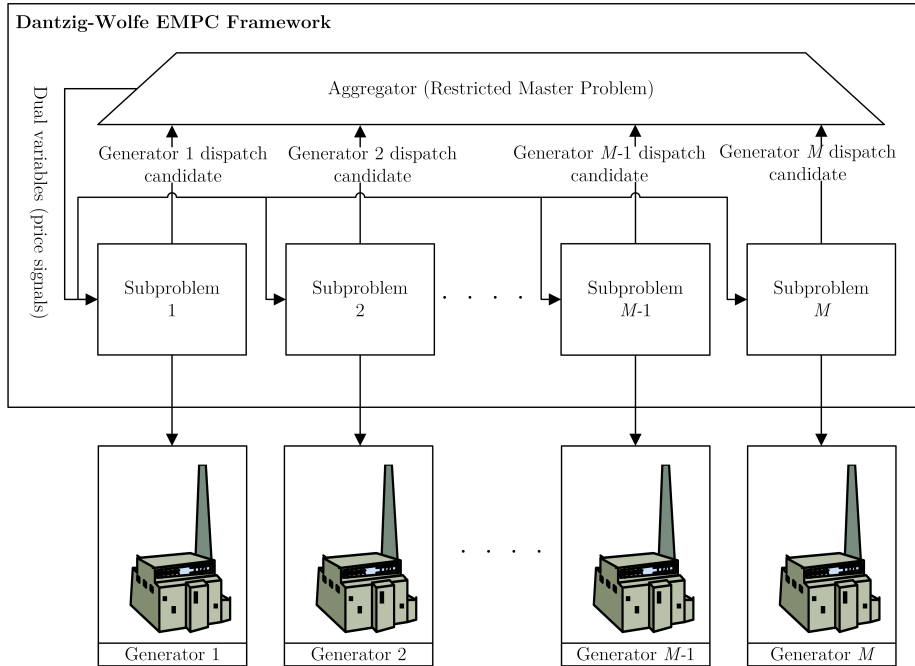


Figure 6.3: Diagram of the Dantzig-Wolfe decomposition algorithm for EMPC of the power portfolio system.

6.3.1 Dantzig-Wolfe Decomposition Algorithm

Algorithm 2 is a Dantzig-Wolfe decomposition algorithm for the solution of (6.10). Fig. 6.3 is a diagram of its application to the OCP (6.9). A subproblem in the form (4.28) is associated with each generator. The subproblems are solved to update the restricted master problem (4.27). This procedure is repeated until a stopping criterion for the Dantzig-Wolfe decomposition algorithm is satisfied. The procedure can be interpreted as follows: An aggregator distributes price signals to the generators. Each generator then generates a candidate production plan (dispatch) based on the price signals. If the aggregator is not satisfied with (a combination of) the candidate production plans, the price signals are updated and the process is repeated.

An advantage of the Dantzig-Wolfe decomposition algorithm is that a feasible suboptimal solution is available in every iteration of the algorithm. Early termination can therefore be applied to trade off computation time and optimality. Upper and lower bounds for the optimal objective value can be determined via

Lagrangian relaxation techniques [DDS05]. This makes it possible to give a qualitative measure of a suboptimal solution. As in (6.8), a shift-initialization strategy is applied to warm-start the Dantzig-Wolfe decomposition algorithm.

6.3.2 ADMM-Based Decomposition Algorithm

Algorithm 3 is an ADMM algorithm for solution of convex optimization problems with separable objective functions. Paper E presents a specialized implementation of the ADMM algorithm for solution of the block-angular LP (6.10). To write (6.10) in ADMM form, we consider the modified problem

$$\min_{t,v} \sum_{j \in \mathcal{J}} g_j^T t_j, \quad (6.11a)$$

$$\text{s.t. } F_{g_j} t_j \leq b_{g_j}, \quad j \in \mathcal{J}, \quad (6.11b)$$

$$F_{l_j} t_j = v_j, \quad j \in \mathcal{J}, \quad (6.11c)$$

$$\sum_{j \in \mathcal{J}} v_j \leq b_l. \quad (6.11d)$$

$v = [v_1^T \ v_2^T \ \dots \ v_{M+1}^T]^T$ is an auxiliary optimization variable. Using the indicator function (4.30), we state the problem (6.11) as

$$\min_{t,v} \sum_{j \in \mathcal{J}} \left(g_j^T t_j + I_{\mathbb{F}_{g_j}}(t_j) \right) + I_{\mathbb{F}_l}(v), \quad (6.12a)$$

$$\text{s.t. } F_{l_j} t_j = v_j, \quad j \in \mathcal{J}, \quad (6.12b)$$

where we have defined the sets $\mathbb{F}_{g_j} = \{t_j | F_{g_j} t_j \leq b_{g_j}\}$ and $\mathbb{F}_l = \{v | \sum_{j \in \mathcal{J}} v_j \leq b_l\}$.

The problem (6.12) is in the standard ADMM form (4.29). The ADMM recursions for solution of (6.12) follow from (4.33). In a simplified form, the recursions to solve (6.12) are

$$t_j^{i+1} = \operatorname{argmin}_{t_j \in \mathbb{F}_{g_j}} g_j^T t_j + \frac{\rho}{2} \|F_{l_j} t_j - v_j^i + u_j^i\|_2^2, \quad j \in \mathcal{J}, \quad (6.13a)$$

$$v^{i+1} = \operatorname{argmin}_{v \in \mathbb{F}_l} \frac{\rho}{2} \sum_{j \in \mathcal{J}} \|F_{l_j} t_j^{i+1} - v_j + u_j^i\|_2^2, \quad (6.13b)$$

$$u_j^{i+1} = u_j^i + F_{l_j} t_j^{i+1} - v_j^{i+1}, \quad j \in \mathcal{J}. \quad (6.13c)$$

Paper E shows that the t -update, (6.13a), can be expressed as the solution to

the convex quadratic program (QP)

$$\min_{t_j} \frac{\rho}{2} t_j^T (F_{l_j})^T F_{l_j} t_j + (g_j + \rho(-v_j^i + u_j^i)^T F_{l_j})^T t_j, \quad (6.14a)$$

$$\text{s.t. } F_{g_j} t_j \leq b_{g_j}, \quad j \in \mathcal{J}, \quad (6.14b)$$

for $j \in \mathcal{J}$. Moreover, the v -update, (6.13b), has the closed-form expression

$$v_j^{i+1} = F_{l_j} t_j^{i+1} + u_j^i - \max(l/(M+1), 0), \quad j \in \mathcal{J},$$

in which

$$l = \sum_{j \in \mathcal{J}} (F_{l_j} t_j^{i+1} + u_j^i) - h. \quad (6.15)$$

The ADMM algorithm is composed of a number of (decoupled) generator-level computations, and a system-level computation. The system-level computation in the ADMM algorithm is the sum (6.15). In comparison, the Dantzig-Wolfe decomposition algorithm requires solution of the LP (4.27). The ADMM algorithm is also attractive since it can be generalized to convex optimization problems, e.g. OCPs with quadratic cost functions [CSZ⁺12, SL12, AHW12]. As the Dantzig-Wolfe decomposition algorithm, the ADMM algorithm can be warm-started using a shift-initialization strategy, and it can be terminated early to obtain a feasible suboptimal solution.

6.3.3 Subproblems

Efficient implementations of the subsystem decomposition algorithms require efficient solution of the subproblems (4.28) and (6.14). Since the subproblems are decoupled in $j \in \mathcal{J}$, they can be solved in parallel. Moreover, a warm-start for the algorithms solving the subproblems is obtained using values from the previous iteration of the respective decomposition algorithm. In the Dantzig-Wolfe decomposition algorithm, the subproblem (4.28) can be expressed as a linear OCP. LPempc is a structure-exploiting IPM for solution of linear OCPs. A crossover procedure can be applied to obtain an optimal extreme point for (4.28), based on an interior-point solution of the subproblem [Mar99, WCS13]. In the ADMM algorithm, the subproblem (6.14) can be expressed as a quadratic OCP. Active-set methods [JRJ04, BB06, FBD08], IPMs [WB10, RWR98, SKC10], and first-order methods [RJM09, JGR⁺14], solve this type of problem efficiently. In particular, Paper D provides an ADMM-based algorithm for solution of input-constrained OCPs with convex objective functions. An implementation of this algorithm is developed for input-constrained extended linear quadratic control problems. Simulations show that the ADMM algorithm is more than an order of magnitude faster than several state-of-the-art quadratic programming algorithms.

Table 6.1: Iteration information table based on closed-loop simulation, with $M = 2$ generators. The minimum, maximum and average number of iterations are listed for both cold-start and for warm-start (in parentheses).

σ	r	DWempc	ADMMempc
0	0	[6(2), 16(17), 12(11)]	[47(2), 485(410), 097(66)]
0	0.01	[6(2), 15(18), 10(09)]	[35(3), 469(410), 088(56)]
0	0.1	[5(2), 15(17), 07(07)]	[33(6), 359(280), 149(48)]
0.01	0	[7(2), 18(19), 13(11)]	[47(2), 485(410), 094(65)]
0.01	0.01	[6(2), 17(17), 10(09)]	[35(2), 469(410), 088(58)]
0.01	0.1	[5(2), 13(16), 07(06)]	[32(6), 380(290), 145(50)]
0.1	0	[7(2), 17(20), 12(11)]	[46(2), 485(410), 091(66)]
0.1	0.01	[6(2), 17(16), 09(09)]	[35(2), 469(410), 084(60)]
0.1	0.1	[5(2), 14(14), 07(06)]	[32(6), 359(279), 144(47)]

6.3.4 Benchmark

The subsystem decomposition algorithms are implemented in MATLAB. We refer to the implementation of the Dantzig-Wolfe decomposition algorithm as `DWempc`, and to the implementation of the ADMM-based decomposition algorithm as `ADMMempc`. Paper E compares `DWempc` and `ADMMempc` using a power portfolio case study with M generators. For this case study, the decomposition algorithms solve the subproblems (4.28) and (6.14) using CPLEX. To get well behaved closed-loop solutions, the OCP objective function (6.9) is augmented by an ℓ_1 -regularization term in the form (5.20). Table 6.1 provides information on the number of iterations for `DWempc` and `ADMMempc`, based on a 10 min closed-loop simulation, with $M = 2$ generators. The closed-loop simulation is performed for different values of the noise parameter, σ , and the regularization parameter, r . The definition of σ in Paper E differs slightly from the definition (5.11). Table 6.1 shows that `DWempc` converges in relatively few iterations compared to `ADMMempc`. The table also shows that regularization reduces the computational time for both `DWempc` and for `ADMMempc`. E.g. for $\sigma = 0.01$ and $r = 0.1$, the average number of iterations for `DWempc` is reduced by more than 40%, compared to the case where $r = 0$. Also observe that while warm-start leads to a marginal improvement in the iteration count for `DWempc`, a substantial reduction in the number of iterations is achieved for `ADMMempc`.

To indicate the performance of a suboptimal solution (suboptimality level), the

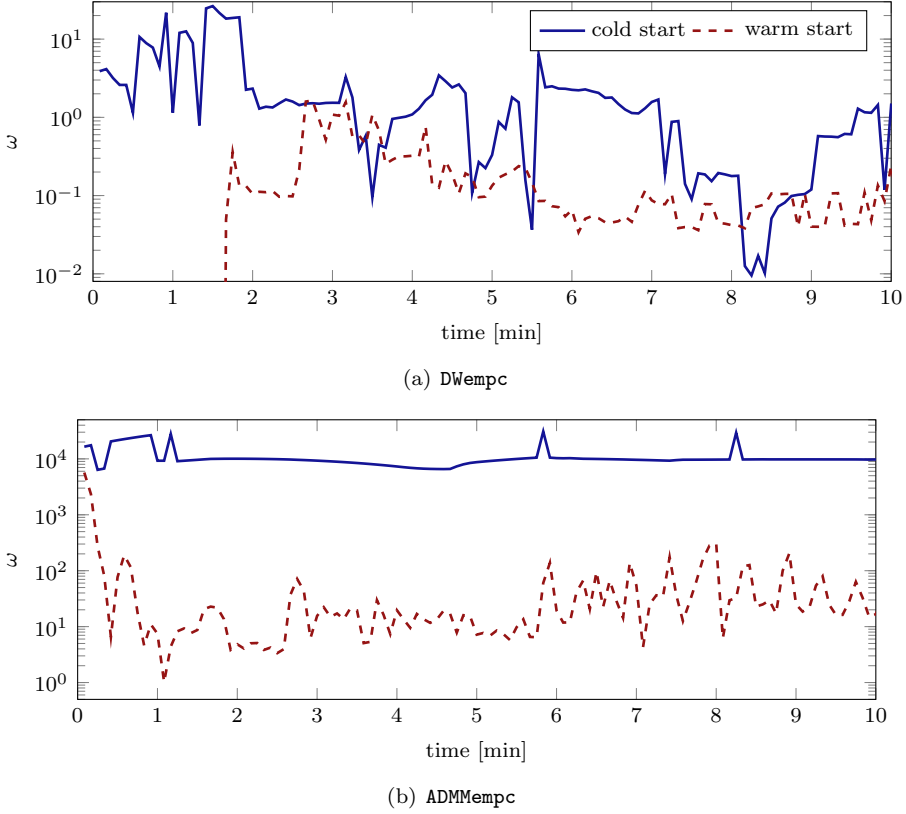


Figure 6.4: Suboptimality measure in a closed-loop solution with $\sigma = 0.01$ and $r = 0.01$. DWempc and ADMMempc are terminated after 0.01 seconds.

following measure is defined

$$\omega = 100 \frac{\tilde{\phi} - \phi^*}{\max(|\phi^*|, 1)}, \quad (6.16)$$

where $\tilde{\phi}$ is the objective value of the OCP (6.9) associated with a suboptimal solution, and ϕ^* is the optimal objective value. We test early-termination in a closed-loop simulation with $\sigma = 0.01$ and $r = 0.01$. The algorithms are terminated after 0.01 seconds. Fig. 6.4 shows the values of ω over the closed-loop simulation. DWempc is up to approximately 30% suboptimal when cold-started, and not more than 5% suboptimal when warm-started. Warm-start also improves the performance of ADMMempc significantly. Fig. 6.5 shows the value of ω as a function of the elapsed CPU time for a single instance of the OCP with

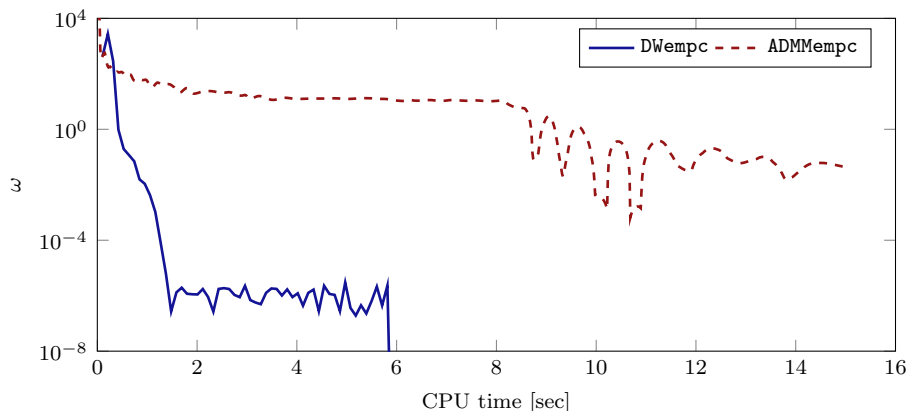


Figure 6.5: Suboptimality measure as a function of the CPU time, for a single instance of the OCP with 128 power generators.

$M = 128$ power generators. The figure shows that `DWempc` converges at a fast rate. After approximately 0.3 seconds, a solution which is less than 1% suboptimal is obtained by `DWempc`. The convergence rate of `ADMMempc` is relatively slow. More than 10 seconds is required to find a 1% suboptimal solution for `ADMMempc`. Fig. 6.6 shows the CPU time to solve (6.9) as a function of M , for `DWempc`, `ADMMempc`, `Gurobi`, `CPLEX`, and `MOSEK`. The reported timings assume that the subproblems (4.28) and (6.14) are solved in parallel. This is done to demonstrate the full parallelization capabilities of the subsystem decomposition algorithms. Case study details and solver specifications are provided in Paper E. Fig. 6.6 shows that for large problems, `DWempc` is 5 times faster than `CPLEX` and more than an order of magnitude faster than `Gurobi` and `MOSEK`. Paper E reports that for high accuracy solutions, `DWempc` is 2 times faster than `CPLEX` and approximately 5 times faster than `Gurobi` and `MOSEK`. Around $M = 3000$ memory becomes an issue for `Gurobi`, `CPLEX` and `MOSEK`. `DWempc` and `ADMMempc` solve OCPs with $M \gg 3000$ without any memory issues.

Table 6.1 reports that `ADMMempc` requires more iterations than `DWempc`. Provided that the number of iterations is small, the computational cost per iteration is approximately equal for `DWempc` and `ADMMempc`. For this reason, `DWempc` outperforms `ADMMempc` by a significant margin. Considering both CPU time and memory requirements, `DWempc` is an attractive optimization algorithm for (6.9), when M is large. For this particular problem ADMM is less attractive, as it requires many iterations to converge to even a moderately accurate solution. In general, the convergence rate of ADMM is very problem-dependent [SLY⁺14, TGS⁺13, GTSJ13].

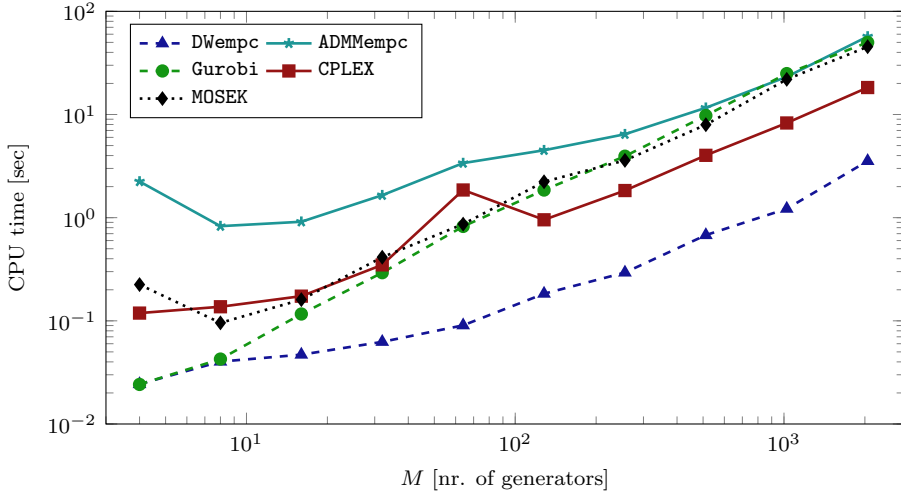


Figure 6.6: CPU time to solve the OCP (6.9) as a function of the number of power generators, M .

6.4 Scenario Decomposition

The size of the OCP solved in MV-EMPC increases with the number of uncertainty scenarios, S . Paper F shows that MV-EMPC usually requires $S > 1000$ to work well. Direct solution of the OCP (5.18) is intractable in real-time, for large S . To overcome this challenge, Paper G presents a novel ADMM-based decomposition algorithm for MV-EMPC of linear stochastic systems. The algorithm decomposes the OCP into S independent convex subproblems, and a number of computationally inexpensive operations. This section summarizes the scenario decomposition algorithm.

The OCP (5.18) is a convex optimization problem when \mathcal{U} is a convex set, and ϕ is an affine function. If the equality constraint (5.18d) is replaced by the inequality constraint

$$\varphi^s \geq \phi(u^s, x^s, z^s), \quad s \in \mathcal{S}, \quad (6.17)$$

the requirement on ϕ can be loosened to convexity. Using the relaxed condition (6.17) is attractive since it preserves convexity of the overall problem for a wide

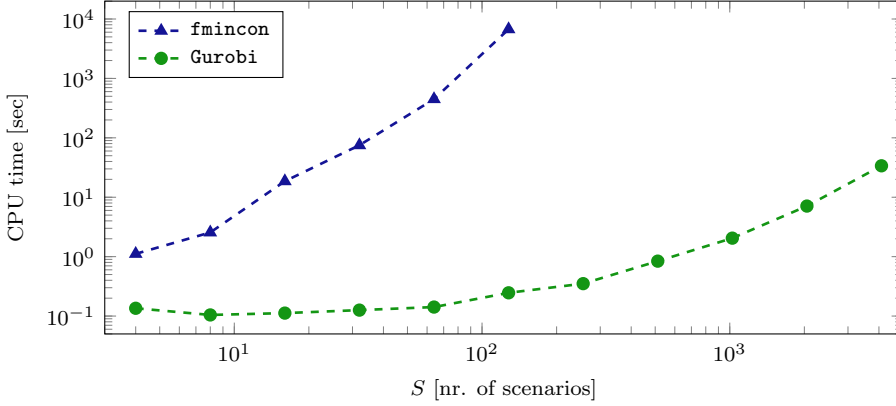


Figure 6.7: CPU time to solve the OCP (5.18) and its convex relaxation (6.18) as a function of the number of uncertainty scenarios, S .

range of cost functions. We write the relaxed OCP as

$$\min_{\{u^s \in \mathcal{U}, x^s, z^s, \varphi^s\}_{s \in \mathcal{S}}, \mu} \alpha \mu + \tilde{\alpha} \sum_{s \in \mathcal{S}} (\varphi^s - \mu)^2, \quad (6.18a)$$

$$\text{s.t. } x_{k+1}^s = Ax_k^s + Bu_k^s + Ed_k + w_k^s, \quad k \in \mathcal{N}_0, \quad s \in \mathcal{S}, \quad (6.18b)$$

$$z_k^s = C_z x_k^s, \quad k \in \mathcal{N}_1, \quad s \in \mathcal{S}, \quad (6.18c)$$

$$\varphi^s \geq \phi(u^s, x^s, z^s), \quad s \in \mathcal{S}, \quad (6.18d)$$

$$\mu = \frac{1}{S} \sum_{s \in \mathcal{S}} \varphi^s, \quad (6.18e)$$

$$u_k^{s_1} = u_k^{s_2}, \quad s_1, s_2 \in \mathcal{S}, \quad k \in \mathcal{Q}. \quad (6.18f)$$

The solution of the OCP (5.18), and the solution of the relaxed OCP (6.18) often only differ when $\alpha \approx 0$ [SDMJ14b]. A small α means that MV-EMPC emphasizes on minimizing the cost variance. When $\alpha \approx 0$, a significant cost reduction can often be achieved by increasing α marginally. For this reason, cases where $\alpha \approx 0$ are generally disregarded in practice [Mar52, Ste01].

Paper F solves the relaxed OCP (6.18) in a conceptual example of MV-EMPC. The example concerns MV-EMPC of the portfolio system (2.9), subject to the constraints (5.3) and the cost function (5.8). The relaxed OCP is expressed as a convex QP. Fig. 6.7 shows the CPU time to solve (5.18) and (6.18) as a function of the number of uncertainty scenarios S . The OCP (5.18) is solved using MATLAB's `fmincon`, while its convex relaxation (6.18) is solved using `Gurobi`. It is verified that both optimization problems yield the same solution (for all practical purposes). For $S = 64$, the CPU time to solve (5.18) is several minutes. The relaxed problem is solved in under 5 seconds, even for $S = 1024$.

For this example, the time to solve the OCP associated with CE-EMPC, (5.10), is approximately 0.1 seconds.

Fig. 6.7 reports CPU times based on an example with a single power generator and a short prediction horizon. For larger problems, the time to solve even the relaxed OCP, is significantly more than 5 seconds. Moreover, memory becomes a problem as S is increased. Paper G presents an ADMM-based decomposition algorithm to solve large instances of the relaxed OCP (6.18), in a reasonable amount of time. To describe the algorithm, (6.18) is written in the compact form

$$\min_{u \in \tilde{\mathcal{U}}, x, z, \varphi, \mu} \quad \alpha\mu + \tilde{\alpha}\varphi^T \varphi + S\tilde{\alpha}\mu^2 - 2\tilde{\alpha}\mu \mathbf{1}^T \varphi, \quad (6.19a)$$

$$\text{s.t.} \quad \tilde{A}x + \tilde{B}u + \tilde{E}d + \tilde{w} = 0, \quad (6.19b)$$

$$z = \tilde{C}x, \quad (6.19c)$$

$$\varphi \geq \tilde{\phi}(u, x, z), \quad (6.19d)$$

$$\mu = \mathbf{1}^T \varphi / S \quad (6.19e)$$

$$\tilde{L}u = 0, \quad (6.19f)$$

where we have defined the stacked vectors

$$u = \begin{bmatrix} u^1 \\ u^2 \\ \vdots \\ u^S \end{bmatrix}, \quad x = \begin{bmatrix} x^1 \\ x^2 \\ \vdots \\ x^S \end{bmatrix}, \quad z = \begin{bmatrix} z^1 \\ z^2 \\ \vdots \\ z^S \end{bmatrix}, \quad \varphi = \begin{bmatrix} \varphi^1 \\ \varphi^2 \\ \vdots \\ \varphi^S \end{bmatrix}. \quad (6.20)$$

$\tilde{\mathcal{U}} = \mathcal{U} \times \mathcal{U} \times \cdots \times \mathcal{U}$ is the Cartesian power of the set \mathcal{U} , such that $u^s \in \mathcal{U}$ for $s \in \mathcal{S}$, can be expressed as $u \in \tilde{\mathcal{U}}$. Constraints (6.19b) and (6.19c) correspond to (6.18b) and (6.18c). Constraint (6.19d) corresponds to (6.18d). Constraint (6.19e) corresponds to (6.18e), and Constraint (6.19f) corresponds to (6.18f). We refer to Paper G for a description of the data structures in (6.19).

Introduce the auxiliary variables $\check{\mu}$, \check{u} and $\check{\varphi}$. Moreover, define the sets

$$\begin{aligned} \mathbb{V}_1 &= \{v_1 | \check{u} \in \tilde{\mathcal{U}}, \tilde{A}\check{x} + \tilde{B}\check{u} + \tilde{E}d + \tilde{w} = 0, z = \tilde{C}\check{x}, \check{\varphi} \geq \tilde{\phi}(\check{u}, \check{x}, z)\}, \\ \mathbb{V}_2 &= \{v_2 | \tilde{L}u = 0\}, \end{aligned}$$

where $v_1 = (\check{u}, \check{x}, z, \check{\varphi}, \check{\mu})$ and $v_2 = (u, \varphi, \mu)$ for compact notation. Using the

indicator function, (6.19) is written as

$$\min_{v_1, v_2} (\alpha \check{\mu} + I_{\mathbb{V}_1}(v_1)) + (\check{\alpha} \varphi^T \varphi + S \check{\alpha} \mu^2 - 2 \check{\alpha} \mu \mathbf{1}^T \varphi + I_{\mathbb{V}_2}(v_2)), \quad (6.21a)$$

$$\text{s.t. } \check{\mu} - \mathbf{1}^T \varphi / S = 0, \quad (6.21b)$$

$$\check{\mu} - \mu = 0, \quad (6.21c)$$

$$\check{u} - u = 0, \quad (6.21d)$$

$$\check{\varphi} - \varphi = 0. \quad (6.21e)$$

Problem (6.21) is in the standard ADMM form (4.29), with variables $v_1 = (\check{u}, x, z, \check{\varphi}, \check{\mu})$ and $v_2 = (u, \varphi, \mu)$. The ADMM recursions for solution of (6.21) are given by (4.29). Paper G develops a computationally efficient formulation of the ADMM recursions that scales linearly in S . To keep the notation simple, we state the recursions for a fixed iteration number and drop superscript i for the iteration number. The v_1 -update in the ADMM algorithm is expressed as the solution of the convex OCPs

$$\min_{\check{u}^s \in \mathcal{U}, x^s, z^s, \check{\varphi}^s} \frac{1}{2} ((\check{u}^s)^T \check{u}^s + (\check{\varphi}^s)^T \check{\varphi}^s) + (m_3^s)^T \check{u}^s + m_4^s \check{\varphi}^s, \quad (6.22a)$$

$$\text{s.t. } x_{k+1}^s = Ax_k^s + Bu_k^s + Ed_k + w^s, \quad k \in \mathcal{N}_0, \quad (6.22b)$$

$$z_k^s = C_z x_k^s, \quad k \in \mathcal{N}_1, \quad (6.22c)$$

$$\check{\varphi}^s \geq \phi(\check{u}^s, x^s, z^s), \quad (6.22d)$$

for $s \in \mathcal{S}$, and computation of

$$\check{\mu}^* = -\frac{1}{2\rho}((m_1 + m_2)\rho + \alpha). \quad (6.23)$$

The vectors m_1, m_2, m_3 and m_4 are updated in every iteration of the ADMM algorithm. m_1^s, m_2^s, m_3^s and $m_4^s, s \in \mathcal{S}$, are components of these vectors. The v_2 -update in the ADMM algorithm is expressed as the solution of the convex optimization problem

$$\min_{u, \varphi, \mu} \frac{1}{2} \rho u^T u + \varphi^T \Theta \varphi + \theta \mu^2 - 2 \check{\alpha} \mathbf{1}^T \mu \varphi - \rho n_2 \mu - \rho n_3^T u, \quad (6.24a)$$

$$\text{s.t. } \tilde{L}u = 0, \quad (6.24b)$$

where $\theta = S \check{\alpha} + \frac{1}{2} \rho$ and $\Theta = \check{\alpha} I + \frac{1}{2} \rho ((1/S^2) \mathbf{1} \mathbf{1}^T + I)$. The vectors n_1, n_2, n_3 and n_4 are updated in every iteration of the ADMM algorithm. Paper G splits (6.24) into an optimization problem in u , and an optimization problem in (φ, μ) . Simple closed-form expressions are derived for the solution of each of these optimization problems.

Solving the S subproblems in the form (6.22) is the main computational bottleneck of the proposed scenario decomposition algorithm. The dimensions of the subproblem, (6.22), are approximately the same as the dimensions of the

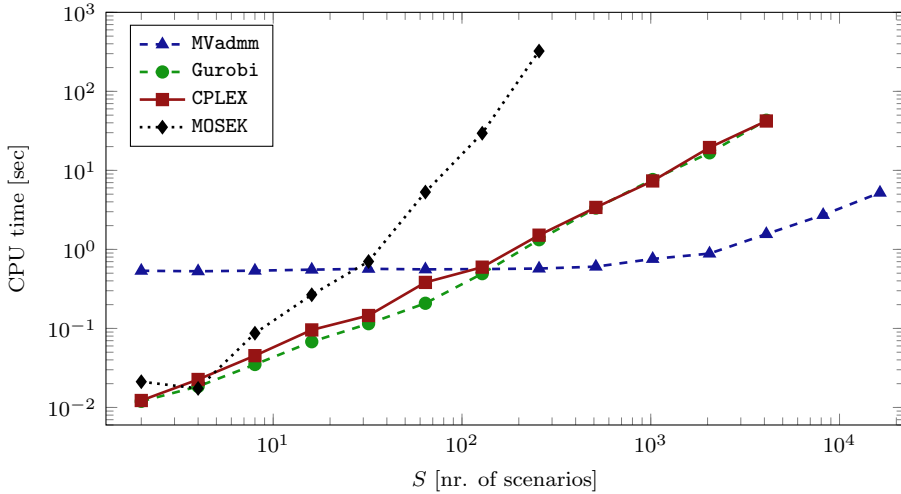


Figure 6.8: CPU time to solve (6.18) as a function of the number of scenarios, S .

OCP solved in CE-EMPC. Warm-started algorithms that are tailored to convex OCPs, e.g. the ADMM algorithm of Paper D, can be used as efficient subproblem solvers for the scenario decomposition algorithm. In MV-EMPC of dynamically decoupled subsystems, the subproblem (6.22) is a block-angular convex optimization problem. `ADMMempc` can be generalized to solve problems of this type. We remark that the subproblems can be solved in parallel.

6.4.1 Benchmark

`MVadmm` is a MATLAB implementation of the scenario decomposition algorithm. The algorithm is specialized to the QP that arises in MV-EMPC of the portfolio system (2.9), subject to the constraints (5.3) and the cost function (5.8). `MVadmm` solves the subproblem (6.22) using `CVXGEN`. Paper G compares `MVadmm` to `CPLEX`, `MOSEK` and `Gurobi` using a small power portfolio case study with a single power generator. The length of the prediction horizon is $N = 40$ time steps. Moreover $q = 1$, i.e. $Q = \{0\}$. In this way, the OCP (6.18) accounts for the possibility of recourse in the following sampling instant (in an approximate manner).

Fig. 6.8 reports the CPU time to solve the relaxed OCP (6.18) for `MVadmm`, `CPLEX`, `MOSEK` and `Gurobi` as a function S . The reported CPU times assume that the subproblems defined by (6.22) are solved in parallel. Fig. 6.8 shows that

`MVadmm` scales better than the general-purpose solvers in terms of computational time. For large S , `MVadmm` is several orders of magnitude faster than the general-purpose solvers. For $S = 8192$, `CPLEX`, `MOSEK` and `Gurobi` fail due to memory issues. `MVadmm` solves the relaxed OCP in approximately 5 seconds for this value of S .

6.5 Summary

In this chapter, we have developed tailored algorithms for EMPC in power production planning. The algorithms can be categorized as follows:

- **General EMPC algorithms:** We presented a homogeneous and self-dual IPM for EMPC of linear systems with linear constraints and linear objective functions. An ADMM-based algorithm was described for input-constrained EMPC of linear systems with convex objective functions. The algorithms scale linearly in the length of the prediction horizon, N . This is important, as stability of EMPC schemes depends on N . The proposed algorithms can be used independently, or as subproblem solvers in decomposition algorithms for EMPC.
- **Subsystem decomposition algorithms:** We presented a Dantzig-Wolfe decomposition algorithm and an ADMM-based decomposition algorithm for EMPC of dynamically decoupled subsystems. While the Dantzig-Wolfe decomposition algorithm is limited to LPs, the ADMM-based decomposition algorithm can be generalized to convex optimization problems. The subsystem decomposition algorithms accommodate the need for EMPC of power systems with a large number of power generators, M . The subsystem decomposition algorithms scale linearly in M .
- **Scenario decomposition algorithms:** An ADMM-based decomposition algorithm was developed for MV-EMPC of linear stochastic systems. The algorithm scales linearly in the number of uncertainty scenarios, S .

Simulations show that the tailored EMPC algorithms are significantly faster than current state-of-the-art solvers, and that the difference in computational time increases with the size of the OCPs. Moreover, the proposed decomposition algorithms can solve much larger problems than general-purpose solvers without any memory issues.

Isolated Power Systems

The contributions of this chapter are methods for power production planning in small isolated power systems. The ORPP is presented for unit commitment and economic dispatch of the system power generators, considering a set of pre-defined contingencies. Frequency control is handled using a reserve activation scheme based on EMPC. The methods proposed in this chapter, are tested using a Faroe Islands simulation case study. The ORPP is currently being tested in the actual Faroese power system.

7.1 Contributions

Small isolated power systems are characterized by low inertia provided by a relatively small number of generators [HCM⁺01, GB11, CFP95, UBA14, KO96, ORF⁺14, TF94, Lal05, LRFO05, LMO05]. This characteristic makes the system frequency in small isolated power systems very sensitive to power imbalances. Imbalances are a result of e.g. loss of power generators, fluctuations in non-controllable production or consumption, and errors in the prediction of renewable energy production. We refer to such power imbalance triggering events as contingencies. Significant frequency deviations from the nominal frequency lead to load-shedding, cascading generator trips, power outages, and ultimately total blackouts.

Due to the limited inertia and the inability to exchange power with neighboring regions, power production planning in small isolated power systems is challenging, especially for systems with a high penetration of renewable energy sources. At the same time, small isolated power systems are ideal for testing smart grid technologies. Full system-level experiments only require a small-scale implementation. Moreover, the volatile conditions in isolated power systems make it possible to test the technologies at their limits.

Paper [H](#) and Paper [I](#) address two related challenges associated with power production planning in small isolated power systems. These challenges are:

- Reserve planning: Reserve planning is an integral part of the UC problem. In small isolated power systems, the system inertia (and reserve requirements) vary significantly with the committed power generators. This is challenging to handle in the UC problem. Paper [H](#) addresses reserve planning in small isolated power systems using a novel formulation of the UC problem, which is referred to as the ORPP. The ORPP guarantees that the system frequency is kept above a pre-defined limit in the event of a contingency.
- Reserve activation: The cost of active reserves is different from generator to generator. This is often neglected by the controllers that activate operational reserves. Using cost information in the reserve activation process is a challenging problem. Paper [I](#) presents an EMPC scheme for activation of reserves. The OCP solved in this EMPC scheme trades off the cost of operation and setpoint tracking.

We have organized this chapter as follows. Section [7.2](#) describes the Faroe Islands' power system and its challenges. Section [7.3](#) defines a single-area model for a small isolated power system. The model consists of a bus connected to a collection of generators and an aggregate of loads. The role of operating reserves in conventional and isolated power systems is discussed in Section [7.4](#). Section [7.4](#) also defines the two main types of operating reserves in isolated power systems: FCR and FRR. Section [7.5](#) describes scheduling of FCR via the ORPP, and Section [7.6](#) gives an overview of EMPC for cost-efficient frequency control using FRR. Section [7.7](#) summarizes the main results in this chapter.

7.2 The Faroe Islands

The Faroe Islands are a group of islands situated in the North Atlantic Ocean. The Faroese power system is isolated; it has no interconnectors to other coun-

tries. The Faroe Islands have a target to increase the amount of renewable energy production from 38% in 2011 to 75% in 2020. The increase in renewable energy is expected to come from a combination of hydro and wind power. In 2009 a joint venture between the Faroe Islands and DONG Energy was formed. The cooperation focuses on methods to integrate renewable energy sources into isolated power systems. Since 2009, DONG Energy has tested several smart grid technologies in the Faroe Islands [Twe13]. This includes the proposed ORPP.

The Faroe Islands are inhabited by almost 50,000 people, and the total area is approximately 1,400 km². The Faroe Islands' electricity demand varies from 15 MW at night time up to 45 MW in the afternoons. In 2014, the installed wind power was 18 MW, corresponding to 122% of the minimum load and 41% of the maximum load. Diesel generators produced 49% of the energy consumed in 2014, while the remaining 51% was produced by hydro generators and wind turbines [SEV15]. There are no liberalized electricity markets in the Faroe Islands. The power system is operated by the municipality-owned company SEV, which is responsible for both generation, transmission and distribution of power.

The Faroe Islands have some of the world's best wind resources, due to their position in the Atlantic Ocean. However, the power system is small and vulnerable with a high number of power outages compared to Continental Europe. Historically, the Faroe Islands have around 30 power outages each year [Twe13]. Power production planning in the Faroe Islands is currently based on manual ad-hoc methods. As more renewable energy is integrated into Faroe Islands' power system, the need for more intelligent power production planning strategies increases.

7.3 Single-Area Model

This section introduces a model of a single-area power system. The level of detail in the model is fit to the proposed control and planning methods. Figure 7.1 is a diagram of the single-area power system. The system consists of three main components: a collection of power generators, a load, and a bus. The balance between production and consumption in the system is

$$\Delta P(t) = \left(\sum_{j \in \mathcal{M}} P_j(t) \right) - P_l(t), \quad (7.1)$$

where $P_j(t)$ is the power production of generator j , and $P_l(t)$ is the system load. We use the swing equation for a synchronous machine to model the frequency in

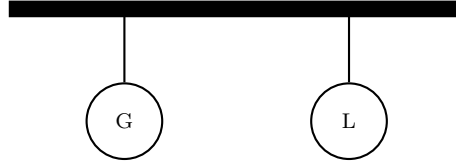


Figure 7.1: Schematic diagram of the single-area power system. The system consists of a bus connected to a collection of generators (G) and an aggregate of loads (L).

the system [And12a, KBL94]. The equation is written as an ordinary differential equation (ODE) in the form

$$\dot{f}(t) = \frac{(f^{\text{nom}})^2}{2HRf(t)} \Delta P(t), \quad (7.2)$$

where

$$H = \sum_{j \in \mathcal{M}} H_j R_j / R, \quad R = \sum_{j \in \mathcal{M}} R_j. \quad (7.3a)$$

In (7.2), $f(t)$ [Hz] is the system frequency, and f^{nom} [Hz] is the nominal frequency. Moreover, H_j [s] is the constant of inertia of generator j , and R_j [MVA] is the rated power of generator j . Model (7.2) assumes that $f_j(t) = f(t)$ for all $j \in \mathcal{M}$, i.e. that the power system is a single-bus system with no line capacity constraints or transmission losses. This assumption can be justified for highly meshed systems, where the relative impedances between nodes in the system are small [Lal05, And12a, UBA14, ORF⁺14, HTM91, KO96]. The Faroese power system is a fairly meshed system, where line capacity constraints and transmission losses are negligible for the applications presented in this chapter. Model (7.2) also assumes that the loads in the system are frequency-independent, i.e. load-damping is neglected. This is a conservative assumption for most control and planning applications, since frequency-dependent loads have a stabilizing effect on the frequency [And12a].

7.4 Operating Reserves

Operating reserves are activated to balance production and consumption in real-time. The European network of transmission system operators (ENTOSO-E) has defined the following three main types of operating reserve [EE12]:

- Frequency containment reserve (FCR): Reserve for containment of frequency deviations (fluctuations) that maintains the power balance in the

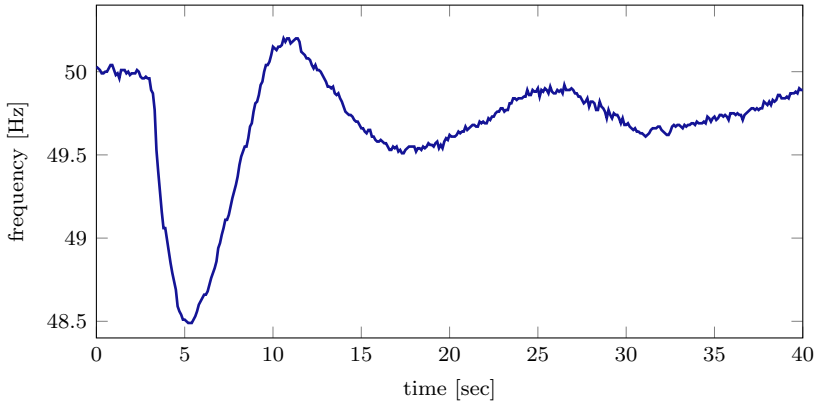


Figure 7.2: Frequency drop in the Faroese power system after intentionally tripping a generator, October 2012.

whole synchronously interconnected system. Activation of FCR results in a restored power balance at a frequency that deviates from the nominal frequency. Activation time for FCR is typically up to 30 seconds. The power generators activate FCR automatically and autonomously using local frequency-based proportional controllers. The FCR is also referred to as the primary reserve.

- Frequency restoration reserve (FRR): Reserve for restoring the frequency to its nominal value. Activation time for FRR is typically up to 15 minutes. The power generators activate FRR manually or automatically. The FRR is also referred to as the secondary reserve.
- Replacement reserve (RR): Reserve for restoring the required level of FCR and FRR. Activation time for RR is typically from 15 minutes up to a number of hours. The RR is also referred to as the tertiary reserve.

The ENTOSO-E reserve specifications are tailored to Continental Europe. In small isolated power systems, the reserve requirements are more strict. Fig. 7.2 shows the frequency in the Faroese power system after intentionally tripping a generator at the Sund power plant in October 2012 [Twe13]. The generator trips around $t = 3$ seconds. Approximately 12% of the total power production in the system is lost due to the generator trip. As a result, the frequency drops more than 1.5 Hz in 3 seconds. In the Faroe Islands, frequency drops of more than 2 Hz are critical. Since the frequency can drop at a rate of 0.5 Hz/s, FCR has to be available within a few seconds to keep the system stable. The nominal frequency in the Faroe Islands' power system is 50Hz. Fig. 7.3 shows a reserve activation diagram for Continental Europe and for the Faroe Islands. Due to the

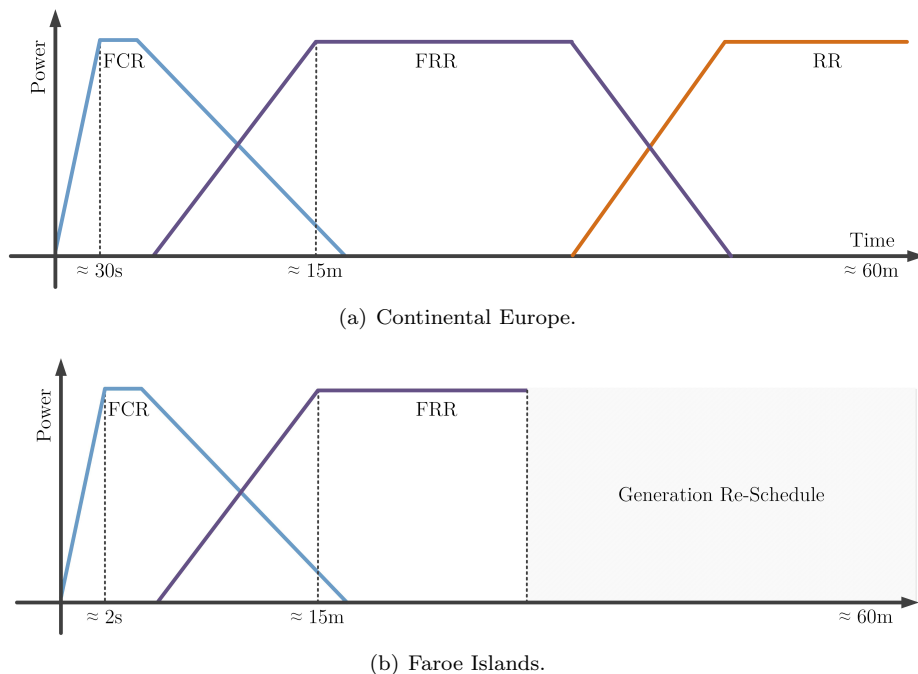


Figure 7.3: Reserve activation diagram.

limited generation capacity, RR is not considered in the Faroe Islands. Instead, a re-optimization of the production plan is performed to restore the FCR and the FRR to their original levels.

7.5 Unit Commitment

The UC problem is solved to determine an hours-ahead production plan for the system generators. The production plan includes the amount of reserve each generator should provide. In contingency-constrained UC problems, the production plan is required to be able to withstand a number of pre-defined contingencies. This means that the system frequency must remain within a safe operating range, in the event of a pre-defined contingency. In small isolated power systems, the frequency dynamics (7.2) depends significantly on the committed power generators [VFF15, SVB⁺15]. This dependence is important to consider in contingency-constrained UC problems for small isolated power systems. The ORPP is a contingency-constrained UC problem, which accounts

for the system frequency dynamics in an explicit way. Minimum frequency constraints are formulated using a model of the system inertia and an FCR activation model for each power generator. The advantages of the ORPP are that it can be formulated as a single MILP, it does not impose any strict assumptions on the generators, and that the parameters in the FCR activation model are simple to obtain. Finally, the ORPP does not require any simulation model of the system.

This section gives an overview of the ORPP. In this thesis, contingencies only refer to loss of power generators. The ORPP generalizes to other types of contingencies as well. Paper H provides proofs and details.

7.5.1 System Dynamics

To determine the minimum frequency resulting from a contingency, we consider the model (7.2). Let $t = 0$ denote the time at which the contingency occurs. The generators that fail during the contingency are indexed by the subset

$$\bar{\mathcal{M}} \subseteq \mathcal{M}.$$

Prior to a contingency, the system is in steady-state. This means that $\Delta P(t) = 0$ for $t < 0$. The power lost in the contingency is

$$P^{\text{lost}} = \sum_{j \in \bar{\mathcal{M}}} P_j^{\text{lost}}.$$

P_j^{lost} is the power production of generator j prior to the contingency. Generators that trip do not contribute to the system inertia. Consequently, H and R in (7.3) are computed as

$$H = \sum_{j \in \mathcal{M} \setminus \bar{\mathcal{M}}} H_j R_j / R, \quad (7.4a)$$

$$R = \sum_{j \in \mathcal{M} \setminus \bar{\mathcal{M}}} R_j. \quad (7.4b)$$

Define the total amount of active FCR

$$P^{\text{FCR}}(t) = \sum_{j \in \mathcal{M}} P_j^{\text{FCR}}(t). \quad (7.5)$$

$P_j^{\text{FCR}}(t)$ is the active FCR at power generator j . Using (7.2), we get

$$\dot{f}(t) = \frac{(f^{\text{nom}})^2}{2HRf(t)} (P^{\text{FCR}}(t) - P^{\text{lost}}), \quad (7.6)$$

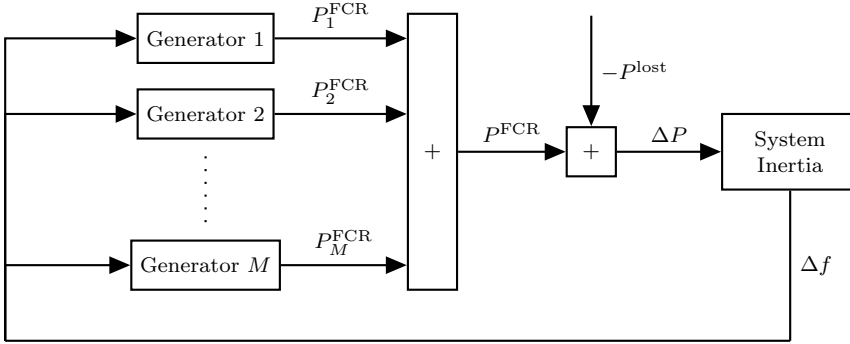


Figure 7.4: Block diagram of the coupled frequency and generator FCR dynamics.

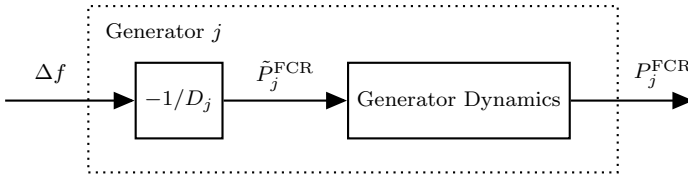


Figure 7.5: Generator FCR activation diagram.

Equation (7.6) is a model of the system frequency in the seconds that follow a contingency. The FRR is activated at a much slower time scale than the FCR. Therefore, FRR is not included in (7.6).

For $t = 0$, the active FCR is zero and $f'(t) < 0$. As time increases, the frequency begins to deviate from the nominal frequency. The generators respond to frequency deviations by activating FCR. The FCR is activated locally at each power generator via frequency-based proportional controllers [And12a, KBL94, Deb88, WW13]. The desired level of active FCR (FCR setpoint) for each generator is

$$\tilde{P}_j^{\text{FCR}}(t) = -(1/D_j) \Delta f(t), \quad j \in \mathcal{M}. \quad (7.7)$$

D_j is the droop of generator j , and $\Delta f(t) = f(t) - f^{\text{nom}}$ is the frequency deviation from the nominal frequency. Fig. 7.4 is a block diagram of the coupled frequency and generator FCR dynamics. Fig. 7.5 illustrates the relationship between the frequency deviation, Δf , the FCR setpoint, $\tilde{P}_j^{\text{FCR}}(t)$, and the active FCR, $P_j^{\text{FCR}}(t)$. The dynamics relating the FCR setpoint and the active FCR are described later in this section.

Provided that the system is stable, the frequency settles at a new steady-state

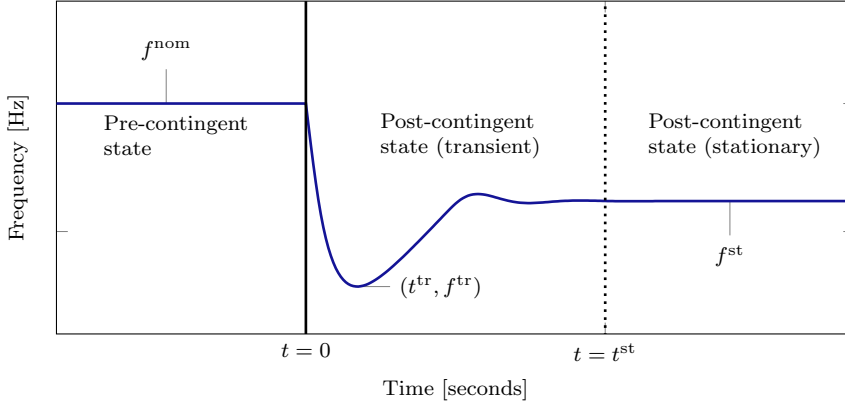


Figure 7.6: Frequency dynamics. The minimum frequency occurs during the transient phase of the post-contingent state.

$f(t) = f^{\text{st}} < f^{\text{nom}}$, for some $t = t^{\text{st}}$ after a contingency has occurred. Fig. 7.6 illustrates a typical system frequency response to a contingency. We refer to the state of the system prior the contingency as the pre-contingent state, and the state of the system after the contingency as a post-contingent state. In the pre-contingent state $f(t) = f^{\text{nom}}$. The post-contingent state is divided into a transient phase and a stationary phase. In the transient phase, the frequency drops to its minimum value f^{tr} , and it then returns to the steady-state f^{st} . The minimum frequency, f^{tr} , may be significantly smaller than the steady-state frequency, f^{st} . The offset $f^{\text{st}} - f^{\text{nom}}$ is eliminated by activating FRR.

Define the steady-state values

$$\begin{aligned}\tilde{P}_j^{\text{FCRst}} &= \tilde{P}_j^{\text{FCR}}(t), & j \in \mathcal{M}, \\ P_j^{\text{FCRst}} &= P_j^{\text{FCR}}(t), & j \in \mathcal{M},\end{aligned}$$

for $t \geq t^{\text{st}}$. Equation (7.7) shows that the steady-state FCR setpoint for each generator is

$$\tilde{P}_j^{\text{FCRst}} = -(1/D_j)(f^{\text{st}} - f^{\text{nom}}), \quad j \in \mathcal{M}.$$

The active FCR at generator j is equal to the minimum of 1) its steady-state FCR setpoint, and 2) the maximum amount of FCR that the generator can deliver. This is written as

$$P_j^{\text{FCRst}} = \min\left(\tilde{P}_j^{\text{FCRst}}, \overline{P}_j^{\text{FCR}}\right), \quad j \in \mathcal{M}, \quad (7.8)$$

where $\overline{P}_j^{\text{FCR}}$ is the maximum amount of FCR that can be activated at generator j . This limit depends on the generator capabilities and the pre-contingent state

of the generator, e.g. a generator that operates at its maximum capacity limit cannot increase its production further.

For convenience, we define the energy contribution from active FCR as

$$E_j^{\text{FCR}}(t) = \int_0^t P_j^{\text{FCR}}(\tau) d\tau, \quad j \in \mathcal{M}, \quad (7.9)$$

and the sum of FCR energy as

$$E^{\text{FCR}}(t) = \sum_{j \in \mathcal{M}} E_j^{\text{FCR}}(t). \quad (7.10)$$

References [RRAG12, GBAR05, RG05, GA14] model (7.8) using mixed-integer constraints. This makes it possible to include constraints for the stationary frequency, f^{st} , in the UC problem. The underlying assumption is that the power system remains in stable operation during the transient part of the post-contingent state. This is often not the case for small isolated power systems, as the minimum frequency, f^{tr} , is critical in such systems. The ORPP includes constraints for f^{tr} .

The minimum frequency, f^{tr} , occurs during the transient part of the post-contingent state. Equation (7.8) is a model for the stationary part of the post-contingent state. Paper H models the transient part of the post-contingent state as a system of ODEs in the form

$$\begin{bmatrix} \mathcal{F}(P^{\text{FCR}}, f, \dot{f}) \\ \mathcal{G}_1 \left(f, P_1^{\text{FCR}}, \dot{P}_1^{\text{FCR}}, \dots, (P_1^{\text{FCR}})^{(n_1)} \right) \\ \vdots \\ \mathcal{G}_M \left(f, P_M^{\text{FCR}}, \dot{P}_M^{\text{FCR}}, \dots, (P_M^{\text{FCR}})^{(n_M)} \right) \end{bmatrix} = \begin{bmatrix} 0 \\ 0 \\ \vdots \\ 0 \end{bmatrix}, \quad (7.11)$$

where $(P_j^{\text{FCR}})^{(n_j)}$ is the n_j 'th derivative of $P_j^{\text{FCR}}(t)$. Moreover

$$\mathcal{F}(P^{\text{FCR}}, f, \dot{f}) = 0, \quad (7.12)$$

is a representation of the frequency dynamics (7.6), where

$$\mathcal{F}(P^{\text{FCR}}, f, \dot{f}) = \dot{f}(t) - \frac{(f^{\text{nom}})^2}{2HRf(t)} (P^{\text{FCR}}(t) - P^{\text{lost}}). \quad (7.13)$$

Finally, the ODE

$$\mathcal{G}_j \left(f, P_j^{\text{FCR}}, \dot{P}_j^{\text{FCR}}, \dots, (P_j^{\text{FCR}})^{(n_j)} \right) = 0, \quad (7.14)$$

is a dynamic model that maps the frequency deviation, Δf , to the active FCR at generator j , P_j^{FCR} , i.e. a model of the dashed block in Fig. 7.5. As an example, consider the case where the generator dynamics are first-order systems in the form

$$T_j(s) = \frac{1}{\tau_j s + 1}, \quad j \in \mathcal{M}. \quad (7.15)$$

For this case

$$\mathcal{G}_j \left(f, P_j^{\text{FCR}}, \dot{P}_j^{\text{FCR}} \right) = \tau_j \dot{P}_j^{\text{FCR}}(t) + P_j^{\text{FCR}}(t) - \tilde{P}_j^{\text{FCR}}(t), \quad j \in \mathcal{M}.$$

where $\tilde{P}_j^{\text{FCR}}(t) = -\frac{1}{D_j} \Delta f(t)$. The model (7.14) is general enough to represent the generators in e.g. [AG14, EMB09, OO96, CB12]. The solution of (7.11) is the frequency, $f(t)$, and the active FCR levels, $P_1^{\text{FCR}}(t), \dots, P_M^{\text{FCR}}(t)$, that follow a contingency.

7.5.2 Minimum Frequency Conditions

Define the minimum frequency condition

$$\min_{t \geq 0} f(t) = f^{\text{tr}} \geq \underline{f} \quad (7.16)$$

where \underline{f} is the lower acceptable limit for the system frequency. Define t^{tr} to be the first time instant at which the power balance is restored

$$t^{\text{tr}} = \min \{ t \mid P^{\text{FCR}}(t) - P^{\text{lost}} = 0 \}. \quad (7.17)$$

Under a simple stability condition it holds that $f(t^{\text{tr}}) = f^{\text{tr}}$. Therefore, a sufficient condition for (7.16), is

$$f(t^{\text{tr}}) \geq \underline{f}. \quad (7.18)$$

Evaluating (7.18) requires the solution of the generally non-linear system (7.11), and subsequent computation of t^{tr} via (7.17). Since the UC problem is an MILP, the condition (7.18) cannot be included directly in this problem. The ORPP is based on a set of conservative conditions derived from (7.18). To state these conditions, define $\mathcal{P}_j^{\text{FCR}}(t; \tilde{f})$ as the solution of (7.14) with the system frequency, f , replaced by the function \tilde{f} . Accordingly, introduce

$$\mathcal{E}_j^{\text{FCR}}(t; \tilde{f}) = \int_0^t \mathcal{P}_j^{\text{FCR}}(\tau; \tilde{f}) d\tau, \quad j \in \mathcal{M}, \quad (7.19)$$

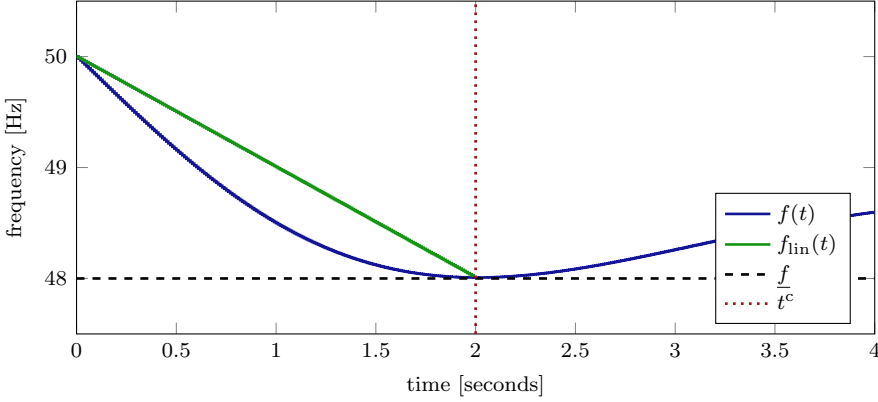


Figure 7.7: The affine function that contains $(0, f^{\text{nom}})$ and (t^c, \underline{f}) is an upper bound for $f(t)$ in the interval $0 \leq t \leq t^{\text{tr}}$.

and the sums

$$\mathcal{P}^{\text{FCR}}(t; \tilde{f}) = \sum_{j \in \mathcal{M}} \mathcal{P}_j^{\text{FCR}}(t; \tilde{f}),$$

$$\mathcal{E}^{\text{FCR}}(t; \tilde{f}) = \sum_{j \in \mathcal{M}} \mathcal{E}_j^{\text{FCR}}(t; \tilde{f}).$$

Note that given $f = \tilde{f}$, ODEs in the form (7.14) become decoupled in $j \in \mathcal{M}$. Define the affine function

$$f_{\text{lin}}(t) = (1 - t/t^c) f^{\text{nom}} + (t/t^c) \underline{f}, \quad (7.20)$$

where t^c is a user-defined parameter. The function f_{lin} provides an upper bound for the frequency, f , in the interval $0 \leq t \leq t^{\text{tr}}$. Fig. 7.7 illustrates this property of f_{lin} , in a simulated contingency example where $t^c = 2\text{s}$ and $\underline{f} = 48\text{Hz}$.

Paper H shows that under reasonable assumptions about \mathcal{P}^{FCR} , the conditions

$$\mathcal{E}^{\text{FCR}}(t; f_{\text{lin}}) + \Delta E^{\text{rot}} \geq P^{\text{lost}} t, \quad t \leq t^c, \quad (7.21a)$$

$$\mathcal{P}^{\text{FCR}}(t^c; f_{\text{lin}}) \geq P^{\text{lost}}, \quad (7.21b)$$

are sufficient conditions for the minimum frequency condition (7.18). Condition (7.21a) ensures that $f(t) \geq \underline{f}$ for $t \leq t^c$, i.e. that the frequency is above \underline{f} for $0 \leq t \leq t^c$. The parameter ΔE^{rot} is related the system inertia. Condition (7.21b) ensures that $t^{\text{tr}} \leq t^c$, i.e. that the minimum frequency occurs before time t^c .

The user-defined parameter t^c is an upper bound for the time at which the minimum frequency occurs. As the power generators activate FCR in proportion to the frequency deviation, the function $\mathcal{E}^{\text{FCR}}(t; f_{\text{lin}})$ is expected to increase as t^c decreases. Consequently, condition (7.21a) becomes less strict when t^c is small. When t^c is small, condition (7.21b) becomes more strict, since the FCR activation time is limited to t^c . The choice of t^c should balance these considerations. The conditions (7.21a) and (7.21b) only need to hold for a single value of t^c , in order to be sufficient for the minimum frequency constraint (7.18).

Conditions (7.21a) and (7.21b) include terms that can be derived from the functions $\mathcal{P}_1^{\text{FCR}}(t; f_{\text{lin}}), \dots, \mathcal{P}_M^{\text{FCR}}(t; f_{\text{lin}})$. The function $\mathcal{P}_j^{\text{FCR}}(t; f_{\text{lin}})$ is the active FCR at generator j in response to the affine frequency drop defined by (7.20). This function depends on the dynamics of the power generator, and the pre-contingent state of the generator. We introduce the notation

$$\mathcal{P}_j^{\text{FCR}}(t; f_{\text{lin}}) = \mathcal{I}(\delta P_j^{\text{FCR}}(t)), \quad j \in \mathcal{M}, \quad (7.22)$$

where $\delta P_j^{\text{FCR}}(t)$ is the amount of active FCR at generator j in response to (7.20), and \mathcal{I} accounts for the implicit limits on $\delta P_j^{\text{FCR}}(t)$ due to the pre-contingent state of the generator. The function $\delta P_j^{\text{FCR}}(t)$ is the open-loop FCR response of power generator j , when $f = f_{\text{lin}}$. This function can be identified based on simulated or experimental data.

7.5.3 Implementation

The ORPP determines a production plan for the system generators. The production plan is optimized over the horizon

$$T = [0, t_s, 2t_s, \dots, Kt_s]. \quad (7.23)$$

t_s [min] is the sampling time and K is the number of time steps. The set of time step indices is denoted

$$\mathcal{K} = \{1, 2, \dots, K\}. \quad (7.24)$$

Table 7.1 lists the ORPP parameters and Table 7.2 lists the ORPP decision variables. The ORPP may be solved in a receding horizon manner to account for updated forecasts of e.g. the wind power production. Paper J develops a computationally efficient EMPC scheme for this approach.

This section describes the implementation of contingency constraints in the ORPP. We refer to Paper H for a full description of the ORPP. The ORPP

Table 7.1: ORPP parameters.

Parameter	Description	Units
d_k	Demand forecast	MW
c_j^P	Production cost	EUR/($t_s \cdot$ MW)
c_j^{on}	Fixed run cost	EUR/ t_s
$(c_j^{\text{su}}, c_j^{\text{sd}})$	Start-up/shut-down cost	EUR
$(c_j^{\text{FRR}}, c_j^{\text{FCR}})$	Reserve capacity costs	EUR/($t_s \cdot$ MW)
$(\underline{p}_j^t, \bar{p}_j^t)$	Technical production limits	MW
$(\underline{p}_j^f, \bar{p}_j^f)$	Forecasted production limits	MW
$(\underline{e}_j, \bar{e}_j)$	Energy limits	MWh
$(\bar{r}_j^{\text{FRR}}, \bar{r}_j^{\text{FCR}})$	Reserve limits	MW
$w_{j,k}$	Disturbance forecast	MW
D_j	Droop	Hz/MW
$I_{l,j}^c$	Contingency matrix	u.l.
Δe_j^{rot}	Rotational energy available	kWh
$\delta p_{j,w}^{\text{FCR}}$	FCR activation parameters	MW
t_w^{FCR}	Discretization points	s
$v_{j,0}^{\text{on}}$	Initial running state	u.l.
$e_{j,0}$	Initial energy level	MWh

Table 7.2: ORPP decision variables.

Variable	Description	Units	Domain
$p_{j,k}$	Production	MW	$\mathbb{R}_{\geq 0}$
$e_{j,k}$	Energy level	MWh	$\mathbb{R}_{\geq 0}$
$v_{j,k}^{\text{on}}$	Running state	u.l.	$\{0, 1\}$
$v_{j,k}^{\text{su}}$	Start-up indicator	u.l.	$\{0, 1\}$
$v_{j,k}^{\text{sd}}$	Shut-down indicator	u.l.	$\{0, 1\}$
$r_{j,k}$	Total reserve	MW	$\mathbb{R}_{\geq 0}$
$r_{j,k}^{\text{FRR}}$	FRR reservation	MW	$\mathbb{R}_{\geq 0}$
$r_{j,k}^{\text{FCR}}$	FCR reservation	MW	$\mathbb{R}_{\geq 0}$
$E_{l,k,w}^{\text{res}}$	Post-contingent FCR energy	kWh	$\mathbb{R}_{\geq 0}$
$\Delta E_{l,k}^{\text{rot}}$	Post-contingent rotational energy	kWh	$\mathbb{R}_{\geq 0}$
$E_{l,k,w}^{\text{con}}$	Post-contingent lost energy	kWh	$\mathbb{R}_{\geq 0}$
$r_{j,k,w}^{\delta p, \text{FCR}}$	Active FCR power	MW	$\mathbb{R}_{\geq 0}$
$r_{j,k,w}^{\delta e, \text{FCR}}$	Active FCR energy	kWh	$\mathbb{R}_{\geq 0}$

considers L different contingencies. The contingencies are indexed by the set

$$\mathcal{L} = \{1, 2, \dots, L\}. \quad (7.25)$$

We define the contingency matrix I^c as

$$I_{l,j}^c = \begin{cases} 1 & \text{if generator } j \in \mathcal{M} \text{ fails in contingency } l \in \mathcal{L}, \\ 0 & \text{otherwise.} \end{cases} \quad (7.26)$$

Minimum frequency constraints based on (7.21) are formulated for each of the contingencies. For this purpose, the FCR activation functions, defined by (7.22), are discretized. Introduce W discretization points $t_1^{\text{FCR}}, \dots, t_W^{\text{FCR}}$ that satisfy

$$t_1^{\text{FCR}} = 0 < t_2^{\text{FCR}} < \dots < t_W^{\text{FCR}} = t^c. \quad (7.27)$$

Also define

$$\delta p_{j,w}^{\text{FCR}} = \delta P_j^{\text{FCR}}(t_w^{\text{FCR}}), \quad j \in \mathcal{M}, \quad w \in \mathcal{W}, \quad (7.28)$$

such that $\delta p_{j,1}^{\text{FCR}}, \dots, \delta p_{j,W}^{\text{FCR}}$ constitute a discretization of the function $\delta P_j^{\text{FCR}}(t)$ in the interval $0 \leq t \leq t^c$. The FCR reservation, $r_{j,k}^{\text{FCR}}$, is restricted by the amount of FCR that can be activated within time t^c . Therefore

$$r_{j,k}^{\text{FCR}} \leq \delta p_{j,W}^{\text{FCR}}, \quad j \in \mathcal{M}, \quad k \in \mathcal{K}. \quad (7.29)$$

The FCR that can be activated at time t_w^{FCR} is modeled as the identified FCR activation parameters $\delta p_{j,w}^{\text{FCR}}$ scaled by $r_{j,k}^{\text{FCR}} / \delta p_{j,W}^{\text{FCR}}$, i.e.

$$r_{j,k,w}^{\delta p, \text{FCR}} = \frac{r_{j,k}^{\text{FCR}}}{\delta p_{j,W}^{\text{FCR}}} \delta p_{j,w}^{\text{FCR}}, \quad j \in \mathcal{M}, \quad k \in \mathcal{K}, \quad w \in \mathcal{W}. \quad (7.30)$$

The energy released during FCR activation is approximated by the area under the line segments that connect the points $r_{j,k,1}^{\delta p, \text{FCR}}, \dots, r_{j,k,W}^{\delta p, \text{FCR}}$. This is expressed as

$$r_{j,k,w}^{\delta e, \text{FCR}} = r_{j,k,w-1}^{\delta e, \text{FCR}} + \lambda (t_w^{\text{FCR}} - t_{w-1}^{\text{FCR}}) r_{j,k,w-1}^{\delta p, \text{FCR}} + \frac{\lambda}{2} (t_w^{\text{FCR}} - t_{w-1}^{\text{FCR}}) (r_{j,k,w}^{\delta p, \text{FCR}} - r_{j,k,w-1}^{\delta p, \text{FCR}}), \quad (7.31)$$

$j \in \mathcal{M}, k \in \mathcal{K}, w \in \mathcal{W} \setminus \{1\}$, and

$$r_{j,k,1}^{\delta e, \text{FCR}} = 0, \quad j \in \mathcal{M}, \quad k \in \mathcal{K}.$$

$\lambda = 5/18$ converts the unit of $r_{j,k,w}^{\delta e, \text{FCR}}$ to $[\text{kW} \cdot \text{h}]$. Fig. 7.8 illustrates the relationship between $\delta P_j^{\text{FCR}}(t)$, $r_{j,k,w}^{\delta p, \text{FCR}}$, $r_{j,k}^{\text{FCR}}$ and $r_{j,k,w}^{\delta e, \text{FCR}}$.

Condition (7.21a) should be satisfied in the discretization points $t_1^{\text{FCR}}, \dots, t_W^{\text{FCR}}$, for each contingency $l \in \mathcal{L}$ and for each time step $k \in \mathcal{K}$. The constraint for this is

$$E_{l,k,w}^{\text{res}} + \Delta E_{l,k}^{\text{rot}} \geq E_{l,k,w}^{\text{con}}, \quad l \in \mathcal{L}, \quad k \in \mathcal{K}, \quad w \in \mathcal{W}. \quad (7.32)$$

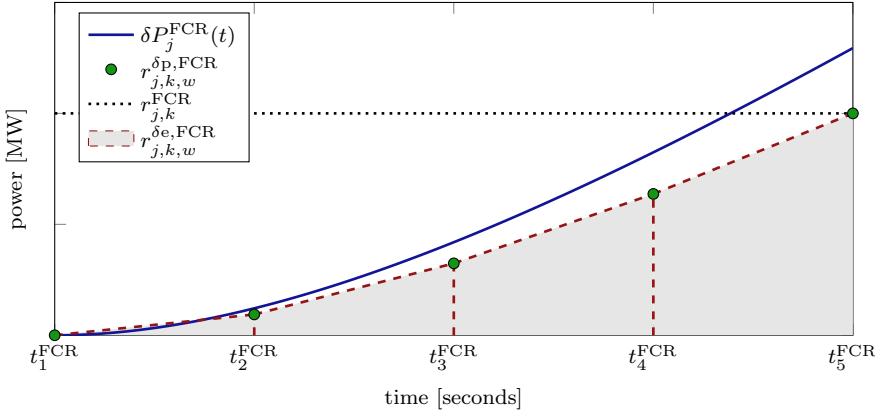


Figure 7.8: Illustration of the relationship between $\delta P_j^{\text{FCR}}(t)$, $r_{j,k,w}^{\delta p, \text{FCR}}$, $r_{j,k}^{\text{FCR}}$ and $r_{j,k,w}^{\delta e, \text{FCR}}$, for a fixed time step $k \in \mathcal{K}$, and a fixed generator $j \in \mathcal{M}$.

$E_{l,k,w}^{\text{res}}$ is the energy provided by the active FCR in time step k , during contingency l , in discretization point w

$$E_{l,k,w}^{\text{res}} = \sum_{j \in \mathcal{M}} (1 - I_{l,j}^c) r_{j,k,w}^{\delta e, \text{FCR}}, \quad l \in \mathcal{L}, \quad k \in \mathcal{K}, \quad w \in \mathcal{W}. \quad (7.33a)$$

$E_{l,k,w}^{\text{con}}$ is the energy lost in time step k , during contingency l , in discretization point w

$$E_{l,k,w}^{\text{con}} = \sum_{j \in \mathcal{M}} I_{l,j}^c p_{j,k} t_m^{\text{FCR}}, \quad l \in \mathcal{L}, \quad k \in \mathcal{K}, \quad w \in \mathcal{W}. \quad (7.33b)$$

$\Delta E_{l,k}^{\text{rot}}$ is the rotational energy available due to the system inertia in time step k , during contingency l

$$\Delta E_{l,k}^{\text{rot}} = \sum_{j \in \mathcal{M}} (1 - I_{l,j}^c) \Delta e_j^{\text{rot}} v_{j,k}^{\text{on}}, \quad l \in \mathcal{L}, \quad k \in \mathcal{K}. \quad (7.33c)$$

Δe_j^{rot} is the rotational energy of generator j , when running. This parameter is computed based on the moment of inertia I_j [$\text{kg} \cdot \text{m}^2$] and the number of poles N_j^p of the generator.

The condition (7.21b) is modeled as

$$\sum_{j \in \mathcal{M}} (1 - I_{l,j}^c) r_{j,k}^{\text{FCR}} \geq \sum_{j \in \mathcal{M}} I_{l,j}^c p_{j,k}, \quad l \in \mathcal{L}, \quad k \in \mathcal{K}. \quad (7.34)$$

Table 7.3: Case study system parameters.

#	Name	Type	I_j	N_j^P	\underline{p}_j^t	\bar{p}_j^t	τ_j
1	Eidisverkid G1	Hydro	5900	8	2.7	6.8	3
2	Eidisverkid G2	Hydro	5900	8	2.7	6.8	3
3	Eidisverkid G3	Hydro	8050	8	3	7.7	3
4	Strond G1	Diesel	2116	14	1	2.2	2
5	Strond G2	Diesel	4375	10	1.3	3.6	2
6	Sundsverkid G1	Diesel	23301	12	4	8.1	5
7	Sundsverkid G2	Diesel	225500	40	7	12.7	5
8	Heygaverkid G1	Hydro	4875	8	2.1	5.3	3
9	Neshagi	Wind	-	-	0	10	0.5

In addition to (7.34), we require that sufficient FRR is available, such that the frequency can be restored to its nominal value. This is expressed similarly to (7.34), expect that we replace $r_{j,k}^{\text{FCR}}$ by $r_{j,k}^{\text{FRR}}$. Paper I presents an EMPC scheme for activation of FRR.

Constraints (7.32) and (7.34) represent the minimum frequency conditions (7.21a) and (7.21b), respectively. Condition (7.21a) needs to hold for all $t \leq t^c$. Constraint (7.32) only ensures that (7.21a) is satisfied for $t = t_1^{\text{FCR}}, \dots, t_W^{\text{FCR}}$. The number and distribution of discretization points are therefore important. In practice, 2-5 evenly spaced points are usually adequate. Provided that there are sufficient discretization points, (7.32) and (7.34) ensure that $f(t) \geq \underline{f}$ in every post-contingent state. Constraint (7.32) may be verified after solving the ORPP for a fine grid of t -values. If it is violated for some t , the ORPP is re-solved with this point included as an extra discretization point. Constraint (7.34) does not depend on the discretization points.

7.5.4 Faroe Islands Case Study #1

Paper H tests the ORPP based on a Faroe Islands simulation case study. A reduced system consisting of $M = 9$ generators is considered. The generator dynamics are modeled as first order systems in the form (7.15). Upper and lower limits for the amount of FCR a generator can provide are accounted for by including saturation limits in the generator model. Table 7.3 lists the case study system parameters. The sampling time is $t_s = 15$ min, and $t^c = 2$ s. We found that $t^c = 2$ s provides a good balance for satisfying both of the minimum frequency conditions in (7.21). The production plan is optimized over 6 hours, corresponding to $K = 24$ time steps. Fig. 7.9 shows the demand forecast,

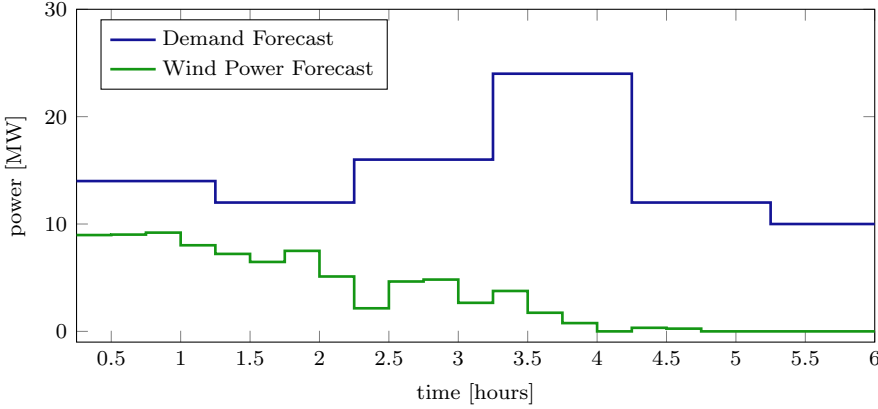


Figure 7.9: Case study demand and wind power forecasts.

and the (maximum) wind power forecast. The wind power production is not allowed to be reduced by more than 5MW compared to the potential wind power production (curtailment limit of 5MW). The production costs and the start-up costs for the generators are

$$c^P = (16.5, 17, 17.5, 18, 18, 18, 18, 16, 1),$$

$$c^{su} = (3000, 3000, 3000, 3000, 3200, 3200, 3200, 3100, 100).$$

The costs c^{on} , c^{sd} , c^{FRR} , and c^{FRR} are zero in this case study. Wind turbines provide the cheapest source of energy. Hydro generators are cheaper to use than diesel generators, when available, but they have limited reservoirs. For simplicity, we consider an example with unlimited reservoirs, and we define the disturbance, $w_{j,k}$, to be zero for all $j \in \mathcal{M}$ and $k \in \mathcal{K}$. Except for Neshagi, the power generators can deliver 100% of their technical maximum production in FCR and FRR. Neshagi does not have any FCR capabilities. The droop is 5% for all the power generators. The minimum frequency is $\underline{f} = 48\text{Hz}$, and the nominal frequency is $f^{\text{nom}} = 50\text{Hz}$.

The functions $\delta P_1^{\text{FCR}}, \dots, \delta P_M^{\text{FCR}}$ are identified based on the generators' simulated open-loop FCR response to the affine frequency drop (7.20). The same approach can, and is, used in actual experiments in the Faroe Islands. The FCR activation functions are discretized using $W = 4$ discretization points with $t^{\text{FCR}} = (0, 2/3, 4/3, 2)$. Figure 7.10 illustrates the identified FCR activation functions. The number of contingencies is $L = 7$ in this case study, and the contingency matrix, (7.26), is

$$I^c = [I_7 \quad \mathbf{0}],$$

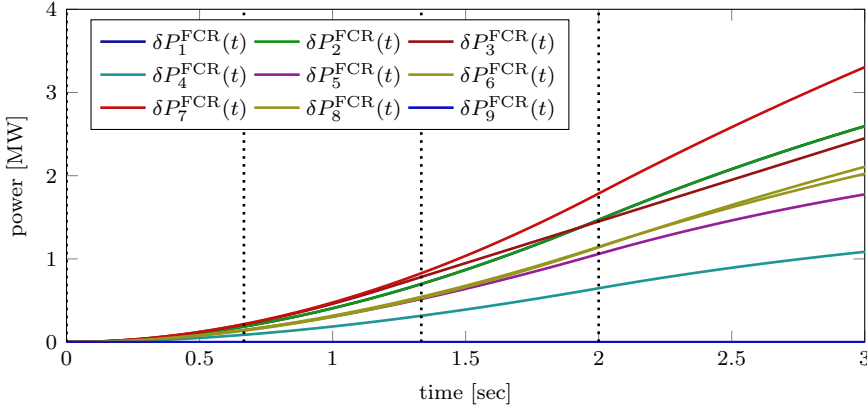


Figure 7.10: The FCR activation functions defined by (7.22). The discretization points $t^{\text{FCR}} = (0, 2/3, 4/3, 2)$ are indicated by vertical black lines.

where I_7 is the identity matrix of size 7. This means that any (single) of the 7 first generators listed in Table 7.3 may trip within one of the 15-minute sampling intervals, during the 6-hour planning horizon. The production plan obtained by solving the ORPP can withstand any of these 7 contingencies. The CPU time to solve the ORPP is approximately 5 seconds using CPLEX.

Paper H compares the ORPP to the UC problem presented in [RRAG12,GBAR05, RG05,GA14], which we refer to as the baseline UC problem (BLUC). The BLUC only includes constraints for the steady-state frequency, f^{st} . Fig. 7.11 illustrates the ORPP production plan and the BLUC production plan. The main differences between the two production plans occur between hours 1-2 and hours 3.5-4.5. Between hours 1-2, the ORPP keeps more generators running than the BLUC, at the expense of reduced wind power production. This increases the system inertia, as well as the available FCR in the system. Between hours 3.5-4.5, Eidisverkid G1 and Heygaverkid G1 are operated at their limits for the BLUC. These generators back-off from their constraints for the ORPP. This increases the available FCR in the system. The ORPP increases the power production of the more expensive generator Eidisverkid G2, to compensate for the back-off. The cost associated with the BLUC is EUR 89039 and the cost associated with the ORPP is EUR 91680. This corresponds to a cost increase of less than 3% for the ORPP.

Contingencies are simulated by numerical solution of the system (7.11). A simulation is performed for each contingency $l \in \mathcal{L}$ and for each time step $k \in \mathcal{K}$. We record the minimum frequency, f^{tr} , and the stationary frequency, f^{st} , for

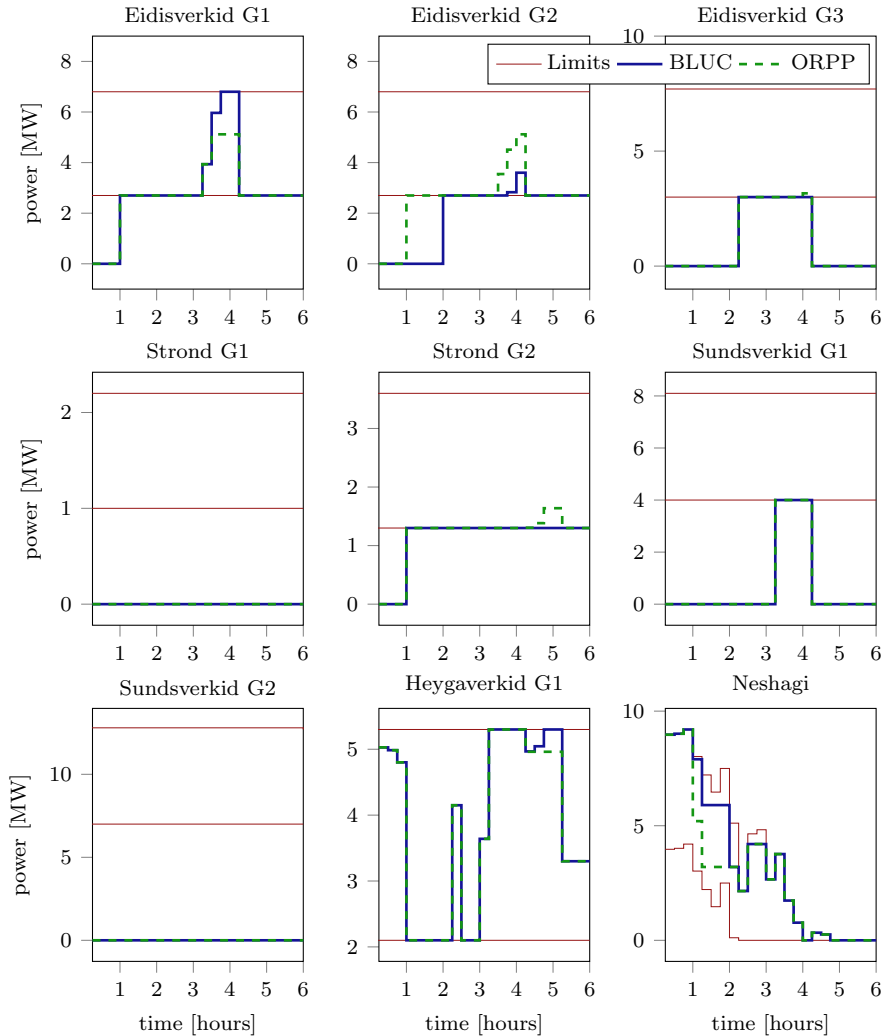


Figure 7.11: Solution of the ORPP and the BLUC.

both the ORPP and the BLUC. Fig. 7.12 reports the worst-case frequencies over the contingencies $l \in \mathcal{L}$, for each time step $k \in \mathcal{K}$. The stationary frequency is maintained above 48Hz for both the ORPP and the BLUC. The ORPP keeps the minimum frequency above 48Hz as well. Potential blackouts and power outages are therefore avoided by the ORPP. Between hours 1-2 and hours 3.5-4.5, the minimum frequency drops below 48Hz for the BLUC. In particular, if Eidisverkid G1 trips between hours 1-2, the frequency drops to 47Hz. This is

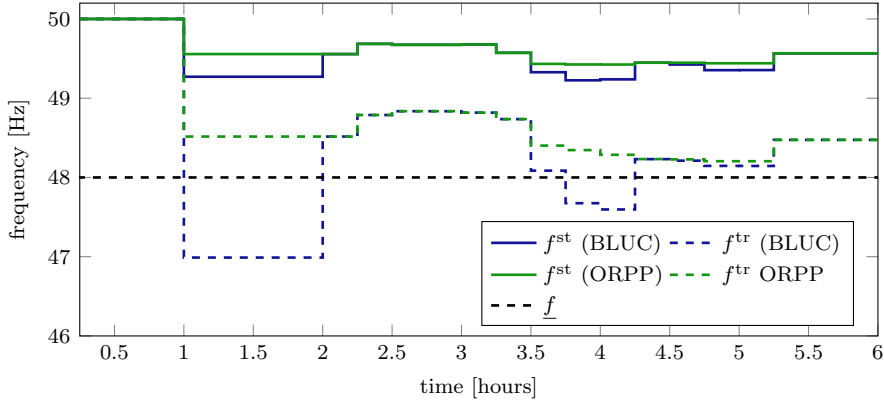


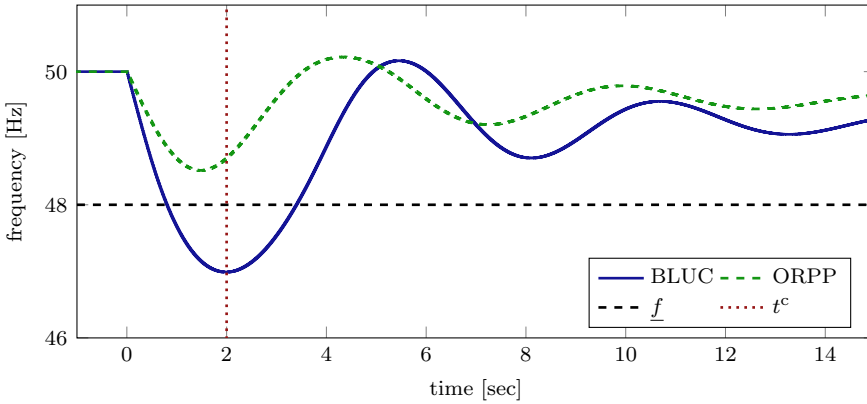
Figure 7.12: Worst-case (stationary and minimum) frequencies over the contingencies $l \in \mathcal{L}$, for each time step $k \in \mathcal{K}$.

very critical for the system stability. Fig. 7.13 illustrates the system frequency and FCR response when Eidisverkid G1 trips between hours 1-2. The actual FCR response, $P^{\text{FCR}}(t)$, and the prediction (7.30) are indicated in Fig 7.13(b). The predicted FCR response underestimates the actual FCR response, without being significantly smaller than the actual FCR response. This indicates that the ORPP is not overly conservative.

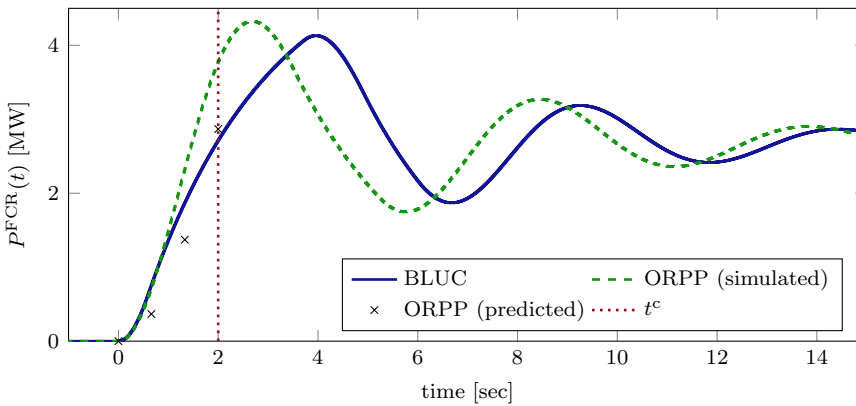
7.6 Frequency Control

The FCR is activated to stabilize the system frequency. The FRR is activated to restore the system frequency to its nominal value. Activation of the FRR is known as automatic generation control (AGC) or as load frequency control (LFC).

Activating reserves has a cost. For generators with a low price of utilization (e.g. wind and hydro turbines), the cost is usually low, and for generators with a high price of utilization (e.g. diesel generators and gas turbines), the cost is usually high. While cost information is included in the UC problem, it is often neglected in the LFC layer. An approximate method to include cost information in the LFC layer is to combine a PI-control structure with so-called participation factors [KNS97, Bev09, Car85, And12a, IKK05]. The participation factor of a generator is a gain that determines its degree of participation in the LFC. The participation factors do not distinguish between up and down regulation, which is a significant economic disadvantage. Moreover, the approach does not consider



(a) System frequency.



(b) System FCR response.

Figure 7.13: System response after Eidisverkid G1 trips (contingency $l = 1$) at hour 1-1.25 (time step $k = 4$).

the frequency dynamics. For example, it is desirable to activate fast (but possibly expensive) generators in situations where the frequency drops at a fast rate. Conversely, slower generators can be activated in situations when the frequency drops at a slow rate. Paper I presents an EMPC scheme for LFC that accounts for both the reserve activation costs and for the system frequency dynamics. The OCP objective function is formulated as a bi-criterion that trades off the cost of operation and setpoint tracking. Setpoint-based MPC have been considered for LFC in [ARF03, KX07, RAF03, VHRW08, MBHH11, MCLA14]. This section provides a summary of the proposed EMPC scheme for cost-effective frequency control.

7.6.1 Model

A combined FCR and FRR model is developed for the single-area system in Fig. 7.1. The model is used for minutes-ahead EMPC of the FRR. On/off decisions are made in advance by solving a UC problem, e.g. the ORPP. This means that unit commitment decisions are fixed in the model. The pre-computed production plan provided by the UC problem is referred to as the nominal production plan. We refer to Paper I for a detailed description of the model.

The system power generators are modelled as state-space systems in the form (2.5). In a continuous-time form, the power generator model is

$$\dot{x}_{g_j}(t) = A_{g_j}x_{g_j}(t) + B_{g_j}u_{g_j}(t), \quad j \in \mathcal{M}, \quad (7.35a)$$

$$z_{g_j}(t) = C_{g_j,z}x_{g_j}(t), \quad j \in \mathcal{M}, \quad (7.35b)$$

where $(A_{g_j}, B_{g_j}, E_{g_j}, C_{g_j,z})$ denote continuous-time state-space matrices. To keep the notation simple, we assume that each generator is a SISO system. $u_{g_j}(t)$ [MW] is the power production setpoint for generator j , and $z_{g_j}(t)$ [MW] is the power production of generator j .

The load in Fig. 7.1 represents an aggregate of all the loads in the system. The aggregate includes the power production of non-controllable power generators, such as non-controllable wind turbines and solar cells. We model the load using a linear state-space model in the form

$$\dot{x}_l(t) = A_lx_l(t) + B_ld_l(t), \quad (7.36a)$$

$$z_l(t) = C_lx_l(t), \quad (7.36b)$$

$d_l(t)$ [MW] is the load setpoint, and $z_l(t)$ [MW] is the load.

The power balance at the bus is

$$z_b(t) = \sum_{j \in \mathcal{M}} z_{g_j}(t) + z_l(t) = \sum_{i \in \mathcal{M}} C_{g_j}x_{g_j}(t) + C_lx_l(t), \quad (7.37)$$

This corresponds to (7.1) with $\Delta P(t) = z_b(t)$, $P_j(t) = z_{g_j}(t)$, and $P_l(t) = -z_l(t)$. Using (7.2), the frequency in the system is modelled as

$$\dot{f}(t) = \frac{(f^{\text{nom}})^2}{2HRf(t)}z_b(t), \quad (7.38)$$

where H and R are computed as in (7.3). The power generator setpoints are composed of two main terms

$$u_{g_j}(t) = \underbrace{\tilde{u}_{g_j}(t)}_{\text{Portfolio Level}} - \underbrace{\frac{1}{D_j}(f(t) - f^{\text{nom}})}_{\text{Generator Level}}, \quad j \in \mathcal{M}. \quad (7.39)$$

The portfolio-level setpoint is determined at a centralized level, in which interactions between the power generators are considered. This component includes the nominal setpoint (production plan), as well as setpoint adjustments provided by active FRR. The generator-level setpoint is the contribution of active FCR. As in (7.7), FCR is activated in direct proportion to frequency deviations from the nominal frequency.

Equations (7.35), (7.36), (7.37), and (7.38), constitute a non-linear model of the single-area power system. Equation (7.39) is a setpoint model that accounts for frequency-based proportional control of FCR. Paper I collects equations (7.35), (7.36), (7.37), (7.38), and (7.39), into a non-linear simulation model. The model is augmented by process and measurement noise. A piecewise constant (unmeasured) disturbance, denoted b_k , is added to the system as well. The random terms model the stochastic nature of renewable energy sources. The non-linear simulation model is linearized for control purposes. The non-linear part of the simulation model is (7.38). Due to tight frequency control via activation of FCR and FRR, it is reasonable to assume that $f(t) \approx f^{\text{nom}}$. Under this assumption, (7.38) can be written as

$$\dot{f}(t) = \frac{f^{\text{nom}}}{2HR} z_b(t), \quad (7.40)$$

or in the state-space form

$$\dot{x}_f(t) = A_f z_b(t), \quad (7.41a)$$

$$z_f(t) = x_f(t), \quad (7.41b)$$

where $z_f(t)$ is the system frequency, and

$$A_f = f^{\text{nom}}/2HS. \quad (7.42)$$

In discrete-time state-space form, the linearized (stochastic) model for the single-area power system is

$$\mathbf{x}_{k+1} = A\mathbf{x}_k + Bu_k + Ed_k + \mathbf{w}_k, \quad (7.43a)$$

$$\mathbf{y}_k = C_y\mathbf{x}_k + \mathbf{v}_k, \quad (7.43b)$$

$$\mathbf{z}_k = C_z\mathbf{x}_k. \quad (7.43c)$$

The process noise and the measurement noise are independent and identically distributed random variables with

$$\mathbf{w}_k \sim N(0, R_w),$$

$$\mathbf{v}_k \sim N(0, R_v).$$

In the system (7.43)

$$u_k = \tilde{u}_{g,k}, \quad d_k = d_{l,k}, \quad \mathbf{x}_k = \begin{bmatrix} x_{g,k} \\ x_{l,k} \\ x_{\Delta f,k} \\ \eta_k \end{bmatrix}, \quad \mathbf{z}_k = \begin{bmatrix} z_{g,k} \\ z_{l,k} \\ z_{b,k} \\ z_{\Delta f,k} \end{bmatrix}, \quad (7.44)$$

where $x_{g,k} = [x_{g_1,k}^T, x_{g_2,k}^T, \dots, x_{g_M,k}^T]^T$, and similarly for $u_{g,k}$ and $z_{g,k}$. Finally

$$z_{\Delta f,k} = x_{\Delta f,k} = z_{f,k} - f^{\text{nom}} = f_k - f^{\text{nom}}.$$

The state variable η_k is included in (7.43) to model piecewise constant disturbances. This makes it possible to estimate and predict the unmeasured disturbance, b_k [PR03, BM07]. We use the Kalman filter defined in Section 3.2 for this purpose.

7.6.2 Nominal Production Plan

The solution of the UC problem provides a nominal production plan for the generators. To account for the nominal production plan in the model (7.43), the input, state, disturbance, and output, are written as

$$u_k = u_k^{\text{nom}} + u_k^{\text{FRR}}, \quad d_k = d_k^{\text{nom}} + d_k^{\text{FRR}}, \quad (7.45a)$$

$$x_k = x_k^{\text{nom}} + x_k^{\text{FRR}}, \quad z_k = z_k^{\text{nom}} + z_k^{\text{FRR}}. \quad (7.45b)$$

The input u_k^{nom} is the pre-computed nominal setpoint, and u_k^{FRR} is the FRR contribution to the setpoint. The FRR contribution, u_k^{FRR} , is computed in real-time using EMPC. The disturbance, d_k , is partitioned into d_k^{nom} , which is known at the time the nominal setpoints are computed, and d_k^{FRR} , which is updated within the proposed EMPC scheme. The nominal state and output, x_k^{nom} and z_k^{nom} , are computed using the state-space model (7.43), with $w_k = v_k = 0$, $u_k = u_k^{\text{nom}}$, and $d_k = d_k^{\text{nom}}$. To keep the presentation simple, the remainder of this section assumes that $u_k^{\text{nom}} = 0$, $d_k^{\text{nom}} = 0$, $x_k^{\text{nom}} = 0$ and $z_k^{\text{nom}} = 0$, i.e. that the nominal production plan is zero. Paper I treats the general case with a non-zero nominal production plan.

7.6.3 Optimal Control Problem

An EMPC scheme is employed to activate FRR. The OCP in this EMPC scheme is defined as

$$\min_{u_k, u_{g,k}, \hat{x}_k, \hat{z}_k} \sum_{k \in \mathcal{N}_0} l_k(u_{g,k}, \hat{z}_{k+1}), \quad (7.46a)$$

$$\text{s.t. } \hat{x}_{k+1} = A\hat{x}_k + Bu_k + Ed_k, \quad k \in \mathcal{N}_0, \quad (7.46b)$$

$$\hat{z}_k = Cz\hat{x}_k, \quad k \in \mathcal{N}_1, \quad (7.46c)$$

$$u_{g,k} = u_k + K\hat{z}_k, \quad k \in \mathcal{N}_0, \quad (7.46d)$$

$$\underline{u}_k \leq u_{g,k} \leq \bar{u}_k, \quad k \in \mathcal{N}_0, \quad (7.46e)$$

where l_k is the stage cost function. The input $u_k = \tilde{u}_{g,k}$ contains the portfolio-level setpoints for the generators. Equations (7.46b) and (7.46c) are the state and output predictions. Equation (7.46d) follows from (7.39). The matrix K is defined such that

$$u_k + K \hat{z}_k = \begin{bmatrix} \tilde{u}_{g_1,k} \\ \tilde{u}_{g_2,k} \\ \vdots \\ \tilde{u}_{M,k} \end{bmatrix} + \begin{bmatrix} -\frac{1}{D_1} \hat{z}_{\Delta f,k} \\ -\frac{1}{D_2} \hat{z}_{\Delta f,k} \\ \vdots \\ -\frac{1}{D_M} \hat{z}_{\Delta f,k} \end{bmatrix}.$$

Equation (7.46d) limits the generator setpoint levels. The limits are time-varying to account for both generator-specific technical limits, as well as limits that are determined by external factors, e.g. the wind speed for wind turbines. The stage cost in the OCP objective function (7.46a) is defined as

$$l_k(u_{g,k}, z_{k+1}) = \beta \varphi^{\text{eco}}(u_{g,k}, z_{k+1}) + (1 - \beta) \varphi^{\text{sp}}(u_{g,k}, z_{k+1}), \quad k \in \mathcal{N}_0. \quad (7.47)$$

The function φ^{eco} is related to the cost of operation and φ^{sp} is a conventional setpoint-based penalty function. The parameter β is a tuning parameter to trade-off cost of operation and setpoint tracking. For the Faroe Islands case study, the cost function φ^{eco} is defined as

$$\varphi^{\text{eco}}(u_{g,k}, z_{k+1}) = r^T |u_{g,k} - u_{g,k-1}| \quad (7.48a)$$

$$+ \bar{c}^T \max(z_{g,k+1}, 0) + \underline{c}^T \max(-z_{g,k+1}, 0) \quad (7.48b)$$

$$+ \bar{q} \max(z_{\Delta f,k+1} - \Delta \bar{f}, 0) + \underline{q} \max(\Delta \underline{f} - z_{\Delta f,k+1}, 0), \quad (7.48c)$$

where r and c are the vectors

$$r = \begin{bmatrix} r_{g_1} \\ r_{g_2} \\ \vdots \\ r_{g_M} \end{bmatrix}, \quad c = \begin{bmatrix} c_{g_1} \\ c_{g_2} \\ \vdots \\ c_{g_M} \end{bmatrix}.$$

The cost function (7.48) consists of three parts. The first term, (7.48a), is an ℓ_1 -regularization term on the input-rate. The parameter r is a price vector associated with wear and tear of the generators. The second two terms, (7.48b), are related to the cost of generation. Let c denote a vector of utilization prices for the generators. The parameter \underline{c} is defined

$$\underline{c} = \begin{bmatrix} 1/c_{g_1} \\ 1/c_{g_2} \\ \vdots \\ 1/c_{g_M} \end{bmatrix}.$$

The price for upward activation of FRR is $\bar{c} = c$. For downward activation of FRR, the price is \underline{c} . We do not use c for downward activation of FRR, to avoid activation of FRR in the nominal case. The final two terms, (7.48c), are related to the cost of frequency deviations. The cost \bar{q} is imposed for frequency deviations larger than \bar{f} , and the cost \underline{q} is imposed for frequency deviations smaller than \underline{f} . The limits $\Delta\underline{f}$ and $\Delta\bar{f}$ are the cut-off frequency deviations, at which critical actions such as load shedding are initiated to avoid a system blackout.

The setpoint-based penalty function, φ^{SP} , is defined as

$$\varphi^{\text{SP}}(u_{g,k}, z_{k+1}) = u_{g,k}^T R^{\text{SP}} u_{g,k} + z_{k+1}^T Q^{\text{SP}} z_{k+1}, \quad (7.49)$$

where R^{SP} and Q^{SP} are weight matrices. The problem (7.46) is as a convex QP. For $\beta = 1$, the quadratic terms (7.49) drop out of the stage cost (7.47). In this special case, the optimization problem is an LP.

7.6.4 Faroe Islands Case Study #2

Paper I presents a Faroe Islands case study with $M = 4$ power generators. A small system is considered to highlight the essential features of the proposed EMPC scheme. A time-varying load over 5 minutes is considered. The load includes non-controllable wind turbines, which give rise to fluctuations from the nominal production plan. In the Faroe Islands, there are several locally owned wind turbines that are not controlled by SEV. Fig. 7.14 illustrates the case study load scenario. The nominal load is $d_k^{\text{nom}} = -21\text{MW}$ over the entire scenario. The load disturbances b_k and d_k^{FRR} are not accounted for in the nominal production plan. A prediction of d_k^{FRR} is available in the EMPC scheme. The unmeasured load disturbance, b_k , is estimated via the Kalman filter. As defined by (7.43), the system is also subject to Gaussian process and measurement noise.

The case study power generators are modeled as first order systems in the form

$$Z_{g_j}(s) = \frac{1}{\tau_{g_j}s + 1} U_{g_j}(s), \quad j \in \mathcal{M}. \quad (7.50)$$

The load has the similar form

$$Z_l(s) = \frac{1}{\tau_l s + 1} U_l(s), \quad (7.51)$$

where $\tau_l < \tau_{g_j}$, for $j \in \mathcal{M}$. We use $\tau_l = 0.5\text{s}$. The transfer functions (7.50) and (7.51) are realized in the state-space forms, (7.35) and (7.36), respectively.

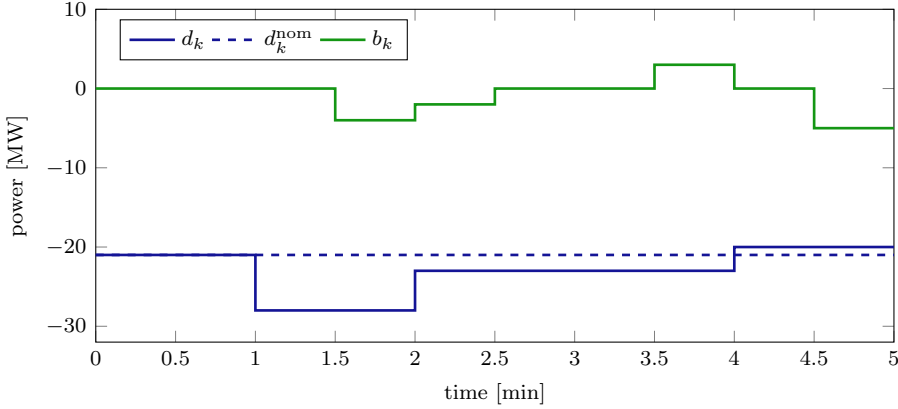


Figure 7.14: Case study load scenario. The UC problem is solved based on the nominal load forecast d^{nom} . The proposed EMPC scheme is a closed-loop strategy for activation of FRR, considering feedback and updated forecasts.

Table 7.4: Case study system parameters.

#	Type	H_j [s]	D_j [Hz/MW]	$\underline{u}_{j,k}$ [MW]	$\bar{u}_{j,k}$ [MW]	τ_{g_j} [s]
1	Hydro	3.1	3/20	3	20	8
2	Hydro	2.5	1/2	2	6	6
3	Diesel	1.8	3/5	1	5	1
4	Diesel	8.2	1/5	5	15	3

Table 7.4 lists the case study system parameters. The data represents actual generators in the Faroe Islands. The inertia provided by each generator is scaled up to better represent a full-scale system. The generator rating, R_j , is defined to have the same magnitude as $\bar{u}_{j,k}$. The price of utilization for the generators in EUR/MWh, are 4, 8, 80, and 60. The input-rate price for each generator is 0.05 EUR/MW. The hydro generators have a lower production cost than the diesel generators. Within each generator group, the smaller and faster generator has the highest utilization cost.

The nominal setpoint is $u_{g,k}^{\text{nom}} = [8, 6, 1, 6]$. The simulation is started from steady-state, such that $z_{g,k}^{\text{nom}} = u_{g,k}^{\text{nom}}$. The sampling time is $T_s = 0.5\text{s}$ and the length of the prediction horizon is $N = 80$ time steps. The cut-off frequency deviations are $\Delta\bar{f} = -\Delta f = 1\text{Hz}$. Frequency deviations larger than $\pm 1\text{Hz}$ have a very high cost. We define the price to be 1000 EUR/(Hz · s). The weight

Table 7.5: Cost of operation and frequency deviations for the different EMPC trade-off specifications, and for PI-control.

	Cost	$\min\{\Delta f\}$	$\max\{\Delta f\}$
EMPC: $\alpha = 0$	15.8	-0.39	0.43
EMPC: $\alpha = 0.1$	10.9	-0.45	0.48
EMPC: $\alpha = 0.2$	7.20	-0.48	0.61
EMPC: $\alpha = 0.3$	4.67	-0.52	0.76
EMPC: $\alpha = 0.5$	2.68	-0.76	0.87
EMPC: $\alpha = 1$	2.10	-1.01	0.91
PI control	14.2	-1.19	1.10

specifications in (7.49) are $Q^{\text{sp}} = \text{blkdiag}(Q_g^{\text{sp}}, Q_l^{\text{sp}}, Q_b^{\text{sp}}, Q_{\Delta f}^{\text{sp}})$, and $R^{\text{sp}} = R_g^{\text{sp}}$. We use $Q_g^{\text{sp}} = I$, $Q_l^{\text{sp}} = Q_b^{\text{sp}} = 0$, $Q_{\Delta f}^{\text{sp}} = 100$, and $R_g^{\text{sp}} = I$. This means that deviations from the nominal frequency have a large penalty, compared to deviations from the generators' production plan. We scale the weights Q^{sp} and R^{sp} by a factor $T_s/3600$, such that the economic criterion, (7.48), and the setpoint-based criterion, (7.49), are in a comparable scale.

Fig. 7.15 and Fig. 7.16 illustrate closed-loop simulations for $\beta = 0$, $\beta = 0.5$ and $\beta = 1$. Fig. 7.15 shows the generator power production levels, and Fig. 7.16 shows the system frequency deviation. The case $\beta = 0$ corresponds to setpoint-based MPC, and $\beta = 1$ corresponds to CE-EMPC with a pure economic objective function. A frequency-based PI-controller is also tested. For $\beta = 0$, all generators with free generation capacity activate a significant amount of FCR. Similar behavior is observed for the PI-controller. For $\beta = 0.5$, low-cost generators are prioritized over high-cost generators, at the expense of slightly larger frequency deviations than for $\beta = 0$. Although the frequency deviations are larger for $\beta = 0.5$ than for $\beta = 0$, no critical deviations occur. When $\beta = 1$, the frequency is operated close to the cut-off frequencies. Since the controlled system is a stochastic system, frequency deviations larger than $\pm 1\text{Hz}$ occur for this value of β . As discussed previously, CE-EMPC (corresponding to $\beta = 1$) does not work well in practice. The use of a setpoint-based term in (7.47) can be interpreted as a heuristic for CE-EMPC, similar to the constraint back-off heuristic (5.19). The heuristic ensures that the frequency is operated with a safety margin from the cut-off frequencies. Paper F achieves similar behavior in a more systematic way using MV-EMPC. In contrast to the proposed EMPC scheme, MV-EMPC guarantees the economic performance of the controller.

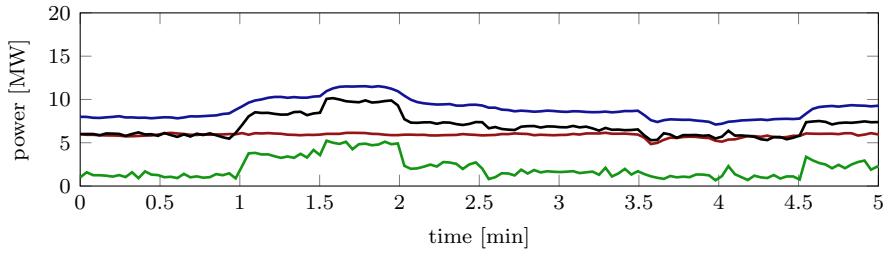
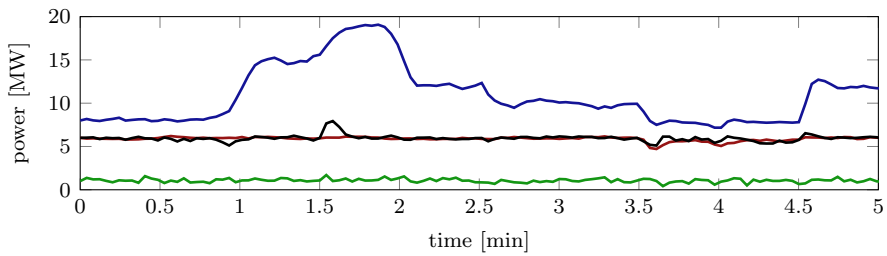
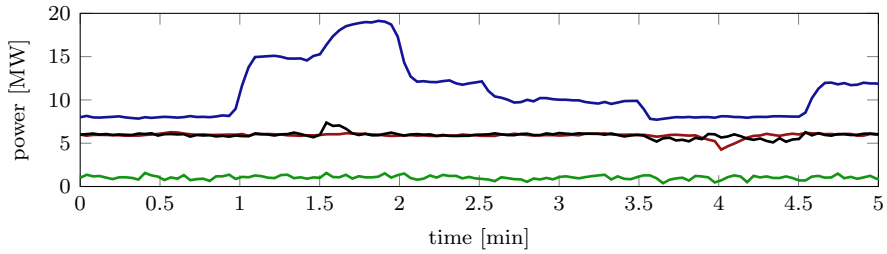
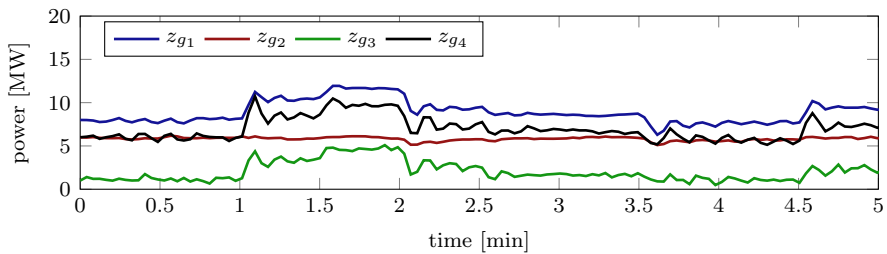
Table 7.5 provides key simulation results for different values of the trade-off parameter β . Over the course of one year, the price difference between setpoint-based MPC and the proposed EMPC scheme with $\beta = 0.5$, sums to over EUR

1.3 million. This corresponds to approximately 3% of the revenues generated by SEV in 2012 [SEV13].

7.7 Summary

In this chapter, we have developed the ORPP for economic dispatch of power generators in a small isolated power system, and an EMPC scheme for frequency control. The ORPP ensures that the systems frequency remains in a safe operating range, in the event of a contingency. The transient dynamics of the frequency response is accounted for in the ORPP, based on a model of the system inertia and an open-loop FCR response of the system generators. The EMPC scheme activates FRR to restore the frequency to the nominal frequency. The EMPC scheme accounts for generator costs and the frequency dynamics. The OCP objective function is a bi-criterion that trades-off the cost of operation and setpoint tracking. The setpoint-based term in the OCP objective function ensures that the stochastic system is operated with a safety margin from the system constraints. This can be viewed as a computationally efficient approach to approximate the behavior of MV-EMPC.

The proposed ORPP and EMPC scheme were tested using a Faroe Island case study. A single-area model of the system was developed. Simulations show that potential blackouts and power outages can be avoided using the ORPP, at a cost increase of less than 3%. The EMPC scheme for frequency control yields a 3% reduction in the yearly operating cost, compared to conventional LFC schemes.

(a) EMPC with $\beta = 0$ (b) EMPC with $\beta = 0.5$ (c) EMPC with $\beta = 1$ 

(d) PI control

Figure 7.15: Closed-loop simulation: Generator power production levels.

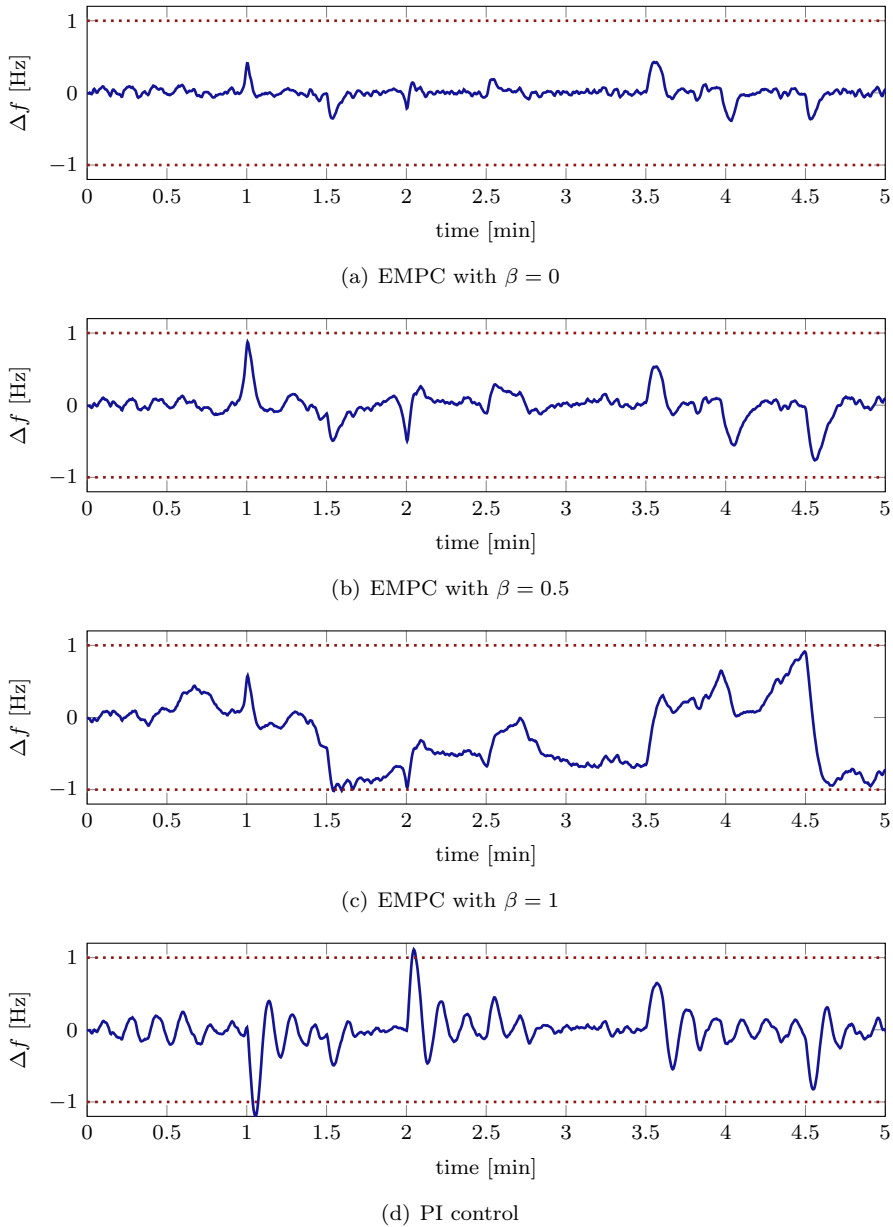


Figure 7.16: Closed-loop simulation: System frequency deviation.

Conclusions

In this thesis, we have developed methods and algorithms for EMPC in power production planning. The formulation and solution of the OCPs that arise in EMPC of linear stochastic systems were given particular attention. We introduced a conceptual portfolio system for demonstration and test purposes. The portfolio system consists of a collection of power generators. Generators represent generic units with the ability to produce power, consume power, or possibly both. The main contributions of this thesis were presented in Chapter 5, Chapter 6, and Chapter 7.

Power generation based on renewable energy sources is inherently uncertain and variable. The power portfolio system is therefore generally a stochastic system. Chapter 5 demonstrated that CE-EMPC performs poorly under uncertainty. Consequently, CE-EMPC is not well suited for control of the portfolio system. For this reason, MV-EMPC was introduced as an extension of CE-EMPC that accounts for the system uncertainty in a more economically efficient manner. In MV-EMPC, the OCP objective function is a trade-off between cost expectation and cost variance. Simulations show that, while CE-EMPC is a high-risk and high-cost strategy, MV-EMPC provides attractive cost/risk trade-off options.

Computationally tractable EMPC schemes require efficient algorithms to solve the OCPs. Chapter 6 presented novel algorithms to solve the OCPs that arise in EMPC. A Riccati-based IPM was developed for CE-EMPC of linear stochastic

systems. The Riccati-based IPM is a specialized algorithm for OCPs with linear constraints and linear objective functions. Input-constrained OCPs with convex objective functions were handled using a tailored ADMM-based algorithm. We demonstrated that the OCP associated with EMPC of dynamically decoupled subsystems can be expressed as a block-angular LP. Subsystem decomposition algorithms based on Dantzig-Wolfe decomposition and ADMM were developed to solve optimization problems of this type. The algorithms facilitate EMPC of energy systems with a large number of generators. General-purpose solvers cannot handle such large-scale systems due to memory limitations. The OCPs that arise in MV-EMPC are large-scale convex optimization problems. To solve these problems in real-time, a scenario decomposition algorithm based on ADMM was presented. Warm-start and early-termination strategies were employed to reduce the computation time of the proposed EMPC algorithms. Simulations demonstrate that the algorithms presented in this thesis are significantly faster than current state-of-the-art solvers, and that the difference in computation time increases with the size of the OCPs.

Chapter 7 concerned planning and control methods for small isolated power systems. A single-area model was introduced to model a small isolated power system. We developed an EMPC scheme for frequency control via activation of operational reserves. The strategy accounts for generation costs and for the system frequency dynamics. Simulations based on a Faroe Islands case study show that significant savings can be achieved using the proposed EMPC scheme. The ORPP was developed for unit commitment and economic dispatch of power generators in a small isolated power system. Frequency constraints in the ORPP ensure that the ORPP production plan is robust against a number of pre-defined contingencies. In a Faroe Islands case study, potential blackouts and power outages are avoided using the ORPP.

8.1 Future Work

Future work involves further investigation and development of the control and planning methods introduced in this thesis. Two main directions for future research are described in the following. In addition to the listed research directions, we plan to improve the proposed planning and control methods for small isolated power systems, based on experimental results. The ORPP is currently being tested in the Faroe Islands. Production plans generated by the ORPP are transmitted directly to the main control room, where the plans are evaluated and validated by the system operators. We would like to test the reserve activation EMPC scheme and a in a similar setting.

8.1.1 Risk Measures in MV-EMPC

This thesis demonstrated that MV-EMPC is a promising strategy for EMPC of linear stochastic systems. MV-EMPC employs variance as a risk measure. We plan to investigate other risk measures than the variance in an MV-EMPC setting. Notably, Conditional Value-at-Risk (CVaR) is a risk measure with many attractive properties; it is a convex and coherent risk measure, which is sensitive to the tail shape of the cost distribution [MCM⁺14, KPU02, SFFM14]. As for MV-EMPC, scenario decomposition algorithms are required for the computational tractability of future Monte Carlo-based EMPC schemes.

8.1.2 Algorithms for EMPC

The algorithms proposed in this thesis have a number of potential extensions to be considered in future work:

- Quadratic programming extensions for LPempc and DWempc: Homogeneous and self dual IPMs can be generalized to conic optimization problems [SAY13, ART03]. We plan to implement a version of LPempc that can handle quadratic terms (and possibly conic terms) in the OCP objective function. Similarly, we would like to extend the Dantzig-Wolfe decomposition algorithm to quadratic programming [Sac80].
- Tuning ADMM: Several ADMM-based algorithms for EMPC have been presented in this thesis. Tuning parameters are critical for the empirical convergence rate of ADMM [BPC⁺11, EF98, GTSJ13, TGS⁺13]. Tuning strategies for ADMM in EMPC applications will be investigated in future work.
- Parallel implementations: The decomposition algorithms developed in this thesis have good parallelization capabilities. Fully parallel implementations of the algorithms are left to future work. The potential of utilizing structure in the subproblems that arise in the decomposition algorithms should also be investigated further.

Bibliography

- [AAR12] D. Angeli, R. Amrit, and J. B. Rawlings. On Average Performance and Stability of Economic Model Predictive Control. *IEEE Transactions on Automatic Control*, 57(7):1615–1626, 2012.
- [AG14] H. Ahmadi and H. Ghasemi. Security-Constrained Unit Commitment with Linearized System Frequency Limit Constraints. *IEEE Transactions on Power Systems*, 29(4):1536–1545, 2014.
- [AGMX96] E. D. Andersen, J. Gondzio, C. Mészáros, and X. Xu. Implementation of Interior Point Methods for Large Scale Linear Programming. In *Interior Point Methods in Mathematical Programming*, pages 189–252. Kluwer Academic Publishers, 1996.
- [AHW12] M. Annergren, A. Hansson, and B. Wahlberg. An ADMM Algorithm for Solving ℓ_1 Regularized MPC. In *51st IEEE Conference on Decision and Control (CDC)*, pages 4486–4491, 2012.
- [AM12] D. Axehill and M. Morari. An Alternative use of the Riccati Recursion for Efficient Optimization. *Systems & Control Letters*, 61(1):37–40, 2012.
- [And12a] G. Andersson. Dynamics and Control of Electric Power Systems. Technical report, Lecture Notes in Electrical Engineering, Power Systems Laboratory, ETH Zurich, 2012. URL: <http://eeh.ee.ethz.ch>.
- [And12b] G. Andersson. Power System Analysis. Technical report, Lecture Notes in Electrical Engineering, Power Systems Laboratory, ETH Zurich, 2012. URL: <http://eeh.ee.ethz.ch>.

- [ARF03] N. Atic, D. H. A. Rerkpreedapong, and A. Feliachi. NERC Compliant Decentralized Load Frequency Control Design Using Model Predictive Control. In *IEEE Power Engineering Society General Meeting*, pages 554–559, 2003.
- [ART03] E. D. Andersen, C. Roos, and T. Terlaky. On Implementing a Primal-Dual Interior-Point Method for Conic Quadratic Optimization. *Mathematical Programming*, 95(2):249–277, 2003.
- [ASS08] E. M. B. Aske, S. Strand, and S. Skogestad. Coordinator MPC for Maximizing Plant Throughput. *Computers & Chemical Engineering*, 32(1-2):195–204, 2008.
- [BB06] R. A. Bartlett and L. T. Biegler. QPSchur: A Dual, Active-Set, Schur-Complement Method for Large-Scale and Structured Convex Quadratic Programming. *Optimization and Engineering*, 7(1):5–32, 2006.
- [Bev09] H. Bevrani. *Robust Power System Frequency Control*. New York: Springer-Verlag, 2009.
- [BGW14] A. Boccia, L. Grüne, and K. Worthmann. Stability and Feasibility of State Constrained MPC without Stabilizing Terminal Constraints. *Systems & Control Letters*, 72:14–21, 2014.
- [BJ76] G. E. P. Box and G. M. Jenkins. *Time Series Analysis: Forecasting and Control*. Holden-Day series in time series analysis and digital processing. Holden-Day, 1976.
- [BK10] K. E. Bakari and W. L. Kling. Virtual power plants: An Answer to Increasing Distributed Generation. In *IEEE/PES Innovative Smart Grid Technologies Conference Europe (ISGT Europe)*, pages 1–6, 2010.
- [BL00] J. Borwein and A. Lewis. *Convex Analysis and Nonlinear Optimization: Theory and Examples*. Canadian Mathematical Society, 2000.
- [BL11] J. R. Birge and F. Louveaux. *Introduction to Stochastic Programming*. Springer Series in Operations Research and Financial Engineering. Springer, 2011.
- [BM07] F. Borrelli and M. Morari. Offset Free Model Predictive Control. In *46th IEEE Conference on Decision and Control (CDC)*, pages 1245–1250, 2007.
- [BMDP02] A. Bemporad, M. Morari, V. Dua, and E. N. Pistikopoulos. The Explicit Linear Quadratic Regulator for Constrained Systems. *Automatica*, 38(1):3–20, 2002.

- [BPC⁺11] S. Boyd, N. Parikh, E. Chu, B. Peleato, and E. Jonathan. Distributed Optimization and Statistical Learning via the Alternating Direction Method of Multipliers. *Foundations and Trends in Machine Learning*, 3(1):1–122, 2011.
- [Bro13] P. Brown. European Union Wind and Solar Electricity Policies: Overview and Considerations. Technical report, Congressional Research Service, 2013. URL: <https://fas.org>.
- [BTS10] J. Bendtsen, K. Trangbaek, and J. Stoustrup. Hierarchical Model Predictive Control for Resource Distribution. In *49th IEEE Conference on Decision and Control (CDC)*, pages 2468–2473, 2010.
- [BV04] S. Boyd and L. Vandenberghe. *Convex Optimization*. Cambridge University Press, 2004.
- [Car85] J. Carpentier. ‘To be or not to be Modern’ that is the Question for Automatic Generation Control (Point of View of a Utility Engineer). *International Journal of Electrical Power & Energy Systems*, 7(2):81–91, 1985.
- [CB07] E. F. Camacho and C. Bordons. *Model Predictive control*. Advanced Textbooks in Control and Signal Processing. Springer London, 2007.
- [CB12] H. Chavez and R. Baldick. Inertia and Governor Ramp Rate Constrained Economic Dispatch to Assess Primary Frequency Response Adequacy. In *International Conference on Renewable Energies and Power Quality*, pages 1–6, 2012.
- [CCMGB06] A. J. Conejo, E. Castillo, R. Minguez, and R. Garcia-Bertrand. *Decomposition Techniques in Mathematical Programming: Engineering and Science Applications*. Springer, 2006.
- [CDPH12] B. Chu, S. Duncan, A. Papachristodoulou, and C. Hepburn. Using Economic Model Predictive Control to Design Sustainable Policies for Mitigating Climate Change. In *51st IEEE Conference on Decision and Control (CDC)*, pages 406–411, 2012.
- [CF13a] G. C. Calafiore and L. Fagiano. Robust Model Predictive Control via Scenario Optimization. *IEEE Transactions on Automatic Control*, 58(1):219–224, 2013.
- [CF13b] G. C. Calafiore and L. Fagiano. Stochastic Model Predictive Control of LPV Systems via Scenario Optimization. *Automatica*, 49(6):1861–1866, 2013.

- [CFP95] C. Concordia, L. H. Fink, and G. Poullikkas. Load Shedding on an Isolated System. *IEEE Transactions on Power Systems*, 10(3):1467–1472, 1995.
- [CSFJ15] A. Capolei, E. Suwartadi, B. Foss, and J. B. Jørgensen. A Mean-Variance Objective for Robust Production Optimization in Uncertain Geological Scenarios. *Journal of Petroleum Science and Engineering*, 125:23–37, 2015.
- [CSZ⁺12] C. Conte, T. Summers, M. N. Zeilinger, M. Morari, and C. N. Jones. Computational Aspects of Distributed Optimization in Model Predictive Control. In *51st IEEE Conference on Decision and Control (CDC)*, pages 6819–6824, 2012.
- [DAR11] M. Diehl, R. Amrit, and J. B. Rawlings. A Lyapunov Function for Economic Optimizing Model Predictive Control. *IEEE Transactions on Automatic Control*, 56(3):703–707, 2011.
- [DDS05] G. Desaulniers, J. Desrosiers, and M. M. Solomon. *Column Generation*. Springer, 2005.
- [Deb88] A. S. Debs. *Modern Power Systems Control and Operation*. Springer US, 1988.
- [DFH09] M. Diehl, H. J. Ferreau, and N. Haverbeke. Efficient Numerical Methods for Nonlinear MPC and Moving Horizon Estimation. In *Nonlinear Model Predictive Control*, volume 384 of *Lecture Notes in Control and Information Sciences*, pages 391–417. Springer Berlin Heidelberg, 2009.
- [DW60] G. B. Dantzig and P. Wolfe. Decomposition Principle for Linear Programs. *Operations Research*, 8(1):101–111, 1960.
- [DZZ⁺12] A. Domahidi, A. U. Zgraggen, M. N. Zeilinger, M. Morari, and C. N. Jones. Efficient Interior Point Methods for Multistage Problems Arising in Receding Horizon Control. In *51st IEEE Conference on Decision and Control (CDC)*, pages 668–674, 2012.
- [EBJ11] K. Edlund, J. D. Bendtsen, and J. B. Jørgensen. Hierarchical Model-Based Predictive Control of a Power Plant Portfolio. *Control Engineering Practice*, 19(10):1126–1136, 2011.
- [ED10] Energinet.dk and DEA. Smart Grid in Denmark. Technical report, 2010. URL: <http://energinet.dk>.
- [ED11] Energinet.dk and DEA. Smart grid in Denmark 2.0. Technical report, 2011. URL: <http://energinet.dk>.

- [EDC14] M. Ellis, H. Durand, and P. D. Christofides. A Tutorial Review of Economic Model Predictive Control Methods. *Journal of Process Control*, 24(8):1156–1178, 2014.
- [Edl10] K. Edlund. *Dynamic Load Balancing of a Power System Portfolio*. Ph.D. thesis, Department of Electronic Systems, Aalborg University, 2010.
- [EE12] ENTSO-E. Operational Reserve Ad Hoc Team Report. Technical report, Bruxelles, Belgium, 2012. URL: <https://entsoe.eu>.
- [EF98] J. Eckstein and M. C. Ferris. Operator-Splitting Methods for Monotone Affine Variational Inequalities, with a Parallel Application to Optimal Control. *Inform Journal on Computing*, 10(2):218–235, 1998.
- [EIA14] EIA. Levelized Cost and Levelized Avoided Cost of New Generation Resources in the Annual Energy Outlook 2014. Technical report, U.S. Energy Information Administration, 2014. URL: <http://eia.gov/forecasts/aeo/>.
- [EMB09] K. Edlund, T. Mølbak, and J. D. Bendtsen. Simple Models for Model-Based Portfolio Load Balancing Controller Synthesis. In *6th IFAC Symposium on Power Plants and Power Systems Control*, pages 173–178, 2009.
- [Ene15] Energinet.dk. Årsrapport 2014. Technical report, 2015. URL: <http://energinet.dk>.
- [ESJ09] K. Edlund, L. E. Sokoler, and J. B. Jørgensen. A Primal-Dual Interior-Point Linear Programming Algorithm for MPC. In *48th IEEE Conference on Decision and Control and 28th Chinese Control Conference (CDC/CCC)*, pages 351–356, 2009.
- [Eur06] European SmartGrids Technology Platform. Vision and Strategy for Europe’s Electricity Networks of the Future. Technical report, European Commission, Directorate-General for Research, 2006. URL: <http://smartgrids.eu>.
- [Eur14] European Commission. Commission Staff Working Document: State of Play on the Sustainability of Solid and Gaseous Biomass used for Electricity, Heating and Cooling in the EU. Technical report, 2014. URL: <http://ec.europa.eu>.
- [Eur15a] European Commission. Report from the Commission to the European Parliament, the Council, the European Economic and

- Social Committee and the Committee of the Regions: Renewable Energy Progress Report. Technical report, 2015. URL: <http://ec.europa.eu>.
- [Eur15b] Eurostat. Share of Renewables in Energy Consumption up to 152013. Technical report, 2015. URL: <http://ec.europa.eu>.
- [FBD08] H. J. Ferreau, H. G. Bock, and M. Diehl. An Online Active Set Strategy to Overcome the Limitations of Explicit MPC. *International Journal of Robust and Nonlinear Control*, 18(8):816–830, 2008.
- [FJ13] G. Frison and J. B. Jørgensen. A Fast Condensing Method for Solving Linear-Quadratic Control Problems. In *52th IEEE Conference on Decision and Control (CDC)*, pages 7715–7720, 2013.
- [GA14] T. Govindaraj and T. Archana. Unit Commitment Based On Frequency Regulating Reserve Constraint Using Dynamic Programming. *IJREAT International Journal of Research in Engineering & Advanced Technology*, 1(6):1–8, 2014.
- [GB11] A. T. Gill and C. B. Black. Status of Hawaii’s Ocean Energy Projects and Permitting Regime. In *OCEANS*, pages 1–8, 2011.
- [GBAR05] F. D. Galiana, F. Bouffard, J. M. Arroyo, and J. F. Restrepo. Scheduling and Pricing of Coupled Energy and Primary, Secondary, and Tertiary Reserve. *Proceedings of the IEEE*, 93(11):1970–1983, 2005.
- [GPSW12] L. Grüne, J. Pannek, M. Seehafer, and K. Worthmann. Analysis of Unconstrained Nonlinear MPC Schemes with Time Varying Control Horizon. In *51st IEEE Conference on Decision and Control (CDC)*, pages 2605–2610, 2012.
- [Grü13] L. Grüne. Economic Receding Horizon Control without Terminal Constraints. *Automatica*, 49(3):725–734, 2013.
- [GSD05] G. C. Goodwin, M. M. Seron, and J. A. De Doná. *Constrained Control and Estimation. An Optimisation Approach*. Springer-Verlag London, 2005.
- [GTSJ13] E. Ghadimi, A. Teixeira, I. Shames, and M. Johansson. Optimal Parameter Selection for the Alternating Direction Method of Multipliers (ADMM): Quadratic Problems. *IEEE Transactions on Automatic Control*, 2013. Submitted.
- [Hal14] R. Halvgaard. *Model Predictive Control for Smart Energy Systems*. Ph.D. thesis, Department of Applied Mathematics and Computer Science, Technical University of Denmark, 2014.

- [HBP⁺12] R. Halvgaard, P. Bacher, B. Perers, E. Andersen, S. Furbo, J. B. Jørgensen, N. K. Poulsen, and H. Madsen. Model Predictive Control for a Smart Solar Tank Based on Weather and Consumption Forecasts. *Energy Procedia*, 30:270–278, 2012.
- [HCM⁺01] N. Hatzigiargyriou, G. Contaxis, M. Matos, J. A. Peas Lopes, M. H. Vasconcelos, G. Kariniotakis, D. Mayer, J. Halliday, G. Dutton, P. Dokopoulos, A. Bakirtzis, J. Stefanakis, A. Gigantidou, P. O'Donnell, D. McCoy, M. J. Fernandes, J. M. S. Cotrim, and A. P. Figueira. Preliminary Results from the More Advanced Control Advice Project for Secure Operation of Isolated Power Systems with Increased Renewable Energy Penetration and Storage. In *IEEE Porto Power Tech*, volume 4, pages 1–6, 2001.
- [HI08] M. Houwing and M. Ilic. The Value of IT for Virtual Power Plants with Micro Cogeneration Systems. In *IEEE International Conference on Systems, Man and Cybernetics*, pages 1–6, 2008.
- [HJB13] L. H. Hansen, J. M. Jensen, and A. Bjerre. EV Portfolio Management. In *Grid Integration of Electric Vehicles in Open Electricity Markets*, pages 129–152. John Wiley & Sons, 2013.
- [HL13] M. Hong and Z.-Q. Luo. On the Linear Convergence of the Alternating Direction Method of Multipliers. *Mathematical Programming*, 2013. Submitted.
- [HLEJ12] T. G. Hovgaard, L. F. S. Larsen, K. Edlund, and J. B. Jørgensen. Model Predictive Control Technologies for Efficient and Flexible Power Consumption in Refrigeration Systems. *Energy*, 44(1):105–116, 2012.
- [HLJ11] T. G. Hovgaard, L. F. S. Larsen, and J. B. Jørgensen. Flexible and Cost Efficient Power Consumption Using Economic MPC a Supermarket Refrigeration Benchmark. In *50th IEEE Conference on Decision and Control and European Control Conference (CDC-ECC)*, pages 848–854, 2011.
- [HLJB12] T. G. Hovgaard, L. F. S. Larsen, J. B. Jørgensen, and S. Boyd. Fast Nonconvex Model Predictive Control for Commercial Refrigeration. In *4th IFAC Nonlinear Model Predictive Control Conference*, pages 514–521, 2012.
- [HLSJ12] T. G. Hovgaard, L. F. S. Larsen, M. J. Skovrup, and J. B. Jørgensen. Optimal Energy Consumption in Refrigeration Systems - Modelling and Non-Convex Optimisation. *The Canadian Journal of Chemical Engineering*, 90(6):1426–1433, 2012.

- [Hov13] T. G. Hovgaard. *Power Management for Energy Systems*. Ph.D. thesis, Department of Applied Mathematics and Computer Science, Technical University of Denmark, 2013.
- [HPJJ12] J. K. Huusom, N. K. Poulsen, S. B. Jørgensen, and J. B. Jørgensen. Tuning SISO Offset-Free Model Predictive Control Based on ARX Models. *Journal of Process Control*, 22(10):1997–2007, 2012.
- [HPM⁺12] R. Halvgaard, N. K. Poulsen, H. Madsen, J. B. Jørgensen, F. Marra, and D. E. M Bondy. Electric Vehicle Charge Planning Using Economic Model Predictive Control. In *IEEE International Electric Vehicle Conference (IEVC)*, pages 1–6, 2012.
- [HPMJ12] R. Halvgaard, N. K. Poulsen, H. Madsen, and J. B. Jørgensen. Economic Model Predictive Control for Building Climate Control in a Smart Grid. In *IEEE/PES Innovative Smart Grid Technologies Conference Europe (ISGT Europe)*, pages 1–6, 2012.
- [HTM91] D. E. Hampton, C. E. Tindall, and J. M. McArdle. Emergency Control of Power System Frequency Using Flywheel Energy Injection. In *International Conference on Advances in Power System Control, Operation and Management*, volume 2, pages 662–667, 1991.
- [HUL01] J.-B. Hiriart-Urruty and C. Lemaréchal. *Fundamentals of Convex Analysis*. Springer, 2001.
- [IKK05] I. Ibraheem, P. Kumar, and D. P. Kothari. Recent Philosophies of Automatic Generation Control Strategies in Power Systems. *IEEE Transactions on Power Systems*, 20(1):346–357, 2005.
- [JFGND12] J. B. Jørgensen, G. Frison, N. F. Gade-Nielsen, and B. Dammann. Numerical Methods for Solution of the Extended Linear Quadratic Control Problem. In *4th IFAC Nonlinear Model Predictive Control Conference*, pages 187–193, 2012.
- [JGR⁺14] J. L. Jerez, P. J. Goulart, S. Richter, G. A. Constantinides, E. C. Kerrigan, and M. Morari. Embedded Online Optimization for Model Predictive Control at Megahertz Rates. *IEEE Transactions on Automatic Control*, 50(12):3009–3018, 2014.
- [JH05] A. Jadbabaie and J. Hauser. On the Stability of Receding Horizon Control with a General Terminal Cost. *IEEE Transactions on Automatic Control*, 50(5):674–678, 2005.
- [JHR11] J. B. Jørgensen, J. K. Huusom, and J. B. Rawlings. Finite Horizon MPC for Systems in Innovation Form. In *50th IEEE Conference*

- on Decision and Control and European Control*, pages 1896–1903, 2011.
- [JJ07] J. B. Jørgensen and S. B. Jørgensen. MPC-Relevant Prediction-Error Identification. In *Proceedings of the American Control Conference*, pages 128–133, 2007.
- [Jør05] J. B. Jørgensen. *Moving Horizon Estimation and Control*. Ph.D. thesis, Department of Chemical Engineering, Technical University of Denmark, 2005.
- [JRJ04] J. B. Jørgensen, J. B. Rawlings, and S. B. Jørgensen. Numerical Methods for Large-Scale Moving Horizon Estimation and Control. In *International Symposium on Dynamics and Control of Process Systems (DYCOPS)*, volume 7, 2004.
- [Kal60] R. E. Kalman. A New Approach to Linear Filtering and Prediction Problems. *Transactions of the ASME, Journal of Basic Engineering*, 82(Series D):35–45, 1960.
- [KBL94] P. Kundur, N. J. Balu, and M. G. Lauby. *Power System Stability and Control*. EPRI power system engineering series. McGraw-Hill, 1994.
- [KCLB14] M. Kraning, E. Chu, J. Lavaei, and S. Boyd. Dynamic Network Energy Management via Proximal Message Passing. *Foundations and Trends in Optimization*, 1(2):73–126, 2014.
- [Ken75] J. W. Kendall. Hard and Soft Constraints in Linear Programming. *Omega*, 3(6):709–715, 1975.
- [KF11] M. Kögel and R. Findeisen. Fast Predictive Control of Linear Systems Combining Nesterov’s Gradient Method and the Method of Multipliers. In *50th IEEE Conference on Decision and Control and European Control Conference (CDC-ECC)*, pages 501–506, 2011.
- [KF12] M. Kögel and R. Findeisen. Parallel Solutions of Model Predictive Control Using the Alternating Direction Method of Multipliers. In *4th IFAC Nonlinear Model Predictive Control Conference*, pages 369–374, 2012.
- [KH05] W. H. Kwon and S. H. Han. *Receding Horizon Control*. Springer-Verlag London, 2005.
- [KM00] E. C. Kerrigan and J. M. Maciejowski. Soft Constraints and Exact Penalty Functions in Model Predictive Control. In *UKACC International Conference (Control 2000)*, 2000.

- [KNS97] J. Kumar, K.-H. Ng, and G. Sheble. AGC Simulator for Price-Based Operation Part 1: A Model. *IEEE Transactions on Power Systems*, 12(2):527–532, 1997.
- [KO96] D. Kottick and O. Or. Neural-Networks for Predicting the Operation of an Under-Frequency Load Shedding System. *IEEE Transactions on Power Systems*, 11(3):1350–1358, 1996.
- [KPU02] P. Krokhmal, J. Palmquist, and S. Uryasev. Portfolio Optimization with Conditional Value-at-Risk Objective and Constraints. *Journal of Risk*, 4(2):43–68, 2002.
- [KX07] L. Kong and L. Xiao. A New Model Predictive Control Scheme-Based Load-Frequency Control. In *IEEE International Conference on Control and Automation*, pages 2514–2518, 2007.
- [Lal05] G. R. Lalor. *Frequency Control on an Island Power System with Evolving Plant Mix*. Ph.D. thesis, School of Electrical, Electronic and Mechanical Engineering University College Dublin, 2005.
- [Lju99] L. Ljung. *System Identification: Theory for the User*. Prentice Hall Information And System Sciences Series. Prentice Hall PTR, 1999.
- [LKMB10] S. Lukovic, I. Kaitovic, M. Mura, and U. Bondi. Virtual Power Plant As a Bridge between Distributed Energy Resources and Smart Grid. In *43rd Hawaii International Conference on System Sciences (HICSS)*, pages 1–8, 2010.
- [LMO05] G. Lalor, A. Mullane, and M. J. O’Malley. Frequency Control and Wind Turbine Technologies. *IEEE Transactions on Power Systems*, 20(4):1905–1913, 2005.
- [LRFO05] G. Lalor, J. Ritchie, D. Flynn, and M. J. O’Malley. The Impact of Combined-Cycle Gas Turbine Short-Term Dynamics on Frequency Control. *IEEE Transactions on Power Systems*, 20(3):1456–1464, 2005.
- [LS15] M. Lazar and V. Spinu. Finite-step Terminal Ingredients for Stabilizing Model Predictive Control. In *5th IFAC Conference on Nonlinear Model Predictive Control*, pages 9–15, 2015.
- [LSE13] S. Lucia, S. Subramanian, and S. Engell. Non-Conservative Robust Nonlinear Model Predictive Control via Scenario Decomposition. In *IEEE International Conference on Control Applications (CCA)*, pages 586–591, 2013.

- [Mac02] J. M. Maciejowski. *Predictive Control with Constraints*. Pearson Education. Prentice Hall, 2002.
- [Mar52] H. Markowitz. Portfolio Selection. *The Journal of Finance*, 7(1):77–91, 1952.
- [Mar99] R. K. Martin. *Large Scale Linear and Integer Optimization: A Unified Approach*. Kluwer Academic Publishers, 1999.
- [MB02] K. R. Muske and T. A. Badgwell. Disturbance Modeling for Offset-Free Linear Model Predictive Control. *Journal of Process Control*, 12(5):617–632, 2002.
- [MB12a] J. Mattingley and S. Boyd. CVXGEN: A Code Generator for Embedded Convex Optimization. *Optimization and Engineering*, 13(1):1–27, 2012.
- [MB12b] J. Matusko and F. Borrelli. Scenario-Based Approach to Stochastic Linear Predictive Control. In *51st IEEE Conference on Decision and Control (CDC)*, pages 5194–5199, 2012.
- [MBHH11] T. H. Mohamed, H. Bevrani, A. A. Hassan, and T. Hiyama. Decentralized Model Predictive Based Load Frequency Control in an Interconnected Power System. *Energy Conversion and Management*, 52(2):1208–1214, 2011.
- [MCLA14] M. Ma, H. Chen, X. Liu, and F. Allgöwer. Distributed Model Predictive Load Frequency Control of Multi-Area Interconnected Power System. *International Journal of Electrical Power & Energy Systems*, 62:289–298, 2014.
- [MCM⁺14] J. M. Morales, A. J. Conejo, H. Madsen, P. Pinson, and M. Zugno. *Integrating Renewables in Electricity Markets*. International Series in Operations Research & Management Science. Springer, 2014.
- [Meh92] S. Mehrotra. On the Implementation of a Primal-Dual Interior Point Method. *SIAM Journal on Optimization*, 2(4):575–601, 1992.
- [ML99] M. Morari and J. H. Lee. Model Predictive Control: Past, Present and Future. *Computers & Chemical Engineering*, 23(4-5):667–682, 1999.
- [Mos95] E. Mosca. *Optimal, Predictive, and Adaptive Control*. Prentice Hall Information and System Sciences Series. Prentice Hall, 1995.

- [MPH⁺15] H. Madsen, J. Parvizi, R. Halvgaard, L. E. Sokoler, J. B. Jørgensen, L. H. Hansen, and K. Hilger. Control of Electricity Loads in Future Electric Energy Systems. In *Handbook of Clean Energy Systems*. John Wiley & Sons, 2015.
- [MQLS11] J. Ma, S. J. Qin, B. Li, and T. Salsbury. Economic Model Predictive Control for Building Energy Systems. In *IEEE/PES Innovative Smart Grid Technologies (ISGT)*, pages 1–6, 2011.
- [MR93] K. R. Muske and J. B. Rawlings. Model Predictive Control with Linear Models. *AIChE Journal*, 39(2):262–287, 1993.
- [MRKG11] J. Mohammadi, A. Rahimi-Kian, and M. S. Ghazizadeh. Joint Operation of Wind Power and Flexible Load as Virtual Power Plant. In *10th International Conference on Environment and Electrical Engineering (EEEIC)*, pages 1–4, 2011.
- [MRRS00] D. Q. Mayne, J. B. Rawlings, C. V. Rao, and P. O. M. Scokaert. Constrained Model Predictive Control: Stability and Optimality. *Automatica*, 36(6):789–814, 2000.
- [MSSVP14] M. Maasoumy, B. M. Sanandaji, A. Sangiovanni-Vincentelli, and K. Poolla. Model Predictive Control of Regulation Services from Commercial Buildings to The Smart Grid. In *American Control Conference (ACC)*, pages 2226–2233, 2014.
- [NW06] J. Nocedal and S. Wright. *Numerical Optimization*. Springer Series in Operations Research and Financial Engineering. Springer, 2006.
- [OO96] J. W. O’Sullivan and M. J. O’Malley. Identification and Validation of Dynamic Global Load Model Parameters for Use in Power System Frequency Simulations. *IEEE Transactions on Power Systems*, 11(2):851–857, 1996.
- [ORF⁺14] J. O’Sullivan, A. Rogers, D. Flynn, P. Smith, A. Mullane, and M. O’Malley. Studying the Maximum Instantaneous Non-Synchronous Generation in an Island System - Frequency Stability Challenges in Ireland. *IEEE Transactions on Power Systems*, 29(26):2943–2951, 2014.
- [PEH⁺13] M. K. Petersen, K. Edlund, L. H. Hansen, J. Bendtsen, and J. Stoustrup. A Taxonomy for Modeling Flexibility and a Computationally Efficient Algorithm for Dispatch in Smart Grids. In *American Control Conference (ACC)*, pages 1150–1156, 2013.
- [PGL12] M. Prandini, S. Garatti, and J. Lygeros. A Randomized Approach to Stochastic Model Predictive Control. In *51st IEEE Conference on Decision and Control (CDC)*, pages 7315–7320, 2012.

- [PHB⁺13] M. K. Petersen, L. H. Hansen, J. Bendtsen, K. Edlund, and J. Stoustrup. Market Integration of Virtual Power Plants. In *52nd IEEE Conference on Decision and Control (CDC)*, pages 2319–2325, 2013.
- [Pin13] P. Pinson. Wind Energy: Forecasting Challenges for Its Operational Management. *Statistical Science*, 28(3):564–585, 2013.
- [Pis12] E. N. Pistikopoulos. From Multi-Parametric Programming Theory to MPC-on-a-Chip Multi-Scale Systems Applications. *Computers & Chemical Engineering*, 47:57–66, 2012.
- [PJ09] G. Prasath and J. B. Jørgensen. Soft Constraints for Robust MPC of Uncertain Systems. In *7th IFAC International Symposium on Advanced Control of Chemical Processes*, pages 225–230, 2009.
- [PN00] J. A. Primbs and V. Nevistić. Feasibility and Stability of Constrained Finite Receding Horizon Control. *Automatica*, 36(7):965–971, 2000.
- [PR03] G. Pannocchia and J. B. Rawlings. Disturbance Models for Offset-Free Model-Predictive Control. *AIChE Journal*, 49(2):426–437, 2003.
- [PRS07] D. Pudjianto, C. Ramsay, and G. Strbac. Virtual Power Plant and System Integration of Distributed Energy Resources. *IET Renewable Power Generation*, 1(1):10–16, 2007.
- [QB03] S. J. Qin and T. A. Badgwell. A Survey of Industrial Model Predictive Control Technology. *Control Engineering Practice*, 11(7):733–764, 2003.
- [RAB12] J. B. Rawlings, D. Angeli, and C. N. Bates. Fundamentals of Economic Model Predictive Control. In *51st IEEE Conference on Decision and Control (CDC)*, pages 3851–3861, 2012.
- [RAF03] D. Rerkpreedapong, N. Atic, and A. Feliachi. Economy Oriented Model Predictive Load Frequency Control. In *Large Engineering Systems Conference on Power Engineering*, pages 12–16, 2003.
- [Raw00] J. B. Rawlings. Tutorial Overview of Model Predictive Control. *IEEE Control Systems*, 20(3):38–52, 2000.
- [RBJ⁺08] J. B. Rawlings, D. Bonne, J. B. Jørgensen, A. N. Venkat, and S. B. Jørgensen. Unreachable Setpoints in Model Predictive Control. *IEEE Transactions on Automatic Control*, 53(9):2209–2215, 2008.

- [RCRW97] C. V. Rao, J. C. Campbell, J. B. Rawlings, and S. J. Wright. Efficient Implementation of Model Predictive Control for Sheet and Film Forming Processes. In *American Control Conference (ACC)*, pages 2940–2944, 1997.
- [RG05] J. F. Restrepo and F. D. Galiana. Unit Commitment with Primary Frequency Regulation Constraints. *IEEE Transactions on Power Systems*, 20(4):1836–1842, 2005.
- [RJM09] S. Richter, C. N. Jones, and M. Morari. Real-Time Input-Constrained MPC Using Fast Gradient Methods. In *48th IEEE Conference on Decision and Control and 28th Chinese Control Conference (CDC/CCC)*, pages 7387–7393, 2009.
- [RM93] J. B. Rawlings and K. R. Muske. The Stability of Constrained Receding Horizon Control. *IEEE Transactions on Automatic Control*, 38(10):1512–1516, 1993.
- [RM09] J. B. Rawlings and D. Q. Mayne. *Model Predictive Control: Theory and Design*. Nob Hill Publishing, 2009.
- [Roc70] R. T. Rockafellar. *Convex Analysis*. Princeton mathematical series. Princeton University Press, 1970.
- [Ros03] J. A. Rossiter. *Model-Based Predictive Control: A Practical Approach*. Control Series. Taylor & Francis, 2003.
- [RRAG12] M. Rouholamini, M. Rashidinejad, A. Abdollahi, and H. Ghasemnejad. Frequency Reserve within Unit Commitment Considering Spinning Reserve Uncertainty. *International Journal of Energy Engineering*, 2(4):177–183, 2012.
- [RSR13] S. Rahnama, J. Stoustrup, and H. Rasmussen. Model Predictive Control for Integration of Industrial Consumers to the Smart Grid under a Direct Control Policy. In *IEEE International Conference on Control Applications (CCA)*, pages 515–520, 2013.
- [Rus07] A. P. Ruszczyński. *Nonlinear Optimization*. Princeton University Press, 2007.
- [RWR98] C. V. Rao, S. J. Wright, and J. B. Rawlings. Application of Interior-Point Methods to Model Predictive Control. *Journal of Optimization Theory and Applications*, 99(3):723–757, 1998.
- [Sac80] R. S. Sacher. A Decomposition Algorithm for Quadratic Programming. *Mathematical Programming*, 18(1):16–30, 1980.

- [SAY13] A. Skajaa, E. D. Andersen, and Y. Ye. Warmstarting the Homogeneous and Self-Dual Interior Point Method for Linear and Conic Quadratic Problems. *Mathematical Programming Computation*, 5(1):1–25, 2013.
- [SC13] M. Soroush and D. J. Chmielewski. Process Systems Opportunities in Power Generation, Storage and Distribution. *Computers & Chemical Engineering*, 51:86–95, 2013.
- [SCFM12] G. Schildbach, G. C. Calafiore, L. Fagiano, and M. Morari. Randomized Model Predictive Control for Stochastic Linear Systems. In *American Control Conference (ACC)*, pages 417–422, 2012.
- [SDG00] M. M. Seron, J. A. De Doná, and G. C. Goodwin. Global Analytical Model Predictive Control with Input Constraints. In *39th IEEE Conference on Decision and Control (CDC)*, pages 154–159, 2000.
- [SDJ15] L. E. Sokoler, P. J. Dinesen, and J. B. Jørgensen. A Hierarchical Algorithm for Integrated Scheduling and Control with Applications to Power Systems. *IEEE Transactions on Control Systems Technology*, 2015. To appear.
- [SDMJ14a] L. E. Sokoler, B. Dammann, H. Madsen, and J. B. Jørgensen. A Decomposition Algorithm for Mean-Variance Economic Model Predictive Control of Stochastic Linear Systems. In *IEEE Multi-conference on Systems and Control*, pages 1086–1093, 2014.
- [SDMJ14b] L. E. Sokoler, B. Dammann, H. Madsen, and J. B. Jørgensen. A Mean-Variance Criterion for Economic Model Predictive Control of Stochastic Linear Systems. In *53rd IEEE Conference on Decision and Control (CDC)*, pages 5907–5914, 2014.
- [SEJ15] L. E. Sokoler, K. Edlund, and J. B. Jørgensen. Application of Economic MPC to Frequency Control in a Single-Area Power System. In *54th IEEE Conference on Decision and Control (CDC)*, pages 2635–2642, 2015.
- [SESJ13] L. E. Sokoler, K. Edlund, L. Standardi, and J. B. Jørgensen. A Decomposition Algorithm for Optimal Control of Distributed Energy Systems. In *4th IEEE/PES Innovative Smart Grid Technologies Europe (ISGT Europe)*, pages 1–5, 2013.
- [SEV13] SEV. SEV: Annual Report and Annual Accounts 2012. Technical report, 2013. URL: <http://sev.fo>.
- [SEV15] SEV. SEV: Annual Report and Annual Accounts 2014. Technical report, 2015. URL: <http://sev.fo>.

- [SFAJ14] L. E. Sokoler, G. Frison, M. S. Andersen, and J. B. Jørgensen. Input-Constrained Model Predictive Control via the Alternating Direction Method of Multipliers. In *European Control Conference (ECC)*, pages 115–120, 2014.
- [SFE⁺13] L. E. Sokoler, G. Frison, K. Edlund, A. Skajaa, and J. B. Jørgensen. A Riccati Based Homogeneous and Self-Dual Interior-Point Method for Linear Economic Model Predictive Control. In *IEEE Multi-conference on Systems and Control*, pages 592–598, 2013.
- [SFFM14] G. Schilb, L. Fagiano, C. Frei, and M. Morari. The Scenario Approach for Stochastic Model Predictive Control with Bounds on Closed-Loop Constraint Violations. *Automatica*, 50(12):3009–3018, 2014.
- [SFS⁺15] L. E. Sokoler, G. Frison, A. Skajaa, R. Halvgaard, and J. B. Jørgensen. A Homogeneous and Self-Dual Interior-Point Linear Programming Algorithm for Economic Model Predictive Control. *IEEE Transactions on Automatic Control*, 2015. To appear.
- [SKC10] A. Shahzad, E. C. Kerrigan, and G. A. Constantinides. A Fast Well-Conditioned Interior Point Method for Predictive Control. In *49th IEEE Conference on Decision and Control (CDC)*, pages 508–513, 2010.
- [SL12] T. H. Summers and J. Lygeros. Distributed Model Predictive Consensus via the Alternating Direction Method of Multipliers. In *50th Annual Allerton Conference on Communication, Control and Computing (Allerton)*, pages 79–84, 2012.
- [SLY⁺14] W. Shi, Q. Ling, K. Yuan, G. Wu, and W. Yin. On the Linear Convergence of the ADMM in Decentralized Consensus Optimization. *IEEE Transactions on Signal Processing*, 62(7):1750–1761, 2014.
- [SMT11] H. Saboori, M. Mohammadi, and R. Taghe. Virtual Power Plant (VPP), Definition, Concept, Components and Types. In *Asia-Pacific Power and Energy Engineering Conference (APPEEC)*, pages 1–4, 2011.
- [SPJS13] L. Standardi, N. K. Poulsen, J. B. Jørgensen, and L. E. Sokoler. Computational Efficiency of Economic MPC for Power Systems Operation. In *4th IEEE/PES Innovative Smart Grid Technologies Europe (ISGT Europe)*, pages 1–5, 2013.

- [SSE⁺14] L. E. Sokoler, L. Standardi, K. Edlund, N. K. Poulsen, H. Madsen, and J. B. Jørgensen. A Dantzig-Wolfe Decomposition Algorithm for Linear Economic Model Predictive Control of Dynamically Decoupled Subsystems. *Journal of Process Control*, 24(8):1225–1236, 2014.
- [SSF⁺13] L. E. Sokoler, A. Skajaa, G. Frison, R. Halvgaard, and J. B. Jørgensen. A Warm-Started Homogeneous and Self-Dual Interior-Point Method for Linear Economic Model Predictive Control. In *52th IEEE Conference on Decision and Control (CDC)*, pages 3677–3683, 2013.
- [Sta15] L. Standardi. *Economic Model Predictive Control for Large-Scale and Distributed Energy Systems*. Ph.D. thesis, Department of Applied Mathematics and Computer Science, Technical University of Denmark, 2015.
- [Ste01] M. C. Steinbach. Markowitz Revisited: Mean-Variance Models in Financial Portfolio Analysis. *SIAM Review*, 43(1):31–85, 2001.
- [Stu02] J. F. Sturm. Implementation of Interior Point Methods for Mixed Semidefinite and Second Order Cone Optimization Problems. *Optimization Methods and Software*, 17(6):1105–1154, 2002.
- [SVB⁺15] L. E. Sokoler, P. Vinter, R. Bærentsen, K. Edlund, and J. B. Jørgensen. Contingency-Constrained Unit Commitment in Meshed Isolated Power Systems. *IEEE Transactions on Power Systems*, 2015. To appear.
- [TF94] J. G. Thompson and B. Fox. Adaptive Load Shedding for Isolated Power Systems. *IEE Proceedings, Generation Transmission and Distribution*, 141(5):491–496, 1994.
- [TGS⁺13] A. Teixeira, E. Ghadimi, I. Shames, H. Sandberg, and M. Johansson. Optimal Scaling of the ADMM Algorithm for Distributed Quadratic Programming. In *52th IEEE Conference on Decision and Control (CDC)*, pages 6868–6873, 2013.
- [TJB03] P. Tøndel, T. A. Johansen, and A. Bemporad. An Algorithm for Multi-Parametric Quadratic Programming and Explicit MPC Solutions. *Automatica*, 39(3):489–497, 2003.
- [Twe13] Twenties. Providing Flexibility with a Virtual Power Plant. Technical report, 2013. URL: <http://twenties-project.eu>.
- [UBA14] A. Ulbig, T. S. Borsche, and G. Andersson. Impact of Low Rotational Inertia on Power System Stability and Operation. In *19th IFAC World Congress*, pages 7290–7297, 2014.

- [VB02] D. H. Van Hessem and O. H. Bosgra. Closed-loop Stochastic Dynamic Process Optimization Under Input and State Constraints. In *American Control Conference (ACC)*, volume 3, pages 2023–2028, 2002.
- [VBN02] L. Vandenberghe, S. Boyd, and M. Nouralishahi. Robust Linear Programming and Optimal Control. In *15th IFAC World Congress*, volume 15, pages 271–276, 2002.
- [VD96] P. Van Overschee and B. De Moor. *Subspace Identification for Linear Systems, Theory, Implementation, Applications*. Kluwer Academic Publishers, 1996.
- [VFF15] P. J. C. Vogler-Finck and W.-G. Früh. Evolution of Primary Frequency Control Requirements in Great Britain with Increasing Wind Generation. *International Journal of Electrical Power & Energy Systems*, 73:377–388, 2015.
- [VHRW08] A. N. Venkat, I. A. Hiskens, J. B. Rawlings, and S. J. Wright. Distributed MPC Strategies with Application to Power System Automatic Generation Control. *IEEE Transactions on Control Systems Technology*, 16(6):1192–1206, 2008.
- [WB10] Y. Wang and S. Boyd. Fast Model Predictive Control Using Online Optimization. *IEEE Transactions on Control Systems Technology*, 18(2):267–278, 2010.
- [WBAW12] B. Wahlberg, S. Boyd, M. Annergren, and Y. Wang. An ADMM Algorithm for a Class of Total Variation Regularized Estimation Problems. In *16th IFAC Symposium on System Identification*, pages 83–88, 2012.
- [WCS13] P. Wei, Y. Cao, and D. Sun. Total Unimodularity and Decomposition Method for Large-Scale Air Traffic Cell Transmission Model. *Transportation Research Part B: Methodological*, 53:1–16, 2013.
- [Wri96] S. J. Wright. *Primal-Dual Interior-Point Methods*. SIAM, 1996.
- [Wri97] S. J. Wright. Applying New Optimization Algorithms to Model Predictive Control. In *5th International Conference on Chemical Process Control*, pages 147–155, 1997.
- [WW13] A. J. Wood and B. F. Wollenberg. *Power Generation, Operation, and Control*. John Wiley & Sons, 3rd edition, 2013.
- [XHY96] X. Xu, P.-F. Hung, and Y. Ye. A Simplified Homogeneous and Self-Dual Linear Programming Algorithm and Its Implementation. *Annals of Operations Research*, 62(1):151–171, 1996.

- [Ye97] Y. Ye. *Interior Point Algorithms*. Wiley-Interscience, New York, 1997.
- [You10] S. You. *Developing Virtual Power Plant for Optimized Distributed Energy Resources Operation and Integration*. Ph.D. thesis, DTU Electrical Engineering, Technical University of Denmark, 2010.
- [YTM94] Y. Ye, M. J. Todd, and S. Mizuno. An $O(\sqrt{n}L)$ -Iteration Homogeneous and Self-Dual Linear Programming Algorithm. *Mathematics of Operations Research*, 19(1):53–67, 1994.
- [YTP09] S. You, C. Træholt, and B. Poulsen. Generic Virtual Power Plants: Management of Distributed Energy Resources under Liberalized Electricity Market. In *8th International Conference on Advances in Power System Control, Operation and Management*, pages 1–6, 2009.
- [ZB09] V. M. Zavala and L. T. Biegler. Nonlinear Model Predictive Control. In Lalo Magni, Davide Martino Raimondo, and Frank Allgöwer, editors, *Control, Nonlinear Programming Strategies for State Estimation and Model Predictive*, volume 384 of *Lecture Notes in Control and Information Sciences*, pages 419–432. Springer Berlin Heidelberg, 2009.
- [ZH14] D. Zhu and G. Hug. Decomposed Stochastic Model Predictive Control for Optimal Dispatch of Storage and Generation. *IEEE Transactions on Smart Grid*, 5(4):2044–2053, 2014.
- [ZJM10] M. N. Zeilinger, C. N. Jones, and M. Morari. Robust Stability Properties of Soft Constrained MPC. In *49th IEEE Conference on Decision and Control (CDC)*, pages 5276–5282, 2010.
- [ZSSM13] X. Zhang, G. Schildbach, D. Sturzenegger, and M. Morari. Scenario-Based MPC for Energy-Efficient Building Climate Control under Weather and Occupancy Uncertainty. In *European Control Conference (ECC)*, pages 1029–1034, 2013.
- [Zug13] M. Zugno. *Optimization Under Uncertainty for Management of Renewables in Electricity Markets*. Ph.D. thesis, Department of Applied Mathematics and Computer Science, Technical University of Denmark, 2013.

Part III

Publications

P A P E R A

A Riccati Based Homogeneous and Self-Dual Interior-Point Method for Linear Economic Model Predictive Control

L. E. Sokoler, G. Frison, K. Edlund, A. Skajaa, and J. B. Jørgensen. A Riccati Based Homogeneous and Self-Dual Interior-Point Method for Linear Economic Model Predictive Control. In *IEEE Multi-conference on Systems and Control*, pages 592–598, 2013.

A Riccati Based Homogeneous and Self-Dual Interior-Point Method for Linear Economic Model Predictive Control

Leo Emil Sokoler, Gianluca Frison, Kristian Edlund, Anders Skajaa and John Bagterp Jørgensen

Abstract—In this paper, we develop an efficient interior-point method (IPM) for the linear programs arising in economic model predictive control of linear systems. The novelty of our algorithm is that it combines a homogeneous and self-dual model, and a specialized Riccati iteration procedure. We test the algorithm in a conceptual study of power systems management. Simulations show that in comparison to state of the art software implementation of IPMs, our method is significantly faster and scales in a favourable way.

I. INTRODUCTION

During the last 30-40 years, model predictive control (MPC) for constrained systems has become the most successful advanced control technology for the process industries [1]–[4]. Technically, MPC is attractive because of its ability to handle constraints, time delays, and multivariate systems in a straightforward and transparent way. The basic idea of MPC is to optimize the forecast of a process model over a finite horizon. At each sampling instant, a new optimization problem is formed and solved. Conventionally, the optimization problems associated with MPC have been formulated as tracking problems that penalize deviations from a set-point. Although this approach ensures that the set-point is reached in a reasonable amount of time, it does not guarantee that the transition between set-points is performed in an economically efficient way. To face this challenge, economic MPC has emerged as a promising technology [5]–[9].

Economic MPC is a variant of MPC that integrates economic information directly in the optimization problem defining the control law. This enables the controller to act based on an economic incentive rather than to deviations from a set-point. Some examples of economic MPC are cost-efficient control of refrigeration systems [10], building climate control [11], [12], and charging batteries in electric vehicles [13]. In linear economic MPC, the optimization problem solved at each sampling instant can be posed as a highly structured linear program. The main contribution of this paper is an efficient algorithm for large-scale problems of this type that combines:

- The homogeneous and self-dual model described in [14]–[17] to facilitate warm-starting
- A specialized and efficiently implemented Riccati iteration procedure to speed-up the most time consuming numerical operations

L. E. Sokoler and K. Edlund are with DONG Energy, DK-2820 Gentofte, Denmark {leoes, kried} @ dongenergy.dk

G. Frison, A. Skajaa and J. B. Jørgensen are with the Department of Informatics and Mathematical Modeling, Technical University of Denmark, DK-2800 Kgs. Lyngby, Denmark {andsk, jbj, giaf} @ imm.dtu.dk

Riccati based IPMs for MPC with ℓ_2 -penalty on set-point deviations have been reported in [18], [19], and similar work for ℓ_1 -penalty in [20]. However, while most modern IPMs are based on the homogeneous and self-dual model, a Riccati iteration procedure for MPC has not previously been developed for such methods.

Our paper is organized as follows. In Section II, we formulate the control law associated with economic MPC as a highly structured linear program. A homogeneous and self-dual IPM for the linear program is derived in Section III. Section IV and Section V show how to implement the IPM efficiently using a highly specialized Riccati iteration procedure and special-purpose linear algebra operations. A MATLAB implementation of our algorithm denoted `LPempc` is compared against state of the art IPMs in Section VI using a small conceptual study in power systems management. Concluding remarks are given in Section VII. Details on our Riccati iteration procedure for economic MPC can be found in the appendix.

II. OPTIMAL CONTROL PROBLEM

We consider linear state space systems in the form

$$\mathbf{x}_{k+1} = \mathbf{A}\mathbf{x}_k + \mathbf{B}u_k + \mathbf{E}d_k, \quad \mathbf{d}_k \sim N(0, \mathbf{R}_d), \quad (1a)$$

$$\mathbf{y}_k = \mathbf{C}_y\mathbf{x}_k + \mathbf{e}_k, \quad \mathbf{e}_k \sim N(0, \mathbf{R}_e), \quad (1b)$$

$$\mathbf{z}_k = \mathbf{C}_z\mathbf{x}_k, \quad (1c)$$

where $\mathbf{x}_0 \sim N(\hat{\mathbf{x}}_0, \mathbf{P}_0)$. Here $(\mathbf{A}, \mathbf{B}, \mathbf{C}_y, \mathbf{C}_z, \mathbf{E})$ are the state space matrices, $\mathbf{x}_k \in \mathbb{R}^{n_x}$ is the state vector, $u_k \in \mathbb{R}^{n_u}$ is the input vector, $\mathbf{y}_k \in \mathbb{R}^{n_z}$ is the measurement vector, $\mathbf{z}_k \in \mathbb{R}^{n_z}$ is the output vector, \mathbf{d}_k is the process noise vector and \mathbf{e}_k is the measurement noise vector. Notice that bold letters indicate stochastic variables.

Economic MPC based on the certainty equivalence principle is a control law for the system (1) that optimizes the control actions with respect to an economic objective function, input limits, input-rate limits and soft output limits. Evaluation of this control law at time step k requires the solution to the following linear program

$$\min_{\mathbf{u}, \hat{\mathbf{x}}, \underline{\mathbf{z}}, \underline{\boldsymbol{\rho}}} \sum_{j \in \mathcal{N}_0} p_{k+j}^T u_{k+j} + q_{k+j+1}^T \rho_{k+j+1}, \quad (2a)$$

$$\text{s.t. } \hat{\mathbf{x}}_{k+j+1|k} = \mathbf{A}\hat{\mathbf{x}}_{k+j|k} + \mathbf{B}u_{k+j}, \quad j \in \mathcal{N}_0, \quad (2b)$$

$$\hat{\mathbf{z}}_{k+j|k} = \mathbf{C}_z\hat{\mathbf{x}}_{k+j|k}, \quad j \in \mathcal{N}_1, \quad (2c)$$

$$\underline{u}_{k+j} \leq u_{k+j} \leq \bar{u}_{k+j}, \quad j \in \mathcal{N}_0, \quad (2d)$$

$$\Delta \underline{u}_{k+j} \leq \Delta u_{k+j} \leq \Delta \bar{u}_{k+j}, \quad j \in \mathcal{N}_0, \quad (2e)$$

$$\underline{z}_{k+j} - \rho_{k+j} \leq \hat{\mathbf{z}}_{k+j|k} \leq \bar{z}_{k+j} + \rho_{k+j}, \quad j \in \mathcal{N}_1, \quad (2f)$$

$$\rho_{k+j} \geq 0, \quad j \in \mathcal{N}_1, \quad (2g)$$

with $(\tilde{w}, \tilde{s}, \tilde{\kappa}, \tilde{\tau}) \geq 0$. We have defined W as a diagonal matrix with diagonal elements w_1, w_2, \dots, w_{m_I} and similarly for S . Moreover, $\mathbf{1}_{m_I}$ is the column vector of all ones of size m_I .

Using the definition (6), the central path may be written as the set

$$\mathcal{C} := \{\phi | V(\phi) = \gamma r^0, \gamma \in [0, 1]\},$$

where $\phi := (\tilde{i}, \tilde{v}, \tilde{w}, \tilde{s}, \tilde{\tau}, \tilde{\kappa})$ and

$$r^k := [V_1(\phi^k)^T \ V_2(\phi^k)^T \ V_3(\phi^k)^T \ V_4(\phi^k)^T \ \mu^k(\mathbf{1}_{m_I})^T \ \mu^k]^T,$$

Here superscript has been introduced to represent the iteration number and $\mu^k := ((\tilde{w}^k)^T s^k + \tilde{\tau}^k \tilde{\kappa}^k) / (m_I + 1)$ is a measure of the duality gap. In addition, $V_i(\phi)$ denotes the i 'th set of components of $V(\phi)$ defined as in (6). Notice, that for fixed $\gamma = 1$ the central path is the initial point, whereas for $\gamma = 0$ the central path is a strict complementary solution of (5).

To track the central path, we use a variant of Mehrotra's predictor-corrector method [22], [23]. The method is based on repeating a two-step procedure. In the first step (affine step) the centering parameter γ is updated and second-order correction terms are computed. Secondly, a corrector step is determined and a new iterate is produced.

The direction associated with the affine step corresponds to a pure Newton direction for (6)

$$J_V(\phi^k) \Delta \phi_{\text{aff}}^k = -V(\phi^k). \quad (7)$$

Here ϕ^k is the current iterate and $\Delta \phi_{\text{aff}}^k$ is the affine direction obtained by solving the system (7).

The Jacobian of V evaluated at ϕ^k is given by

$$J_V(\phi^k) = \begin{bmatrix} 0 & F^T & H^T & 0 & g & 0 \\ -F & 0 & 0 & 0 & b & 0 \\ -H & 0 & 0 & -I & c & 0 \\ -g^T & -b^T & -c^T & 0 & 0 & 1 \\ 0 & 0 & S^k & \tilde{W}^k & 0 & 0 \\ 0 & 0 & 0 & 0 & \tilde{\kappa}^k & \tilde{\tau}^k \end{bmatrix}. \quad (8)$$

Having solved for $\Delta \phi_{\text{aff}}^k$, the affine variables \tilde{w}_{aff}^k , s_{aff}^k , $\tilde{\tau}_{\text{aff}}^k$ and $\tilde{\kappa}_{\text{aff}}^k$ are computed

$$\begin{aligned} \tilde{w}_{\text{aff}}^k &:= \tilde{w}^k + \alpha_{\text{aff}}^k \Delta \tilde{w}_{\text{aff}}^k, & s_{\text{aff}}^k &:= s^k + \beta_{\text{aff}}^k \Delta s_{\text{aff}}^k, \\ \tilde{\tau}_{\text{aff}}^k &:= \tilde{\tau}^k + \alpha_{\text{aff}}^k \Delta \tilde{\tau}_{\text{aff}}^k, & \tilde{\kappa}_{\text{aff}}^k &:= \tilde{\kappa}^k + \beta_{\text{aff}}^k \Delta \tilde{\kappa}_{\text{aff}}^k. \end{aligned}$$

The damping parameters α_{aff} and β_{aff} are introduced to ensure that the non-negative constraints (5f) remain satisfied

$$\begin{aligned} \alpha_{\text{aff}}^k &:= \max \left\{ a_{\text{aff}} \in [0, 1] \left[\begin{array}{c} \tilde{w}_{\text{aff}}^k \\ \tilde{\tau}_{\text{aff}}^k \end{array} \right] + a_{\text{aff}} \left[\begin{array}{c} \Delta \tilde{w}_{\text{aff}}^k \\ \Delta \tilde{\tau}_{\text{aff}}^k \end{array} \right] \geq 0 \right\}, \\ \beta_{\text{aff}}^k &:= \max \left\{ b_{\text{aff}} \in [0, 1] \left[\begin{array}{c} s_{\text{aff}}^k \\ \tilde{\kappa}_{\text{aff}}^k \end{array} \right] + b_{\text{aff}} \left[\begin{array}{c} \Delta s_{\text{aff}}^k \\ \Delta \tilde{\kappa}_{\text{aff}}^k \end{array} \right] \geq 0 \right\}. \end{aligned}$$

To update the centering parameter γ^k , we compare the affine duality gap μ_{aff}^k with the current duality gap μ^k [22]

$$\gamma^k := \left(\frac{\mu_{\text{aff}}^k}{\mu^k} \right)^3 = \left(\frac{((\tilde{w}_{\text{aff}}^k)^T s_{\text{aff}}^k + \tilde{\tau}_{\text{aff}}^k \tilde{\kappa}_{\text{aff}}^k)}{((\tilde{w}^k)^T s^k + \tilde{\tau}^k \tilde{\kappa}^k)} \right)^3. \quad (9)$$

In the second step of Mehrotra's predictor-corrector method, (7) is solved with a modified right hand side.

The resulting linear system of equations is written as

$$J_V(\phi^k) \Delta \phi^k = -\bar{V}(\phi^k),$$

where $\bar{V}_i(\phi) := (1 - \gamma^k) V_i(\phi)$ for $i = 1, 2, 3, 4$ and

$$\begin{aligned} \bar{V}_5(\phi^k) &:= V_5(\phi^k) - \gamma^k \mu^k (\mathbf{1}_{m_I})^T + \Delta \tilde{W}_{\text{aff}}^k \Delta S_{\text{aff}}^k \mathbf{1}_{m_I}, \\ \bar{V}_6(\phi^k) &:= V_6(\phi^k) - \gamma^k \mu^k + \Delta \tilde{\tau}_{\text{aff}}^k \Delta \tilde{\kappa}_{\text{aff}}^k. \end{aligned}$$

Here $\Delta \tilde{W}_{\text{aff}}^k$ and ΔS_{aff}^k are second-order correction terms defined as diagonal matrices with the elements of \tilde{w}_{aff} and s_{aff} appearing on their respective diagonals. Similarly $\Delta \tilde{\tau}_{\text{aff}}^k$ and $\Delta \tilde{\kappa}_{\text{aff}}^k$ are scalar second-order correction terms. Finally, the terms involving γ^k are used to orient the search direction towards the central path based on the updating formula (9).

As in [24], an iterate is classified as optimal if

$$\rho_E^k \leq \varepsilon_E, \quad \rho_I^k \leq \varepsilon_I, \quad \rho_D^k \leq \varepsilon_D, \quad \rho_O^k \leq \varepsilon_O, \quad (10a)$$

and infeasible if $\tilde{\tau}^k \leq \varepsilon_{\tilde{\tau}} \max(1, \tilde{\kappa}^k)$ and

$$\rho_E^k \leq \varepsilon_E, \quad \rho_I^k \leq \varepsilon_I, \quad \rho_D^k \leq \varepsilon_D, \quad \rho_G^k \leq \varepsilon_G. \quad (11a)$$

The parameters $\varepsilon_{\tilde{\tau}}$, ε_E , ε_I , ε_D , ε_O and ε_G are small user-defined tolerances and

$$\begin{aligned} \rho_D &:= \|V_1(\phi)\|_{\infty} / \max(1, \| [H^T \ F^T \ g] \|_{\infty}), \\ \rho_E &:= \|V_2(\phi)\|_{\infty} / \max(1, \| [F \ b] \|_{\infty}), \\ \rho_I &:= \|V_3(\phi)\|_{\infty} / \max(1, \| [H \ I \ c] \|_{\infty}), \\ \rho_G &:= |L - \tilde{\kappa}| / \max(1, \| [g^T \ b^T \ c^T \ 1] \|_{\infty}), \\ \rho_O &:= |L| / (|\tilde{\tau}| + |-b^T \tilde{v} - c^T \tilde{w}|). \end{aligned}$$

where $L := g^T \tilde{v} - (-b^T \tilde{v} - c^T \tilde{w})$ is the duality gap. An implementation of the procedure described above is summarized in Algorithm 1. Notice that a parameter $v \in [0.95; 0.999]$ is introduced to keep the iterates away from the boundary of the feasible region. In `LPempc`, $v = 0.995$.

IV. RICCATI ITERATION PROCEDURE

Solving the linear systems involving the Jacobian matrix (8) is the main computational bottleneck of Algorithm 1. For an arbitrary right hand side, the operations can be written as

$$F^T \Delta \tilde{v} + H^T \Delta \tilde{w} + g \Delta \tilde{\tau} = r_1, \quad (12a)$$

$$b \Delta \tilde{\tau} - F \Delta \tilde{v} = r_2, \quad (12b)$$

$$c \Delta \tilde{\tau} - H \Delta \tilde{v} - \Delta \tilde{s} = r_3, \quad (12c)$$

$$g^T \Delta \tilde{v} + b^T \Delta \tilde{v} + c^T \Delta \tilde{w} - \Delta \tilde{\kappa} = r_4, \quad (12d)$$

$$\tilde{W} \Delta \tilde{s} + \tilde{S} \Delta \tilde{w} = r_5, \quad (12e)$$

$$\tilde{\kappa} \Delta \tilde{\tau} + \tilde{\tau} \Delta \tilde{\kappa} = r_6. \quad (12f)$$

We remark that this system is different from the case of conventional IPMs, due to our introduction of the homogeneous and self-dual model. In particular, a Riccati iteration procedure for MPC has not previously been developed for solving (12) efficiently.

The following proposition shows that the solution of (12) can be obtained by solving a smaller linear system, and a number of computationally inexpensive operations.

Algorithm 1 Homogeneous and self-dual IPM for (5)

Require: $\begin{cases} \text{DATA} & (g, F, b, H, c) \\ \text{INITIAL POINT} & (\tilde{r}, \tilde{v}, \tilde{w}, \tilde{s}, \tilde{\tau}, \tilde{\kappa}) \\ \text{PARAMETERS} & \nu \end{cases}$

```

// initialize
 $\mu \leftarrow (\tilde{w}^T \tilde{s} + \tilde{\tau} \tilde{\kappa}) / (m_I + 1)$ 
while not CONVERGED do
  // affine step
   $\Delta\phi_{\text{aff}} \leftarrow -J_V(\phi)^{-1}V(\phi)$ 
  // center parameter
   $\alpha_{\text{aff}} \leftarrow \max \left\{ a_{\text{aff}} \in [0, 1] \left[ \begin{array}{c} \tilde{w} \\ \tilde{\tau} \end{array} \right] + a_{\text{aff}} \left[ \begin{array}{c} \Delta\tilde{w}_{\text{aff}} \\ \Delta\tilde{\tau}_{\text{aff}} \end{array} \right] \geq 0 \right\}$ 
   $\beta_{\text{aff}} \leftarrow \max \left\{ b_{\text{aff}} \in [0, 1] \left[ \begin{array}{c} \tilde{s} \\ \tilde{\kappa} \end{array} \right] + b_{\text{aff}} \left[ \begin{array}{c} \Delta\tilde{s}_{\text{aff}} \\ \Delta\tilde{\kappa}_{\text{aff}} \end{array} \right] \geq 0 \right\}$ 
   $\tilde{s}_{\text{aff}} \leftarrow \tilde{s} + \beta_{\text{aff}} \Delta\tilde{s}_{\text{aff}}, \quad \tilde{\kappa}_{\text{aff}} \leftarrow \tilde{\kappa} + \beta_{\text{aff}} \Delta\tilde{\kappa}_{\text{aff}}$ 
   $\tilde{w}_{\text{aff}} \leftarrow \tilde{w} + \alpha_{\text{aff}} \Delta\tilde{w}_{\text{aff}}, \quad \tilde{\tau}_{\text{aff}} \leftarrow \tilde{\tau} + \alpha_{\text{aff}} \Delta\tilde{\tau}_{\text{aff}}$ 
   $\mu_{\text{aff}} \leftarrow (\tilde{w}_{\text{aff}}^T \tilde{s}_{\text{aff}} + \tilde{\tau}_{\text{aff}} \tilde{\kappa}_{\text{aff}}) / (m_I + 1)$ 
   $\gamma \leftarrow (\mu_{\text{aff}} / \mu)^3$ 
  // predictor-corrector step
   $\Delta\phi \leftarrow -J_V(\phi)^{-1}\tilde{V}(\phi)$ 
  // step update
   $\alpha \leftarrow \max \left\{ a \in [0, 1] \left[ \begin{array}{c} \tilde{w} \\ \tilde{\tau} \end{array} \right] + a \left[ \begin{array}{c} \Delta\tilde{w} \\ \Delta\tilde{\tau} \end{array} \right] \geq 0 \right\}$ 
   $\beta \leftarrow \max \left\{ b \in [0, 1] \left[ \begin{array}{c} \tilde{s} \\ \tilde{\kappa} \end{array} \right] + b \left[ \begin{array}{c} \Delta\tilde{s} \\ \Delta\tilde{\kappa} \end{array} \right] \geq 0 \right\}$ 
   $\tilde{r} \leftarrow \tilde{r} + \nu\beta\Delta\tilde{r}, \quad \tilde{s} \leftarrow \tilde{s} + \nu\beta\Delta\tilde{s}, \quad \tilde{\kappa} \leftarrow \tilde{\kappa} + \nu\beta\Delta\tilde{\kappa}$ 
   $\tilde{v} \leftarrow \tilde{v} + \nu\alpha\Delta\tilde{v}, \quad \tilde{w} \leftarrow \tilde{w} + \nu\alpha\Delta\tilde{w}, \quad \tilde{\tau} \leftarrow \tilde{\tau} + \nu\alpha\Delta\tilde{\tau}$ 
   $\mu \leftarrow (\tilde{w}^T \tilde{s} + \tilde{\tau} \tilde{\kappa}) / (m_I + 1)$ 
end while

```

Proposition 2: The solution to (12) can be obtained by solving

$$\begin{bmatrix} 0 & F^T & H^T \\ -F & 0 & 0 \\ -H & 0 & \tilde{W}^{-1}\tilde{S} \end{bmatrix} \begin{bmatrix} f_1 & h_1 \\ f_2 & h_2 \\ f_3 & h_3 \end{bmatrix} = \begin{bmatrix} r_1 & -g \\ r_2 & -b \\ \hat{r}_3 & -c \end{bmatrix}, \quad (13)$$

and subsequent computation of

$$\begin{aligned} \Delta\tilde{\tau} &= \frac{\hat{r}_6 - \tilde{\tau}(g^T f_1 + b^T f_2 + c^T f_3)}{\tilde{\kappa} + \tilde{\tau}(g^T h_1 + b^T h_2 + c^T h_3)}, \\ \Delta\tilde{r} &= f_1 + h_1 \Delta\tilde{\tau}, \\ \Delta\tilde{v} &= f_2 + h_2 \Delta\tilde{\tau}, \\ \Delta\tilde{w} &= f_3 + h_3 \Delta\tilde{\tau}, \\ \Delta\tilde{\kappa} &= g^T \Delta\tilde{r} + b^T \Delta\tilde{v} + c^T \Delta\tilde{w} - r_4, \\ \Delta\tilde{s} &= \tilde{W}^{-1}(r_C - \tilde{S} \Delta\tilde{w}), \end{aligned}$$

where $\hat{r}_3 := r_3 + \tilde{W}^{-1}r_5$ and $\hat{r}_6 := r_6 + \tilde{\tau}r_4$.

Proof: See [24]. ■

To solve (13) efficiently, we have developed a Riccati iteration procedure specifically tailored to economic MPC. The procedure exploits the problem structure by reducing the original system into a much smaller system, which is then solved by a standard recursive approach. For further details, we refer to the appendix.

The proposed method has order of complexity $O(N(n_u + n_x + n_y)^3)$ per iteration. In comparison, a general purpose solver based on dense linear algebra yields $O(N^3(n_u + n_x + n_y)^3)$. Thus, the computational cost per iteration is reduced by two orders of magnitude in N . However, as described in [25], the complexity of IPMs based on direct sparse linear algebra is linear to quadratic for problems such as (2). Notice also, that if the number of states n_x is very large, condensing methods using state-elimination have an advantage over a Riccati based solver [19].

V. SPECIAL OPERATORS

To speed-up the numerical computations and reduce the storage requirements of Algorithm 1, operations involving the structured matrices F and H are implemented as specialized linear algebra routines. Denote the Lagrange multipliers associated with the inequality constraints (2d)-(2g) as $\Delta\eta$, $\Delta\lambda$, Δv , $\Delta\omega$, $\Delta\gamma$, $\Delta\zeta$ and $\Delta\xi$ where $\Delta\eta := [\Delta\eta_0^T \ \Delta\eta_1^T \ \dots \ \Delta\eta_{N-1}^T]^T$, and similarly for $\Delta\lambda$, Δv , $\Delta\omega$, $\Delta\gamma$, $\Delta\zeta$ and $\Delta\xi$. $\Delta\eta$ and $\Delta\lambda$ are multipliers for the input limits (2d), Δv and $\Delta\omega$ are multipliers for the input-rate limits (2e), $\Delta\gamma$ and $\Delta\zeta$ are multipliers for the output limits (2f) and $\Delta\xi$ is the vector of multipliers for the non-negative constraints (2g). Using this notation, the optimization variables \tilde{r} , \tilde{v} , and \tilde{w} can be stated in the form

$$\begin{aligned} \tilde{r} &= [u_0^T \ \hat{x}_1^T \ \rho_1^T \ \dots \ u_{N-1}^T \ \hat{x}_N^T \ \rho_N^T]^T, \\ \tilde{v} &= [\tilde{v}_1^T \ \dots \ \tilde{v}_N^T]^T, \\ \tilde{w} &= [\eta^T \ \lambda^T \ v^T \ \omega^T \ \gamma^T \ \zeta^T \ \xi^T]^T. \end{aligned}$$

As an example consider the case $N = 2$. In this case the specialized linear algebra routines are

$$\begin{aligned} F^T \tilde{v} &= [\tilde{v}_1^T B \ \tilde{v}_2^T A - \tilde{v}_1^T \ 0 \ \tilde{v}_2^T B \ -\tilde{v}_2^T \ 0]^T, \\ H^T \tilde{w} &= \begin{bmatrix} \eta_0 - \lambda_0 + v_0 - \omega_0 \\ D^T(\omega_1 - v_1) + C^T(\gamma_1 - \zeta_1) \\ -\gamma_1 - \zeta_1 - \eta_1 \\ \eta_1 - \lambda_1 + v_1 - \omega_1 \\ C^T(\gamma_2 - \zeta_2) \\ -\gamma_2 - \zeta_2 - \eta_2 \end{bmatrix}, \end{aligned}$$

and

$$\begin{aligned} H\tilde{r} &= [u^T \ -u^T \ u_0^T \ (u_1 - D\hat{x}_1)^T \ -u_0^T \ (D\hat{x}_1 - u_1)^T \\ &\quad (C\hat{x}_1 - \rho_1)^T \ (C\hat{x}_2 - \rho_2)^T \ (-C\hat{x}_1 - \rho_1)^T \\ &\quad \quad \quad (-C\hat{x}_2 - \rho_2)^T \ -\tilde{\rho}^T]^T, \\ Ft &= [(Bu_0 - \hat{x}_1)^T \ (A\hat{x}_1 + Bu_1 - \hat{x}_2)^T]^T, \end{aligned}$$

VI. CASE STUDY - POWER SYSTEM

We now present a case study of economic MPC, which is used to compare LP_{emPC} against state of the art IPMs. The tolerance parameters in (10)-(11) are set to 10^{-8} . It has been verified that for this setup, approximately the same accuracy in the solution is achieved for all other solvers using their default tolerance settings. The study is performed on an Intel(R) Core(TM) i5-2520M CPU @ 2.50GHz with 4 GB RAM running a 64-bit Ubuntu 12.04.1 LTS operating system.

TABLE I

CASE STUDY PARAMETERS. THE PORTFOLIO CONSISTS OF A FAST AND EXPENSIVE GENERATOR, AND A SLOW AND CHEAP GENERATOR.

	τ	p_k	u_k	\bar{u}_k	Δu_k	$\Delta \bar{u}_k$
Power Generator 1	90	100	0	200	-20	20
Power Generator 2	30	200	0	150	-40	40

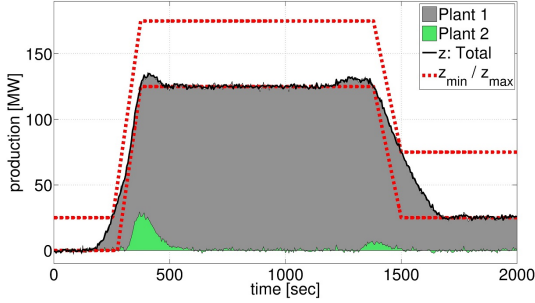


Fig. 1. Closed-loop simulation of a stochastic power system controlled by economic MPC. A majority of the production is produced by the cheap (slow) power generator, while the expensive unit (fast) is used only when extra flexibility is required to satisfy the constraints.

In our study, we consider generic power generators in the form [26]

$$Y_i(s) = \frac{1}{(\tau_i s + 1)^3} U_i(s), \quad i = 1, 2, \dots, m. \quad (14)$$

Here $U_i(s)$ is the units of fuel supplied to generator i and $Y_i(s)$ is its power production. Moreover, the total power production is given by

$$Z(s) = \sum_{i=1}^m Y_i(s) = \sum_{i=1}^m \frac{1}{(\tau_i s + 1)^3} U_i(s). \quad (15)$$

The system (14)-(15) is realized as a state space system in the form (1), where $u_k \in \mathbb{R}^m$ is the units of fuel supplied to the power generators, $y_k \in \mathbb{R}^m$ is the measured power production of each generator and $z_k \in \mathbb{R}$ is the total power production.

Fig. 1 illustrates an example with $m = 2$ power generators. The simulation is performed in closed-loop over $N = 400$ time steps using a sampling time of $T_s = 5$ seconds. Thus, the optimization problem (2) is solved 400 times. The controller objective is to keep the total power production within a certain pre-defined range, while minimizing input costs and respecting capacity constraints. The case study parameters are listed in Table I. Aside the parameters listed in the table, we have fixed the length of the prediction horizon to $N = 80$ and $q_k = 10^4$ over the entire scenario. Moreover, full information about the initial state is given $\mathbf{x}_0 \sim (0, 0)$ and $R_d = R_e = I$.

The closed-loop solution depicted in Fig. 1 was computed using LP_{empc} , and IPMs from the following software packages: SeDuMi , MOSEK , LIPSOL and GLPK . These solvers are mainly written in low-level language such as FORTRAN or C and rely on sparse linear algebra routines that are specifically tailored to the solution of large-scale

TABLE II

COMPARISON OF THE NUMBER OF ITERATIONS, BASED ON OUR CLOSED-LOOP SIMULATION.

	Min	Max	Mean	Std.	Fail Rate (%)
LP_{empc} (HSD)	11	23	17.4	2.35	0
MOSEK (HSD)	12	53	22.1	8.17	0
SeDuMi (HSD)	15	23	19.3	1.55	0
LIPSOL	12	45	19.2	9.63	11.25
GLPK	15	26	19.42	1.72	8.25

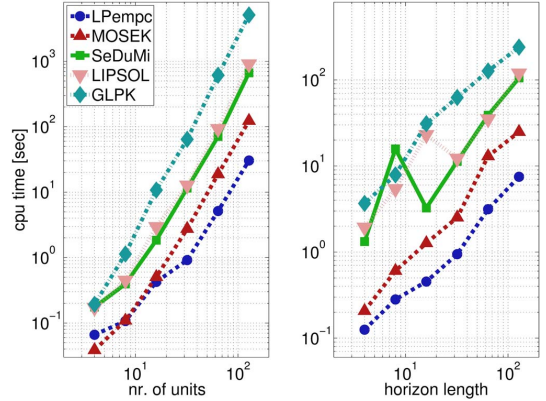


Fig. 2. CPU-time for the different solvers as a function of the number of power generators m (fixed $N = 32$) and the length of the prediction horizon N (fixed $m = 32$).

sparse linear and conic programs. In comparison, LP_{empc} is written in MATLAB with a separate MEX-file performing the Riccati iteration procedure.

Table II lists selected results from the closed loop simulation. We have tagged the IPMs based on the homogeneous and self-dual model by (HSD).

The fail rate accounts for the cases in which numerical instabilities occurred, or more than 100 iterations were used. Thus, the table indicates that the homogeneous and self-dual IPMs are more reliable than the conventional IPMs. Moreover, our simulations show that LP_{empc} and SeDuMi use a smaller and less fluctuating number of iterations than MOSEK .

In Fig. 2 we have compared the CPU-time for the different solvers, as a function of the number of power generators and the length of the prediction horizon. The figure shows that the advantage of using LP_{empc} increases with the problem size. E.g. for 16 units, MOSEK and LP_{empc} are approximately equally fast, but for 128 units the difference is a factor 4. For 128 units LP_{empc} is about 150 times faster than GLPK . Similar results is observed for an increasing prediction horizon N .

VII. CONCLUSION & FUTURE WORK

In this paper, we have developed an efficient Riccati based homogeneous and self-dual IPM for linear economic MPC. Simulations show that a MATLAB implementation of our algorithm, LP_{empc} , is significantly faster than state of

the art IPMs based on direct sparse linear algebra. As the problems become larger LP_{empc} becomes relatively faster. We have also observed that for our problem, homogeneous and self-dual IPMs are more reliable (100% convergence) than conventional IPMs (90-95% convergence).

Although the advantages of homogeneous and self-dual IPMs have been widely accepted in the field of optimization, they have not yet been adopted by the MPC community. Our work on extending Riccati based solvers for MPC to homogeneous and self dual IPMs is therefore a significant contribution that allows for MPC-based controllers to exploit important features of the homogeneous and self-dual model. One example is the warm-starting approach of [17] which will be implemented in the next edition of LP_{empc} . Since the optimization problems solved at successive sampling instants in MPC are very similar, we expect that this method will reduce the number of iterations for LP_{empc} significantly.

APPENDIX

Riccati Iteration Procedure for Economic MPC

Consider the system (13)

$$\begin{bmatrix} 0 & F^T & H^T \\ -F & 0 & 0 \\ -H & 0 & \tilde{W}^{-1}\tilde{S} \end{bmatrix} \begin{bmatrix} f_1 & h_1 \\ f_2 & h_2 \\ f_3 & h_3 \end{bmatrix} = \begin{bmatrix} r_1 & -g \\ r_2 & -b \\ \hat{r}_3 & -c \end{bmatrix}.$$

For a single arbitrary right hand side, we may write this system as

$$\begin{bmatrix} 0 & F^T & H^T \\ -F & 0 & 0 \\ -H & 0 & \tilde{W}^{-1}\tilde{S} \end{bmatrix} \begin{bmatrix} \Delta\tilde{r} \\ \Delta\tilde{v} \\ \Delta\tilde{w} \end{bmatrix} = \begin{bmatrix} r_D \\ r_E \\ r_I \end{bmatrix}. \quad (16)$$

Using the same notation as in Section V, we write the solution to (16) in the form

$$\begin{aligned} \Delta\tilde{r} &= [\Delta u_0^T \quad \Delta\hat{x}_1^T \quad \Delta\rho_1^T \quad \dots \quad \Delta u_{N-1}^T \quad \Delta\hat{x}_N^T \quad \Delta\rho_N^T]^T, \\ \Delta\tilde{v} &= [\Delta\tilde{v}_0^T \quad \Delta\tilde{v}_1^T \quad \dots \quad \Delta\tilde{v}_{N-1}^T]^T, \\ \Delta\tilde{w} &= [\Delta\eta^T \quad \Delta\lambda^T \quad \Delta v^T \quad \Delta\omega^T \quad \Delta\gamma^T \quad \Delta\zeta^T \quad \Delta\xi^T]^T. \end{aligned}$$

Accordingly, we partition the right hand side such that

$$\begin{aligned} r_D &= [r_{u,0}^T \quad r_{x,1}^T \quad r_{w,1}^T \quad \dots \quad r_{u,N-1}^T \quad r_{x,N}^T \quad r_{w,N}^T]^T, \\ r_E &= [R_{v,0}^T \quad R_{v,1}^T \quad \dots \quad R_{v,N-1}^T]^T, \\ r_I &= [r_\eta^T \quad r_\lambda^T \quad r_v^T \quad r_\omega^T \quad r_\gamma^T \quad r_\zeta^T \quad r_\xi^T]^T, \end{aligned}$$

and write the diagonal matrix $\tilde{W}^{-1}\tilde{S}$ in terms of diagonal submatrices

$$\tilde{W}^{-1}\tilde{S} = \mathbf{diag} \left(\Sigma_\eta^T, \Sigma_\lambda^T, \Sigma_v^T, \Sigma_\omega^T, \Sigma_\gamma^T, \Sigma_\zeta^T, \Sigma_\xi^T \right).$$

The linear system of equations (16) can now be stated in the form

$$\begin{aligned} \Delta\eta_i - \Delta\lambda_i + \Delta v_i - \Delta\omega_i + B^T \Delta\tilde{v}_i &= r_{u,i}, & i \in \mathcal{N}_0, \\ -\Delta u_i + \Sigma_{\eta,i} \Delta\eta_i &= r_{\eta,i}, & i \in \mathcal{N}_0, \\ \Delta u_i + \Sigma_{\lambda,i} \Delta\lambda_i &= r_{\lambda,i}, & i \in \mathcal{N}_0, \\ -\Delta u_i + D \Delta\hat{x}_i + \Sigma_{v,i} \Delta v_i &= r_{v,i}, & i \in \mathcal{N}_0, \\ \Delta u_i - D \Delta\hat{x}_i + \Sigma_{\omega,i} \Delta\omega_i &= r_{\omega,i}, & i \in \mathcal{N}_0, \\ \Delta\hat{x}_{i+1} - A \Delta\hat{x}_i - B \Delta u_i &= R_{v,i}, & i \in \mathcal{N}_0, \\ \Delta\rho_i - C_z \Delta\hat{x}_i + \Sigma_{\gamma,i} \Delta\gamma_i &= r_{\gamma,i}, & i \in \mathcal{N}_1, \\ \Delta\rho_i + C_z \Delta\hat{x}_i + \Sigma_{\zeta,i} \Delta\zeta_i &= r_{\zeta,i}, & i \in \mathcal{N}_1, \\ \Delta\rho_i + \Sigma_{\xi,i} \Delta\xi_i &= r_{\xi,i}, & i \in \mathcal{N}_1, \\ -\Delta\gamma_i - \Delta\zeta_i - \Delta\xi_i &= r_{w,i}, & i \in \mathcal{N}_1, \\ -\Delta\tilde{v}_i + C_z^T (\Delta\gamma_{i+1} - \Delta\zeta_{i+1}) + A^T \Delta\tilde{v}_i \\ + D^T (\omega_i - \Delta v_i) &= r_{x,i}, & i \in \mathcal{N}_0, \end{aligned}$$

with $\mathcal{N}_0 := \mathcal{N} \setminus 0$ and the special cases

$$\begin{aligned} -\Delta u_0 + \Sigma_{v,0} \Delta v_0 &= r_{v,0}, \\ \Delta u_0 + \Sigma_{\omega,0} \Delta\omega_0 &= r_{\omega,0}, \\ \Delta\hat{x}_1 - B \Delta u_0 &= R_{v,0}, \\ -\Delta\tilde{v}_{N-1} + C_z^T (\Delta\gamma_N - \Delta\zeta_N) &= r_{x,N}. \end{aligned}$$

By eliminating the Lagrange multipliers for the inequality constrains $\Delta\eta$, $\Delta\lambda$, Δv , $\Delta\omega$, $\Delta\gamma$, $\Delta\zeta$ and $\Delta\xi$ we get the reduced set of equations

$$B^T \Delta\tilde{v}_0 + U_0 \Delta u_0 = R_{u,0}, \quad (17a)$$

$$B^T \Delta\tilde{v}_i + U_i \Delta u_i + G_i \Delta\hat{x}_i = R_{u,i}, \quad i \in \mathcal{N}_0, \quad (17b)$$

$$-\Delta\hat{x}_1 + B \Delta u_0 = R_{v,0}, \quad (17c)$$

$$-\Delta\hat{x}_{i+1} + A \Delta\hat{x}_i + B \Delta u_i = R_{v,i}, \quad i \in \mathcal{N}_0, \quad (17d)$$

$$W_i \Delta\rho_i + M_i^T \Delta\hat{x}_i = R_{w,i}, \quad i \in \mathcal{N}_1, \quad (17e)$$

$$\begin{aligned} -\Delta\tilde{v}_{i-1} + M_i \Delta\rho_i + \bar{X}_i \Delta\hat{x}_i \\ + G_i^T \Delta u_i + A^T \Delta\tilde{v}_i &= \bar{R}_{x,i}, \quad i \in \mathcal{N}_0, \end{aligned} \quad (17f)$$

$$-\Delta\tilde{v}_{N-1} + M_N \Delta\rho_N + \bar{X}_N \Delta\hat{x}_N = \bar{R}_{x,N}, \quad (17g)$$

where we have defined

$$U_i := \Sigma_{\eta,i}^{-1} + \Sigma_{\lambda,i}^{-1} + \Sigma_{\omega,i}^{-1} + \Sigma_{v,i}^{-1}, \quad i \in \mathcal{N}_0,$$

$$G_i := -(\Sigma_{\omega,i}^{-1} + \Sigma_{v,i}^{-1})D, \quad i \in \mathcal{N}_0,$$

$$W_i := \Sigma_{\zeta,i}^{-1} + \Sigma_{\xi,i}^{-1} + \Sigma_{\gamma,i}^{-1}, \quad i \in \mathcal{N}_1,$$

$$M_i := C_z^T (\Sigma_{\zeta,i}^{-1} - \Sigma_{\gamma,i}^{-1}), \quad i \in \mathcal{N}_1,$$

$$\bar{X}_i := C_z^T (\Sigma_{\zeta,i}^{-1} + \Sigma_{v,i}^{-1})C_z + D^T (\Sigma_{\gamma,i}^{-1} + \Sigma_{\omega,i}^{-1})D, \quad i \in \mathcal{N}_0,$$

$$\bar{X}_N := C_z^T (\Sigma_{\zeta,N}^{-1} + \Sigma_{v,N}^{-1})C_z.$$

Furthermore

$$R_{u,i} := r_{u,i} + \bar{r}_{\lambda,i} + \bar{r}_{\omega,i} - \bar{r}_{\eta,i} - \bar{r}_{v,i}, \quad i \in \mathcal{N}_0,$$

$$R_{v,i} := -R_{v,i}, \quad i \in \mathcal{N}_0,$$

$$R_{w,i} := r_{w,i-1} + \bar{r}_{\zeta,i-1} + \bar{r}_{\xi,i} + \bar{r}_{\gamma,i}, \quad i \in \mathcal{N}_1,$$

$$\bar{R}_{x,i} := r_{x,i} + C_z^T (\bar{r}_{\zeta,i} - \bar{r}_{\gamma,i}) + D^T (\bar{r}_{v,i} - \bar{r}_{\omega,i}), \quad i \in \mathcal{N}_0,$$

$$\bar{R}_{x,N} := r_{x,N} + C_z^T (\bar{r}_{\zeta,N} - \bar{r}_{\gamma,N}).$$

P A P E R B

A Decomposition Algorithm for Optimal Control of Distributed Energy Systems

L. E. Sokoler, K. Edlund, L. Standardi, and J. B. Jørgensen. A Decomposition Algorithm for Optimal Control of Distributed Energy Systems. In *4th IEEE/PES Innovative Smart Grid Technologies Europe (ISGT Europe)*, pages 1–5, 2013.

A Decomposition Algorithm for Optimal Control of Distributed Energy Systems

Leo Emil Sokoler and Kristian Edlund
DONG Energy, DK-2820 Gentofte, Denmark
Email: {leoes,kried}@dongenergy.dk

Laura Standardi and John Bagterp Jørgensen
Department of Applied Mathematics and Computer Science
Technical University of Denmark, DK-2800 Kgs. Lyngby, Denmark
Email: {laus, jbjø}@dtu.dk

Abstract—In economic model predictive control of distributed energy systems, the constrained optimal control problem can be expressed as a linear program with a block-angular structure. In this paper, we present an efficient Dantzig-Wolfe decomposition algorithm specifically tailored to problems of this type. Simulations show that a MATLAB implementation of the algorithm is significantly faster than several state-of-the-art linear programming solvers and that it scales in a favorable way.

I. INTRODUCTION

Due to global concerns related to environmental issues and security of supply, an increasing share of electricity is being produced by renewable energy sources. Accordingly, methods for power production planning that can handle the volatile and unpredictable power generation associated with technologies such as wind, solar and wave power are required. For this reason, energy systems management has emerged as a promising application area for economic model predictive control (MPC).

In economic MPC of energy systems, the power production planning is handled in real-time by an optimization algorithm that computes an optimal production plan based on the most recent information available such as forecasts of energy prices, wind power production, and district heating consumption. Examples of economic MPC in energy systems management include cost-efficient control of refrigeration systems [1], building climate control [2], [3], and optimal charging strategies for batteries in electric vehicles [4].

Economic MPC requires the solution of a linear program at every sampling instant. In energy systems management, the solution to this linear problem, known as the optimal control problem, provides a sequence of control moves that yields the most cost-efficient power generation, with respect to a process model of the power system. To compensate for non-predictable disturbances and discrepancies between the process model and the true system, only the first input in the sequence of control moves is applied to the system, and the optimization procedure is repeated using updated information at the following sampling instant.

As the control moves are computed in real-time, one of the key challenges in economic MPC is to solve the optimal control problem in an efficient and reliable way. The main contribution of this paper is an algorithm for control of distributed energy systems that satisfies these criteria. Our algorithm exploits that the units in a distributed energy system

are dynamically decoupled. This gives rise to a block-angular structure in the optimal control problem, that allows it to be decomposed into a master problem and a number of subproblems, using Dantzig-Wolfe decomposition [5], [6]. To solve the decomposed problem efficiently we use a column generation procedure, which is warm-started by a strategy that utilizes problem specific features. Similar algorithms have been applied to coordinate the target calculation in set-point based MPC [7], [8], building climate control [9], and hierarchical MPC-based control [10].

A. Paper Organization

This paper is organized as follows. In Section II, we introduce the optimal control problem solved in economic MPC and a compact problem formulation is derived. We decompose the problem using Dantzig-Wolfe decomposition in Section III, and optimality conditions are derived in Section IV. In this section we also present a warm-started column generation procedure for solving the optimization problem. Performance benchmarks for the proposed algorithm based on a conceptual energy systems management case study are provided in Section V. We give concluding remarks in Section VI.

II. PROBLEM DEFINITION

We consider an electrical grid with M dynamically decoupled power generating units. The units are modelled as discrete state space systems in the form

$$x_{j,k+1} = A_j x_{j,k} + B_j u_{j,k}, \quad j \in \mathcal{M}, \quad (1a)$$

$$y_{j,k} = C_j x_{j,k}, \quad j \in \mathcal{M}, \quad (1b)$$

where $\mathcal{M} = \{1, 2, \dots, M\}$. The state space matrices are denoted as (A_j, B_j, C_j) , the states as $x_{j,k} \in \mathbb{R}^{n_x(j)}$, the inputs as $u_{j,k} \in \mathbb{R}^{n_u(j)}$, and the outputs as $y_{j,k} \in \mathbb{R}^{n_y(j)}$.

Assuming that the power production is available as a linear combination of the outputs in (1), the total power production can be written as

$$y_{T,k} = \sum_{j \in \mathcal{M}} \Upsilon_j y_{j,k} = \sum_{j \in \mathcal{M}} \Upsilon_j C_j x_{j,k}, \quad (2)$$

in which $\Upsilon_j \in \mathbb{R}^{1 \times n_y(j)}$ is a row vector such that $\Upsilon_j C_j x_{j,k}$ is the power production of unit j at time step k .

Economic MPC defines a control law for the generating units (1), that optimizes the inputs (control moves) with

respect to an economic objective function, input limits, input rate limits and soft output limits. Evaluating this control law requires the solution to the minimization problem

$$\min_{u,x,y,T,\rho,\gamma} \sum_{k \in \mathcal{N}_0} q_{k+1}^T \rho_{k+1} + \sum_{j \in \mathcal{M}} p_{j,k}^T u_{j,k} + r_{j,k+1}^T \gamma_{j,k+1}, \quad (3a)$$

subject to the constraints

$$x_{j,k+1} = A_j x_{j,k} + B_j u_{j,k}, \quad k \in \mathcal{N}_0, \quad j \in \mathcal{M}, \quad (3b)$$

$$y_{j,k} = C_j x_{j,k}, \quad k \in \mathcal{N}_1, \quad j \in \mathcal{M}, \quad (3c)$$

$$y_{T,k} = \sum_{j \in \mathcal{M}} \Upsilon_j C_j x_{j,k}, \quad k \in \mathcal{N}_1, \quad (3d)$$

$$\underline{u}_{j,k} \leq u_{j,k} \leq \bar{u}_{j,k}, \quad k \in \mathcal{N}_0, \quad j \in \mathcal{M}, \quad (3e)$$

$$\Delta \underline{u}_{j,k} \leq u_{j,k} - u_{j,k-1} \leq \Delta \bar{u}_{j,k}, \quad k \in \mathcal{N}_0, \quad j \in \mathcal{M}, \quad (3f)$$

$$\underline{y}_{j,k} - \gamma_{j,k} \leq y_{j,k} \leq \bar{y}_{j,k} + \gamma_{j,k}, \quad k \in \mathcal{N}_1, \quad j \in \mathcal{M}, \quad (3g)$$

$$0 \leq \gamma_{j,k} \leq \bar{\gamma}_{j,k}, \quad k \in \mathcal{N}_1, \quad j \in \mathcal{M}, \quad (3h)$$

$$\underline{y}_{T,k} - \rho_k \leq y_{T,k} \leq \bar{y}_{T,k} + \rho_k, \quad k \in \mathcal{N}_1, \quad (3i)$$

$$0 \leq \rho_k \leq \bar{\rho}_k, \quad k \in \mathcal{N}_1, \quad (3j)$$

where $\mathcal{N}_i = \{0 + i, 1 + i, \dots, N - 1 + i\}$, with N being the length of the prediction horizon. The input data are the input limits, $(\underline{u}_{j,k}, \bar{u}_{j,k})$, the input rate limits, $(\Delta \underline{u}_{j,k}, \Delta \bar{u}_{j,k})$, the output limits associated with the generating units, $(\underline{y}_{j,k}, \bar{y}_{j,k})$, the output limits associated with the total power production, $(\underline{y}_{T,k}, \bar{y}_{T,k})$, the input prices, $p_{j,k}$, the price for violating the output limits associated with the generating units, $r_{j,k}$, and the price for violating the output limits associated with the total power production q_k . The slack variables $\gamma_{j,k}$ and ρ_k represent the violation of the output constraints. We include upper limits, $(\bar{\gamma}_{j,k}, \bar{\rho}_k)$, on these variables, as this simplifies later computations considerably.

A. Compact Formulation

By eliminating the states using equation (1a), we can write the output equation, (1b), as

$$y_{j,k} = C_j A_j^k x_{j,0} + \sum_{i \in \mathcal{N}_0} H_{j,k-i} u_{j,i}, \quad j \in \mathcal{M},$$

where the impulse response coefficients are given by

$$H_{j,k} = C_j A_j^{k-1} B_j, \quad j \in \mathcal{M}.$$

Consequently

$$y_{T,k} = \sum_{j \in \mathcal{M}} \left(\Upsilon_j C_j A_j^k x_{j,0} + \sum_{i \in \mathcal{N}_0} \Upsilon_j H_{j,k-i} u_{j,i} \right).$$

Define the vectors

$$y_j = [y_{j,1}^T \quad y_{j,2}^T \quad \cdots \quad y_{j,N}^T]^T, \quad j \in \mathcal{M}, \quad (4a)$$

$$u_j = [u_{j,0}^T \quad u_{j,1}^T \quad \cdots \quad u_{j,N-1}^T]^T, \quad j \in \mathcal{M}, \quad (4b)$$

and the matrices

$$\Gamma_j = \begin{bmatrix} H_{j,1} & 0 & \cdots & 0 \\ H_{j,2} & H_{j,1} & & \\ \vdots & \vdots & \ddots & \\ H_{j,N} & H_{j,N-1} & \cdots & H_{j,1} \end{bmatrix}, \quad \Phi_j = \begin{bmatrix} C_j A_j \\ C_j A_j^2 \\ \vdots \\ C_j A_j^{N-1} \end{bmatrix},$$

for $j \in \mathcal{M}$.

We can then write the outputs, (4a), for each of the generating units as

$$y_j = \Gamma_j u_j + \Phi_j x_{j,0}, \quad j \in \mathcal{M}. \quad (5)$$

Moreover, by introducing $\tilde{\Gamma}_j$ and $\tilde{\Phi}_j$ accordingly, it follows that $y_T = \sum_{j \in \mathcal{M}} \tilde{\Gamma}_j u_j + \tilde{\Phi}_j x_{j,0}$. We simplify the notation further by introducing

$$\underline{u}_j = [\underline{u}_{j,0}^T \quad \underline{u}_{j,1}^T \quad \cdots \quad \underline{u}_{j,N-1}^T]^T, \quad j \in \mathcal{M},$$

$$\bar{u}_j = [\bar{u}_{j,0}^T \quad \bar{u}_{j,1}^T \quad \cdots \quad \bar{u}_{j,N-1}^T]^T, \quad j \in \mathcal{M},$$

and similarly we define $\Delta \underline{u}_j$, $\Delta \bar{u}_j$, \underline{y}_j , \bar{y}_j , \underline{y}_T , \bar{y}_T , $\bar{\gamma}_j$, $\bar{\rho}$, ρ , q , p_j , r_j and γ_j . Using this notation, the optimal control problem, (3), can be written as

$$\min_{u,\rho,\gamma} q^T \rho + \sum_{j \in \mathcal{M}} p_j^T u_j + r_j^T \gamma_j, \quad (6a)$$

subject to a set of decoupled constraints

$$\underline{u}_j \leq u_j \leq \bar{u}_j, \quad j \in \mathcal{M}, \quad (6b)$$

$$\Delta \underline{u}_j \leq \Delta u_j \leq \Delta \bar{u}_j, \quad j \in \mathcal{M}, \quad (6c)$$

$$\underline{y}_j - \gamma_j \leq \Gamma_j u_j + \Phi_j x_{j,0} \leq \bar{y}_j + \gamma_j, \quad j \in \mathcal{M}, \quad (6d)$$

$$0 \leq \gamma_j \leq \bar{\gamma}_j, \quad j \in \mathcal{M}, \quad (6e)$$

$$0 \leq \rho \leq \bar{\rho}, \quad (6f)$$

and a set of linking constraints

$$\underline{y}_T - \rho \leq \sum_{j \in \mathcal{M}} \tilde{\Gamma}_j u_j + \tilde{\Phi}_j x_{j,0} \leq \bar{y}_T + \rho. \quad (6g)$$

In a compact form, (6) can be stated by

$$\min_z \sum_{j \in \mathcal{M}} c_j^T z_j, \quad (7a)$$

$$\text{s.t. } G_j z_j \geq g_j, \quad j \in \mathcal{M}, \quad (7b)$$

$$\sum_{j \in \mathcal{M}} H_j z_j \geq h, \quad (7c)$$

where $\mathcal{M} = 1, 2, \dots, M+1$ and

$$z_j = [u_j^T \quad \gamma_j^T]^T, \quad c_j = [p_j^T \quad r_j^T]^T, \quad j \in \mathcal{M}$$

$$z_{M+1} = \rho^T, \quad c_{M+1} = q^T.$$

In (7), (7b) represents the decoupled constraints (6b)-(6f), and (7c) represents the linking constraints (6g). The data structures in (7) are defined as

$$G_j = \begin{bmatrix} \bar{G}_j \\ -\bar{G}_j \end{bmatrix}, \quad g_j = \begin{bmatrix} \underline{g}_j \\ -\bar{g}_j \end{bmatrix}, \quad H_j = \begin{bmatrix} \bar{H}_j \\ -\bar{H}_j \end{bmatrix}, \quad h = \begin{bmatrix} \underline{h} \\ -\bar{h} \end{bmatrix},$$

where

$$\left[\bar{G}_j \mid \underline{g}_j \mid \bar{g}_j \right] = \left[\begin{array}{cc|c|c} I & 0 & \underline{u}_j & \bar{u}_j \\ \Lambda & 0 & \Delta \underline{u}_j & \Delta \bar{u}_j \\ \Gamma_j & I & \underline{y}_j & \infty \\ \Gamma_j & -I & -\infty & \bar{y}_j \\ 0 & I & 0 & \bar{\gamma}_j \end{array} \right],$$

$$\left[\bar{H}_j \mid \underline{h} \mid \bar{h} \right] = \left[\begin{array}{cc|c} \tilde{\Gamma}_j & 0 & \underline{y}_T \\ \tilde{\Gamma}_j & 0 & -\infty \end{array} \mid \begin{array}{c} \infty \\ \bar{y}_T \end{array} \right],$$

for $j \in \mathcal{M}$, with

$$\begin{aligned} \underline{y}_T &= \underline{y}_T - \sum_{j \in \mathcal{M}} \tilde{\Phi}_j x_{j,0}, & \tilde{y}_T &= \tilde{y}_T - \sum_{j \in \mathcal{M}} \tilde{\Phi}_j x_{j,0}, \\ \underline{y}_j &= \underline{y}_j - \Phi_j x_{j,0}, & \tilde{y}_j &= \tilde{y}_j - \Phi_j x_{j,0}, & j \in \mathcal{M}, \\ \Delta \underline{u}_j &= \Delta \underline{u}_j + I_0 u_{j,-1}, & \Delta \tilde{u}_j &= \Delta \tilde{u}_j + I_0 u_{j,-1}, & j \in \mathcal{M}, \end{aligned}$$

and Λ and I_0 defined as

$$\Lambda_j = \begin{bmatrix} I & & & & \\ -I & I & & & \\ & & \ddots & & \\ & & & \ddots & \\ & & & & -I & I \end{bmatrix}, \quad I_0 = \begin{bmatrix} I \\ 0 \\ \vdots \\ 0 \end{bmatrix}.$$

In the special case $j = M+1$, $\tilde{H}_{M+1} = [I \quad -I]^T$ and

$$\left[\tilde{G}_{M+1} \mid \underline{g}_{M+1} \mid \bar{g}_{M+1} \right] = \left[I \mid 0 \mid \bar{p} \right].$$

III. DANTZIG-WOLFE DECOMPOSITION

Dantzig-Wolfe decomposition exploits that a convex set can be characterized by its extreme points and its extreme rays [5], [6]. For each $j \in \mathcal{M}$, the set of points satisfying the decoupled constraints (7b), $\mathcal{G}_j = \{z_j \mid G_j z_j \geq g_j\}$, may be written as

$$\mathcal{G}_j = \left\{ z_j \mid z_j = \sum_{i \in \mathcal{P}} \lambda_j^i z_j^i, \sum_{i \in \mathcal{P}} \lambda_j^i = 1, \lambda_j^i \geq 0 \quad \forall i \in \mathcal{P} \right\},$$

where z_j^i are the extreme points of \mathcal{G}_j , and λ_j^i are convex combination multipliers. Notice that since each of the sets \mathcal{G}_j are bounded, extreme rays are not needed in their representation.

By replacing the decision variables in (7) by convex combination multipliers, we obtain the master problem formulation

$$\min_{\lambda \geq 0} \phi = \sum_{j \in \mathcal{M}} \sum_{i \in \mathcal{P}} c_j^i \lambda_j^i, \quad (8a)$$

$$\text{s.t.} \quad \sum_{j \in \mathcal{M}} \sum_{i \in \mathcal{P}} H_j^i \lambda_j^i \geq h, \quad (8b)$$

$$\sum_{i \in \mathcal{P}} \lambda_j^i = 1, \quad j \in \mathcal{M}, \quad (8c)$$

where we have defined $H_j^i = H_j z_j^i$ and $c_j^i = c_j^T z_j^i$ for each $j \in \mathcal{M}$ and $i \in \mathcal{P}$.

Given a solution, λ^* , to the master problem (8), a solution to the original problem, (7), can be obtained as

$$z_j^* = \sum_{i \in \mathcal{P}} (\lambda^*)^i z_j^i, \quad j \in \mathcal{M}.$$

Since the number of extreme points, $|\mathcal{P}|$, can increase exponentially with the size of the original problem, solving the master problem directly is inefficient. As demonstrated in the following section however, the problem can be solved efficiently using a column generation procedure that replaces \mathcal{P} by a subset $\tilde{\mathcal{P}}$.

IV. COLUMN GENERATION PROCEDURE

The dual linear program of (8) can be stated as

$$\max_{\alpha \geq 0, \beta} h^T \alpha + \sum_{j \in \mathcal{M}} \beta_j, \quad (9a)$$

$$\text{s.t.} \quad (H_j^i)^T \alpha + \beta_j \leq c_j^i, \quad j \in \mathcal{M}, i \in \mathcal{P}, \quad (9b)$$

in which $\alpha \in \mathbb{R}^{4N}$ and $\beta \in \mathbb{R}^{M+1}$ are the Lagrange multipliers associated with the linking constraints, (8b), and the convexity constraints, (8c), respectively. The necessary and sufficient optimality conditions for (8) and (9) are

$$\sum_{j \in \mathcal{M}} \sum_{i \in \mathcal{P}} H_j^i \lambda_j^i \geq h, \quad (10a)$$

$$\sum_{i \in \mathcal{P}} \lambda_j^i = 1, \quad j \in \mathcal{M}, \quad (10b)$$

$$\lambda_j^i \geq 0, \quad j \in \mathcal{M}, i \in \mathcal{P}, \quad (10c)$$

$$c_j^i - (H_j^i)^T \alpha - \beta_j \geq 0, \quad j \in \mathcal{M}, i \in \mathcal{P}, \quad (10d)$$

$$\alpha \geq 0, \quad (10e)$$

$$\lambda_j^i (c_j^i - (H_j^i)^T \alpha - \beta_j) = 0, \quad j \in \mathcal{M}, i \in \mathcal{P}, \quad (10f)$$

In Proposition 1 we derive conditions for which a solution satisfying this set of optimality conditions, can be obtained by solving the master problem (8) over a subset of the original variables.

Proposition 1: Let $\tilde{\mathcal{P}} \subseteq \mathcal{P}$, and define $(\tilde{\lambda}, \tilde{\alpha}, \tilde{\beta})$ as a primal-dual solution to (8) and (9) restricted to the subset $\tilde{\mathcal{P}}$. Then the solution

$$\alpha^* = \tilde{\alpha},$$

$$\beta_j^* = \tilde{\beta}_j, \quad j \in \mathcal{M},$$

$$(\lambda^*)^i_j = \begin{cases} \tilde{\lambda}_j^i & \text{if } i \in \tilde{\mathcal{P}} \\ 0 & \text{if } i \in \mathcal{P} \setminus \tilde{\mathcal{P}} \end{cases}, \quad j \in \mathcal{M}, i \in \mathcal{P},$$

satisfies the conditions, (10), if the optimal objective value of the subproblem

$$\varphi_j = \min_{\tilde{z}_j} \{ (c_j - H_j^T \alpha^*)^T \tilde{z}_j - \beta_j^* \mid G_j \tilde{z}_j \geq g_j \}, \quad (11)$$

is non-negative for each $j \in \mathcal{M}$.

Proof The solution $(\lambda^*, \alpha^*, \beta^*)$ satisfies (10a) since

$$\sum_{j \in \mathcal{M}} \sum_{i \in \mathcal{P}} H_j^i (\lambda^*)^i_j = \sum_{j \in \mathcal{M}} \sum_{i \in \tilde{\mathcal{P}}} H_j^i \tilde{\lambda}_j^i \geq h,$$

which follows from the definition of $(\tilde{\lambda}, \tilde{\alpha}, \tilde{\beta})$. Similarly, it is easy to verify that the conditions (10c), (10b), (10e) and (10f) are fulfilled.

Provided that $(\lambda^*, \alpha^*, \beta^*)$ is optimal, (10d) yields

$$c_j^i - (H_j^i)^T \alpha^* - \beta_j^* = (c_j - H_j^T \alpha^*)^T z_j^i - \beta_j^* \geq 0, \quad (12)$$

for all $j \in \mathcal{M}$ and $i \in \mathcal{P}$. By construction of the solution, (12) is satisfied for all $i \in \tilde{\mathcal{P}}$. To check that the condition holds for all $i \in \mathcal{P} \setminus \tilde{\mathcal{P}}$, we consider the optimization problem (11). Since this linear program minimizes the left hand side of (12) over all possible extreme points, \tilde{z}_j , of \mathcal{G}_j , the solution

$(\lambda^*, \alpha^*, \beta^*)$ also satisfies the remaining optimality condition (12) if φ_j is non-negative for all $j \in \mathcal{M}$. ■

In Algorithm 1, we have outlined a column generation procedure based on Proposition 1. The algorithm exploits that if (12) is violated, then the solution to the subproblems, (11), provides a set of extreme points that can be added to the master problem. Notice that when \mathcal{P} is restricted to the subset $\tilde{\mathcal{P}}$, the master problem (8) is much smaller than the original problem. Therefore, the column generation procedure requires less memory than conventional linear programming methods. Moreover, solving the subproblems is computationally inexpensive as they do not grow with the number of units M . We remark that this step may be performed in parallel.

Algorithm 1 Column generation procedure for solving (8).

Require: $\{z_j^0\}_{j=1}^{\mathcal{M}}$
 $i = 0$, converged = false
while not converged **do**
 $\tilde{\mathcal{P}} = \{0, 1, \dots, i\}$
 for $j \in \mathcal{M}, i \in \tilde{\mathcal{P}}$ **do**
 $H_j^i = H_j z_j^i, c_j^i = c_j^T z_j^i$
 end for
 $(\phi^*, \lambda^*, \alpha^*, \beta^*) \leftarrow$ solve (8) with $\mathcal{P} = \tilde{\mathcal{P}}$
 for $j \in \mathcal{M}$ **do**
 $(\varphi_j^*, \tilde{z}_j^*) \leftarrow$ solve (11)
 end for
 if $\varphi_j \geq 0 \forall j \in \mathcal{M}$ **then**
 converged = true
 else
 for $j \in \mathcal{M}$ **do**
 $z_j^{i+1} = \tilde{z}_j^*$
 end for
 $i = i + 1$
 end if
end while

A. Warm-Starting

Algorithm 1 requires a set of initial points $\{z_j^0\}_{j=1}^{\mathcal{M}}$ that are feasible for both the subproblems (11) and the original problem (7). As economic MPC is a receding horizon strategy, we can generate such a set of points by exploiting the solution from a previous time step.

Given the solution to (11)

$$z_j^* = [u_{j,0}^{*T} \quad \dots \quad u_{j,N-1}^{*T} \quad \gamma_{j,1}^{*T} \quad \dots \quad \gamma_{j,N}^{*T}]^T,$$

$$z_{M+1}^* = [\rho_1^{*T} \quad \dots \quad \rho_N^{*T}]^T,$$

we build a set of initial points in the following sampling instant as

$$z_j^0 = [u_{j,1}^{*T} \quad \dots \quad u_{j,N-1}^{*T} \quad \check{u}_j^T \quad \check{\gamma}_{j,2}^{*T} \quad \dots \quad \check{\gamma}_{j,N}^{*T} \quad \check{\gamma}_j^T]^T,$$

$$z_{M+1}^0 = [\rho_2^{*T} \quad \dots \quad \rho_N^{*T} \quad \check{\rho}^T]^T,$$

for each $j \in \mathcal{M}$. Hence, the original solution values are shifted forward in time, and the variables \check{u}_j , $\check{\gamma}_j$ and $\check{\rho}$ are appended

to the initial points. In our implementation, we let

$$\check{u}_j = u_{j,N-1}^*, \quad j \in \mathcal{M}, \quad (13)$$

which leads to an initial input sequence with constant input in the two final sampling intervals. Using the state space equations (1)-(2), we compute the outputs $\check{y}_{j,N}$ and $\check{y}_{T,N}$ associated with this input sequence. Based on these values we let

$$\check{\gamma}_j = \max(y_{j,N} - \check{y}_{j,N}, 0) + \max(\check{y}_{j,N} - \bar{y}_{j,N}, 0),$$

$$\check{\rho} = \max(y_{T,N} - \check{y}_{T,N}, 0) + \max(\check{y}_{T,N} - \bar{y}_{T,N}, 0),$$

where the maximum function is evaluated element-wise.

Assuming that the inputs (13) satisfy the input constraints for the updated problem data, and that the upper limits on γ_j and ρ are sufficiently large, the strategy above yields a set of feasible initial points for Algorithm 1, $\{z_j^0\}_{j=1}^{\mathcal{M}}$, which exploits the solution obtained in the previous time step. As the solution in successive time steps are closely related in MPC applications, this approach provides a warm-start for Algorithm 1. In case no previous solution is available, a similar strategy can be used to adjust the slack variables for an arbitrary feasible input sequence.

V. RESULTS

In this section, we compare a MATLAB implementation of Algorithm 1, denoted DWempc, to linear programming solvers from the following software packages: CPLEX, Gurobi and MOSEK. The algorithms are run on an Intel(R) Core(TM) i5-2520M CPU @ 2.50GHz with 4 GB RAM running a 64-bit Windows 7 Enterprise operating system. In DWempc, the restricted master problem and the subproblems are solved using CPLEX.

As a conceptual case study, we consider a collection of power generating units in the form

$$Y_j(s) = 1/(\tau_j s + 1)^3 U_j(s), \quad j \in \mathcal{M}, \quad (14)$$

where $U_j(s)$ is the fuel input and the $Y_j(s)$ is the power production. The third order model, (14), has been validated against actual measurement data in [11]. In our study, we vary the time constant, τ_j , to represent different types of power generating units. Time constants in the range 80-120 are associated with slow units, such as centralized thermal power plants, while time constants in the range 20-60 represent units with faster dynamics such as diesel generators and gas turbines. To control the units, (14), using economic MPC, we realize the system in the discrete state space form (1)-(2) using a sampling time of $T_s = 5$ seconds. In the resulting model structure, $u_{j,k} \in \mathbb{R}$ is fuel input, $y_{j,k} \in \mathbb{R}$ is the power production, and $y_{T,k} \in \mathbb{R}$ is the total power production. Thus, $Y_j = 1$, for all $j \in \mathcal{M}$. Fig. 1 demonstrates the production plan obtained using economic MPC in a case study with $M = 3$ power generating units. The graphs show the individual outputs, as well as the output limits for the total power production. The case study parameters are listed in Table I. All parameters listed in the table, are kept constant over the entire

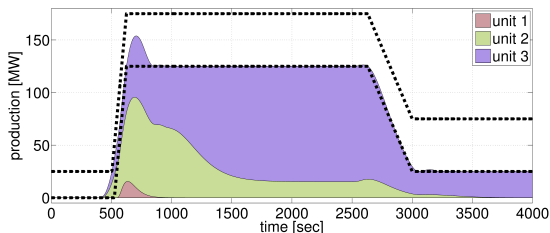


Fig. 1. Closed-loop simulation study of economic MPC.

TABLE I
CASE STUDY PARAMETERS

	τ_j	$p_{j,k}$	$u_{j,k}$	$\bar{u}_{j,k}$	$\Delta u_{j,k}$	$\Delta \bar{u}_{j,k}$
Generating Unit 1	40	24	0	50	-30	30
Generating Unit 2	90	12	0	100	-20	20
Generating Unit 3	100	6	0	200	-5	5

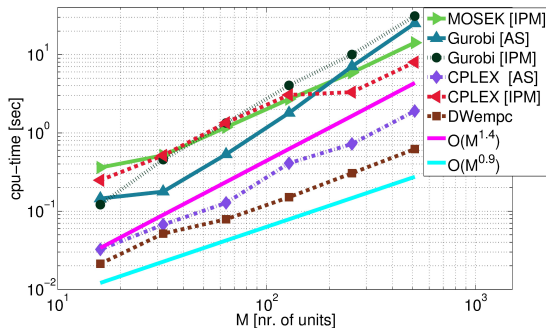


Fig. 2. CPU-time for solving (3) as a function of the number of power generating units, and fixed $N = 50$. Active-set methods are denoted by (AS) and interior-point methods are denoted by (IPM).

horizon. The values, $p_{j,k}$, are the prices pr. unit of fuel (e.g oil, natural gas or coal). We have defined these parameters such that the fuel price for fast units is higher than the fuel price for slow units. The price for imbalances is fixed to $q_k = 10000$.

Based on a similar case study as above, we have solved the constrained optimal control problem, (3), for an increasing number of generating units. The computation time is depicted in Fig. 2. In the simulations $DWempc$ outperforms conventional linear programming solvers with a significant margin, and the difference in computing time grows with the number of units controlled. As the subproblems are solved sequentially in our implementation, the performance of $DWempc$ can be improved even further using parallel computing. To make a fair comparison, we have initialized all algorithms using their default cold-starting point. For $DWempc$ we define such a cold-starting point by setting all inputs, $u_{j,k}$ to zero, and increase the slack variables, $\gamma_{j,k}$ and ρ_k , to their upper bounds. In Table II, we have listed the iteration numbers associated with Figure 2. For $DWempc$, increasing the number of generating

TABLE II
COMPARISON OF THE NUMBER OF ITERATIONS

M	MOS [IPM]	GUR [AS]	GUR [IPM]	CPL [AS]	CPL [IPM]	$DWempc$
16	19	692	22	590	20	30
32	33	700	49	486	44	31
64	34	902	55	559	43	25
128	36	1452	46	1058	40	24
256	36	2221	60	1168	47	23
512	42	3087	65	1737	62	20

units decreases the number of iterations, while for all other solvers the number of iterations increases. We expect that the number of iterations can be reduced additionally in closed-loop by employing the warm-starting strategy proposed in Section IV-A.

VI. CONCLUSIONS

In this paper, we have presented a warm-started Dantzig-Wolfe decomposition algorithm for economic MPC of distributed energy systems. Our results show that a MATLAB implementation of the algorithm is significantly faster than both active-set methods and interior-point methods, provided by MOSEK, CPLEX and Gurobi. Moreover, $DWempc$ has several desirable features, such as low memory costs and parallelization capabilities, which makes it favorable for real-time applications such as economic MPC.

REFERENCES

- [1] T. G. Hovgaard, L. F. S. Larsen, and J. B. Jørgensen, "Flexible and cost efficient power consumption using economic MPC a supermarket refrigeration benchmark," in *50th IEEE Conference on Decision and Control and European Control Conference (CDC-ECC)*, 2011, pp. 848–854.
- [2] J. Ma, S. J. Qin, B. Li, and T. Salsbury, "Economic model predictive control for building energy systems," in *IEEE/PES Innovative Smart Grid Technologies (ISGT)*, 2011, pp. 1–6.
- [3] R. Halvgaard, N. K. Poulsen, H. Madsen, and J. B. Jørgensen, "Economic Model Predictive Control for building climate control in a Smart Grid," in *IEEE/PES Innovative Smart Grid Technologies Conference Europe (ISGT Europe)*, 2012, pp. 1–6.
- [4] R. Halvgaard, N. K. Poulsen, H. Madsen, J. B. Jørgensen, F. Marra, and D. E. M. Bondy, "Electric vehicle charge planning using Economic Model Predictive Control," in *IEEE International Electric Vehicle Conference (IEVC)*, 2012, pp. 1–6.
- [5] G. B. Dantzig and P. Wolfe, "Decomposition Principle for Linear Programs," *Operations Research*, vol. 8, no. 1, pp. 101–111, 1960.
- [6] R. K. Martin, *Large Scale Linear and Integer Optimization: A Unified Approach*. Kluwer Academic Publishers, 1999.
- [7] R. Cheng, J. F. Forbes, and W. S. Yip, "Dantzig-Wolfe decomposition and plant-wide MPC coordination," *Computers & Chemical Engineering*, vol. 32, no. 7, pp. 1507–1522, 2008.
- [8] —, "Dantzig-Wolfe Decomposition and Large-Scale Constrained MPC Problems," in *International Symposium on Dynamics and Control of Process Systems (DYCOPS)*, 2004.
- [9] P.-D. Morosan, R. D. Bourdais, and J. Didier Buisson, "Distributed MPC for Multi-Zone Temperature Regulation with Coupled Constraints," in *18th IFAC World Congress*, 2011, pp. 1552–2557.
- [10] K. Edlund, J. D. Bendtsen, and J. B. Jørgensen, "Hierarchical model-based predictive control of a power plant portfolio," *Control Engineering Practice*, vol. 19, no. 10, pp. 1126–1136, 2011.
- [11] K. Edlund, T. Mølbaek, and J. D. Bendtsen, "Simple models for model-based portfolio load balancing controller synthesis," in *6th IFAC Symposium on Power Plants and Power Systems Control*, 2009, pp. 173–178.

P A P E R C

A Warm-Started Homogeneous and Self-Dual Interior-Point Method for Linear Economic Model Predictive Control

L. E. Sokoler, A. Skajaa, G. Frison, R. Halvgaard, and J. B. Jørgensen. A Warm-Started Homogeneous and Self-Dual Interior-Point Method for Linear Economic Model Predictive Control. In *52th IEEE Conference on Decision and Control (CDC)*, pages 3677–3683, 2013.

A Warm-Started Homogeneous and Self-Dual Interior-Point Method for Linear Economic Model Predictive Control

Leo Emil Sokoler, Anders Skajaa, Gianluca Frison, Rasmus Halvgaard, and John Bagterp Jørgensen

Abstract—In this paper, we present a warm-started homogeneous and self-dual interior-point method (IPM) for the linear programs arising in economic model predictive control (MPC) of linear systems. To exploit the structure in the optimization problems, our algorithm utilizes a Riccati iteration procedure which is adapted to the non-standard system solved in homogeneous and self-dual IPMs, and specifically tailored to economic MPC. Fast convergence is further achieved by means of a recent warm-starting strategy for homogeneous and self-dual IPMs that has not previously been applied to MPC. We implement our algorithm in MATLAB and its performance is analyzed based on a smart grid power management case study. Closed loop simulations show that 1) our algorithm is significantly faster than state-of-the-art IPMs based on sparse linear algebra routines, and 2) warm-starting reduces the number of iterations by approximately 15-35%.

I. INTRODUCTION

In conventional linear model predictive control (MPC), the control problem is formulated as a convex program that penalizes deviations between a desired set-point and the controlled output(s) [1]–[4]. Although this classical approach has become the standard way of formulating the control problem in MPC applications, recent studies show that for energy systems it is often more convenient to use an MPC-based controller with a pure economic objective function [5]–[9]. This variant of MPC, known as economic MPC, guarantees that the set-point is reached in the most profitable way (which is not necessarily the fastest). Applications where economic MPC have been applied to minimize operating costs include control of refrigeration systems [10], building climate control [11], [12], charging batteries in electric vehicles [13], as well as control of non-linear chemical processes [14]. Stability of economic MPC has been addressed in [8] and [6].

Aside the requirement of a predictive model, the main challenge in linear economic MPC is that a linear program has to be solved at each sampling instant. For large systems, the computation time of solving this optimization problem may render the method infeasible. To overcome this problem, our paper develops an efficient and reliable IPM for the linear programs arising in linear economic MPC. The proposed algorithm is a homogeneous and self-dual variant of Mehrotra’s predictor-corrector method [15], [16] that exploits the following problem specific features:

- **Structure:** The optimal control problem solved in linear economic MPC can be posed as a highly structured

The authors are with the Department of Applied Mathematics and Computer Science, Technical University of Denmark, DK-2800 Kgs. Lyngby, Denmark. L. E. Sokoler and A. Skajaa are also affiliated with DONG Energy, DK-2820 Gentofte, Denmark. Email: {leso, andsk, giaf, rhal, jbjjo} at dtu.dk

linear program. We utilize this structure to speed-up the most time consuming numerical operations using a Riccati iteration procedure specifically tailored to economic MPC.

- **Warm-Start:** In MPC applications, the optimization problems solved at successive time steps are closely related. To take advantage of the solution from the previous sampling instant, we implement a recently developed warm-starting strategy for homogeneous and self-dual IPMs. This method does not introduce any additional significant computations and has been reported to reduce the number of iterations by 30-75% for an extensive amount of linear programs and quadratic conic problems [17].

Although Riccati based IPMs have been developed in [18]–[21] for set-point based MPC with ℓ_2 -penalty, and ℓ_1 -penalty in [22], these results are not directly applicable to the homogeneous and self-dual model, which has become widely adopted by state-of-the-art IPMs for linear programming. In our previous work [23], the main emphasis was to develop a Riccati iteration procedure specifically tailored to economic MPC, while the focus of this paper is to further improve our algorithm using the warm-starting strategy of [17].

We have organized the paper as follows. In Section II, we introduce the control problem solved in economic MPC. A homogeneous and self-dual IPM for solving this problem tailored to economic MPC is derived in Section III-IV, and warm-starting is discussed in Section V. Finally, section VI presents simulation results based on a MATLAB implementation of our algorithm denoted LP_{empc}. Concluding remarks are given in Section VII.

II. PROBLEM DEFINITION

In linear economic MPC, the constrained optimal control problem solved at each sampling instant may be formulated as

$$\min_{u,x,\rho} \sum_{k=0}^{N-1} p_k^T u_k + q_{k+1}^T \rho_{k+1}, \quad (1a)$$

$$\text{s.t. } x_{k+1} = Ax_k + Bu_k, \quad k = 0, 1, \dots, N-1, \quad (1b)$$

$$u_k \leq u_k \leq \bar{u}_k, \quad k = 0, 1, \dots, N-1, \quad (1c)$$

$$\Delta u_k \leq \Delta u_k \leq \Delta \bar{u}_k, \quad k = 0, 1, \dots, N-1, \quad (1d)$$

$$\underline{z}_k - \rho_k \leq Cx_k \leq \bar{z}_k + \rho_k, \quad k = 1, 2, \dots, N, \quad (1e)$$

$$\rho_k \geq 0, \quad k = 1, 2, \dots, N, \quad (1f)$$

where N is the length of the prediction horizon. The problem data are the state-space matrices, (A, B, C) , defining the

linear system controlled, the initial state, x_0 , the input limits, $(\underline{u}_k, \bar{u}_k)$, the input-rate limits, $(\Delta \underline{u}_k, \Delta \bar{u}_k)$, the output limits, $(\underline{z}_k, \bar{z}_k)$, the input prices, p_k , and the price for violating the output constraints q_k . As an example, in power systems p_k may be the cost of fuel and q_k may be the cost of not meeting the power demand.

The input-rate is defined in terms of the backward difference operator

$$\Delta u_k := u_k - u_{k-1}, \quad k = 0, 1, \dots, N-1.$$

By augmenting the state-space system such that

$$A := \begin{bmatrix} A & 0 \\ 0 & 0 \end{bmatrix}, \quad x_k := \begin{bmatrix} x_k \\ u_{k-1} \end{bmatrix}, \quad B := \begin{bmatrix} B \\ I \end{bmatrix},$$

$$E := \begin{bmatrix} E \\ 0 \end{bmatrix}, \quad C := \begin{bmatrix} C & 0 \end{bmatrix},$$

we can express (1d) as

$$\Delta u_k \leq u_k - D x_k \leq \Delta \bar{u}_k, \quad k = 0, 1, \dots, N-1$$

in which $D := \begin{bmatrix} 0 & I \end{bmatrix}$. This formulation simplifies computations in our Riccati iteration procedure considerably.

III. HOMOGENEOUS AND SELF-DUAL MODEL

By aggregating the problem data into the structures $g \in \mathbb{R}^n$, $F \in \mathbb{R}^{m_E \times n}$, $b \in \mathbb{R}^{m_E}$, $H \in \mathbb{R}^{m_I \times n}$ and $c \in \mathbb{R}^{m_I}$, (1) can be written as the linear program

$$\min_t \{g^T t \mid Ft = b, Ht \leq c\}, \quad (2)$$

where $n := N(n_u + n_x + n_z)$, $m_E := Nn_x$ and $m_I := N(4n_u + 3n_z)$. As an example, consider the case for $N = 2$

$$t := \begin{bmatrix} u_0^T & x_1^T & \rho_1^T & u_1^T & x_2^T & \rho_2^T \end{bmatrix}^T,$$

$$g := \begin{bmatrix} p_0^T & 0 & q_1^T & p_1^T & 0 & q_2^T \end{bmatrix}^T,$$

and

$$[F \mid b] := \begin{bmatrix} B & -I & 0 & 0 & 0 & 0 & -Ax_0 \\ 0 & A & 0 & B & -I & 0 & 0 \end{bmatrix},$$

$$[H \mid c] := \begin{bmatrix} I & 0 & 0 & 0 & 0 & 0 & \bar{u}_0 \\ 0 & 0 & 0 & I & 0 & 0 & \bar{u}_1 \\ -I & 0 & 0 & 0 & 0 & 0 & -\underline{u}_0 \\ 0 & 0 & 0 & -I & 0 & 0 & -\underline{u}_1 \\ I & 0 & 0 & 0 & 0 & 0 & \Delta \bar{u}_0 \\ 0 & -D & 0 & I & 0 & 0 & \Delta \bar{u}_1 \\ -I & 0 & 0 & 0 & 0 & 0 & -\Delta \underline{u}_0 \\ 0 & D & 0 & -I & 0 & 0 & -\Delta \underline{u}_1 \\ 0 & C & -I & 0 & 0 & 0 & \bar{z}_1 \\ 0 & 0 & 0 & 0 & 0 & C & -I \\ 0 & -C & -I & 0 & 0 & 0 & -\bar{z}_1 \\ 0 & 0 & 0 & 0 & -C & -I & -\bar{z}_2 \\ 0 & 0 & -I & 0 & 0 & 0 & 0 \\ 0 & 0 & 0 & 0 & 0 & -I & 0 \end{bmatrix},$$

in which we have defined

$$\Delta \bar{u}_0 := \Delta \bar{u}_0 + Dx_0,$$

$$\Delta \underline{u}_0 := \Delta \underline{u}_0 + Dx_0.$$

Hence, the control problem (1) can be posed as a highly structured linear program.

The dual of the linear program (2) is

$$\max_{v,w} \{-b^T v - c^T w \mid -F^T v - H^T w = g, w \geq 0\}. \quad (3)$$

In homogeneous and self-dual IPMs, the solution to (2)-(3) is obtained by solving a related homogeneous and self-dual linear program [24]–[26]. Aside from an inherent ability to detect infeasibility, recent advances show that IPMs based on this approach can be warm-started efficiently [17].

If we introduce a new set of optimization variables $(\tilde{t}, \tilde{v}, \tilde{w}, \tilde{s})$, and the additional scalar variables $(\tilde{\tau}, \tilde{\kappa})$, the self-dual and homogeneous problem associated with (2)-(3), may be stated as the linear feasibility problem

$$\min_{\tilde{t}, \tilde{v}, \tilde{w}, \tilde{s}, \tilde{\tau}, \tilde{\kappa}} 0, \quad (4a)$$

$$\text{s.t. } F^T \tilde{v} + H^T \tilde{w} + g \tilde{\tau} = 0, \quad (4b)$$

$$b \tilde{\tau} - F \tilde{t} = 0, \quad (4c)$$

$$c \tilde{\tau} - H \tilde{t} - \tilde{s} = 0, \quad (4d)$$

$$-g^T \tilde{t} - b^T \tilde{v} - c^T \tilde{w} + \tilde{\kappa} = 0, \quad (4e)$$

$$(\tilde{w}, \tilde{s}, \tilde{\tau}, \tilde{\kappa}) \geq 0, \quad (4f)$$

Proposition 1 shows that the solution to (2)-(3), can be obtained by solving (4).

Proposition 1: The linear feasibility problem (4) always has a strict complimentary solution $(\tilde{t}^*, \tilde{v}^*, \tilde{w}^*, \tilde{s}^*, \tilde{\tau}^*, \tilde{\kappa}^*)$ satisfying $\tilde{s}_j^* \tilde{w}_j^* = 0$ for $j = 1, 2, \dots, m_I$ and $\tilde{\tau}^* \tilde{\kappa}^* = 0$. For such a solution, one of the following conditions hold

- **I.** $\tilde{\tau}^* > 0, \tilde{\kappa}^* = 0$: The scaled solution $(t^*, v^*, w^*, s^*) = (\tilde{t}^*, \tilde{v}^*, \tilde{w}^*, \tilde{s}^*) / \tilde{\tau}^*$ is a primal-dual optimal solution to (2)-(3).
- **II.** $\tilde{\tau}^* = 0, \tilde{\kappa}^* > 0$: The problem (2) is infeasible or unbounded; either $-b^T \tilde{v}^* - c^T \tilde{w}^* > 0$ (implies primal infeasibility), or $g^T \tilde{t}^* < 0$ (implies dual infeasibility).

Proof: See [26]. ■

A. Interior Point Method

We now present a homogeneous and self-dual IPM for solving (4). For compact notation, we denote the optimization variables by $\phi := (\tilde{t}, \tilde{v}, \tilde{w}, \tilde{s}, \tilde{\tau}, \tilde{\kappa})$, and introduce superscript k to indicate a particular iteration number.

The necessary and sufficient optimality conditions for (4) are $(\tilde{w}, \tilde{s}, \tilde{\kappa}, \tilde{\tau}) \geq 0$ and

$$V(\phi) := \begin{bmatrix} F^T \tilde{v} + H^T \tilde{w} + g \tilde{\tau} \\ b \tilde{\tau} - F \tilde{t} \\ c \tilde{\tau} - H \tilde{t} - \tilde{s} \\ -g^T \tilde{t} - b^T \tilde{v} - c^T \tilde{w} + \tilde{\kappa} \\ \tilde{W} \tilde{S} \mathbf{1}_{m_I} \\ \tilde{\tau} \tilde{\kappa} \end{bmatrix} = \begin{bmatrix} 0 \\ 0 \\ 0 \\ 0 \\ 0 \\ 0 \end{bmatrix}, \quad (5)$$

W is a diagonal matrix with the elements of w on its diagonal, and similarly for S . Moreover, $\mathbf{1}_{m_I}$ is the column vector of all ones of size m_I .

To find a point satisfying the optimality conditions, we use a variant of Mehrotra's predictor-corrector method [15], [16]. The method tracks the central path \mathcal{C} , which connects

an initial point ϕ^0 satisfying $(\tilde{w}^0, \tilde{s}^0, \tilde{\kappa}^0, \tilde{\tau}^0) \geq 0$ to a strict complementary solution of (4), denoted ϕ^* . Formally, we can write the central path as

$$\mathcal{C} := \{ \phi | V(\phi) = \gamma r^0, (\tilde{w}, \tilde{s}, \tilde{\kappa}, \tilde{\tau}) \geq 0, \gamma \in [0, 1] \}.$$

In this definition

$$r^0 := [V_1(\phi^0)^T \ V_2(\phi^0)^T \ V_3(\phi^0)^T \ V_4(\phi^0)^T \ \mu^0(\mathbf{1}_{m_I})^T \ \mu^0]^T,$$

where $\mu^0 := ((\tilde{w}^0)^T \tilde{s}^0 + \tilde{\tau}^0 \tilde{\kappa}^0) / (m_I + 1)$ is a measure of the duality gap, and $V_i(\phi)$ is the i 'th set of components of $V(\phi)$, defined as in (5).

The basic idea in IPMs is to generate a sequence of iterates along the central path $\{\phi^0, \phi^1, \dots, \phi^k, \dots, \phi^N\}$, such that $\phi^N \rightarrow \phi^*$ as $N \rightarrow \infty$. In Mehrotra's predictor-corrector method, the iterates are computed by repeating a two-step procedure. The first part of this procedure, known as the affine step, updates the value of γ and computes second-order correction terms. Secondly, a corrector step is determined and a new iterate is produced.

1) *Affine Step*: The affine direction $\Delta\phi_{\text{aff}}^k$ is obtained by solving the linear system

$$J_V(\phi^k)\Delta\phi_{\text{aff}}^k = -V(\phi^k), \quad (6)$$

which corresponds to the Newton direction for (5). The Jacobian of V evaluated at ϕ^k is

$$J_V(\phi^k) = \begin{bmatrix} 0 & F^T & H^T & 0 & g & 0 \\ -F & 0 & 0 & 0 & b & 0 \\ -H & 0 & 0 & -I & c & 0 \\ -g^T & -b^T & -c^T & 0 & 0 & 1 \\ 0 & 0 & \tilde{S}^k & \tilde{W}^k & 0 & 0 \\ 0 & 0 & 0 & 0 & \tilde{\kappa}^k & \tilde{\tau}^k \end{bmatrix}. \quad (7)$$

Given the solution to (6), we compute the maximum step length in the affine direction for the primal and dual variables, such that (4f) remains satisfied

$$\alpha_{\text{aff}}^k := \max \left\{ a_{\text{aff}} \in [0, 1] \left[\begin{array}{l} \tilde{w}^k \\ \tilde{\tau}^k \end{array} \right] + a_{\text{aff}} \left[\begin{array}{l} \Delta\tilde{w}_{\text{aff}}^k \\ \Delta\tilde{\tau}_{\text{aff}}^k \end{array} \right] \geq 0 \right\},$$

$$\beta_{\text{aff}}^k := \max \left\{ b_{\text{aff}} \in [0, 1] \left[\begin{array}{l} \tilde{s}^k \\ \tilde{\kappa}^k \end{array} \right] + b_{\text{aff}} \left[\begin{array}{l} \Delta\tilde{s}_{\text{aff}}^k \\ \Delta\tilde{\kappa}_{\text{aff}}^k \end{array} \right] \geq 0 \right\}.$$

Accordingly, affine variables are computed

$$\begin{aligned} \tilde{w}_{\text{aff}}^k &:= \tilde{w}^k + \alpha_{\text{aff}}^k \Delta\tilde{w}_{\text{aff}}^k, & \tilde{s}_{\text{aff}}^k &:= \tilde{s}^k + \beta_{\text{aff}}^k \Delta\tilde{s}_{\text{aff}}^k, \\ \tilde{\tau}_{\text{aff}}^k &:= \tilde{\tau}^k + \alpha_{\text{aff}}^k \Delta\tilde{\tau}_{\text{aff}}^k, & \tilde{\kappa}_{\text{aff}}^k &:= \tilde{\kappa}^k + \beta_{\text{aff}}^k \Delta\tilde{\kappa}_{\text{aff}}^k. \end{aligned}$$

The affine variables provide a measure of the relative reduction in the duality gap, in the affine direction. This information is used to update the centering parameter γ . For this purpose, we use the heuristic [16]

$$\gamma^k := \left[\frac{\mu_{\text{aff}}^k}{\mu^k} \right]^3 = \left[\frac{((\tilde{w}_{\text{aff}}^k)^T \tilde{s}_{\text{aff}}^k + \tilde{\tau}_{\text{aff}}^k \tilde{\kappa}_{\text{aff}}^k)}{((\tilde{w}^k)^T \tilde{s}^k + \tilde{\tau}^k \tilde{\kappa}^k)} \right]^3. \quad (8)$$

2) *Predictor-Corrector Step*: In the predictor-corrector step, we compute the search direction $\Delta\phi^k$ by solving (6) with a modified right hand side

$$J_V(\phi^k)\Delta\phi^k = -\tilde{V}(\phi^k). \quad (9)$$

$\tilde{V}_i(\phi) := (1 - \gamma^k)V_i(\phi)$ for $i = 1, 2, 3, 4$ and

$$\begin{aligned} \tilde{V}_5(\phi^k) &:= V_5(\phi^k) + \Delta\tilde{W}_{\text{aff}}^k \Delta\tilde{S}_{\text{aff}}^k \mathbf{1}_{m_I} - \gamma^k \mu^k \mathbf{1}_{m_I}^T, \\ \tilde{V}_6(\phi^k) &:= V_6(\phi^k) + \Delta\tilde{\tau}_{\text{aff}}^k \Delta\tilde{\kappa}_{\text{aff}}^k - \gamma^k \mu^k. \end{aligned}$$

The diagonal matrices $\Delta\tilde{W}_{\text{aff}}^k$ and $\Delta\tilde{S}_{\text{aff}}^k$ are defined in a similar way to W and S . Terms involving these matrices are, as well as $\Delta\tilde{\tau}_{\text{aff}}^k$ and $\Delta\tilde{\kappa}_{\text{aff}}^k$, included to compensate for linearization errors [16]. We also notice that by employing the heuristic (8), the search direction is forced towards the central path if $\mu_{\text{aff}}^k \approx \mu^k$, meaning that only a small step in the non-negative orthant $(\tilde{w}, \tilde{s}, \tilde{\kappa}, \tilde{\tau}) \geq 0$ is available in the affine direction.

3) *Stopping Criteria*: To classify a solution as optimal, we adopt the criteria proposed in [27]

$$\rho_E^k \leq \varepsilon_E, \quad \rho_I^k \leq \varepsilon_I, \quad \rho_D^k \leq \varepsilon_D, \quad \rho_O^k \leq \varepsilon_O. \quad (10)$$

Moreover, the problem is considered to be infeasible if $\tilde{\tau}^k \leq \varepsilon_\tau \max(1, \tilde{\kappa}^k)$, and

$$\rho_E^k \leq \varepsilon_E, \quad \rho_I^k \leq \varepsilon_I, \quad \rho_D^k \leq \varepsilon_D, \quad \rho_G^k \leq \varepsilon_G. \quad (11)$$

$\varepsilon_\tau, \varepsilon_E, \varepsilon_I, \varepsilon_D, \varepsilon_O$ and ε_G are small user-defined tolerances and

$$\begin{aligned} \rho_D &:= \|V_1(\phi)\|_\infty / \max(1, \| [H^T \ F^T \ g] \|_\infty), \\ \rho_E &:= \|V_2(\phi)\|_\infty / \max(1, \| [F \ b] \|_\infty), \\ \rho_I &:= \|V_3(\phi)\|_\infty / \max(1, \| [H \ I \ c] \|_\infty), \\ \rho_G &:= |L - \tilde{\kappa}| / \max(1, \| [g^T \ b^T \ c^T \ 1] \|_\infty), \\ \rho_O &:= |L| / (\tilde{\tau} + |-b^T \tilde{v} - c^T \tilde{w}|). \end{aligned}$$

where $L := g^T \tilde{\tau} - (-b^T \tilde{v} - c^T \tilde{w})$ is the duality gap.

4) *Algorithm*: Algorithm 1 summarizes the homogeneous and self-dual IPM described in this paper. We use a damping parameter, ν , to keep the iterates well inside the interior of the non-negative orthant $(\tilde{w}, \tilde{s}, \tilde{\tau}, \tilde{\kappa}) \geq 0$, as they approach the solution. To speed-up numerical computations and reduce the storage requirements of `LPemrc`, operations involving the structured matrices F and H are implemented as specialized linear algebra routines [28].

IV. RICCATI ITERATION PROCEDURE

The main computational efforts in Algorithm 1 are the solution of the linear systems (6) and (9). In a generic form, we can write these operations as

$$F^T \Delta\tilde{v} + H^T \Delta\tilde{w} + g \Delta\tilde{\tau} = r_1, \quad (12a)$$

$$b \Delta\tilde{\tau} - F \Delta\tilde{v} = r_2, \quad (12b)$$

$$c \Delta\tilde{\tau} - H \Delta\tilde{v} - \Delta\tilde{s} = r_3, \quad (12c)$$

$$g^T \Delta\tilde{v} + b^T \Delta\tilde{v} + c^T \Delta\tilde{w} - \Delta\tilde{\kappa} = r_4, \quad (12d)$$

$$\tilde{W} \Delta\tilde{s} + \tilde{S} \Delta\tilde{w} = r_5, \quad (12e)$$

$$\tilde{\kappa} \Delta\tilde{\tau} + \tilde{\tau} \Delta\tilde{\kappa} = r_6. \quad (12f)$$

Algorithm 1 Homogeneous and self-dual IPM for (4)

Require: $\begin{cases} \text{DATA} & (g, F, b, H, c) \\ \text{INITIAL POINT} & (\bar{t}, \bar{v}, \bar{w}, \bar{s}, \bar{\tau}, \bar{\kappa}) \\ \text{PARAMETERS} & v \in [0.95; 0.999] \end{cases}$

```

// initialize
 $\mu \leftarrow (\bar{w}^T \bar{s} + \bar{\tau} \bar{\kappa}) / (m_l + 1)$ 
while not CONVERGED do
  // affine step
   $\Delta \phi_{\text{aff}} \leftarrow -J_V(\phi)^{-1} V(\phi)$ 
   $\alpha_{\text{aff}} \leftarrow \max \left\{ a_{\text{aff}} \in [0, 1] \left[ \begin{array}{l} \bar{w} \\ \bar{\tau} \end{array} \right] + a_{\text{aff}} \left[ \begin{array}{l} \Delta \bar{w}_{\text{aff}} \\ \Delta \bar{\tau}_{\text{aff}} \end{array} \right] \geq 0 \right\}$ 
   $\beta_{\text{aff}} \leftarrow \max \left\{ b_{\text{aff}} \in [0, 1] \left[ \begin{array}{l} \bar{s} \\ \bar{\kappa} \end{array} \right] + b_{\text{aff}} \left[ \begin{array}{l} \Delta \bar{s}_{\text{aff}} \\ \Delta \bar{\kappa}_{\text{aff}} \end{array} \right] \geq 0 \right\}$ 
   $\bar{s}_{\text{aff}} \leftarrow \bar{s} + \beta_{\text{aff}} \Delta \bar{s}_{\text{aff}}, \quad \bar{\kappa}_{\text{aff}} \leftarrow \bar{\kappa} + \beta_{\text{aff}} \Delta \bar{\kappa}_{\text{aff}}$ 
   $\bar{w}_{\text{aff}} \leftarrow \bar{w} + \alpha_{\text{aff}} \Delta \bar{w}_{\text{aff}}, \quad \bar{\tau}_{\text{aff}} \leftarrow \bar{\tau} + \alpha_{\text{aff}} \Delta \bar{\tau}_{\text{aff}}$ 
   $\mu_{\text{aff}} \leftarrow (\bar{w}_{\text{aff}}^T \bar{s}_{\text{aff}} + \bar{\tau}_{\text{aff}} \bar{\kappa}_{\text{aff}}) / (m_l + 1)$ 
   $\gamma \leftarrow (\mu_{\text{aff}} / \mu)^3$ 
  // predictor-corrector step
   $\Delta \phi \leftarrow -J_V(\phi)^{-1} V(\phi)$ 
   $\alpha \leftarrow \max \left\{ a \in [0, 1] \left[ \begin{array}{l} \bar{w} \\ \bar{\tau} \end{array} \right] + a \left[ \begin{array}{l} \Delta \bar{w} \\ \Delta \bar{\tau} \end{array} \right] \geq 0 \right\}$ 
   $\beta \leftarrow \max \left\{ b \in [0, 1] \left[ \begin{array}{l} \bar{s} \\ \bar{\kappa} \end{array} \right] + b \left[ \begin{array}{l} \Delta \bar{s} \\ \Delta \bar{\kappa} \end{array} \right] \geq 0 \right\}$ 
   $\bar{t} \leftarrow \bar{t} + v \beta \Delta \bar{t}, \quad \bar{s} \leftarrow \bar{s} + v \beta \Delta \bar{s}, \quad \bar{\kappa} \leftarrow \bar{\kappa} + v \beta \Delta \bar{\kappa}$ 
   $\bar{v} \leftarrow \bar{v} + v \alpha \Delta \bar{v}, \quad \bar{w} \leftarrow \bar{w} + v \alpha \Delta \bar{w}, \quad \bar{\tau} \leftarrow \bar{\tau} + v \alpha \Delta \bar{\tau}$ 
   $\mu \leftarrow (\bar{w}^T \bar{s} + \bar{\tau} \bar{\kappa}) / (m_l + 1)$ 
end while

```

We notice that the system (12) is different from the system solved in standard IPMs. Consequently, existing Riccati iteration procedures for MPC cannot be applied directly. However, as shown in Proposition 2, the solution to (12) can be obtained by solving a reduced linear system and a number of computationally inexpensive operations.

Proposition 2: The solution to (12) can be computed as

$$\begin{bmatrix} 0 & F^T & H^T \\ -F & 0 & 0 \\ -H & 0 & \tilde{W}^{-1} \tilde{S} \end{bmatrix} \begin{bmatrix} f_1 & h_1 \\ f_2 & h_2 \\ f_3 & h_3 \end{bmatrix} = \begin{bmatrix} r_1 & -g \\ r_2 & -b \\ r_3 & -c \end{bmatrix}, \quad (13)$$

and subsequent computation of

$$\begin{aligned} \Delta \bar{\tau} &= \frac{r_6 - \bar{\tau}(g^T f_1 + b^T f_2 + c^T f_3)}{\bar{\kappa} + \bar{\tau}(g^T h_1 + b^T h_2 + c^T h_3)}, \\ \Delta \bar{t} &= f_1 + h_1 \Delta \bar{\tau}, \\ \Delta \bar{v} &= f_2 + h_2 \Delta \bar{\tau}, \\ \Delta \bar{w} &= f_3 + h_3 \Delta \bar{\tau}, \\ \Delta \bar{\kappa} &= g^T \Delta \bar{t} + b^T \Delta \bar{v} + c^T \Delta \bar{w} - r_4, \\ \Delta \bar{s} &= \tilde{W}^{-1} (r_3 - \tilde{S} \Delta \bar{w}), \end{aligned}$$

where $r_3 := r_3 + \tilde{W}^{-1} r_5$ and $r_6 := r_6 + \bar{\tau} r_4$.

Proof: See [27]. \blacksquare

In the appendix, an efficient solution procedure for (13) using a Riccati iteration procedure specifically tailored to economic MPC is derived. The order of complexity of the

proposed method is $O(N(n_u + n_x + n_z)^3)$. In comparison, the complexity of solving the system directly using sparse linear algebra routines is linear to quadratic in N . Finally, a general purpose dense solver yields the complexity $O(N^3(n_u + n_x + n_z)^3)$ which is two orders of magnitude larger in N compared to our approach.

V. WARM-STARTING

We apply the warm-starting strategy from [17] to pick an initial point for Algorithm 1. The main idea is to construct such a point by combining a guess of the solution (candidate point) with a standard cold starting point. The initial point is defined as

$$\begin{aligned} w^0 &= \lambda \bar{w} + (1 - \lambda) \mathbf{1}_{m_l}, & s^0 &= \lambda \bar{s} + (1 - \lambda) \mathbf{1}_{m_l}, \\ t^0 &= \lambda \bar{t}, & v^0 &= \lambda \bar{v}, \\ \tau^0 &= 1, & \kappa^0 &= (w^0)^T s^0 / N, \end{aligned}$$

where $(\bar{t}, \bar{v}, \bar{w}, \bar{s})$ is the candidate point and $\lambda \in [0, 1[$ is a tuning parameter. Notice that in case $\lambda = 0$, the initial point becomes the standard cold-starting point $\phi^0 = (0, 0, \mathbf{1}_{m_l}, \mathbf{1}_{m_l}, 1, 1)$. Conversely, $\lambda = 1$ corresponds to using the candidate point as the initial solution. Since this point typically lies close to the boundary of the non-negative orthant $(\bar{w}, \bar{s}, \bar{\kappa}, \bar{\tau}) \geq 0$, $\lambda = 1$ can lead to ill-conditioned linear systems and/or blocking of the search direction [29].

For MPC applications, a good choice of the candidate point at time k can be constructed using the solution from the previous time step. As an example consider the solution at time step $k = 0$, for $N = 3$

$$t := [u_0^{*T} \quad x_1^{*T} \quad \rho_1^{*T} \quad u_1^{*T} \quad x_2^{*T} \quad \rho_2^{*T} \quad u_2^{*T} \quad x_3^{*T} \quad \rho_3^{*T}]^T.$$

In this case we use the following candidate point at time step $k = 1$

$$\bar{t} := [u_1^{*T} \quad x_2^{*T} \quad \rho_2^{*T} \quad u_2^{*T} \quad x_3^{*T} \quad \rho_3^{*T} \quad u_2^{*T} \quad x_3^{*T} \quad \rho_3^{*T}]^T.$$

Similarly, we left-shift the slack variables, s , and the dual variables, v and w .

VI. CASE STUDY - SMART GRID POWER MANAGEMENT

In this section we compare LPempc against IPMs from the following software packages: Gurobi, SeDuMi and MOSEK. These state-of-the-art IPMs are mainly written in low-level language such as FORTRAN and C, and rely on sparse linear algebra that are specifically tailored to the solution of large-scale sparse linear and conic programs. We also include CPLEX in our comparison.

The tolerance parameters for LPempc in (10)-(11) are set to 10^{-8} . With these settings LPempc achieves the same solution accuracy as the other solvers using their default tolerance settings. We have performed our simulations on an Intel(R) Core(TM) i5-2520M CPU @ 2.50GHz with 4 GB RAM running a 64-bit Ubuntu 12.04.1 LTS operating system.

TABLE I
CASE STUDY PARAMETERS

	τ_i	p_k	\underline{u}_k	\bar{u}_k	$\Delta \underline{u}_k$	$\Delta \bar{u}_k$
Power Plant 1	90	100	0	200	-20	20
Power Plant 2	30	200	0	150	-40	40

In the case study, we represent a system of m power generating units by a collection of simple third order systems in the form

$$Y_i(s) = \frac{1}{(\tau_i s + 1)^3} U_i(s), \quad i = 1, 2, \dots, m. \quad (14)$$

where $U_i(s)$ is the amount of fuel fed to the i 'th power unit and $Y_i(s)$ is its power production. In [30] the model (14) has been validated against actual measurement data.

The total production from the m power generating units is the sum

$$Z(s) = \sum_{i=1}^m Y_i(s) = \sum_{i=1}^m \frac{1}{(\tau_i s + 1)^3} U_i(s). \quad (15)$$

In state space form, the system (14)-(15) can be written as

$$\mathbf{x}_{k+1} = \mathbf{A}\mathbf{x}_k + \mathbf{B}u_k + \mathbf{E}\mathbf{d}_k, \quad \mathbf{d}_k \sim N(0, R_d), \quad (16a)$$

$$\mathbf{y}_k = \mathbf{C}_y \mathbf{x}_k + \mathbf{e}_k, \quad \mathbf{e}_k \sim N(0, R_e), \quad (16b)$$

$$\mathbf{z}_k = \mathbf{C}_z \mathbf{x}_k. \quad (16c)$$

$u_k \in \mathbb{R}^{n_u}$ is the amount of fuel fed to the power generating units, $\mathbf{y}_k \in \mathbb{R}^{n_y}$ is the measured power production from each of the units and $\mathbf{z}_k \in \mathbb{R}^{n_z}$ is the total power production. Notice that we have introduced process noise \mathbf{d}_k , and measurement noise \mathbf{e}_k . To control the stochastic system (16), we use economic MPC based on the certainty equivalence principle. Hence, stochastic variables are replaced by estimates of their conditional mean value in (1). The estimates are computed using the Kalman filter.

A. Closed-Loop Simulation

The following results are generated using an example with two power generating units; a cheap/slow unit, and an expensive/fast unit. This can represent a common situation in the power industry where large thermal power plants often produce a majority of the electricity, while units with faster dynamics such as diesel generators are used only in critical peak periods.

In our example, the controller objective is to coordinate the most cost-efficient power production, respecting capacity constraints and a time-varying electricity demand. It is assumed that full information about the initial state is given $\mathbf{x}_0 \sim (0, 0)$, and that the penalty of violating the output constraints is $q_k = 10^4$ for all time steps. The system and controller parameters are listed in Table I. We set the prediction horizon to $N = 80$ time steps and use a sampling time of $T_s = 5$ seconds. Moreover, we let $R_d = R_e = \sigma I$. A closed-loop simulation with $\sigma = 1$ is depicted in Fig. 1. The plot illustrates how the work load is distributed among the power generating units. It can be read that the cheap unit accounts for the main load, while the expensive unit is

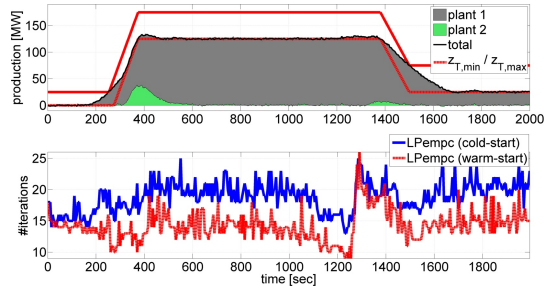


Fig. 1. Closed-loop simulation of a power system controlled by economic MPC. Warm-starting ($\lambda = 0.99$) yields a significant reduction in the number of iterations.

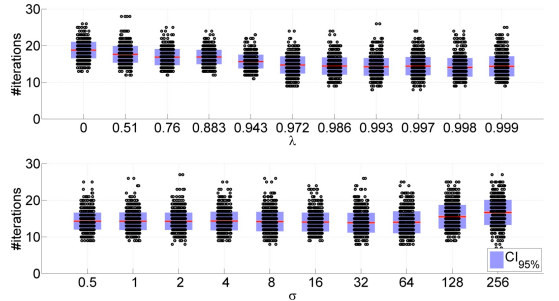


Fig. 2. Number of iterations needed to converge as a function of the tuning parameter λ , and the noise parameter σ . Each box-plot has been generated based on an entire closed-loop simulation. In the top plot we have fixed $\sigma = 1$, and in the bottom plot $\lambda = 0.99$.

activated only when faster dynamics are needed to satisfy the electricity demand. The figure also shows that warm-starting LPempc reduces the number of iterations needed to find a solution with the desired accuracy. On average the number of iterations is reduced by approximately 35%, which is significant as it is achieved without introducing any additional expensive computations. To tune λ , we have generated the box-plots depicted in Fig. 2. The case $\lambda = 0$ corresponds to a cold-start. Thus, in all cases warm-starting reduces the average number of iterations. We have chosen $\lambda = 0.99$ for our controller. For this value of λ , the initial point lies well inside the interior of the non-negative orthant, $(\bar{w}, \bar{s}, \bar{\kappa}, \bar{\tau}) \geq 0$, while it still maintains characteristics of the candidate point. Fig 2 shows that for this value of λ the number of iterations is reduced even when the variance of the noise is increased significantly.

Fig. 3 shows CPU-timings based on a closed-loop simulation with 10 power generating units and a prediction horizon of $N = 200$ time steps. In this simulation LPempc is up to an order of magnitude faster than CPLEX, Gurobi, SeDuMi and MOSEK, depending on the problem data. On average, LPempc is approximately 7 times faster than Gurobi, 5 times faster than MOSEK and 15 times faster than both SeDuMi and CPLEX. As demonstrated in [23], this difference grows with the problem size, as LPempc scales in a

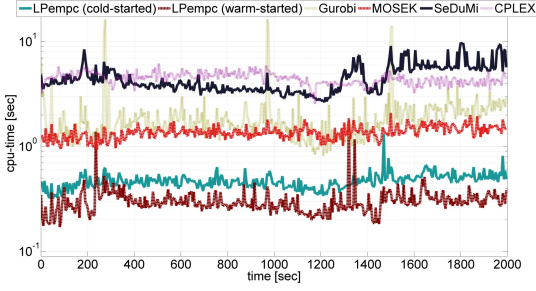


Fig. 3. CPU-time for solving (1) with 10 power generating units and a prediction horizon of 200 time steps.

favourable way.

VII. CONCLUSIONS

In this paper, we have developed an efficient IPM for linear economic MPC. The algorithm combines a homogeneous and self-dual model, and a Riccati iteration procedure specifically tailored to MPC. To speed up convergence, a recent warm-starting strategy for homogeneous and self-dual IPMs was implemented. Our simulations show that this strategy reduces the number of iterations by 10-35%, and that a MATLAB implementation of our algorithm, LPempc, is up to an order of magnitude faster than CPLEX, Gurobi, SeDuMi and MOSEK.

APPENDIX

RICCATI ITERATION PROCEDURE FOR ECONOMIC MPC

Following the derivation in [23], we write the system (13) in the form

$$\begin{bmatrix} 0 & F^T & H^T \\ -F & 0 & 0 \\ -H & 0 & \tilde{W}^{-1}\tilde{S} \end{bmatrix} \begin{bmatrix} \tilde{t} \\ \tilde{v} \\ \tilde{w} \end{bmatrix} = \begin{bmatrix} \bar{r}_1 \\ \bar{r}_2 \\ \bar{r}_3 \end{bmatrix}. \quad (17)$$

where we have only included a single right hand side. We write the solution to this system as

$$\begin{aligned} \tilde{t} &= [u_0^T \quad x_1^T \quad \rho_1^T \quad \dots \quad u_{N-1}^T \quad x_N^T \quad \rho_N^T]^T, \\ \tilde{v} &= [\tilde{v}_0^T \quad \tilde{v}_1^T \quad \dots \quad \tilde{v}_{N-1}^T]^T, \\ \tilde{w} &= [\eta^T \quad \lambda^T \quad v^T \quad \omega^T \quad \gamma^T \quad \zeta^T \quad \xi^T]^T. \end{aligned}$$

$\eta := [\eta_0^T \quad \eta_1^T \quad \dots \quad \eta_{N-1}^T]^T$, and similarly for λ , v , ω , γ , ζ and ξ . Accordingly, the right hand side is partitioned such that

$$\begin{aligned} \bar{r}_1 &= [r_{u,0}^T \quad r_{x,1}^T \quad r_{w,1}^T \quad \dots \quad r_{u,N-1}^T \quad r_{x,N}^T \quad r_{w,N}^T]^T, \\ \bar{r}_2 &= [R_{v,0}^T \quad R_{v,1}^T \quad \dots \quad R_{v,N-1}^T]^T, \\ \bar{r}_3 &= [r_\eta^T \quad r_\lambda^T \quad r_v^T \quad r_\omega^T \quad r_\gamma^T \quad r_\zeta^T \quad r_\xi^T]^T. \end{aligned}$$

The diagonal matrix $\tilde{W}^{-1}\tilde{S}$ is written in terms of diagonal submatrices

$$\tilde{W}^{-1}\tilde{S} = \text{diag}(\Sigma_\eta^T, \Sigma_\lambda^T, \Sigma_v^T, \Sigma_\omega^T, \Sigma_\gamma^T, \Sigma_\zeta^T, \Sigma_\xi^T)$$

For compact notation, we also introduce $\mathcal{A}_i := \{0 + i, 1 + i, \dots, N-1 + i\}$.

Based on the notation above and the definition of F and H , the linear system of equations (17) can be stated in the form

$$\begin{aligned} \eta_i - \lambda_i + v_i - \omega_i + B^T \tilde{v}_i &= r_{\eta,i}, & i \in \mathcal{A}_0, \\ -u_i + \Sigma_{\eta,i} \eta_i &= r_{\eta,i}, & i \in \mathcal{A}_0, \\ u_i + \Sigma_{\lambda,i} \lambda_i &= r_{\lambda,i}, & i \in \mathcal{A}_0, \\ -u_i + Dx_i + \Sigma_{v,i} v_i &= r_{v,i}, & i \in \tilde{\mathcal{A}}_0, \\ u_i - Dx_i + \Sigma_{\omega,i} \omega_i &= r_{\omega,i}, & i \in \tilde{\mathcal{A}}_0, \\ x_{i+1} - Ax_i - Bu_i &= R_{v,i}, & i \in \tilde{\mathcal{A}}_0, \\ \rho_i - Cx_i + \Sigma_{\gamma,i} \gamma_i &= r_{\gamma,i}, & i \in \mathcal{A}_1, \\ \rho_i + Cx_i + \Sigma_{\zeta,i} \zeta_i &= r_{\zeta,i}, & i \in \mathcal{A}_1, \\ \rho_i + \Sigma_{\xi,i} \xi_i &= r_{\xi,i}, & i \in \mathcal{A}_1, \\ -\gamma_i - \zeta_i - \xi_i &= r_{w,i}, & i \in \mathcal{A}_1, \\ -\tilde{v}_i + C^T(\gamma_{i+1} - \zeta_{i+1}) + A^T \tilde{v}_i & & \\ + D^T(\omega_i - v_i) &= r_{x,i}, & i \in \tilde{\mathcal{A}}_0, \end{aligned}$$

with $\tilde{\mathcal{A}}_0 := \mathcal{A}_0 \setminus 0$ and the special cases

$$\begin{aligned} -u_0 + \Sigma_{v,0} v_0 &= r_{v,0}, \\ u_0 + \Sigma_{\omega,0} \omega_0 &= r_{\omega,0}, \\ x_1 - Bu_0 &= R_{v,0}, \\ -\tilde{v}_{N-1} + C^T(\gamma_N - \zeta_N) &= r_{x,N}. \end{aligned}$$

By eliminating η , λ , v , ω , γ , ζ and ξ we get

$$B^T \tilde{v}_0 + U_0 u_0 = R_{u,0}, \quad (18a)$$

$$B^T \tilde{v}_i + U_i u_i + G_i x_i = R_{u,i}, \quad i \in \tilde{\mathcal{A}}_0, \quad (18b)$$

$$-x_1 + Bu_0 = R_{v,0}, \quad (18c)$$

$$-x_{i+1} + Ax_i + Bu_i = R_{v,i}, \quad i \in \tilde{\mathcal{A}}_0, \quad (18d)$$

$$W_i \rho_i + M_i^T x_i = R_{w,i}, \quad i \in \mathcal{A}_1, \quad (18e)$$

$$-\tilde{v}_{i-1} + M_i \rho_i + \tilde{X}_i x_i + G_i^T u_i + A^T \tilde{v}_i = \tilde{R}_{x,i}, \quad i \in \tilde{\mathcal{A}}_0, \quad (18f)$$

$$-\tilde{v}_{N-1} + M_N \rho_N + \tilde{X}_N x_N = \tilde{R}_{x,N}, \quad (18g)$$

where we have defined

$$U_i := \Sigma_{\eta,i}^{-1} + \Sigma_{\lambda,i}^{-1} + \Sigma_{\omega,i}^{-1} + \Sigma_{v,i}^{-1}, \quad i \in \mathcal{A}_0,$$

$$G_i := -(\Sigma_{\omega,i}^{-1} + \Sigma_{v,i}^{-1})D, \quad i \in \tilde{\mathcal{A}}_0,$$

$$W_i := \Sigma_{\zeta,i}^{-1} + \Sigma_{\xi,i}^{-1} + \Sigma_{\gamma,i}^{-1}, \quad i \in \mathcal{A}_1,$$

$$M_i := C^T(\Sigma_{\zeta,i}^{-1} - \Sigma_{\gamma,i}^{-1}), \quad i \in \mathcal{A}_1,$$

$$\tilde{X}_i := C^T(\Sigma_{\zeta,i}^{-1} + \Sigma_{v,i}^{-1})C + D^T(\Sigma_{\gamma,i}^{-1} + \Sigma_{\omega,i}^{-1})D, \quad i \in \tilde{\mathcal{A}}_0,$$

$$\tilde{X}_N := C^T(\Sigma_{\zeta,N}^{-1} + \Sigma_{v,N}^{-1})C.$$

Furthermore

$$R_{u,i} := r_{u,i} + \bar{r}_{\lambda,i} + \bar{r}_{\omega,i} - \bar{r}_{\eta,i} - \bar{r}_{v,i}, \quad i \in \mathcal{A}_0,$$

$$R_{v,i} := -R_{v,i}, \quad i \in \mathcal{A}_0,$$

$$R_{w,i} := r_{w,i-1} + \bar{r}_{\zeta,i-1} + \bar{r}_{\xi,i} + \bar{r}_{\gamma,i}, \quad i \in \mathcal{A}_1,$$

$$\tilde{R}_{x,i} := r_{x,i} + C^T(\bar{r}_{\zeta,i} - \bar{r}_{\gamma,i}) + D^T(\bar{r}_{v,i} - \bar{r}_{\omega,i}), \quad i \in \mathcal{A}_0,$$

$$\tilde{R}_{x,N} := r_{x,N} + C^T(\bar{r}_{\zeta,N} - \bar{r}_{\gamma,N}).$$

$\bar{r}_{\lambda,i} := \Sigma_{\lambda,i}^{-1} r_{\lambda,i}$, and similarly for $\bar{r}_{\omega,i}$, $\bar{r}_{\eta,i}$, $\bar{r}_{v,i}$, $\bar{r}_{\xi,i}$, $\bar{r}_{\zeta,i}$ and $\bar{r}_{\gamma,i}$. Solving (18e) for \tilde{w} gives

$$\rho_i = W_i^{-1}(R_{w,i} - M_i^T x_i), \quad i \in \mathcal{N}_1. \quad (19)$$

Substituting back into (18) yields the equations

$$\begin{aligned} B^T \tilde{v}_0 + U_0 u_0 &= R_{u,0} \\ B^T \tilde{v}_i + U_i u_i + G_i x_i &= R_{u,i}, & i \in \mathcal{N}_0^{\tilde{v}} \\ -x_1 + B u_0 &= R_{v,0} \\ -x_{i+1} + A x_i + B u_i &= R_{v,i}, & i \in \mathcal{N}_0^{\tilde{v}} \\ -\tilde{v}_{i-1} + X_i x_i + G_i^T u_i + A^T \tilde{v}_i &= R_{x,i}, & i \in \mathcal{N}_0^{\tilde{v}} \\ -\tilde{v}_{N-1} + X_N x_N &= R_{x,N} \end{aligned}$$

where $X_i := \bar{X}_i - M_i W_i^{-1} M_i^T$ and $R_{x,i} := \bar{R}_{x,i} - M_i W_i^{-1} R_{w,i}$. This set of equations can be solved efficiently by a Riccati iteration procedure [18]–[22]. Thus, by utilizing the structure of (1) we have reduced (13) to a smaller system which can be solved efficiently using a recursive approach.

REFERENCES

- [1] S. J. Qin and T. A. Badgwell, "A survey of industrial model predictive control technology," *Control Engineering Practice*, vol. 11, no. 7, pp. 733–764, 2003.
- [2] J. B. Rawlings and D. Q. Mayne, *Model Predictive Control: Theory and Design*. Nob Hill Publishing, 2009.
- [3] J. B. Rawlings, "Tutorial overview of model predictive control," *IEEE Control Systems*, vol. 20, no. 3, pp. 38–52, 2000.
- [4] J. M. Maciejowski, *Predictive Control: With Constraints*. Pearson Education, Prentice Hall, 2002.
- [5] M. Diehl, R. Amrit, and J. B. Rawlings, "A Lyapunov Function for Economic Optimizing Model Predictive Control," *IEEE Transactions on Automatic Control*, vol. 56, no. 3, pp. 703–707, 2011.
- [6] L. Grüne, "Economic receding horizon control without terminal constraints," *Automatica*, vol. 49, no. 3, pp. 725–734, 2013.
- [7] J. B. Rawlings, D. Angeli, and C. N. Bates, "Fundamentals of economic model predictive control," in *2012 IEEE 51st Annual Conference on Decision and Control (CDC)*, pp. 3851–3861, 2012.
- [8] D. Angeli, R. Amrit, and J. B. Rawlings, "On Average Performance and Stability of Economic Model Predictive Control," *IEEE Transactions on Automatic Control*, vol. 57, no. 7, pp. 1615–1626, 2012.
- [9] J. B. Rawlings, D. Bonne, J. B. Jørgensen, A. N. Venkat, and S. B. Jørgensen, "Unreachable Setpoints in Model Predictive Control," *IEEE Transactions on Automatic Control*, vol. 53, no. 9, pp. 2209–2215, 2008.
- [10] T. G. Hovgaard, L. F. S. Larsen, and J. B. Jørgensen, "Flexible and cost efficient power consumption using economic MPC a supermarket refrigeration benchmark," in *2011 50th IEEE Conference on Decision and Control and European Control Conference (CDC-ECC)*, pp. 848–854, 2011.
- [11] J. Ma, S. J. Qin, B. Li, and T. Salsbury, "Economic model predictive control for building energy systems," in *2011 IEEE PES Innovative Smart Grid Technologies (ISGT)*, pp. 1–6, 2011.
- [12] R. Halvgaard, N. K. Poulsen, H. Madsen, and J. B. Jørgensen, "Economic Model Predictive Control for building climate control in a Smart Grid," in *2012 IEEE PES Innovative Smart Grid Technologies (ISGT)*, pp. 1–6, 2012.
- [13] R. Halvgaard, N. K. Poulsen, H. Madsen, J. B. Jørgensen, F. Marra, and D. E. M. Bondy, "Electric vehicle charge planning using Economic Model Predictive Control," in *2012 IEEE International Electric Vehicle Conference (IEVC)*, pp. 1–6, 2012.
- [14] R. Amrit, J. B. Rawlings, and L. T. Biegler, "Optimizing process economics online using model predictive control," *Computers & Chemical Engineering*, vol. 58, no. 0, pp. 334 – 343, 2013.
- [15] S. Mehrotra, "On the Implementation of a Primal-Dual Interior Point Method," *SIAM Journal on Optimization*, vol. 2, no. 4, pp. 575–601, 1992.
- [16] J. Nocedal and S. Wright, *Numerical Optimization*. Springer Series in Operations Research and Financial Engineering, Springer, 2006.
- [17] A. Skajaa, E. D. Andersen, and Y. Ye, "Warmstarting the homogeneous and self-dual interior point method for linear and conic quadratic problems," *Mathematical Programming Computation*, vol. 5, no. 1, pp. 1–25, 2013.
- [18] C. V. Rao, S. J. Wright, and J. B. Rawlings, "Application of Interior-Point Methods to Model Predictive Control," *Journal of Optimization Theory and Applications*, vol. 99, no. 3, pp. 723–757, 1998.
- [19] J. B. Jørgensen, G. Frison, N. F. Gade-Nielsen, and B. Dammann, "Numerical Methods for Solution of the Extended Linear Quadratic Control Problem," in *4th IFAC Nonlinear Model Predictive Control Conference*, pp. 187–193, 2012.
- [20] J. B. Jørgensen, J. B. Rawlings, and S. B. Jørgensen, "Numerical Methods for Large-Scale Moving Horizon Estimation and Control," in *International Symposium on Dynamics and Control Process Systems (DYCOPS)*, vol. 7, 2004.
- [21] J. B. Jørgensen, *Moving Horizon Estimation and Control*. Ph.D. thesis, Department of Chemical Engineering, Technical University of Denmark, 2005.
- [22] L. Vandenbergh, S. Boyd, and M. Nouralishahi, "Robust linear programming and optimal control," in *Proceedings of the 15th IFAC World Congress*, vol. 15, pp. 271–276, 2002.
- [23] L. E. Sokoler, G. Frison, K. Edlund, and J. B. Anders Skajaa and Jørgensen, "A Riccati Based Homogeneous and Self-Dual Interior-Point Method for Linear Economic Model Predictive Control," in *2013 IEEE Multi-conference on Systems and Control*, pp. 592 – 598, 2013.
- [24] E. D. Andersen, J. Gondzio, C. Meszaros, and X. Xu, "Implementation of Interior Point Methods for Large Scale Linear Programming," Papers 96.3, Ecole des Hautes Etudes Commerciales, Université de Geneve, 1996.
- [25] X. Xu, P.-F. Hung, and Y. Ye, "A simplified homogeneous and self-dual linear programming algorithm and its implementation," *Annals of Operations Research*, vol. 62, no. 1, pp. 151–171, 1996.
- [26] Y. Ye, M. J. Todd, and S. Mizuno, "An $O(\sqrt{n}L)$ -Iteration Homogeneous and Self-Dual Linear Programming Algorithm," *Mathematics of Operations Research*, vol. 19, no. 1, pp. 53–67, 1994.
- [27] E. D. Andersen, C. Roos, and T. Terlaky, "On implementing a primal-dual interior-point method for conic quadratic optimization," *Mathematical Programming*, vol. 95, no. 2, pp. 249–277, 2003.
- [28] K. Edlund, L. E. Sokoler, and J. B. Jørgensen, "A primal-dual interior-point linear programming algorithm for MPC," in *Proceedings of the 48th IEEE Conference on Decision and Control, 2009 held jointly with the 2009 28th Chinese Control Conference. CDC/CCC 2009*, pp. 351–356, 2009.
- [29] J. Gondzio and A. Grothey, "A New Unblocking Technique to Warmstart Interior Point Methods Based on Sensitivity Analysis," *SIAM Journal on Optimization*, vol. 19, no. 3, pp. 1184–1210, 2008.
- [30] K. Edlund, T. Mølbak, and J. D. Bendtsen, "Simple models for model-based portfolio load balancing controller synthesis," in *6th IFAC Symposium on Power Plants and Power Systems Control*, pp. 173–178, 2009.

P A P E R D

Input-Constrained Model Predictive Control via the Alternating Direction Method of Multipliers

L. E. Sokoler, G. Frison, M. S. Andersen, and J. B. Jørgensen. Input-Constrained Model Predictive Control via the Alternating Direction Method of Multipliers. In *European Control Conference (ECC)*, pages 115–120, 2014.

Input-Constrained Model Predictive Control via the Alternating Direction Method of Multipliers

Leo Emil Sokoler, Gianluca Frison, Martin S. Andersen, and John Bagterp Jørgensen

Abstract—This paper presents an algorithm, based on the alternating direction method of multipliers, for the convex optimal control problem arising in input-constrained model predictive control. We develop an efficient implementation of the algorithm for the extended linear quadratic control problem (LQCP) with input and input-rate limits. The algorithm alternates between solving an extended LQCP and a highly structured quadratic program. These quadratic programs are solved using a Riccati iteration procedure, and a structure-exploiting interior-point method, respectively. The computational cost per iteration is quadratic in the dimensions of the controlled system, and linear in the length of the prediction horizon. Simulations show that the approach proposed in this paper is more than an order of magnitude faster than several state-of-the-art quadratic programming algorithms, and that the difference in computation time grows with the problem size. We improve the method further using a warm-start procedure.

I. INTRODUCTION

In model predictive control (MPC) an optimal control problem (OCP) is solved to optimize the predicted behavior of a dynamic model over a finite horizon. The solution to the OCP provides a sequence of inputs, of which only the first input is applied to the controlled system. At the following sampling instant the procedure is repeated, such that the inputs are computed in a closed-loop fashion. Model predictive control is one of the most industrially successful advanced control technology for constrained dynamic systems [1]–[3].

Since MPC requires the solution of the OCP at every sampling instant, its use has conventionally been limited to systems with slow dynamics. In addition to increased available computing power, however, the development of new algorithms have extended the use of MPC to systems with dynamics even in the kHz range. These algorithms are based on multi-parametric programming [4], [5], interior-point methods [6]–[11] and first-order methods [11], [12]. Another emerging research area within computational methods for MPC is the alternating direction method of multipliers (ADMM) [13]–[15]. Numerical examples show that ADMM often outperforms accelerated gradient methods [12], [13], [16]. Applications of ADMM for MPC include distributed MPC for dynamically coupled systems [17], [18], ℓ_1 -regularized MPC [19], as well as state and input-constrained MPC [12], [20], [21]. In [20] the OCP arising in state and input-constrained MPC is solved by decomposing the optimization problem into smaller subproblems along the time-axis, while [21] handles the optimization problem

via a combination of ADMM and Nesterov’s fast gradient method. A more general class of convex OCPs is discussed in relation to ADMM in [22]. The ADMM method proposed in [22] introduces a set of auxiliary input and state variables, which allows both input and state constraints to be handled efficiently. Finally, [12] provides a comprehensive study on first-order methods for MPC on resource-constrained embedded platforms

The algorithm presented in this paper is specifically tailored to input-constrained MPC. We split the OCP into a part related to the dynamic state constraints, and a part related to the input constraints. In contrast to [22], auxiliary state variables are not introduced. Moreover, we provide an efficient implementation of the ADMM algorithm for the extended linear quadratic control problem (LQCP) [23] with input and input-rate limits. The optimization problem associated with the dynamic state constraints is solved using a Riccati iteration procedure, whereas the input constraints are handled by a structure-exploiting interior-point method.

A. Paper Organization

This paper is organized as follows. Section II presents a generic ADMM algorithm for the OCP arising in input-constrained MPC. Section III develops an efficient implementation of the algorithm for the extended LQCP with limits on the input and the input-rate. Section IV tests a C version of the algorithm, denoted ADMM_{MPC} , using a closed-loop simulation study of a simple mass-spring system. This section also presents a large-scale benchmark that compares ADMM_{MPC} to state-of-the-art quadratic programming algorithms. Concluding remarks are given in Section V.

II. PROBLEM DEFINITION

Let $\{u_k\}_{k=0}^{N-1}$ denote a sequence of control variables with $u_k \in \mathbb{R}^{n_u}$, and $\{x_k\}_{k=0}^N$ denote a sequence of system states with $x_k \in \mathbb{R}^{n_x}$. In addition introduce the optimization vectors

$$u = [u_0^T \quad u_1^T \quad \dots \quad u_{N-1}^T]^T, \quad x = [x_1^T \quad x_2^T \quad \dots \quad x_N^T]^T.$$

The OCP associated with input-constrained MPC may be stated as

$$\min_{\{u_k, x_{k+1}\}_{k=0}^{N-1}} \{V(x, u) \mid u \in \mathbb{U}, (x, u) \in \mathbb{X}\}. \quad (1)$$

We assume that $V(x, u)$ is a convex function, and that \mathbb{X} is a convex set accounting for dynamic state constraints such that

$$\mathbb{X} = \{(x, u) \mid x_{k+1} = f_k(x_k, u_k), k \in \mathcal{N}\}, \quad (2)$$

The authors are with the Department of Applied Mathematics and Computer Science, Technical University of Denmark, DK-2800 Kgs. Lyngby, Denmark. Email: {leso, gjaef, mskan, jbjjo}@dtu.dk

where x_0 is a known (or estimated) initial state, $\mathcal{N} = \{0, 1, \dots, N-1\}$ is the prediction horizon, and $f_k : \mathbb{R}^{n_x} \times \mathbb{R}^{n_u} \mapsto \mathbb{R}^{n_x}$. It is further assumed that the input constraint set, \mathbb{U} , is a convex set.

A. Optimization Algorithm

The optimization problem (1) can be written as

$$\min_{\{u_k, v_{k+1}, v_k\}_{k=0}^{N-1}} \{V(x, u) + I_{\mathbb{X}}(x, u) + I_{\mathbb{U}}(v) \mid u = v\} \quad (3)$$

where $I_{\mathbb{A}}$ is the indicator function of a set \mathbb{A} and $v = [v_0^T \ v_1^T \ \dots \ v_{N-1}^T]^T$, $v_k \in \mathbb{R}^{n_u}$, is a vector of auxiliary variables.

The Lagrangian, $\mathcal{L}(x, u, v, z)$, associated with (3) is

$$\mathcal{L}(x, u, v, z) = V(x, u) + I_{\mathbb{X}}(x, u) + I_{\mathbb{U}}(v) + z^T(u - v), \quad (4)$$

and a stationary point of the Lagrangian satisfies

$$0 \in \partial_x \mathcal{L}(x, u, v, z) = \partial_x(V(x, u) + I_{\mathbb{X}}(x, u)), \quad (5a)$$

$$0 \in \partial_u \mathcal{L}(x, u, v, z) = \partial_u(V(x, u) + I_{\mathbb{X}}(x, u)) + z, \quad (5b)$$

$$0 \in \partial_v \mathcal{L}(x, u, v, z) = \partial_v(I_{\mathbb{U}}(v)) - z, \quad (5c)$$

where $z = [z_0^T \ z_1^T \ \dots \ z_{N-1}^T]^T$, $z_k \in \mathbb{R}^{n_u}$, denotes the Lagrange multipliers associated with the equality constraints of (3), and ∂ is the subdifferential operator. Hence, the necessary and sufficient optimality conditions for (3) may be stated as the primal feasibility condition, $u = v$, and the stationarity condition (5). For details and proofs, see e.g. [13]–[15].

In ADMM a point satisfying the optimality conditions for (3), is obtained via the recursions

$$(u, x)^{i+1} = \underset{\{u_k, x_{k+1}\}_{k=0}^{N-1}}{\operatorname{argmin}} \mathcal{L}_\rho(x, u, v^i, z^i), \quad (6a)$$

$$v^{i+1} = \underset{\{v_k\}_{k=0}^{N-1}}{\operatorname{argmin}} \mathcal{L}_\rho(x^{i+1}, u^{i+1}, v, z^i), \quad (6b)$$

$$z^{i+1} = z^i + \rho(u^{i+1} - v^{i+1}), \quad (6c)$$

in which $\mathcal{L}_\rho(x, u, v, z) = \mathcal{L}(x, u, v, z) + \frac{\rho}{2} \|u - v\|_2^2$ is the augmented Lagrangian with penalty parameter $\rho > 0$ [13]. Using the definition (4), we get

$$(u, x)^{i+1} = \underset{\{u_k, x_{k+1}\}_{k=0}^{N-1}}{\operatorname{argmin}} (V(x, u) + I_{\mathbb{X}}(x, u) + \frac{\rho}{2} \|u - v^i + w^i\|_2^2), \quad (7a)$$

$$v^{i+1} = \underset{\{v_k\}_{k=0}^{N-1}}{\operatorname{argmin}} (I_{\mathbb{U}}(v) + \frac{\rho}{2} \|u^{i+1} - v + w^i\|_2^2), \quad (7b)$$

$$w^{i+1} = w^i + u^{i+1} - v^{i+1}, \quad (7c)$$

where $w = \frac{1}{\rho} z$ is a scaled dual variable.

To speed up convergence u^{i+1} is replaced by $\tilde{u}^{i+1} = \alpha^i u^{i+1} + (1 - \alpha)(-v^i)$ in the recursions for v and w [13], [24]. The relaxation parameter $\alpha \in (0, 2)$ is tuned to the particular application.

B. Stopping Criteria

To detect an optimal solution in (3), we adopt the stopping criteria proposed in [13]. For the specific problem formulation, (3), these criteria are

$$\|u^i - v^i\|_2 \leq \varepsilon_P, \quad (8a)$$

$$\rho \|v^{i+1} - v^i\|_2 \leq \varepsilon_D. \quad (8b)$$

The conditions test primal and dual feasibility of the updated values in (7), i.e. if the necessary and sufficient optimality conditions for (3) are satisfied. The tolerance levels, ε_P and ε_D , are updated with respect to an absolute tolerance parameter, ε_A , and a relative tolerance parameter, ε_R , as follows

$$\varepsilon_P = \sqrt{N n_u} \varepsilon_A + \varepsilon_R \max\{\|u^i\|_2, \|v^i\|_2\},$$

$$\varepsilon_D = \sqrt{N n_u} \varepsilon_A + \varepsilon_R \rho \|w^i\|_2,$$

where n_u is the dimension of the control variables, and N is the length of the prediction horizon.

C. Warm-Start Procedure

The ADMM recursions (7) are initialized using the values v^0 and w^0 . As MPC requires solving the OCP in every sampling instant, a warm start is usually available for these initial values. Such a warm start is obtained by shifting the solution from the previous sampling instant forward in time. As an example consider the solution at sampling interval $k = 0$

$$v^* = [v_0^{*T} \ v_1^{*T} \ \dots \ v_{N-2}^{*T} \ v_{N-1}^{*T}]^T,$$

$$w^* = [w_0^{*T} \ w_1^{*T} \ \dots \ w_{N-2}^{*T} \ w_{N-1}^{*T}]^T.$$

We use the following initial values at sampling interval $k = 1$

$$v^* = [v_1^{*T} \ v_2^{*T} \ \dots \ v_{N-1}^{*T} \ v_{N-1}^{*T}]^T,$$

$$w^* = [w_1^{*T} \ w_2^{*T} \ \dots \ w_{N-1}^{*T} \ w_{N-1}^{*T}]^T.$$

As can be read, the last components of these vectors occur twice. This means that the initial guess for the final input move is the input move from the previous time step.

If no warm start is available, we use the standard cold-starting point $(v^0, w^0) = (\mathbf{0}, \mathbf{0})$.

D. Summary

Algorithm 1 summarizes the solution method for input-constrained MPC outlined above.

The convergence rate of Algorithm 1 can be very sensitive to the penalty parameter ρ [12], [13], [16], [25]. To overcome this issue, updating strategies for ρ have been proposed in e.g. [13], [25]. We also remark that Algorithm 1 requires the solution of two convex optimization problems in each iteration. As illustrated in the subsequent section, the overall complexity of Algorithm 1 is often attractive due to the structure of these problems.

Algorithm 1 ADMM Algorithm for Input-Constrained MPC

Require: ρ , (v^0, w^0) , $(\varepsilon_P, \varepsilon_D)$
 $i = 0$, converged = false

while not converged **do**

$$(x, u)^{i+1} = \arg \min_{\{u_k, x_{k+1}\}_{k=0}^{N-1}} V(x, u) + I_{\mathbb{X}}(x, u) + \frac{\rho}{2} \|u - v^i + w^i\|_2^2$$

$$v^{i+1} = \arg \min_{\{v_k\}_{k=0}^{N-1}} I_{\mathbb{V}}(v) + \frac{\rho}{2} \|u^{i+1} - v + w^i\|_2^2$$

$$w^{i+1} = w^i + u^{i+1} - v^{i+1}$$

$$r_P^{i+1} = u^{i+1} - v^{i+1}, \quad r_D^{i+1} = \rho(v^{i+1} - v^i)$$

if $\|r_P^{i+1}\|_2 \leq \varepsilon_P$ **and** $\|r_D^{i+1}\|_2 \leq \varepsilon_D$ **then**
 converged = true

end if
 $i \leftarrow i + 1$
end while

III. INPUT-CONSTRAINED EXTENDED LINEAR QUADRATIC CONTROL PROBLEM

As a special case of input-constrained MPC, we consider the extended LQCP [23]. The dynamic state constraints, (2), are governed by the parameters $\{A_k, B_k, b_k\}_{k=0}^{N-1}$, such that

$$\mathbb{X} = \{(x, u) \mid x_{k+1} = A_k x_k + B_k u_k + b_k, \quad k \in \mathcal{N}\}.$$

Moreover, the objective function is given by $V(x, u) = \sum_{k=0}^{N-1} \ell_k(x_k, u_k) + \ell_N(x_N)$, with the stage cost defined as

$$\ell_k(x_k, u_k) = \frac{1}{2} \begin{bmatrix} x_k \\ u_k \end{bmatrix}^T \begin{bmatrix} Q_k & M_k^T \\ M_k & R_k \end{bmatrix} \begin{bmatrix} x_k \\ u_k \end{bmatrix} + \begin{bmatrix} q_k \\ s_k \end{bmatrix}^T \begin{bmatrix} x_k \\ u_k \end{bmatrix} + \sigma_k,$$

and the terminal cost $\ell_N(x_N) = \frac{1}{2} x_N^T P x_N + p^T x_N + \sigma_N$. We impose box constraints on both the input and the input-rate. This is achieved by defining the input constraint set, \mathbb{U} , as

$$\mathbb{U} = \{u \mid \underline{u}_k \leq u_k \leq \bar{u}_k, \Delta \underline{u}_k \leq \Delta u_k \leq \Delta \bar{u}_k, \quad k \in \mathcal{N}\},$$

where the input-rate is given by $\Delta u_k = u_k - u_{k-1}$.

For the input-constrained extended LQCP defined above, the optimization problem for computing the (x, u) -update, (7a), becomes

$$\min_{\{u_k, x_{k+1}\}_{k=0}^{N-1}} \sum_{k=0}^{N-1} \ell_k(x_k, u_k) + \ell_N(x_N) + \frac{\rho}{2} \|u - v^i + w^i\|_2^2, \quad (9a)$$

$$\text{s.t. } x_{k+1} = A_k x_k + B_k u_k + b_k, \quad k \in \mathcal{N}, \quad (9b)$$

and for the v -update, (7b), we have

$$\min_{\{v_k\}_{k=0}^{N-1}} \frac{\rho}{2} \|u^{i+1} - v + w^i\|_2^2, \quad (10a)$$

$$\text{s.t. } \underline{v}_k \leq v_k \leq \bar{v}_k, \quad k \in \mathcal{N}, \quad (10b)$$

$$\Delta \underline{v}_k \leq \Delta v_k \leq \Delta \bar{v}_k, \quad k \in \mathcal{N}. \quad (10c)$$

The following results show that the optimization problems (9) and (10) can be solved with high efficiency.

A. The (x, u) -update

By re-defining the stage cost, $\ell_k(x_k, u_k)$, such that

$$R_k \leftarrow R_k + \rho I,$$

$$s_k \leftarrow s_k + \rho(-v_k^i + w_k^i),$$

the optimization problem (9) can be posed as an instance of the extended LQCP (with no input constraints) [23]. As demonstrated in [8], [23], [26]–[29], Riccati-based algorithms may be applied to solve such problems efficiently. These algorithms consist of a factorization part, and a backward and forward substitution part. The factorizations require $\mathcal{O}(N(n_x + n_u)^3)$ operations, while the substitutions require $\mathcal{O}(N(n_x + n_u)^2)$ operations.

In the context of Algorithm 1, it is important to note that only s_k changes as a function of the iteration number. This means that the factorizations can be computed outside the inner iteration loop, and that subsequent (x, u) -updates only require $\mathcal{O}(N(n_x + n_u)^2)$ operations.

B. The v -update

Let $v = [v_0 \ v_1 \ \dots \ v_{N-1}]^T$, and further denote $v_k^j \in \mathbb{R}$ as the j 'th input component of the vector $v_k \in \mathbb{R}^{n_u}$. Then the optimization vector v may be written as

$$v = [(v_0^0 \ \dots \ v_0^{n_u}) \ \dots \ (v_{N-1}^0 \ \dots \ v_{N-1}^{n_u})].$$

The problem (10) is separable across the input components. Therefore a problem in the form (10) may be solved for each $v^j = [v_0^j \ \dots \ v_{N-1}^j]$. Consequently, a solution method for (10) can assume that $n_u = 1$.

To write the optimization problem in a more compact form, we define the structures

$$\Lambda = \begin{bmatrix} 1 & & & & \\ -1 & 1 & & & \\ & & \ddots & & \\ & & & -1 & 1 \end{bmatrix}, \quad I_0 = \begin{bmatrix} 1 \\ 0 \\ \vdots \\ 0 \end{bmatrix},$$

and express (10) as the constrained quadratic program

$$\min_{\{v_k\}_{k=0}^{N-1}} \left\{ \frac{1}{2} v^T H v + g^T v \mid F v \geq f \right\}, \quad (11)$$

in which the problem data are

$$H = \rho I, \quad g = \rho(-u^{i+1} - w^i),$$

$$F = [\Lambda^T \quad -\Lambda^T \quad I \quad -I]^T,$$

$$f = [(\Delta \bar{u}_k + I_0 u_{-1})^T \quad -(\Delta \underline{u}_k - I_0 u_{-1})^T \quad \bar{u}_k^T \quad -\underline{u}_k^T]^T.$$

The main computational bottleneck in solving (11) using an interior-point method is solving a linear system of equations (in each iteration of the interior-point method) [30]. One way to express the linear system of equations solved is

$$(H + F^T D F) \Delta v = r, \quad (12)$$

where D is a diagonal matrix, r is a residual vector, and Δv is the optimization search direction. Proposition 1 provides a method for solving the structured system (12), that scales linearly in the length of the prediction horizon.

TABLE I
COMPLEXITY OF ALGORITHM 1 FOR THE INPUT-CONSTRAINED
EXTENDED LQCP.

	(x, u) -update	v -update	w -update	Total
Off-line	$\mathcal{O}(N(n_x + n_u)^3)$	-	-	$\mathcal{O}(N(n_x + n_u)^3)$
On-line	$\mathcal{O}(N(n_x + n_u)^2)$	$\mathcal{O}(Nn_u)$	$\mathcal{O}(Nn_u)$	$\mathcal{O}(N(n_x + n_u)^2)$

Proposition 1: The operation (12) can be performed in $\mathcal{O}(N)$ operations.

Proof: We write (12) as $\tilde{H}\tilde{D}v = r$ where $\tilde{H} = H + F^TDF$. Let $D = \mathbf{blkdiag}(D_1, D_2, D_3, D_4)$ denote block partitions of the diagonal matrix D . Then $\tilde{H} = (H + F^TDF) = \tilde{D}_1 + \Lambda^T\tilde{D}_2\Lambda$, where $\tilde{D}_1 = \rho I + D_3 + D_4$ and $\tilde{D}_2 = D_1 + D_2$ are diagonal matrices. Since \tilde{D}_1 is diagonal and $\Lambda^T\tilde{D}_2\Lambda$ is symmetric tridiagonal, \tilde{H} is tridiagonal. Each iteration of the interior-point method, thus requires the solution of a symmetric tridiagonal system. Such a system can be solved in $\mathcal{O}(N)$ operations [31]. ■

Since solving (10) for each input component, v^j , requires $\mathcal{O}(N)$ operations, the overall complexity of solving (10) is $\mathcal{O}(Nn_u)$. Note however, that the problems can be solved in parallel for each $j = 0, 1, \dots, n_u$.

C. Summary

Table I summarizes the computational complexity of Algorithm 1 for the input-constrained extended LQCP. As discussed previously, the matrix factorizations computed in the (x, u) -update are constant for all iterations of the ADMM algorithm. These factorizations can be reused every time a new OCP is solved, meaning that the computations with cubic complexity can be performed off-line. This is a big advantage, since the on-line computation time is critical in MPC applications. In this regard the ADMM algorithm requires $\mathcal{O}(N(n_x + n_u)^2)$ operations per iteration.

IV. NUMERICAL EXAMPLES

This section tests the warm-start procedure introduced in Section II-C, and provides a large-scale benchmark that compares `ADMMmpc` against state-of-the-art quadratic programming algorithms. `ADMMmpc` is implemented in C with the use of BLAS and LAPACK linear algebra routines. We access `ADMMmpc` from MATLAB via a MEX-interface. The tolerance specifications in (8) are set to $\epsilon_A = \epsilon_R = 10^{-4}$. These tolerance levels yield, in the worst case, less than a 1% relative increase in the objective function compared to a high accuracy solution.

A. Closed-Loop Simulation

As a special case of the extended LQCP, we consider an ℓ_2 -based tracking objective that penalizes deviations from a desired set-point, \bar{y}_k , with

$$\ell(x_k, u_k) = \frac{1}{2}(y_k - \bar{y}_k)^T Q_k (y_k - \bar{y}_k) + \frac{1}{2}\Delta u_k^T R_k \Delta u_k, \quad k \in \mathcal{N},$$

$$\ell_N(x_N) = \frac{1}{2}(y_N - \bar{y}_N)^T Q_N (y_N - \bar{y}_N),$$

where the system output is given by $y_k = Cx_k$. As demonstrated in [23], a problem with the cost functions defined

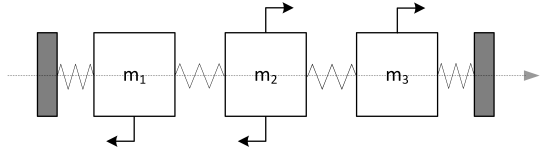


Fig. 1. Illustration of the mass-spring system.

TABLE II
CONTROLLER PARAMETERS.

j	\underline{u}_k^j	\bar{u}_k^j	$\Delta \underline{u}_k^j$	$\Delta \bar{u}_k^j$	r_k^j
1	-0.4	0	-0.15	0.15	0.1
2	-0.1	0.1	-0.05	0.05	0.1
3	0	0.4	-0.15	0.15	0.1

above can be transformed into an instance of the extended LQCP.

Fig. 1 illustrates the dynamic system considered in this case study. The system is a mass-spring system [6], [9], which consists of three 1 kg masses connected by springs, and walls at the end. No damping is assumed and the spring constant is 1 N/m. Actuators are attached to each of the masses. The first actuator can apply a force only in the negative direction, whereas the last actuator can apply a force only in the positive direction. The second actuator can apply a force in both directions, but its operating range is very limited. Table II lists the input limits, $(\underline{u}_k^j, \bar{u}_k^j)$, the input-rate limits, $(\Delta \underline{u}_k^j, \Delta \bar{u}_k^j)$, and the regularization parameters, $R_k = \mathbf{diag}(r_k)$. These values are fixed over the entire prediction horizon $k \in \mathcal{N}$. The controller objective is to control the displacement of the second mass, y_k , with respect to a time-varying reference \bar{y}_k . The penalty for deviating from the reference is $Q_k = 1$ for all time steps, and the length of the prediction horizon is $N = 120$. The system is realized in a discrete state space form (A, B, C) using a sampling time of $T_s = 0.5$ seconds.

Fig. 2 illustrates a closed-loop simulation with 2400 sampling intervals. For each of the 2400 OCPs solved, we use the penalty parameter $\rho = 1$ and the relaxation parameter $\alpha = 1.8$. To make warm-start non-trivial in periods with a constant reference, we include Gaussian process and measurement noise in the simulation.

Fig. 2 shows that the displacement of the second mass tracks the desired reference very well, and that there are periods in which the input limits are reached. As the dynamic state constraints and the input constraints are handled separately in the ADMM recursions, (7), active constraints make the OCP more challenging for `ADMMmpc`.

Fig. 3 depicts the number of iterations used by the ADMM algorithm for a cold start and a warm start, respectively, as well as the number of active constraints in the solution. We observe that warm-start reduces the number of iterations significantly, even when a large fraction of the constraints is active. On average the time saved per problem solved is 80%. Fig. 3 also shows that the advantage over cold start is less significant in time steps where the active set changes

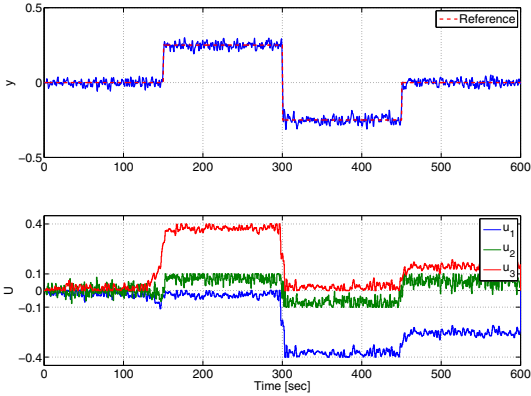


Fig. 2. Closed-loop simulation of the mass-spring system controlled by input-constrained MPC with an ℓ_2 penalty on deviations from the reference, and an ℓ_2 regularization term on the input-rate.

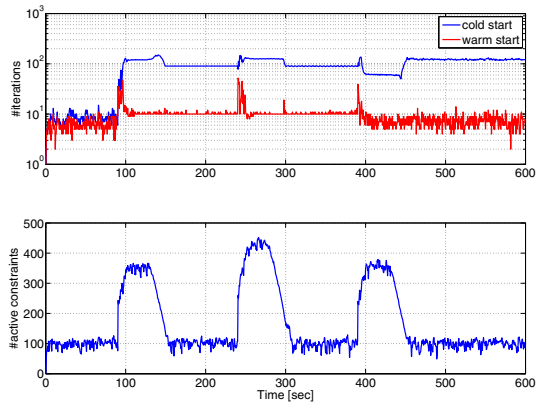


Fig. 3. Number of iterations used by ADMM_{mpc} to converge to a solution with the desired accuracy, and the number of active constraints in the solution.

dramatically compared to the previous time step.

B. Large-Scale Benchmark

We compare ADMM_{mpc} to the general purpose interior-point methods provided by CPLEX, MOSEK and Gurobi, in an open-loop simulation. The comparison also includes an implementation of the structure exploiting primal barrier interior-point method for MPC, fast_mpc , provided in [6], as well as the automatic code generation based interior-point method FORCES [32]. Similar to ADMM_{mpc} , these algorithms are run in MATLAB via MEX interfaces using low accuracy settings. All simulations are performed on an Intel(R) Xenon(R) CPU X5650 @ 2.67GHz with 12 GB RAM running a 64-bit Ubuntu 12.04 operating system. Warm-start is not employed in the benchmark.

As a scalable dense test problem, we construct a random dynamic system with the largest eigenvalue close to the unit

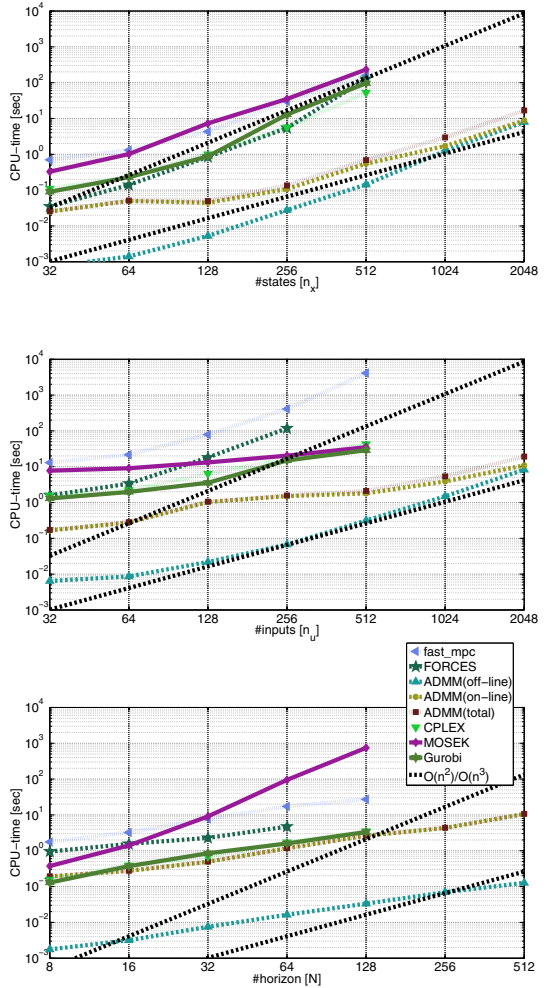


Fig. 4. Computation time of solving the OCP, (1), as a function of the number of states, n_x ($n_u = 16$, $N = 16$), the number of inputs, n_u ($n_x = 128$, $N = 16$), and the length of the prediction horizon, N ($n_x = 64$, $n_u = 64$).

circle. The state transition matrix $A \in \mathbb{R}^{n_x \times n_x}$ is build as a dense random matrix with non-negative elements, which is then scaled by the largest row (column) sum [33]. We generate $B \in \mathbb{R}^{n_u \times n_x}$ and $C \in \mathbb{R}^{n_y \times n_x}$ as random dense matrices as well, and set $n_y = n_x$. Using a similar problem setting as in the mass-spring system case study, we ensure that a large fraction of the constraints is active in the solution to make the problem challenging for ADMM_{mpc} .

Fig. 4 shows the computation time of solving the OCP, (1), as a function of the problem size. The optimization problems are solved using the penalty parameter $\rho = \sqrt{n_x/n_u}(1/\log(N))$, which we found to work well in practice. The relaxation parameter is set to $\alpha = 1.9$. For these parameter specifications, the number of iterations used by

ADMM_{MPC} fluctuates between 100-200 for all problem sizes considered. Fig. 4 shows that the ADMM algorithm is more than an order of magnitude faster than the interior-point methods for large problems (although the interior-point methods only require 10-20 iterations, the computational cost per iteration is much more expensive than for ADMM_{MPC}).

Fig. 4 also shows that the off-line computation time of ADMM_{MPC} grows faster than its on-line computation time. The off-line computation time is however, not critical in MPC applications. We note that although ADMM_{MPC} converges faster than the interior-point methods to a solution with the tolerance levels $\epsilon_A = \epsilon_R = 10^{-4}$, the number of iterations required for a highly accurate solution may be very large [13]. In this case, we suggest to combine the ADMM algorithm with a higher order optimization method.

V. CONCLUSIONS

This paper presented a generic ADMM algorithm for solving the convex optimal control problem arising in input-constrained MPC. As a special case, we focused on an efficient implementation of the algorithm for the extended LQCP with limits on the inputs and the input-rate. Simulations show that for this classical MPC formulation, a C version of the algorithm denoted ADMM_{MPC} is faster than several state-of-the-art quadratic programming algorithms with a significant margin, and that it scales in a favorable way. Moreover, we also demonstrated that by reusing information from the previous sampling instant, the computation time can be reduced further using a simple warm-start procedure.

REFERENCES

- [1] D. Q. Mayne, J. B. Rawlings, C. V. Rao, and P. O. M. Scokaert, "Constrained model predictive control: Stability and optimality," *Automatica*, vol. 36, no. 6, pp. 789–814, 2000.
- [2] J. B. Rawlings, "Tutorial overview of model predictive control," *IEEE Control Systems*, vol. 20, no. 3, pp. 38–52, 2000.
- [3] S. J. Qin and T. A. Badgwell, "A survey of industrial model predictive control technology," *Control Engineering Practice*, vol. 11, no. 7, pp. 733–764, 2003.
- [4] E. N. Pistikopoulos, "From multi-parametric programming theory to MPC-on-a-chip multi-scale systems applications," *Computers & Chemical Engineering*, vol. 47, no. 0, pp. 57–66, 2012.
- [5] H. J. Ferreau, H. G. Bock, and M. Diehl, "An online active set strategy to overcome the limitations of explicit MPC," *International Journal of Robust and Nonlinear Control*, vol. 18, no. 8, pp. 816–830, 2008.
- [6] Y. Wang and S. Boyd, "Fast Model Predictive Control Using Online Optimization," *IEEE Transactions on Control Systems Technology*, vol. 18, no. 2, pp. 267–278, 2010.
- [7] L. E. Sokoler, G. Frison, K. Edlund, A. Skajaa, and J. B. Jørgensen, "A Riccati Based Homogeneous and Self-Dual Interior-Point Method for Linear Economic Model Predictive Control," in *2013 IEEE Multi-conference on Systems and Control*, pp. 592–598, 2013.
- [8] C. V. Rao, S. J. Wright, and J. B. Rawlings, "Application of Interior-Point Methods to Model Predictive Control," *Journal of Optimization Theory and Applications*, vol. 99, no. 3, pp. 723–757, 1998.
- [9] A. Shahzad and G. A. Kerrigan, E. C. Constantinides, "A fast well-conditioned interior point method for predictive control," in *2010 49th IEEE Conference on Decision and Control (CDC)*, pp. 508–513, 2010.
- [10] K. Edlund, L. E. Sokoler, and J. B. Jørgensen, "A primal-dual interior-point linear programming algorithm for MPC," in *48th IEEE Conference on Decision and Control, held jointly with 28th Chinese Control Conference*, pp. 351–356, 2009.
- [11] S. Richter, C. N. Jones, and M. Morari, "Real-time input-constrained MPC using fast gradient methods," in *48th IEEE Conference on Decision and Control, held jointly with 28th Chinese Control Conference*, pp. 7387–7393, 2009.
- [12] J. L. Jerez, P. J. Goulart, S. Richter, G. A. Constantinides, E. C. Kerrigan, and M. Morari, "Embedded Online Optimization for Model Predictive Control at Megahertz Rates," *IEEE Transactions on Automatic Control*, p. Accepted, 2013.
- [13] S. Boyd, N. Parikh, E. Chu, B. Peleato, and E. Jonathan, "Distributed optimization and statistical learning via the alternating direction method of multipliers," *Foundations and Trends in Machine Learning*, vol. 3, no. 1, pp. 1–122, 2011.
- [14] S. Boyd and L. Vandenberghe, *Convex Optimization*. Cambridge University Press, 2004.
- [15] R. T. Rockafellar, *Convex Analysis*. Princeton mathematical series, Princeton University Press, 1970.
- [16] M. Hong and Z.-Q. Luo, "On the Linear Convergence of the Alternating Direction Method of Multipliers," *Mathematical Programming*, p. Submitted, 2013.
- [17] C. Conte, T. Summers, M. N. Zeilinger, M. Morari, and C. N. Jones, "Computational aspects of distributed optimization in model predictive control," in *2012 IEEE 51st Annual Conference on Decision and Control (CDC)*, pp. 6819–6824, 2012.
- [18] T. H. Summers and J. Lygeros, "Distributed model predictive consensus via the Alternating Direction Method of Multipliers," in *2012 50th Annual Allerton Conference on Communication, Control and Computing (Allerton)*, pp. 79–84, 2012.
- [19] M. Annergren, A. Hansson, and B. Wahlberg, "An ADMM algorithm for solving ℓ_1 regularized MPC," in *2012 IEEE 51st Annual Conference on Decision and Control (CDC)*, pp. 4486–4491, 2012.
- [20] M. Kögel and R. Findeisen, "Parallel Solutions of Model Predictive Control Using the Alternating Direction Method of Multipliers," in *4th IFAC Nonlinear Model Predictive Control Conference*, pp. 369–374, 2012.
- [21] M. Kögel and R. Findeisen, "Fast predictive control of linear systems combining Nesterov's gradient method and the method of multipliers," in *2011 50th IEEE Conference on Decision and Control and European Control Conference (CDC-ECC)*, pp. 501–506, 2011.
- [22] B. O'Donoghue, G. Stathopoulos, and S. Boyd, "A Splitting Method for Optimal Control," *IEEE Transactions on Control Systems Technology*, vol. 21, no. 6, pp. 2432–2442, 2013.
- [23] J. B. Jørgensen, G. Frison, N. F. Gade-Nielsen, and B. Dammann, "Numerical Methods for Solution of the Extended Linear Quadratic Control Problem," in *4th IFAC Nonlinear Model Predictive Control Conference*, pp. 187–193, 2012.
- [24] J. Eckstein and M. C. Ferris, "Operator-Splitting Methods for Monotone Affine Variational Inequalities, with a Parallel Application to Optimal Control," *Inform Journal on Computing*, vol. 10, no. 2, pp. 218–235, 1998.
- [25] E. Ghadimi, A. Teixeira, I. Shames, and M. Johansson, "Optimal parameter selection for the alternating direction method of multipliers (ADMM): quadratic problems," *IEEE Transactions on Automatic Control*, p. Submitted, 2013.
- [26] J. B. Jørgensen, J. B. Rawlings, and S. B. Jørgensen, "Numerical Methods for Large-Scale Moving Horizon Estimation and Control," in *International Symposium on Dynamics and Control Process Systems (DYCOPS)*, vol. 7, 2004.
- [27] J. B. Jørgensen, *Moving Horizon Estimation and Control*. Ph.D. thesis, Department of Chemical Engineering, Technical University of Denmark, 2005.
- [28] L. Vandenberghe, S. Boyd, and M. Nourlshahi, "Robust linear programming and optimal control," in *Proceedings of the 15th IFAC World Congress*, vol. 15, pp. 271–276, 2002.
- [29] G. Frison and J. B. Jørgensen, "Efficient Implementation of the Riccati Recursion for Solving Linear-Quadratic Control Problems," in *2013 IEEE Multi-conference on Systems and Control*, pp. 1117–1122, 2013.
- [30] J. Nocedal and S. Wright, *Numerical Optimization*. Springer Series in Operations Research and Financial Engineering, Springer, 2006.
- [31] G. H. Golub and C. F. Van Loan, *Matrix Computations*. Johns Hopkins Studies in the Mathematical Sciences, Johns Hopkins University Press, 2012.
- [32] A. Domahidi, A. Zraggen, M. N. Zeilinger, M. Morari, and C. N. Jones, "Efficient Interior Point Methods for Multistage Problems Arising in Receding Horizon Control," in *51st IEEE Conference on Decision and Control (CDC)*, pp. 668–674, 2012.
- [33] C. D. Meyer, *Matrix analysis and applied linear algebra*. Society for Industrial and Applied Mathematics, 2000.

P A P E R E

A Dantzig-Wolfe Decomposition Algorithm for Linear Economic Model Predictive Control of Dynamically Decoupled Subsystems

L. E. Sokoler, L. Standardi, K. Edlund, N. K. Poulsen, H. Madsen, and J. B. Jørgensen. A Dantzig-Wolfe Decomposition Algorithm for Linear Economic Model Predictive Control of Dynamically Decoupled Subsystems. *Journal of Process Control*, 24(8):1225–1236, 2014.



A Dantzig–Wolfe decomposition algorithm for linear economic model predictive control of dynamically decoupled subsystems



L.E. Sokoler^{a,b}, L. Standardi^a, K. Edlund^b, N.K. Poulsen^a, H. Madsen^a, J.B. Jørgensen^{a,*}

^a Department of Applied Mathematics and Computer Science, Technical University of Denmark, DK-2800 Kgs. Lyngby, Denmark

^b DONG Energy, DK-2820 Gentofte, Denmark

ARTICLE INFO

Article history:

Received 10 January 2014

Received in revised form 20 May 2014

Accepted 20 May 2014

Available online 3 July 2014

Keywords:

Optimization

Dantzig–Wolfe decomposition

Regularization

Linear programming

Distributed model predictive control

Energy management

ABSTRACT

This paper presents a warm-started Dantzig–Wolfe decomposition algorithm tailored to economic model predictive control of dynamically decoupled subsystems. We formulate the constrained optimal control problem solved at each sampling instant as a linear program with state space constraints, input limits, input rate limits, and soft output limits. The objective function of the linear program is related directly to the cost of operating the subsystems, and the cost of violating the soft output constraints. Simulations for large-scale economic power dispatch problems show that the proposed algorithm is significantly faster than both state-of-the-art linear programming solvers, and a structure exploiting implementation of the alternating direction method of multipliers. It is also demonstrated that the control strategy presented in this paper can be tuned using a weighted ℓ_1 -regularization term. In the presence of process and measurement noise, such a regularization term is critical for achieving a well-behaved closed-loop performance.

© 2014 Elsevier Ltd. All rights reserved.

1. Introduction

Conventionally, the optimal control problem (OCP) solved in model predictive control (MPC) is formulated as a convex program that penalizes deviations between the controlled output and a setpoint [1–4]. While this approach ensures that the setpoint is reached in a reasonable amount of time, it does not guarantee that the transition between setpoints is performed in an economically efficient way. To overcome this problem, MPC has been extended to solve OCPs with more general cost functions, providing a systematic method for optimizing economic performance [5–11]. Stability and other properties of such economic MPC (EMPC) schemes have been addressed in [5–9,12–14].

The main contribution of this paper is a Dantzig–Wolfe decomposition algorithm for EMPC of dynamically decoupled subsystems that solves the OCP in an efficient and reliable way. As the control law is computed in real-time, such an algorithm allows EMPC to be employed even for applications with thousands of subsystems. In particular, we consider an ℓ_1 -regularized linear type of OCP with input constraints, input rate constraints and soft

output constraints. Each subsystem is governed by a discrete state space model. The coupling of the subsystems occurs through a set of aggregated variables.

The Dantzig–Wolfe decomposition algorithm, presented in this paper, exploits that dynamically decoupled subsystems give rise to a block-angular structure in the OCP constraint matrix. This allows the OCP to be decomposed into a master problem and a number of subproblems [15–17]. The master problem includes a set of linking constraints which couples the subsystems, whereas the subproblems are concerned only with the individual subsystems. Using an iterative approach illustrated in Fig. 1, the decomposed problem can be solved via a delayed column generation procedure. Such techniques have previously been applied to conventional norm-based MPC in [18–20].

The block-angular constraint matrix structure appears for dynamically decoupled subsystems with linking constraints [21]. Dynamic multi-plant models as well as dynamic multi-product models are examples of such models [22]. Dynamic multi-plant models occur e.g. in the production planning for multiple refineries [23]. For process systems, dynamically decoupled systems with linking constraints occur when independent units are connected to shared process equipment such as pipes. A boiler-turbine system producing high pressure (HP), middle pressure (MP) and low pressure (LP) steam as well as electricity is a common example of a system that can be modeled as dynamically decoupled subsystems (the boilers) that have linking constraints (the demand for

* Corresponding author. Tel.: +45 45253088.

E-mail addresses: leso@dtu.dk (L.E. Sokoler), laus@dtu.dk (L. Standardi), kried@dongenergy.dk (K. Edlund), nkpo@dtu.dk (N.K. Poulsen), hmad@dtu.dk (H. Madsen), jbjo@dtu.dk (J.B. Jørgensen).

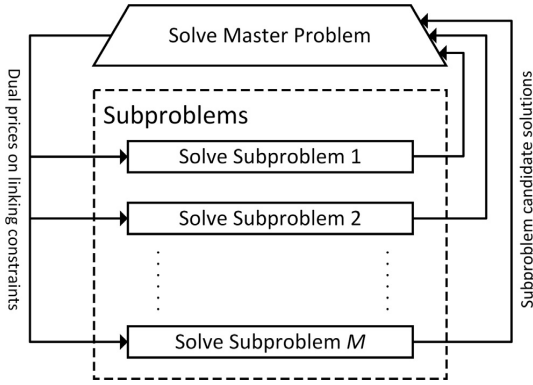


Fig. 1. Flowchart of the delayed column generation procedure used in the Dantzig–Wolfe decomposition algorithm for EMPC of dynamically decoupled subsystems with linking constraints. In each iteration, dual prices associated with the linking constraints are obtained by solving the master problem. These prices are used by the subsystems to compute an updated solution that improves the overall objective function.

various steam qualities and electrical power) [18,24]. In upstream offshore oil production, the compressors and pumps of a number of production wells share the pipeline, separators and compressors to bring the oil onshore [25,26]. This is also an example of a system that can be modeled as dynamically decoupled subsystems with linking constraints. Smart Grid systems in which a number of independent energy producers and consumers are controlled to balance power production and consumption represent yet another instance of dynamically decoupled systems with linking constraints [20,27]. The temperature regulation of multi-room buildings can also be formulated as dynamically decoupled subsystems with linking constraints [28]. As is evident by this list of examples, dynamically decoupled subsystems with linking constraints are common in process systems.

To test a MATLAB implementation of the Dantzig–Wolfe decomposition algorithm, denoted DW_{EMPC} , a simple energy systems management case study is presented. We show that as more units are added to a network of controllable generators, DW_{EMPC} becomes increasingly favorable over state-of-the-art sparse linear programming solvers provided by Gurobi, CPLEX, and MOSEK. It is further demonstrated that a nearly optimal solution can be acquired, even if DW_{EMPC} is terminated early. This is an attractive property in real-time applications such as EMPC, since only a limited amount of time is available for solving the OCP.

In addition to the general purpose solvers, DW_{EMPC} is compared to a structure exploiting implementation of the alternating direction method of multipliers (ADMM) [29–32], denoted $ADMM_{EMPC}$, with similar parallelization capabilities to DW_{EMPC} . Simulations illustrate that unless a highly suboptimal control performance is tolerated, DW_{EMPC} outperforms $ADMM_{EMPC}$ with a significant margin. Results also show that for both algorithms, a simple warm-start strategy yields a substantial improvement over cold start, and that the performance of this strategy increases with the weights on the ℓ_1 -regularization term. Inclusion of the regularization term is critical for the controller performance in the face of stochastic process and measurement noise as well as model-plant mismatch.

1.1. Paper organization

We have organized the paper as follows. In Section 2, the OCP solved in this paper is introduced. We decompose the problem using Dantzig–Wolfe decomposition in Section 3, and a column

generation procedure for solving the decomposed problem is presented. Section 4 describes a distributed implementation of ADMM for solving the OCP. Section 5 reports performance indicators for the proposed algorithms. These performance indicators are computed using a conceptual energy systems management case study. Concluding remarks are given in Section 6.

2. Problem definition

We consider M dynamically decoupled discrete state space models in the form

$$x_{j,k+1} = A_j x_{j,k} + B_j u_{j,k}, \quad j \in \mathcal{M}, \quad (1a)$$

$$y_{j,k} = C_j x_{j,k}, \quad j \in \mathcal{M}, \quad (1b)$$

where $\mathcal{M} = \{1, 2, \dots, M\}$. The state space matrices are denoted by (A_j, B_j, C_j) , the states by $x_{j,k} \in \mathbb{R}^{n_x(j)}$, the inputs by $u_{j,k} \in \mathbb{R}^{n_u(j)}$, and the outputs by $y_{j,k} \in \mathbb{R}^{n_y(j)}$. Moreover, we define the aggregated variables

$$y_{T,k} = \sum_{j \in \mathcal{M}} \Upsilon_j y_{j,k} = \sum_{j \in \mathcal{M}} \Upsilon_j C_j x_{j,k}, \quad (2)$$

in which $\Upsilon_j \in \mathbb{R}^{n_{yT} \times n_{y(j)}}$ are subsystem multipliers.

The OCP defining the EMPC control law for the subsystems (1), is in this paper defined as

$$\min_{u,x,y,y_T,\rho,\gamma} \psi = \psi_{eco} + \psi_{reg}, \quad (3a)$$

with

$$\psi_{eco} = \sum_{k \in \mathcal{N}_0} \left(q_{k+1}^T \rho_{k+1} + \sum_{j \in \mathcal{M}} p_{j,k}^T u_{j,k} + r_{j,k+1}^T \Upsilon_j y_{j,k+1} \right), \quad (3b)$$

$$\psi_{reg} = \sum_{k \in \mathcal{N}_0} \sum_{j \in \mathcal{M}} w_{j,k} \|\Delta u_{j,k}\|_1, \quad (3c)$$

and subject to the constraints

$$x_{j,k+1} = A_j x_{j,k} + B_j u_{j,k}, \quad k \in \mathcal{N}_0, \quad j \in \mathcal{M}, \quad (3d)$$

$$y_{j,k} = C_j x_{j,k}, \quad k \in \mathcal{N}_1, \quad j \in \mathcal{M}, \quad (3e)$$

$$y_{T,k} = \sum_{j \in \mathcal{M}} \Upsilon_j C_j x_{j,k}, \quad k \in \mathcal{N}_1, \quad (3f)$$

$$\underline{u}_{j,k} \leq u_{j,k} \leq \bar{u}_{j,k}, \quad k \in \mathcal{N}_0, \quad j \in \mathcal{M}, \quad (3g)$$

$$\Delta \underline{u}_{j,k} \leq \Delta u_{j,k} \leq \Delta \bar{u}_{j,k}, \quad k \in \mathcal{N}_0, \quad j \in \mathcal{M}, \quad (3h)$$

$$y_{-j,k} - \gamma_{j,k} \leq y_{j,k} \leq \bar{y}_{j,k} + \gamma_{j,k}, \quad k \in \mathcal{N}_1, \quad j \in \mathcal{M}, \quad (3i)$$

$$0 \leq \gamma_{j,k} \leq \bar{\gamma}_{j,k}, \quad k \in \mathcal{N}_1, \quad j \in \mathcal{M}, \quad (3j)$$

$$\underline{y}_{T,k} - \rho_k \leq y_{T,k} \leq \bar{y}_{T,k} + \rho_k, \quad k \in \mathcal{N}_1, \quad (3k)$$

$$0 \leq \rho_k \leq \bar{\rho}_k, \quad k \in \mathcal{N}_1, \quad (3l)$$

where \leq and \geq denote element-wise inequalities. The input rate is defined as $\Delta u_k = u_k - u_{k-1}$ and $\mathcal{N}_i = \{0 + i, 1 + i, \dots, N - 1 + i\}$, with N being the length of the control and prediction horizon.

The input data to (3) are the input limits, $(\underline{u}_{j,k}, \bar{u}_{j,k})$, the input rate limits, $(\Delta \underline{u}_{j,k}, \Delta \bar{u}_{j,k})$, the subsystem output limits, $(y_{-j,k}, \bar{y}_{j,k})$, the aggregated variable limits, $(\underline{y}_{T,k}, \bar{y}_{T,k})$, the input prices, $p_{j,k}$, the price for violating the subsystem output limits, $r_{j,k}$, and the price for violating the aggregated variable limits, q_k . The slack variables, $\gamma_{j,k}$ and ρ_k , account for the violation of the soft output constraints. We impose upper limits, $(\bar{\gamma}_{j,k}, \bar{\rho}_k)$, on these variables, as this simplifies later computations considerably.

The objective function (3a) consists of an economic term (3b) and a regularization term (3c). The economic term (3b) represents the cost of operating the subsystems and the cost of violating the soft output constraints. The regularization term (3c) is included to obtain a well behaved solution. In our paper, the regularization term is formulated as a weighted ℓ_1 -penalty on the input rate. Using an ℓ_1 -penalty ensures that the resulting OCP is a linear program that can be solved using Dantzig–Wolfe decomposition.

Remark 1. An alternative way of expressing the OCP objective function (3a) is as a trade-off between the economic term and the regularization term, such that

$$\psi = \alpha \psi_{\text{eco}} + (1 - \alpha) \psi_{\text{reg}}, \quad \alpha \in [0, 1], \quad (4)$$

where α is a user-defined parameter. Amrit et al. [12] discuss the trade-off between the economic term and an ℓ_2 -regularization term.

The regularization term (3c) is a special case of

$$\psi_{\text{reg}} = \sum_{k \in \mathcal{N}_0} \left(\sum_{j \in \mathcal{M}} w_{j,k+1}^x \|x_{j,k+1} - \bar{x}_{j,k+1}\|_1 + \sum_{j \in \mathcal{M}} w_{j,k}^u \|u_{j,k} - \bar{u}_{j,k}\|_1 + w_{j,k}^{\Delta u} \|\Delta u_{j,k}\|_1 \right), \quad (5)$$

in which $(\bar{x}_{j,k+1}, \bar{u}_{j,k})_{k \in \mathcal{N}_0, j \in \mathcal{M}}$ are target values that may be computed by a target calculator or a real-time optimization layer. An objective function consisting only of (5) corresponds to conventional ℓ_1 norm-based MPC. Edlund et al. [20] solves such problems using Dantzig–Wolfe decomposition.

Remark 2. The objective function (4) is similar to the mean-variance-based economic objective function introduced in [33] for production optimization in an oil field. For a random cost variable, ψ_{eco} , the mean-variance optimization criterion is

$$\psi_{\text{MV}} = \alpha E[\psi_{\text{eco}}] + (1 - \alpha) V[\psi_{\text{eco}}].$$

$E[\psi_{\text{eco}}]$ is the cost expectation and $V[\psi_{\text{eco}}]$ is the cost variance. In (4), ψ_{eco} can be interpreted as a certainty-equivalent approximation of the mean of the random cost variable, ψ_{eco} , while the regularization term, ψ_{reg} , is included to make the controller less sensitive to noise. The key advantage in using the deterministic formulation (4) is that the computational load is significantly reduced compared to a mean-variance approach based on Monte Carlo simulations. Other measures of risk than the mean-variance formulation that can be used to regularize the solution are Value-at-Risk (VaR) and Conditional Value-at-Risk (CVaR) [34].

Remark 3. The Dantzig–Wolfe decomposition algorithm is an algorithm for solving linear programs. Consequently, the approach described in this paper is limited to solve OCPs with a linear objective function, linear dynamics, and linear constraints. Rao and Rawlings [35] provide a number of penalty functions that can be expressed as linear programs. Penalty functions based on ℓ_1 norms, such as (3c) and (5), as well as ℓ_∞ norms can be expressed as linear programs. Piecewise linear approximations accommodate the need for solving OCPs with more general convex economic cost functions [26,36,37]. The disadvantage of using piecewise linear approximations is that the size of the resulting linear program may increase considerably.

Remark 4. The expression (2) for the aggregated variables is tailored to dynamically decoupled subsystems that collaborate to

meet a common objective. The expression (2) is a special case of the more general expression

$$y_{T,k} = \sum_{j \in \mathcal{M}} \gamma_j^y y_{j,k} + \gamma_j^u u_{j,k}, \quad k \in \mathcal{N}_1, \quad (6)$$

for the aggregated variables. The general expression (6) may be used to describe couplings between subsystems (e.g. interactions between 1) process units in a process system; and 2) the transmission lines coupling producers and consumers in a power system) [18]. When the number of aggregated variables increases, the number of linking constraints increases. The Dantzig–Wolfe decomposition algorithm is most efficient when the number of linking constraints is small compared to the total number of constraints.

2.1. Compact formulation

By eliminating the states using Eq. (1a), we can write the output Eq. (1b), as

$$y_{j,k} = C_j A_j^k x_{j,0} + \sum_{i \in \mathcal{N}_0} H_{j,k-i} u_{j,i}, \quad j \in \mathcal{M}, \quad k \in \mathcal{N}_1,$$

where the impulse response coefficients are given by

$$H_{j,k} = C_j A_j^{k-1} B_j, \quad j \in \mathcal{M}, \quad k \in \mathcal{N}_1.$$

Consequently

$$y_{T,k} = \sum_{j \in \mathcal{M}} \left(\gamma_j C_j A_j^k x_{j,0} + \sum_{i \in \mathcal{N}_0} \gamma_j H_{j,k-i} u_{j,i} \right), \quad k \in \mathcal{N}_1.$$

Define the vectors

$$y_j = [y_{j,1}^T \quad y_{j,2}^T \quad \cdots \quad y_{j,N}^T]^T, \quad j \in \mathcal{M}, \quad (7a)$$

$$u_j = [u_{j,0}^T \quad u_{j,1}^T \quad \cdots \quad u_{j,N-1}^T]^T, \quad j \in \mathcal{M}, \quad (7b)$$

and the matrices

$$\Gamma_j = \begin{bmatrix} H_{j,1} & 0 & \cdots & 0 \\ H_{j,2} & H_{j,1} & & \\ \vdots & \vdots & \ddots & \\ H_{j,N} & H_{j,N-1} & \cdots & H_{j,1} \end{bmatrix}, \quad \Phi_j = \begin{bmatrix} C_j A_j \\ C_j A_j^2 \\ \vdots \\ C_j A_j^{N-1} \end{bmatrix},$$

for $j \in \mathcal{M}$. Then, for each of the subsystems (7a)

$$y_j = \Gamma_j u_j + \Phi_j x_{j,0}, \quad j \in \mathcal{M}. \quad (8)$$

By introducing $\tilde{\Gamma}_j$ and $\tilde{\Phi}_j$ accordingly, it follows that $y_T = \sum_{j \in \mathcal{M}} \tilde{\Gamma}_j u_j + \tilde{\Phi}_j x_{j,0}$.

The notation is simplified further with

$$u_j = [u_{j,0}^T \quad u_{j,1}^T \quad \cdots \quad u_{j,N-1}^T]^T, \quad j \in \mathcal{M},$$

$$\bar{u}_j = [\bar{u}_{j,0}^T \quad \bar{u}_{j,1}^T \quad \cdots \quad \bar{u}_{j,N-1}^T]^T, \quad j \in \mathcal{M},$$

and similarly we define Δu_j , $\Delta \bar{u}_j$, y_j , \bar{y}_j , y_T , \bar{y}_T , $\bar{\rho}$, ρ , $\bar{\eta}_j$, η_j , q , p_j , r_j , w_j and γ_j . Using these definitions, the OCP (3) may be written in the form

$$\min_{u, \rho, \gamma, \eta} \psi = q^T \rho + \sum_{j \in \mathcal{M}} p_j^T u_j + r_j^T \gamma_j + w_j^T \eta_j \quad (9a)$$

subject to a set of decoupled constraints

$$u_j \leq u_j \leq \bar{u}_j, \quad j \in \mathcal{M}, \quad (9b)$$

$$\Delta u_j - l_0 u_{j,-1} \leq \Lambda u_j \leq \Delta \bar{u}_j - l_0 u_{j,-1}, \quad j \in \mathcal{M}, \quad (9c)$$

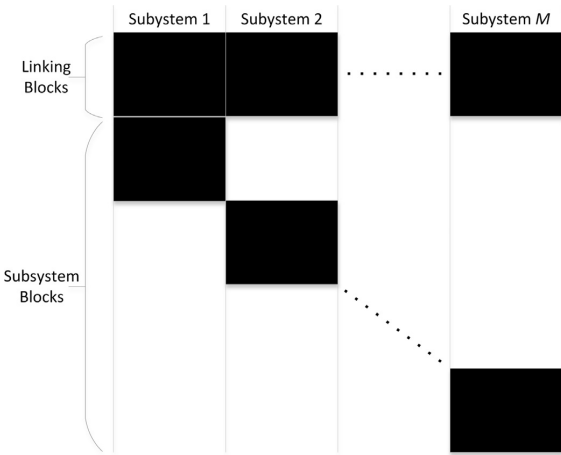


Fig. 2. The block-angular structure of the constraint matrix in (9). The efficiency of the Dantzig–Wolfe decomposition method depends on this structure.

$$y_j - \gamma_j \leq \Gamma_j u_j + \Phi_j x_{j,0} \leq \bar{y}_j + \gamma_j, \quad j \in \mathcal{M}, \tag{9d}$$

$$I_0 u_{j,-1} - \eta_j \leq \Lambda u_j \leq I_0 u_{j,-1} + \eta_j, \quad j \in \mathcal{M}, \tag{9e}$$

$$0 \leq \eta_j \leq \bar{\eta}, \quad j \in \mathcal{M}, \tag{9f}$$

$$0 \leq \gamma_j \leq \bar{\gamma}, \quad j \in \mathcal{M}, \tag{9g}$$

and a set of linking constraints

$$y_T - \rho \leq \sum_{j \in \mathcal{M}} \tilde{\Gamma}_j u_j + \tilde{\Phi}_j x_{j,0} \leq \bar{y}_T + \rho. \tag{9h}$$

$$0 \leq \rho \leq \bar{\rho}, \tag{9i}$$

where Λ and I_0 are defined as

$$\Lambda_j = \begin{bmatrix} I & & & & \\ -I & I & & & \\ & & \ddots & & \\ & & & \ddots & \\ & & & & -I & I \end{bmatrix}, \quad I_0 = \begin{bmatrix} I \\ 0 \\ \vdots \\ 0 \end{bmatrix}.$$

We remark that (9e) and (9f) imply that $\eta_{j,k} \geq |\Delta u_{j,k}|$. Note also, that the structure of the constraint matrix in (9), can be stated in the block-angular form illustrated in Fig. 2.

In particular, (9) is written as

$$\min_z \psi = \sum_{j \in \bar{\mathcal{M}}} c_j^T z_j, \tag{10a}$$

$$\text{s.t. } G_j z_j \geq g_j, \quad j \in \bar{\mathcal{M}}, \tag{10b}$$

$$\sum_{j \in \bar{\mathcal{M}}} H_j z_j \geq h, \tag{10c}$$

with $\bar{\mathcal{M}} = 1, 2, \dots, M + 1$, and

$$z_j = [u_j^T \quad \gamma_j^T \quad \eta_j^T]^T, \quad c_j = [p_j^T \quad r_j^T \quad w_j^T]^T, \quad j \in \mathcal{M},$$

$$z_{M+1} = \rho^T, \quad c_{M+1} = q^T.$$

(10b) represents the decoupled constraints (9b)–(9g), and (10c) represents the linking constraints (9h) and (9i).

The data structures in (10) are defined as

$$G_j = \begin{bmatrix} \bar{G}_j \\ -\bar{G}_j \end{bmatrix}, \quad g_j = \begin{bmatrix} \underline{g}_j \\ -\bar{g}_j \end{bmatrix}, \quad H_j = \begin{bmatrix} \bar{H}_j \\ -\bar{H}_j \end{bmatrix}, \quad h = \begin{bmatrix} \underline{h} \\ -\bar{h} \end{bmatrix},$$

in which

$$[\bar{G}_j \quad \underline{g}_j \quad \bar{g}_j] = \begin{bmatrix} I & 0 & 0 & u_j & \bar{u}_j \\ \Lambda & 0 & 0 & \Delta u_j & \Delta \bar{u}_j \\ \Gamma_j & I & 0 & y_j & \infty \\ \tilde{\Gamma}_j & -I & 0 & -\infty & \tilde{y}_j \\ 0 & I & 0 & 0 & \bar{y}_j \\ -\Lambda & 0 & I & -I_0 u_{j,-1} & \infty \\ \Lambda & 0 & I & I_0 u_{j,-1} & \infty \\ 0 & 0 & I & 0 & \bar{\eta}_j \end{bmatrix},$$

$$[\bar{H}_j \quad \underline{h} \quad \bar{h}] = \begin{bmatrix} \tilde{\Gamma}_j & 0 & y_T & \infty \\ \tilde{\Gamma}_j & 0 & -\infty & \tilde{y}_T \end{bmatrix},$$

for $j \in \mathcal{M}$, with

$$y_T = \underline{y}_T - \sum_{j \in \mathcal{M}} \tilde{\Phi}_j x_{j,0}, \quad \tilde{y}_T = \bar{y}_T - \sum_{j \in \mathcal{M}} \tilde{\Phi}_j x_{j,0},$$

$$y_j = \underline{y}_j - \Phi_j x_{j,0}, \quad \tilde{y}_j = \bar{y}_j - \Phi_j x_{j,0}, \quad j \in \mathcal{M},$$

$$\Delta u_j = \Delta u_j + I_0 u_{j,-1}, \quad \Delta \bar{u}_j = \Delta \bar{u}_j + I_0 u_{j,-1}, \quad j \in \mathcal{M},$$

In the special case $j = M + 1$

$$[\bar{G}_{M+1} \quad \underline{g}_{M+1} \quad \bar{g}_{M+1}] = [I \quad 0 \quad \bar{\rho}],$$

$$\bar{H}_{M+1} = [I \quad -I]^T.$$

Remark 5. We only use (10) to have a convenient notation. In the actual solution of all the linear and quadratic programs reported in this paper, the bound constraints are exploited.

3. Dantzig–Wolfe decomposition

Dantzig–Wolfe decomposition utilizes the fact that a convex set can be characterized by its extreme points and its extreme rays [15–17]. In particular, for each $j \in \bar{\mathcal{M}}$, the set of points satisfying the decoupled constraints (10b) may be written as

$$\mathcal{G}_j = \{z_j | G_j z_j \geq g_j\} = \left\{ z_j | z_j = \sum_{i \in \mathcal{P}} \lambda_j^i z_j^i, \sum_{i \in \mathcal{P}} \lambda_j^i = 1, \lambda_j^i \geq 0 \quad \forall i \in \mathcal{P} \right\}, \tag{11}$$

where z_j^i are the extreme points of \mathcal{G}_j , and λ_j^i are convex combination multipliers. Note that since each of the sets \mathcal{G}_j are bounded, extreme rays are not needed in their representation. \mathcal{P} is a set defined such that all extreme points of the set defined by (10b) can be represented as $z^i = [z_j^i]_{j \in \bar{\mathcal{M}}} = [z_1^i; z_2^i; \dots; z_{|\bar{\mathcal{M}}|}^i]$ for $i \in \mathcal{P}$. Note that with this definition, the same extreme point, z_j^i , may appear several times in (11). This mathematical representation, with the possibility that the same subproblem extreme point, z_j^i , is represented several times, facilitates a computationally efficient implementation of the Dantzig–Wolfe decomposition algorithm.

By replacing the decision variables in (10) by convex combination multipliers, we obtain the master problem formulation

$$\min_{\lambda} \psi = \sum_{j \in \overline{\mathcal{M}}} \sum_{i \in \mathcal{P}} c_j^i \lambda_j^i, \tag{12a}$$

$$\text{s.t.} \sum_{j \in \overline{\mathcal{M}}} \sum_{i \in \mathcal{P}} H_j^i \lambda_j^i \geq h, \tag{12b}$$

$$\sum_{i \in \mathcal{P}} \lambda_j^i = 1, \quad j \in \overline{\mathcal{M}}, \tag{12c}$$

$$\lambda_j^i \geq 0, \quad j \in \overline{\mathcal{M}}, i \in \mathcal{P}, \tag{12d}$$

where we have defined

$$H_j^i = H_j z_j^i, \quad j \in \overline{\mathcal{M}}, i \in \mathcal{P}, \tag{13a}$$

$$c_j^i = c_j^T z_j^i, \quad j \in \overline{\mathcal{M}}, i \in \mathcal{P}. \tag{13b}$$

Given a solution, λ^* , to the master problem (12), a solution to the original problem (10) can be obtained as

$$z_j^* = \sum_{i \in \mathcal{P}} (\lambda^*)^i z_j^i, \quad j \in \overline{\mathcal{M}}.$$

The number of extreme points, $|\mathcal{P}|$, can increase exponentially with the size of the original problem. In such cases, it is computationally inefficient to solve the master problem directly. In the following section, we overcome this issue by employing a column generation procedure that replaces \mathcal{P} by a subset $\tilde{\mathcal{P}}$.

3.1. Column generation procedure

The dual linear program of (12) may be stated as

$$\max_{\alpha, \beta} \phi = \alpha^T h + \sum_{j \in \overline{\mathcal{M}}} \beta_j, \tag{14a}$$

$$\text{s.t.} (H_j^*)^T \alpha + \beta_j \leq c_j^i, \quad j \in \overline{\mathcal{M}}, i \in \mathcal{P}, \tag{14b}$$

$$\alpha \geq 0. \tag{14c}$$

$\alpha \in \mathbb{R}^{4N}$ and $\beta \in \mathbb{R}^{M+1}$ are the Lagrange multipliers associated with the linking constraints (12b) and the convexity constraints (12c), respectively.

The necessary and sufficient optimality conditions for (12) and (14) are

$$\sum_{j \in \overline{\mathcal{M}}} \sum_{i \in \mathcal{P}} H_j^i \lambda_j^i \geq h, \tag{15a}$$

$$\sum_{i \in \mathcal{P}} \lambda_j^i = 1, \quad j \in \overline{\mathcal{M}}, \tag{15b}$$

$$\lambda_j^i \geq 0, \quad j \in \overline{\mathcal{M}}, i \in \mathcal{P}, \tag{15c}$$

$$c_j^i - (H_j^i)^T \alpha - \beta_j \geq 0, \quad j \in \overline{\mathcal{M}}, i \in \mathcal{P}, \tag{15d}$$

$$\alpha \geq 0, \tag{15e}$$

$$\lambda_j^i (c_j^i - (H_j^i)^T \alpha - \beta_j) = 0, \quad j \in \overline{\mathcal{M}}, i \in \mathcal{P}, \tag{15f}$$

Proposition 1 shows that a solution to the master problem (12) can be obtained by solving a restricted master problem in which \mathcal{P} in (12) is replaced by $\tilde{\mathcal{P}} \subseteq \mathcal{P}$. This implies that a solution to (12) can be obtained by solving a linear program that is often much smaller than (12).

Proposition 1. Let $\tilde{\mathcal{P}} \subseteq \mathcal{P}$ and define $(\tilde{\lambda}, \tilde{\alpha}, \tilde{\beta})$ as a primal-dual solution to (12) and (14) with \mathcal{P} replaced by $\tilde{\mathcal{P}}$. Define $(\lambda^*, \alpha^*, \beta^*)$ as

$$\begin{aligned} \alpha^* &= \alpha, \\ \beta_j^* &= \beta_j, \quad j \in \overline{\mathcal{M}}, \\ (\lambda^*)^i_j &= \begin{cases} \tilde{\lambda}_j^i & \text{if } i \in \tilde{\mathcal{P}} \\ 0 & \text{if } i \in \mathcal{P} \setminus \tilde{\mathcal{P}}, \end{cases} \quad j \in \overline{\mathcal{M}}, i \in \mathcal{P}. \end{aligned}$$

If the optimal objective value of the subproblem

$$\min_{\tilde{z}_j} \varphi_j = (c_j - H_j^T \alpha^*)^T \tilde{z}_j - \beta_j^* \tag{16a}$$

$$\text{s.t.} G_j \tilde{z}_j \geq g_j, \tag{16b}$$

is non-negative for each $j \in \overline{\mathcal{M}}$, i.e. $\varphi_j^* \geq 0 \forall j \in \overline{\mathcal{M}}$, then $(\lambda^*, \alpha^*, \beta^*)$ satisfies the necessary and sufficient optimality conditions (15), λ^* is a minimizer of (12), and (α^*, β^*) is a maximizer of (14).

Proof. The solution $(\lambda^*, \alpha^*, \beta^*)$ satisfies (15a) since

$$\sum_{j \in \overline{\mathcal{M}}} \sum_{i \in \mathcal{P}} H_j^i (\lambda^*)^i_j = \sum_{j \in \overline{\mathcal{M}}} \sum_{i \in \tilde{\mathcal{P}}} H_j^i \tilde{\lambda}_j^i \geq h,$$

which follows from the definition of $(\tilde{\lambda}, \tilde{\alpha}, \tilde{\beta})$. Similarly, it can be verified that the conditions (15b), (15c), (15e) and (15f) are fulfilled.

Provided that $(\lambda^*, \alpha^*, \beta^*)$ is optimal, (15d) yields

$$c_j^i - (H_j^i)^T \alpha^* - \beta_j^* = (c_j - H_j^T \alpha^*)^T z_j^i - \beta_j^* \geq 0, \tag{17}$$

for all $j \in \overline{\mathcal{M}}$ and $i \in \mathcal{P}$. By construction of $(\lambda^*, \alpha^*, \beta^*)$, (17) is satisfied for all $i \in \tilde{\mathcal{P}}$. To check that the condition holds for all $i \in \mathcal{P} \setminus \tilde{\mathcal{P}}$, we consider the optimization problem (16). Since this linear program minimizes the left hand side of (17) over all possible extreme points, \tilde{z}_j , of G_j , $(\lambda^*, \alpha^*, \beta^*)$ also satisfies the remaining optimality condition (17) if φ_j is non-negative for all $j \in \overline{\mathcal{M}}$. \square

Algorithm 1 summarizes a column generation procedure based on Proposition 1.

Remark 6. The problem (16) is an OCP with linear constraints and a linear objective function. Refs. [10,11,38,39] provide an efficient

Algorithm 1. Column generation procedure for solution of (12).

```

Require:  $(i_{\max}, \varepsilon), \{z_j^0\}_{j \in \overline{\mathcal{M}}}$ 
 $i = 0, \text{ converged} = \text{false}$ 
while not converged and  $i < i_{\max}$  do
     $\tilde{\mathcal{P}} = \{0, 1, \dots, i\}$ 
    COMPUTE PROBLEM DATA
    for  $j \in \overline{\mathcal{M}}$  do
         $H_j^i = H_j z_j^i$ 
         $c_j^i = c_j^T z_j^i$ 
    end for
    SOLVE RESTRICTED MASTER PROBLEM
     $(\phi^*, \lambda^*, \alpha^*, \beta^*) \leftarrow \text{solve (12) with } \mathcal{P} = \tilde{\mathcal{P}}$ 
    SOLVE SUBPROBLEMS
    for  $j \in \overline{\mathcal{M}}$  do
         $(\varphi_j^*, \tilde{z}_j^*) \leftarrow \text{solve (16)}$ 
    end for
    CHECK IF CONVERGED
    if  $|\varphi_j| \geq \varepsilon \quad \forall j \in \overline{\mathcal{M}}$  then
         $\text{converged} = \text{true}$ 
    else
        UPDATE EXTREME POINTS
        for  $j \in \overline{\mathcal{M}}$  do
             $z_j^{i+1} = \tilde{z}_j^*$ 
        end for
    end if
     $i = i + 1$ 
end while
    
```

Riccati-based homogeneous and self-dual interior-point linear programming algorithm for such problems. Using the optimal interior point solution found by this algorithm, crossover methods can be applied to obtain an optimal extreme point for the column generation procedure [17].

3.2. Warm-start

A sequence of closely related OCPs are solved in a moving horizon implementation of EMPC. Therefore, in Algorithm 1 the feasible initial guess of the solution, $\{z_j^0\}_{j \in \overline{\mathcal{M}}}$, at the current sampling instant is constructed from the solution at the previous sampling instant. Given the solution to (16)

$$\begin{aligned} u_j^* &= [u_{j,0}^{*T} \cdots u_{j,N-1}^{*T}]^T, \quad j \in \mathcal{M}, \\ \gamma_j^* &= [\gamma_{j,1}^{*T} \cdots \gamma_{j,N}^{*T}]^T, \quad j \in \mathcal{M}, \\ \eta_j^* &= [\eta_{j,0}^{*T} \cdots \eta_{j,N-1}^{*T}]^T, \quad j \in \mathcal{M}, \\ \rho^* &= [\rho_1^{*T} \cdots \rho_N^{*T}]^T, \end{aligned}$$

we construct an initial point for the following sampling instant as

$$z_j^0 = [(u_j^0)^T \ (\gamma_j^0)^T \ (\eta_j^0)^T]^T, \quad j \in \mathcal{M},$$

where

$$\begin{aligned} u_j^0 &= [u_{j,1}^{*T} \cdots u_{j,N-1}^{*T} \ (u_{j,N}^0)^T]^T, \quad j \in \mathcal{M}, \\ \gamma_j^0 &= [\gamma_{j,2}^{*T} \cdots \gamma_{j,N}^{*T} \ (\gamma_j^0)^T]^T, \quad j \in \mathcal{M}, \\ \eta_j^0 &= [\eta_{j,1}^{*T} \cdots \eta_{j,N-1}^{*T} \ (\eta_j^0)^T]^T, \quad j \in \mathcal{M}. \end{aligned}$$

Finally

$$z_{M+1}^0 = \rho^0 = [\rho_2^{*T} \cdots \rho_N^{*T} \ (\rho^0)^T]^T.$$

The original solution values are thus shifted forward in time, and $u_{j,N}^0, \gamma_{j,N+1}^0, \eta_{j,N}^0$ and ρ_{N+1}^0 are appended to the resulting initial point.

In our implementation, we use

$$\begin{aligned} u_{j,N}^0 &= u_{j,N-1}^*, \quad j \in \mathcal{M}, \\ \eta_{j,N}^0 &= 0, \quad j \in \mathcal{M}. \end{aligned}$$

We use the state space equations (1) and (2) to compute $y_{j,N+1}^0$ and $y_{T,N+1}^0$ associated with the input sequence $\{u_j^0\}_{j \in \overline{\mathcal{M}}}$. We construct the initial slack values as

$$\gamma_{j,N+1}^0 = \max(y_{j,N+1} - y_{j,N+1}^0, 0) + \max(y_{j,N+1}^0 - \bar{y}_{j,N+1}, 0),$$

for each $j \in \mathcal{M}$, and

$$\rho_{N+1}^0 = \max(y_{T,N+1} - y_{T,N+1}^0, 0) + \max(y_{T,N+1}^0 - \bar{y}_{T,N+1}, 0).$$

As the solution to the OCP often only differs slightly between successive sampling instants, the initial point generated as above provides a warm-start for Algorithm 1.

3.3. Cold-start

In the case that no previous solution is available for generating a warm start, a feasible initial guess of the solution, $\{z_j^0\}_{j \in \overline{\mathcal{M}}}$, in Algorithm 1 can be constructed by adjusting the slack variables, γ_j^0 and ρ^0 . Let $\{u_j^0\}_{j \in \overline{\mathcal{M}}}$ be feasible with respect to the input constraints and the input-rate constraints. Such a point is easily obtained in

practice. As an example consider $u_j^0 = \underline{u}_j$ for each $j \in \mathcal{M}$. Then, in a similar way as for the warm-start strategy, we compute

$$\gamma_{j,k}^0 = \max(y_{j,k} - y_{j,k}^0, 0) + \max(y_{j,k}^0 - \bar{y}_{j,k}, 0),$$

$$\rho_k^0 = \max(y_{T,k} - y_{T,k}^0, 0) + \max(y_{T,k}^0 - \bar{y}_{T,k}, 0),$$

where $k \in \mathcal{N}_1, j \in \mathcal{M}$. The values, $y_{j,k}^0$ and $y_{T,k}^0$ are the subsystem outputs and the aggregated variables associated with the inputs, $\{u_j^0\}_{j \in \overline{\mathcal{M}}}$, computed via (1) and (2). Finally, $\eta_j^0 = \Delta u_j^0$ for each $j \in \mathcal{M}$.

4. The alternating direction method of multipliers

ADMM has been demonstrated as a powerful algorithm for solving large-scale structured convex optimization problems [29]. The problems successfully solved by ADMM includes a range of OCPs arising in MPC applications [30–32]. In this section, we present a distributed ADMM scheme for solving the OCP (10) that exploits the block-angular structure of (10). We refer to [29] for details and proofs related to ADMM.

To solve (10) via ADMM, we first introduce the auxiliary variables $v_j \in \mathbb{R}^{4N y_T}$ for $j=1, 2, \dots, M$ and $v_{M+1} \in \mathbb{R}^{4N}$, and write the OCP as

$$\begin{aligned} \min_{z,v} \quad & \psi = \sum_{j \in \overline{\mathcal{M}}} c_j^T z_j, \\ \text{s.t.} \quad & G_j z_j \geq g_j, \quad j \in \overline{\mathcal{M}}, \\ & H_j z_j = v_j, \quad j \in \overline{\mathcal{M}}, \\ & \sum_{j \in \overline{\mathcal{M}}} v_j \geq h, \end{aligned}$$

Using indicator functions, this problem can be stated in the standard ADMM form

$$\min_{z,v} \psi = \sum_{j \in \overline{\mathcal{M}}} (c_j^T z_j + I_{Z_j}(z_j)) + I_V(v), \tag{18a}$$

$$\text{s.t. } H_j z_j = v_j, \quad j \in \overline{\mathcal{M}} \tag{18b}$$

where $Z_j = \{z_j | G_j z_j \geq g_j\}$, $V = \{v | \sum_{j \in \overline{\mathcal{M}}} v_j \geq h\}$, and I_A is the indicator function of a set A defined as

$$I_A(x) = \begin{cases} 0 & \text{if } x \in A, \\ \infty & \text{otherwise.} \end{cases}$$

For the problem (18), the ADMM recursions described in [29] becomes

$$z_j^{i+1} = \underset{z_j \in Z_j}{\operatorname{argmin}} c_j^T z_j + \frac{\rho}{2} \|H_j z_j - v_j^i + u_j^i\|_2^2, \quad j \in \overline{\mathcal{M}}, \tag{19a}$$

$$v^{i+1} = \underset{v \in V}{\operatorname{argmin}} \frac{\rho}{2} \sum_{j \in \overline{\mathcal{M}}} \|H_j z_j^{i+1} - v_j + u_j^i\|_2^2, \tag{19b}$$

$$u_j^{i+1} = u_j^i + H_j z_j^{i+1} - v_j^{i+1}, \quad j \in \overline{\mathcal{M}}, \tag{19c}$$

where u^i is a scaled dual variable.

The update of z_j , (19a), thus consists of solving the constrained quadratic program

$$\min_{z_j} \frac{\rho}{2} z_j^T H_j^T H_j z_j + (c_j + \rho(-v_j^i + u_j^i)^T H_j) z_j, \tag{20a}$$

$$\text{s.t. } G_j z_j \geq g_j \tag{20b}$$

for each $j \in \overline{\mathcal{M}}$.

The update for v , (19b), yields the explicit solution

$$v_j^{i+1} = H_j z_j^{i+1} + u_j^i + \max(l/(M+1), 0), \quad j \in \overline{\mathcal{M}},$$

Algorithm 2. ADMM algorithm for the solution of (10)

Require: $(\rho, \alpha, i_{\max}, \epsilon_p, \epsilon_D), (v^0, u^0), (\epsilon_p, \epsilon_D)$
 $i=0, \text{converged} = \text{false}$
while $\text{converged} = \text{false}$ **and** $i < i_{\max}$ **do**
 UPDATE VARIABLES
 for $j \in \mathcal{M}$ **do**
 $z_j^{i+1} = \underset{z_j}{\text{argmin}} c_j^T z_j + \frac{\rho}{2} \|H_j z_j - v_j^i + u_j^i\|_2^2$
 end for
 $l = h - \sum_{j \in \mathcal{M}} \alpha H_j z_j^{i+1} - (1 - \alpha)(-v_j^i) + u_j^i$
 for $j \in \mathcal{M}$ **do**
 $v_j^{i+1} = \alpha H_j z_j^{i+1} - (1 - \alpha)(-v_j^i) + u_j^i + \max(l/(M+1), 0)$
 $u_j^{i+1} = u_j^i + \alpha H_j z_j^{i+1} - (1 - \alpha)(-v_j^i) - v_j^{i+1}$
 end for
 COMPUTE RESIDUALS
 for $j \in \mathcal{M}$ **do**
 $r_j^{i+1} = \rho H_j z_j^{i+1} - v_j^{i+1}$
 $s_j^{i+1} = -\rho H_j^T (v_j^{i+1} - v_j^i)$
 end for
 CHECK IF CONVERGED
 if $\|r^{i+1}\|_2 \leq \epsilon_p$ **and** $\|s^{i+1}\|_2 \leq \epsilon_D$ **then**
 $\text{converged} = \text{true}$
 end if
 $i \leftarrow i + 1$
end while

where $l = h - \sum_{j \in \mathcal{M}} \alpha H_j z_j^{i+1} + u_j^i$. Each subsystem can thus perform its own update of z_j . Having computed l with a contribution from all the subsystems, v_j and u_j can be determined individually as well.

Algorithm 2 provides an overview of the ADMM steps described above. Under mild assumptions, the ADMM algorithm converges with a linear convergence rate to the optimal solution of the OCP [29,40]. Note that we have replaced $H_j z_j^{i+1}$ with $\alpha H_j z_j^{i+1} - (1 - \alpha)(-v_j^i)$ in the recursions for v_j and u_j . As described in [29,41] such a relaxation often speeds up convergence. The relaxation parameter $\alpha \in [0, 2]$ is tuned to the particular application.

To detect an optimal solution in Algorithm 2, we have adopted the stopping criteria proposed in [29]. For the specific problem formulation (18), these criteria can be written as

$$\|r^i\|_2 \leq \epsilon_p, \quad \|s^i\|_2 \leq \epsilon_d,$$

in which

$$s_j^{i+1} = -\rho H_j^T (v_j^{i+1} - v_j^i), \quad r_j^{i+1} = \rho H_j z_j^{i+1} - v_j^{i+1},$$

measure the primal and dual residual. These stopping criteria may be extended to include a relative measure as well [29].

As for the Dantzig–Wolfe decomposition algorithm, a warm start for Algorithm 2 can be constructed by shifting the closed-loop solution values, v^* and u^* , forward in time. If such a solution is not available, the standard cold-starting point $(v^0, u^0) = (\mathbf{0}, \mathbf{0})$ is used. We remark that in comparison to the Dantzig–Wolfe decomposition algorithm, the initial point does not need to be feasible. Moreover, the extensions of Algorithm 2 are not restricted only to linear programming [30–32]. One could consider more general regularization terms in (4), e.g. ℓ_2 -regularization terms.

Remark 7. The optimization problem (20) is an OCP with a quadratic cost function and linear constraints. Efficient algorithms for such structured QPs include active-set methods [42–44], interior-point methods [10,45–50] and first-order methods [49,51].

5. Smart energy systems case study

To handle the volatile and unpredictable power generation associated with technologies such as wind, solar and wave power, energy systems management has emerged as a promising application area for EMPC. In EMPC of energy systems, the power

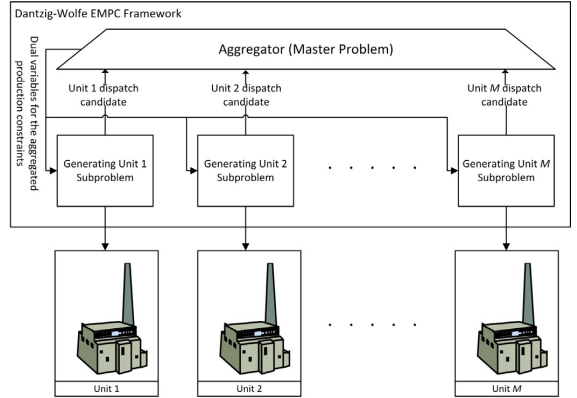


Fig. 3. EMPC diagram for the Dantzig–Wolfe decomposition algorithm for a dynamic multi-plant system with linking constraints.

production planning is handled in real-time by computing an optimal production plan based on the most recent information available such as forecasts of energy prices, wind power production, and district heating consumption [52–57].

In this section we use a conceptual energy systems management case study to test a MATLAB implementation of Algorithm 1, DW_{empc} , and a MATLAB implementation of Algorithm 2, $ADMM_{empc}$. The energy system considered, consists of a collection of power generating units in the form

$$Y_j(s) = \frac{1}{(\tau_j s + 1)^3} (U_j(s) + D_j(s)) + E_j(s), \quad j \in \mathcal{M}, \quad (21)$$

where $D_j(s)$ is the process noise, $E_j(s)$ is the measurement noise, $U_j(s)$ is the input (power production setpoint) to the j th power unit and $Y_j(s)$ is its power production. The third order model, (21), has been validated against actual measurement data in [58]. This system is a dynamic multi-plant system. Fig. 3 illustrates the Dantzig–Wolfe decomposition algorithm for a dynamic multi-plant system.

To represent different types of power generating units, we vary the time constants, τ_j ; values in the range 40–80 are associated with slow units such as centralized thermal power plants, while values in the range 20–40 represent units with faster dynamics such as diesel generators and gas turbines.

In the case study, the controller must compute the most cost-efficient feasible power setpoint for each power generating unit such that the total power production satisfies the time varying power demand.

The total power produced by the M generating units is

$$Y_T(s) = \sum_{j=1}^M \frac{1}{(\tau_j s + 1)^3} (U_j(s) + D_j(s)). \quad (22)$$

Using a discrete state space representation, (21) and (22) may be expressed as

$$x_{j,k+1} = A_j x_{j,k} + B_j u_{j,k} + E_j d_{j,k}, \quad j \in \mathcal{M}, \quad (23a)$$

$$y_{j,k} = C_j x_{j,k} + e_{j,k}, \quad j \in \mathcal{M}, \quad (23b)$$

$$y_{T,k} = \sum_{j \in \mathcal{M}} C_j x_{j,k}, \quad (23c)$$

In the resulting model structure, $u_{j,k} \in \mathbb{R}$ is the unit input (power setpoint), $y_{j,k} \in \mathbb{R}$ is the unit power production, and $y_{T,k} \in \mathbb{R}$ is the total power production. We assume that $x_{j,0} \sim N(\bar{x}_{j,0}, P_{j,0})$,

$\mathbf{d}_{j,k} \sim N(0, R_{j,d})$, and that $\mathbf{e}_{j,k} \sim N(0, R_{j,e})$. By employing the Kalman filter, the separation principle, and the certainty equivalence principle, the OCP in EMPC for (23) can be stated in the form (3) with $\gamma_j = 1$ for all $j \in \mathcal{M}$, see e.g. [38].

5.1. Suboptimality measure

The Dantzig–Wolfe decomposition algorithm and the ADMM algorithm satisfy the subsystem constraints (10b) in every iteration. Therefore, a set of feasible but not necessarily optimal inputs, $\{\hat{u}_j\}_{j=1}^M$, is available for the power generating units at each iteration of the algorithms. Consequently, the algorithms may be terminated early and still provide a feasible suboptimal solution. Using (9), we can compute the cost associated with the suboptimal inputs as

$$\hat{\psi} = \mathbf{q}^T \hat{\rho} + \sum_{j \in \mathcal{M}} p_j^T \hat{u}_j + \mathbf{r}_j^T \hat{\gamma}_j + \mathbf{w}_j^T \hat{\eta}_j,$$

where $\hat{\rho}$, $\hat{\gamma}_j$ and $\hat{\eta}_j$ are completely determined by \hat{u}_j . Based on $\hat{\psi}$ and the optimal value ψ^* , we define the level of suboptimality as

$$\omega = 100 \frac{\hat{\psi} - \psi^*}{\max(|\psi^*|, 1)}. \quad (24)$$

This definition of suboptimality provides a quality measure of the current available inputs.

Remark 8. In Dantzig–Wolfe decomposition, the solution to the restricted master problem, (12) with \mathcal{P} replaced by $\hat{\mathcal{P}} \subset \mathcal{P}$, provides an upper bound on the optimal objective value. Moreover, a lower bound can be determined without much extra work via the Lagrangian relaxation techniques described in [59]. Therefore, a bound on (24) can be computed in each iteration of Algorithm 1.

5.2. Simulation parameters

In the simulations presented below, the control and prediction horizon is $N=60$ time steps, and a sampling time of $T_s=5$ s is used. Each generating unit is represented by a system in the form (21) with a time constant, τ_j , sampled from the uniform distribution over the interval [20, 80]. For simplicity, it is assumed that $\mathbf{d}_{j,k} \sim N(0, (10\sigma)^2 I)$, $\mathbf{e}_{j,k} \sim N(0, \sigma^2 I)$, and that full initial state information is given such that $x_{j,0} \sim (0, 0)$.

The power generating unit input price is $p_{j,k} = 1/\tau_j$. This implies that fast units are more expensive to use than slow units. The conflict between response time and operating costs represents a common situation in the power industry: Large thermal power plants often produce a majority of the electricity, while the use of units with faster dynamics such as diesel generators and gas turbines are limited to critical peak periods.

We define the input limits and the input rate limits as

$$(\underline{u}_{j,k}, \bar{u}_{j,k}, \Delta \underline{u}_{j,k}, \Delta \bar{u}_{j,k}) = (0, 8/M, -M/4, M/4).$$

In this way, the possible contribution from each unit to the overall power production diminishes as the number of units is increased. Local output constraints in the form (3i) and (3j) are not present. The local output variables, $y_{j,k}$, and the local slack variables, $\gamma_{j,k}$, are thus excluded from the optimization problem.

The penalty for not satisfying the electricity demand (3k) is fixed to $\rho_k = 10$. For ADMM_{mpc}, we use the algorithm parameters $\rho = 1$ and $\alpha = 1.8$. These parameters have been carefully tuned to this particular application. The tolerance parameter for DW_{mpc} is set to $\varepsilon = 1e-4$. ADMM_{mpc} uses the following primal and dual tolerance specification: $\epsilon_p = \epsilon_D = 1e-2$. Both DW_{mpc} and ADMM_{mpc} use CPLEX for solving the subproblems. Although the subproblems are solved sequentially, we refer to their effective CPU time in this paper, assuming that the subproblems are solved in parallel. The

Table 1
Case study simulation and controller parameters.

	τ_i	p_k	\underline{u}_k	\bar{u}_k	$\Delta \underline{u}_k$	$\Delta \bar{u}_k$
Generating Unit 1	65	1/65	0	4	-1	1
Generating Unit 2	75	1/75	0	4	-1	1

reason for this is to report the full potential of the distributed optimization algorithms.

5.3. Closed-loop simulations

We first consider an example with $M=2$ power generating units. Table 1 lists the system and controller parameters.

Fig. 4 illustrates closed-loop simulations for different values of the noise parameter, σ , and the regularization weights, $w = w_{j,k}$. As indicated in Fig. 4(b), the closed-loop input variance increases significantly if no penalty is imposed on the input rate. This happens even for small values of the noise parameter. By assigning a penalty to the input-rate, the solution becomes more well-behaved and better suited for practical applications. Table 2 shows that the addition of regularization also reduces the computing time for DW_{mpc} as well as for ADMM_{mpc}. E.g. for scenario s_6 , corresponding to $\sigma = 0.01$ and $w = 0.1$, the average number of iterations performed by DW_{mpc} is reduced by more than 40% compared to the case without regularization, i.e. the case with $w = 0$. Also observe that while warm-start only leads to a marginal improvement in the iteration count for DW_{mpc}, a substantial reduction in the number of iterations is achieved for ADMM_{mpc}.

Fig. 5 shows the level of suboptimality, ω , computed via (24), for scenario s_5 when the run time of DW_{mpc} and ADMM_{mpc} is limited to 0.01 s.

We observe that DW_{mpc} is up to approximately 30% suboptimal when cold-started, and not more than 5% suboptimal when warm-started. Hence, although the number of iterations only decreases slightly when DW_{mpc} is warm-started, the quality of the solution obtained after terminating early improves significantly. By the same token, warm-start reduces the level of suboptimality for ADMM_{mpc} by several orders of magnitude.

Provided that the number of iterations is small, the effort per iteration is approximately equal for DW_{mpc} and ADMM_{mpc}. Table 2 reports that ADMM_{mpc} requires many more iterations than DW_{mpc}. Accordingly, we expect DW_{mpc} to provide a more accurate solution than ADMM_{mpc} within the same time frame. This is confirmed by Fig. 5. Note however, that the computing time per iteration is constant for ADMM_{mpc}, while each iteration of DW_{mpc} requires an increasing work-load since extreme points are added to the restricted master problem on the fly. Nonetheless, in all our simulations DW_{mpc} outperforms ADMM_{mpc} by a significant margin.

Fig. 6 depicts the level of suboptimality as a function of the CPU time for DW_{mpc} and ADMM_{mpc}. A single instance of the OCP with 128 generating units is solved.

Table 2
Iteration information table for the closed-loop simulation scenarios depicted in Fig. 4. The minimum, maximum and average number of iterations is listed for both cold start and for warm start (in parentheses).

	σ	w	DW _{mpc}	ADMM _{mpc}
s_1	0	0	[6(2), 16(17), 12(11)]	[47(2), 485(410), 097(66)]
s_2	0	0.01	[6(2), 15(18), 10(09)]	[35(3), 469(410), 088(56)]
s_3	0	0.1	[5(2), 15(17), 07(07)]	[33(6), 359(280), 149(48)]
s_4	0.01	0	[7(2), 18(19), 13(11)]	[47(2), 485(410), 094(65)]
s_5	0.01	0.01	[6(2), 17(17), 10(09)]	[35(2), 469(410), 088(58)]
s_6	0.01	0.1	[5(2), 13(16), 07(06)]	[32(6), 380(290), 145(50)]
s_7	0.1	0	[7(2), 17(20), 12(11)]	[46(2), 485(410), 091(66)]
s_8	0.1	0.01	[6(2), 17(16), 09(09)]	[35(2), 469(410), 084(60)]
s_9	0.1	0.1	[5(2), 14(14), 07(06)]	[32(6), 359(279), 144(47)]

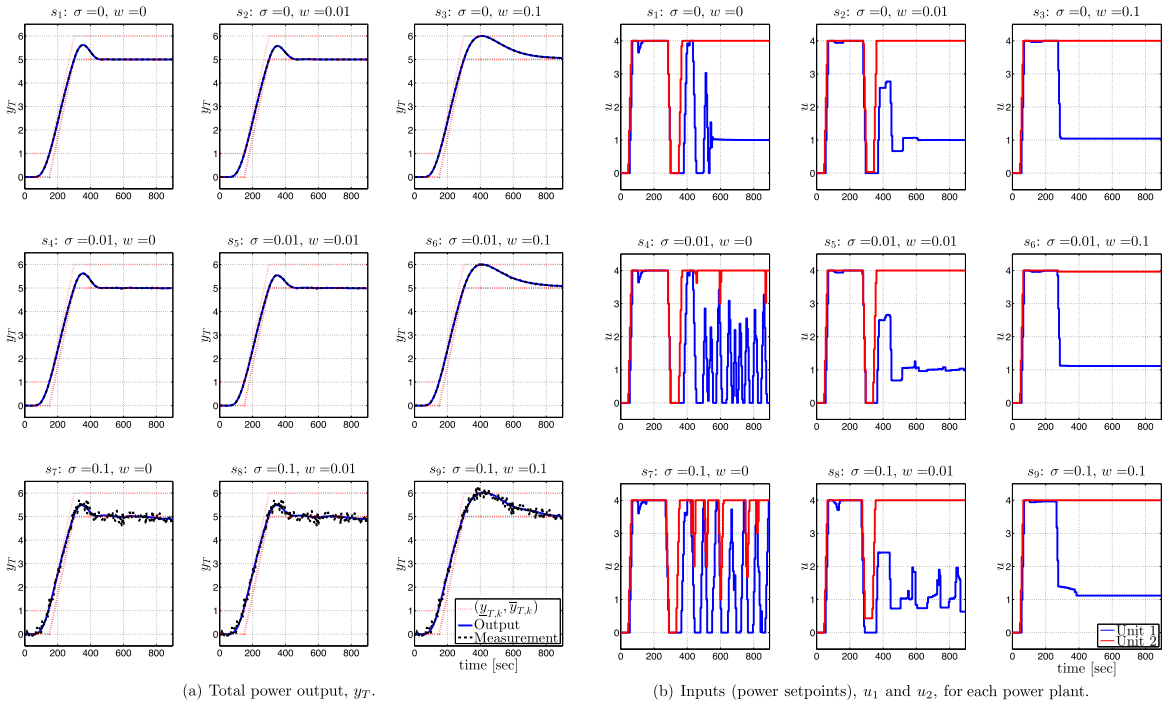


Fig. 4. Closed-loop simulations of the system (23) controlled by EMPC. The OCP (3) representing the EMPC is solved to a specified tolerance using CPLEX. The figures illustrate the total output and the inputs for different values of the noise parameter, σ , and the regularization weights, w . The effect of the regularization is most clearly observed in the inputs. At the expense of slightly less tight control on the total power output, the inputs become less volatile when the regularization weight is increased.

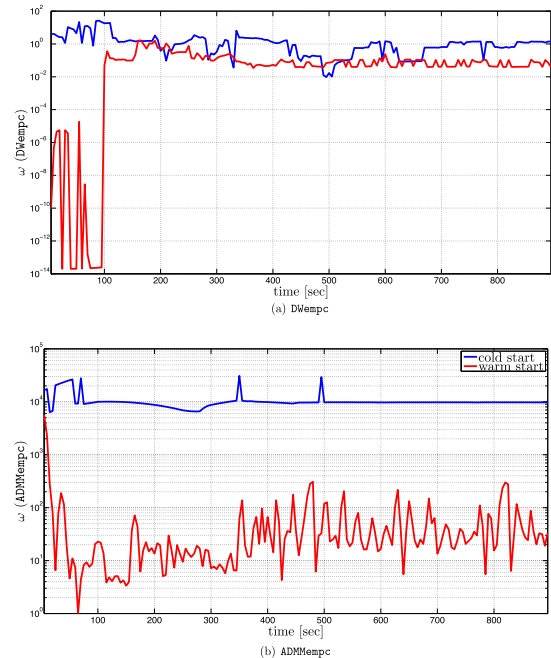


Fig. 5. Suboptimality level of the closed-loop solution obtained by $DWempc$ and $ADMempc$ when terminated after 0.01 s.

Initially, $ADMempc$ finds the best solution. The quality of this solution is however far from optimal, making it economically very inefficient. For $DWempc$, fast convergence is observed after 0.2 s, and at 0.3 s a solution which is less than 1% suboptimal is found. Moreover, while $DWempc$ keeps improving until a highly accurate solution is found, $ADMempc$ suffers from a much slower convergence rate. Only after 10 s is a solution with a suboptimality level of 1% found by this algorithm.

5.4. Large-scale simulations

We compare the performance of the algorithms presented in this paper to the performance of $Gurobi$, $Cplex$ and $Mosek$. These state-of-the-art linear programming solvers are invoked via a

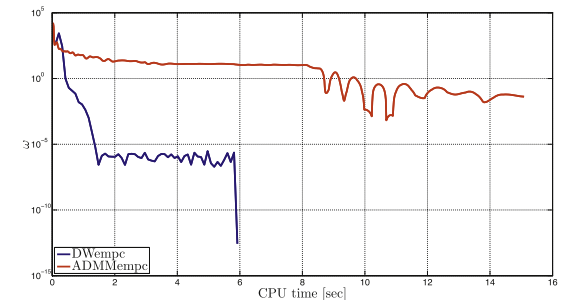


Fig. 6. Level of suboptimality as a function of the CPU time, for a single instance of the OCP with 128 generating units.

Table 3
Tolerance specifications for DWempc and ADMMempc.

Accuracy	ϵ	ϵ_p	ϵ_D
High (h)	1e-6	1e-4	1e-4
Medium (m)	1e-5	1e-3	1e-3
Low (l)	1e-4	1e-2	1e-2

MEX interface in MATLAB. We use their default tolerance settings. The algorithms are run on an Intel(R) Core(TM) i7-4770K CPU @ 3.50 GHz with 16 GB RAM running a 64-bit Windows 8.1 Pro operating system. For each solver, the computation time of solving the OCP (3) is reported as a function of the number of generating units. Table 3 lists the different accuracy settings used by DWempc and ADMMempc in our benchmarks.

Fig. 7 and Table 4 report the CPU time of solving the OCP for different number of generating units and optimization algorithms. For large problems, ADMMempc does not converge to high accuracy solutions within a reasonable amount of time. Therefore, Table 4 is incomplete.

For large problems, DWempc is faster than all other solvers tested in our case study. Observe also that Gurobi, CPLEX and MOSEK perform almost as well as DWempc in terms of CPU time. For high accuracy solutions, DWempc is 2 times faster than CPLEX and 5 times faster than Gurobi. DWempc and ADMMempc can easily accommodate very large problems in memory while Gurobi, CPLEX and MOSEK fail due to insufficient memory. The threshold when memory becomes an issue is around $M = 3000$ generating units. Consequently, when considering both CPU time and memory requirements, DWempc is

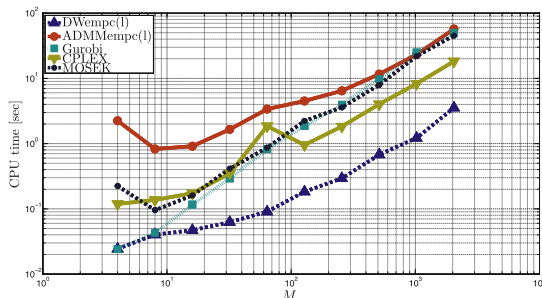


Fig. 7. CPU time for the different solvers as a function of the number of power generating units, M .

an attractive optimization algorithm for large scale dynamically decoupled energy management problems.

Note from Fig. 6 that ADMMempc needs many more iterations to converge than DWempc for the high accuracy tolerance specification, (h). Table 5 further shows that the number of iterations increases with the problem size for ADMMempc. Therefore, ADMMempc is less attractive from a scalability point of view. Apparently, the number of iterations used by DWempc does not depend on the number of generating units, M .

Table 6 lists the suboptimality level of the solution determined by DWempc and ADMMempc for different values of M . As observed from Table 6, DWempc is not only faster than ADMMempc for the tolerance specifications listed in Table 3, but the solution accuracy is also significantly better.

Table 4
CPU time for solving (3) with an increasing number of generating units, M .

solver/ M	16	32	64	128	256	512	1024	2048
Gurobi	1.16e-1	2.93e-1	8.22e-1	1.85	3.94	9.76	2.49e1	5.00e1
CPLEX	1.73e-1	3.49e-1	1.86	9.54e-1	1.83	4.02	8.28	1.83e1
MOSEK	1.60e-1	4.14e-1	8.66e-1	2.23	3.59	7.96	2.19e1	4.54e1
DWempc (l)	4.70e-2	6.25e-2	9.04e-2	1.83e-1	2.94e-1	6.78e-1	1.22	3.54
DWempc (m)	4.95e-2	7.20e-2	1.54e-1	2.61e-1	4.59e-1	1.28	2.78	5.20
DWempc (h)	6.48e-2	9.48e-2	2.03e-1	3.58e-1	6.74e-1	1.80	4.91	9.61
ADMMempc (l)	9.13e-1	1.65	3.38	4.50	6.44	1.16e1	2.32e1	5.70e1
ADMMempc (m)	1.76	3.06	4.28	1.03e1	2.45e1	7.76e1	2.58e2	-
ADMMempc (h)	8.49	7.88e1	5.59e2	-	-	-	-	-

Table 5
The number of iterations performed by DWempc and ADMMempc in solving (3) for an increasing number of generating units, M .

solver/ M	16	32	64	128	256	512	1024	2048
DWempc (l)	9	8	7	7	6	6	5	5
DWempc (m)	10	9	10	9	8	9	8	6
DWempc (h)	12	12	11	12	11	10	11	11
ADMMempc (l)	93	157	303	352	395	436	530	615
ADMMempc (m)	178	286	370	705	1,284	2,520	4,994	-
ADMMempc (h)	865	7,468	50,000	-	-	-	-	-

Table 6
Suboptimality level of DWempc and ADMMempc in the solution of (3) for an increasing number of generating units, M .

solver/ M	16	32	64	128	256	512	1024	2048
DWempc (l)	2.08e-2	1.67e-2	1.53e-1	1.86e-1	9.65e-1	9.44e-1	3.18	3.13
DWempc (m)	1.66e-5	3.87e-3	7.40e-3	1.94e-2	4.74e-2	5.29e-2	1.63e-1	9.37e-1
DWempc (h)	-2.46e-10	-1.13e-9	6.46e-6	1.98e-4	7.55e-4	1.06e-3	2.32e-3	4.82e-2
ADMMempc (l)	4.58e-1	6.65e-1	7.92e1	2.09e2	2.84e2	5.50e2	8.13e2	1.33e3
ADMMempc (m)	8.16e-2	8.36e-2	9.97	1.38e-1	1.53e1	6.62e-1	6.96	-
ADMMempc (h)	1.87e-1	1.86e-2	3.36e-5	-	-	-	-	-

6. Conclusions

In this paper, we developed and presented a warm-started possibly early terminated Dantzig–Wolfe decomposition algorithm for ℓ_1 -regularized linear EMPC of dynamically decoupled subsystems. Simulations show that a MATLAB implementation of the proposed algorithm, denoted DW_{empc} , is faster than $CPLEX$, $Gurobi$ and $MOSEK$, as well as a special-purpose implementation of ADMM denoted $ADMM_{empc}$. Both DW_{empc} and $ADMM_{empc}$ have similar parallelization capabilities. They are able to handle much larger problems than the general purpose solvers. The simulations also demonstrate that in combination with warm-start, early termination of DW_{empc} yields a highly accurate solution after only a few iterations. In contrast to $ADMM_{empc}$, the number of iterations required by DW_{empc} to achieve a certain tolerance level does not grow with the problem size.

For cases when the number of DW_{empc} iterations is large, DW_{empc} may be slower than $ADMM_{empc}$. The reason is that the computing time per iteration of DW_{empc} grows with the iteration number. Conversely, the time spent per iteration by $ADMM_{empc}$ is constant. Although this is a potential drawback of the Dantzig–Wolfe decomposition algorithm that favors the ADMM algorithm, we have not observed this being the case in any of our simulations. In all our simulations, DW_{empc} outperforms $ADMM_{empc}$; in some cases by several orders of magnitude.

Acknowledgements

This work was funded in part by (1) the Danish Ministry of Higher Education and Science in the industrial PhD project “Stochastic MPC with Applications in Smart Energy Systems” (11-117435); (2) the Southern Denmark Growth Forum and the European Regional Development Fund in the project “Smart & Cool” (ERDFD-10-0083); and (3) The Danish Council for Strategic Research in the project “CITIES – Centre for IT-Intelligent Energy Systems in Cities” (1305-00027B).

References

- [1] D.Q. Mayne, J.B. Rawlings, C.V. Rao, P.O.M. Scokaert, Constrained model predictive control: stability and optimality, *Automatica* 36 (6) (2000) 789–814.
- [2] J.B. Rawlings, Tutorial overview of model predictive control, *IEEE Control Syst.* 20 (3) (2000) 38–52.
- [3] S.J. Qin, T.A. Badgwell, A survey of industrial model predictive control technology, *Control Eng. Pract.* 11 (7) (2003) 733–764.
- [4] J.B. Rawlings, D.Q. Mayne, *Model Predictive Control: Theory and Design*, Nob Hill Publishing, Madison, 2009.
- [5] M. Diehl, R. Amrit, J.B. Rawlings, A Lyapunov function for economic optimizing model predictive control, *IEEE Trans. Autom. Control* 56 (3) (2011) 703–707.
- [6] L. Grüne, Economic receding horizon control without terminal constraints, *Automatica* 49 (3) (2013) 725–734.
- [7] J.B. Rawlings, D. Angeli, C.N. Bates, Fundamentals of economic model predictive control, in: 2012 IEEE 51st Annual Conference on Decision and Control (CDC), 2012, pp. 3851–3861.
- [8] D. Angeli, R. Amrit, J.B. Rawlings, On average performance and stability of economic model predictive control, *IEEE Trans. Autom. Control* 57 (7) (2012) 1615–1626.
- [9] J.B. Rawlings, D. Bonne, J.B. Jørgensen, A.N. Venkat, S.B. Jørgensen, Unreachable setpoints in model predictive control, *IEEE Trans. Autom. Control* 53 (9) (2008) 2209–2215.
- [10] L.E. Sokoler, G. Frison, K. Edlund, A. Skajaa, J.B. Jørgensen, A Riccati based homogeneous and self-dual interior-point method for linear economic model predictive control, in: 2013 IEEE Multi-conference on Systems and Control, 2013, pp. 592–598.
- [11] L.E. Sokoler, A. Skajaa, G. Frison, R. Halvgaard, J.B. Jørgensen, A warm-started homogeneous and self-dual interior-point method for linear economic model predictive control, in: 2013 IEEE 52nd Annual Conference on Decision and Control (CDC), 2013, pp. 3677–3683.
- [12] R. Amrit, J.B. Rawlings, L.T. Biegler, Optimizing process economics online using model predictive control, *Comput. Chem. Eng.* 58 (0) (2013) 334–343.
- [13] R. Huang, E. Harinath, L.T. Biegler, Lyapunov stability of economically oriented NMPC for cyclic processes, *J. Process Control* 21 (4) (2011) 501–509.
- [14] M. Heidarinejad, J. Liu, P.D. Christofides, Economic model predictive control of nonlinear process systems using Lyapunov techniques, *AIChE J.* 58 (3) (2012) 855–870.
- [15] A.J. Conejo, E. Castillo, R. Minguez, R. Garcia-Bertrand, *Decomposition Techniques in Mathematical Programming: Engineering and Science Applications*, Springer, Berlin, Heidelberg, 2006.
- [16] G.B. Dantzig, P. Wolfe, Decomposition principle for linear programs, *Operat. Res.* 8 (1) (1960) 101–111.
- [17] R.K. Martin, *Large Scale Linear and Integer Optimization: A Unified Approach*, Kluwer Academic Publishers, Dordrecht, The Netherlands, 1999.
- [18] R. Cheng, J.F. Forbes, W.S. Yip, Dantzig–Wolfe decomposition and plant-wide MPC coordination, *Comput. Chem. Eng.* 32 (7) (2008) 1507–1522.
- [19] J.M. Maestre, R.R. Negenborn, Distributed MPC under coupled constraints based on Dantzig–Wolfe decomposition, in: *Distributed Model Predictive Control Made Easy, Intelligent Systems, Control and Automation: Science and Engineering*, Springer-Verlag GmbH, Berlin, Heidelberg, 2013, pp. 101–115 (Chapter 6).
- [20] K. Edlund, J.D. Bendtsen, J.B. Jørgensen, Hierarchical model-based predictive control of a power plant portfolio, *Control Eng. Pract.* 19 (10) (2011) 1126–1136.
- [21] L.S. Lasdon, *Optimization Theory for Large Systems*, Dover Publications, Inc., 2002.
- [22] H.P. Williams, *Model Building in Mathematical Programming*, 3rd ed., John Wiley & Sons, New York, 1995.
- [23] A. Alabi, J. Castro, Dantzig–Wolfe and block coordinate-descent decomposition in large-scale integrated refinery-planning, *Comput. Operat. Res.* 36 (8) (2009) 2472–2483.
- [24] J.J. Sirola, T.F. Edgar, Process energy systems: control economic and sustainability objectives, *Comput. Chem. Eng.* 47 (2012) 134–144.
- [25] V. Gunnerud, B. Foss, E. Tognes, Parallel Dantzig–Wolfe decomposition for real-time optimization—applied to a complex oil field, *J. Process Control* 20 (9) (2010) 1019–1026.
- [26] V. Gunnerud, B. Foss, Oil production optimization—a piecewise linear model solved with two decomposition strategies, *Comput. Chem. Eng.* 34 (11) (2010) 1803–1812.
- [27] M. Soroush, D.J. Chmielewski, Process systems opportunities in power generation, storage and distribution, *Comput. Chem. Eng.* 51 (0) (2013) 86–95.
- [28] P.-D. Morosan, R.D. Bourdais, J. Didier Buisson, Distributed MPC for multi-zone temperature regulation with coupled constraints, in: *Proceedings of the 18th IFAC World Congress*, 2011, pp. 1552–2557.
- [29] S. Boyd, N. Parikh, E. Chu, B. Peleato, E. Jonathan, Distributed optimization and statistical learning via the alternating direction method of multipliers, *Found. Trends Mach. Learn.* 3 (1) (2011) 1–122.
- [30] C. Conte, T. Summers, M.N. Zeilinger, M. Morari, C.N. Jones, Computational aspects of distributed optimization in model predictive control, in: 2012 IEEE 51st Annual Conference on Decision and Control (CDC), 2012, pp. 6819–6824.
- [31] T.H. Summers, J. Lygeros, Distributed model predictive consensus via the alternating direction method of multipliers, in: 2012 50th Annual Allerton Conference on Communication, Control and Computing (Allerton), 2012, pp. 79–84.
- [32] M. Annergren, A. Hansson, B. Wahlberg, An ADMM algorithm for solving ℓ_1 regularized MPC, in: 2012 IEEE 51st Annual Conference on Decision and Control (CDC), 2012, pp. 4486–4491.
- [33] A. Capolei, E. Suwardati, B. Foss, J.B. Jørgensen, A mean-variance objective for robust production optimization in uncertain geological scenarios, *J. Petrol. Sci. Eng.* (2013) (in press).
- [34] J.M. Morales, A.J. Conejo, H. Madsen, P. Pinson, Marco Zugno, *Integrating Renewables in Electricity Markets*, International Series in Operations Research & Management Science, Springer, Berlin, Heidelberg, 2014.
- [35] C.V. Rao, J.B. Rawlings, Linear programming and model predictive control, *J. Process Control* 10 (2–3) (2000) 283–289.
- [36] A. Frangioni, B. Gendron, *A Stabilized Structured Dantzig–Wolfe Decomposition Method*, Technical report, CIRRELT, Montreal, Canada, 2010, <https://www.cirrelt.ca/documents/travail/cirrelt-2010-02.pdf>
- [37] J.C. Enamorado, A. Ramos, T. Gómez, Multi-area decentralized optimal hydro-thermal coordination by the Dantzig–Wolfe decomposition method, in: *IEEE Power Engineering Society Summer Meeting*, 2000, vol. 4, 2000, pp. 2027–2032.
- [38] L.E. Sokoler, G. Frison, A. Skajaa, R. Halvgaard, J.B. Jørgensen, A homogeneous and self-dual interior-point linear programming algorithm for economic model predictive control, *IEEE Trans. Autom. Control* (2013) (submitted for publication).
- [39] G. Frison, J.B. Jørgensen, A fast condensing method for solving linear-quadratic control problems, in: 2013 IEEE 52nd Annual Conference on Decision and Control (CDC), 2013, pp. 7715–7720.
- [40] M. Hong, Z.-Q. Luo, On the linear convergence of the alternating direction method of multipliers, *Math. Program.* (2013), arXiv:1208.3922v3.
- [41] J. Eckstein, M.C. Ferris, Operator-splitting methods for monotone affine variational inequalities with a parallel application to optimal control, *Inf. J. Comput.* 10 (2) (1998) 218–235.
- [42] J.B. Jørgensen, J.B. Rawlings, S.B. Jørgensen, Numerical methods for large-scale moving horizon estimation and control, in: *International Symposium on Dynamics and Control Process Systems (DYCOPS)*, vol. 7, 2004.
- [43] R.A. Bartlett, L.T. Biegler, QPSchur: a dual, active-set, Schur-complement method for large-scale and structured convex quadratic programming, *Optimiz. Eng.* 7 (1) (2006) 5–32.

- [44] H.J. Ferreau, H.G. Bock, M. Diehl, An online active set strategy to overcome the limitations of explicit MPC, *Int. J. Robust Nonlinear Control* 18 (8) (2008) 816–830.
- [45] Y. Wang, S. Boyd, Fast model predictive control using online optimization, *IEEE Trans. Control Syst. Technol.* 18 (2) (2010) 267–278.
- [46] C.V. Rao, S.J. Wright, J.B. Rawlings, Application of interior-point methods to model predictive control, *J. Optimiz. Theory Appl.* 99 (3) (1998) 723–757.
- [47] A. Shahzad, G.A. Kerrigan, E.C. Constantinides, A fast well-conditioned interior point method for predictive control, in: 2010 49th IEEE Conference on Decision and Control (CDC), 2010, pp. 508–513.
- [48] K. Edlund, L.E. Sokoler, J.B. Jørgensen, A primal-dual interior-point linear programming algorithm for MPC, in: 48th IEEE Conference on Decision and Control, held jointly with 28th Chinese Control Conference, 2009, pp. 351–356.
- [49] S. Richter, C.N. Jones, M. Morari, Real-time input-constrained MPC using fast gradient methods, in: 48th IEEE Conference on Decision and Control, held jointly with 28th Chinese Control Conference, 2009, pp. 7387–7393.
- [50] J.B. Jørgensen, G. Frison, N.F. Gade-Nielsen, B. Dammann, Numerical methods for solution of the extended linear quadratic control problem, in: 4th IFAC Nonlinear Model Predictive Control Conference, 2012, pp. 187–193.
- [51] J.L. Jerez, P.J. Goulart, S. Richter, G.A. Constantinides, E.C. Kerrigan, M. Morari, Embedded online optimization for model predictive control at megahertz rates, *IEEE Trans. Autom. Control* (2014) (in press), available from <http://control.lee.ethz.ch/index.cgi?page=publications&action=details&id=4342>
- [52] T.G. Hovgaard, L.F.S. Larsen, J.B. Jørgensen, Flexible and cost efficient power consumption using economic MPC a supermarket refrigeration benchmark, in: 2011 50th IEEE Conference on Decision and Control and European Control Conference (CDC-ECC), 2011, pp. 848–854.
- [53] J. Ma, S.J. Qin, B. Li, T. Salsbury, Economic model predictive control for building energy systems, in: 2011 IEEE PES Innovative Smart Grid Technologies (ISGT), 2011, pp. 1–6.
- [54] R. Halvgaard, N.K. Poulsen, H. Madsen, J.B. Jørgensen, Economic model predictive control for building climate control in a smart grid, in: 2012 IEEE PES Innovative Smart Grid Technologies (ISGT), 2012, pp. 1–6.
- [55] R. Halvgaard, N.K. Poulsen, H. Madsen, J.B. Jørgensen, F. Marra, D.E.M. Bondy, Electric vehicle charge planning using economic model predictive control, in: 2012 IEEE International Electric Vehicle Conference (IEVC), 2012, pp. 1–6.
- [56] L. Standardi, N.K. Poulsen, J.B. Jørgensen, L.E. Sokoler, Computational efficiency of economic MPC for power systems operation, in: 2013 4th IEEE/PES Innovative Smart Grid Technologies Europe (ISGT EUROPE), IEEE, Kgs. Lyngby, Denmark, 2013, pp. 1–5.
- [57] L.E. Sokoler, K. Edlund, L. Standardi, J.B. Jørgensen, A decomposition algorithm for optimal control of distributed energy systems, in: 2013 4th IEEE/PES Innovative Smart Grid Technologies Europe (ISGT EUROPE), vol. 2013, IEEE, Kgs. Lyngby, Denmark, 2013, pp. 1–5.
- [58] K. Edlund, T. Mølbak, J.D. Bendtsen, Simple models for model-based portfolio load balancing controller synthesis, in: 6th IFAC Symposium on Power Plants and Power Systems Control, 2009, pp. 173–178.
- [59] G. Desaulniers, J. Desrosiers, M.M. Solomon, *Column Generation*, Springer, Berlin, Heidelberg, 2005.

P A P E R F

A Mean-Variance Criterion for Economic Model Predictive Control of Stochastic Linear Systems

L. E. Sokoler, B. Dammann, H. Madsen, and J. B. Jørgensen. A Mean-Variance Criterion for Economic Model Predictive Control of Stochastic Linear Systems. In *53rd IEEE Conference on Decision and Control (CDC)*, pages 5907–5914, 2014.

A Mean-Variance Criterion for Economic Model Predictive Control of Stochastic Linear Systems

Leo Emil Sokoler, Bernd Dammann, Henrik Madsen and John Bagterp Jørgensen

Abstract—Stochastic linear systems arise in a large number of control applications. This paper presents a mean-variance criterion for economic model predictive control (EMPC) of such systems. The system operating cost and its variance is approximated based on a Monte-Carlo approach. Using convex relaxation, the tractability of the resulting optimal control problem is addressed. We use a power management case study to compare different variations of the mean-variance strategy with EMPC based on the certainty equivalence principle. The certainty equivalence strategy is much more computationally efficient than the mean-variance strategies, but it does not account for the variance of the uncertain parameters. Open-loop simulations suggest that a single-stage mean-variance approach yields a significantly lower operating cost than the certainty equivalence strategy. In closed-loop, the single-stage formulation is overly conservative, which results in a high operating cost. For this case, a two-stage extension of the mean-variance approach provides the best trade-off between the expected cost and its variance. It is demonstrated that by using a constraint back-off technique in the specific case study, certainty equivalence EMPC can be modified to perform almost as well as the two-stage mean-variance formulation. Nevertheless, we argue that the mean-variance approach can be used both as a strategy for evaluating less computational demanding methods such as the certainty equivalence method, and as an individual control strategy when heuristics such as constraint back-off do not perform well.

I. INTRODUCTION

Model predictive control (MPC) is a class of algorithms for control of dynamic systems. Due to its ability to handle multiple-input multiple-output (MIMO) systems and constraints in a straightforward and transparent way, MPC has become the leading advanced control methodology in a number of industries [1]–[3]. The basic idea of MPC is to optimize the predicted behavior of a dynamic model over a finite horizon. At each sampling instant, an optimal control problem (OCP) is solved to obtain an open-loop input trajectory. The first input in the trajectory is then applied to the controlled system, and the procedure is repeated at the following sampling instant. This way, the MPC control strategy is synthesized in a closed-loop manner using feedback.

Conventionally, the OCP solved in MPC is formulated as a convex program that penalizes deviations between the controlled variable and a setpoint [1], [2], [4], [5]. While this approach ensures that the setpoint is reached in a reasonable amount of time, it does not guarantee that the transition between setpoints is performed in an economically efficient

The authors are with the Department of Applied Mathematics and Computer Science, Technical University of Denmark, DK-2800 Kgs. Lyngby, Denmark. L. E. Sokoler is also affiliated with DONG Energy, DK-2820 Gentofte, Denmark. Email: {leso, beda, hmad, jbjjo} at dtu.dk

way. To overcome this problem, MPC has been modified to solve OCPs with more general cost functions. In this way, EMPC provides a systematic method for optimizing economic performance [6]–[12]. Stability and other properties of economic MPC (EMPC) schemes have been addressed in [6]–[10], [13].

In EMPC, the OCP solved to obtain the open-loop input trajectory aims to minimize the system operating cost over a finite horizon. Due to uncertain system parameters such as process noise, the operating cost will often be a random variable. A common way of handling the uncertainty is simply to replace the uncertain parameters with their mean values, such that the OCP reduces to a standard deterministic form. This approach is known as certainty equivalence EMPC (CE-EMPC) [14], [15].

This paper shows that although CE-EMPC is attractive from a computational point of view, disregarding the variance of the uncertain parameters may lead to poor economic performance. To overcome this issue, we introduce a mean-variance based OCP that allows a specific trade-off between the expected cost and the cost variance. The novelties of this paper can be summarized as follows:

- A mean-variance based OCP is introduced and extended to a two-stage stochastic program. The two-stage stochastic program accounts for the feedback structure of MPC. We denote the resulting control strategy as MV-EMPC(M).
- To increase computational speed, we approximate MV-EMPC(M) using a convex relaxation of the two-stage stochastic program. For the cost function considered in this paper, the convex relaxation can be formulated as a convex quadratic program. We refer to the EMPC control strategy based on solving the convex quadratic program as MVQP-EMPC(M).
- We provide open-loop and closed-loop simulations that compare three special cases of MV-EMPC(M), including a back-off based modification of CE-EMPC.

Simulations demonstrate that while MV-EMPC(M) outperforms CE-EMPC in open-loop, the back-off based modification of CE-EMPC works almost as well in closed-loop. Nevertheless, the performance of MV-EMPC(M) provides important information that can be utilized to evaluate the performance of less computational demanding control strategies. We also emphasize that the preliminary results presented in this paper are based on a single test system. Other examples may show that the performance gap between MV-EMPC(M) and CE-EMPC can be much larger.

A. Related Work

Monte Carlo methods have previously been combined with classical MPC in [16]–[21]. The OCPs considered by these methods consist of standard state and input penalty objective functions subject to probabilistic constraints. In [21], a value-at-risk variation of the standard cost function is suggested, and [22] introduces a single-stage mean-variance criterion for EMPC of a non-linear system with uncertain model parameters. The OCP defined in [22] is solved using sequential quadratic programming. The method proposed in this paper is specialized to linear systems and only requires solving a single convex quadratic program. Also, the results in [22] are limited to open-loop performance, while we consider closed-loop performance as well.

B. Paper Organization

This paper is organized as follows. Section II defines the OCPs solved in CE-EMPC and MV-EMPC(M). Section III introduces a particular cost function and describes solution methods to the resulting OCPs. This section also provides a constraint back-off technique for CE-EMPC. Section IV presents a simple power management case study that compares three special cases of MV-EMPC(M), including CE-EMPC. Concluding remarks are given in Section V.

II. PROBLEM DEFINITION

In this section, a formal definition of CE-EMPC and MV-EMPC(M) is given. Although CE-EMPC is a special case of MV-EMPC(M), this case is treated separately.

A. Stochastic Linear Systems

We consider stochastic linear state space systems in the form

$$x_{k+1} = Ax_k + Bu_k + w_k, \quad (1a)$$

$$y_k = C_y x_k + v_k, \quad (1b)$$

$$z_k = C_z x_k, \quad (1c)$$

where (A, B, C_y, C_z) are the state space matrices, $x_k \in \mathbb{R}^{n_x}$ is the state, $u_k \in \mathbb{R}^{n_u}$ is the input, $y_k \in \mathbb{R}^{n_y}$ is the measured output, and $z_k \in \mathbb{R}^{n_z}$ is the controlled variable. Moreover, $w_k \in \mathbb{R}^{n_x}$ is the process noise, and $v_k \in \mathbb{R}^{n_y}$ is the measurement noise. We will assume that realizations of w_k and v_k can be generated.

The system description (1) may be derived from realization of input-output models such as finite impulse response (FIR) models, autoregressive moving average exogenous (ARMAX) models, Box-Jenkins models, and transfer function models. In addition, (1) arises from the discretization of linear continuous differential equations.

Fig. 1 is a schematic diagram of the EMPC employed in this paper. The EMPC controller consists of an estimator and a regulator. The estimator estimates the current state, x_k , and the regulator determines the open-loop input trajectory, $\{u_j^*\}_{j=k}^{k+N-1}$. We denote the estimate of x_k by \hat{x}_k .

Remark 1: We do not discuss the problem of computing the estimate \hat{x}_k in this paper. Note that when w_k and v_k are

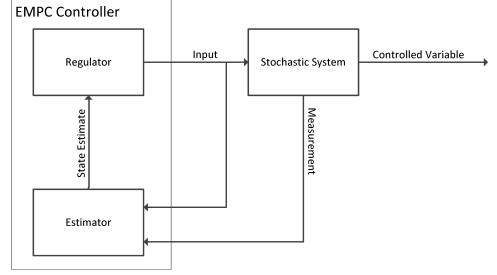


Fig. 1. Schematic diagram of the EMPC framework.

normally distributed, the Kalman filter provides an estimate with minimum state prediction error variance [23].

B. Cost Function

Without loss of generality, let \bar{x}_0 denote the current state. Moreover, define $\mathcal{N}_i = \{0 + i, 1 + i, \dots, N - 1 + i\}$ with N being the length of the prediction horizon, and introduce the vectors

$$u = \begin{bmatrix} u_0 \\ u_1 \\ \vdots \\ u_{N-1} \end{bmatrix}, \quad x = \begin{bmatrix} x_1 \\ x_2 \\ \vdots \\ x_N \end{bmatrix}, \quad z = \begin{bmatrix} z_1 \\ z_2 \\ \vdots \\ z_N \end{bmatrix}, \quad w = \begin{bmatrix} w_0 \\ w_1 \\ \vdots \\ w_{N-1} \end{bmatrix},$$

Also, define the cost function

$$\Psi_{\text{eco}}(u; \bar{x}_0, w) = \{\phi(u, x, z) | x_0 = \bar{x}_0, x_{k+1} = Ax_k + Bu_k + w_k, z_{k+1} = C_z x_{k+1}, k \in \mathcal{N}_0\}, \quad (2)$$

in which $\phi(u, x, z)$ measures e.g. input costs, input rate costs, output costs, terminal costs, tracking error costs, and costs of violating soft output constraints. Terminal constraints may also be included in (2) by further restricting the domain of Ψ_{eco} .

When \bar{x}_0 and w are deterministic variables, $\Psi_{\text{eco}} = \Psi_{\text{eco}}(u; \bar{x}_0, w)$, is deterministic in u . Conversely, if w and \bar{x}_0 are random variables, Ψ_{eco} is a random variable as well. In this case, the distribution of Ψ_{eco} depends on u . We describe different strategies to select u in the stochastic case. For simplicity, the estimate, \hat{x}_0 , of the initial state, $x_0 = \bar{x}_0$, is assumed to be perfect (the method presented in this paper can be extended to handle the case in which x_0 is uncertain as well).

C. Certainty Equivalence Economic Model Predictive Control

In CE-EMPC, the uncertain parameters in the cost function (2) are replaced by their mean values, i.e.

$$\Psi_{\text{CE}} = \Psi_{\text{eco}}(u; \hat{x}_0, \mathbb{E}_w[w]). \quad (3)$$

Consequently, the open-loop input trajectory in CE-EMPC is defined as

$$u_{\text{CE}}^* = \arg \min_{u \in \mathcal{U}} \Psi_{\text{CE}}. \quad (4)$$

Note that u is restricted to the input constraint set \mathcal{U} . A drawback of CE-EMPC is that in general $E_w[\Psi_{\text{eco}}(u; \hat{x}_0, w)] \neq \Psi_{\text{eco}}(u; \hat{x}_0, E_w[w])$, i.e. the minimizer of (3), u_{CE}^* , does not necessarily minimize the expected cost.

Remark 2: Provided that $\phi(u, x, z)$ is a convex function and that \mathcal{U} is a convex set, u_{CE}^* can often be obtained efficiently by special-purpose optimization algorithms [24], [25].

D. Mean-Variance Economic Model Predictive Control

As an alternative to the certainty equivalence criterion, (3), this paper considers a mean-variance trade-off criterion. The criterion is formulated as

$$\Psi_{\text{MV}} = \lambda E_w[\Psi_{\text{eco}}] + (1 - \lambda) \text{Var}_w[\Psi_{\text{eco}}], \quad (5)$$

where λ is a risk aversion parameter that controls the trade-off between the expected system operating cost and its variance. The formulation (5) can be interpreted as a classical Markowitz mean-variance optimization approach [26], [27].

Closed form expressions for the mean, $E_w[\Psi_{\text{eco}}]$, and the variance, $\text{Var}_w[\Psi_{\text{eco}}]$, are generally not available. To evaluate (5), we therefore introduce the sample estimates

$$E_w[\Psi_{\text{eco}}] \approx \mu = \frac{1}{S} \sum_{i \in \mathcal{S}} \Psi_{\text{eco}}(u; \hat{x}_0, w^i), \quad (6a)$$

$$\text{Var}_w[\Psi_{\text{eco}}] \approx s^2 = \frac{1}{S-1} \sum_{i \in \mathcal{S}} (\Psi_{\text{eco}}(u; \hat{x}_0, w^i) - \mu)^2, \quad (6b)$$

where $\{w^i\}_{i=1}^S$ is a set of samples from the distribution of w and $\mathcal{S} = \{1, 2, \dots, S\}$. It follows that for a sufficiently large number of scenarios, S

$$\Psi_{\text{MV}} \approx \lambda \mu + (1 - \lambda) s^2, \quad (7)$$

i.e. the right hand side of (7) is a sample estimate of the mean-variance criterion (5). With some abuse of notation, the remainder of this paper simply denotes the sample estimate by Ψ_{MV} . Moreover, we refer to MV-EMPC as the variation of EMPC in which

$$u_{\text{MV}}^* = \underset{u \in \mathcal{U}}{\text{argmin}} \Psi_{\text{MV}}, \quad (8)$$

is the open-loop input trajectory. Later in this section, we introduce MV-EMPC(M) as a two-stage generalization of MV-EMPC.

To develop efficient algorithms for evaluating (8), it is convenient to state u_{MV}^* as (part of) the solution, u^* , to the OCP

$$\underset{u \in \mathcal{U}, \{x^i, z^i, v^i\}_{i=1}^S}{\text{minimize}} \quad \Psi_{\text{MV}} = \lambda \mu + \tilde{\lambda} \sum_{j \in \mathcal{S}} (v^j - \mu)^2, \quad (9a)$$

$$\text{subject to } (x^i, u, z^i) \in \mathcal{X}(\hat{x}_0, w^i), \quad (9b)$$

$$v^i = \phi(u, x^i, z^i), \quad (9c)$$

$$\mu = \frac{1}{S} \sum_{j \in \mathcal{S}} v^j, \quad (9d)$$

where $k \in \mathcal{N}_0$, $i \in \mathcal{S}$ and $\tilde{\lambda} = (1 - \lambda)/(S - 1)$. For compact notation, we have defined

$$\mathcal{X}(\hat{x}_0, w) = \{(x, u, z) | x_0 = \hat{x}_0, x_{k+1} = Ax_k + Bu_k + w_k, \\ z_{k+1} = C_z x_{k+1}, k \in \mathcal{N}_0\}.$$

One issue with the criterion (7) is that the estimates μ and s^2 are based on open-loop performance, i.e. the formulation (9) assumes that no recourse exists in the future. Therefore, MV-EMPC may be overly conservative when applied in a receding horizon manner [21]. To account for the fact that new information becomes available at each sampling instant, we introduce scenario dependent input variables $u^i \in \mathcal{U}$ for $i \in \mathcal{S}$. In addition, the constraints (9c) and (9b) are replaced with

$$(x^i, u^i, z^i) \in \mathcal{X}(\hat{x}_0, w^i), \quad i \in \mathcal{S}, \quad (10a)$$

$$v^i = \phi(u^i, x^i, z^i), \quad i \in \mathcal{S}, \quad (10b)$$

$$u_k^i = u_k^j, \quad i, j \in \mathcal{S}, k \in \mathcal{M}, \quad (10c)$$

where $\mathcal{M} = \{0, 1, \dots, M\}$ and $M \leq N$. The constraint (10c) states that in the first $k = 0, 1, \dots, M$ time steps, the input should be equal for all the scenarios. In the view of stochastic optimization, the modification (10) can be interpreted as extending (9) to a two-stage stochastic optimization problem [28], [29]. At the first stage ($k = 0, 1, \dots, M$), we fix u_k^i over the entire set of scenarios $i \in \mathcal{S}$, i.e. ‘‘a here-and-now decision’’. At the second stage, ($k = M + 1, M + 2, \dots, N$), the inputs adapt to the scenarios. We refer to EMPC based on the extended formulation, (10), as MV-EMPC(M). Note that (9) corresponds to the special case $M = N$. The other extreme case is MV-EMPC(1). This case assumes that the full realization of w becomes available in the following time step.

Remark 3: The dimensions of the OCP solved in MV-EMPC(M), (9)-(10), grow with the number of scenarios. From a computational point of view, CE-EMPC is therefore less demanding than MV-EMPC(M). In particular, the OCP solved in CE-EMPC corresponds to MV-EMPC(M) with $M = N$ and a single scenario ($S = 1$).

III. OPTIMIZATION METHODS

This section presents optimization methods for solving the OCP (9), under the two-stage modification (10). Moreover, a simple back-off heuristic for CE-EMPC is introduced.

A. Cost Function Example

We study the non-linear cost function

$$\phi(u, x, z) = \sum_{k \in \mathcal{N}_0} c_k^T u_k + \sum_{k \in \mathcal{N}_1} q_k^T ((z_k - \bar{z}_k)_+ + (z_k - \bar{z}_k)_-), \quad (11)$$

where $v_+ = \max\{0, v_i\}$ for $i = 1, 2, \dots, n_v$, with $v \in \mathbb{R}^{n_v}$ (the non-negative part of a vector). The parameter c_k is the marginal input price and q_k is the marginal price for not maintaining the controlled variable, z_k , within an acceptable operating range $(\underline{z}_k, \bar{z}_k)$. The latter can be interpreted as soft output constraints [30]. We assume that the input constraint set, \mathcal{U} , limits the input and the input-rate such that

$$\mathcal{U} = \{u | \underline{u}_k \leq u_k \leq \bar{u}_k, \Delta \underline{u}_k \leq \Delta u_k \leq \Delta \bar{u}_k, k \in \mathcal{N}_0\}, \quad (12)$$

where $\Delta u_k = u_k - u_{k-1}$. Based on the specifications above, the OCP solved in MV-EMPC(M), (9)-(10), may be posed as

$$\underset{\{u^i \in \mathcal{U}, x^i, z^i, v^i, \rho^i \geq 0\}_{i=1, \mu}^S}{\text{minimize}} \quad \Psi_{\text{MV}} = \lambda \mu + \tilde{\lambda} \sum_{j \in \mathcal{S}} (v^j - \mu)^2, \quad (13a)$$

subject to the constraints

$$(x^i, u^i, z^i) \in \mathcal{X}(\hat{x}_0, w^i), \quad i \in \mathcal{S}, \quad (13b)$$

$$v^i = \sum_{k \in \mathcal{N}_0} c_k^T u_k^i + q_{k+1}^T \rho_{k+1}^i, \quad i \in \mathcal{S}, \quad (13c)$$

$$\mu = \frac{1}{S} \sum_{j \in \mathcal{S}} v^j, \quad (13d)$$

$$u_k^i = u_k^j, \quad k \in \mathcal{M}, i, j \in \mathcal{S}, \quad (13e)$$

$$\rho_k^i = (z_k - z_k^i)_+ + (z_k^i - \bar{z}_k)_+, \quad k \in \mathcal{N}_1, i \in \mathcal{S}. \quad (13f)$$

Note that we have introduced the auxiliary optimization vectors ρ^i for $i \in \mathcal{S}$. The input data to the OCP, (13), are the state space matrices (A, B, C_z), the estimate of the initial state, \hat{x}_0 , the input cost, c_k , the soft output constraint violation cost, q_k , the input limits, $(\underline{u}_k, \bar{u}_k)$, the input rate limits, $(\Delta \underline{u}_k, \Delta \bar{u}_k)$, the output limits, $(\underline{z}_k, \bar{z}_k)$, and the process noise scenarios, w^i .

B. Convex Relaxation of Mean-Variance Optimal Control Problem

The problem (13) is non-convex due to the constraint (13f). Consider the relaxation

$$\rho_k^i \geq (z_k - z_k^i)_+ + (z_k^i - \bar{z}_k)_+, \quad k \in \mathcal{N}_1, i \in \mathcal{S}, \quad (14)$$

which replaces a set of equality constraints by a set of inequality constraints. We can model (14) using the linear inequalities

$$\underline{z}_k - \rho_k^i \leq z_k^i \leq \bar{z}_k + \rho_k^i, \quad k \in \mathcal{N}_1, i \in \mathcal{S}, \quad (15a)$$

$$\rho_k^i \geq 0, \quad k \in \mathcal{N}_1, i \in \mathcal{S}. \quad (15b)$$

Appendix I shows that by using the model (15), (13) may be expressed as a highly structured convex quadratic program. We refer to the EMPC strategy based on solving the two-stage OCP (13), with the relaxed model (15) as MVQP-EMPC(M).

For $\lambda = 1$ ($\tilde{\lambda} = 0$), the objective function, (13a), is non-decreasing in ρ . Consequently, a solution to the relaxed problem will always satisfy (14) with equality. When $\lambda < 1$ ($\tilde{\lambda} > 0$) the deviation terms $\tilde{\lambda}(v^j - \mu)^2$ in (13a) may possibly be reduced by increasing ρ_k^j further than the bound, (14), for some $k \in \mathcal{N}_1$ and $j \in \mathcal{S}$. If this can be done without increasing $\lambda \mu$ by a larger amount, the solution will satisfy (14) with strict inequality for some $k \in \mathcal{N}_1$ and $j \in \mathcal{S}$. Clearly this situation is likely to occur for $\lambda = 0$. As λ is increased towards one, we expect the solution to the relaxed problem to become a better approximation of the solution to the original problem (13).

Remark 4: Using the same line of arguments as above, the solution to the general problem (9) can be approximated by solving a convex optimization problem, provided that \mathcal{U} is a convex set and that $\phi(u, x, z)$ is a convex function. This is

done by replacing (9c) with the relaxed constraint $v_i \geq \Psi_{\text{eco}}^i$ for $i \in \mathcal{S}$.

C. Constraint Back-Off Heuristic for Certainty Equivalence Economic Model Predictive Control

With the model specifications (11) and (12), the open-loop input trajectory associated with CE-EMPC, (4), can be determined by solving the OCP

$$\underset{u \in \mathcal{U}, x, z, \rho \geq 0}{\text{minimize}} \quad \Psi_{\text{CE}} = \sum_{k \in \mathcal{N}_0} c_k^T u_k + q_{k+1}^T \rho_{k+1}, \quad (16a)$$

$$\text{subject to } (x, u, z) \in \mathcal{X}(\hat{x}_0, E_w[w]) \quad (16b)$$

$$\underline{z}_k - \rho_k \leq z_k \leq \bar{z}_k + \rho_k, \quad k \in \mathcal{N}_1, \quad (16c)$$

We can regard (16) as a special case of the OCP solved in MV-EMPC(M), (13), with $M = N$, $S = 1$, and $w^1 = E_w[w]$. Hence, the dimension of the problem (16) is substantially smaller than the dimension of the OCP solved in MV-EMPC(M). Also observe that (16) is a linear program.

A disadvantage of only accounting for the scenario in which the uncertain parameters attain their mean values, is that the controller can become too aggressive. To avoid this situation, we introduce constraint back-off. Let γ be a back-off parameter, and replace the output limits in (16c) by

$$\underline{z}_k^{\text{BO}} = \bar{z}_k - \gamma(\bar{z}_k - \underline{z}_k)/2, \quad \underline{z}_k^{\text{BO}} = \underline{z}_k - \gamma(\underline{z}_k - \bar{z}_k)/2,$$

for $k \in \mathcal{N}_1$. We interpret γ in a similar way as λ , i.e. a risk aversion parameter that controls the trade-off between the expected cost and the cost variance. Note that $\gamma = 0$ corresponds to the case with no back-off, while $\gamma = 1$ yields $\underline{z}_k^{\text{BO}} = \bar{z}_k^{\text{BO}} = (\underline{z}_k + \bar{z}_k)/2$.

IV. SIMULATION CASE STUDY

In this section, we present a simple power management case study. The cost function and the input constraint set are defined as in (11) and (12). We compare the following EMPC strategies:

- CE-EMPC: Certainty equivalence EMPC with back-off parameter γ , see (16).
- MV-EMPC(M): Two-stage mean-variance EMPC with risk aversion parameter λ , we test the extreme cases $M = 1$ and $M = N$, see (13).
- MVQP-EMPC(M): The same as MV-EMPC(M), but with the convex relaxation (14), again we test $M = 1$ and $M = N$.

Note that these strategies are all special cases of (9) (under the modification (10)).

A. Case Study System Definition

The following system is considered

$$Y(s) = \frac{1}{(\tau s + 1)^3} (U(s) + W(s)) + V(s), \quad (17a)$$

$$Z(s) = \frac{1}{(\tau s + 1)^3} (U(s) + W(s)), \quad (17b)$$

where $U(s)$ is the input, $Y(s)$ is the measurement, $Z(s)$ is the controlled variable, $W(s)$ is the process noise, and $V(s)$ is the measurement noise. In [31], the third order transfer function

TABLE I
CASE STUDY CONTROLLER AND SYSTEM PARAMETERS

p_k	q_k	\underline{u}_k	\bar{u}_k	$\Delta \underline{u}_k$	$\Delta \bar{u}_k$	\underline{z}_k	\bar{z}_k	N	τ
1	10	0	2	-1	1	0	1	10	8

model (17) is identified to describe the power production of a thermal power plant.

We convert the transfer function model, (17), into a discrete state space model of the form (1) using a sampling time of $T_s = 5$ seconds. In the resulting model structure, u_k is the power reference, z_k is the controlled variable, and y_k is the measured power production. The distributions of the process and measurement noise are

$$w_k \sim N(0, 0.1I), \quad v_{k+1} \sim N(0, 0.01), \quad k \in \mathcal{N}_0.$$

Table I lists the case study system and controller parameters. The parameters are kept constant for all k . We define the lower and upper output limit to be zero and one. This can be interpreted as a situation in which deviations from the steady-state power production is allowed to be no more than 1 MW, and no less than the current production level. The input price, p_k , can be interpreted as the fuel cost, and q_k can be interpreted as the cost of buying power in the electricity market. Finally, the initial state, x_0 , is a vector of all zeros.

B. Open-Loop Simulations

We consider the effect of varying the number of scenarios, S , the risk aversion parameter, λ , and the back-off parameter, γ , in an open-loop situation, i.e. a simulation without feedback. Moreover, the effect of approximating (13) using the convex relaxation (14) is investigated. The estimated mean operating cost and its standard deviation are denoted $\bar{\mu}$, and $\bar{\sigma}$, respectively. These values are computed using (6). Different realizations of the process noise, w , are generated for optimization purpose, and for computing $\bar{\mu}$ and $\bar{\sigma}$.

As an example, let $\lambda = 0.5$, and $\gamma = 0.3$. Fig. 2 shows the expected cost and its 95% normal confidence interval ($\bar{\mu} \pm 1.96\bar{\sigma}$), as a function of the number of scenarios, S , for MV-EMPC(N) and CE-EMPC. The performance of CE-EMPC is independent of the number of scenarios. As the number of scenarios, S , is increased, the cost, $\bar{\mu}$, and the standard deviation, $\bar{\sigma}$, associated with MV-EMPC(N) converge. For $S \geq 1000$, MV-EMPC(N) operates the system with the same expected cost as CE-EMPC but at a reduced risk level (smaller standard deviation). In the following simulations, we fix $S = 1000$.

To observe the effect of the risk aversion parameter, λ , and the back-off parameter, γ , we consider the mean-variance efficient frontier [26], [27]. Fig. 3 shows a plot of $\bar{\mu}$ as a function of $\bar{\sigma}$, for 1000 different values of λ and γ in the range $[0, 1]$. The graphs associated with MV-EMPC(N) and MVQP-EMPC(N) coincide for most values of λ . The case $\lambda = 1$ corresponds to the right endpoint of the two graphs. For values of λ close to zero (small values of $\bar{\sigma}$), the relaxed OCP solved in MVQP-EMPC(N) produces a different solution than the OCP solved in MV-EMPC(N). For example, the

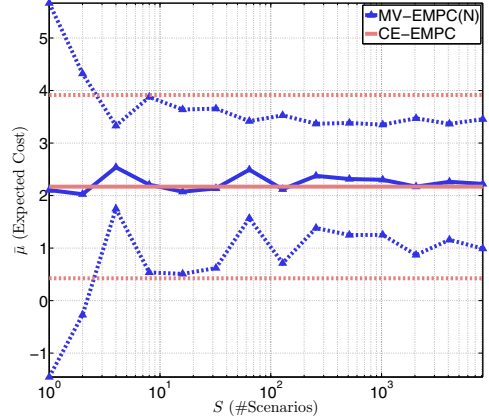


Fig. 2. Open-loop simulation: The expected cost and its 95% normal confidence interval for MV-EMPC(N) and CE-EMPC, as a function of the number of scenarios, S .

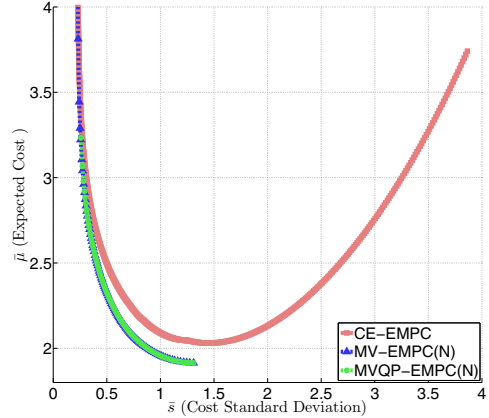
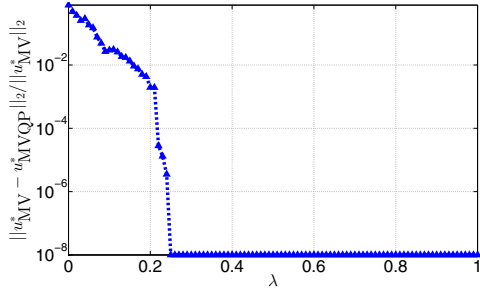


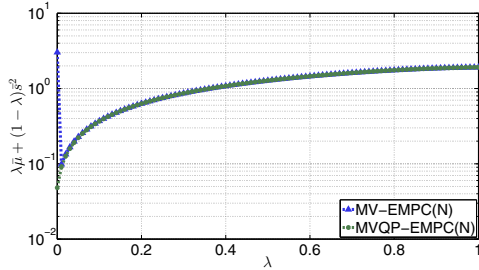
Fig. 3. Open-loop simulation: The expected cost, $\bar{\mu}$, as a function of the cost standard deviation, $\bar{\sigma}$, for 1000 values of λ and γ in the range $[0, 1]$.

left endpoint ($\lambda = 0$) of the graph associated with MVQP-EMPC(N) lies within the plotted cost interval, while the left endpoint associated with MV-EMPC(N) lies well above this interval. In most practical applications, these high-cost/low-variance solutions are disregarded, since accepting a small increase in the variance leads to a large cost reduction.

Fig. 3 also shows that the mean-variance strategies operate the system at a reduced cost compared to CE-EMPC. For example, given the standard deviation $\bar{\sigma} = 0.4$, a 6% decrease in the expected cost is obtained. The right endpoint of the graph associated with CE-EMPC corresponds to the case when $\gamma = 0$, meaning that no constraint back-off is used. As discussed previously, disregarding the variance may cause the controller to become too aggressive. We observe that the case $\gamma = 0$ results in a high-cost/high-variance situation. Evidently, a much better mean-variance cost trade-off can be



(a) Relative difference between u_{MVQP}^* and u_{MV}^* measured in the 2-norm, as a function of λ .



(b) Value of the mean-variance criterion, (7), for MV-EMPC(N) and MVQP-EMPC(N)

Fig. 4. Open-loop simulation: Comparison of the solution obtained by solving the OCP associated with MV-EMPC(N) and its relaxation, for 1000 different values of λ .

obtained with CE-EMPC when $\gamma > 0$.

Fig. 4(a) illustrates the relative difference between the input obtained by solving the OCP associated with MV-EMPC(N), (13), denoted u_{MV}^* , and the input obtained when using the relaxed model (15), denoted u_{MVQP}^* , as a function of λ . The values of the mean-variance criterion, (7), associated with these open-loop input trajectories are shown in Fig. 4(b). The relaxed problem yields a nearly optimal solution to the original problem for most choices of λ . As λ approaches zero, the difference between the two solutions grow. As illustrated in Fig. 3, the values of λ for which the solutions differ, usually have no practical interest.

Fig. 5 depicts the solution time of the OCP solved in MV-EMPC(N), MVQP-EMPC(N) and CE-EMPC, as a function of the number of scenarios S . The OCP associated with MV-EMPC(N), (13), is solved using MATLABs `fmincon`, whereas its relaxation based on (14) is solved via Gurobi using the formulation derived in Appendix I. The algorithms are run on a cluster of dual-socket Intel(R) Xeon(R) E5-2665 @ 2.40GHz servers, each equipped with 64 GB of memory, and running Scientific Linux 6.4. Eight cores are dedicated to solve each optimization problem. Fig. 5 shows that already for $S = 64$ scenarios, the computation time of solving the OCP associated with MV-EMPC(N), (13), is several minutes. In contrast to this, the relaxed problem can be solved in under 5 seconds, even for $S = 1024$ scenarios. This is an important result, as EMPC requires computing the open-loop

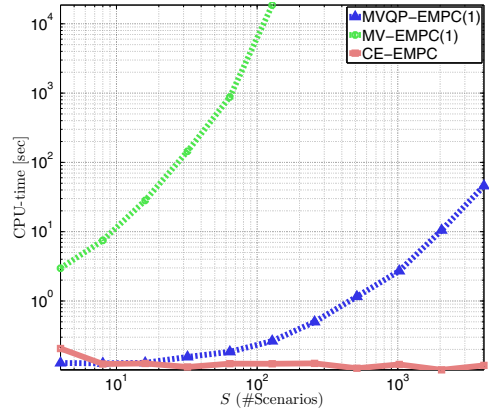


Fig. 5. Open-loop simulation: CPU-time for solving (13) using MATLABs `fmincon`, and CPU-time for solving its convex relaxation using Gurobi, as a function of the number of scenarios S . The figure also shows the CPU-time of solving the linear program (16), associated with CE-EMPC.

input trajectory in real-time. For CE-EMPC, the computation time of solving the OCP, (16), does not change with the number of scenarios.

Remark 5: Appendix I shows that the OCP associated with MVQP-EMPC(M) is highly structured. We therefore expect that the computation times reported in this paper can be reduced significantly using special purpose algorithms. Moreover, decomposition techniques may be applied to solve the problem more efficiently [32].

C. Closed-Loop Simulations

In the remainder of this paper we consider a closed-loop situation, meaning that the inputs are applied in a receding horizon manner (the OCP is solved at every time step). To study the effect of feedback, the mean-variance strategy, MVQP-EMPC(M), is tested for both $M = 1$ and $M = N$. When $M = 1$, the OCP (13) can be viewed as a two-stage stochastic optimization problem that accounts for future information in an approximate manner. The closed-loop simulation is performed over 50 time steps, and for 20 different values of λ and γ in the range $[0,1]$. The Kalman filter is used for closed-loop state estimation.

We label the estimated expected cost and its standard deviation as $\bar{\mu}_{CL}$ and $\bar{\sigma}_{CL}$. These quantities are computed based on 5000 closed-loop simulations. This implies that $50 \cdot 20 \cdot 5000 = 5$ million convex quadratic programs are solved. To reduce the computation time of solving the quadratic programs, we run the closed-loop simulations in parallel using the above mentioned high performance computing cluster. Only the approximation, MVQP-EMPC(M), is considered in closed loop.

Fig. 6 depicts the closed-loop mean-variance efficient frontier for MVQP-EMPC(N), MVQP-EMPC(1) and CE-EMPC. The figure shows that the operating cost associated with CE-EMPC is lower than the cost of MVQP-EMPC(N) and only slightly higher than the cost of MVQP-EMPC(1).

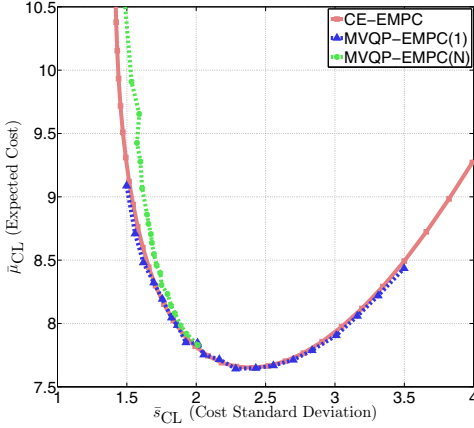


Fig. 6. Closed-loop simulation: The expected cost, $\bar{\mu}_{CL}$, as a function of the cost standard deviation, \bar{s}_{CL} , for 20 values of λ and γ in the range $[0, 1]$.

For a given standard deviation, \bar{s} , MVQP-EMPC(N) operates the system at an increased expected cost compared to the other strategies. MVQP-EMPC(N) works poorly in closed-loop because the controller is overly conservative. The less conservative two-stage approach, MVQP-EMPC(1), is thus better suited for closed-loop applications. It is also important to note that CE-EMPC performs almost as well as MVQP-EMPC(1). This indicates that in the presence of feedback, conventional certainty equivalence strategies may be modified to work well for stochastic systems as well. Using such an approach reduces the computational costs significantly. We emphasize the importance of comparing the different methods before deciding on a particular control strategy, since the performance gap between MVQP-EMPC(1) and CE-EMPC may be larger in other cases than in the example provided in this paper. The mean-variance approach can be used both as a control strategy, and as a performance indicator.

V. CONCLUSION

We have formulated a two-stage mean-variance based OCP for EMPC of stochastic linear systems. This strategy is denoted MV-EMPC(M). A cost function consisting of input cost and cost for violating soft output constraints was considered. For computational efficiency, a solution to the stochastic problem was approximated by solving a convex relaxation of the OCP. Simulations based on a power management case study show that MV-EMPC(M) has the potential of reducing the system operating cost compared to CE-EMPC. By using a simple back-off heuristic, however, the mean-variance efficient frontier of CE-EMPC and MV-EMPC(M) becomes almost identical in closed-loop. This may not be the case in general. Hence, MV-EMPC(M) provides both a systematic method for validating the economic performance of more simple methods, and an independent control strategy.

APPENDIX I

COMPACT FORMULATION OF THE RELAXED MEAN-VARIANCE OPTIMAL CONTROL PROBLEM

We consider the problem, (13), under the relaxation, (15). For convenience, define

$$z = \begin{bmatrix} z_1 \\ z_2 \\ \vdots \\ z_N \end{bmatrix}, \bar{z} = \begin{bmatrix} \bar{z}_1 \\ \bar{z}_2 \\ \vdots \\ \bar{z}_N \end{bmatrix}, u = \begin{bmatrix} u_0 \\ u_1 \\ \vdots \\ u_{N-1} \end{bmatrix}, \bar{u} = \begin{bmatrix} \bar{u}_0 \\ \bar{u}_1 \\ \vdots \\ \bar{u}_{N-1} \end{bmatrix},$$

and similarly for p and q . We also introduce the stacked vectors \bar{z} , \bar{u} , $\Delta\bar{u}$, \bar{z} , \bar{u} , and $\Delta\bar{u}$, consisting of S copies of the above.

The objective function, (13a), is written in the form

$$\psi_{MV} = \lambda\mu + \tilde{\lambda}v^T v + S\tilde{\lambda}\mu^2 - 2\tilde{\lambda}\mu\mathbf{1}^T v,$$

where $\mathbf{1}^T$ is a vector of all ones. In a compact form, the state space constraints, (13b), can be formulated as

$$\tilde{A}x + \tilde{B}u + \tilde{w} = 0, \quad z = \tilde{C}x,$$

where $\tilde{A} = \mathbf{blkdiag}(\tilde{A}, \tilde{A}, \dots, \tilde{A})$, and \tilde{B} and \tilde{C} are defined in the same way with

$$\tilde{A} = \begin{bmatrix} -I & & & & \\ A & -I & & & \\ & & \ddots & & \\ & & & A & -I \end{bmatrix}, \tilde{w}^i = \begin{bmatrix} w_0^i \\ w_1^i \\ \vdots \\ w_{N-1}^i \end{bmatrix} + \begin{bmatrix} Ax_0 \\ 0 \\ \vdots \\ 0 \end{bmatrix}, i \in \mathcal{S},$$

and $\tilde{B} = \mathbf{blkdiag}(B, B, \dots, B)$, $\tilde{C} = \mathbf{blkdiag}(C, C, \dots, C)$. Finally, $\tilde{w} = [(\tilde{w}^1)^T (\tilde{w}^2)^T \dots (\tilde{w}^S)^T]^T$, with \tilde{w}^i defined as above.

The input limits and the input rate limits, $u^i \in \mathcal{U}$, $i \in \mathcal{S}$, can be put in the form $\tilde{u} \leq u \leq \bar{\tilde{u}}$ and $\Delta\tilde{u} \leq \tilde{\Lambda}u \leq \Delta\bar{\tilde{u}}$, where $\tilde{\Lambda} = \mathbf{blkdiag}(\Lambda, \Lambda, \dots, \Lambda)$ and

$$\tilde{\Lambda} = \begin{bmatrix} I & & & & \\ -I & I & & & \\ & & \ddots & & \\ & & & \ddots & \\ & & & & -I & I \end{bmatrix}$$

Let $\tilde{p} = \mathbf{diag}(p, p, \dots, p)$, and $\tilde{q} = \mathbf{diag}(q, q, \dots, q)$, then (13c) and (13d) can be written as

$$v = \tilde{p}^T u + \tilde{q}^T \rho, \quad \mu = \frac{1}{S}\mathbf{1}^T v,$$

In place of (13f), we have the relaxed constraints (15), $\bar{z} - \rho \leq z \leq \bar{z} + \rho$ and $\rho \geq 0$. Finally, (13e) stating that the input should be equal over the different scenarios up to time step M is formulated as $\tilde{L}u = 0$, where

$$\tilde{L} = \begin{bmatrix} L & -L & & & \\ & L & -L & & \\ & & \ddots & \ddots & \\ & & & L & -L \end{bmatrix},$$

and the matrix L is defined as $L = [I \ 0]$ such that $Lu^i = [(u_1^i)^T (u_2^i)^T \dots (u_M^i)^T]^T$. By aggregating the data structures defined above into H , g , A , b , C , d , \bar{x} and \bar{x} ,

the optimization problem can be posed as a convex quadratic program in the standard form

$$\begin{aligned} & \text{minimize} \quad \frac{1}{2}x^T Hx + g^T x \\ & \text{subject to} \quad Ax = b, \quad Cx \leq d, \quad \underline{x} \leq x \leq \bar{x}, \end{aligned}$$

where $x = [u^T \quad x^T \quad z^T \quad \rho^T \quad v^T \quad \mu]^T$ is the optimization vector, and

$$H = 2 \begin{bmatrix} 0 & 0 & 0 & 0 & 0 & 0 \\ 0 & 0 & 0 & 0 & 0 & 0 \\ 0 & 0 & 0 & 0 & 0 & 0 \\ 0 & 0 & 0 & 0 & 0 & 0 \\ 0 & 0 & 0 & 0 & \tilde{\lambda}I & -\tilde{\lambda}\mathbf{1} \\ 0 & 0 & 0 & 0 & -\tilde{\lambda}\mathbf{1}^T & S\tilde{\lambda} \end{bmatrix}, \quad g = \begin{bmatrix} 0 \\ 0 \\ 0 \\ 0 \\ 0 \\ \lambda \end{bmatrix}.$$

In addition

$$C = \begin{bmatrix} 0 & 0 & I & -I & 0 & 0 \\ 0 & 0 & -I & -I & 0 & 0 \\ \tilde{\Lambda} & 0 & 0 & 0 & 0 & 0 \\ -\tilde{\Lambda} & 0 & 0 & 0 & 0 & 0 \end{bmatrix}, \quad d = \begin{bmatrix} z_{\text{max}} \\ -z_{\text{min}} \\ \Delta\tilde{u} \\ -\Delta\tilde{u} \end{bmatrix},$$

and

$$A = \begin{bmatrix} \tilde{B} & \tilde{A} & 0 & 0 & 0 & 0 \\ 0 & \tilde{C} & -I & 0 & 0 & 0 \\ \tilde{p}^T & 0 & 0 & \tilde{q}^T & -I & 0 \\ 0 & 0 & 0 & 0 & \frac{1}{S}\mathbf{1}^T & -I \\ \tilde{L} & 0 & 0 & 0 & 0 & 0 \end{bmatrix}, \quad b = \begin{bmatrix} -\tilde{w} \\ 0 \\ 0 \\ 0 \\ 0 \end{bmatrix}.$$

The lower and upper bounds are

$$\begin{aligned} \underline{x} &= [\tilde{u}^T \quad -\infty \quad -\infty \quad 0 \quad -\infty \quad -\infty]^T, \\ \bar{x} &= [\tilde{u}^T \quad \infty \quad \infty \quad \infty \quad \infty \quad \infty]^T. \end{aligned}$$

REFERENCES

- [1] S. J. Qin and T. A. Badgwell, "A survey of industrial model predictive control technology," *Control Engineering Practice*, vol. 11, no. 7, pp. 733–764, 2003.
- [2] J. B. Rawlings, "Tutorial overview of model predictive control," *IEEE Control Systems*, vol. 20, no. 3, pp. 38–52, 2000.
- [3] J. M. Maciejowski, *Predictive Control: With Constraints*, ser. Pearson Education. Prentice Hall, 2002.
- [4] D. Q. Mayne, J. B. Rawlings, C. V. Rao, and P. O. M. Scokaert, "Constrained model predictive control: Stability and optimality," *Automatica*, vol. 36, no. 6, pp. 789–814, 2000.
- [5] J. B. Rawlings and D. Q. Mayne, *Model Predictive Control: Theory and Design*. Nob Hill Publishing, 2009.
- [6] M. Diehl, R. Amrit, and J. B. Rawlings, "A Lyapunov Function for Economic Optimizing Model Predictive Control," *IEEE Transactions on Automatic Control*, vol. 56, no. 3, pp. 703–707, 2011.
- [7] L. Grüne, "Economic receding horizon control without terminal constraints," *Automatica*, vol. 49, no. 3, pp. 725–734, 2013.
- [8] J. B. Rawlings, D. Angeli, and C. N. Bates, "Fundamentals of economic model predictive control," in *2012 IEEE 51st Annual Conference on Decision and Control (CDC)*, 2012, pp. 3851–3861.
- [9] D. Angeli, R. Amrit, and J. B. Rawlings, "On Average Performance and Stability of Economic Model Predictive Control," *IEEE Transactions on Automatic Control*, vol. 57, no. 7, pp. 1615–1626, 2012.
- [10] J. B. Rawlings, D. Bonne, J. B. Jørgensen, A. N. Venkat, and S. B. Jørgensen, "Unreachable Setpoints in Model Predictive Control," *IEEE Transactions on Automatic Control*, vol. 53, no. 9, pp. 2209–2215, 2008.
- [11] L. E. Sokoler, G. Frison, K. Edlund, A. Skajaa, and J. B. Jørgensen, "A Riccati Based Homogeneous and Self-Dual Interior-Point Method for Linear Economic Model Predictive Control," in *2013 IEEE Multi-conference on Systems and Control*, 2013, pp. 592–598.
- [12] L. E. Sokoler, A. Skajaa, G. Frison, R. Halvgaard, and J. B. Jørgensen, "A Warm-Started Homogeneous and Self-Dual Interior-Point Method for Linear Economic Model Predictive Control," in *2013 IEEE 52th Annual Conference on Decision and Control (CDC)*, 2013, pp. 3677–3683.
- [13] R. Amrit, J. B. Rawlings, and L. T. Biegler, "Optimizing process economics online using model predictive control," *Computers & Chemical Engineering*, vol. 58, no. 0, pp. 334–343, 2013.
- [14] D. P. Bertsekas, "Dynamic Programming and Suboptimal Control: A Survey from ADP to MPC," *European Journal of Control*, vol. 11, no. 45, pp. 310–334, 2005.
- [15] —, *Dynamic Programming and Optimal Control*, 2nd ed. Athena Scientific, 2000.
- [16] G. Calafiore and L. Fagiano, "Robust Model Predictive Control via Scenario Optimization," *IEEE Transactions on Automatic Control*, vol. 58, no. 1, pp. 219–224, 2013.
- [17] G. C. Calafiore and L. Fagiano, "Stochastic model predictive control of LPV systems via scenario optimization," *Automatica*, vol. 49, no. 6, pp. 1861–1866, 2013.
- [18] J. Matusko and F. Borrelli, "Scenario-based approach to stochastic linear predictive control," in *2012 IEEE 51st Annual Conference on Decision and Control (CDC)*, 2012, pp. 5194–5199.
- [19] M. Prandini, S. Garatti, and J. Lygeros, "A randomized approach to Stochastic Model Predictive Control," in *2012 IEEE 51st Annual Conference on Decision and Control (CDC)*, 2012, pp. 7315–7320.
- [20] G. Schildbach, G. C. Calafiore, L. Fagiano, and M. Morari, "Randomized Model Predictive Control for stochastic linear systems," in *2012 American Control Conference (ACC)*, 2012, pp. 417–422.
- [21] G. Schildbach, L. Fagiano, C. Frei, and M. Morari, "The Scenario Approach for Stochastic Model Predictive Control with Bounds on Closed-Loop Constraint Violations," *Automatica*, p. Submitted, 2013.
- [22] A. Capolei, E. Suwartadi, B. Foss, and J. B. Jørgensen, "A Mean-Variance Objective for Robust Production Optimization in Uncertain Geological Scenarios," *Journal of Petroleum Science and Engineering*, p. Submitted, 2013.
- [23] R. Kalman, "A New Approach to Linear Filtering and Prediction Problems," *Transactions of the ASME, Journal of Basic Engineering*, vol. 82, no. Series D, pp. 35–45, 1960.
- [24] L. E. Sokoler, G. Frison, A. Skajaa, R. Halvgaard, and J. B. Jørgensen, "A Homogeneous and Self-Dual Interior-Point Linear Programming Algorithm for Economic Model Predictive Control," *IEEE Transactions on Automatic Control*, p. Submitted, 2013.
- [25] L. E. Sokoler, L. Standardi, K. Edlund, N. K. Poulsen, H. Madsen, and J. B. Jørgensen, "A Dantzig-Wolfe decomposition algorithm for linear economic model predictive control of dynamically decoupled subsystems," *Journal of Process Control*, vol. 24, no. 8, pp. 1225–1236, 2014.
- [26] M. C. Steinbach, "Markowitz Revisited: Mean-Variance Models in Financial Portfolio Analysis," *SIAM Review*, vol. 43, no. 1, pp. 31–85, 2001.
- [27] H. Markowitz, "Portfolio Selection," *The Journal of Finance*, vol. 7, no. 1, pp. 77–91, 1952.
- [28] J. R. Birge and F. Louveaux, *Introduction to Stochastic Programming*, ser. Springer Series in Operations Research and Financial Engineering. Springer, 2011.
- [29] P. Kall and J. Mayer, *Stochastic Linear Programming: Models, Theory, and Computation*, ser. International series in operations research & management science. Springer, 2010.
- [30] G. Prasath and J. B. Jørgensen, "Soft constraints for robust MPC of uncertain systems," in *7th IFAC International Symposium on Advanced Control of Chemical Processes*, 2009, pp. 225–230.
- [31] K. Edlund, T. Mølbak, and J. D. Bendtsen, "Simple models for model-based portfolio load balancing controller synthesis," in *6th IFAC Symposium on Power Plants and Power Systems Control*, 2009, pp. 173–178.
- [32] L. E. Sokoler, B. Dammann, H. Madsen, and J. B. Jørgensen, "A Decomposition Algorithm for Mean-Variance Economic Model Predictive Control of Stochastic Linear Systems," in *2014 IEEE Multi-conference on Systems and Control*, 2014, p. Accepted.

P A P E R G

A Decomposition Algorithm for Mean-Variance Economic Model Predictive Control of Stochastic Linear Systems

L. E. Sokoler, B. Dammann, H. Madsen, and J. B. Jørgensen. A Decomposition Algorithm for Mean-Variance Economic Model Predictive Control of Stochastic Linear Systems. In *IEEE Multi-conference on Systems and Control*, pages 1086–1093, 2014.

A Decomposition Algorithm for Mean-Variance Economic Model Predictive Control of Stochastic Linear Systems

Leo Emil Sokoler, Bernd Dammann, Henrik Madsen, and John Bagterp Jørgensen

Abstract—This paper presents a decomposition algorithm for solving the optimal control problem (OCP) that arises in Mean-Variance Economic Model Predictive Control of stochastic linear systems. The algorithm applies the alternating direction method of multipliers to a reformulation of the OCP that decomposes into small independent subproblems. We test the decomposition algorithm using a simple power management case study, in which the OCP is formulated as a convex quadratic program. Simulations show that the decomposition algorithm scales linearly in the number of uncertainty scenarios. Moreover, a parallel implementation of the algorithm is several orders of magnitude faster than state-of-the-art convex quadratic programming algorithms, provided that the number of uncertainty scenarios is large.

I. INTRODUCTION

Economic Model Predictive Control (EMPC) is a variation of MPC that aims at optimizing the economic performance of the controlled dynamic system [1]–[6]. At each sampling instant, the current state of the system is estimated, followed by the solution of an optimal control problem (OCP). The solution to the OCP yields an open-loop input trajectory that minimizes the predicted operating cost (maximizes profit) over a finite horizon. Only the first input in the open-loop input trajectory is applied to the controlled system, and the procedure is repeated in the next sampling instant. This way, a closed-loop input trajectory is synthesized using feedback.

When the controlled system is stochastic, the operating cost is generally uncertain. The most common way to overcome this issue is to replace random variables in the OCP with their mean value. This approach is known as Certainty Equivalence EMPC (CE-EMPC) [7], [8]. An advantage of CE-EMPC is that the OCP can be expressed in a standard deterministic form that (often) can be solved efficiently. However, disregarding the variance of the uncertain parameters may be economically inefficient [9], [10].

To include information about the probabilistic distribution of the operating cost in the OCP, [9] and [10] employ an objective function that trades off the expected operating cost and its variance. The cost expectation and the cost variance are estimated via sample scenarios of the uncertain parameters. This approach is referred to as Mean-Variance EMPC (MV-EMPC).

One of the main challenges in MV-EMPC is that the dimensions of the OCP solved online grow with the number

of uncertainty scenarios. Consequently, MV-EMPC may be intractable in real time for applications that require a large number of scenarios to achieve a well-behaved closed-loop performance. The novelty of this paper is an algorithm based on the Alternating Direction Method of Multipliers (ADMM) that decomposes the OCP arising in MV-EMPC of stochastic linear systems into small independent subproblems that can be solved in parallel. Each subproblem is related to a single uncertainty scenario and has the same dimensions as the OCP solved in CE-EMPC. Solving the subproblems in parallel reduces the time and memory requirements of MV-EMPC significantly.

Previously, ADMM has been combined with conventional deterministic MPC of dynamically coupled systems [11], [12], dynamically decoupled systems [13], as well as state and input-constrained MPC [14]–[17], and ℓ_1 -regularized MPC [18]. To the best of the authors' knowledge, no prior work has applied ADMM to solve the OCP that arises in stochastic variations of MPC. In particular, this paper presents the first decomposition algorithm for the OCP that occurs in MV-EMPC of stochastic linear systems.

We have organized the paper as follows. Section II provides a formal definition of MV-EMPC and demonstrates its application to stochastic linear systems. Section III introduces a decomposition algorithm based on ADMM, for solving the OCP associated with MV-EMPC. A MATLAB implementation of the decomposition algorithm, denoted `MVadmm`, is tested in Section IV using a simple power management case study. Section V concludes the paper.

II. MEAN-VARIANCE BASED ECONOMIC MPC

This section formalizes MV-EMPC and describes its application to stochastic linear systems.

A. Stochastic Linear Systems

We consider stochastic linear state space systems in the form

$$x_{k+1} = Ax_k + Bu_k + w_k, \quad (1a)$$

$$y_k = C_y x_k + v_k, \quad (1b)$$

$$z_k = C_z x_k, \quad (1c)$$

where (A, B, C_y, C_z) are the state space matrices, $x_k \in \mathbb{R}^{n_x}$ is the state vector, $u_k \in \mathbb{R}^{n_u}$ is the input vector, $y_k \in \mathbb{R}^{n_y}$ is the vector of measured outputs, $z_k \in \mathbb{R}^{n_z}$ is the vector of controlled variables, $w_k \in \mathbb{R}^{n_x}$ is the process noise vector, and $v_k \in \mathbb{R}^{n_y}$ is the vector of measurement noise. To keep the notation simple, the remainder of this paper assumes that the

The authors are with the Department of Applied Mathematics and Computer Science, Technical University of Denmark, DK-2800 Kgs. Lyngby, Denmark. L. E. Sokoler is also affiliated with DONG Energy, DK-2820 Gentofte, Denmark. Email: {leso, beda, hmad, jbjjo} at dtu.dk

current time step is $k = 0$. The estimate of the current state, $x_0 = \bar{x}_0$, is denoted \hat{x}_0 .

B. Cost Function

Let $\mathcal{N}_i = \{0 + i, 1 + i, \dots, N - 1 + i\}$, with N being the length of the prediction and control horizon. Also introduce the vectors

$$u = [u_0^T \quad u_1^T \quad \dots \quad u_{N-1}^T]^T, \quad x = [x_1^T \quad x_2^T \quad \dots \quad x_N^T]^T,$$

and similarly define z and w . Moreover, define the cost function

$$\Psi_{\text{eco}}(u; \bar{x}_0, w) = \{\phi(u, x, z) | x_0 = \bar{x}_0, \\ x_{k+1} = Ax_k + Bu_k + w_k, z_{k+1} = Cx_{k+1}, k \in \mathcal{N}_0\}, \quad (2)$$

which measures the cost (or negative profit) of operating the system (1) in the following N time steps. The function ϕ can, for example, include an input cost, an input rate cost, an output cost, a tracking error cost, and a cost of violating soft output constraints.

Generally, the initial state, \bar{x}_0 , and the process noise, w , are random variables. The system operating cost, $\Psi_{\text{eco}} = \Psi_{\text{eco}}(u; \bar{x}_0, w)$, is therefore a random variable as well. MV-EMPC provides a way to select u that trades off the expected value of Ψ_{eco} and its variance.

For simplicity, it is assumed throughout this paper that the initial state, \bar{x}_0 , is known, i.e. that the current state estimate, \hat{x}_0 , is perfect. This simplifies notation considerably. The results extend to the case with uncertain initial state in a straightforward way.

C. Optimal Control Problem

In MV-EMPC, the OCP objective function approximates the criterion

$$\Psi_{\text{MV}} = \lambda E_w[\Psi_{\text{eco}}] + (1 - \lambda) \text{Var}_w[\Psi_{\text{eco}}], \quad (3)$$

where $\lambda \in [0, 1]$ is a risk aversion parameter that determines the trade-off between the expected cost and the cost variance [9], [10].

Explicit expressions of the expected value, $E_w[\Psi_{\text{eco}}]$, and the variance, $\text{Var}_w[\Psi_{\text{eco}}]$, are usually not available. For this reason, their sample estimates are introduced

$$E_w[\Psi_{\text{eco}}] \approx \mu = \frac{1}{S} \sum_{i \in \mathcal{S}} \Psi_{\text{eco}}(u; \hat{x}_0, w^i), \quad (4a)$$

$$\text{Var}_w[\Psi_{\text{eco}}] \approx s^2 = \frac{1}{S-1} \sum_{i \in \mathcal{S}} (\Psi_{\text{eco}}(u; \hat{x}_0, w^i) - \mu)^2, \quad (4b)$$

where w^i is sampled from the distribution of w and $\mathcal{S} = \{1, 2, \dots, S\}$.

Provided that the number of scenarios, S , is large, then

$$\Psi_{\text{MV}} \approx \tilde{\Psi}_{\text{MV}} = \lambda \mu + (1 - \lambda) s^2. \quad (5)$$

The open-loop input trajectory in MV-EMPC is defined as the trajectory, $u_{\text{MV}}^* \in \mathcal{U}$, that minimizes (5). Here \mathcal{U} is some input constraint set representing e.g. input limits and input-rate limits.

For the stochastic linear system (1), $u^* = u_{\text{MV}}^*$ can be expressed as (a part of) the solution to the OCP

$$\underset{u \in \mathcal{U}, \{\psi^j, z^j, \psi^j\}_{j=1}^S, \mu}{\text{minimize}} \quad \lambda \mu + \tilde{\lambda} \sum_{j \in \mathcal{S}} (\psi^j - \mu)^2, \quad (6a)$$

$$\text{subject to} \quad (x^j, u, z^j) \in \mathcal{X}(\hat{x}_0, w^j), \quad i \in \mathcal{S}, \quad (6b)$$

$$\psi^j = \phi(u, x^j, z^j), \quad i \in \mathcal{S}, \quad (6c)$$

$$\mu = \frac{1}{S} \sum_{j \in \mathcal{S}} \psi^j, \quad (6d)$$

where $\tilde{\lambda} = (1 - \lambda)/(S - 1)$, and

$$\mathcal{X}(\hat{x}_0, w) = \{(x, u, z) | x_0 = \hat{x}_0, \\ x_{k+1} = Ax_k + Bu_k + w_k, z_{k+1} = Cx_{k+1}, k \in \mathcal{N}_0\}. \quad (7)$$

In [9], a two-stage extension of the problem (6) is introduced. The extended problem is

$$\underset{\{u^j \in \mathcal{U}, x^j, z^j, \psi^j\}_{j=1}^S, \mu}{\text{minimize}} \quad \lambda \mu + \tilde{\lambda} \sum_{j \in \mathcal{S}} (\psi^j - \mu)^2, \quad (8a)$$

subject to

$$(x^j, u^j, z^j) \in \mathcal{X}(\hat{x}_0, w^j), \quad i \in \mathcal{S}, \quad (8b)$$

$$\psi^j = \phi(u^j, x^j, z^j), \quad i \in \mathcal{S}, \quad (8c)$$

$$\mu = \frac{1}{S} \sum_{j \in \mathcal{S}} \psi^j, \quad (8d)$$

$$u_k^j = u_k^i, \quad i, j \in \mathcal{S}, k \in \mathcal{M}. \quad (8e)$$

where $\mathcal{M} = \{0, 1, \dots, M\}$ and $M \leq N$. The formulation (8) uses scenario-dependent input variables, $u^i \in \mathcal{U}$, to account for the fact that recourse exists in the future, i.e. that MV-EMPC applies the open-loop input trajectory to the controlled system in a receding horizon manner. This results in a less conservative controller and may reduce both cost variance and cost expectation in closed-loop operation [9].

The OCP (8) is a convex optimization problem when \mathcal{U} is a convex set, and ϕ is an affine function. If the equality constraint (8c) is replaced by the inequality constraint

$$\psi^j \geq \phi(u^j, x^j, z^j), \quad i \in \mathcal{S}, \quad (9)$$

the requirement on ϕ can be loosened to convexity. Using the relaxed condition (9) is attractive since it can handle a large variety of cost functions, while preserving convexity of the overall problem.

The solution to (8), and the solution obtained under the relaxed condition (9), often differ only for very small values of λ [9]. In most practical applications, these high-cost/low-variance solutions are disregarded, since accepting a small increase in the variance (increasing λ by a small amount) leads to a large cost reduction [19], [20].

The remainder of this paper describes an efficient algorithm for solving the problem (8) under the relaxed condition (9). It is assumed that \mathcal{U} is a convex set, and that ϕ is a convex function.

Remark 1: We can regard the extended problem (8) as a two-stage stochastic optimization problem. In the first stage ($k = 0, 1, \dots, M$), (8e) requires that the inputs, u_k^i , are equal

in all the scenarios, $i \in \mathcal{S}$. In the second stage ($k > M$), the inputs adapt to the uncertainty scenarios, w^i , assuming that w_k^i are known for $k > M$. Note that (6) is a special case of (8) with $M = N$ (no second stage). The OCP solved in CE-EMPC is the special case of (6), in which $S = 1$ and $w^1 = E_w[w]$.

III. DECOMPOSITION ALGORITHM

In this section, we present an ADMM-based decomposition algorithm for solving the OCP (8) under the relaxed condition (9). The algorithm is first presented in a general ADMM form, which is thereafter specialized to the specific problem structure. It is outside the scope of this paper to give a detailed description of ADMM. For details and proofs, we therefore refer to [21]–[23].

A. Variable Splitting

In a compact form (8), under the condition (9), may be written as

$$\underset{u \in \mathcal{U}, x, z, \psi, \mu}{\text{minimize}} \quad \lambda \mu + \tilde{\lambda} \psi^T \psi + S \tilde{\lambda} \mu^2 - 2 \tilde{\lambda} \mu^T \psi, \quad (10a)$$

$$\text{subject to} \quad \tilde{A}x + \tilde{B}u + \tilde{w} = 0, \quad (10b)$$

$$z = \tilde{C}x \quad (10c)$$

$$\psi \geq \tilde{\phi}(u, x, z), \quad (10d)$$

$$\mu = \mathbf{1}^T \psi / S \quad (10e)$$

$$\tilde{L}u = 0, \quad (10f)$$

where we have used the data structures defined in Appendix I.

We transform the optimization problem (10), into the following ADMM form

$$\underset{y_1, y_2}{\text{minimize}} \quad f_1(y_1) + f_2(y_2), \quad (11a)$$

$$\text{subject to} \quad M_1 y_1 + M_2 y_2 = 0, \quad (11b)$$

where the optimization variables are

$$y_1 = [\tilde{u}^T \quad x^T \quad z^T \quad \tilde{\psi}^T \quad \tilde{\mu}^T]^T, \quad (12a)$$

$$y_2 = [u^T \quad \psi^T \quad \mu^T]^T. \quad (12b)$$

Problem (10) is thus split into two different parts. The auxiliary variables $\tilde{\mu}$, \tilde{u} and $\tilde{\psi}$, are introduced to formulate each part of the optimization problem in a way that allows exploitation of the problem structure in an efficient way.

The problem data in (11) are

$$g = [0 \quad 0 \quad 0 \quad 0 \quad \lambda]^T, H = \begin{bmatrix} 0 & 0 & 0 \\ 0 & \tilde{\lambda}I & -\tilde{\lambda}\mathbf{1}^T \\ 0 & -\tilde{\lambda}\mathbf{1} & S\tilde{\lambda} \end{bmatrix}, \quad (13)$$

and

$$M_1 = \begin{bmatrix} 0 & 0 & 0 & 0 & 1 \\ 0 & 0 & 0 & 0 & 1 \\ I & 0 & 0 & 0 & 0 \\ 0 & 0 & 0 & I & 0 \end{bmatrix}, M_2 = \begin{bmatrix} 0 & -\frac{\mathbf{1}^T}{S} & 0 \\ 0 & 0 & -1 \\ -I & 0 & 0 \\ 0 & -I & 0 \end{bmatrix}. \quad (14)$$

In (13)-(14), $\mathbf{1}$ is a vector of all ones. The functions f_1 and f_2 are convex, with

$$f_1(y_1) = g^T y_1 + I_{\mathbb{Y}_1}(y_1), \quad (15a)$$

$$f_2(y_2) = y_2^T H y_2 + I_{\mathbb{Y}_2}(y_2), \quad (15b)$$

where $I_{\mathbb{A}}$ is the indicator function of a set \mathbb{A} , and

$$\mathbb{Y}_1 = \{y_1 | \tilde{A}x + \tilde{B}u + \tilde{w} = 0, z = \tilde{C}x, \tilde{\psi} \geq \tilde{\phi}(\tilde{u}, x, z)\}, \quad (16a)$$

$$\mathbb{Y}_2 = \{y_2 | \tilde{L}u = 0\}. \quad (16b)$$

B. Recursion Formulas

The Lagrangian of (11) is

$$\mathcal{L}(y_1, y_2, \zeta) = f_1(y_1) + f_2(y_2) + \zeta^T (M_1 y_1 + M_2 y_2), \quad (17)$$

where ζ is a vector of Lagrange multipliers (dual variables) associated with the constraint (11b).

A stationary point of the Lagrangian, (y_1^*, y_2^*, ζ^*) , satisfies

$$0 \in \partial_{y_1} \mathcal{L}(y_1^*, y_2^*, \zeta^*) = \partial f_1(y_1^*) + M_1^T \zeta^*, \quad (18a)$$

$$0 \in \partial_{y_2} \mathcal{L}(y_1^*, y_2^*, \zeta^*) = \partial f_2(y_2^*) + M_2^T \zeta^*, \quad (18b)$$

where ∂ is the subdifferential operator. Hence, the necessary and sufficient optimality conditions of (11) may be stated as the primal feasibility condition, $M_1 y_1 + M_2 y_2 = 0$, and the stationarity condition (18).

In ADMM, a point satisfying the optimality conditions for (11), is obtained via the recursions

$$\begin{aligned} y_1(j+1) &= \arg \min_{y_1} \mathcal{L}_\rho(y_1, y_2(j), \zeta(j)) \\ &= \arg \min_{y_1} f_1(y_1) + \frac{\rho}{2} \|M_1 y_1 + M_2 y_2(j) + \eta(j)\|_2^2, \end{aligned} \quad (19a)$$

$$\begin{aligned} y_2(j+1) &= \arg \min_{y_2} \mathcal{L}_\rho(y_1(j+1), y_2, \zeta(j)) \\ &= \arg \min_{y_2} f_2(y_2) + \frac{\rho}{2} \|M_1 y_1(j+1) + M_2 y_2 + \eta(j)\|_2^2, \end{aligned} \quad (19b)$$

$$\eta(j+1) = \eta(j) + (M_1 y_1(j+1) + M_2 y_2(j+1)), \quad (19c)$$

in which $\mathcal{L}_\rho(y_1, y_2, \zeta) = \mathcal{L}(y_1, y_2, \zeta) + \frac{\rho}{2} \|M_1 y_1 + M_2 y_2\|_2^2$ is the augmented Lagrangian, with penalty parameter $\rho > 0$. Note that j indicates the iteration number. The final expressions in (19) are written in terms of the scaled dual variable $\eta = \frac{1}{\rho} \zeta$. This is done to achieve a more compact notation.

A stopping criterion for an algorithm based on (19) is

$$\|M_1 y_1(j) + M_2 y_2(j)\|_2 \leq \varepsilon_P, \quad (20a)$$

$$\rho \|M_1^T M_2(y_2(j+1) - y_2(j))\|_2 \leq \varepsilon_D. \quad (20b)$$

where ε_P and ε_D are small user defined tolerance levels. The conditions (20) test for primal and dual feasibility (in an absolute sense) of the updated values in (19). Accordingly, the algorithm can be stopped when the necessary and sufficient optimality conditions for (11) are satisfied with a certain level of accuracy.

Remark 2: To speed up convergence of the ADMM recursions (19), $M_1 y_1(j+1)$ can be replaced by $\alpha M_1 y_1(j+1) - (1-\alpha) M_2 y_2(j)$, in the recursions for y_2 , (19b), and η ,

(19c), where $\alpha \in [0, 2]$ is a relaxation parameter [22], [24]. Adaptive updating strategies for the penalty parameter, ρ , are proposed in [25], [26]. We also remark that it is often convenient to extend the stopping criterions (20), to include a relative optimality measure [22].

C. Problem Structure

The following results provide an efficient way to exploit the problem structure (13)-(14), in an implementation of the ADMM recursions (19).

We write the scaled dual variable η , as

$$\eta = [\eta_1^T \quad \eta_2^T \quad \eta_3^T \quad \eta_4^T]^T,$$

such that each of its components are associated with a particular set of constraints in (11b); η_1 is associated with the constraint $\tilde{\mu} = \mathbf{1}^T \psi / S$, η_2 is associated with the constraint $\tilde{\mu} = \mu$, η_3 is associated with the constraint $\tilde{u} = u$, and η_4 is associated with the constraint $\tilde{\psi} = \psi$. The dual variables η_3 and η_4 , are further split into the components

$$\begin{aligned} \eta_3 &= [(\eta_3^1)^T \quad (\eta_3^2)^T \quad \dots \quad (\eta_3^S)^T]^T, \\ \eta_4 &= [(\eta_4^1)^T \quad (\eta_4^2)^T \quad \dots \quad (\eta_4^S)^T]^T, \end{aligned}$$

where η_3^i and η_4^i are associated with the constraints $\tilde{u}^i = u^i$ and $\tilde{\psi}^i = \psi^i$, respectively.

Proposition 1 shows that the update of $y_1 = (\tilde{u}, x, z, \tilde{\psi}, \tilde{\mu})$, (19a), can be performed by solving S small independent optimization problems. The number of constraints and the number of variables in each subproblem is reduced by a factor of S , compared to a naive approach that handles the y_1 -update in a centralized manner. Proposition 2 states that the update of $y_2 = (u, \psi, \mu)$, (19b), can be split into an optimization problem in u , and an optimization problem in (ψ, μ) . Proposition 3 and Proposition 4 demonstrate that both problems have simple closed form solutions.

Proposition 1: The ADMM update of $y_1 = (\tilde{u}, x, z, \tilde{\psi}, \tilde{\mu})$, (19a), can be performed by, for each $i \in \mathcal{S}$, solving the subproblem

$$\underset{\tilde{u}^i \in \mathcal{U}, x^i, z^i, \tilde{\psi}^i}{\text{minimize}} \quad \frac{1}{2} ((\tilde{u}^i)^T \tilde{u}^i + (\tilde{\psi}^i)^T \tilde{\psi}^i) + (m_3^i)^T \tilde{u}^i + m_4^i \tilde{\psi}^i \quad (21a)$$

subject to

$$\tilde{A}x^i + \tilde{B}\tilde{u}^i + \tilde{w}^i = 0, z^i = \tilde{C}x^i, \quad (21b)$$

$$\tilde{\psi}^i \geq \phi(\tilde{u}^i, x^i, z^i), \quad (21c)$$

and computation of

$$\tilde{\mu}^* = -\frac{1}{2\rho} ((m_1 + m_2)\rho + \lambda), \quad (22)$$

where

$$m = \begin{bmatrix} m_1 \\ m_2 \\ m_3 \\ m_4 \end{bmatrix} = M_2 y_2(j) + \eta(j) = \begin{bmatrix} \mathbf{1}^T \psi(j) \\ -\mu(j) \\ -u(j) \\ -\psi(j) \end{bmatrix} + \begin{bmatrix} \eta_1(j) \\ \eta_2(j) \\ \eta_3(j) \\ \eta_4(j) \end{bmatrix},$$

with $m_3^i = -u^i(j) + \eta_3^i(j)$ and $m_4^i = -\psi^i(j) + \eta_4^i(j)$.

Proof: The update of y_1 , (19a), may be expressed as the solution to the optimization problem

$$\underset{y_1 \in \mathbb{Y}_1}{\text{minimize}} \quad g^T y_1 + \frac{\rho}{2} \|M_1 y_1 + m\|_2^2, \quad (23)$$

which follows directly from the definition of f_1 , (15a). Using the fact that \tilde{A} , \tilde{B} and \tilde{C} , are block diagonal (see Appendix I), and the definition of $\tilde{\phi}$, (42), $y_1 \in \mathbb{Y}_1$ can be stated as (21b)-(21c), for each $i \in \mathcal{S}$. Inserting the expressions of g , M_1 , (13)-(14), and y_1 , (12a), in the objective function of (23), gives

$$\begin{aligned} g^T y_1 + \frac{\rho}{2} \|M_1 y_1 + m\|_2^2 &= \lambda \tilde{\mu} + \frac{\rho}{2} ((y_1^T M_1^T + 2m^T) M_1 y_1) + d \\ &= \Theta + \rho \tilde{\mu}^2 + ((m_1 + m_2)\rho + \lambda) \tilde{\mu} + d, \end{aligned} \quad (24)$$

where d represents a constant term, and Θ is the sum

$$\Theta = \frac{\rho}{2} \sum_{i \in \mathcal{S}} [(\tilde{u}^i)^T \tilde{u}^i + (\tilde{\psi}^i)^T \tilde{\psi}^i + 2((m_3^i)^T \tilde{u}^i + (m_4^i)^T \tilde{\psi}^i)].$$

The constant term d can be left out of (23), as it does not change the optimal solution to the optimization problem. The variable $\tilde{\mu}$ is unconstrained, and independent of all other variables in (24). Setting the derivative of (24) with respect to $\tilde{\mu}$ equal to zero, and solving for $\tilde{\mu}$, gives the optimal value (22). For fixed, $\tilde{\mu} = \tilde{\mu}^*$, (24) is separable in $i \in \mathcal{S}$. As both the constraints and the objective function of (23) are separable in the uncertainty scenarios, the problem can be decomposed into S independent subproblems in the form (21). ■

Proposition 2: The ADMM update of $y_2 = (u, \psi, \mu)$, (19b), may be split into the constrained minimization problem in u

$$\underset{u \in \{u | \tilde{L}u = 0\}}{\text{minimize}} \quad \frac{1}{2} \rho u^T u - \rho n_3^T u, \quad (25)$$

and the unconstrained minimization problem in (ψ, μ)

$$\underset{\psi, \mu}{\text{minimize}} \quad \psi^T \Upsilon \psi + \omega \mu^2 - 2\tilde{\lambda} \mathbf{1}^T \mu \psi - \rho n_2 \mu, \quad (26)$$

where $\Upsilon = \tilde{\lambda} I + \frac{1}{2} \rho ((1/S^2) \mathbf{1} \mathbf{1}^T + I)$, $\omega = S\tilde{\lambda} + \frac{1}{2} \rho$, $\delta = \frac{1}{2} \rho (-2/Sn_1 \mathbf{1} - 2n_4)$, and

$$n = \begin{bmatrix} n_1 \\ n_2 \\ n_3 \\ n_4 \end{bmatrix} = M_1 y_1(j+1) + \eta(j) = \begin{bmatrix} \tilde{\mu}(j+1) \\ \tilde{\mu}(j+1) \\ \tilde{u}(j+1) \\ \tilde{\psi}(j+1) \end{bmatrix} + \begin{bmatrix} \eta_1(j) \\ \eta_2(j) \\ \eta_3(j) \\ \eta_4(j) \end{bmatrix},$$

with $n_3^i = \tilde{u}^i(j+1) + \eta_3^i(j)$ and $n_4^i = \tilde{\psi}^i(j+1) + \eta_4^i(j)$.

Proof: The update of y_2 , (19b), can be expressed as the solution to the optimization problem

$$\underset{y_2 \in \mathbb{Y}_2}{\text{minimize}} \quad y_2^T H y_2 + \frac{\rho}{2} \|M_2 y_2 + n\|_2^2, \quad (27)$$

which follows directly from the definition of f_2 , (15b). Moreover, (16b) shows that constraint, $y_2 \in \mathbb{Y}_2$, is equivalent to $u \in \{u | \tilde{L}u = 0\}$. Inserting the definitions of H , M_2 , (13)-(14), and y_2 , (12b), in the objective function of (27), gives

$$\begin{aligned} y_2^T H y_2 + \frac{\rho}{2} \|M_2 y_2 + n\|_2^2 &= \frac{1}{2} \rho u^T u + \psi^T \Upsilon \psi + \omega \mu^2 \\ &\quad - 2\tilde{\lambda} \mathbf{1}^T \mu \psi - \rho n_2 \mu - \rho n_3^T u + d. \end{aligned}$$

where d is a constant term. As this expression involves no cross terms in u and (ψ, μ) , and since (ψ, μ) are unconstrained, (27) can be split into the constrained minimization problem in u (25), and the unconstrained minimization problem in (ψ, μ) (26). ■

Proposition 3: The analytical solution of (25) is

$$(\bar{u}^1)^* = (\bar{u}^2)^* = \dots = (\bar{u}^S)^* = \frac{1}{S} \sum_{i \in \mathcal{S}} \bar{n}_3^i, \quad (28a)$$

$$(\hat{u}^i)^* = \hat{n}_3^i, \quad i \in \mathcal{S}, \quad (28b)$$

where $u^i = [(\bar{u}^i)^T \quad (\hat{u}^i)^T]^T$, for $i \in \mathcal{S}$, such that

$$\bar{u}^i = [(u_1^i)^T \quad (u_2^i)^T \quad \dots \quad (u_M^i)^T]^T, \\ \hat{u}^i = [(u_{M+1}^i)^T \quad (u_{M+2}^i)^T \quad \dots \quad (u_N^i)^T]^T,$$

i.e. \bar{u}^i consists of the first M inputs in the open-loop input trajectory, u^i , and \hat{u}^i consists of the remaining $N - M$ inputs (we use a similar notation for n_3).

Proof: Inserting the definitions of \bar{u}^i and \hat{u}^i , in the objective function of (25) gives

$$\frac{1}{2} \rho u^T u - \rho n_3^T u = \frac{\rho}{2} \sum_{i \in \mathcal{S}} \|u^i - \bar{n}_3^i\|_2^2 + d \\ = \frac{\rho}{2} \sum_{i \in \mathcal{S}} [\|\bar{u}^i - \bar{n}_3^i\|_2^2 + \|\hat{u}^i - \hat{n}_3^i\|_2^2] + d. \quad (29)$$

Definition (43) implies that the constraint $\bar{L}u = 0$ can be stated as $Lu^1 = Lu^2 = \dots = Lu^S$. Since $Lu^i = \bar{u}^i$, this is equivalent to $\bar{u} = \bar{u}^1 = \bar{u}^2 = \dots = \bar{u}^S$. By inserting $\bar{u} = \bar{u}^i$ for each $i \in \mathcal{S}$, in (25), the constraint $\bar{L}u = 0$ can therefore be eliminated. After eliminating the constraint, the optimization problem is stated as

$$\text{minimize}_{\bar{u}, \{\hat{u}^i\}_{i=1}^S} \sum_{i \in \mathcal{S}} \|\bar{u} - \bar{n}_3^i\|_2^2 + \|\hat{u}^i - \hat{n}_3^i\|_2^2, \quad (30)$$

where we have scaled the objective function by 2ρ and removed the constant term, d . Equation (30) is an unconstrained convex quadratic program. Setting the gradient of the objective function equal to zero, and solving for \bar{u} and $\{\hat{u}^i\}_{i=1}^S$ yields $(\hat{u}^i)^* = \hat{n}_3^i$ for $i \in \mathcal{S}$ and $\bar{u}^* = \frac{1}{S} \sum_{i \in \mathcal{S}} \bar{n}_3^i$. Since $\bar{u}^* = (\bar{u}^1)^* = (\bar{u}^2)^* = \dots = (\bar{u}^S)^*$, the result (28) follows. ■

Proposition 4: The solution of (26) can be obtained by first computing

$$\psi^* = \frac{(\gamma_1 + S\gamma_2)I - \gamma_2 \mathbf{1}\mathbf{1}^T}{\gamma_1(S\gamma_2 + \gamma_1)} (\rho \tilde{\lambda} \mathbf{1} n_2 - \omega \delta) \\ = \theta_2 \left[\mathbf{1} \left(\gamma_2 \omega \mathbf{1}^T \delta + (\theta_1 \rho - \gamma_2 \rho S) \tilde{\lambda} n_2 \right) - \theta_1 \omega \delta \right], \quad (31)$$

and subsequent computation of

$$\mu^* = \frac{2\tilde{\lambda} \mathbf{1}^T \psi^* + n_2 \rho}{2\omega}, \quad (32)$$

in which $\gamma_1 = \omega(2\tilde{\lambda} + \rho)$, $\gamma_2 = (\omega\rho/S^2 - 2\tilde{\lambda}^2)$, $\theta_1 = S\gamma_2 + \gamma_1$, and $\theta_2 = 1/(\gamma_1 \theta_1)$.

Proof: Equation (26) is an unconstrained convex quadratic program. The result (32) is obtained by setting the derivative of the objective function with respect to μ equal to zero and solving for μ . Inserting the expression for μ

Algorithm 1 ADMM-based decomposition algorithm for the two-stage OCP, (8)-(9), that arises in MV-EMPC

```

while not converged do
  // ADMM update of  $y_1 = (\check{u}, x, z, \check{\psi}, \check{\mu})$ 
  for  $i \in \mathcal{S}$  do
     $(\check{u}^i, x^i, z^i, \check{\psi}^i) \leftarrow$  compute via (21)
  end for
   $\check{\mu}^* \leftarrow$  compute via (22) [O(1)]
  // ADMM update of  $y_2 = (u, \psi, \mu)$ 
   $u \leftarrow$  compute via (28) [O(SMn_u)]
   $\psi \leftarrow$  compute via (31) [O(S)]
   $\mu \leftarrow$  compute via (32) [O(S)]
  // ADMM update of  $\eta$ 
   $\eta \leftarrow$  compute via (19c) [O(2 + SNn_u + 2S)]
end while

```

back into the objective function of (26), yields the reduced optimization problem

$$\text{minimize}_{\psi} \psi^T (\omega Y - \tilde{\lambda}^2 \mathbf{1}\mathbf{1}^T) \psi + (\omega \delta - \rho \tilde{\lambda} \mathbf{1} n_2)^T \psi.$$

Setting the derivative of the objective function equal to zero, results in the linear system of equations

$$2(\omega Y - \tilde{\lambda}^2 \mathbf{1}\mathbf{1}^T) \psi^* = \rho \tilde{\lambda} \mathbf{1} n_2 - \omega \delta. \quad (33)$$

The matrix to be inverted in solving this system can be written as

$$2(\omega Y - \tilde{\lambda}^2 \mathbf{1}\mathbf{1}^T) = \omega(2\tilde{\lambda} + \rho)I + (\omega\rho/S^2 - 2\tilde{\lambda}^2) \mathbf{1}\mathbf{1}^T \\ = \gamma_1 I + \gamma_2 \mathbf{1}\mathbf{1}^T, \quad (34)$$

where we have used the definitions of Y , γ_1 , and γ_2 . Using the Sherman-Morrison formula [27] to invert a matrix in the form (34), i.e. the sum of a diagonal matrix plus a rank one matrix, gives

$$(\gamma_1 I + \gamma_2 \mathbf{1}\mathbf{1}^T)^{-1} = \frac{1}{\gamma_1} I - \frac{\frac{1}{\gamma_1} \gamma_2 \mathbf{1}\mathbf{1}^T \frac{1}{\gamma_1}}{1 + \frac{\gamma_2}{\gamma_1} \mathbf{1}^T \mathbf{1}} = \frac{(\gamma_1 + S\gamma_2)I - \gamma_2 \mathbf{1}\mathbf{1}^T}{\gamma_1(S\gamma_2 + \gamma_1)}.$$

This shows that ψ^* can be determined via (31). ■

D. Summary

Algorithm 1 summarizes an implementation of the ADMM recursions (19) based on Proposition 1-4. As indicated, the algorithm scales linearly in the number of scenarios, S . The main computational bottleneck in Algorithm 1 is solving S subproblems in the form (21). The dimensions of each subproblem do not depend on S . In comparison, the number of constraints and the number of variables in the full OCP (10) grow linearly with S .

Remark 3: Algorithm 1 solves S subproblems in the form (21) in every iteration. A significant speed-up can be achieved by solving the subproblems in parallel, and by warm-starting the optimization method that solves the subproblems. Utilizing the high degree of structure in the subproblems may also reduce the computational effort [13], [16], [28]–[33].

IV. CASE STUDY

This section compares a MATLAB implementation of Algorithm 1, `MVadmm`, against `MOSEK`, `Gurobi` and `CPLEX`. These state-of-the-art convex optimization algorithms solve the OCP (10) directly using standard tolerance specifications. We let `MVadmm` run 500 iterations. It has been verified that the solution obtained after 500 iterations satisfies the primal and dual residual criteria (20) with at least $\varepsilon_P = \varepsilon_D = 0.01$ in all our simulations. Remark 2 provides suggestions for reducing the number of iterations. The subproblems (21) are solved by `CVXGEN`. The simulations are performed on an Intel(R) Core(TM) i5-2520M CPU @ 2.50GHz with 4 GB RAM running a 64-bit Ubuntu 12.04.1 LTS operating system.

A. System Definition

We consider a third order transfer function model introduced in [34] to describe the power production of a thermal power plant. The model is

$$Y(s) = \frac{1}{(\tau s + 1)^3} (U(s) + W(s)) + V(s), \quad (35a)$$

$$Z(s) = \frac{1}{(\tau s + 1)^3} (U(s) + W(s)), \quad (35b)$$

where $U(s)$ is the power reference (input), $Y(s)$ is the measured power production (measured output), $Z(s)$ is the actual power production (controlled variable), $W(s)$ is the process noise, and $V(s)$ is the measurement noise. The transfer function model (35) is converted to a discrete state space model of the form (1) using a sampling time of $T_s = 5$ seconds. We assume that the input constraint set, \mathcal{U} , limits the power reference, u_k , and changes in the power reference, $\Delta u_k = u_k - u_{k-1}$, such that

$$\mathcal{U} = \{u | u_k \leq u_k \leq \bar{u}_k, \Delta u_k \leq \Delta u_k \leq \Delta \bar{u}_k, k \in \mathcal{N}_0\}, \quad (36)$$

B. Cost Function

The case study cost function is defined as in (2) with

$$\phi(u, z) = \sum_{k \in \mathcal{N}_0} c_k^T u_k + \sum_{k \in \mathcal{N}_1} q_k^T ((z_k^i - z_k)_+ + (z_k - \bar{z}_k)_+), \quad (37)$$

where subscript $+$ refers to the non-negative part of a vector, i.e. $v_+ = \max\{0, v_i\}$ for $i = 1, 2, \dots, n_v$, with $v \in \mathbb{R}^{n_v}$. The input price, c_k , can be interpreted as the fuel cost, and q_k can be interpreted as the cost of buying power in the electricity market.

Using (37) leads to ADMM subproblems (21) with the following cost constraint

$$\Psi^i \geq \sum_{k \in \mathcal{N}_0} c_k^T \tilde{u}_k^i + \sum_{k \in \mathcal{N}_1} q_k^T ((z_k^i - z_k)_+ + (z_k^i - \bar{z}_k)_+), \quad (38)$$

for each $i \in \mathcal{S}$. As in [9], we replace this set of non-linear constraints by

$$\Psi^i \geq \sum_{k \in \mathcal{N}_0} c_k^T \tilde{u}_k^i + q_{k+1}^T \beta_{k+1}^i, \quad i \in \mathcal{S}, \quad (39a)$$

$$\bar{z}_k - \beta_k^i \leq z_k^i \leq \bar{z}_k + \beta_k^i, \quad k \in \mathcal{N}_1, \quad i \in \mathcal{S}, \quad (39b)$$

$$\beta_k^i \geq 0, \quad k \in \mathcal{N}_1, \quad i \in \mathcal{S}, \quad (39c)$$

TABLE I

CASE STUDY CONTROLLER AND SYSTEM PARAMETERS									
p_k	q_k	u_k	\bar{u}_k	Δu_k	$\Delta \bar{u}_k$	z_k	\bar{z}_k	τ	N
1	20	0	10	-3	3	5	6	10	40

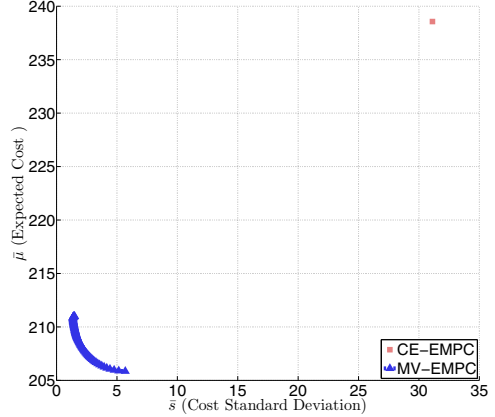


Fig. 1. Open-loop efficient frontier for $\lambda = [0, 1]$. The efficient frontier is obtained by solving (10) with $S = 2048$ uncertainty scenarios.

where β_k^i are auxiliary optimization variables. Similarly, a vector representation of (39) is introduced to replace the cost function constraint (10d) in the full formulation of the OCP (10). The resulting optimization problem is a convex quadratic program. Replacing the non-linear constraint (38) by the convex constraints (39) yields a good approximation for non-zero values of λ . For details, we refer to [9].

C. Case Study Parameters

Table I lists the case study system and controller parameters. The parameters are kept constant for all k . The process noise and the measurement noise are uncorrelated, and normally distributed with $w_k \sim N_{iid}(0, 0.25I)$ and $v_{k+1} \sim N_{iid}(0, 0.01)$, for $k \in \mathcal{N}_0$.

D. Simulations

First consider a situation without feedback. We use $M = N$ in (8e) to represent that no recourse exists in the future. Let $\bar{\mu}$ and \bar{s} denote the open-loop cost expectation and its standard deviation. These values are computed via the sample estimates (4). We use different scenarios of w to compute $\bar{\mu}$ and \bar{s} , and in solving (10). Fig. 1 shows a plot of the expected cost, $\bar{\mu}$, as a function of the standard deviation, \bar{s} , i.e. the efficient frontier [19]. To compute the frontier, we have solved (10) with $S = 2048$ uncertainty scenarios, and λ values in the range $[0, 1]$. Fig. 1 shows that MV-EMPC reduces both cost variance and cost expectation in open-loop, compared to CE-EMPC. Each point on the graph associated with MV-EMPC provides a different mean-variance trade-off option. The rightmost point corresponds to $\lambda = 1$ and the leftmost point corresponds to $\lambda = 0$.

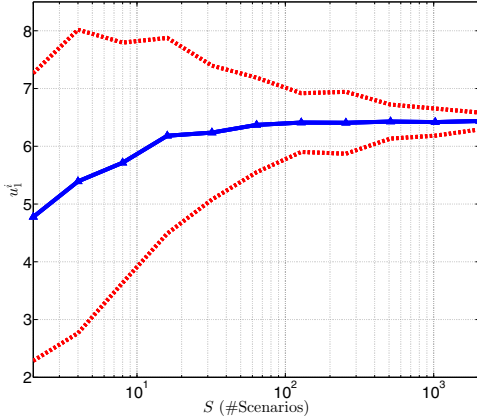


Fig. 2. Sample expectation of u_1^i and its 95% normal confidence interval.

In closed-loop, we set $M = 1$ in (8e) to account for the fact that a new state estimate becomes available at the next sampling instant. This allows u_k^i to vary over the scenarios, $i \in \mathcal{S}$, for $k \geq 2$. Fig. 2 illustrates the mean value of u_1^i and its 95% normal confidence interval as a function of S , over 100 different realizations of the uncertainty scenarios $\{w^i\}_{i=1}^S$. Large variations in $u_1^i = u_1^1 = u_1^2 = \dots = u_1^S$ occur if the number of uncertainty scenarios is too small, i.e. the input becomes very sensitive to the particular realization of uncertainty scenarios. This is likely to cause undesirable oscillations in the resulting closed-loop input-trajectory. The number of scenarios required to avoid this problem depends on the application. For the specific case study, $S = 1000 - 2048$ scenarios are sufficient to obtain u_1^i with a reasonable small variance.

Fig. 3 illustrates the CPU time of solving the OCP (10) for CPLEX, MOSEK, Gurobi and MVadmm, as a function S . We report the solution time for a sequential implementation of MVadmm (seq.) and for a pseudo parallel implementation of MVadmm (par.). The timings for the pseudo parallel implementation are obtained from the sequential CPU-time results, assuming that the independent subproblems (21) are solved in parallel. Fig. 3 shows that MVadmm scales linearly in the number of uncertainty scenarios, which yields an improvement over the general purpose solvers. Solving the subproblems in parallel reduces the computation time of MVadmm significantly. For large S , the pseudo parallel implementation of MVadmm is several orders of magnitude faster than CPLEX, MOSEK and Gurobi. Remark 3 provides suggestions to improve the computational performance of MVadmm even further. When $S \geq 8192$, MVadmm is the only algorithm that does not fail to come up with a solution due to memory issues.

V. CONCLUSION

We have presented an ADMM-based decomposition algorithm for MV-EMPC of stochastic linear systems that

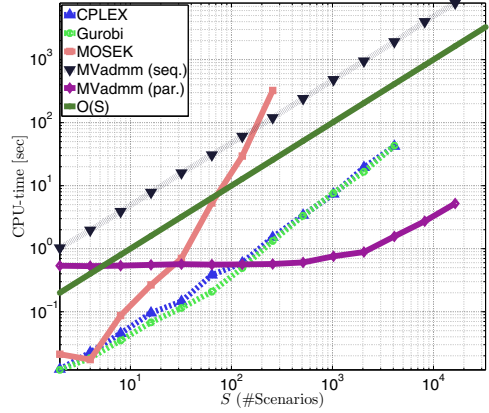


Fig. 3. CPU time for solving (10) as a function of the number of scenarios, S .

scales linearly in the number of uncertainty scenarios. At every iteration, the algorithm solves a number of small independent subproblems. Simulations based on a simple power management case study show that when the number of uncertainty scenarios is large, a parallel implementation of the decomposition algorithm is several orders of magnitude faster than state-of-the-art convex quadratic programming algorithms. Furthermore, the decomposition algorithm reduces memory requirements of MV-EMPC significantly.

APPENDIX I

MV-EMPC OPTIMAL CONTROL PROBLEM

This appendix introduces data structures to express the two-stage OCP (8) under the relaxed condition (9) in a more compact form. Define the stacked vectors

$$u = \begin{bmatrix} u^1 \\ u^2 \\ \vdots \\ u^S \end{bmatrix}, \quad x = \begin{bmatrix} x^1 \\ x^2 \\ \vdots \\ x^S \end{bmatrix}, \quad z = \begin{bmatrix} z^1 \\ z^2 \\ \vdots \\ z^S \end{bmatrix}, \quad \psi = \begin{bmatrix} \psi^1 \\ \psi^2 \\ \vdots \\ \psi^S \end{bmatrix}. \quad (40)$$

and let $\tilde{\mathcal{U}} = \mathcal{U}^S = \mathcal{U} \times \mathcal{U} \times \dots \times \mathcal{U}$ be the Cartesian power of the set \mathcal{U} such that $u^i \in \mathcal{U}$ with $i \in \mathcal{S}$ can be expressed as $u \in \tilde{\mathcal{U}}$. The objective function, (8a), is written in the form $\lambda \mu + \tilde{\lambda} v^T v + S \tilde{\lambda} \mu^2 - 2 \tilde{\lambda} \mu \mathbf{1}^T v$ where $\mathbf{1}$ is a vector of all ones. As a compact notation for the state space constraints, (8b), we use

$$\tilde{A}x + \tilde{B}u + \tilde{w} = 0, \quad z = \tilde{C}x, \quad (41)$$

where \tilde{A} , \tilde{B} , and \tilde{C} , are block diagonal matrices, such that $\tilde{A} = \mathbf{blkdiag}(\tilde{A}, \tilde{A}, \dots, \tilde{A})$ and similarly for \tilde{B} and \tilde{C} . Moreover $\tilde{B} = \mathbf{blkdiag}(B, B, \dots, B)$, $\tilde{C} = \mathbf{blkdiag}(C, C, \dots, C)$ and

$$\tilde{A} = \begin{bmatrix} -I & & & & \\ A & -I & & & \\ & & \ddots & \ddots & \\ & & & A & -I \end{bmatrix}, \quad \tilde{w}^i = \begin{bmatrix} w_0^i \\ w_1^i \\ \vdots \\ w_{N-1}^i \end{bmatrix} + \begin{bmatrix} Ax_0 \\ 0 \\ \vdots \\ 0 \end{bmatrix}, \quad i \in \mathcal{S}.$$

P A P E R H

Contingency-Constrained Unit Commitment in Meshed Isolated Power Systems

L. E. Sokoler, P. Vinter, R. Bærentsen, K. Edlund, and J. B. Jørgensen. Contingency-Constrained Unit Commitment in Meshed Isolated Power Systems. *IEEE Transactions on Power Systems*, 2015. To appear.

Contingency-Constrained Unit Commitment in Meshed Isolated Power Systems

Leo Emil Sokoler, Peter Vinter, Runi Bærentsen, Kristian Edlund, and John Bagterp Jørgensen

Abstract—This paper presents a mixed-integer linear optimization problem for unit commitment and economic dispatch of power generators in a meshed isolated power system. The optimization problem is referred to as the optimal reserve planning problem (ORPP). The ORPP guarantees that the system frequency is kept above a predefined limit in the event of a contingency. The minimum frequency constraints are formulated using novel sufficient conditions that take into account the system inertia and the dynamics of the power generators. The proposed sufficient conditions are attractive from both a computational and a modelling point of view. We compare the ORPP to a unit commitment problem that only considers the stationary behavior of the frequency. Simulations based on a Faroe Islands case study show that, without being overly conservative, potential blackouts and power outages can be avoided using the ORPP. In the particular case study, the cost increase associated with the additional security provided by the ORPP is less than 3%.

Index Terms—Energy management, power generation planning, optimal scheduling, integer linear programming, islanding.

I. INTRODUCTION

POWER production planning is an important task in power system operations. This task involves solving a mixed-integer linear program (MILP) for unit commitment and economic dispatch of the system power generators. The solution of the MILP provides an hours-ahead production plan for each generator, including the amount of operating reserves they should provide. Operating reserves are important to balance production and consumption in real-time. Imbalances occur due to e.g., loss of power generators, fluctuations in non controllable production or consumption, and errors in the prediction of renewable energy production. We refer to these events as contingencies.

Manuscript received January 26, 2015; revised February 04, 2015, June 16, 2015, and August 14, 2015; accepted September 29, 2015. This work was supported in part by the Danish Ministry of Higher Education and Science in the industrial Ph.D. project “Stochastic MPC with Applications in Smart Energy Systems” (11-117435); and in part by The Danish Council for Strategic Research in the project “CITIES—Centre for IT-Intelligent Energy Systems in Cities” (1305-00027B). Paper no. TPWRS-00102-2015.

L. E. Sokoler is with the Department of Applied Mathematics and Computer Science, Technical University of Denmark, DK-2800 Kgs. Lyngby, Denmark, and also with DONG Energy, DK-2830 Virum, Denmark (e-mail: les@dtu.dk).

J. B. Jørgensen is with the Department of Applied Mathematics and Computer Science, Technical University of Denmark, DK-2800 Kgs. Lyngby, Denmark (e-mail: jbj@dtu.dk).

P. Vinter is with Ingeniørfirmaet P. A. Pedersen A/S, DK-1970 Frederiksberg C, Denmark.

R. Bærentsen and K. Edlund are with DONG Energy, DK-2830 Virum, Denmark.

Color versions of one or more of the figures in this paper are available online at <http://ieeexplore.ieee.org>.

Digital Object Identifier 10.1109/TPWRS.2015.2485781

Small isolated power systems are characterized by low inertia provided by a relatively small number of generators. The frequency in such systems is much more sensitive to power imbalances than large interconnected power systems. Moreover, the system inertia varies significantly with the committed units [1]. For these reasons, it is necessary to include minimum frequency constraints in the production planning problem for small isolated power systems. Frequency constraints are very challenging to handle in the unit commitment (UC) problem, since there is generally no linear expression for the minimum frequency. References [2]–[5] introduce constraints in the UC problem that keep the steady state frequency above a predefined limit. The underlying assumption is that the power system remains in stable operation during the transient part of the system dynamics that follow a contingency. This is often not the case in isolated power systems. For such systems, it is necessary to consider constraints for the minimum frequency that occurs during the transient part of the system dynamics as well. The minimum frequency depends on the system inertia and the dynamics of the power generators. Several heuristics have been proposed to account for the minimum frequency in the UC problem. References [6] and [7] use a multi-level approach that alternates between solving the UC problem and a grid simulation. References [8]–[11] couple the system dynamics and the reserve requirements using a load-frequency sensitivity index (LFSI). The LFSI is estimated from frequency data recorded during forced generator outages. A significant limitation is that the LFSI is regarded as a fixed parameter in the UC problem. In [12] the system inertia and the size of the contingency are mapped into reserve requirements in the UC problem using a piecewise linear function. The piecewise linear function is fitted to data generated by a comprehensive simulation model. Reference [13] derives a non-linear expression of the minimum frequency using a simplified model of the system dynamics. The model assumes that all the power generators have the same underlying simple model structure. Market designs that consider the minimum frequency in large synchronous interconnected systems are discussed in [14].

This paper presents novel sufficient conditions that guarantee that the minimum frequency is kept above a predefined limit. The conditions are based on a model of the system inertia and a generic power generator model. The power generator model describes the activation of primary reserves for each power generator. Secondary reserves are not considered in the power generator model, as they have no significant effect on the minimum frequency. We use the proposed sufficient conditions to develop a UC problem with minimum frequency constraints. The problem is referred to as the optimal reserve planning

problem (ORPP). The advantages of the ORPP are that it can be formulated as a single MILP, it does not impose any strict assumptions on the generators, and that the parameters in the power generator model are simple to obtain. Finally, the proposed approach does not require any simulation model of the system.

We have organized this paper as follows. Section II derives sufficient conditions for the minimum frequency. Section III formulates the ORPP as a MILP. Simulations based on a Faroe Islands case study are provided in Section IV. Section V concludes the paper.

A. Faroe Islands Case Study

The Faroe Islands make up a 1,400 km² group of islands situated in the North Atlantic Ocean and inhabited by almost 50,000 people. The Faroe Islands have some of the world's best wind resources due to their position in the Atlantic Ocean. However, the power system is small, isolated, and vulnerable, with a high number of blackouts. Historically, the Faroe Islands have around 30 power outages each year [15]. Some of these outages are total blackouts (1–3). In 2014, a load-shedding strategy was implemented to avoid critical frequency drops. This strategy has already prevented several blackouts [16]. The Faroe Islands have a target to increase the amount of renewable energy production from 38% in 2011 to 75% in 2020. A significant part of the increased renewable energy production is expected to come from wind turbines. In 2014 the installed wind power was 18% of the total capacity, corresponding to 122% of the minimum load and 41% of the maximum load. Operating reserves in the Faroe Islands are planned on the basis of the $n - 1$ criterion combined with other ad-hoc rules. The $n - 1$ criterion is only concerned with the amount of reserve that is available in the system, and does not account for the system frequency [17]. As more renewable energy is integrated into the Faroe Islands' power system, the need for a more intelligent reserve planning strategy increases. The strategy proposed in this paper will be tested in the Faroe Islands during 2015 as part of the GRANI project [15].

II. PROBLEM FORMULATION

This section derives sufficient conditions, which guarantee that the minimum frequency resulting from a contingency is kept above a predefined limit, denoted f .

We consider two types of operating reserves in this paper; frequency containment reserve (FCR) and frequency restoration reserve (FRR). The FCR is a reserve for containment of frequency deviations (primary reserve), and the FRR is a reserve for restoring the frequency to the nominal frequency (secondary reserve). Activation time for FRR is up to several minutes. In low-inertia systems, such as small isolated power systems, the FCR activation time must in the order of a few seconds. E.g., [15] shows that the frequency in the Faroese power system may drop at a rate of 1 Hz/s after a contingency. In the Faroe Islands, frequency drops of more than 2 Hz are critical. This means that sufficient FCR has to be available within 2 seconds in order to keep the system stable.

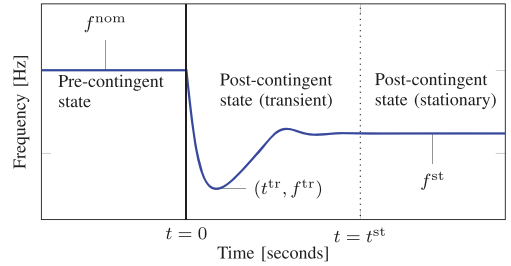


Fig. 1. Frequency dynamics. The minimum frequency occurs during the transient phase of the post-contingent state.

We refer to the state of the system prior to a contingency as the pre-contingent state, and the state of the system after a contingency as a post-contingent state. The type of contingency considered in this paper is limited to loss of power generators. The proposed ORPP can, however, easily be generalized to other types of contingencies as well. Fig. 1 illustrates the frequency dynamics in the event that one or more power generators fail. The system is operated at its nominal frequency f^{nom} in the pre-contingent state. The post-contingent state is divided into a transient phase and a stationary phase. In the transient phase, the frequency drops to its minimum value f^{tr} , and it then returns to a steady state value f^{st} . The minimum frequency, f^{tr} , may be significantly smaller than the steady state frequency, f^{st} . The offset $f^{\text{st}} - f^{\text{nom}}$ is eliminated by activating FRR. The FRR does not have any effect on f^{st} and f^{tr} , since reserves in this category are activated at a much slower time scale than the FCR.

Define the set $\mathbb{J} = \{1, 2, \dots, J\}$, with J being the number of power generators. The generators respond to frequency deviations from the nominal frequency by activating FCR. The FCR is activated locally at each power generator via frequency-based proportional controllers [18], [19]. We denote the FCR activation signal (set-point) provided to each generator as $\tilde{P}_j^{\text{FCR}}(t)$. The FCR activated (output) at each generator is denoted $P_j^{\text{FCR}}(t)$. The energy released during FCR activation is $E_j^{\text{FCR}}(t) = \int_0^t P_j^{\text{FCR}}(\tau) d\tau$. The FCR set-point provided to each of the generators is

$$\tilde{P}_j^{\text{FCR}}(t) = -(1/D_j)\Delta f(t), \quad j \in \mathbb{J}. \quad (1)$$

D_j is the local droop of generator j , and $\Delta f(t) = f(t) - f^{\text{nom}}$ is the frequency deviation from the nominal frequency. Let t^{st} denote the time instant at which the frequency settles at its steady state value f^{st} . For $t \geq t^{\text{st}}$, the FCR set-point is $\tilde{P}_j^{\text{FCR}}(t) = \tilde{P}_j^{\text{FCR, st}} = -(1/D_j)(f^{\text{st}} - f^{\text{nom}})$, where $\tilde{P}_j^{\text{FCR, st}}$ is the steady state FCR set-point for generator j . The FCR activated at generator j in steady state is equal to the minimum of 1) the steady state FCR set-point, and 2) the maximum amount of FCR that the generator can deliver. Hence

$$P_j^{\text{FCR}}(t) = P_j^{\text{FCR, st}} = \min\left(\tilde{P}_j^{\text{FCR, st}}, \bar{P}_j^{\text{FCR}}\right), \quad j \in \mathbb{J}, \quad (2)$$

$t \geq t^{\text{st}}$. The parameter \bar{P}_j^{FCR} is the maximum amount of FCR that can be activated at generator j . This limit depends on the generator capabilities and the pre-contingent state of the system,

e.g., a generator that operates at its maximum level cannot increase its production further.

For convenience, we define the sums

$$P^{\text{FCR}}(t) = \sum_{j \in \mathcal{J}} P_j^{\text{FCR}}(t), \quad E^{\text{FCR}}(t) = \sum_{j \in \mathcal{J}} E_j^{\text{FCR}}(t). \quad (3)$$

References [2]–[5] model (2) using mixed-integer constraints. This allows constraints for the stationary frequency, f^{st} , to be included in the UC problem. We derive constraints for the minimum frequency, f^{tr} , which is critical in island operations. The minimum frequency, f^{tr} , depends on $P^{\text{FCR}}(t)$ for $t < t^{\text{st}}$ (transient part of the post-contingent state). Equation (2) describes the generator dynamics for $t \geq t^{\text{st}}$ (stationary part of the post-contingent state).

We model the frequency dynamics resulting from a contingency using the swing equation for a synchronous machine [18], [19]. The equation is written as an implicit ordinary differential equation (ODE) in the form

$$\mathcal{F}(P^{\text{FCR}}, f, \dot{f}) = 0, \quad (4)$$

where

$$\mathcal{F}(P^{\text{FCR}}, f, \dot{f}) = \dot{f}(t) - \frac{(f^{\text{nom}})^2}{2HRf(t)}(P^{\text{FCR}}(t) - P^{\text{lost}}), \quad (5)$$

and

$$H = \sum_{j \in \mathcal{J} \setminus \bar{\mathcal{J}}} H_j R_j / R, \quad R = \sum_{j \in \mathcal{J} \setminus \bar{\mathcal{J}}} R_j, \quad (6a)$$

$$P^{\text{FCR}}(t) = \sum_{j \in \mathcal{J} \setminus \bar{\mathcal{J}}} P_j^{\text{FCR}}(t), \quad P^{\text{lost}} = \sum_{j \in \bar{\mathcal{J}}} P_j^{\text{lost}} \quad (6b)$$

Power generator j has constant of inertia H_j [s], and rated power R_j [MVA]. The FCR activated at generator j is $P_j^{\text{FCR}}(t)$ [MW], and the lost power resulting from the contingency is denoted P_j^{lost} [MW]. Time $t = 0$ denotes the time instant at which the contingency occurs. The subset $\bar{\mathcal{J}} \subseteq \mathcal{J}$ refers to the tripped generators. These generators do not provide any inertia to the system. Note also that $P_j^{\text{FCR}}(t) = 0$ for $j \in \bar{\mathcal{J}}$, and $P_j^{\text{lost}}(t) = 0$ for $j \in \mathcal{J} \setminus \bar{\mathcal{J}}$.

It holds that $H_j = E_j^{\text{rot}}(\omega_j^{\text{nom}}) / R_j$, in which

$$E_j^{\text{rot}}(\omega_j) = \frac{1}{2} I_j \omega_j^2, \quad (7)$$

maps the angular velocity ω_j [rad/s] to the rotational energy $E_j^{\text{rot}}(\omega_j)$ [J]. I_j [kg · m²] is the moment of inertia. The relation between angular velocity and frequency is

$$f_j(t) = \frac{1}{4\pi} \omega_j(t) N_j^p, \quad j \in \mathcal{J}, \quad (8)$$

where N_j^p is the number of poles in the generator. The minimum desired angular velocity for generator j , $\underline{\omega}_j$, is derived from the predefined frequency limit \underline{f} using (8).

The generator dynamics during FCR activation, P_j^{FCR} , is modeled as the implicit ODE

$$\mathcal{G}_j(f, P_j^{\text{FCR}}, \dot{P}_j^{\text{FCR}}, \dots, (P_j^{\text{FCR}})^{(n_j)}) = 0, \quad (9)$$

$(P_j^{\text{FCR}})^{(n_j)}$ is the n_j 'th derivative of $P_j^{\text{FCR}}(t)$. The formulation (9) is general enough to represent the models in e.g. [13],

[20]–[22]. We provide an example of (9) in Section IV. Equations (4) and (9) define a system of ODEs that describes the coupled frequency and power generator dynamics that follow a contingency. The system is

$$\begin{bmatrix} \mathcal{F}(P^{\text{FCR}}, f, \dot{f}) \\ \mathcal{G}_1(f, P_1^{\text{FCR}}, \dot{P}_1^{\text{FCR}}, \dots, (P_1^{\text{FCR}})^{(n_1)}) \\ \vdots \\ \mathcal{G}_J(f, P_J^{\text{FCR}}, \dot{P}_J^{\text{FCR}}, \dots, (P_J^{\text{FCR}})^{(n_J)}) \end{bmatrix} = \begin{bmatrix} 0 \\ 0 \\ \vdots \\ 0 \end{bmatrix}. \quad (10)$$

The solution of (10) is the system frequency, $f(t)$, and the FCR response of the power generators $\{P_j^{\text{FCR}}(t)\}_{j \in \mathcal{J}}$, resulting from the contingency.

Remark 1: Model (5) assumes that $f_j(t) = f(t)$ for all $j \in \mathcal{J}$, i.e., that the power system is a single-bus system with no line capacity constraints or transmission losses. This assumption can be justified for highly meshed systems where the relative impedances between nodes in the system are small [18], [23], [24]. Single-bus models for transient frequency analysis in highly meshed isolated power systems are described in [25]–[27]. The Faroese power grid is a fairly meshed system, where line capacity constraints and transmission losses are negligible for the application considered in this paper. Model (5) also assumes that all loads are frequency-independent, i.e., load-damping is neglected. This is a conservative assumption for the application considered in this paper, since frequency-dependent loads have a stabilizing effect on the frequency [18].

A. Minimum Frequency Conditions

We use model (10) to derive sufficient conditions for $f(t) \geq \underline{f}$. Assumption 1 is that the frequency extreme values are non-increasing over time. This stability condition is a standard power system design criterion.

Assumption 1: For any $t_1 \geq 0$ and $t_2 \geq 0$, with $t_2 \geq t_1$ and $\dot{f}(t_1) = \dot{f}(t_2) = 0$

$$|f(t_2) - f^{\text{st}}| \leq |f(t_1) - f^{\text{st}}|. \quad (11)$$

Define t^{tr} to be the first time instant at which the power balance is restored

$$t^{\text{tr}} = \min \{t \mid P^{\text{FCR}}(t) - P^{\text{lost}} = 0\}. \quad (12)$$

It follows from (4) that $\dot{f}(t^{\text{tr}}) = 0$, and due to Assumption 1, $f(t^{\text{tr}}) = f^{\text{tr}}$. This shows that a sufficient condition for the minimum frequency condition, $f^{\text{tr}} \geq \underline{f}$, is

$$f(t^{\text{tr}}) \geq \underline{f}. \quad (13)$$

Evaluating (13) requires the solution of the generally non-linear system (10), and subsequent computation of t^{tr} via (12). Since the UC problem is a MILP, which is restricted to linear constraints, Condition (13) can not be included in the UC problem. To overcome this issue, we replace (13) by a set of more conservative conditions that can be modelled using mixed-integer linear programming. For this purpose, it is convenient to define the function $\mathcal{P}_j^{\text{FCR}}(t; \tilde{f})$ to be the solution of (9) with the system frequency, f , replaced by the function \tilde{f} . Accordingly, introduce $\mathcal{E}_j^{\text{FCR}}(t; \tilde{f}) = \int_0^t \mathcal{P}_j^{\text{FCR}}(\tau; \tilde{f}) d\tau$. Note that

$\mathcal{P}_j^{\text{FCR}}(t; f) = P_j^{\text{FCR}}(t)$ and $\mathcal{E}_j^{\text{FCR}}(t; f) = E_j^{\text{FCR}}(t)$. Similar to (3), we also introduce the sums $\mathcal{P}^{\text{FCR}}(t; \tilde{f})$ and $\mathcal{E}^{\text{FCR}}(t; \tilde{f})$ such that $\mathcal{P}^{\text{FCR}}(t; f) = P^{\text{FCR}}(t)$ and $\mathcal{E}^{\text{FCR}}(t; f) = E^{\text{FCR}}(t)$.

The functions $\{\mathcal{G}_j\}_{j \in \mathcal{J}}$ are coupled only in f . Provided that \tilde{f} is a known function, $\mathcal{P}_j^{\text{FCR}}(t; \tilde{f})$ can be determined independently for each $j \in \mathcal{J}$ by solving the ODEs

$$\mathcal{G}_j \left(\tilde{f}, P_j^{\text{FCR}}, \dot{P}_j^{\text{FCR}}, \dots, (P_j^{\text{FCR}})^{(n_j)} \right) = 0, \quad j \in \mathcal{J}.$$

Appendix B introduces a number of reasonable assumptions about \mathcal{P}^{FCR} that we exploit in the following.

Introduce the affine function

$$f_{\text{lin}}(t) = (1 - t/t^c)f^{\text{nom}} + (t/t^c)\underline{f}, \quad (14)$$

such that $f_{\text{lin}}(0) = f^{\text{nom}}$ and $f_{\text{lin}}(t^c) = \underline{f}$. We refer to t^c [s] as the critical time. Propositions 1 and 2 provide sufficient conditions for the minimum frequency constraint (13). These conditions are conservative conditions that exploit the properties of f_{lin} to decouple the generator and frequency dynamics. A similar idea is introduced in [28] for computing the maximum frequency deviation in small isolated power systems. Condition (15) ensures that $f(t) \geq \underline{f}$ for $t \leq t^c$, and (19) ensures that $t^{\text{tr}} \leq t^c$, i.e., that the minimum frequency occurs before time t^c . The critical time t^c is a user-defined parameter that specifies an upper bound for the time at which the minimum frequency can occur. Note that $\dot{f}_{\text{lin}}(t) = (\underline{f} - f^{\text{nom}})/t^c$. This shows that the slope of f_{lin} is inversely proportional to t^c . As the power generators activate FCR in proportion to the frequency deviation, the function $\mathcal{E}^{\text{FCR}}(t; f_{\text{lin}})$ is expected to increase as t^c decreases. Consequently, condition (15) becomes less strict when t^c is small. This observation agrees with Assumption 3. When t^c is small, condition (19) becomes more strict, since the activation time for the required amount of FCR is limited to t^c . This observation agrees with Assumption 4. The choice of t^c should take the above-mentioned considerations into account. As a rule of thumb, t^c should be chosen such that 1) $\mathcal{P}^{\text{FCR}}(t^c; f_{\text{lin}})$ is large, and 2) $\mathcal{E}^{\text{FCR}}(t; f_{\text{lin}})$ increases at a relatively high rate for $t \leq t^c$. The conditions (15) and (19) only need to hold for a single value of t^c , in order to be sufficient for the minimum frequency constraint (13). Usually, the conditions can be satisfied for a wide range of t^c values. Several values of t^c may be used in practice, as the system inertia and the response of the generators vary with the committed units.

Proposition 1: The condition

$$\mathcal{E}^{\text{FCR}}(t; f_{\text{lin}}) + \Delta E^{\text{rot}} \geq P^{\text{lost}}t, \quad t \leq t^c, \quad (15)$$

is a sufficient condition for

$$f(t) \geq \underline{f}, \quad t \leq t^c. \quad (16)$$

Proof: Appendix A shows that condition (16) can be stated as $E^{\text{FCR}}(t) + \Delta E^{\text{rot}} \geq P^{\text{lost}}t$, for $t \leq t^c$. ΔE^{rot} is the energy contribution from the system inertia, $E^{\text{FCR}}(t)$ is the energy contribution from the activated FCR, and $P^{\text{lost}}t^{\text{tr}}$ is the energy lost as a result of the contingency. Suppose (15) is satisfied and (16) is violated. If (16) is violated there exists a $\tilde{t} \leq t^{\text{tr}}$ such that $f(\tilde{t}) = \underline{f}$ and $f(\tilde{t} + \Delta t) < \underline{f}$ with $\tilde{t} + \Delta t \leq t^c$. Assumption 5

states that $f(t)$ is convex in the time interval $[0, t^{\text{tr}}]$. Therefore it holds that

$$f(t) \leq (1 - t/\tilde{t})f^{\text{nom}} + (t/\tilde{t})\underline{f}, \quad t \leq \tilde{t}. \quad (17)$$

As $\tilde{t} \leq t^c$ we have

$$(1 - t/\tilde{t})f^{\text{nom}} + (t/\tilde{t})\underline{f} \leq f_{\text{lin}}(t). \quad (18)$$

It follows from Assumption 3 that $E^{\text{FCR}}(t) \geq \mathcal{E}(t; f_{\text{lin}})$ for $t \leq \tilde{t}$. Since (15) is satisfied by assumption

$$E^{\text{FCR}}(t) \geq \mathcal{E}^{\text{FCR}}(t; f_{\text{lin}}) \geq P^{\text{lost}}t - \Delta E^{\text{rot}}, \quad t \leq \tilde{t},$$

which contradicts the assumption that (16) is violated. ■

Proposition 2: Provided that (15) is satisfied, a sufficient condition for (13) is

$$\mathcal{P}^{\text{FCR}}(t^c; f_{\text{lin}}) \geq P^{\text{lost}}. \quad (19)$$

Proof: Since (15) is satisfied, (16) holds. This shows that two cases can occur: case 1) $f(t^c) = \underline{f}$ and case 2) $f(t^c) > \underline{f}$. Define the functions f_1 and f_2 that satisfy Assumption 1 to represent these cases. Let $f_1(t^c) = \underline{f}$, and $f_2(t^c + \Delta t) = \underline{f}$. It follows from Assumption 4 that

$$\mathcal{P}^{\text{FCR}}(t^c; f_1) \leq \mathcal{P}^{\text{FCR}}(t^c + \Delta t; f_2). \quad (20)$$

By definition, $f_{\text{lin}}(t) \geq f_1(t)$. Assumption 3 therefore gives $\mathcal{P}^{\text{FCR}}(t^c; f_{\text{lin}}) \leq \mathcal{P}^{\text{FCR}}(t^c; f_1)$. If (19) is satisfied, then using the inequalities above

$$\begin{aligned} \mathcal{P}^{\text{FCR}}(t^c + \Delta t; f_2) &\geq \mathcal{P}^{\text{FCR}}(t^c; f_1) \\ &\geq \mathcal{P}^{\text{FCR}}(t^c; f_{\text{lin}}) \geq P^{\text{lost}}. \end{aligned}$$

This means that the power balance is restored by no later than the time at which $f(t) = \underline{f}$. It follows that $t^{\text{tr}} \geq \underline{f}$. ■

Conditions (15) and (19) include terms that can be derived from $\{\mathcal{P}_j^{\text{FCR}}(t; f_{\text{lin}})\}_{j \in \mathcal{J}}$. The function $\mathcal{P}_j^{\text{FCR}}(t; f_{\text{lin}})$ is the activated FCR at generator j in response to the affine frequency drop (14). This function depends on the dynamics of the power generator j , and the pre-contingent state of the system. It is useful to separate the effect of these two components. We therefore introduce the notation

$$\mathcal{P}_j^{\text{FCR}}(t; f_{\text{lin}}) = \mathcal{I}(\delta P_j^{\text{FCR}}(t)), \quad j \in \mathcal{J} \quad (21)$$

where $\delta P_j^{\text{FCR}}(t)$ is the amount of FCR that is activated at generator j in response to (14), and \mathcal{I} accounts for the implicit limits on $\delta P_j^{\text{FCR}}(t)$ due to the pre-contingent state of the system. The function $\delta P_j^{\text{FCR}}(t)$ is determined by recording the response of the power generator to the affine frequency drop f_{lin} . This can be done by simulation or in simple experiments. Such experiments are currently being conducted on the Faroe Islands.

III. OPTIMAL RESERVE PLANNING PROBLEM

In this section, we formulate the ORPP as a MILP. The results derived in Section II are used to formulate the minimum frequency constraints. Table I lists the ORPP parameters and Table II lists the ORPP decision variables. The production plan is optimized over the horizon $T = [0, t^s, 2t^s, \dots, Kt^s]$, where t^s [min] is the sampling time and K is the number of time steps.

TABLE I
 ORPP PARAMETERS

Parameter	Description	Units
d_k	Demand forecast	MW
c_j^p	Production cost	EUR/(t_s ·MW)
c_j^{on}	Fixed run cost	EUR/ t_s
$(c_j^{\text{su}}, c_j^{\text{sd}})$	Start-up/shut-down cost	EUR
$(c_j^{\text{FRR}}, c_j^{\text{FCR}})$	Reserve capacity costs	EUR/(t_s ·MW)
$(\underline{p}_j^t, \bar{p}_j^t)$	Technical production limits	MW
$(\underline{p}_j^f, \bar{p}_j^f)$	Forecasted production limits	MW
$(\underline{e}_j, \bar{e}_j)$	Energy limits	MWh
$(\bar{r}_j^{\text{FRR}}, \bar{r}_j^{\text{FCR}})$	Reserve limits	MW
$w_{j,k}$	Disturbance forecast	MW
D_j	Droop	Hz/MW
$I_{i,j}^c$	Contingency matrix	u.l.
ΔE_j^{rot}	Rotational energy available	kWh
$\delta p_{j,m}^{\text{FCR}}$	FCR activation parameters	MW
t_j^{FCR}	Discretization points	s
$v_{j,0}^{\text{on}}$	Initial running state	u.l.
$e_{j,0}$	Initial energy level	MWh

 TABLE II
 ORPP DECISION VARIABLES

Variable	Description	Units	Domain
$p_{j,k}$	Production	MW	$\mathbb{R}_{\geq 0}$
$e_{j,k}$	Energy level	MWh	$\mathbb{R}_{\geq 0}$
$v_{j,k}^{\text{on}}$	Running state	u.l.	$\{0, 1\}$
$v_{j,k}^{\text{su}}$	Start-up indicator	u.l.	$\{0, 1\}$
$v_{j,k}^{\text{sd}}$	Shut-down indicator	u.l.	$\{0, 1\}$
$r_{j,k}$	Total reserve	MW	$\mathbb{R}_{\geq 0}$
$r_{j,k}^{\text{FRR}}$	FRR reservation	MW	$\mathbb{R}_{\geq 0}$
$r_{j,k}^{\text{FCR}}$	FCR reservation	MW	$\mathbb{R}_{\geq 0}$
$E_{j,k}^{\text{res}}$	Post-contingent FCR energy	kWh	$\mathbb{R}_{\geq 0}$
$\Delta E_{j,k}^{\text{rot}}$	Post-contingent rotational energy	kWh	$\mathbb{R}_{\geq 0}$
$E_{j,k}^{\text{con}}$	Post-contingent lost energy	kWh	$\mathbb{R}_{\geq 0}$
$r_{j,k}^{\text{dp,FCR}}$	FCR power activation	MW	$\mathbb{R}_{\geq 0}$
$r_{j,k}^{\text{de,FCR}}$	FCR energy activation	kWh	$\mathbb{R}_{\geq 0}$

The ORPP may be solved using a rolling-horizon approach, in order to take into account the most recent forecasts of e.g., the wind power production.

The ORPP objective function is to minimize the cost of operation over the horizon T . We define the cost function as

$$\phi = \sum_{j \in \mathbb{J}} \sum_{k \in \mathbb{K}} (t_s c_j^p p_{j,k} + t_s c_j^{\text{on}} v_{j,k}^{\text{on}} + c_j^{\text{su}} v_{j,k}^{\text{su}} + c_j^{\text{sd}} v_{j,k}^{\text{sd}} + t_s c_j^{\text{FRR}} r_{j,k}^{\text{FRR}} + t_s c_j^{\text{FCR}} r_{j,k}^{\text{FCR}}), \quad (22)$$

where $\mathbb{K} = \{1, 2, \dots, K\}$. When the reserve costs are non-zero, the model in [4] is used to account for the fact that the FCR is activated automatically.

The total power production is required to equal the consumption at every time interval

$$\sum_{j \in \mathbb{J}} p_{j,k} = d_k, \quad k \in \mathbb{K}. \quad (23)$$

We impose capacity constraints on the generators

$$\underline{p}_j^t v_{j,k}^{\text{on}} \leq p_{j,k} \leq \bar{p}_j^t v_{j,k}^{\text{on}}, \quad j \in \mathbb{J}, k \in \mathbb{K}, \quad (24a)$$

$$\underline{p}_{j,k}^f \leq p_{j,k} \leq \bar{p}_{j,k}^f, \quad j \in \mathbb{J}, k \in \mathbb{K}, \quad (24b)$$

$$\underline{e}_j \leq e_{j,k} \leq \bar{e}_j, \quad j \in \mathbb{J}, k \in \mathbb{K}. \quad (24c)$$

Constraint (24a) states that the power production of a running generator has to be within its technical limits, and that the power production of a generator not running is zero. Constraint (24b) states that the power production of every generator is within some forecast limits. If the lower forecast limit is positive, the generator is forced to be running. An application of (24b) is to model the production of wind turbines that are required to utilize (part of) their potential production. Constraint (24c) limits the energy reservoirs of the generators. Examples of limited reservoirs are batteries in electric vehicles, water storage for generation of hydroelectricity, and district heating accumulation tanks that are connected to combined heat and power plants. The energy balance equation is

$$e_{j,k} = e_{j,k-1} - t_s/60(p_{j,k} - w_{j,k}), \quad j \in \mathbb{J}, k \in \mathbb{K}, \quad (25)$$

which is used in e.g., [29] as a generic energy model for power generators in a Smart Grid system. We have included the parameter $w_{j,k}$ in (25) to model the impact of non-controllable inputs on the energy levels, e.g., the rainfall on the reservoir level in a hydro power plant. The binary decision variables in the ORPP are coupled by the constraints

$$v_{j,k}^{\text{on}} - v_{j,k-1}^{\text{on}} \leq v_{j,k}^{\text{su}}, \quad j \in \mathbb{J}, k \in \mathbb{K}, \quad (26a)$$

$$v_{j,k-1}^{\text{su}} - v_{j,k}^{\text{sd}} \leq v_{j,k}^{\text{sd}}, \quad j \in \mathbb{J}, k \in \mathbb{K}. \quad (26b)$$

The total reserve of each power generator is

$$r_{j,k} = r_{j,k}^{\text{FRR}} + r_{j,k}^{\text{FCR}}, \quad j \in \mathbb{J}, k \in \mathbb{K}. \quad (27)$$

The generators should respect their capacity constraints, even when the reserves are activated. This means that

$$p_{j,k} + r_{j,k} \leq \bar{p}_j^t v_{j,k}^{\text{on}}, \quad j \in \mathbb{J}, k \in \mathbb{K}, \quad (28a)$$

$$p_{j,k} + r_{j,k} \leq \bar{p}_{j,k}^f, \quad j \in \mathbb{J}, k \in \mathbb{K}, \quad (28b)$$

$$\frac{t_s}{60} r_{j,k} \leq e_{j,k}, \quad j \in \mathbb{J}, k \in \mathbb{K}. \quad (28c)$$

The FRR and the FCR are further limited by

$$r_{j,k}^{\text{FRR}} \leq \bar{r}_j^{\text{FRR}} v_{j,k}^{\text{on}}, \quad j \in \mathbb{J}, k \in \mathbb{K}, \quad (29a)$$

$$r_{j,k}^{\text{FCR}} \leq \bar{r}_j^{\text{FCR}} v_{j,k}^{\text{on}}, \quad j \in \mathbb{J}, k \in \mathbb{K}, \quad (29b)$$

where $\bar{r}_j^{\text{FCR}} \leq \bar{p}_j^t$ and $\bar{r}_j^{\text{FRR}} \leq \bar{p}_j^t$. References [4], [30] provide more details on the UC problem.

A. Minimum Frequency Constraints

We use the sufficient conditions (15) and (19) to formulate minimum frequency constraints in the ORPP. For this purpose, we discretize the FCR activation functions, $\{\delta P_j^{\text{FCR}}(t)\}_{j \in \mathbb{J}}$, defined by (21). Introduce M discretization points $\{t_m^{\text{FCR}}\}_{m \in \mathbb{M}}$ with $\mathbb{M} = \{1, 2, \dots, M\}$ that satisfy $t_1^{\text{FCR}} = 0 < t_2^{\text{FCR}} < \dots < t_M^{\text{FCR}} = t^c$. Also define

$$\delta p_{j,m}^{\text{FCR}} = \delta P_j^{\text{FCR}}(t_m^{\text{FCR}}), \quad j \in \mathbb{J}, m \in \mathbb{M}, \quad (30)$$

such that $\{\delta p_{j,m}^{\text{FCR}}\}_{m \in \mathbb{M}}$ is a discretization of the function $\delta P_j^{\text{FCR}}(t)$. The FCR reservation, $r_{j,k}^{\text{FCR}}$, is restricted by the

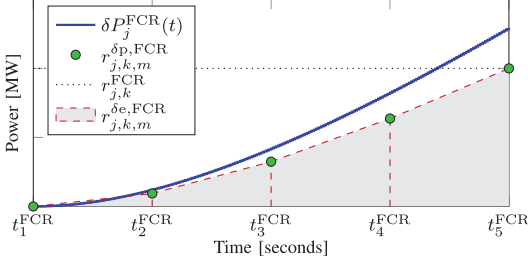


Fig. 2. Example of the relationship between $\delta P_j^{\text{FCR}}(t)$, $r_{j,k}^{\text{FCR}}$, $r_{j,k}^{\text{FCR}}$ and $r_{j,k}^{\text{FCR}}$, for a fixed time step $k \in \mathbb{K}$, and a fixed generator $j \in \mathbb{J}$.

amount of FCR that can be activated within time t^c . Therefore

$$r_{j,k}^{\text{FCR}} \leq \delta p_{j,M}^{\text{FCR}}, \quad j \in \mathbb{J}, k \in \mathbb{K}. \quad (31)$$

The FCR that can be activated at time t_m^{FCR} after a contingency has occurred is modeled as the identified FCR activation parameters $\delta p_{j,m}^{\text{FCR}}$ scaled by $r_{j,k}^{\text{FCR}} / \delta p_{j,M}^{\text{FCR}}$, i.e.,

$$r_{j,k}^{\delta p, \text{FCR}} = \frac{r_{j,k}^{\text{FCR}}}{\delta p_{j,M}^{\text{FCR}}} \delta p_{j,m}^{\text{FCR}}, \quad j \in \mathbb{J}, k \in \mathbb{K}, m \in \mathbb{M}. \quad (32)$$

The energy released during FCR activation is approximated by the area under the line segments that connect the points $\{r_{j,k}^{\delta p, \text{FCR}}\}_{m \in \mathbb{M}}$. This is expressed as

$$r_{j,k}^{\delta e, \text{FCR}} = r_{j,k,m-1}^{\delta e, \text{FCR}} + \lambda (t_m^{\text{FCR}} - t_{m-1}^{\text{FCR}}) r_{j,k,m-1}^{\delta p, \text{FCR}} + \frac{\lambda}{2} (t_m^{\text{FCR}} - t_{m-1}^{\text{FCR}}) (r_{j,k,m}^{\delta p, \text{FCR}} - r_{j,k,m-1}^{\delta p, \text{FCR}}), \quad (33)$$

$j \in \mathbb{J}, k \in \mathbb{K}, m \in \mathbb{M} \setminus \{1\}$ and $r_{j,k,1}^{\delta e, \text{FCR}} = 0$. The parameter $\lambda = 5/18$ converts the unit of $r_{j,k}^{\delta e, \text{FCR}}$ to [kW · h]. Fig. 2 illustrates the relationship between $\delta P_j^{\text{FCR}}(t)$, $r_{j,k}^{\delta p, \text{FCR}}$, $r_{j,k}^{\text{FCR}}$ and $r_{j,k}^{\delta e, \text{FCR}}$.

Let L denote the number of contingencies and $\mathbb{L} = \{1, 2, \dots, L\}$ be a set of indices associated with the contingencies. Define the contingency matrix I^c as

$$I_{l,j}^c = \begin{cases} 1 & \text{if generator } j \text{ fails in contingency } l, \\ 0 & \text{otherwise.} \end{cases} \quad (34)$$

We require condition (15) to be satisfied in the points defined by t_m^{FCR} , for each contingency $l \in \mathbb{L}$ and for each time step $k \in \mathbb{K}$. The constraint for this is

$$E_{l,k,m}^{\text{res}} + \Delta E_{l,k}^{\text{rot}} \geq E_{l,k,m}^{\text{con}}, \quad l \in \mathbb{L}, k \in \mathbb{K}, m \in \mathbb{M}. \quad (35)$$

The variable $E_{l,k,m}^{\text{res}}$ is the energy provided by the activated FCR in time step k , during contingency l , in discretization point m . This is expressed as

$$E_{l,k,m}^{\text{res}} = \sum_{j \in \mathbb{J}} (1 - I_{l,j}^c) r_{j,k}^{\delta e, \text{FCR}}, \quad (36a)$$

$l \in \mathbb{L}, k \in \mathbb{K}, m \in \mathbb{M}$. Note that including the contingency matrix, $I_{l,j}^c$, in (36a) ensures that only generators that do no trip

during a contingency may provide reserve during that particular contingency. Moreover, it follows from (29b) and (32) that $r_{j,k}^{\delta e, \text{FCR}} = 0$ if a generator is not running. The variable $E_{l,k,m}^{\text{con}}$ is the energy lost in time step k , during contingency l , in discretization point m . This is expressed as

$$E_{l,k,m}^{\text{con}} = \sum_{j \in \mathbb{J}} I_{l,j}^c p_{j,k} t_m^{\text{FCR}}, \quad l \in \mathbb{L}, k \in \mathbb{K}, m \in \mathbb{M}. \quad (36b)$$

In the expression (36b), the contingency matrix ensures that only power from the generators that fail during a contingency is assigned to $E_{l,k,m}^{\text{con}}$. The variable $\Delta E_{l,k}^{\text{rot}}$ is the rotational energy available due to the system inertia in time step k , during contingency l . This is expressed as

$$\Delta E_{l,k}^{\text{rot}} = \sum_{j \in \mathbb{J}} (1 - I_{l,j}^c) \Delta e_j^{\text{rot}} v_{j,k}^{\text{on}}, \quad l \in \mathbb{L}, k \in \mathbb{K}. \quad (36c)$$

Δe_j^{rot} is the parameter defined by

$$\Delta e_j^{\text{rot}} = E_j^{\text{rot}} (\omega_j^{\text{nom}} - \omega_j), \quad j \in \mathbb{J}. \quad (37)$$

E_j^{rot} is the function introduced in (7). Equation (36c) takes into account that the system inertia changes with the committed units. This is achieved using the indicator variable $v_{j,k}^{\text{on}}$. Including the contingency matrix in (36c) ensures that generators that drip do not contribute with inertia during a contingency.

The condition (19) is modeled as

$$\sum_{j \in \mathbb{J}} (1 - I_{l,j}^c) r_{j,k}^{\text{FCR}} \geq \sum_{j \in \mathbb{J}} I_{l,j}^c p_{j,k}, \quad l \in \mathbb{L}, k \in \mathbb{K}. \quad (38)$$

In addition to (38), we require that sufficient reserve in the FRR category is available, such that the frequency can be restored to its nominal value after a contingency has occurred. This is expressed similarly to (38) expect that we replace $r_{j,k}^{\text{FCR}}$ by $r_{j,k}^{\text{FRR}}$. Strategies for dispatching FRR are discussed in e.g., [31], [32].

The ORPP minimizes (22) subject to (23)–(29) and (31)–(38). Constraints (35) and (38) represent the minimum frequency conditions (15) and (19), respectively. Condition (15) needs to hold for all $t \leq t^c$. Constraint (35) however, only ensures that (15) is satisfied for $t \in \{t_m^{\text{FCR}}\}_{m \in \mathbb{M}}$. The number and distribution of the discretization points are therefore important. In practice, 2–5 evenly spaced points are usually sufficient. Provided that there are sufficient discretization points, (35) and (38) ensure that $f(t) \geq \underline{f}$ in every post-contingent state. Constraint (35) may be verified after solving the ORPP for a fine grid of t -values. If it is violated for some t , the ORPP is re-solved with this point included as an extra discretization point. Constraint (38) does not depend on the discretization points.

IV. CASE STUDY

In this section, we test the ORPP using a simulation case study based on the Faroe Islands' power system. A reduced system consisting of $J = 9$ units is considered.

Contingencies are simulated using a non-linear simulation model [18]. Fig. 3 is a block diagram of this model, and (10) is the model in differential equation form. We use the model to simulate the frequency and generator dynamics for a fixed

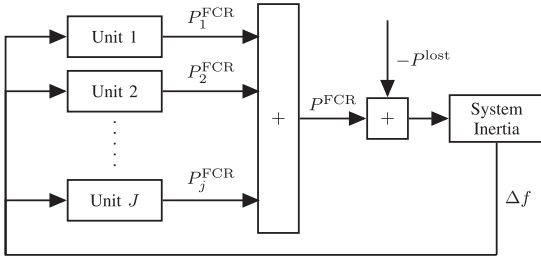


Fig. 3. Simulation model block diagram of the system (10). The model simulates the frequency and FCR response to a contingency.

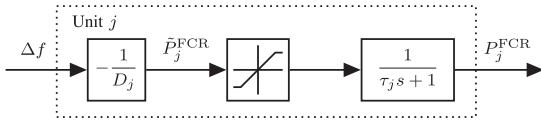


Fig. 4. Generator dynamics representing (9) for the particular case study.

contingency $l \in \mathbb{L}$, and a fixed time step $k \in \mathbb{K}$. The system inertia block represents (5), and the unit blocks represent (9). The post-contingent state of the system depends on the pre-contingent state of the system, e.g., the system inertia depends on the committed units, and the FCR that can be activated on a specific generator depends on its current production. Therefore, the solution of the ORPP is an input to the non-linear simulation model. Fig. 4 is a model of the generator dynamics in the specific case study. This model replaces the unit blocks in Fig. 3. The saturation block in Fig. 4 represents limits on the FCR that can be activated due to the unit capabilities as defined by the constraints (24), (28) and (29). We denote this limit by \bar{P}_j^{FCR} . For this study, the generators are assumed to have first order dynamics. The time constant associated with each generator is denoted τ_j [s]. In the form (9), the case study generator dynamics are

$$\mathcal{G}_j \left(f, P_j^{\text{FCR}}, \dot{P}_j^{\text{FCR}}, \dots, (P_j^{\text{FCR}})_{(n_j)} \right) = \tau_j \dot{P}_j^{\text{FCR}}(t) + P_j^{\text{FCR}}(t) - \bar{P}_j^{\text{FCR}}(t), \quad j \in \mathcal{J}, \quad (39)$$

where $\bar{P}_j^{\text{FCR}}(t) = \min(-1/D_j \Delta f(t), \bar{P}_j^{\text{FCR}})$ and $n_j = 1$ for all $j \in \mathcal{J}$.

Note that the models described by Figs. 3 and 4 are used for simulation only, and that they are not required to formulate and solve the ORPP.

Table III lists the case study system parameters. The data has been partly modified due to confidentiality reasons. The sampling time is $t^s = 15$ min, and $t^c = 2$ s. The parameter t^c was determined using a trial-and-error approach, considering the dynamics of the generators. We found that $t^c = 2$ s, provides a good balance for satisfying the minimum frequency sufficient conditions (15) and (19). We optimize over 6 hours, corresponding to $K = 24$ time steps. Fig. 5 shows the demand forecast, and the (maximum) wind power forecast. These quantities correspond to $\{d_k\}_{k \in \mathbb{K}}$ and $\{p_{9,k}^f\}_{k \in \mathbb{K}}$ in the ORPP, respectively. The maximum amount of wind power that is allowed to be curtailed is 5 MW. This lower limit is modeled

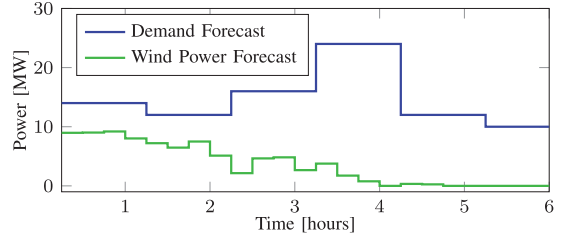


Fig. 5. Case study demand and wind power forecasts.

TABLE III
CASE STUDY SYSTEM PARAMETERS

#	Name	Type	I_j	N_j^p	p_j^t	\bar{p}_j^t	τ_j
1	Eidisverkid G1	Hydro	5900	8	2.7	6.8	3
2	Eidisverkid G2	Hydro	5900	8	2.7	6.8	3
3	Eidisverkid G3	Hydro	8050	8	3	7.7	3
4	Strond G1	Diesel	2116	14	1	2.2	2
5	Strond G2	Diesel	4375	10	1.3	3.6	2
6	Sundsverkid G1	Diesel	23301	12	4	8.1	5
7	Sundsverkid G2	Diesel	225500	40	7	12.7	5
8	Heygaverkid G1	Hydro	4875	8	2.1	5.3	3
9	Neshagi	Wind	-	-	0	10	0.5

using $\{p_{9,k}^f\}_{k \in \mathbb{K}} = \{\bar{p}_{9,k}^f - 5\}_{k \in \mathbb{K}}$. The production cost and the start-up cost are $c^p = (16.5, 17, 17.5, 18, 18, 18, 18, 16, 1)$ and $c^{\text{su}} = (3000, 3000, 3000, 3000, 3200, 3200, 3200, 3100, 100)$. The costs c^{om} , c^{sd} , c^{FRR} , and c^{FRR} are zero in this case study. Wind turbines provide the cheapest source of energy. Hydro generators are cheaper to use than diesel generators, when available, but they have limited reservoirs. For simplicity, we consider an example with unlimited reservoirs, and we define the disturbance, $w_{j,k}$, to be zero. Except for Neshagi, the power generators can deliver 100% of their technical maximum production in FCR and FRR. Neshagi does not provide FCR. The droop is 5% for all units. The minimum frequency is $f = 48$ Hz, and the nominal frequency is $f^{\text{nom}} = 50$ Hz. The rotational energy, Δe_j^{rot} , is computed as in (37).

The functions $\{\delta P_j^{\text{FCR}}\}_{j \in \mathcal{J}}$ are identified by simulation using the model illustrated in Fig. 4. As described in Section II, this is done by recording the FCR activation response of each power generator to the affine frequency drop defined by (14). Note that this can be done in experiments without any model of the generators. We set $M = 4$ and use the discretization points $t^{\text{FCR}} = (0, 2/3, 4/3, 2)$. The parameters $\{\delta p_{j,m}^{\text{FCR}}\}_{j \in \mathcal{J}}$ are defined as in (30). Table IV lists the identified parameters for the units that can deliver FCR. The number of contingencies considered in this case study is $L = 7$, and the contingency matrix is $I^c = [I_7 \ 0]$, where I_7 is the identity matrix of size 7. As defined by (34), this means that any (single) of the 7 first generators listed in Table III may trip within one of the 15-minute sampling intervals, during the entire 6 hours planning horizon. The production plan obtained by solving the ORPP is robust against any of these 7 contingencies. Neshagi is not part of a contingency in this case study. Fluctuating wind power production can be handled simply by including the

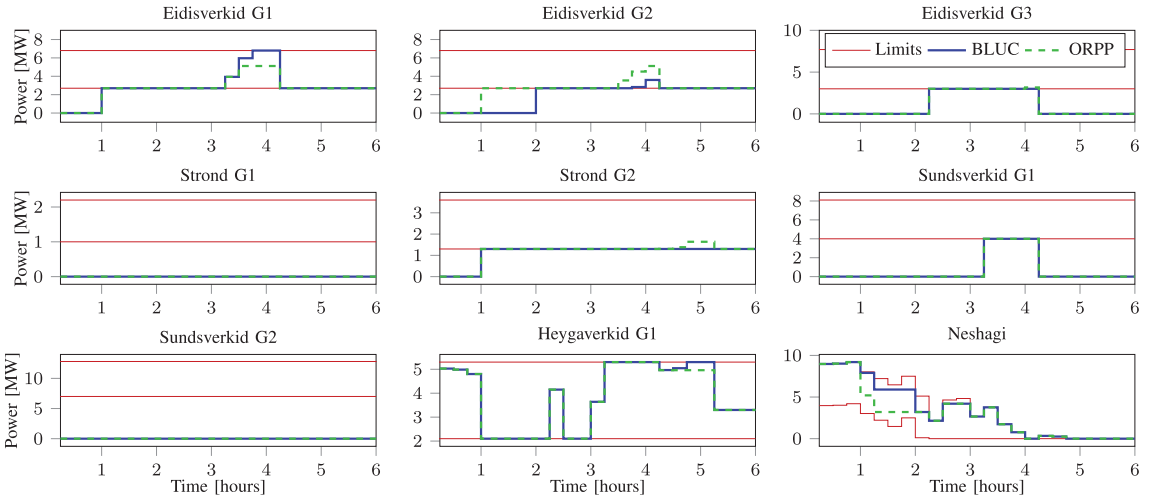


Fig. 6. Solution of the ORPP and the BLUC.

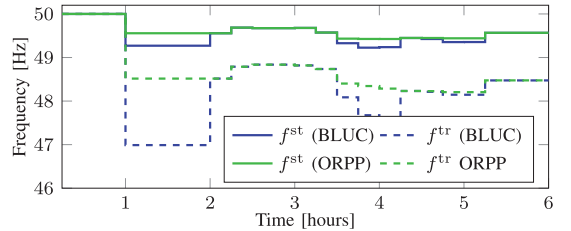
TABLE IV
CASE STUDY IDENTIFIED PARAMETERS

	1	2	3	4	5	6	7	8
$\delta p_{i,1}^{\text{FCR}}$	0	0	0	0	0	0	0	0
$\delta p_{i,2}^{\text{FCR}}$	0.18	0.18	0.21	0.086	0.14	0.14	0.21	0.14
$\delta p_{i,3}^{\text{FCR}}$	0.7	0.7	0.78	0.32	0.52	0.53	0.82	0.54
$\delta p_{i,4}^{\text{FCR}}$	1.5	1.5	1.4	0.65	1.1	1.1	1.8	1.1

uncertain fraction of the wind power production as a separate generator in the ORPP.

The ORPP is solved using CPLEX. In this particular case study, the ORPP is a MILP with 6692 variables (657 binary variables) and 7531 constraints. The solution time of the ORPP is approximately 5 seconds. We only solve the ORPP one single time, as no violations of the minimum frequency constraints occur for the specified discretization points.

We compare the ORPP against the optimization problem presented in [2]–[5], which we refer to as the baseline unit commitment problem (BLUC). The difference between the ORPP and the BLUC is that, while the ORPP limits the minimum frequency, f^{tr} , the BLUC only limits the steady state frequency, f^{st} . Fig. 6 compares the solutions determined by the ORPP and the BLUC. The main differences between the two solutions occur between hours 1–2 and hours 3.5–4.5. Between hours 1–2 the ORPP provides a solution with more generators running, at the expense of curtailing the wind power production. Eidisverkid G2 increases the system inertia, and at the same time it provides additional FCR that can be activated. Between hours 3.5–4.5 the BLUC provides a solution where Eidisverkid G1 and Heygaverkid G1 produce at their maximum capacity for a significant amount of time. In the solution provided by the ORPP, these generators back-off from their constraints such that more FCR can be activated in the event of a contingency. This increases cost of operation, since the more expensive power generator, Eidisverkid G2, increases its production to compensate for the back-off. The cost associated with the BLUC solu-

Fig. 7. Simulated worst-case frequency drops (both stationary and minimum) over all contingencies $l \in \mathbb{L}$ for each time step $k \in \mathbb{K}$.

tion is EUR 89039 and the cost associated with the ORPP solution is EUR 91680. This corresponds to a cost increase of less than 3%.

The robustness of the solutions provided by the ORPP and the BLUC is tested using the non-linear simulation model illustrated in Fig. 3 (and represented by the system of differential equations (10)). The generator dynamics are defined as in (39), and the frequency dynamics are defined as in (5). The upper and lower limits for the saturation block in Fig. 4 are computed from the solution of the ORPP and the BLUC. A simulation is run for every contingency $l \in \mathbb{L}$, and for each time step $k \in \mathbb{K}$. Each simulation produces an output similar to Fig. 1. In each simulation, we record the minimum frequency, f^{tr} , and stationary frequency, f^{st} , for both the ORPP and the BLUC.

Fig. 7 depicts the most critical frequency drops over all the contingencies, for each $k \in \mathbb{K}$. The figure shows that both the ORPP and the BLUC ensure that the stationary frequency is maintained above 48 Hz. Only the ORPP keeps the minimum frequency above 48 Hz as well. Thus, potential blackouts and power outages are avoided using the ORPP.

Between hours 1–2 and hours 3.5–4.5, the frequency associated with the BLUC drops significantly below 48 Hz. The worst-case for the BLUC occurs if Eidisverkid G1 fails between hours 1–2, which results in a minimum frequency just below 47

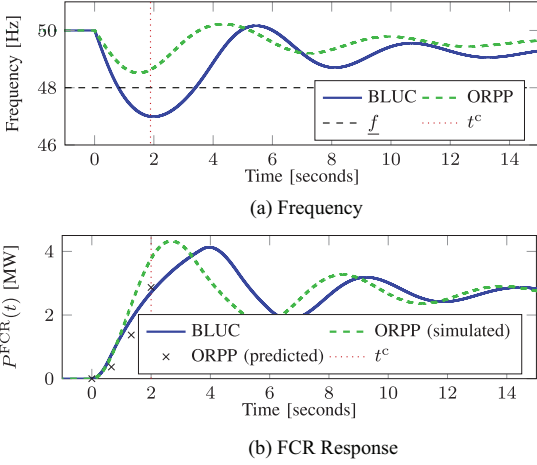


Fig. 8. System response after Eidisverkid G1 trips (contingency $l = 1$) at hour 1–1.25 (time step $k = 4$).

Hz. This situation is illustrated in Fig. 8. Fig. 8(a) shows the simulated system frequency, and Fig. 8(b) shows the simulated FCR response, $P^{\text{FCR}}(t)$, and the FCR response predicted by the ORPP via (32). The predicted FCR response underestimates the actual FCR response, without being significantly smaller than the actual FCR response. This indicates that the ORPP is not overly conservative. This observation is supported by Fig. 7: The solutions provided by the BLUC and the ORPP are very similar in situations where the minimum frequency does not drop below 48 Hz for the BLUC. Moreover, in hours 3.5–5 the frequency drops almost to the minimum frequency of 48 Hz for the ORPP, which shows that the ORPP does not introduce a significant amount of slack in the minimum frequency constraint.

Remark 2: In addition to the BLUC, we have compared the ORPP to a conventional UC problem using the $n - 1$ criterion for reserve planning. In this model, we simply require that there are sufficient FCR and FRR reserves to compensate for the lost production from any of the first 7 generators listed in Table III. In the particular case study, the production plan obtained with the conventional UC problem, coincides with the solution obtained by solving the BLUC.

V. CONCLUSION

In this paper, we have presented a mixed-integer linear program for unit commitment (UC) and economic dispatch of power generators in a meshed isolated power system. The optimization problem provides a production plan which ensures that the minimum frequency is maintained above a predefined limit in the event of a contingency. The transient dynamics of the frequency response are accounted for using a novel way to include information on the system dynamics in the UC problem. Simulations based on a Faroe Islands case study show that potential blackouts and power outages can be avoided using the proposed approach, at a cost increase of less than 3%.

APPENDIX A SOLUTION OF THE SWING EQUATION

The non-negative solution of (4) with initial value $f(0) = f^{\text{nom}}$ is

$$f(t) = \sqrt{(f^{\text{nom}})^2 (E^{\text{FCR}}(t) - P^{\text{lost}}t + HR)} / \sqrt{HR}.$$

The constraint $f(t) \geq \underline{f}$ may therefore be expressed in the form $HR((f/f^{\text{nom}})^2 - 1) \leq E^{\text{FCR}}(t) - P^{\text{lost}}t$. Simplifying using the relations (6), (7), and (8) yields

$$E^{\text{FCR}}(t) + \Delta E^{\text{rot}} \geq P^{\text{lost}}t,$$

in which $\Delta E^{\text{rot}} = \sum_{j \in J} E_j^{\text{rot}}(\omega_j^{\text{nom}} - \underline{\omega}_j)$ is defined in terms of the function (7).

APPENDIX B ASSUMPTIONS

Assumption 2 is that the FCR activated is non-decreasing in the interval $t \leq t^{\text{tr}}$.

Assumption 2:

$$\dot{P}^{\text{FCR}}(t) = \dot{\mathcal{P}}^{\text{FCR}}(t; f) \geq 0, \quad t \leq t^{\text{tr}}.$$

Assumption 3 is that the FCR activated is non-increasing with respect to f in the interval $t \leq t^{\text{tr}}$.

Assumption 3: For a non-negative function ϵ

$$P^{\text{FCR}}(t) = \mathcal{P}^{\text{FCR}}(t; f) \geq \mathcal{P}^{\text{FCR}}(t; f + \epsilon), \quad t \leq t^{\text{tr}},$$

and consequently

$$E^{\text{FCR}}(t) = \mathcal{E}^{\text{FCR}}(t; f) \geq \mathcal{E}^{\text{FCR}}(t; f + \epsilon), \quad t \leq t^{\text{tr}}.$$

Assumptions 2 and 3 are justified as $f(t)$ is decreasing for $t < t^{\text{tr}}$ due to Assumption 1, and that the FCR activation set-point (1) is proportional to the frequency deviation from the nominal frequency. As demonstrated in [33], some generators may be inverse response systems. For such units $\dot{P}_j^{\text{FCR}}(t) < 0$ during the first few seconds that follow a contingency. Due to the vulnerability of small isolated power systems, it is reasonable to assume that the effect of these inverse response systems is negligible in the total FCR response, such that $\dot{P}^{\text{FCR}}(t) > 0$. In practice, this is achieved by limiting the FCR response from the inverse response systems. Fig. 9 is an illustration of Assumption 3.

Assumption 4 is that, for a fixed frequency drop, $f^{\text{nom}} - f_1^{\text{tr}}$, more (or an equal amount) of FCR is activated if the time at which f_1^{tr} occurs is increased.

Assumption 4: For f_1 and f_2 that satisfy Assumption 1 and

$$f_1(t_1^{\text{tr}}) = f_1^{\text{tr}}, \quad f_2(t_1^{\text{tr}} + \Delta t) = f_1^{\text{tr}},$$

with $t_1^{\text{tr}} + \Delta t \leq t_2^{\text{tr}}$, then

$$\mathcal{P}^{\text{FCR}}(t^{\text{tr}}; f_1) \leq \mathcal{P}^{\text{FCR}}(t^{\text{tr}} + \Delta t; f_2).$$

Assumption 4 is reasonable, since the FCR provided by a generator is limited by its response time. When a generator has more time to respond, we expect FCR for that generator to increase. Assumption 5 is that the frequency is convex for $t \leq t^{\text{tr}}$.

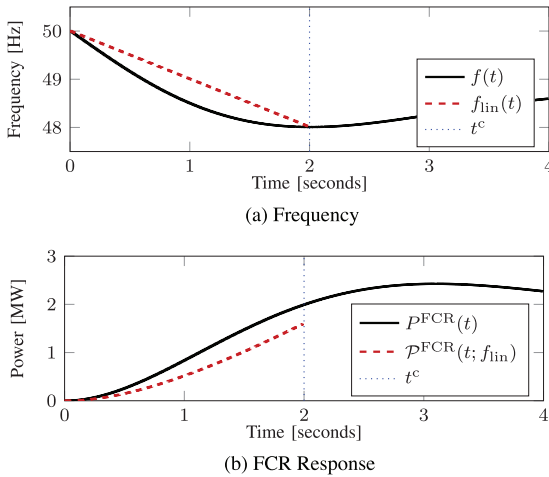


Fig. 9. Illustration of Assumption 3. We consider a situation with two generators. Generator 1 trips at time $t = 0$, with $P^{\text{lost}} = P_1^{\text{lost}} = 2$ MW. This means that $P^{\text{FCR}}(t) = P_2^{\text{FCR}}(t)$. The parameters in (6) are specified to be $H = 10$ s and $R = 2.85$ MVA. The generator dynamics are given by (39), with $\tau_1 = \tau_2 = 1$ s, and $D_1 = D_2 = 0.7$ Hz/MW. The nominal frequency is $f_0 = 50$ Hz. For this illustration, we assume that the generators have unlimited generation capacity, such that $\dot{P}_i^{\text{FCR}} = -1/D_i \Delta f(t)$. Consequently, $\mathcal{P}^{\text{FCR}}(t; f_{\text{lin}}) = \delta P^{\text{FCR}}(t)$. We define $f^{\text{lin}}(t)$ as in (14), with $t_c = 2$ s and $f = 48$ Hz. The functions $f(t)$ and $P(t)$ are determined by solving the system of differential equations (10). The function $\mathcal{P}^{\text{FCR}}(t; f_{\text{lin}})$ does not depend on the frequency. Note that Assumption 2 is satisfied.

Assumption 5: For $t_1 \leq t^{\text{tr}}$ and $t_2 \leq t^{\text{tr}}$, $f(xt_1 + (1-x)t_2) \leq xf(t_1) + (1-x)f(t_2)$, where $x \in [0, 1]$.

A sufficient condition for convexity is $\dot{f}(t) \geq 0$. For $f(t) \approx f^{\text{nom}}$, it follows from (4) that $\dot{f}(t) \approx (f^{\text{nom}})/(2HR)(P^{\text{FCR}}(t) - P^{\text{lost}})$ and consequently $\dot{f}(t) \approx 1/(2HR)f_0\dot{P}^{\text{FCR}}(t)$, which is non-negative for $t \leq t^{\text{tr}}$ due to Assumption 2. Assumption 5 is justified since we constrain the frequency to be close to its nominal value. Actual measurement data supports the convexity assumption [15].

REFERENCES

- P. J. C. Vogler-Finck and W.-G. Fröh, "Evolution of primary frequency control requirements in Great Britain with increasing wind generation," *Int. J. Elect. Power Energy Syst.*, vol. 73, pp. 377–388, 2015.
- M. Rouholamini, M. Rashidinejad, A. Abdollahi, and H. Ghasemnejad, "Frequency reserve within unit commitment considering spinning reserve uncertainty," *Int. J. Energy Eng.*, vol. 2, no. 4, pp. 177–183, 2012.
- F. D. Galiana, F. Bouffard, J. M. Arroyo, and J. F. Restrepo, "Scheduling and pricing of coupled energy and primary, secondary, and tertiary reserve," *Proc. IEEE*, vol. 93, no. 11, pp. 1970–1983, Nov. 2005.
- J. F. Restrepo and F. D. Galiana, "Unit commitment with primary frequency regulation constraints," *IEEE Trans. Power Syst.*, vol. 20, no. 4, pp. 1836–1842, Nov. 2005.
- T. Govindaraj and T. Archana, "Unit commitment based on frequency regulating reserve constraint using dynamic programming," *IJREAT Int. J. Res. Eng. Adv. Technol.*, vol. 1, no. 6, pp. 1–8, 2014.
- X. Lei, E. Lerch, and D. Povh, "Unit commitment at frequency security condition," *Eur. Trans. Elect. Power*, vol. 11, no. 2, pp. 89–96, 2001.
- X. Lei, E. Lerch, and C. Y. Xie, "Frequency security constrained short-term unit commitment," *Elect. Power Syst. Res.*, vol. 60, no. 3, pp. 193–200, 2002.
- C. C. Wu and N. Chen, "Frequency-based method for fast-response reserve dispatch in isolated power systems," in *IEE Proc., Gener., Transm., Distrib.*, 2004, vol. 151, no. 1, pp. 73–77.
- C. C. Wu and N. Chen, "Online methodology to determine reasonable spinning reserve requirement for isolated power systems," *IEE Proc., Gener., Transm., Distrib.*, vol. 150, no. 4, pp. 455–461, 2003.
- G. W. Chang, C.-S. Chuang, T.-K. Lu, and C.-C. Wu, "Frequency-regulating reserve constrained unit commitment for an isolated power system," *IEEE Trans. Power Syst.*, vol. 28, no. 2, pp. 578–586, May 2013.
- C. S. Chuang and G. W. Chang, "Lagrangian relaxation-based unit commitment considering fast response reserve constraints," *Energy Power Eng.*, vol. 5, no. 4, pp. 970–974, 2013.
- R. Doherty, G. Lalor, and M. O'Malley, "Frequency control in competitive electricity market dispatch," *IEEE Trans. Power Syst.*, vol. 20, no. 3, pp. 1588–1596, Aug. 2005.
- H. Ahmadi and H. Ghasemi, "Security-constrained unit commitment with linearized system frequency limit constraints," *IEEE Trans. Power Syst.*, vol. 29, no. 4, pp. 1536–1545, Jul. 2014.
- E. Ela, V. Gevorgian, A. Tuohy, B. Kirby, M. Milligan, and M. O'Malley, "Market designs for the primary frequency response ancillary service—Part I: Motivation and design," *IEEE Trans. Power Syst.*, vol. 29, no. 1, pp. 421–431, Jan. 2014.
- Twenties, Providing Flexibility With a Virtual Power Plant, Tech. Rep., 2013 [Online]. Available: <http://twenties-project.eu>
- SEV, SEV: Annual Report and Annual Accounts 2014, Tech. Rep., 2015 [Online]. Available: <http://sev.fi>
- M. Zima and G. Andersson, "On security criteria in power systems operation," in *Proc. IEEE Power Eng. Soc. General Meeting*, 2005, pp. 3089–3093.
- G. Andersson, Dynamics and Control of Electric Power Systems, Lecture Notes in Electrical Engineering, Power Systems Laboratory, ETH Zurich, Tech. Rep., 2012 [Online]. Available: <http://eeh.ee.ethz.ch>
- P. Kundur, N. J. Balu, and M. G. Lauby, *Power System Stability and Control*, ser. EPRI Power System Engineering Series. New York, NY, USA: McGraw-Hill, 1994.
- K. Edlund, T. Mølbak, and J. D. Bendtsen, "Simple models for model-based portfolio load balancing controller synthesis," in *Proc. 6th IFAC Symp. Power Plants and Power Systems Control*, 2009, pp. 173–178.
- J. W. O'Sullivan and M. J. O'Malley, "Identification and validation of dynamic global load model parameters for use in power system frequency simulations," *IEEE Trans. Power Syst.*, vol. 11, no. 2, pp. 851–857, May 1996.
- H. Chavez and R. Baldick, "Inertia and governor ramp rate constrained economic dispatch to assess primary frequency response adequacy," in *Proc. Int. Conf. Renewable Energies and Power Quality*, 2012, pp. 1–6.
- G. R. Lalor, "Frequency control on an island power system with evolving plant mix," Ph.D. dissertation, Sch. Elect., Electron., Mech. Eng., Univ. College Dublin, Dublin, Ireland, 2005.
- A. Ulbig, T. S. Borsche, and G. Andersson, "Impact of low rotational inertia on power system stability and operation," in *Proc. 19th IFAC World Congr.*, pp. 7290–7297, 20014.
- J. O'Sullivan, A. Rogers, D. Flynn, P. Smith, A. Mullane, and M. O'Malley, "Studying the maximum instantaneous non-synchronous generation in an island system—Frequency stability challenges in Ireland," *IEEE Trans. Power Syst.*, vol. 29, no. 6, pp. 2943–2951, Nov. 2014.
- D. E. Hampton, C. E. Tindall, and J. M. McArdle, "Emergency control of power system frequency using flywheel energy injection," in *Proc. Int. Conf. Advances in Power System Control, Operation and Management*, 1991, vol. 2, pp. 662–667.
- D. Kottick and O. Or, "Neural-networks for predicting the operation of an under-frequency load shedding system," *IEEE Trans. Power Syst.*, vol. 11, no. 3, pp. 1350–1358, Aug. 1996.
- I. Egidio, F. Fernandez-Bernal, P. Centeno, and L. Rouco, "Maximum frequency deviation calculation in small isolated power systems," *IEEE Trans. Power Syst.*, vol. 24, no. 4, pp. 1731–1738, Nov. 2009.
- M. K. Petersen, K. Edlund, L. H. Hansen, J. Bendtsen, and J. Stoustrup, "A taxonomy for modeling flexibility and a computationally efficient algorithm for dispatch in smart grids," in *Proc. Amer. Control Conf. (ACC)*, 2013, pp. 1150–1156.
- M. Carrión and J. M. Arroyo, "A computationally efficient mixed-integer linear formulation for the thermal unit commitment problem," *IEEE Trans. Power Syst.*, vol. 21, no. 3, pp. 1371–1378, Aug. 2006.
- G. Andersson, Power System Analysis, Lecture Notes in Electrical Engineering, Power Systems Laboratory, ETH Zurich, Tech. Rep., 2012 [Online]. Available: <http://eeh.ee.ethz.ch>
- H. Bevrani, *Robust Power System Frequency Control*. New York, NY, USA: Springer-Verlag, 2009.

- [33] IEEE PES Working Group, "Hydraulic turbine and turbine control models for system dynamic studies," *IEEE Trans. Power Syst.*, vol. 7, no. 1, pp. 167–179, Feb. 1992.



Leo Emil Sokoler received the (honours) M.Sc. degree in industrial mathematics from the Technical University of Denmark (DTU), Kgs. Lyngby, Denmark, in 2012. He is currently pursuing the Ph.D. degree at the Department of Applied Mathematics and Computer Science of the DTU. The Ph.D. project is a collaboration between DTU and the Danish utility company DONG Energy.

His research interests include convex optimization, power system modeling, and model predictive control.



Peter Vinter received the M.Sc. degree in electrical engineering from the Technical University of Denmark (DTU), Kgs. Lyngby, Denmark, in 1992.

He is currently a consulting engineer at P. A. Pedersen, Frederiksberg C, Denmark, working with power system planning, protection and control, and large-scale renewable integration in island systems. Previously, he worked in the fields of planning, control, protection and operation of 10–400 kV power systems at the Danish electric utilities NESA and DONG Energy. Over the years, he has supervised a

number of diploma and master students at DTU. He has contributed to research papers on virtual power plants, grid planning and distribution automation at CIRÉD conferences and other occasions.



Runi Bærentsen received the M.Sc. degree in applied mathematics from the Technical University of Denmark (DTU), Kgs. Lyngby, Denmark, in 2012.

He works as system architect for the flexibility program, providing commercial smart-grid and flexibility solutions from the Danish utility company DONG Energy. His main research interests are operations research, large data analysis, and algorithms for cost-effective control of energy systems.



Kristian Edlund received the M.Sc. EE degree in control engineering from Aalborg University, Aalborg, Denmark, in 2006 and the Ph.D. degree in control engineering from the Aalborg University, Aalborg, Denmark, in 2010.

He works as product manager for the flexibility program, providing commercial smart-grid and flexibility solutions from the Danish utility company DONG Energy. His research interests cover the fields of mathematical optimization modelling, control of energy systems and commodity market

trading in a smart grid context.



John Bagterp Jørgensen received the M.Sc. in engineering from the Technical University of Denmark (DTU), Kgs. Lyngby, Denmark, in 1997. He received the Ph.D. degree in chemical engineering in 2005 at the Department of Chemical Engineering of DTU.

He is an associate professor at the Department of Applied Mathematics and Computer Science of DTU. He is also a faculty member at DTU's Center for Energy Resources Engineering (CERE). His research concentrates on optimization and model predictive control including computational aspects

and applications. The applications include industrial processes, intelligent control of smart energy systems, production optimization and closed-loop reservoir management of oil fields, and an artificial pancreas for people with type 1 diabetes. His research is to a large extent conducted in collaboration with industrial companies. He is also a co-founder of and a partner in 2-control ApS and has significant experience in online optimization and control of industrial processes.

P A P E R I

Application of Economic MPC to Frequency Control in a Single-Area Power System

L. E. Sokoler, K. Edlund, and J. B. Jørgensen. Application of Economic MPC to Frequency Control in a Single-Area Power System. In *54th IEEE Conference on Decision and Control (CDC)*, pages 2635–2642, 2015.

Application of Economic MPC to Frequency Control in a Single-Area Power System

Leo Emil Sokoler, Kristian Edlund and John Bagterp Jørgensen

Abstract—This paper presents a novel model predictive control scheme for frequency control in a single-area power system. The proposed controller provides set-point corrections to the system power generators, based on the solution to an optimal control problem. The optimal control problem directly incorporates the cost of operation into its objective function. A trade-off parameter is used to balance set-point tracking and cost minimization. Simulations based on a Faroe Islands case study show that the proposed approach reduces cost of operation by almost an order of magnitude, compared to both set-point based model predictive control as well as conventional frequency-based PI-control.

I. INTRODUCTION

Power production planning is an important task in power system operations. The task involves solving a mixed-integer optimization problem for unit commitment and economic dispatch of the system power generators [1], [2]. This optimization problem is a computationally challenging problem that may take up to several minutes, or even hours, to solve. To compensate for real-time fluctuations in the power production and the power consumption, a second control layer is used. This layer is responsible for the activation of operational reserves. Planning the operational reserves is an integral part of the unit commitment problem. In this paper, we refer to the solution of the unit commitment problem as the nominal production plan.

In small isolated power systems, a single operator is often responsible for both power transmission and power production. An example of such an isolated power system is the Faroe Islands. Here the municipality-owned company SEV acts both as the transmission system operator (TSO) and as the sole power generating company. This means that SEV is responsible for balancing production and consumption, including the activation of operational reserves.

In the Faroe Islands, the operational reserves can be categorized into two main categories: automatic reserves and manual reserves. The automatic reserves are frequency controlled reserves that are activated in direct proportion to frequency deviations from the nominal frequency (primary control). Primary control stabilizes the frequency at a steady-state that deviates from the nominal frequency. The manual reserves are activated to eliminate the steady-state error, such that the frequency is returned to its nominal value (secondary control). Secondary control is also known as load frequency control (LFC). Following the activation of manual reserves,

a re-dispatch of the generating units may be performed to free up the required operational reserves.

Activating reserves is associated with a cost. Some generators have a low marginal production cost (e.g. wind turbines and hydro turbines), and others have a high marginal production cost (e.g. diesel generators and gas turbines). While this information is accounted for in the unit commitment problem, it is often neglected by the controllers that activate the operational reserves. An approximate method to use information on the reserve activation cost, is to combine a PI-control structure for LFC with so-called participation factors [3]–[7]. The participation factor of a generator is a gain that determines its degree of participation in the LFC. The participation factors do not distinguish between up and down regulation, which is a significant drawback from an economical point of view. Moreover, the approach does not consider the frequency dynamics. As an example, it is desirable to activate fast but expensive power generators in situations where the frequency drops significantly below the nominal frequency. Conversely, it is attractive to activate cheaper generators when the frequency drop is less significant.

In this paper, we present an economic model predictive (EMPC) based strategy for activation of operational reserves. The reserves are activated based on the solution to an optimal control problem (OCP), which takes into account real-time measurements, and updated forecasts of e.g. renewable energy production. Reference [8] provides an example of short-term forecasts that can be used for improved frequency control. The OCP objective function is formulated as a bi-objective criterion that trades off the cost of operation and set-point tracking.

Set-point based MPC have been considered for LFC in [9]–[11], and for tertiary control in [12]. References [13]–[15] develop distributed algorithms for such conventional MPC schemes. In the previous work [9]–[15], quadratic penalty functions are used to ensure 1) that the load flows on the tie-lines to other areas are restored to their scheduled values, and 2) that the frequency is returned to its nominal value. References [9] and [11] include an input-rate regularization term in the OCP objective function, to reduce wear and tear on the power generators. The main novelty of this paper, is to introduce a generalized OCP that directly incorporates the cost of operation into the MPC layer. Moreover, while existing work focus on multi-area and interconnected power systems, the proposed EMPC scheme is tailored to isolated power systems. In such systems, no power is exchanged with neighboring regions and no

L. E. Sokoler and J. B. Jørgensen are affiliated with the Department of Applied Mathematics and Computer Science, Technical University of Denmark, DK-2800 Kgs. Lyngby, Denmark {leso, jbjjo}@dtu.dk
K. Edlund are affiliated with DONG Energy, DK-2830 Virum, Denmark.

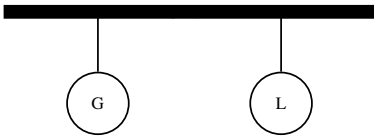


Fig. 1. Schematic diagram of the single-area power system. The system consists of a bus, which is connected to a number of generators (G), and an aggregation of loads (L).

markets are available for trading energy. The emphasis on isolated power systems is motivated by the GRANI project [16]. The GRANI project is a collaboration between DONG Energy and the Faroe Islands. The Faroe Islands acts as a live demonstration laboratory for testing new power system control technologies.

To test the proposed EMPC scheme, a non-linear simulation model of an isolated power system is developed. We linearize the non-linear model for prediction and control. To estimate non-predictable disturbances, the linear model is augmented by a disturbance model. Simulations are performed using a case study based on the Faroe Islands' power system. We compare EMPC to set-point based MPC and frequency-based PI-control. Set-point based MPC occurs as a special case of the proposed EMPC scheme. Simulations show that significant cost reductions can be achieved by trading off cost of operations and set-point tracking, even without compromising the high quality frequency control associated with set-point based MPC.

We have organized this paper as follows. Section II derives a non-linear simulation model of an isolated power system. Section III introduces an EMPC scheme for frequency control in this system, and Section IV presents a Faroe Islands case study. Section V concludes the paper.

II. MODEL

This section presents a stochastic non-linear simulation model of a small isolated power system. The system is represented by a single-area power system, in which the frequency is equal for all the power generators. The Faroe Islands is a fairly meshed system, where line capacity constraints and transmission losses are negligible for the application considered in this paper. A linearized model of the single-area power system is derived for control purpose. We provide the Kalman filter equations for state estimation in the stochastic linear system.

A. Simulation Model

Figure 1 is a diagram of the single-area power system. The system consists of three main components: a collection of power generators, a load, and a bus. By convention, negative sign is used for power consumption and positive sign is used for power production.

Power generators are modeled with different levels of detail, depending on the application of interest. Linear models

are often well suited to describe the relation between generator power set-point, and generator power production [4]–[6], [17]–[19]. Reference [20] validates such linear models against actual measurement data. Similar models have been used for MPC in [9]–[11], [14], [15], [17].

In this paper, a collection of M power generators is modeled by the linear state space model

$$\dot{x}_{g_i}(t) = A_{g_i}x_{g_i}(t) + B_{g_i}u_{g_i}(t), \quad i \in \mathcal{M}, \quad (1a)$$

$$z_{g_i}(t) = C_{g_i}x_{g_i}(t), \quad i \in \mathcal{M}, \quad (1b)$$

with $\mathcal{M} = \{1, 2, \dots, M\}$. In Equation (1), $u_{g_i}(t)$ is the power set-point of generator i , $x_{g_i}(t)$ is the state of generator i , and $z_{g_i}(t)$ is the power production of generator i .

The power set-point, $u_{g_i}(t)$, is separated into the following two components

$$u_{g_i}(t) = \underbrace{\tilde{u}_{g_i}(t)}_{\text{System Level}} - \underbrace{K_i(z_f(t) - f_0)}_{\text{Local Level}}, \quad i \in \mathcal{M}. \quad (2)$$

The system level control component is determined at a centralized level, in which interactions between the power generators are accounted for. This component includes the nominal set-point, as well as set-point adjustments resulting from secondary control. The local level control component models the primary control of each power generator. Primary control is activated in direct proportion to frequency deviations from the nominal frequency [6], [18], [19]. The nominal frequency is denoted f_0 , the current frequency is denoted $z_f(t)$, and the proportional gain associated with the primary control of generator i is denoted K_i . The model (1) is valid for set-points in the the interval $\underline{u}_{g_i}(t) \leq u_{g_i}(t) \leq \bar{u}_{g_i}(t)$. The parameter $\underline{u}_{g_i}(t)$ is the minimum production of generator i , and $\bar{u}_{g_i}(t)$ is the maximum production of generator i .

The load in Fig. 1 represents an aggregate of all the loads in the system. The aggregate may include the power production of non-controllable power generators, such as non-controllable wind-turbines and solar cells. We model the load using a linear state space model in the form

$$\dot{x}_l(t) = A_l x_l(t) + B_l d_l(t), \quad (3a)$$

$$z_l(t) = C_l x_l(t), \quad (3b)$$

The input $d_l(t)$ is the load set-point, $x_l(t)$ is the load state, and $z_l(t)$ is the actual load. Later in this paper, the load set-point is replaced by a piecewise constant load forecast. Modeling the load using the filtered value $z_l(t)$, instead of the load forecast, better represents the physical behavior of the system, since the load does not change instantaneously.

The power balance at the bus is

$$\begin{aligned} z_b(t) &= \sum_{i \in \mathcal{M}} z_{g_i}(t) + z_l(t) \\ &= \sum_{i \in \mathcal{M}} C_{g_i}x_{g_i}(t) + C_l x_l(t), \end{aligned} \quad (4)$$

Using the swing equation for a synchronous machine [6], [18], [19], the following model for the system frequency is

derived

$$\dot{x}_f(t) = A_f(x_f(t))z_b(t), \quad (5a)$$

$$z_f(t) = x_f(t), \quad (5b)$$

where $z_f(t)$ is the system frequency, and

$$A_f(x_f(t)) = f_0^2 / (2HSx_f(t)). \quad (6)$$

Note that (5) is a non-linear system, since $A_f(x_f(t))$ is a function of the system frequency. In Equation (6)

$$H = \sum_{i \in \mathcal{M}} H_i S_i / S, \quad S = \sum_{i \in \mathcal{M}} S_i.$$

Generator i has constant of inertia H_i and rating S_i . Reference [21] lists these values for different types of generators.

Collect the generator subsystems (1) into a single linear state space model with block-angular matrices (A_g, B_g, C_g) , such that $x_g = [x_{g1}, x_{g2}, \dots, x_{gM}]$, and similarly introduce u_g and z_g . Also define the frequency deviation variables

$$z_{\Delta f}(t) = x_{\Delta f}(t) = z_f(t) - f_0,$$

Equations (1), (2), (3), (4) and (5) are combined to form the system model

$$\dot{x}(t) = f(x(t), u(t), d(t)), \quad (7a)$$

$$z(t) = g(x(t)), \quad (7b)$$

$u(t) = \tilde{u}_g(t)$, $x(t) = [x_g(t)^T, x_l(t)^T, x_{\Delta f}(t)^T]^T$, $z(t) = [z_g(t)^T, z_l(t), z_b(t), z_{\Delta f}(t)]^T$, and $d(t) = d_l(t)$. Define the vector function

$$L(x(t)) = \begin{bmatrix} A_g & 0 & -B_g K \\ 0 & A_d & 0 \\ A_{\Delta f}(x(t))e^T C_g & A_{\Delta f}(x(t))C_l & 0 \end{bmatrix} x(t),$$

where e is a vector of all ones, $K = [K_1, K_2, \dots, K_M]^T$, and $A_{\Delta f}(x(t)) = A_f(f_0 + x_{\Delta f}(t))$. Moreover, define the matrices

$$B = \begin{bmatrix} B_g \\ 0 \\ 0 \end{bmatrix}, \quad E = \begin{bmatrix} 0 \\ B_d \\ 0 \end{bmatrix}, \quad C_z = \begin{bmatrix} C_g & 0 & 0 \\ 0 & C_l & 0 \\ e^T C_g & C_l & 0 \\ 0 & 0 & 1 \end{bmatrix}. \quad (8)$$

Using these definitions, the system model may be written in the form (7) with

$$\begin{aligned} f(x(t), u(t), d(t)) &= L(x(t)) + Bu(t) + Ed(t), \\ g(x(t)) &= C_z x(t). \end{aligned}$$

The deterministic model is augmented by stochastic terms. The stochastic model is

$$\begin{aligned} \mathbf{x}(t_k + T_s) &= F(\mathbf{x}(t_k), u(t_k) + \mathbf{w}_u(t_k), \\ &\quad d(t_k) + b(t_k) + \mathbf{w}_d(t_k)), \end{aligned} \quad (9a)$$

$$\mathbf{y}(t_k) = h(\mathbf{x}(t_k)) + \mathbf{v}(t_k), \quad (9b)$$

$$\mathbf{z}(t_k) = g(\mathbf{x}(t_k)). \quad (9c)$$

$\mathbf{y}(t_k)$ is a vector of measurements, $\mathbf{w}_u(t_k)$ is the generator process noise, $\mathbf{w}_d(t_k)$ is the load process noise, and $\mathbf{v}(t_k)$ is the measurement noise. The available measurements are the

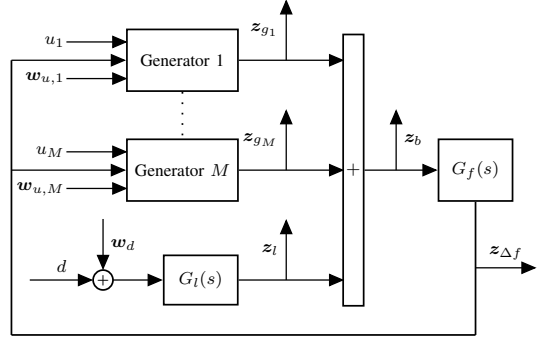


Fig. 2. System dynamics in the linear stochastic model (10). The transfer functions $G_l(s)$ and $G_f(s)$ represent the load and linearized frequency dynamics, respectively.

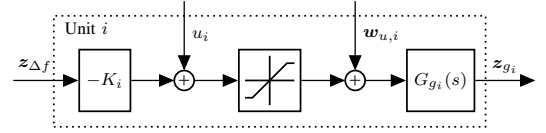


Fig. 3. Generator dynamics in the linear stochastic model (10). The transfer function $G_{g_i}(s)$ represents the dynamics of generator i .

power production of each generator, the power balance at the bus, and the system frequency. This means that $h(x(t)) = C_y x(t)$, where C_y is a sub-matrix of C_z . The sampling time is denoted T_s . We use $T_s = 0.1$ s. Bold letters indicate random variables. The system noise is assumed to consist of independent and identically distributed random variables with $\mathbf{w}_u(t_k) \sim N(0, R_{w_u})$, $\mathbf{w}_d(t_k) \sim N(0, R_{w_d})$, and $\mathbf{v}(t_k) \sim N(0, R_v)$.

In the stochastic model (9), $d(t_k)$ is interpreted as a piecewise constant load forecast. The parameters $b(t_k)$ and $\mathbf{w}_d(t_k)$ account for the forecast errors. The term $b(t_k)$ models unpredictable disturbances due to e.g. generator trips and non-zero mean forecast errors, and the term $\mathbf{w}_d(t_k)$ accounts for random fluctuations from the mean. We simulate the system using `ode45` in MATLAB.

B. Control Model

The controller proposed in this paper keeps the system frequency, $z_f(t)$, close to its nominal value, f_0 . Equation (6) shows that when $x_f(t) \approx f_0$, then $A_f(x_f(t)) \approx f_0 / (2HS)$. It follows that $L(x(t)) \approx A x(t)$, with A defined accordingly. For the application presented in this paper, it is therefore adequate to use a linearization of (9) in the controller. Fig. 2 and Fig. 3 provide a block-diagram of the linearized system. The saturation block in Fig. 3 illustrates that the generator model is valid only for set-points within the generator production limits.

With some abuse of notation, the linearized system is

written as

$$\mathbf{x}_{k+1} = A\mathbf{x}_k + B(u_k + \mathbf{w}_{u,k}) + E(d_k + \mathbf{w}_{d,k}), \quad (10a)$$

$$\mathbf{y}_k = C_y \mathbf{x}_k + \mathbf{v}_k, \quad (10b)$$

$$\mathbf{z}_k = C_z \mathbf{x}_k, \quad (10c)$$

where (A, B, E) have been redefined to denote discrete-time state space matrices. These matrices are computed from the continuous-time state space matrices using the matrix exponential. The matrices C_z and C_y are not redefined. The disturbance $b(t_k)$ is not included in (10a), as this parameter is unknown to the controller. Assuming that the sampling time is $T_s = 0.1$ as in the continuous-time case, then $\mathbf{w}_{u,k} \sim N(0, R_{w_u})$, $\mathbf{w}_{d,k} \sim N(0, R_{w_d})$, and $\mathbf{v}_k \sim N(0, R_v)$. We derive a representation of (10), with sampling time $\bar{T}_s = nT_s = n0.1$, for some integer $n \geq 1$. Increasing the sampling time may be necessary to accommodate the proposed controller to an existing control system, or to reduce the computation time of solving the OCP.

When $\bar{T}_s = nT_s$, the control input, u_k , is constant for $knT_s \leq t \leq (k+1)nT_s$. The controller assumes that the demand forecast, d_k , is constant in this interval as well. Average values can be fed into the controller if this is not the case.

Using Equation (10a), the state evolution from time $t = knT_s$ to time $t = (k+1)nT_s$, is

$$\mathbf{x}_{(k+1)n} = \tilde{A}\mathbf{x}_{kn} + \tilde{B}u_{kn} + \tilde{E}d_{kn} + \tilde{\mathbf{w}}_{kn}, \quad (11)$$

where

$$\tilde{A} = A^n, \quad \tilde{B} = \sum_{i=1}^n A^{i-1}B, \quad \tilde{E} = \sum_{i=1}^n A^{i-1}E. \quad (12)$$

In addition, $\tilde{\mathbf{w}}_{kn} \sim N(0, \tilde{R}_w)$, with covariance matrix

$$\tilde{R}_w = \sum_{i=1}^n A^{k-1} (BR_{w_u}B^T + ER_{w_d}E^T) (A^{k-1})^T.$$

By letting $k := nk$, Equations (10b), (10c), and (11) provide a discrete-time linear state space model for the linearization of (9), with sampling time $\bar{T}_s = nT_s$.

C. State Estimation

The system (9) is a stochastic system. We estimate the system state using the Kalman filter [22]. The Kalman filter is implemented based on the linearized model defined by $(\tilde{A}, \tilde{B}, \tilde{E}, C_z, C_y, \tilde{R}_w, R_v)$. To estimate the unknown disturbance, $b(t_k)$, we augment the model by a disturbance model [23], [24], such that

$$\mathbf{x}_k := \mathbf{x}_k + \tilde{E}\boldsymbol{\eta}_k. \quad (13)$$

The disturbance model is $\boldsymbol{\eta}_{k+1} = \boldsymbol{\eta}_k + \mathbf{w}_{\eta,k}$, with $\mathbf{w}_{\eta,k} \sim N(0, R_\eta)$. We denote the augmented state space system by

$$\mathbf{x}_{k+1} = A\mathbf{x}_k + Bu_k + Ed_k + \mathbf{w}_k, \quad (14a)$$

$$\mathbf{y}_k = C_y \mathbf{x}_k + \mathbf{v}_k, \quad (14b)$$

$$\mathbf{z}_k = C_z \mathbf{x}_k. \quad (14c)$$

Algorithm 1 Economic Model Predictive Control Algorithm

Filter

$$e_k = y_k - C_y \hat{\mathbf{x}}_{k|k-1}$$

$$R_{e,k} = C_y P_{k|k-1} C_y^T + R_v$$

$$\kappa_k = P_{k|k-1} C_y^T R_{e,k}^{-1}$$

$$P_{k|k} = P_{k|k-1} - \kappa_k (R_v + C_y P_{k|k-1} C_y^T) \kappa_k^T$$

$$\hat{\mathbf{x}}_{k|k} = \hat{\mathbf{x}}_{k|k-1} + \kappa_k e_k$$

Regulator

$$u_k = \mu(\mathcal{P})$$

Predictor

$$\hat{\mathbf{x}}_{k+1|k} = A\hat{\mathbf{x}}_{k|k} + Bu_k + Ed_k$$

$$P_{k+1|k} = AP_{k|k}A^T + R_w$$

In this system

$$\mathbf{x}_k := \begin{bmatrix} \mathbf{x}_k \\ \boldsymbol{\eta}_k \end{bmatrix}, \quad A := \begin{bmatrix} \tilde{A} & \tilde{E} \\ 0 & 1 \end{bmatrix}, \quad B := \begin{bmatrix} \tilde{B} \\ 0 \end{bmatrix}, \quad E := \begin{bmatrix} \tilde{E} \\ 0 \end{bmatrix},$$

$C_z := [C_z \ 0]$, and $C_y := [C_y \ 0]$. Finally, $\mathbf{w}_k \sim N(0, R_w)$ with $R_w := \text{blkdiag}(R_w, R_\eta)$, using MATLAB notation.

Define $\mathcal{I}_k = \{\mathcal{I}_{k-1}, u_{k-1}, d_{k-1}, y_k\}$, with $\mathcal{I}_0 = y_0$. Moreover, introduce the conditional means $\hat{\mathbf{x}}_{k+j|k} = E[\mathbf{x}_{k+j}|\mathcal{I}_k]$, $\hat{y}_{k+j|k} = E[y_{k+j}|\mathcal{I}_k]$, $\hat{\mathbf{z}}_{k+j|k} = E[\mathbf{z}_{k+j}|\mathcal{I}_k]$, and the conditional covariance matrix $P_{k+j|k} = V[\mathbf{x}_{k+j}|\mathcal{I}_k]$. The filtered estimate, $\hat{\mathbf{x}}_{k|k}$, and the covariance matrix, $P_{k|k}$, is computed as

$$e_k = y_k - \hat{y}_{k|k-1} = y_k - C_y \hat{\mathbf{x}}_{k|k-1}, \quad (15a)$$

$$R_{e,k} = C_y P_{k|k-1} C_y^T + R_v, \quad (15b)$$

$$\kappa_k = P_{k|k-1} C_y^T R_{e,k}^{-1}, \quad (15c)$$

$$P_{k|k} = P_{k|k-1} - \kappa_k R_{e,k} \kappa_k^T, \quad (15d)$$

$$\hat{\mathbf{x}}_{k|k} = \hat{\mathbf{x}}_{k|k-1} + \kappa_k e_k, \quad (15e)$$

κ is the Kalman filter gain, e_k is the innovation, and $R_{e,k}$ is the innovation covariance matrix. The j -step ahead prediction for $j \geq 0$ is

$$\hat{\mathbf{x}}_{k+1+j|k} = A\hat{\mathbf{x}}_{k+j|k} + Bu_{k+j} + Ed_{k+j}, \quad (16a)$$

$$P_{k+1+j|k} = AP_{k+j|k}A^T + R_w. \quad (16b)$$

Finally, $\hat{\mathbf{z}}_{k+j} = C_z \hat{\mathbf{x}}_{k+j|k}$, for $j \geq 0$.

III. ECONOMIC MODEL PREDICTIVE CONTROL

This section presents an EMPC scheme for controlling the single-area power system (9). Algorithm 1 list the EMPC scheme. The function μ solves the OCP, and returns the first element in the optimal input sequence $\{u_{k+j}^*\}_{j=0}^N$. The input argument \mathcal{P} denotes a set of input parameters to the OCP. The OCP solved in this paper is formulated as a convex quadratic program.

A. Nominal Solution

The nominal production plan is computed by solving a unit-commitment and economic dispatch problem. To account for the nominal production plan in the EMPC scheme,

we separate the inputs, states, disturbances, and outputs, in (14), into two components

$$\begin{aligned} u_k &= u_k^{\text{nom}} + u_k^{\text{mpc}}, & d_k &= d_k^{\text{nom}} + d_k^{\text{mpc}}, \\ x_k &= x_k^{\text{nom}} + x_k^{\text{mpc}}, & z_k &= z_k^{\text{nom}} + z_k^{\text{mpc}}. \end{aligned}$$

The input u_k^{nom} is the pre-computed nominal set-point, and u_k^{mpc} is the set-point correction computed in real-time. Accordingly, the disturbance d_k is partitioned into d_k^{nom} , which is known at the time the nominal set-point is computed, and d_k^{mpc} , which is known only by the real-time controller. Using the state space model (14), with $w_k = v_k = 0$, $u_k = u_k^{\text{nom}}$, and $d_k = d_k^{\text{nom}}$, we compute the nominal state and output values, x_k^{nom} and z_k^{nom} , respectively. Similarly, the generator set-points that include the effect of primary control, as defined by (2), is written as

$$u_{g,k} = u_{g,k}^{\text{nom}} + u_{g,k}^{\text{mpc}}, \quad (17)$$

where the individual components are

$$u_{g,k}^{\text{nom}} = \bar{u}_{g,k}^{\text{nom}} + K z_{\Delta f,k}^{\text{nom}}, \quad (18a)$$

$$u_{g,k}^{\text{mpc}} = \bar{u}_{g,k}^{\text{mpc}} + K z_{\Delta f,k}^{\text{mpc}}. \quad (18b)$$

B. Optimal Control Problem

The OCP solved at every sampling time is defined as

$$\min_X \phi = \sum_{j=0}^{N-1} l_j \left(u_{g,k+j}^{\text{mpc}}, \hat{z}_{k+j+1|k}^{\text{mpc}} \right), \quad (19a)$$

subject to

$$\hat{x}_{k+j+1|k}^{\text{mpc}} = A \hat{x}_{k+j|k}^{\text{mpc}} + B u_{k+j}^{\text{mpc}} + E d_{k+j}^{\text{mpc}}, \quad j \in \mathcal{N}, \quad (19b)$$

$$\hat{z}_{k+j+1|k}^{\text{mpc}} = C_z \hat{x}_{k+j+1|k}^{\text{mpc}}, \quad j \in \mathcal{N}, \quad (19c)$$

$$u_{g,k+j} = u_{g,k+j}^{\text{nom}} + u_{g,k+j}^{\text{mpc}}, \quad j \in \mathcal{N}, \quad (19d)$$

$$u_{g,k+j}^{\text{mpc}} = \bar{u}_{k+j}^{\text{mpc}} + K z_{\Delta f,k+j|k}^{\text{mpc}}, \quad j \in \mathcal{N}, \quad (19e)$$

$$\underline{u}_{k+j} \leq u_{g,k+j} \leq \bar{u}_{k+j}, \quad j \in \mathcal{N}. \quad (19f)$$

The prediction horizon is $\mathcal{N} = \{0, 1, 2, \dots, N\}$, with N being the length of the horizon. The optimization variables in (19) are

$$X = \{u_{g,k+j}, u_{g,k+j}^{\text{mpc}}, \hat{x}_{k+j+1|k}^{\text{mpc}}, \hat{z}_{k+j+1|k}^{\text{mpc}}\}_{k \in \mathcal{N}}.$$

As defined by (7), the frequency deviation, $\hat{z}_{\Delta f,k+j|k}^{\text{mpc}}$, is available as part of the output vector $\hat{z}_{k+j|k}^{\text{mpc}}$, and $\bar{u}_{g,k+j}^{\text{mpc}} = u_{k+j}^{\text{mpc}}$. The input parameters to (19) are the state space matrices (A, B, E, C_z), the nominal set-point $u_{g,k+j}^{\text{nom}}$, the load forecast correction d_{k+j}^{mpc} , the gain vector K , the generation limits ($\underline{u}_{k+j}, \bar{u}_{k+j}$), the filtered estimate $\hat{x}_{k|k}^{\text{mpc}}$, and the output $\hat{z}_{k|k}^{\text{mpc}}$. The stage cost $l_j(u_{g,k+j}, \hat{z}_{k+j|k}^{\text{mpc}})$ is defined subsequently.

Equations (19b) and (19c) are the state and output predictions. These constraints are governed by the Kalman filter equations (16). Equations (19d) and (19e) follow from (17) and (18). Equations (19e) limits the generator set-points. The limits are time-varying to account for both generator-specific technical limits, as well as limits that are determined by external factors, e.g. the wind speed for wind turbines.

C. Objective Function

The stage cost in the OCP objective function (19a) is defined as

$$\begin{aligned} l_k(u_{g,k}^{\text{mpc}}, z_{k+1}^{\text{mpc}}) &= \alpha \phi^{\text{eco}}(u_{g,k}^{\text{mpc}}, z_{k+1}^{\text{mpc}}) \\ &\quad + (1 - \alpha) \phi^{\text{sp}}(u_{g,k}^{\text{mpc}}, z_{k+1}^{\text{mpc}}), \quad k \in \mathcal{N}. \end{aligned} \quad (20)$$

The function ϕ^{eco} is an economic cost function, which is related directly to the cost of operation. The function ϕ^{sp} is a conventional set-point based penalty function. The parameter α is a tuning-parameter to trade-off cost of operation and set-point tracking. In this paper, the economic cost function is defined as

$$\phi^{\text{eco}}(u_{g,k}^{\text{mpc}}, z_{k+1}^{\text{mpc}}) = r^T \left| u_{g,k}^{\text{mpc}} - u_{g,k-1}^{\text{mpc}} \right| \quad (21a)$$

$$+ c^T \max \left(z_{g,k+1}^{\text{mpc}}, 0 \right) + \bar{c}^T \max \left(-z_{g,k+1}^{\text{mpc}}, 0 \right) \quad (21b)$$

$$+ \bar{q} \max \left(z_{\Delta f,k+1}^{\text{mpc}} - \bar{f}, 0 \right) + \underline{q} \max \left(\underline{f} - z_{\Delta f,k+1}^{\text{mpc}}, 0 \right). \quad (21c)$$

The max function and the absolute value function are evaluated element-wise. The frequency deviation, $z_{\Delta f,k+1|k}^{\text{mpc}}$, and the generator outputs, $z_{g,k+1|k}^{\text{mpc}}$, are available as part of the output vector z_{k+1}^{mpc} .

The cost function (21) consists of three terms. The first term, (21a), is an ℓ_1 -regularization term on the input-rate. The parameter $r = [r_{g_1}, r_{g_2}, \dots, r_{g_M}]$ is a cost vector associated with wear and tear on the generators. The second term, (21a), is related to the cost of generation, $c = [c_{g_1}, c_{g_2}, \dots, c_{g_M}]$ for each generator. We define \bar{c}_i , such that $\bar{c}_i = 1/c_{g_i}$, for $i \in \mathcal{M}$. For upward activation of operational reserves the penalty is c , and for downward activation of operational reserves the penalty is \bar{c} . We do not use c for downward activation, as the operational reserves should be activated only to compensate for the load not accounted for in the nominal production plan. The final term, (21c), is related to the cost of frequency deviations. The cost \bar{q} is imposed for frequency deviations smaller than \bar{f} , and the cost \underline{q} is imposed for frequency deviations larger than \underline{f} . The limits \underline{f} and \bar{f} are the cut-off frequency deviations, at which critical actions such as load shedding are initiated to avoid a blackout. In case the nominal production plan contains frequency deviations, these limits should be modified accordingly.

The set-point based penalty function, ϕ^{eco} , is defined as

$$\begin{aligned} \phi^{\text{sp}}(u_{g,k}^{\text{mpc}}, z_{k+1}^{\text{mpc}}) &= (u_{g,k}^{\text{mpc}})^T R^{\text{sp}} u_{g,k}^{\text{mpc}} \\ &\quad + (z_{k+1}^{\text{mpc}})^T Q^{\text{sp}} z_{k+1}^{\text{mpc}}. \end{aligned} \quad (22)$$

Note that $u_{g,k}^{\text{mpc}} = u_{g,k} - u_{g,k}^{\text{nom}}$, and $z_k^{\text{mpc}} = z_k - z_k^{\text{nom}}$, such that (22) penalizes deviations from the nominal production plan.

The problem (19) is formulated as a convex quadratic program. For $\alpha = 1$, the quadratic terms (22) drop out of the stage cost (20). In this special case, the optimization problem is a linear program. We solve the OCP using Gurobi.

IV. CASE STUDY

In this section, we test the proposed EMPC scheme using a simulation case study based on the Faroe Islands' power

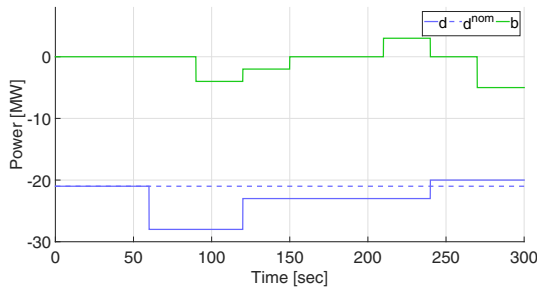


Fig. 4. Case study simulation scenario. The unit-commitment problem is solved based on the nominal load forecast d^{nom} . Updated forecasts and measurements are used in the EMPC scheme to control the system frequency in real-time.

system. The system is a reduced system that consists of $M = 4$ power generators. The EMPC based controller is compared to set-point based MPC and conventional frequency-based PI-control. The simulations are performed using an Intel(R) Xeon(R) CPU @ 2.67GHz with 12 GB RAM running a 64-bit Windows 7 Enterprise operating system.

We consider a time-varying load over 300 seconds. The load is assumed to include a portfolio of non-controllable wind-turbines. In the Faroe Islands, there are several locally owned wind-turbines that are not controlled by SEV. Fig. 4 shows the scenario set-up.

The nominal load forecast is $d_k^{\text{nom}} = -21$ MW over the entire simulation scenario. The deviations, b_k and $d_k^{\text{mpc}} = d_k - d_k^{\text{nom}}$, from the nominal forecast occur due to fluctuations in the power production and the power consumption. A significant part of the deviations is due to the non-controllable wind-turbines. The component d_k^{mpc} is predictable during real time control, and the component, b_k , is estimated based on measurements. In addition to these piece-wise constant deviations, the load and the generators are affected by process noise, as defined in (9). In our simulations the process noise covariance matrix is $R_w = I_4$, where I_4 is the identity matrix of size 4×4 . The measurement noise covariance matrix is $R_v = \text{blkdiag}(0.1I_6, 0)$. Thus, only the frequency measurement is noise-free. We have provided the noise covariance matrices for (9), such that the values can be related directly to the physical system. The nominal frequency in the Faroe Islands' power system is $f_0 = 50$ Hz.

A. System Parameters

The case study power generators are modeled as first order systems in the form

$$Z_{g_i}(s) = \frac{1}{\tau_{g_i}s + 1} U_{g_i}(s), \quad i = 1, 2, \dots, 4, \quad (23)$$

where Z_{g_i} [MW] is the power production of generator i , and U_{g_i} [MW] is the power set-point of generator i . The load has the similar form

$$Z_l(s) = \frac{1}{\tau_l s + 1} U_l(s), \quad (24)$$

TABLE I
CASE STUDY SYSTEM PARAMETERS.

Name	Type	H_i [s]	$\underline{u}_{i,k}$ [MW]	$\bar{u}_{i,k}$ [MW]	τ_i [s]
Gen. 1	Hydro	3.1	3	20	8
Gen. 2	Hydro	2.5	2	6	6
Gen. 3	Diesel	1.8	1	5	1
Gen. 4	Diesel	8.2	5	15	3

$\tau_l < \tau_{g_i}$, for $i \in \mathcal{M}$. We use $\tau_l = 0.5$ s. In (24), $U_l(s)$ [MW] is the load set-point, and $Z_l(s)$ [MW] is the actual load. The transfer functions (23) and (24) are realized in state space form, to form the system (9).

Table I lists the case study system parameters. The data represents actual generators in the Faroe Islands. Due to confidentiality reasons, the data has been partly modified. Moreover, the inertia provided by each generator is scaled up to better represent the full scale system. The parameters listed in Table I are constant over the entire simulation scenario. The unit rating, S_i [MVA], is defined to have the same magnitude as $\bar{u}_{i,k}$. The primary control gain vector is $K = [20/3, 2, 5/3, 5]^T$ [MW/Hz]. These gains are computed based on a 6% speed droop for each of the generators [4]. The power generator production costs in Euro/MWh are 4, 8, 80, and 60, respectively. Therefore, $c = \bar{T}_s/3600 \cdot [4, 8, 80, 60]^T$, where $\bar{T}_s = nT_s$ is the sampling time of the controller. The prices defined here are similar to the estimates provided in [25]. The input-rate cost is defined to be 0.05 Euro/MW, such that $r = 0.05 \cdot [1, 1, 1, 1]^T$. The hydro generators have a lower production cost than the diesel generators, but they have limited reservoirs. For this case study, the reservoirs are assumed not to have any limits. Within each generator group, the smaller and faster generator has the highest operating cost.

The nominal set-point is $u_{g,k}^{\text{nom}} = [8, 6, 1, 6]$. These set-points are computed by solving an economic dispatch problem, considering operational reserve requirements [1], [2]. The simulation is started from steady-state, such that $z_{g,k}^{\text{nom}} = u_{g,k}^{\text{nom}}$. For the disturbance model defined in (13), we use the noise covariance matrix $R_\eta = 0.1$.

B. Controller

The controller sampling time is $\bar{T}_s = 0.5$ seconds, and we define the prediction horizon to be $N = 80$ time steps. The cut-off frequency deviations are $\bar{f} = -\underline{f} = 1$ Hz. Frequency deviations larger than ± 1 Hz has a very high cost, as it involves potential load-shedding, cascading generator trips, and ultimately a total blackout. We define the price to be 1000 Euro/(Hz · s). Accordingly, $q = \bar{q} = 1000\bar{T}_s$. We note that the economic criterion, (21), may be modified to include several cut-off frequencies with different costs.

The weights in the set-point based criterion (22) are partitioned as $Q^{\text{sp}} = \text{blkdiag}(Q_g^{\text{sp}}, Q_l^{\text{sp}}, Q_b^{\text{sp}}, Q_{\Delta f}^{\text{sp}})$, and $R^{\text{sp}} = R_g^{\text{sp}}$. We use $Q_g^{\text{sp}} = I_4$, $Q_l^{\text{sp}} = Q_b^{\text{sp}} = 0$, $Q_{\Delta f}^{\text{sp}} = 100$, and $R_g^{\text{sp}} = I_4$. This means that deviations from the nominal frequency have a much higher penalty, compared to generator deviations from their nominal production plan. We scale the

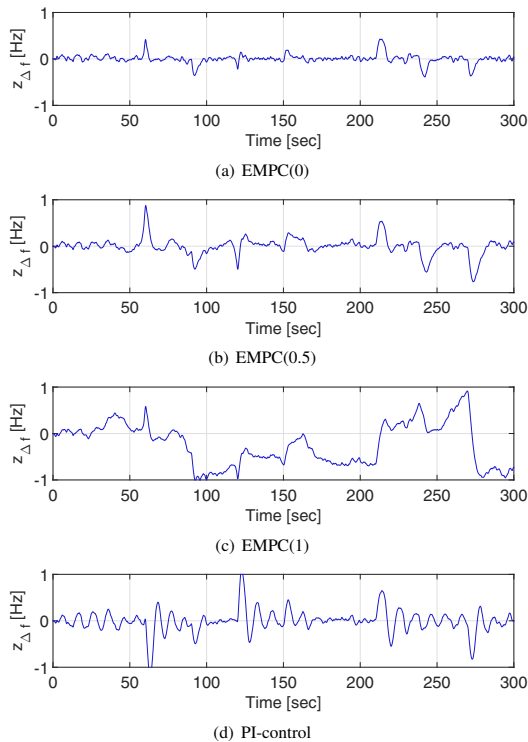


Fig. 5. System frequency associated with the closed loop simulations in Fig. 6.

weights Q^{SP} and R^{SP} by a factor $\bar{T}_s/3600$, such that the economic criterion, (21), and the set-point based criterion, (22), is in a comparable scale.

C. Simulations

Closed-loop simulations are performed using the trade-off specifications $\alpha = 0$, $\alpha = 0.5$ and $\alpha = 1$. The case $\alpha = 0$ corresponds to set-point based MPC, and $\alpha = 1$ only considers cost minimization. The case $\alpha = 0.5$ balances the two extreme cases. For compact notation, we use $\text{EMPC}(\alpha)$ to denote EMPC with trade-off parameter α . We also include a conventional frequency-based PI-controller in our comparison. We have tuned the PI-controller by trial and error.

Fig. 5 and Fig. 6 illustrate closed-loop simulations for the four different strategies described above. Fig. 5 shows the system frequency, and Fig. 6 shows the power production of the generators

For $\alpha = 0$, the EMPC scheme coincides with set-point based MPC. In this case, all the generators with free generation capacity participate in keeping the frequency close to its nominal value. Similar behavior is observed for the PI-controller. For $\alpha = 0.5$, slightly larger frequency deviations are allowed than for set-point based MPC, such that slower and less expensive units can be prioritized over the fast and

TABLE II
KEY SIMULATION RESULTS: COST OF OPERATION AND FREQUENCY DEVIATIONS FOR DIFFERENT EMPC TRADE-OFF SPECIFICATIONS, AND FOR PI-CONTROL.

	Cost of operation	$\min\{z_{\Delta,f,k}\}$	$\max\{z_{\Delta,f,k}\}$
EMPC(0)	15.8	-0.39	0.43
EMPC(0.1)	10.9	-0.45	0.48
EMPC(0.2)	7.20	-0.48	0.61
EMPC(0.3)	4.67	-0.52	0.76
EMPC(0.5)	2.68	-0.76	0.87
EMPC(1)	2.10	-1.01	0.91
PI-control	14.2	-1.19	1.10

expensive generators. Note that the frequency deviation never exceeds the cut-off frequency deviations ± 1 Hz. For $\alpha = 1$, the generators act similar to the case $\alpha = 0.5$. The frequency is however, operated close to a cut-off frequency a significant part of the time. Since the controlled system is a stochastic system, EMPC with $\alpha = 1$ is high risk strategy. By reducing α , the risk is reduced at the expense of the operating cost.

Table II provides key data from the illustrated simulations, and for additional values of the trade-off parameter α . The costs reported in this table are computed as

$$\pi = \sum_k c^T z_{g,k+1}^{\text{mpc}} + r^T \left| u_{g,k}^{\text{mpc}} - u_{g,k-1}^{\text{mpc}} \right|, \quad (25)$$

The cost (25) is the actual cost of operation. Compared to the criterion (21b), generator costs can be negative in (25) when operational reserves are activated in the downward direction.

The cost associated with set-point based MPC is approximately 16 Euro. Over the course of one year, the price difference between this strategy and EMPC with $\alpha = 0.5$, sums to over 1.3 million Euro, which is approximately 3 % of the revenues generated by SEV in 2012. Although the case $\alpha = 1$ results in even lower generation costs, it is disregarded due to its high risk. A systematic method for trading-off cost variance and cost expectation may be achieved for $\alpha = 1$, by combining the proposed strategy with mean-variance EMPC [26], [27].

V. CONCLUSIONS

We develop a novel economic model predictive control scheme for frequency control in a single-area power system. The scheme is a generalization of set-point based MPC, that trades off cost minimization and set-point tracking. Simulations based on a Faroe Islands case study show that the proposed controller reduces cost of operation by almost an order of magnitude, while maintaining a high quality frequency control.

ACKNOWLEDGEMENT

This work was funded in part by 1) the Danish Ministry of Higher Education and Science in the industrial PhD project "Stochastic MPC with Applications in Smart Energy Systems" (11-117435); and 2) The Danish Council for Strategic Research in the project "CITIES - Centre for IT-Intelligent Energy Systems in Cities" (1305-00027B).

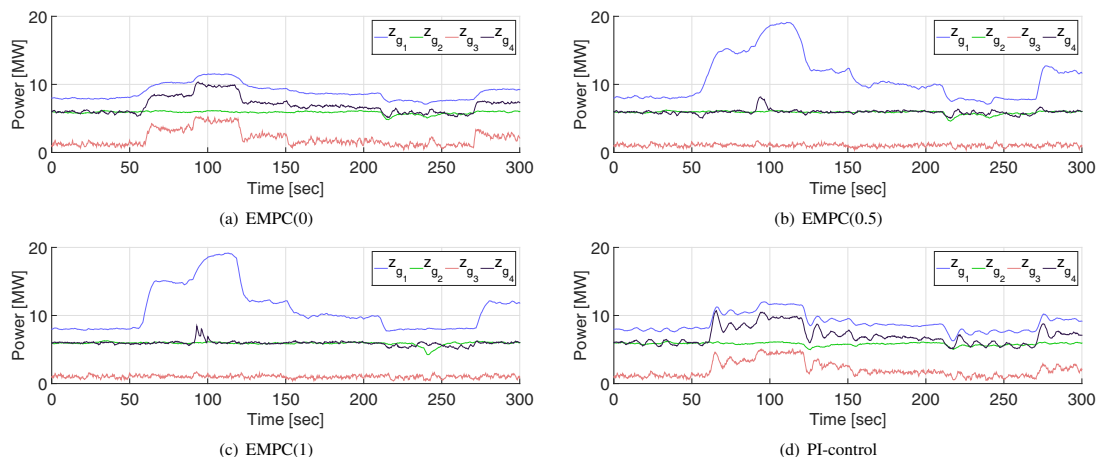


Fig. 6. Closed-loop simulation for EMPC and frequency-based PI-control. The EMPC scheme is tested using the trade-off specifications $\alpha = 0$, $\alpha = 0.5$, and $\alpha = 1$.

REFERENCES

- [1] J. F. Restrepo and F. D. Galiana, "Unit Commitment With Primary Frequency Regulation Constraints," *IEEE Transactions on Power Systems*, vol. 20, no. 4, pp. 1836–1842, 2005.
- [2] M. Carrión and J. M. Arroyo, "A computationally efficient mixed-integer linear formulation for the thermal unit commitment problem," *IEEE Transactions on Power Systems*, vol. 21, no. 3, pp. 1371–1378, 2006.
- [3] J. Kumar, K.-H. Ng, and G. Sheble, "AGC simulator for price-based operation. I. A model," *IEEE Transactions on Power Systems*, vol. 12, no. 2, pp. 527–532, 1997.
- [4] H. Bevrani, *Robust Power System Frequency Control*. New York: Springer-Verlag, 2009.
- [5] J. Carpentier, "'To be or not to be modern' that is the question for automatic generation control (point of view of a utility engineer)," *International Journal of Electrical Power & Energy Systems*, vol. 7, no. 2, pp. 81–91, 1985.
- [6] G. Andersson, "Dynamics and Control of Electric Power Systems," Lecture Notes in Electrical Engineering, Power Systems Laboratory, ETH Zurich, Tech. Rep., 2012. [Online]. Available: <http://www.eeh.ee.ethz.ch>
- [7] I. Ibraheem, P. Kumar, and D. P. Kothari, "Recent philosophies of automatic generation control strategies in power systems," *IEEE Transactions on Power Systems*, vol. 20, no. 1, pp. 346–357, 2005.
- [8] D. J. Trudnowski, W. L. McReynolds, and J. Johnson, "Real-time very short-term load prediction for power-system automatic generation control," *IEEE Transactions on Control Systems Technology*, vol. 9, no. 2, pp. 254–260, 2001.
- [9] N. Atic, D. H. A. Rerkpreedapong, and A. Feliachi, "NERC compliant decentralized load frequency control design using model predictive control," in *2003 IEEE Power Engineering Society General Meeting*, 2003, pp. 554–559.
- [10] L. Kong and L. Xiao, "A New Model Predictive Control Scheme-Based Load-Frequency Control," in *IEEE International Conference on Control and Automation*, 2007, 2007, pp. 2514–2518.
- [11] D. Rerkpreedapong, N. Atic, and A. Feliachi, "Economy oriented model predictive load frequency control," in *2003 Large Engineering Systems Conference on Power Engineering*, 2003, pp. 12–16.
- [12] F. Abbaspourbarati, M. Scherer, A. Ulbig, and G. Andersson, "Towards an optimal activation pattern of tertiary control reserves in the power system of Switzerland," in *American Control Conference (ACC)*, 2012, 2012, pp. 3629–3636.
- [13] A. N. Venkat, I. A. Hiskens, J. B. Rawlings, and S. J. Wright, "Distributed MPC Strategies With Application to Power System Automatic Generation Control," *IEEE Transactions on Control Systems Technology*, vol. 16, no. 6, pp. 1192–1206, 2008.
- [14] T. H. Mohamed, H. Bevrani, A. A. Hassan, and T. Hiyama, "Decentralized model predictive based load frequency control in an interconnected power system," *Energy Conversion and Management*, vol. 52, no. 2, pp. 1208–1214, 2011.
- [15] M. Ma, H. Chen, X. Liu, and F. Allgöwer, "Distributed model predictive load frequency control of multi-area interconnected power system," *International Journal of Electrical Power & Energy Systems*, vol. 62, no. 0, pp. 289–298, 2014.
- [16] Twenties, "Providing Flexibility with a Virtual Power Plant," Tech. Rep., 2013. [Online]. Available: <http://www.twenties-project.eu/node/18>
- [17] M. Maasoumy, A. Sanandaji, B. M. Sangiovanni-Vincentelli, and K. Poolla, "Model Predictive Control of regulation services from commercial buildings to the smart grid," in *2014 American Control Conference (ACC)*, 2014, pp. 2226–2233.
- [18] A. S. Debs, *Modern Power Systems Control and Operation*. Springer US, 1988.
- [19] A. J. Wood and B. F. Wollenberg, *Power Generation, Operation, and Control*, 3rd ed. John Wiley & Sons, 2013.
- [20] K. Edlund, T. Mølbak, and J. D. Bendtsen, "Simple models for model-based portfolio load balancing controller synthesis," in *6th IFAC Symposium on Power Plants and Power Systems Control*, 2009, pp. 173–178.
- [21] P. Kundur, N. J. Balu, and M. G. Lauby, *Power System Stability and Control*, ser. EPRI power system engineering series. McGraw-Hill, 1994.
- [22] R. Kalman, "A New Approach to Linear Filtering and Prediction Problems," *Transactions of the ASME, Journal of Basic Engineering*, vol. 82, no. Series D, pp. 35–45, 1960.
- [23] G. Pannocchia and J. B. Rawlings, "Disturbance Models for Offset-Free Model-Predictive Control," *AIChE Journal*, vol. 49, no. 2, pp. 426–437, 2003.
- [24] F. Borrelli and M. Morari, "Offset Free Model Predictive Control," in *2007 46th IEEE Conference on Decision and Control (CDC)*, 2007, pp. 1245–1250.
- [25] EIA, "Levelized Cost and Levelized Avoided Cost of New Generation Resources in the Annual Energy Outlook 2014," U.S. Energy Information Administration, Tech. Rep., 2014. [Online]. Available: <http://www.eia.gov/forecasts/aeo/er/index.cfm>
- [26] L. E. Sokoler, B. Dammann, H. Madsen, and J. B. Jørgensen, "A Mean-Variance Criterion for Economic Model Predictive Control of Stochastic Linear Systems," in *2014 IEEE 53rd Annual Conference on Decision and Control (CDC)*, 2014, pp. 5907–5914.
- [27] —, "A Decomposition Algorithm for Mean-Variance Economic Model Predictive Control of Stochastic Linear Systems," in *2014 IEEE Multi-conference on Systems and Control*, 2014, pp. 1086–1093.

P A P E R J

A Hierarchical Algorithm for Integrated Scheduling and Control with Applications to Power Systems

L. E. Sokoler, P. J. Dinesen, and J. B. Jørgensen. A Hierarchical Algorithm for Integrated Scheduling and Control with Applications to Power Systems. *IEEE Transactions on Control Systems Technology*, 2015. To appear.

A Hierarchical Algorithm for Integrated Scheduling and Control With Applications to Power Systems

Leo Emil Sokoler, Peter Juhler Dinesen, and John Bagterp Jørgensen

Abstract—The contribution of this paper is a hierarchical algorithm for integrated scheduling and control via model predictive control of hybrid systems. The controlled system is a linear system composed of continuous control, state, and output variables. Binary variables occur as scheduling decisions in the optimal control problem (OCP). The scheduling decisions are made on a slow time scale compared with the system dynamics. This gives rise to a temporal separation of the scheduling and control variables in the OCP. Accordingly, the proposed hierarchical algorithm consists of two optimization levels. The upper level (scheduling level) solves a mixed-integer linear program (MILP) with a low frequency. The lower level (control level) solves an LP with a high frequency. The main advantage of the proposed approach is that it requires online solution of an LP rather than an MILP. Simulations based on a power portfolio case study show that the hierarchical algorithm reduces the computation to solve the OCP by several orders of magnitude. The improvement in computation time is achieved without a significant increase in the overall cost of operation.

Index Terms—Hybrid power systems, mixed-integer linear programming (MILP), model predictive control (MPC), production scheduling.

I. INTRODUCTION

MODEL PREDICTIVE CONTROL (MPC) has become one of the most popular industrial control strategies [1]–[5]. The basic idea of MPC is to optimize the predicted behavior of a process model over a finite horizon. At each sampling instant, the current state is estimated based on measurements, and an optimal control problem (OCP) is formed and solved. The solution of the OCP provides a sequence of inputs. Only the first input in this sequence is applied to the controlled system, and the procedure is repeated at the

following sampling instant. In this way, a closed-loop input trajectory is synthesized using feedback by solving a sequence of open-loop OCPs.

The control of hybrid systems is an emerging application area for MPC. Examples are traction control [6], control of refrigeration systems [7]–[9], control of cogenerating power plants [10], water treatment control [11], and supply chain management [12]. The main limitation of MPC for hybrid systems is that it requires the solution of a computationally challenging OCP in real time [13]–[17]. References [18]–[20] establish important properties for MPC of hybrid systems, such as closed-loop stability. Fault detection and state estimation in hybrid systems are described in [21].

Hybrid systems are often represented as mixed logical dynamical (MLD) systems [13], [22]–[26]. MLD systems are composed of continuous and binary inputs, states, outputs, and auxiliary variables. The OCP that arises in MPC of MLD systems is a mixed-integer linear program (MILP) or a mixed-integer quadratic program (MIQP). Computationally tractable MPC schemes require algorithms that can solve the OCP in real time. Efficient algorithms for MPC of MLD systems have been proposed in [13]–[17]. Reference [16] develops a structure-exploiting gradient projection algorithm for the subproblems that occur in a branch-and-bound algorithm for the OCP. References [13]–[15] and [27] express the OCP as a multiparametric MILP, which is solved offline. The main issue with this explicit approach is that the computation time can grow exponentially with the problem size (horizon length, number of states, and number of inputs). Explicit methods are, therefore, usually limited to small-dimensional problems. Larger problems have been solved efficiently using convex relaxation techniques [28], [29] and Lagrangian decomposition [30], [31]. The performance of these methods is very problem-dependent.

In this paper, we address a special case of MPC of MLD systems where decisions are made on two time scales. Binary scheduling decisions are made on a slow time scale, while continuous control decisions are made on a fast time scale. The novelty of this paper is a hierarchical algorithm for solution of the OCP that occurs for this special case. The algorithm consists of an upper optimization level, which we refer to as the scheduling optimization level, and a lower optimization level, which we refer to as the control optimization level. The scheduling optimization level solves an MILP with a low frequency. The control optimization level solves an LP with a high frequency. Binary decisions, made by the upper optimization level, are fixed in the lower optimization level. In the hierarchical algorithm, the time-critical computation is the solution of an LP. Without the hierarchical decomposition

Manuscript received October 6, 2015; revised April 10, 2016; accepted April 23, 2016. Manuscript received in final form May 3, 2016. This work was supported in part by the Danish Ministry of Higher Education and Science within the Industrial Ph.D. Project entitled Stochastic MPC with Applications in Smart Energy Systems under Grant 11-117435, in part by the Danish Council for Strategic Research within the Project entitled Centre for IT-Intelligent Energy Systems in Cities under Grant 1305-00027B, and in part by the Southern Denmark Growth Forum and the European Regional Development Fund within the Project Smart & Cool under Grant ERDFD-10-0083. Recommended by Associate Editor A. Horch. (Corresponding author: John Bagterp Jørgensen.)

L. E. Sokoler is with the Department of Applied Mathematics and Computer Science, Technical University of Denmark, Kongens Lyngby DK-2800, Denmark, and also with DONG Energy, Virum DK-2830, Denmark (e-mail: les@dtu.dk).

P. J. Dinesen was with the Technical University of Denmark, Kongens Lyngby DK-2800, Denmark. He is now with the PA Consulting Group, Copenhagen 2150, Denmark (e-mail: pjdi@dtu.dk).

J. B. Jørgensen is with the Department of Applied Mathematics and Computer Science, Technical University of Denmark, Kongens Lyngby DK-2800, Denmark (e-mail: jbj@dtu.dk).

Color versions of one or more of the figures in this paper are available online at <http://ieeexplore.ieee.org>.

Digital Object Identifier 10.1109/TCST.2016.2565382

of the MPC scheme, the time-critical computation is the solution of an MILP.

The main assumption of the proposed approach is that the binary decisions are made on a slow time scale compared with the system dynamics. The application of the decomposition algorithm is, therefore, limited to solve the OCPs that satisfy this assumption. However, such systems are ubiquitous in integrated scheduling and control [32]–[36]. Reference [37] shows that a range of production management problems related to the control of chemical processes, e.g., batch operations, blending operations, and supply chain optimization, fits well into the proposed framework. Motion planning problems in robotics are another application area that involves decisions on two time scales (geometric path planning and real-time feedback control) [38], [39]. The hierarchical separation of the scheduling layer and the control layer is similar to the separation of the real-time optimization (RTO) layer and the control layer (MPC) commonly used in the chemical process industries [40]–[43]. The main difference is that the scheduling problem is a dynamic optimization problem involving both the continuous and discrete variables, while the RTO is a steady-state optimization problem involving continuous variables only.

This paper is motivated by the application of economic MPC (EMPC) to integrated scheduling and control in power system operations [35], [44]. In EMPC, the OCP objective function is directly related to the cost of operation [45]. For this reason, we focus on the OCPs with a linear cost function rather than a conventional setpoint-based quadratic cost function. The proposed approach generalizes to the OCPs with a quadratic cost function as well. As an illustrative example, we consider a power portfolio case study. The case study involves unit commitment (UC) and economic dispatch of a collection of power generators. An MPC scheme is employed for cost-efficient control of the power generators. The MPC scheme integrates production scheduling and balance control [46]. The ON/OFF decisions occur as binary variables in the OCP. Direct solution of the OCP is, therefore, intractable in real time. Simulations show that the proposed hierarchical algorithm reduces the computation time to solve the OCP by several orders of magnitude. The improvement in computation time is achieved without a significant increase in the overall cost of operation. The algorithm also establishes a formal relationship between the OCP and the well-known UC problem [34], [47], [48], which has not previously been described in the literature. Related problems where a similar approach can be applied are, e.g., control of cogeneration power plants [10], [23], control of wind farms for power optimization [49], and utility systems in the chemical process industries [34], [35], [50].

A. Paper Organization

This paper is organized as follows. Section II defines the OCP for integrated scheduling and control. Section III presents the hierarchical algorithm for efficient solution of the OCP. Section IV introduces the power portfolio problem. Section V provides the simulations and results, and Section VI concludes this paper.

II. PROBLEM DEFINITION

We consider continuous-time linear state-space models in the form

$$\dot{x}(t) = A_c x(t) + B_c u(t) + E_c d(t) \quad (1a)$$

$$z(t) = C_z x(t) + F_z d(t). \quad (1b)$$

The state-space matrices are denoted by $(A_c, B_c, E_c, C_z, F_z)$, the control variable is denoted by $u(t) : \mathbb{R} \mapsto \mathbb{R}^{n_u}$, the system state is denoted by $x(t) : \mathbb{R} \mapsto \mathbb{R}^{n_x}$, the disturbance is denoted by $d(t) : \mathbb{R} \mapsto \mathbb{R}^{n_d}$, and the output is denoted by $z(t) : \mathbb{R} \mapsto \mathbb{R}^{n_z}$. MPC is applied to control the system (1). The prediction horizon is $T = [t_0, t_f]$.

A. Optimal Control Problem

This section defines the OCP for integrated scheduling and control. The OCP includes binary scheduling variables and continuous control variables. We partition the prediction horizon, T , into L equidistant subintervals $T_l = [\tau_l, \tau_{l+1}]$, $l = 0, 1, \dots, L-1$, such that $T = T_0 \cup T_1 \cup \dots \cup T_{L-1}$. The length of each subinterval is $\Delta\tau = (t_f - t_0)/L$. $\tau_0 = t_0$ and $\tau_L = t_f$. Let $\mathcal{L} = \{0, 1, \dots, L\}$ denote the set of indices associated with time instants $\tau_0, \tau_1, \dots, \tau_L$. A vector of binary scheduling variables, $b_l \in \{0, 1\}^q$, is associated with each time step, τ_l .

The OCP is defined as

$$\min_{X(\cdot), v(\cdot), b} f_{\mathbb{R}}(X, v) + f_{\mathbb{Z}}(b) \quad (2a)$$

$$\text{s.t. } \dot{x}(t) = A_c x(t) + B_c u(t) + E_c d(t), \quad t \in T \quad (2b)$$

$$z(t) = C_z x(t) + F_z d(t), \quad t \in T \quad (2c)$$

$$c_{\mathbb{R}}(X(t), v(t), t) \leq 0, \quad t \in T \quad (2d)$$

$$c_{\mathbb{Z}}(b) \leq 0 \quad (2e)$$

$$\gamma(v(t), b) = 0, \quad t \in T. \quad (2f)$$

The decision variables in (2) are the continuous-time functions $X(t) = [u(t)^T \ x(t)^T \ z(t)^T]^T : \mathbb{R} \mapsto \mathbb{R}^{n_u+n_x+n_z}$ and $v(t) : \mathbb{R} \mapsto \mathbb{R}^q$, and the vector of binary variables

$$b = [b_0^T \ b_1^T \ \dots \ b_L^T]^T. \quad (3)$$

In general, $X(t)$ may also contain auxiliary continuous-time functions. Constraints (2b) and (2c) are the state-space constraints. The initial state, $x(0) = x_0$, is a fixed parameter. Equation (2d) represents the continuous-time constraints. These constraints are related to the continuous control decisions for the system (1). Equation (2e) represents the discrete-time constraints. These constraints are related to the binary scheduling decisions for the system (1). We assume that $c_{\mathbb{R}}$ and $c_{\mathbb{Z}}$ are the affine functions.

In the objective function (2a), $f_{\mathbb{R}}(X, v)$ is the cost associated with the continuous control decisions, and $f_{\mathbb{Z}}(b)$ is the cost associated with the binary scheduling decisions. We assume that $f_{\mathbb{R}}$ and $f_{\mathbb{Z}}$ are the linear functions. Moreover

$$f_{\mathbb{R}}(X, v) = \int_{t_0}^{t_f} g_{\mathbb{R}}(X(t), v(t), t) dt. \quad (4)$$

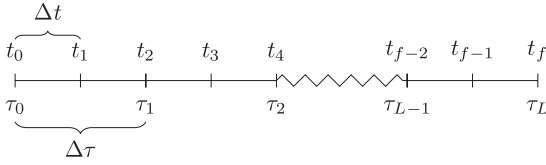


Fig. 1. Two time scales associated with the OCP (7). The sampling time of the continuous-time system, (1), is Δt . The time between the binary decisions, (3), is $\Delta \tau$. This paper addresses the case where Δt is small compared with $\Delta \tau$.

Constraint (2f) couples the vector of binary variables, b , and the continuous-time function $v(t)$. The coupling function, γ , is defined as

$$\gamma(v(t), b) = \begin{cases} v(t) - b_0 & \text{if } \tau_0 \leq t \leq \tau_1 \\ \vdots & \\ v(t) - b_{L-1} & \text{if } \tau_{L-1} \leq t \leq \tau_L. \end{cases} \quad (5)$$

This means that any feasible solution of (2) satisfies

$$v(t) = b_l, \quad \tau_l \leq t \leq \tau_{l+1}$$

for $l \in \mathcal{L} \setminus \{L\}$. The main purpose of the coupling function, γ , is to decouple the binary and continuous variables in $c_{\mathbb{R}}$ and $c_{\mathbb{Z}}$, as well as in $f_{\mathbb{R}}$ and $f_{\mathbb{Z}}$. Note that the system dynamics, (2b), does not depend on the binary variables.

B. Discretization

To solve (2), we discretize the optimization problem. The sampling time is $\Delta t = \Delta \tau / K$, for some positive integer K . The discretization points are denoted by t_0, t_1, \dots, t_N . We let $\mathcal{N} = \{0, 1, \dots, N\}$ denote the set of indices associated with the discretization points. Note that

$$\tau_l = t_{Kl}, \quad l \in \mathcal{L}. \quad (6)$$

Fig. 1 shows the relation (6) for $K = 2$.

We consider the case where binary decisions are made on a slow time scale, compared with the system dynamics. This means that Δt is small compared with $\Delta \tau$, i.e., $N \gg L$. The discrete-time formulation of (2) is

$$\min_{X, v, b} \tilde{f}_{\mathbb{R}}(X, v) + f_{\mathbb{Z}}(b) \quad (7a)$$

$$\text{s.t. } x_{k+1} = Ax_k + Bu_k + Ed_k, \quad k \in \mathcal{N} \setminus \{N\} \quad (7b)$$

$$z_k = C_z x_k + F_z d_k, \quad k \in \mathcal{N} \setminus \{0\} \quad (7c)$$

$$c_{\mathbb{R}}(X_k, v_k, t_k) \leq 0, \quad k \in \mathcal{N} \quad (7d)$$

$$c_{\mathbb{Z}}(b) \leq 0 \quad (7e)$$

$$\gamma(v_k, b) = 0, \quad k \in \mathcal{N}. \quad (7f)$$

Constraints (7b) and (7c) are the discrete-time equivalents of (2b) and (2c), respectively. The discrete-time state-space matrices are denoted by A , B , and E . $u_k \in \mathbb{R}^{n_u}$ is the control variable, $x_k \in \mathbb{R}^{n_x}$ is the system state, $d_k \in \mathbb{R}^{n_d}$ is the disturbance, and $z_k \in \mathbb{R}^{n_z}$ is the output. The initial state, x_0 , is a fixed parameter. As in the continuous-time case, we use $X_k = [u_k^T \ x_k^T \ z_k^T]^T$ for compact notation. This vector may

also contain additional auxiliary variables. In the objective function (7a), we have defined

$$\tilde{f}_{\mathbb{R}}(X, v) = \sum_{k \in \mathcal{N} \setminus \{N\}} g_{\mathbb{R}}(X_k, v_k, t_k) \Delta t$$

which is an Euler approximation of the integral (4).

III. HIERARCHICAL ALGORITHM

Problem (7) is an MILP. Solving (7) in real time is, therefore, challenging, especially since N is large. To reduce the computation time to solve (7), we consider a hierarchical approach. The idea is to decompose the solution of (7) into two separate optimization levels. The upper optimization level (scheduling level) is associated with the binary decisions that are made on a slow time scale, and the lower optimization level (control level) is associated with the control decisions that are made on a fast time scale. Binary variables are fixed at the lower optimization level. For this reason, the lower level optimization problem can be expressed as an LP. We refer to the upper level MILP as the UL-OCP, and to the lower level LP as the LL-OCP. The UL-OCP is solved with a low frequency, and the LL-OCP is solved with a high frequency.

A. Upper Level Optimal Control Problem

The UL-OCP is simply (7), where we replace the sampling time, Δt , with some $\Delta \bar{t}$ that satisfies

$$\Delta t \leq \Delta \bar{t} \leq \Delta \tau$$

with $\Delta \tau / \Delta \bar{t}$ integer. We use bar notation to denote the variables and the parameters associated with the UL-OCP. In the case $\Delta \bar{t} = \Delta t$, the UL-OCP coincides with (7). When $\Delta \bar{t} = \Delta \tau$, the sampling time is the time between binary decisions. By assumption, the system dynamics occurs at a much faster time scale than $\Delta \tau$. Therefore, the state transition matrix, \bar{A} , resulting from a discretization with $\Delta \bar{t} = \Delta \tau$, satisfies $\bar{A} \approx 0$. In addition

$$\bar{z}_k \approx C_z(\bar{B}\bar{u}_{k-1} + \bar{E}\bar{d}_{k-1}) + F_z\bar{d}_k, \quad k \in \mathcal{N}. \quad (8)$$

Consequently, the state variables $\bar{x}_1, \bar{x}_2, \dots, \bar{x}_{\bar{N}}$ can be eliminated from the UL-OCP, for a sufficiently large $\Delta \bar{t}$.

B. Lower Level Optimal Control Problem

The LL-OCP is (7) with fixed binary variables, $b = \bar{b}$. As the binary variables are fixed, we do not include $f_{\mathbb{Z}}(\bar{b})$ in the LL-OCP objective function. Similarly, constraint (7e) is excluded from the LL-OCP. The LL-OCP is

$$\min_X \sum_{k \in \tilde{\mathcal{N}} \setminus \{\tilde{N}\}} g_{\mathbb{R}}(X_k, \bar{v}_k, t_k) \Delta t \quad (9a)$$

$$\text{s.t. } x_{k+1} = Ax_k + Bu_k + Ed_k, \quad k \in \tilde{\mathcal{N}} \setminus \{\tilde{N}\} \quad (9b)$$

$$z_k = C_z x_k + F_z d_k, \quad k \in \tilde{\mathcal{N}} \setminus \{0\} \quad (9c)$$

$$c_{\mathbb{R}}(X_k, \bar{v}_k, t_k) \leq 0, \quad k \in \tilde{\mathcal{N}} \quad (9d)$$

where $\tilde{\mathcal{N}} = \{0, 1, \dots, \tilde{N}\}$. The variables $v_1 = \bar{v}_1, v_2 = \bar{v}_2, \dots, v_N = \bar{v}_N$ are fixed parameters in (9). These parameters are determined by the coupling function (5), for fixed $b = \bar{b}$. Since the system dynamics occurs on a relatively fast time scale, \tilde{N} may be chosen significantly smaller than N .

Algorithm 1 MPC of (10) via Hierarchical Solution of the OCP

```

k = 0, l = 0
for t = t0, t1, . . . , ∞ do
  k ← k + 1
  yk ← measure system output
  x̂k|k ← estimate system state
  {d̂k+j|k}j∈N ← update disturbance forecast
  ===== HIERARCHICAL ALGORITHM =====
  if t = τl then
    if Ilb = 1 then
      // UPPER OPTIMIZATION LEVEL
      {b̂l+j}j∈L ← solve UL-OCP (MILP).
    end if
    l ← l + 1
  end if
  // LOWER OPTIMIZATION LEVEL
  uk ← solve LL-OCP (LP)
  =====
  apply uk to the system (10)
end for

```

C. Algorithm

Consider the stochastic system

$$\mathbf{x}_{k+1} = \mathbf{A}\mathbf{x}_k + \mathbf{B}u_k + \mathbf{E}\mathbf{d}_k + \mathbf{G}\mathbf{w}_k \quad (10a)$$

$$\mathbf{z}_k = \mathbf{C}_z\mathbf{x}_k + \mathbf{F}_z\mathbf{d}_k \quad (10b)$$

$$\mathbf{y}_k = \mathbf{C}_y\mathbf{x}_k + \mathbf{F}_y\mathbf{d}_k + \mathbf{v}_k \quad (10c)$$

where $\mathbf{w}_k \sim N(0, \mathbf{R}_w)$ is the process noise, $\mathbf{v}_k \sim N(0, \mathbf{R}_v)$ is the measurement noise, and $\mathbf{d}_k \sim N(\check{\mathbf{d}}_k, \mathbf{R}_d)$ is an unknown disturbance. We use bold letters to denote random variables.

Define $\mathcal{I}_k = \{\mathcal{I}_{k-1}, u_{k-1}, \mathbf{d}_{k-1}, y_k\}$, with $\mathcal{I}_0 = y_0$. Moreover, introduce the conditional means $\hat{\mathbf{x}}_{k+j|k} = E[\mathbf{x}_{k+j}|\mathcal{I}_k]$, $\hat{\mathbf{y}}_{k+j|k} = E[y_{k+j}|\mathcal{I}_k]$, and $\hat{\mathbf{z}}_{k+j|k} = E[\mathbf{z}_{k+j}|\mathcal{I}_k]$, and the conditional covariance matrix $\mathbf{P}_{k+j|k} = V[\mathbf{x}_{k+j}|\mathcal{I}_k]$. These values are computed using the Kalman filter. The disturbance forecast is denoted by $\hat{\mathbf{d}}_{k+j|k}$. We assume that a disturbance forecast is generated by some external procedure.

In MPC, based on the separation and certainty equivalence principle, uncertain parameters are replaced by their conditional expectations. We use this approach to control the stochastic system (10). The OCP solved at every sampling instant, $k = 0, 1, \dots, \infty$, is (7), with $x_0 = \hat{x}_{k|k}$, and $d_j = \hat{d}_{k+j|k}$ for $j \in \mathcal{N}$. Algorithm 1 is an MPC scheme for the control of the stochastic system (10), using the hierarchical algorithm for the solution of the OCP. The indicator variables $I_1^b, I_2^b, \dots, I_\infty^b$ trigger the solution of the UL-OCP. The indicator variables can be predefined or updated online, e.g., it is reasonable to update the scheduling decisions if a significant change in the disturbance forecast arises. The lower optimization level requires that the values for the binary variables are available within its control horizon. Therefore, $I_0^b = 1$.

There are several parameters in Algorithm 1 that can be tuned to tradeoff optimality and computation time. Increasing the sampling time, $\Delta\bar{t}$, reduces the size of the UL-OCP.

Reducing the length of the prediction horizon, \bar{N} , reduces the size of the LL-OCP. As an example, \bar{N} may be chosen just large enough to ensure that the controller is stable [51]–[53]. We suggest to use a fairly long prediction horizon to achieve stable and cost-efficient operation of the system.

IV. POWER PORTFOLIO PROBLEM

Electricity is bought and sold in electricity markets. A majority of the energy is usually traded in a day-ahead energy market. When the market is cleared, the power producers receive a 24 h-ahead reference profile specifying the amount of electricity they have sold. Scheduling the generation of available power generators is a challenging task for the power producers, as it involves decisions across different time scales and scheduling horizons. Hours-ahead to days-ahead scheduling (scheduling level) is handled by solving an MILP for UC and economic dispatch of the power generators. To account for imbalances between the power production and the reference profile, a balance control layer (control level) can be employed. The control level is important to account for the inherent uncertainties associated with the generation of renewable energy sources [44], [46]. We show that the proposed approach facilitates the integration of the scheduling and the control level. This makes it possible to tradeoff computation time and optimality in a systematic way.

A collection of M power generators is controlled using the proposed MPC scheme. The M power generators represent a portfolio of generators that is operated by a single power producer. The generators are modeled as transfer functions in the form

$$Z_i(s) = G_{u,i}(s)U_i(s), \quad i \in \mathcal{M} \quad (11)$$

where $\mathcal{M} = \{1, 2, \dots, M\}$. $U_i(s)$ is the power production setpoint, and $Z_i(s)$ is the power production. We define $D(s)$ to be the aggregated power production from uncontrollable generators, such as photovoltaic generators and uncontrollable wind turbines. The net power production is the sum

$$Z_T(s) = \sum_{i \in \mathcal{M}} Z_i(s) + D(s). \quad (12)$$

We collect (11) and (12) into a single model in the form

$$Z(s) = G_u(s)U(s) + G_d(s)D(s) \quad (13)$$

where $U(s) = [U_1(s)^T, \dots, U_M(s)^T]^T$ is the control variable, and $Z(s) = [Z_1(s)^T, \dots, Z_M(s)^T, Z_T(s)^T]^T$ is the output

$$G_u(s) = [\mathbf{blkdiag}(G_{u,1}, \dots, G_{u,M}); [G_{u,1}, \dots, G_{u,M}]]$$

and $G_d(s) = [0, \dots, 0, 1]^T$ are the transfer functions. The model (13) is realized in the continuous-time state-space form (1). In the resulting model structure

$$\mathbf{A}_c = \mathbf{blkdiag}(\mathbf{A}_{c,1}, \mathbf{A}_{c,2}, \dots, \mathbf{A}_{c,M})$$

$$\mathbf{B}_c = \mathbf{blkdiag}(\mathbf{B}_{c,1}, \mathbf{B}_{c,2}, \dots, \mathbf{B}_{c,M})$$

$$\mathbf{C}_z = [\mathbf{blkdiag}(\mathbf{C}_{z,1}, \dots, \mathbf{C}_{z,M}); [\mathbf{C}_{z,1}, \dots, \mathbf{C}_{z,M}]]$$

$\mathbf{E}_c = 0$, and $\mathbf{F}_z = [0, \dots, 0, 1]^T$. Moreover, $x(t)$ is the system state, $u(t) = [u_1(t)^T, \dots, u_M(t)^T]^T$ is the vector of power production setpoints, and $z(t) = [z_1(t)^T, \dots, z_{M+1}(t)^T]^T$ is

the vector of power production outputs. This vector contains the power production of each generator, as well as the total power production, $z_{M+1}(t) = z_T(t)$. Finally, $d(t)$ is the power production from noncontrollable generators.

The power generators can be turned ON and OFF in the time instants $t \in \{\tau_0, \tau_1, \dots, \tau_L\}$. Define the binary variables

$$b_{i,l}^s = \begin{cases} 1, & \text{if generator } i \text{ is running at time } \tau_l \\ 0, & \text{otherwise} \end{cases}$$

$i \in \mathcal{M}$ and $l \in \mathcal{L}$. Similarly, define $b_{i,l}^u$ to indicate if a generator is turned ON, and $b_{i,l}^d$ to indicate if a generator is turned OFF. In addition

$$v_i^s(t) = b_{i,l}^s, \quad \tau_l \leq t \leq \tau_{l+1} \quad (14)$$

for $i \in \mathcal{M}$ and $l \in \mathcal{L} \setminus \{L\}$, i.e., $v_i^s(t)$ is a piecewise constant representation of $b_{i,l}^s$. We define $v_i^u(t)$ and $v_i^d(t)$ in the same manner.

The cost of operation is defined as

$$\psi = \int_{t_0}^{t_f} \left(\sum_{i \in \mathcal{M}} (p_i^z z_i(t) + p_i^s v_i^s(t)) + p^\rho \rho(t) \right) dt + \sum_{i \in \mathcal{M}} \sum_{l \in \mathcal{L}} (p_i^u b_{i,l}^u + p_i^d b_{i,l}^d) \quad (15)$$

where p_i^z is the marginal production price for power generator i , p_i^s is the fixed running cost for power generator i , p_i^u is the start-up cost for power generator i , and p_i^d is the shutdown cost for power generator i . p^ρ is the marginal price for power imbalances. Imbalance costs are imposed when the power production deviates from a predefined reference (e.g., the power demand or the power sold in the day-ahead electricity market), denoted by $r(t)$. This is expressed as

$$r(t) - \rho(t) \leq z_{M+1}(t) \leq r(t) + \rho(t), \quad t \in T. \quad (16)$$

To keep the notation simple, we use one single price, p^ρ , for both the positive and negative imbalances. Asymmetric prices can represent a market situation where power is traded on an electricity exchange.

The power production setpoint for a generator is limited by its capacity limits. This is modeled by the constraint

$$\underline{z}_i v_i^s(t) \leq u_i(t) \leq \bar{z}_i v_i^s(t), \quad i \in \mathcal{M}, \quad t \in T. \quad (17)$$

The lower and upper capacity limits for power generator i are \underline{z}_i and \bar{z}_i , respectively. The setpoint for a generator not running is zero. This is enforced by multiplying each of the capacity limits in (17) by $v_i^s(t)$. A constraint on the input-rate is defined to avoid drastic setpoint changes

$$\partial \underline{u}_i - Q v_i^d(t) \leq \frac{du_i(t)}{dt} \leq \partial \bar{u}_i + Q v_i^u(t) \quad (18)$$

$i \in \mathcal{M}$, $t \in T$. The upper and lower input-rate limits for generator i are $\partial \underline{u}_i$ and $\partial \bar{u}_i$, respectively. The terms involving Q relax the constraint (18) when a generator is turned ON or OFF. This is necessary to avoid infeasibility of the OCP, e.g., when $\underline{u}_i \geq \Delta \bar{u}_i$ for some $i \in \mathcal{M}$. The binary decision variables are coupled by the constraints

$$b_{i,l}^s = b_{i,l-1}^s + (b_{i,l}^u - b_{i,l}^d), \quad i \in \mathcal{M}, \quad l \in \mathcal{L} \quad (19a)$$

$$b_{i,l}^u + b_{i,l}^d \leq 1, \quad i \in \mathcal{M}, \quad l \in \mathcal{L}. \quad (19b)$$

These constraints model the start-up and shutdown logic. We refer to [47] for a detailed description of the logical constraints in UC and economic dispatch problems. The OCP associated with the power portfolio problem is to minimize (15) subject to the constraints (16)–(19).

A. Standard Form

The OCP associated with the power portfolio problem is written in the standard form (7). The components of the binary vector, (3), are

$$b_l = [b_{1,l}^s \quad b_{1,l}^u \quad b_{1,l}^d \quad \dots \quad b_{M,l}^s \quad b_{M,l}^u \quad b_{M,l}^d]$$

for $l \in \mathcal{L}$. We define the components of v accordingly. In the objective function (2a)

$$f_{\mathbb{R}}(X, v) = \int_{t_0}^{t_f} \left(\sum_{i \in \mathcal{M}} (p_i^z z_i(t) + p_i^s v_i^s(t)) + p^\rho \rho(t) \right) dt$$

$$f_{\mathbb{Z}}(b) = \sum_{i \in \mathcal{M}} \sum_{l \in \mathcal{L}} p_i^u b_{i,l}^u + p_i^d b_{i,l}^d$$

such that

$$g_{\mathbb{R}}(X(t), v(t), t) = \sum_{i \in \mathcal{M}} (p_i^z z_i(t) + p_i^s v_i^s(t)) + p^\rho \rho(t)$$

and $X(t) = [u(t)^T \quad x(t)^T \quad z(t)^T \quad \rho(t)^T]^T$. The function associated with the constraint (2d) is

$$c_{\mathbb{R}}(X(t), v(t), t) = \begin{bmatrix} \bar{c}_{\mathbb{R}}(X(t), v(t), t) \\ c_{\mathbb{R}}^0(X(t), v(t), t) \\ \vdots \\ c_{\mathbb{R}}^N(X(t), v(t), t) \end{bmatrix} \quad (20)$$

where

$$\bar{c}_{\mathbb{R}}(X(t), v(t), t) = \begin{bmatrix} z_{M+1}(t) - r(t) - \rho(t) \\ r(t) - z_{M+1}(t) - \rho(t) \\ u_i(t) - \bar{z}_i v_i^s(t) \\ \underline{z}_i v_i^s(t) - u_i(t) \end{bmatrix}$$

$$c_{\mathbb{R}}^i(X(t), v(t), t) = \begin{bmatrix} \frac{du_i(t)}{dt} - \Delta \bar{u}_i - Q v_i^u(t) \\ \Delta \underline{u}_i - Q v_i^d(t) - \frac{du_i(t)}{dt} \end{bmatrix}, \quad i \in \mathcal{M}.$$

$c_{\mathbb{Z}}(b)$ is constructed by stacking the constraints (19). The coupling constraint (2f) follows from the definition (5).

In the discretized OCP, (7), we use the backward-difference approximation

$$\frac{du_i(t)}{dt} \approx \frac{u_{i,k} - u_{i,k-1}}{\Delta t}, \quad i \in \mathcal{M}, \quad k \in \mathcal{N}.$$

The constraints for the discretized OCP are expressed as in (20) with

$$\bar{c}_{\mathbb{R}}(X_k, v_k, t_k) = \begin{bmatrix} z_{M+1,k} - r_k - \rho_k \\ r_k - z_{M+1,k} - \rho_k \\ u_{i,k} - \bar{z}_{i,k} v_{i,k}^s \\ \underline{z}_{i,k} v_{i,k}^s - u_{i,k} \end{bmatrix}$$

$$c_{\mathbb{R}}^i(X_k, v_k, t_k) = \begin{bmatrix} \frac{u_{i,k} - u_{i,k-1}}{\Delta t} - \partial \bar{u}_i - Q v_{i,k}^u \\ \partial \underline{u}_i - Q v_{i,k}^d - \frac{u_{i,k} - u_{i,k-1}}{\Delta t} \end{bmatrix}, \quad i \in \mathcal{M}.$$

The discretized OCP is an MILP. To get well-behaved closed-loop solutions, the OCP objective function can be augmented by ℓ_1 - and ℓ_2 -penalty terms on the input-rate [54]. For ℓ_2 -regularization, the OCP becomes an MIQP. It is straightforward to generalize the hierarchical algorithm to this case.

B. Relationship to the Unit Commitment Problem

The transfer function (11) maps the power production setpoint for a generator to its actual power production. It is reasonable to assume that the gain in this system is 1. This means that

$$z_i(t) \rightarrow u_i(t), \quad i \in \mathcal{M} \quad (21a)$$

$$z_{M+1}(t) \rightarrow \sum_{i \in \mathcal{M}} u_i(t) + d(t) \quad (21b)$$

for $t \rightarrow \infty$. Consider the approximation (8) for the UL-OCP. Based on (21), we can further assume that

$$C_z \bar{B} \approx [\mathbf{blkdiag}(I, \dots, I); [1, 1, 1]]$$

where we use that $E = 0$ and $F_z = [0, \dots, 0, 1]^T$. Consequently

$$\begin{bmatrix} \bar{z}_{1,k} \\ \vdots \\ \bar{z}_{M,k} \\ \bar{z}_{T,k} \end{bmatrix} = \begin{bmatrix} \bar{u}_{1,k-1} \\ \vdots \\ \bar{u}_{M,k} \end{bmatrix} + \begin{bmatrix} 0 \\ \vdots \\ 0 \\ \bar{d}_k \end{bmatrix}, \quad k \in \mathcal{N}. \quad (22)$$

Equation (22) is used to eliminate the power production variables, $\bar{z}_1, \bar{z}_2, \dots, \bar{z}_N$ from the UL-OCP. In this way, the UL-OCP can be expressed without the state and output variables, as well as without the state-space constraint (7b) and (7c). The resulting optimization problem is a UC problem [34], [47], [48], i.e., for a sufficiently coarse temporal discretization, the UL-OCP coincides with the UC problem. Hierarchical decomposition of UC and balance control is widely adopted in power system operations [34], [48]. This paper shows that the hierarchical approach can be interpreted as an approximate way to solve the OCP (7). The approximation provides a computationally efficient scheme to obtain suboptimal solutions of (7). This makes it possible to employ MPC, based on (7), for integrated scheduling and control.

V. CASE STUDY

We consider an example of the power portfolio problem, with $M = 3$ generators in the form

$$G_{u,i}(s) = \frac{1}{(1 + \kappa_i s)^3}, \quad i \in \mathcal{M}. \quad (23)$$

Reference [55] validates the model (23) against actual measurement data. Note that the gain in the system (23) is 1. The controlled system is a stochastic system in the form (10). The disturbance, d_k , is the noncontrollable wind power production. For this case study, we do not consider process noise nor measurement noise.

Table I lists the case study parameters for each of the three generators in convenient display units. Generator 1 has a small time constant, i.e., the generator is fast. It has a high marginal production price and a high fixed running cost.

TABLE I
CASE STUDY GENERATOR PARAMETERS

Parameter/Generator	Gen. 1	Gen. 2	Gen. 3
κ_i [s]	20	25	40
p_i^z [EUR/MWh]	80	40	10
p_i^b [EUR/h]	25	10	5
p_i^u [EUR]	100	150	200
p_i^d [EUR]	0	0	0
$(\partial \underline{u}_i, \partial \bar{u}_i)$ [MW/s]	(-0.2, 0.2)	(-0.1, 0.1)	(-0.05, 0.05)
$(\bar{z}_i, \underline{z}_i)$ [MW]	(0.5, 5)	(2, 10)	(5, 25)

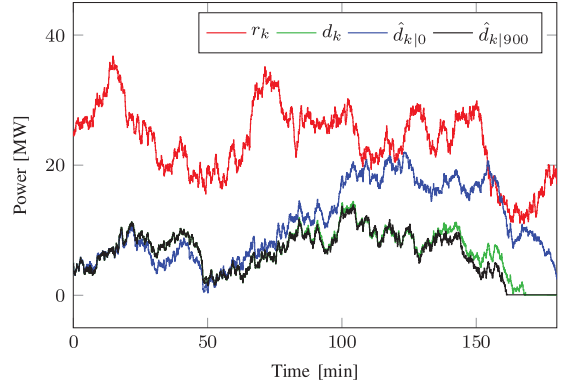


Fig. 2. Case study power demand (reference, r_k), wind power production (disturbance, d_k), and wind power forecasts (disturbance forecasts, $\hat{d}_{k|0}$ and $\hat{d}_{k|900}$).

Moreover, Generator 1 has a very limited capacity. In contrast to this, Generator 3 is a slow low-cost generator with a large capacity. Generator 2 is a medium-sized generator. The contrast between the generator agility and the production price is a common situation in power systems, where large thermal power plants often produce a majority of the electricity, while the use of smaller gas turbines is limited to critical peak periods.

The imbalance price, p^ρ , is 400 EUR/MWh. The time between binary decisions is $\Delta \tau = 900$ s. This means that the generators can be turned ON or OFF every 15 min. The length of the prediction horizon is $t_f = 3$ h. The sampling time for the system dynamics is $\Delta t = 5$ s, which is adequate for dynamics in the time scale listed in Table I. As a result of these parameter specifications, $N = 2160$ and $L = 12$. UC is often performed with a prediction horizon of more than 24 h. We use a 3 h-ahead horizon to be able to solve the full size OCP (7) using a general-purpose solver in a reasonable amount of time. Fig. 2 shows the case study reference, r_k , the wind power production, d_k , the initial wind power production forecast, $\hat{d}_{k|0}$, and an updated wind power production forecast, $\hat{d}_{k|900}$. The wind power forecasts should be interpreted as $\{\hat{d}_{k|0}\}_{k=0}^{2160}$ and $\{\hat{d}_{k|900}\}_{k=0}^{2160}$, respectively. Note that $\hat{d}_{k|900} = d_k$ for $k \leq 900$. For $t > 75$ min ($k > 900$), the initial wind power forecast, $\hat{d}_{k|0}$, is not very accurate. This suggests that the UL-OCP should be resolved when the updated forecast, $\hat{d}_{k|900}$, becomes available at $t = 75$ min ($k = 900$).

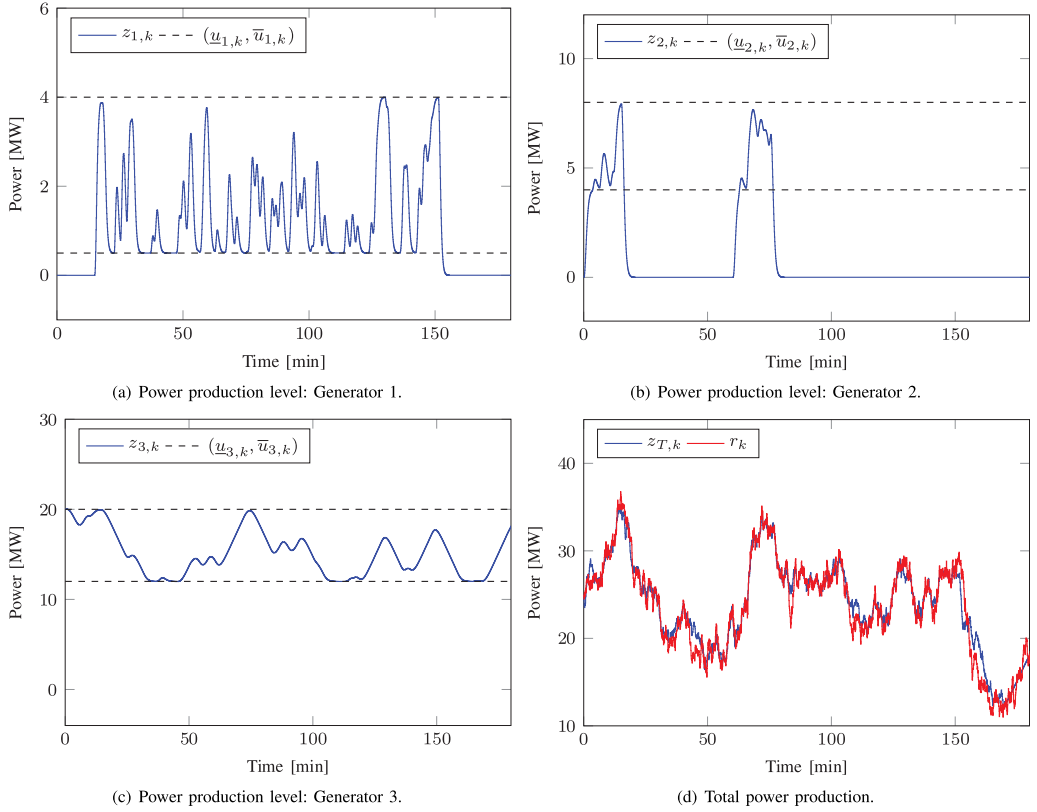


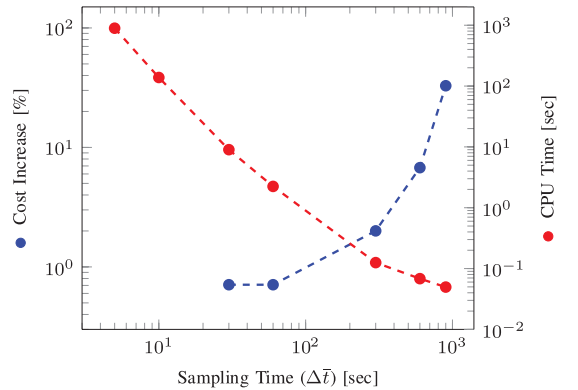
Fig. 3. Open-loop simulation: generator power production levels and total power production.

A. Known Disturbance

Assume that the disturbance, \mathbf{d}_k , is known over the entire 24-h prediction horizon. Fig. 3 shows the open-loop production plan obtained by the direct solution of the OCP (7). Fig. 3(d) shows that the total power production follows the reference well. Large imbalance costs are, therefore, avoided when \mathbf{d}_k is known. The total cost of operation is EUR 2426.

The computation time to solve the OCP (7) is approximately 15 min using Gurobi. Direct solution of (7) is, thus, intractable in real time. To overcome this issue, (7) is solved using Algorithm 1. We consider a situation with a fixed horizon length, $\tilde{N} = 2160$, in the LL-OCP, and varying sampling time, $\Delta\tilde{t}$, in the UL-OCP. Average values are used for \bar{r}_k and \bar{d}_k in the UL-OCP. For each value of $\Delta\tilde{t}$, we record the cost of operation over the entire simulation scenario, as well as the time to solve the UL-OCP. Fig. 4 shows the simulation results.

For $\Delta\tilde{t} = 5$ s and $\Delta\tilde{t} = 10$ s, the hierarchical algorithm obtains the same solution as Gurobi. This means that the cost increase is 0%. As the sampling time increases, the computation time decreases and the cost of operation increases. In the extreme case, $\Delta\tilde{t} = 900$ s, the relative cost increase compared with the direct solution of the OCP is 33%. For $\Delta\tilde{t} = 60$ s,


 Fig. 4. Relative cost increase and computation time to solve the UL-OCP with $t_f = 3$ h, as a function of the sampling time $\Delta\tilde{t}$.

the cost increase is $<1\%$, while the computation time is reduced by two orders of magnitude. We conclude that the binary decision variables, (3), can be determined efficiently by solving the UL-OCP on a coarse temporal time-scale, without a significant increase in the cost of operation.

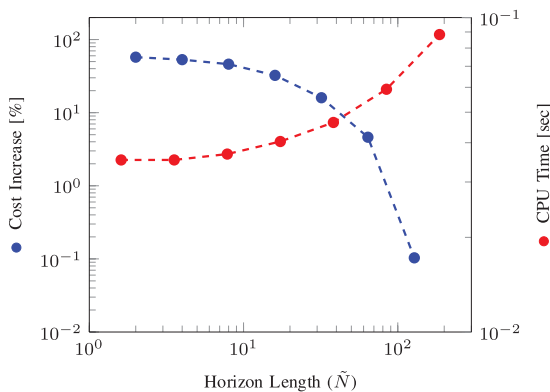


Fig. 5. Relative cost increase and average computation time to solve the LL-OCP with $\Delta t = 5$ s, as a function of the prediction horizon \tilde{N} .

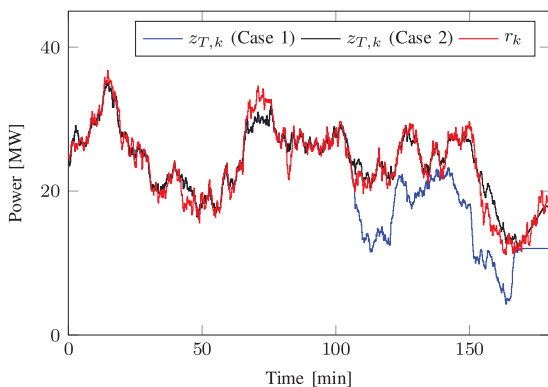


Fig. 6. Closed-loop simulation: total power production. In Case 1, the binary scheduling variables are only updated at the beginning of the simulation. In Case 2, the binary scheduling variables are also updated at time step $k = 900$ using the updated forecast $\hat{d}_{k|900}$.

The average computation time to solve the LL-OCP with $\tilde{N} = N = 2160$ is 3 s. This is critical, as the LL-OCP is solved as part of the (high frequency) lower optimization level in Algorithm 1. We, therefore, fix the sampling time to $\Delta \tilde{t} = 30$ s in the UL-OCP, and vary the horizon length \tilde{N} in the LL-OCP. Fig. 5 shows the average computation time to solve the LL-OCP and the cost of operation, as a function of \tilde{N} . For small \tilde{N} , the cost is significantly larger than for $\tilde{N} = 2160$. When $\tilde{N} = 64$, the cost increase is $< 5\%$, and for $\tilde{N} = 128$, the cost increase is $< 1\%$. Compared with the case where $\tilde{N} = N = 2160$, the computation time to solve the LL-OCP is reduced by one order of magnitude for $\tilde{N} = 64$. For $\Delta \tilde{t} = 60$ s and $\tilde{N} = 128$, the UL-OCP is solved in 2 s and the LL-OCP is solved in 0.1 s. In comparison, the time to solve the OCP (7) directly is ~ 15 min.

B. Unknown Disturbance

Consider the more realistic case where only forecasts of the disturbance, d_k , are available. Two closed-loop simulations

are performed. In the first simulation (Case 1), the UL-OCP is solved one single time using the initial forecast, $\hat{d}_{k|0}$. In the second simulation (Case 2), the UL-OCP is resolved at time step $k = 900$ using the updated forecast, $\hat{d}_{k|900}$. The parameter specifications for Algorithm 1 are $\Delta \tilde{t} = 60$ s and $\tilde{N} = 128$.

We assume that a perfect disturbance forecast is available in the LL-OCP. This means that d_k is known 10 min ahead of time for the LL-OCP. Fig. 6 shows the total power production for Case 1 and for Case 2. In Case 1, significant deficits in the total power production occur for $t \geq 75$ min. This is because two of the three generators are turned OFF for $t \geq 75$ min, as a result of the binary scheduling decisions made at time $t = 0$ min. As the binary variables are fixed in the LL-OCP, the generators cannot be turned ON. For Case 2, the power deficits are avoided. Based on the updated forecast, $\hat{d}_{k|900}$, the UL-OCP modifies the initial plan to have more generators turned ON for $t \geq 75$ min. This reduces costs by 75% compared with Case 1. In practice, the UL-OCP may be solved, e.g., every 5 min using the most recent forecasts. It is important to note that this is only possible using the hierarchical algorithm.

VI. CONCLUSION

In this paper, we have developed a hierarchical algorithm for MPC of a subclass of hybrid systems. The algorithm decomposes the OCP into an upper level MILP and a lower level LP. Binary scheduling variables are determined by solving the upper level MILP, and continuous control variables are determined by solving the lower level LP. The binary variables occur as fixed parameters in the lower level LP. The proposed approach reduces the most time-critical numerical operations in solving the OCP to the solution of the lower level LP and allows frequent solution of the upper level MILP. The performance of the hierarchical algorithm was tested using a power portfolio case study. For this case study, the computation time to solve the open-loop OCP using the hierarchical algorithm is in the order of seconds. In comparison, the time to solve the OCP directly using the state-of-the-art MILP solver is more than 15 min. The performance improvement in computation time is achieved at the expense of less than a 1% increase in the MILP objective function.

REFERENCES

- [1] J. B. Rawlings, "Tutorial overview of model predictive control," *IEEE Control Syst.*, vol. 20, no. 3, pp. 38–52, Jun. 2000.
- [2] D. Q. Mayne, J. B. Rawlings, C. V. Rao, and P. O. M. Scokaert, "Constrained model predictive control: Stability and optimality," *Automatica*, vol. 36, no. 6, pp. 789–814, 2000.
- [3] J. B. Rawlings and D. Q. Mayne, *Model Predictive Control Theory and Design*. Madison, WI, USA: Nob Hill Publishing, 2009.
- [4] F. Borrelli, A. Bemporad, and M. Morari, *Predictive Control for Linear and Hybrid Systems*. Cambridge, U.K.: Cambridge Univ. Press, 2015.
- [5] R. Amrit, J. B. Rawlings, and L. T. Biegler, "Optimizing process economics online using model predictive control," *Comput. Chem. Eng.*, vol. 58, pp. 334–343, Nov. 2013.
- [6] F. Borrelli, A. Bemporad, M. Fodor, and D. Hrovat, "An MPC/hybrid system approach to traction control," *IEEE Trans. Control Syst. Technol.*, vol. 14, no. 3, pp. 541–552, May 2006.
- [7] L. F. S. Larsen, T. Geyer, and M. Morari, "Hybrid model predictive control in supermarket refrigeration systems," in *Proc. 16th IFAC World Congr.*, 2005.

- [8] D. Sarabia, F. Capraro, L. F. S. Larsen, and C. de Prada, "Hybrid NMPC of supermarket display cases," *Control Eng. Pract.*, vol. 17, no. 4, pp. 428–441, 2009.
- [9] L. F. S. Larsen, R. Izadi-Zamanabadi, and R. Wisniewski, "Supermarket refrigeration system—Benchmark for hybrid system control," in *Proc. Eur. Control Conf. (ECC)*, 2007, pp. 113–120.
- [10] G. Ferrari-Trecate, E. Galleste, P. Letizia, M. Spedicato, M. Morari, and M. Antoine, "Modeling and control of co-generation power plants: A hybrid system approach," *IEEE Trans. Control Syst. Technol.*, vol. 12, no. 5, pp. 694–705, Sep. 2004.
- [11] J. L. Villa, M. Duque, A. Gauthier, and N. Rakoto-Ravalontsalama, "Supervision and optimal control of a class of industrial processes," in *Proc. IEEE Conf. Emerg. Technol. Factory Autom.*, vol. 2, Sep. 2003, pp. 177–180.
- [12] E. Mestan, M. Türkay, and Y. Arkun, "Optimization of operations in supply chain systems using hybrid systems approach and model predictive control," *Ind. Eng. Chem. Res.*, vol. 45, no. 19, pp. 6493–6503, 2006.
- [13] A. Bemporad, F. Borrelli, and M. Morari, "Optimal controllers for hybrid systems: Stability and piecewise linear explicit form," in *Proc. 39th IEEE Conf. Decision Control (CDC)*, vol. 2, Dec. 2000, pp. 1810–1815.
- [14] A. Bemporad, "Explicit model predictive control," in *Encyclopedia of Systems and Control*, J. Baillieul and T. Samad, Eds. London, U.K.: Springer, 2014, pp. 1–9.
- [15] D. Axehill, T. Besselmann, D. M. Raimondo, and M. Morari, "A parametric branch and bound approach to suboptimal explicit hybrid MPC," *Automatica*, vol. 50, no. 1, pp. 240–246, 2014.
- [16] D. Axehill and A. Hansson, "A dual gradient projection quadratic programming algorithm tailored for model predictive control," in *Proc. 47th IEEE Conf. Decision Control (CDC)*, Dec. 2008, pp. 3057–3064.
- [17] C. Kirches, "Fast numerical methods for mixed-integer nonlinear model-predictive control," Ph.D. dissertation, Ruprecht-Karls-Universität Heidelberg, Heidelberg, Germany, 2010. [Online]. Available: <http://archiv.ub.uni-heidelberg.de/volltextserver/11636>
- [18] A. Bemporad, W. P. M. H. Heemels, and B. De Schutter, "On hybrid systems and closed-loop MPC systems," *IEEE Trans. Autom. Control*, vol. 47, no. 5, pp. 863–869, May 2002.
- [19] M. Lazar, W. P. M. H. Heemels, S. Weiland, and A. Bemporad, "Stabilizing model predictive control of hybrid systems," *IEEE Trans. Autom. Control*, vol. 51, no. 11, pp. 1813–1818, Nov. 2006.
- [20] M. Lazar and W. P. M. H. Heemels, "Predictive control of hybrid systems: Input-to-state stability results for sub-optimal solutions," *Automatica*, vol. 45, no. 1, pp. 180–185, 2009.
- [21] A. Bemporad, D. Mignone, and M. Morari, "Moving horizon estimation for hybrid systems and fault detection," in *Proc. Amer. Control Conf. (ACC)*, vol. 4, 1999, pp. 2471–2475.
- [22] M. Morari and M. Barić, "Recent developments in the control of constrained hybrid systems," *Comput. Chem. Eng.*, vol. 30, nos. 10–12, pp. 1619–1631, 2006.
- [23] M. Morari, M. Baotic, and F. Borrelli, "Hybrid systems modeling and control," *Eur. J. Control*, vol. 9, nos. 2–3, pp. 177–189, 2003.
- [24] J. Lunze and F. Lamnabhi-Lagarigue, Eds., *Handbook of Hybrid Systems Control: Theory, Tools, Applications*. Cambridge, U.K.: Cambridge Univ. Press, 2009.
- [25] A. Bemporad and M. Morari, "Verification of hybrid systems via mathematical programming," in *Hybrid Systems: Computation and Control* (Lecture Notes in Computer Science), vol. 1569, F. W. Vaandrager and J. H. van Schuppen, Eds. Berlin, Germany: Springer, 1999, pp. 31–45.
- [26] O. Slupphaug and B. A. Foss, "Model predictive control for a class of hybrid systems," in *Proc. Eur. Control Conf. (ECC)*, 1997, pp. 3095–3100.
- [27] P. Rivotti and E. N. Pistikopoulos, "A dynamic programming based approach for explicit model predictive control of hybrid systems," *Comput. Chem. Eng.*, vol. 72, pp. 126–144, Jan. 2015.
- [28] D. Axehill, L. Vandenbergh, and A. Hansson, "Convex relaxations for mixed integer predictive control," *Automatica*, vol. 46, no. 9, pp. 1540–1545, 2010.
- [29] M. Schmitt, R. Vujanic, J. Warrington, and M. Morari, "An approach for model predictive control of mixed integer-input linear systems based on convex relaxations," in *Proc. 52nd IEEE Conf. Decision Control (CDC)*, Dec. 2013, pp. 6428–6433.
- [30] A. G. Becutti, T. Geyer, and M. Morari, "Temporal Lagrangian decomposition of model predictive control for hybrid systems," in *Proc. 43rd IEEE Conf. Decision Control (CDC)*, vol. 3, Dec. 2004, pp. 2509–2514.
- [31] L. Zukui and M. G. Ierapetritou, "Production planning and scheduling integration through augmented Lagrangian optimization," *Comput. Chem. Eng.*, vol. 34, no. 6, pp. 996–1006, 2010.
- [32] M. Baldea and I. Harjankoski, "Integrated production scheduling and process control: A systematic review," *Comput. Chem. Eng.*, vol. 71, pp. 377–390, Dec. 2014.
- [33] J. Du, J. Park, I. Harjankoski, and M. Baldea, "A time scale-bridging approach for integrating production scheduling and process control," *Comput. Chem. Eng.*, vol. 79, pp. 59–69, Aug. 2015.
- [34] M. Soroush and D. J. Chmielewski, "Process systems opportunities in power generation, storage and distribution," *Comput. Chem. Eng.*, vol. 51, pp. 86–95, Apr. 2013.
- [35] S. Engell and I. Harjankoski, "Optimal operation: Scheduling, advanced control and their integration," *Comput. Chem. Eng.*, vol. 47, pp. 121–133, Dec. 2012.
- [36] J. Zhuge and M. G. Ierapetritou, "An integrated framework for scheduling and control using fast model predictive control," *AIChE J.*, vol. 61, no. 10, pp. 3304–3319, 2015.
- [37] R. L. Tousain, "Dynamic optimization in business-wide process control," Ph.D. dissertation, Faculty Design, Eng. Production, Delft Univ. Technol., Delft, The Netherlands, 2002. [Online]. Available: <http://repository.tudelft.nl>
- [38] L. Messner, H. Gattringer, and H. Bremer, "Efficient online computation of smooth trajectories along geometric paths for robotic manipulators," in *Multibody System Dynamics, Robotics and Control*, H. Gattringer and J. Gerstmayr, Eds. Vienna, Austria: Springer, 2013, pp. 17–30.
- [39] K. B. Reed, V. Kallem, R. Alterovitz, K. Goldberg, A. M. Okamura, and N. J. Cowan, "Integrated planning and image-guided control for planar needle steering," in *Proc. 2nd IEEE/RAS EMBS Int. Conf. Biomed. Robot. Biomechatron.*, Oct. 2008, pp. 819–824.
- [40] T. E. Marlin and A. N. Hrymak, "Real-time operations optimization of continuous processes," in *Proc. 5th Int. Conf. Chem. Process Control*, 1996, pp. 156–164.
- [41] M. L. Darby, M. Nikolaou, J. Jones, and D. Nicholson, "RTO: An overview and assessment of current practice," *J. Process Control*, vol. 21, no. 6, pp. 874–884, 2011.
- [42] G. François, S. Costello, and D. Bonvin, "Application of real-time optimization methods to energy systems in the presence of uncertainties and disturbances," *TMC Acad. J.*, vol. 9, no. 2, pp. 19–40, 2015.
- [43] S. Engell, "Feedback control for optimal process operation," *J. Process Control*, vol. 17, no. 3, pp. 203–219, 2007.
- [44] L. E. Sokoler, "Methods and algorithms for economic MPC in power production planning," Ph.D. dissertation, Dept. Appl. Math. Comput. Sci., Tech. Univ. Denmark, Kongens Lyngby, Denmark, 2016. [Online]. Available: <http://orbit.dtu.dk>
- [45] T. G. Hovgaard, K. Edlund, and J. B. Jørgensen, "The potential of economic MPC for power management," in *Proc. 49th IEEE Conf. Decision Control (CDC)*, Dec. 2010, pp. 7533–7538.
- [46] K. Edlund, J. D. Bendtsen, and J. B. Jørgensen, "Hierarchical model-based predictive control of a power plant portfolio," *Control Eng. Pract.*, vol. 19, no. 10, pp. 1126–1136, 2011.
- [47] M. Carrión and J. M. Arroyo, "A computationally efficient mixed-integer linear formulation for the thermal unit commitment problem," *IEEE Trans. Power Syst.*, vol. 21, no. 3, pp. 1371–1378, Aug. 2006.
- [48] A. J. Wood, B. F. Wollenberg, and G. B. Sheblé, *Power Generation, Operation and Control*, 3rd ed. New York, NY, USA: Wiley, 2013.
- [49] V. Spudić, M. Jelavić, M. Baotic, and N. Perić, "Hierarchical wind farm control for power/load optimization," in *Proc. Torque*, 2010, pp. 681–692.
- [50] J. J. Sirola and T. F. Edgar, "Process energy systems: Control, economic, and sustainability objectives," *Comput. Chem. Eng.*, vol. 47, pp. 134–144, Dec. 2012.
- [51] L. Grüne, "Economic receding horizon control without terminal constraints," *Automatica*, vol. 49, no. 3, pp. 725–734, 2013.
- [52] K. Worthmann, "Estimates of the prediction horizon length in MPC: A numerical case study," in *Proc. 4th IFAC Nonlinear Model Predict. Control Conf.*, 2012, pp. 232–237.
- [53] A. Jadbabaie and J. Hauser, "On the stability of receding horizon control with a general terminal cost," *IEEE Trans. Autom. Control*, vol. 50, no. 5, pp. 674–678, May 2005.
- [54] L. E. Sokoler, L. Standardi, K. Edlund, N. K. Poulsen, H. Madsen, and J. B. Jørgensen, "A Dantzig-Wolfe decomposition algorithm for linear economic model predictive control of dynamically decoupled subsystems," *J. Process Control*, vol. 24, no. 8, pp. 1225–1236, 2014.
- [55] K. Edlund, T. Mølbak, and J. D. Bendtsen, "Simple models for model-based portfolio load balancing controller synthesis," in *Proc. 6th IFAC Symp. Power Plants Power Syst. Control*, 2009, pp. 173–178.



Leo Emil Sokoler received the M.Sc. (Hons.) degree in industrial mathematics from the Technical University of Denmark (DTU), Kongens Lyngby, Denmark, in 2012, and the Ph.D. degree in applied mathematics from the Department of Applied Mathematics and Computer Science, DTU, in 2016. His Ph.D. project was conducted in a collaboration between DTU and DONG Energy, Fredericia, Denmark, the Danish utility company.

His current research interests include convex optimization, power system modeling, and model

predictive control.



Peter Juhler Dinesen received the M.Sc. (Hons.) degree in industrial mathematics from the Technical University of Denmark, Kongens Lyngby, Denmark, in 2015. His M.Sc. thesis with the Technical University of Denmark.

He was a Research Assistant with the Technical University of Denmark, for two months. He is currently a Management Consultant with the PA Consulting Group, Copenhagen, Denmark, where he is involved in process optimization, large data analysis, and project management. He combines his

experience within mathematical optimization modeling and consultancy to solve complex real life challenges in various industries. His current research interests include applied mathematical modeling, scientific computing, numerical optimization, and model predictive control.



John Bagterp Jørgensen received the M.Sc. degree in engineering from the Technical University of Denmark (DTU), Kongens Lyngby, Denmark, in 1997, and the Ph.D. degree in chemical engineering from the Department of Chemical Engineering, DTU, in 2005.

He is currently an Associate Professor with the Department of Applied Mathematics and Computer Science, DTU. He is also a Faculty Member with the Center for Energy Resources Engineering, DTU.

His research is to a large extent conducted in collaboration with industrial companies. He is also a Co-Founder and a Partner with 2-control ApS and has significant experience in online optimization and control of industrial processes. His current research interests include optimization and model predictive control, including computational aspects and applications.

P A P E R **K**

A Homogeneous and Self-Dual Interior-Point Linear Programming Algorithm for Economic Model Predictive Control

L. E. Sokoler, G. Frison, A. Skajaa, R. Halvgaard, and J. B. Jørgensen. A Homogeneous and Self-Dual Interior-Point Linear Programming Algorithm for Economic Model Predictive Control. *IEEE Transactions on Automatic Control*, 2015. To appear.

A Homogeneous and Self-Dual Interior-Point Linear Programming Algorithm for Economic Model Predictive Control

Leo Emil Sokoler, Gianluca Frison, Anders Skajaa, Rasmus Halvgaard, John Bagterp Jørgensen

Abstract—We develop an efficient homogeneous and self-dual interior-point method (IPM) for the linear programs arising in economic model predictive control of constrained linear systems with linear objective functions. The algorithm is based on a Riccati iteration procedure, which is adapted to the linear system of equations solved in homogeneous and self-dual IPMs. Fast convergence is further achieved using a warm-start strategy. We implement the algorithm in MATLAB and C. Its performance is tested using a conceptual power management case study. Closed loop simulations show that 1) the proposed algorithm is significantly faster than several state-of-the-art IPMs based on sparse linear algebra, and 2) warm-start reduces the average number of iterations by 35-40%.

Index Terms—Optimization algorithms, Linear programming algorithms, Predictive control for linear systems, Riccati iterations, Energy systems

I. INTRODUCTION

In economic model predictive control (EMPC) of linear systems with a linear objective function and linear constraints, the optimal control problem (OCP) can be posed as a linear program (LP). As the optimization problem is solved online, the performance and reliability of the optimization algorithm solving the LP is important. The homogeneous and self-dual model has become widely adopted by state-of-the-art IPMs to solve LPs. This paper presents a homogeneous and self-dual variant of Mehrotra's predictor-corrector method [1], [2] for EMPC. The algorithm combines the following methods for computational efficiency:

- **Riccati Iteration Procedure:** The most time consuming numerical operations in the IPM are handled by a Riccati iteration procedure tailored to EMPC. Riccati iteration procedures have not previously been combined with the homogeneous and self-dual model.
- **Warm-Start:** The warm-start strategy of [3] is applied to reduce the number of IPM iterations. This strategy, which is designed for homogeneous and self-dual IPMs, has not been applied to MPC problems in the existing literature. In [3] warm-start reduces the number of iterations by 30-75% based on the NETLIB collection of test problems.

Riccati-based IPMs have been developed for set-point based MPC with an ℓ_2 -penalty [4], [5] and with an ℓ_1 -penalty [6]. The main contributions of this paper are 1) to combine the

The authors are with the Department of Applied Mathematics and Computer Science, DTU, DK-2800 Kgs. Lyngby, Denmark. L. E. Sokoler and A. Skajaa are also affiliated with DONG Energy, DK-2830 Virum, Denmark (e-mail: {leso, gjaf, andsk, rhal, jbjjo}@dtu.dk)

homogeneous and self dual model with a Riccati iteration procedure, 2) to test the warm-start procedure of [3] in an MPC framework, and 3) to report performance results for an efficient implementation of the proposed algorithm.

This paper is organized as follows. Section II formulates the OCP solved in EMPC as a highly structured LP. Section III develops a special purpose homogeneous and self-dual IPM for EMPC. Warm-start is introduced in Section IV. Section V compares a MATLAB and C implementation of the proposed algorithm denoted LP_{empc} to several state-of-the-art IPMs using a simple power management case study¹. Concluding remarks are given in Section VI.

II. OPTIMAL CONTROL PROBLEM

We consider linear state space systems in the form

$$\mathbf{x}_{k+1} = A\mathbf{x}_k + B\mathbf{u}_k + E\mathbf{d}_k, \quad \mathbf{d}_k \sim N(0, R_d), \quad (1a)$$

$$\mathbf{y}_k = C_y\mathbf{x}_k + \mathbf{e}_k, \quad \mathbf{e}_k \sim N(0, R_e), \quad (1b)$$

$$\mathbf{z}_k = C_z\mathbf{x}_k, \quad (1c)$$

where $\mathbf{x}_0 \sim N(\hat{\mathbf{x}}_0, P_0)$. (A, B, C_y, C_z, E) are the state space matrices, $\mathbf{x}_k \in \mathbb{R}^{n_x}$ is the state vector, $\mathbf{u}_k \in \mathbb{R}^{n_u}$ is the input vector, $\mathbf{y}_k \in \mathbb{R}^{n_y}$ is the measurement vector, $\mathbf{z}_k \in \mathbb{R}^{n_z}$ is the output vector, \mathbf{d}_k is the process noise vector, and \mathbf{e}_k is the measurement noise vector. We use bold letters to denote stochastic variables. In this paper, the OCP solved at every sampling instant is defined as

$$\min_{\mathbf{u}, \hat{\mathbf{x}}, \hat{\mathbf{z}}, \rho} \sum_{j \in \mathcal{N}_0} p_{k+j}^T \mathbf{u}_{k+j} + q_{k+j+1}^T \rho_{k+j+1}, \quad (2a)$$

s.t.

$$\hat{\mathbf{x}}_{k+j+1|k} = A\hat{\mathbf{x}}_{k+j|k} + B\mathbf{u}_{k+j}, \quad j \in \mathcal{N}_0, \quad (2b)$$

$$\hat{\mathbf{z}}_{k+j|k} = C_z\hat{\mathbf{x}}_{k+j|k}, \quad j \in \mathcal{N}_1, \quad (2c)$$

$$\underline{\mathbf{u}}_{k+j} \leq \mathbf{u}_{k+j} \leq \bar{\mathbf{u}}_{k+j}, \quad j \in \mathcal{N}_0, \quad (2d)$$

$$\Delta \underline{\mathbf{u}}_{k+j} \leq \mathbf{u}_{k+j} - \mathbf{u}_{k+j-1} \leq \Delta \bar{\mathbf{u}}_{k+j}, \quad j \in \mathcal{N}_0, \quad (2e)$$

$$\underline{\mathbf{z}}_{k+j} - \rho_{k+j} \leq \hat{\mathbf{z}}_{k+j|k} \leq \bar{\mathbf{z}}_{k+j} + \rho_{k+j}, \quad j \in \mathcal{N}_1, \quad (2f)$$

$$\rho_{k+j} \geq 0, \quad j \in \mathcal{N}_1, \quad (2g)$$

where $\mathcal{N}_i := \{0 + i, 1 + i, \dots, N - 1 + i\}$, with N being the length of the prediction horizon. The problem data are the state-space matrices, (A, B, C_z) , the filtered estimate, $\hat{\mathbf{x}}_{k|k}$, the input limits, $(\underline{\mathbf{u}}_{k+j}, \bar{\mathbf{u}}_{k+j})$, the input-rate limits, $(\Delta \underline{\mathbf{u}}_{k+j}, \Delta \bar{\mathbf{u}}_{k+j})$, the output limits, $(\underline{\mathbf{z}}_{k+j}, \bar{\mathbf{z}}_{k+j})$, the input

¹Software is available via <http://www2.imm.dtu.dk/~jbjjo/publications>

prices, p_{k+j} , and the price for violating the output constraints, q_{k+j} . We use soft output constraints, defined by (2f) and (2g), to ensure feasibility of the OCP. For compact notation, the optimization variables in (2) are written as u, \hat{x}, \hat{z} and ρ , where $u = [u_k^T \ u_{k+1}^T \ \dots \ u_{k+N-1}^T]^T$, and similarly for \hat{x} , \hat{z} , and ρ . The filtered estimate, $\hat{x}_{k|k} := E[x_k|Y_k]$, is the conditional expectation of x_k given the observations $Y_k := [y_0^T \ y_1^T \ y_2^T \ \dots \ y_k^T]^T$. We obtain this value using the Kalman filter. By augmenting the state-space system such that

$$A := \begin{bmatrix} A & 0 \\ 0 & 0 \end{bmatrix}, \quad \hat{x}_k := \begin{bmatrix} \hat{x}_k \\ u_{k-1} \end{bmatrix}, \quad B := \begin{bmatrix} B \\ I \end{bmatrix}, \quad E := \begin{bmatrix} E \\ 0 \end{bmatrix},$$

$$C_z := [C_z \ 0], \quad C_y := [C_y \ 0],$$

$$\Delta \underline{u}_{k+j} \leq u_{k+j} - D\hat{x}_{k+j|k} \leq \Delta \bar{u}_{k+j}, \quad j \in \mathcal{N}_0,$$

in which $D := [0 \ I]$. This formulation simplifies later computations considerably. To keep the notation simple we assume that the current time step is $k = 0$, and write $\hat{x}_j := \hat{x}_{0+j|0}$ for conditional expressions. The problem data is collected in the structures g, F, b, H and c , and (2) is put into the form

$$\min_{t,s} \{g^T t | Ft = b, Ht + s = c, s \geq 0\}. \quad (3)$$

As an example, consider the case for $N = 2$

$$t := [u_0^T \ \hat{x}_1^T \ \rho_1^T \ u_1^T \ \hat{x}_2^T \ \rho_2^T]^T,$$

$$g := [p_0^T \ 0 \ q_1^T \ p_1^T \ 0 \ q_2^T]^T,$$

and

$$[F \mid b] := \begin{bmatrix} B & -I & 0 & 0 & 0 & 0 & | & -A\hat{x}_0 \\ 0 & A & 0 & B & -I & 0 & | & 0 \\ I & 0 & 0 & 0 & 0 & 0 & | & \bar{u}_0 \\ 0 & 0 & 0 & I & 0 & 0 & | & \bar{u}_1 \\ -I & 0 & 0 & 0 & 0 & 0 & | & -\underline{u}_0 \\ 0 & 0 & 0 & -I & 0 & 0 & | & -\underline{u}_1 \\ I & 0 & 0 & 0 & 0 & 0 & | & \Delta \bar{u}_0 \\ 0 & -D & 0 & I & 0 & 0 & | & \Delta \bar{u}_1 \\ -I & 0 & 0 & 0 & 0 & 0 & | & -\Delta \underline{u}_0 \\ 0 & D & 0 & -I & 0 & 0 & | & -\Delta \underline{u}_1 \\ 0 & C_z & -I & 0 & 0 & 0 & | & \bar{z}_1 \\ 0 & 0 & 0 & 0 & C_z & -I & | & \bar{z}_2 \\ 0 & -C_z & -I & 0 & 0 & 0 & | & -\bar{z}_1 \\ 0 & 0 & 0 & 0 & -C_z & -I & | & -\bar{z}_2 \\ 0 & 0 & -I & 0 & 0 & 0 & | & 0 \\ 0 & 0 & 0 & 0 & 0 & -I & | & 0 \end{bmatrix},$$

where $\Delta \bar{u}_0 := \Delta \bar{u}_0 + D\hat{x}_0$ and $\Delta \underline{u}_0 := \Delta \underline{u}_0 + D\hat{x}_0$. The problem (2) can thus be posed as a highly structured LP with $n := N(n_u + n_x + n_z)$ variables, $m_E := Nn_x$ equality constraints, and $m_I := N(4n_u + 3n_z)$ inequality constraints. We have eliminated \hat{z}_j from the optimization problem using the linear relation (2c).

Remark 1: We restrict the OCP (2) to a fairly narrow class of problems. This is done to show the full potential of a special purpose Riccati-based homogenous and self-dual IPM. It is straightforward to accommodate the proposed algorithm to

handle more general OCPs with linear objective functions and linear constraints, e.g. OCPs with combined input and state constraints, as well as state and output costs in the objective function.

III. HOMOGENEOUS AND SELF-DUAL INTERIOR-POINT METHOD

The dual of the LP (3) is

$$\max_{v,w} \{-b^T v - c^T w\} - F^T v - H^T w = g, w \geq 0, \quad (4)$$

where $v \in \mathbb{R}^{m_E}$ and $w \in \mathbb{R}^{m_I}$ are dual variables corresponding to the Lagrange multipliers for the equality constraints and the inequality constraint of (3), respectively. We assume that F has full row rank. This is always the case for the problem (3).

Homogeneous and self-dual IPMs solve (3) and (4) indirectly. The idea is to replace (3) and (4) by a closely related LP with a number of special properties, which are utilized by homogeneous and self-dual IPMs. Aside from an inherent ability to detect infeasibility, [3] shows that IPMs based on the homogeneous and self-dual model can be warm-started efficiently. We refer to [7]–[9] for proofs and details.

Introduce a new set of optimization variables $(\tilde{t}, \tilde{v}, \tilde{w}, \tilde{s})$, and the additional scalar variables $(\tilde{\tau}, \tilde{\kappa})$. Then the LP solved in homogenous and self-dual IPMs may be stated as the linear feasibility problem

$$\text{find } \tilde{t}, \tilde{v}, \tilde{w}, \tilde{s}, \tilde{\tau}, \tilde{\kappa}, \quad (5a)$$

$$\text{s.t. } F^T \tilde{v} + H^T \tilde{w} + g\tilde{\tau} = 0, \quad (5b)$$

$$b\tilde{\tau} - F\tilde{t} = 0, \quad (5c)$$

$$c\tilde{\tau} - H\tilde{t} - \tilde{s} = 0, \quad (5d)$$

$$-g^T \tilde{t} - b^T \tilde{v} - c^T \tilde{w} + \tilde{\kappa} = 0, \quad (5e)$$

$$(\tilde{w}, \tilde{s}, \tilde{\tau}, \tilde{\kappa}) \geq 0, \quad (5f)$$

Proposition 1 shows that the solution to (3) and (4) can be obtained by solving (5).

Proposition 1: The linear feasibility problem (5) always has a strict complimentary solution $(\tilde{t}^*, \tilde{v}^*, \tilde{w}^*, \tilde{s}^*, \tilde{\tau}^*, \tilde{\kappa}^*)$ satisfying $\tilde{s}_j^* \tilde{w}_j^* = 0$ for $j = 1, 2, \dots, m_I$ and $\tilde{\tau}^* \tilde{\kappa}^* = 0$. For such a solution, one of the following conditions hold

- 1) $\tilde{\tau}^* > 0, \tilde{\kappa}^* = 0$: The scaled solution $(t^*, v^*, w^*, s^*) = (\tilde{t}^*, \tilde{v}^*, \tilde{w}^*, \tilde{s}^*)/\tilde{\tau}^*$ is a primal-dual optimal solution to (3) and (4).
- 2) $\tilde{\tau}^* = 0, \tilde{\kappa}^* > 0$: The problem (3) is infeasible or unbounded; either $-b^T \tilde{v}^* - c^T \tilde{w}^* > 0$ (primal infeasible), or $g^T \tilde{t}^* < 0$ (dual infeasible).

Proof: See [9], [10]. ■

A. Riccati Iteration Procedure for EMPC

The necessary and sufficient optimality conditions for (5) are $(\tilde{w}, \tilde{s}, \tilde{\kappa}, \tilde{\tau}) \geq 0$ and

$$\begin{bmatrix} F^T \tilde{v} + H^T \tilde{w} + g\tilde{\tau} \\ b\tilde{\tau} - F\tilde{t} \\ c\tilde{\tau} - H\tilde{t} - \tilde{s} \\ -g^T \tilde{t} - b^T \tilde{v} - c^T \tilde{w} + \tilde{\kappa} \\ \tilde{W} \tilde{S} \mathbf{1}_{m_I} \\ \tilde{\tau} \tilde{\kappa} \end{bmatrix} = \begin{bmatrix} 0 \\ 0 \\ 0 \\ 0 \\ 0 \\ 0 \end{bmatrix}, \quad (6)$$

\tilde{W} is a diagonal matrix with the elements of \tilde{w} in its diagonal, and \tilde{S} is defined similarly. Moreover, $\mathbf{1}_{m_I}$ is a column vector of all ones of size m_I .

The main computational bottleneck in homogeneous and self-dual IPMs is solving a linear system of equations. The equations are solved to determine a feasible search direction for the solution of (6) with $(\tilde{w}, \tilde{s}, \tilde{\kappa}, \tilde{\tau}) \geq 0$. In every IPM iteration a new system is formed and solved. For an arbitrary right hand side, we can write the linear system of equations solved as

$$F^T \Delta \tilde{v} + H^T \Delta \tilde{w} + g \Delta \tilde{\tau} = r_1, \quad (7a)$$

$$b \Delta \tilde{\tau} - F \Delta \tilde{t} = r_2, \quad (7b)$$

$$c \Delta \tilde{\tau} - H \Delta \tilde{t} - \Delta \tilde{s} = r_3, \quad (7c)$$

$$g^T \Delta \tilde{t} + b^T \Delta \tilde{v} + c^T \Delta \tilde{w} - \Delta \tilde{\kappa} = r_4, \quad (7d)$$

$$\tilde{W} \Delta \tilde{s} + \tilde{S} \Delta \tilde{w} = r_5, \quad (7e)$$

$$\tilde{\kappa} \Delta \tilde{\tau} + \tilde{\tau} \Delta \tilde{\kappa} = r_6. \quad (7f)$$

The search direction is denoted $(\Delta \tilde{t}, \Delta \tilde{v}, \Delta \tilde{w}, \Delta \tilde{s}, \Delta \tilde{\tau}, \Delta \tilde{\kappa})$. In Equation (7e) and Equation (7f), $\tilde{W} = \tilde{W}_j$, $\tilde{S} = \tilde{S}_j$, $\tilde{\kappa} = \tilde{\kappa}_j$, and $\tilde{\tau} = \tilde{\tau}_j$, are fixed. Subscript j denotes the IPM iteration number.

The equations (7) are different from the equations solved in standard IPMs [1], [2]. Conventional Riccati iteration procedures can therefore not be applied directly to solve the system (7).

Proposition 2 shows that the solution of (7) can be computed by solving the reduced linear system of equations (8), and a number of computationally inexpensive operations. Proposition 3 shows that the reduced linear system can be solved using a Riccati iteration procedure that scales as $O(N(n_u + n_x + n_z)^3)$. This is achieved by eliminating variables from the reduced system (8), such that it can be expressed in the standard form (11). The proof of Proposition 3 provides details for efficiently eliminating variables from the system.

Remark 2: The complexity of solving the system (7) directly using sparse linear algebra routines is linear to quadratic in the length of the prediction horizon, N , while a general purpose solver using dense linear algebra scales cubically in N [11]. It is convenient to have an algorithm that scales linearly in N , as stability of MPC schemes often may be achieved by selecting a sufficiently large value of N [12], [13]. For systems where the state dimension, n_x , is relatively large compared to the number of inputs, n_u , condensing methods may be more efficient to solve (8) than Riccati-based solvers [5], [14]. These methods eliminate the state variables from the system to form and solve a smaller but less structured system. Condensing methods scale quadratically to cubically in N . Condensing-based solvers are therefore not well suited to handle problems with a large prediction horizon. As a rule of thumb, condensing-based solvers are more efficient than Riccati-based solvers roughly when $n_x \geq N n_u$ [14]. Reference [14] provides a highly efficient condensing method, which may replace the proposed Riccati iteration procedure to solve (7), when $n_x \geq N n_u$.

Remark 3: The reduced linear system (8) is a special case of the system solved in the primal-dual Riccati-based IPMs

[4], [5]. The results in these papers may be utilized to derive special-purpose homogenous and self-dual IPMs algorithms, when the matrices F and H have a more general structure, than for the particular problem (2).

Proposition 2: The solution to (7) can be obtained by solving

$$\begin{bmatrix} 0 & F^T & H^T \\ -F & 0 & 0 \\ -H & 0 & \tilde{W}^{-1} \tilde{S} \end{bmatrix} \begin{bmatrix} f_1 & h_1 \\ f_2 & h_2 \\ f_3 & h_3 \end{bmatrix} = \begin{bmatrix} r_1 & -g \\ r_2 & -b \\ r_3 & -c \end{bmatrix}, \quad (8)$$

and subsequent computation of

$$\Delta \tilde{\tau} = \frac{r_6 - \tilde{\tau}(g^T f_1 + b^T f_2 + c^T f_3)}{\tilde{\kappa} + \tilde{\tau}(g^T h_1 + b^T h_2 + c^T h_3)},$$

$$\Delta \tilde{t} = f_1 + h_1 \Delta \tilde{\tau},$$

$$\Delta \tilde{v} = f_2 + h_2 \Delta \tilde{\tau},$$

$$\Delta \tilde{w} = f_3 + h_3 \Delta \tilde{\tau},$$

$$\Delta \tilde{\kappa} = g^T \Delta \tilde{t} + b^T \Delta \tilde{v} + c^T \Delta \tilde{w} - r_4,$$

$$\Delta \tilde{s} = \tilde{W}^{-1}(r_5 - \tilde{S} \Delta \tilde{w}),$$

where $r_3 := r_3 + \tilde{W}^{-1} r_5$ and $r_6 := r_6 + \tilde{\tau} r_4$.

Proof: See [10]. ■

Proposition 3: The system (8) can be solved in $O(N(n_u + n_x + n_z)^3)$ operations using a Riccati iteration procedure.

Proof: For a single arbitrary right hand side, we may write the system (8) as

$$\begin{bmatrix} 0 & F^T & H^T \\ -F & 0 & 0 \\ -H & 0 & \tilde{W}^{-1} \tilde{S} \end{bmatrix} \begin{bmatrix} \Delta \tilde{t} \\ \Delta \tilde{v} \\ \Delta \tilde{w} \end{bmatrix} = \begin{bmatrix} r_D \\ r_E \\ r_I \end{bmatrix}. \quad (9)$$

Denote the Lagrange multipliers associated with the inequality constraints (2d) and (2g) as $\eta, \delta, v, \omega, \gamma, \zeta$ and ξ where $\eta := [\eta_0^T \ \eta_1^T \ \dots \ \eta_{N-1}^T]^T$, and similarly for δ, v, γ, ζ and ξ . The multipliers (η, δ) are associated with the input limits (2d), (v, ω) are associated with the input-rate limits (2e), (γ, ζ) are associated with the output limits (2f), and ξ is associated with the non-negative constraints (2g). The system variables are written in the form

$$\begin{aligned} \Delta \tilde{t} &= [\Delta u_0^T \ \Delta \hat{x}_1^T \ \Delta \rho_1^T \ \dots \ \Delta u_{N-1}^T \ \Delta \hat{x}_N^T \ \Delta \rho_N^T]^T, \\ \Delta \tilde{v} &= [\Delta \tilde{v}_0^T \ \Delta \tilde{v}_1^T \ \dots \ \Delta \tilde{v}_{N-1}^T]^T, \\ \Delta \tilde{w} &= [\Delta \eta^T \ \Delta \delta^T \ \Delta v^T \ \Delta \omega^T \ \Delta \gamma^T \ \Delta \zeta^T \ \Delta \xi^T]^T. \end{aligned}$$

Accordingly, we partition the right hand side such that

$$\begin{aligned} r_D &= [r_{u,0}^T \ r_{x,1}^T \ r_{w,1}^T \ \dots \ r_{u,N-1}^T \ r_{x,N}^T \ r_{w,N}^T]^T, \\ r_E &= [R_{v,0}^T \ R_{v,1}^T \ \dots \ R_{v,N-1}^T]^T, \\ r_I &= [r_\eta^T \ r_\delta^T \ r_v^T \ r_\omega^T \ r_\gamma^T \ r_\zeta^T \ r_\xi^T]^T, \end{aligned}$$

and write the diagonal matrix $\tilde{W}^{-1} \tilde{S}$ in terms of diagonal submatrices

$$\tilde{W}^{-1} \tilde{S} = \mathbf{diag}(\Sigma_\eta^T, \Sigma_\delta^T, \Sigma_v^T, \Sigma_\omega^T, \Sigma_\gamma^T, \Sigma_\zeta^T, \Sigma_\xi^T).$$

The Lagrange multipliers $\Delta \eta, \Delta \delta, \Delta v, \Delta \omega, \Delta \gamma, \Delta \zeta$ and $\Delta \xi$, are eliminated from the system (9). This is computationally inexpensive as the matrices to be inverted in the process are

TABLE I
CASE STUDY PARAMETERS

	τ_i	p_k	\underline{u}_k	\bar{u}_k	$\Delta \underline{u}_k$	$\Delta \bar{u}_k$
Power Plant 1	90	100	0	200	-20	20
Power Plant 2	30	200	0	150	-40	40

our comparisons, as well as FORCES that is an IPM based on automatic code generation [17]. All solvers are called from MATLAB using MEX interfaces. We have performed our simulations using an Intel(R) Core(TM) i5-2520M CPU @ 2.50GHz with 4 GB RAM running a 64-bit Ubuntu 12.04.1 LTS operating system.

The test system is a system of m generic power generating units in the form identified by [18]. For $i = 1, 2, \dots, m$

$$Y_i(s) = \frac{1}{(\tau_i s + 1)^3} (U_i(s) + D_i(s)) + E_i(s). \quad (12)$$

$D_i(s)$ is the process noise, $E_i(s)$ is the measurement noise, $U_i(s)$ is the power set-point and $Y_i(s)$ is the power production. The total production from the m power generating units is the sum $Z(s) = \sum_{i=1}^m \frac{1}{(\tau_i s + 1)^3} (U_i(s) + D_i(s))$. We convert the transfer function model into the state space form (1) using a sampling time of $T_s = 5$ seconds. In the resulting model structure, $u_k \in \mathbb{R}^{n_u}$ is the n_u power set-points, $y_k \in \mathbb{R}^{n_y}$ is the measured power production, and $z_k \in \mathbb{R}^{n_z}$ is the total power production. Note that $n_u = n_y = m$ and $n_z = 1$. It is assumed that $d_k \sim N(0, \sigma I)$ and $e_k \sim N(0, \sigma I)$.

A. Simulations

An example with two power generating units is considered; a cheap/slow unit, and an expensive/fast unit. This conflict between response time and operating costs represents a common situation in the power industry where large thermal power plants often produce a majority of the electricity, while the use of units with faster dynamics such as diesel generators and gas turbines are limited to critical peak periods. The controller objective is to coordinate the most cost-efficient power production, respecting capacity constraints and a time-varying electricity demand. It is assumed that full information about the initial state is given $x_0 \sim (0, 0)$, and that the penalty of violating the output constraints is $q_k = 10^4$ for all time steps. Table I lists the system and controller parameters. We set the prediction horizon to $N = 80$ time steps. It has been verified by simulation that the controller is stable for this value of N .

Fig. 1 is a closed-loop simulation with noise parameter $\sigma = 1$. The figure illustrates the power production of each power generating unit. The cheap unit produces 97% of the energy, while the expensive unit is activated only to avoid power imbalances. Fig. 1 also shows that warm-start yields a significant reduction in the number of iterations. On average the number of iterations is reduced by approximately 37%.

Fig. 2 shows a number of box-plots for tuning the warm-start parameter λ . The case $\lambda = 0$ corresponds to a cold start. For all values of λ , warm-start reduces the average number of iterations. We have chosen $\lambda = 0.99$ for our controller.

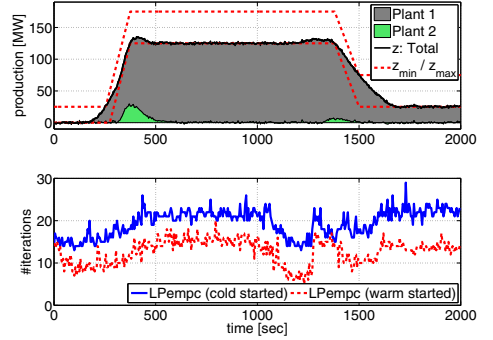


Fig. 1. Closed-loop simulation of a power system controlled by EMPC. Warm-start ($\lambda = 0.99$) yields a significant reduction in the number of iterations.

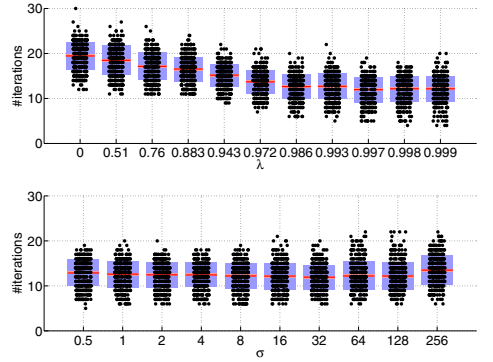
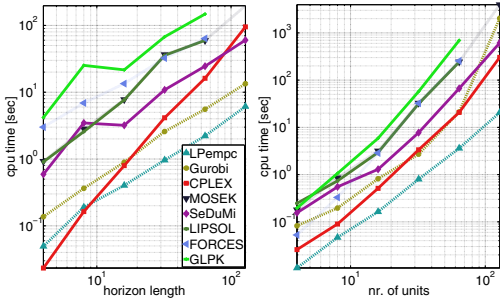


Fig. 2. Number of iterations as a function of the tuning parameter λ and the noise parameter σ . Each box-plot has been generated based on a full closed-loop simulation. In the top plot we have fixed $\sigma = 1$, and in the bottom plot $\lambda = 0.99$.

This value of λ yields an initial point which is both close to the candidate point and lies well inside the interior of the non-negative orthant, $(\tilde{w}, \tilde{s}, \tilde{k}, \tilde{\tau}) \geq 0$. Fig. 2 shows that for $\lambda = 0.99$, the number of iterations is reduced even when the noise parameter is increased significantly.

Fig. 3 is a plot of the computation time to solve LP (2) as a function of the number of power generating units, m , and the length of the horizon, N . The figure shows that LPempc is faster than all other solvers with a significant margin. In addition to the algorithms compared in Fig. 3, the problem (2) is solved using the code generation based IPM CVXGEN [19]. For problems larger than $m = 4$ and $N = 12$, code generation in CVXGEN fails due to the problem size. Therefore, we have not included results for CVXGEN in our benchmark. In general, code generation based solvers such as CVXGEN and FORCES are most competitive for small-dimensional problems [17]. Fig. 4 compares the computation time for different algorithms in a closed-loop simulation with 15 power generating units and a prediction horizon of $N = 200$ time steps. Only the most competitive solvers for this problem are included. In this simulation LPempc is up to an order of magnitude faster than



(a) Increasing N and fixed $m = 32$. (b) Increasing m and fixed $N = 32$.

Fig. 3. Computation time to solve (2), as a function of the horizon length, N , and the number of power generators, m .

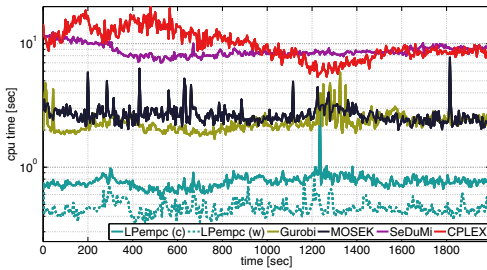


Fig. 4. Computation time to solve (2) with 15 power generating units and a prediction horizon of 200 time steps. Warm-start reduces the average number of iterations by approximately 40%. Only the most competitive solvers are included in this figure.

CPLEX, Gurobi, SeDuMi and MOSEK, depending on the problem data. On average, LPempc is approximately 5 times faster than Gurobi, 6 times faster than MOSEK, 19 times faster than SeDuMi, and 22 times faster than CPLEX.

VI. CONCLUSIONS

In this paper, we develop a computationally efficient homogeneous and self-dual IPM for EMPC of linear systems with a linear objective function and linear constraints. The computation time per IPM iteration is reduced using a Riccati iteration procedure specifically tailored to EMPC. The combination of a Riccati iteration procedure and the homogeneous and self-dual model has not been studied in the existing literature. We reduce the number of IPM iterations using a warm-start strategy that has not previously been applied to MPC problems. Simulations show that warm-start reduces the average number of iterations by 35-40%, and that a MATLAB and C implementation of the proposed algorithm, LPempc, is significantly faster than several state-of-the-art IPMs, as well as automatic code generation based IPMs for MPC. In the particular case study, LPempc is up to an order of magnitude faster than CPLEX, Gurobi, SeDuMi and MOSEK.

ACKNOWLEDGEMENT

This work was funded in part by 1) the Danish Ministry of Higher Education and Science in the industrial Ph.D. project

"Stochastic MPC with Applications in Smart Energy Systems" (11-117435); and 2) the Danish Council for Strategic Research in the project "CITIES - Centre for IT-Intelligent Energy Systems in Cities" (1305-00027B).

REFERENCES

- [1] S. Mehrotra, "On the Implementation of a Primal-Dual Interior Point Method," *SIAM Journal on Optimization*, vol. 2, no. 4, pp. 575-601, 1992.
- [2] J. Nocedal and S. Wright, *Numerical Optimization*, ser. Springer Series in Operations Research and Financial Engineering. Springer, 2006.
- [3] A. Skajaa, E. D. Andersen, and Y. Ye, "Warmstarting the homogeneous and self-dual interior point method for linear and conic quadratic problems," *Mathematical Programming Computation*, vol. 5, no. 1, pp. 1-25, 2013.
- [4] C. V. Rao, S. J. Wright, and J. B. Rawlings, "Application of Interior-Point Methods to Model Predictive Control," *Journal of Optimization Theory and Applications*, vol. 99, no. 3, pp. 723-757, 1998.
- [5] J. B. Jørgensen, G. Frison, N. F. Gade-Nielsen, and B. Dammann, "Numerical Methods for Solution of the Extended Linear Quadratic Control Problem," in *4th IFAC Nonlinear Model Predictive Control Conference*, 2012, pp. 187-193.
- [6] L. Vandenbergh, S. Boyd, and M. Nouralishahi, "Robust linear programming and optimal control," in *15th IFAC World Congress*, vol. 15, 2002, pp. 271-276.
- [7] E. D. Andersen, J. Gondzio, C. Meszaros, and X. Xu, "Implementation of Interior Point Methods for Large Scale Linear Programming," Ecole des Hautes Etudes Commerciales, Universite de Geneve, Papers 96.3, 1996.
- [8] X. Xu, P.-F. Hung, and Y. Ye, "A simplified homogeneous and self-dual linear programming algorithm and its implementation," *Annals of Operations Research*, vol. 62, no. 1, pp. 151-171, 1996.
- [9] Y. Ye, M. J. Todd, and S. Mizuno, "An $O(\sqrt{n}L)$ -Iteration Homogeneous and Self-Dual Linear Programming Algorithm," *Mathematics of Operations Research*, vol. 19, no. 1, pp. 53-67, 1994.
- [10] E. D. Andersen, C. Roos, and T. Terlaky, "On implementing a primal-dual interior-point method for conic quadratic optimization," *Mathematical Programming*, vol. 95, no. 2, pp. 249-277, 2003.
- [11] V. M. Zavala and L. T. Biegler, "Nonlinear Model Predictive Control," in *Control, Nonlinear Programming Strategies for State Estimation and Model Predictive*, ser. Lecture Notes in Control and Information Sciences, L. Magni, D. M. Raimondo, and F. Allgöwer, Eds. Springer Berlin Heidelberg, 2009, vol. 384, pp. 419-432.
- [12] M. Diehl, R. Amrit, and J. B. Rawlings, "A Lyapunov Function for Economic Optimizing Model Predictive Control," *IEEE Transactions on Automatic Control*, vol. 56, no. 3, pp. 703-707, 2011.
- [13] L. Grüne, "Economic receding horizon control without terminal constraints," *Automatica*, vol. 49, no. 3, pp. 725-734, 2013.
- [14] G. Frison and J. B. Jørgensen, "A Fast Condensing Method for Solving Linear-Quadratic Control Problems," in *52th IEEE Conference on Decision and Control (CDC)*, 2013, pp. 7715-7720.
- [15] L. E. Sokoler, G. Frison, A. Skajaa, R. Halvgaard, and J. B. Jørgensen, "A Homogeneous and Self-Dual Interior-Point Linear Programming Algorithm for Economic Model Predictive Control," Department of Applied Mathematics and Computer Science, Technical University of Denmark, Tech. Rep., 2014. [Online]. Available: <http://www2.imm.dtu.dk/~jbjo>
- [16] M. Diehl, H. J. Ferreau, and N. Haverbeke, "Efficient Numerical Methods for Nonlinear MPC and Moving Horizon Estimation," in *Nonlinear Model Predictive Control*, ser. Lecture Notes in Control and Information Sciences. Springer Berlin Heidelberg, 2009, vol. 384, pp. 391-417.
- [17] A. Domahidi, A. U. Zgraggen, M. N. Zeilinger, M. Morari, and C. N. Jones, "Efficient Interior Point Methods for Multistage Problems Arising in Receding Horizon Control," in *51st IEEE Conference on Decision and Control (CDC)*, 2012, pp. 668-674.
- [18] K. Edlund, T. Molbak, and J. D. Bendtsen, "Simple models for model-based portfolio load balancing controller synthesis," in *6th IFAC Symposium on Power Plants and Power Systems Control*, 2009, pp. 173-178.
- [19] J. Mattingley and S. Boyd, "CVXGEN: a code generator for embedded convex optimization," *Optimization and Engineering*, vol. 13, no. 1, pp. 1-27, 2012.

[This page intentionally left blank]

[This page intentionally left blank]